COLLEGE DOCTORAL PAYS DE LA LOIRE — SCIENCES DE L'INGENIERIE ET DES SYSTEMES

Oniris VetAgroBio Nantes ÉCOLE NATIONALE

THÈSE DE DOCTORAT

ONIRIS

ÉCOLE DOCTORALE N°602
Sciences de l'Ingénierie et des Systèmes
Spécialité *« Génie des procédés et Bioprocédés »*

Par

Christy RAAD

« Mixing sandwich bread dough under pressurised gas »

Thèse présentée et soutenue à Nantes, le 15 Décembre 2025
Unité de recherche : GEPEA CNRS 6144

Rapporteurs avant soutenance :

Bernard CUQ	Professeur in Institut Agro – Montpellier Supagro
Stéphane DESOBRY	Professeur in Université de Lorraine

Composition du Jury :

Président :	Bernard CUQ	Professeur in Institut Agro – Montpellier Supagro
Examinateurs :	Stéphane DESOBRY	Professeur in Université de Lorraine
	Reine BARBAR	Maîtresse de Conférence – Montpellier Supagro
	Alain RIAUBLANC	Chargé de recherche – INRAE, Nantes
Dir. de thèse :	Alain LE-BAIL	Professeur in Oniris – UMR GEPEA CNRS 6144 - Nantes
Co-dir. de thèse :	Patricia LE-BAIL	Directrice de Recherches – INRAE BIA, Nantes

ACKNOWLEDGEMENT

I would like to express my sincere gratitude to my reporters Bernard CUQ, Stephane DESOBRY, and jury members Reine BARBAR and Alain RIAUBLANC for agreeing to participate as my revision committee and as reporters. I deeply appreciate your willingness to contribute your time and effort to the evaluation of my work. It is a privilege to have such esteemed professionals accompany me during this significant step in my academic life.

For my supervisors Alain and Patricia, I would like to immensely thank them for believing in me and in my capabilities. For being a great support and for guiding me throughout this crazy journey. Thank you for always pushing me to always be and do my best. For Alain, I am in awe of how much knowledge you have and shared with me during these 3 years. To Patricia, not only as my co-director but also as an inspiring individual your encouragement and support have played a vital role in my personal growth. I deeply admire your strength and wisdom, and I am truly grateful for the kindness and openness with which you welcomed me.

I would like to thank God for his plan to bring me here, to pursue this PhD in France against all odds. I want to give a special thanks to my parents for always being here for me, for encouraging me and for praying for me. Of course my siblings, Aimee, Martin and Calvin, my sister-in-law Nour and brother-in-law Joseph for all your love and support and knowing I have a great and solid support system back home and here in France. Martin and Nour for giving me a sense of home here in France and walking with me in every step of these years.

To my best friend Joy, not just for being there during the easy times, but especially for standing by me when things were tough. Your unwavering support, your ability to listen without judgment, and your constant encouragement have meant the world to me. I am endlessly grateful for your long friendship, for the laughter, the late-night talks, the shared silences, and the strength you have given me just by being yourself.

I would like to thank all the people that I have met in Oniris, I hope this won't take long. I would like to start with our head of department Michel HAVET for always encouraging me. I would like to thank Delphine QUEVEAU and Anthony OGE for not only being my technical referrals but also for being my emotional support and for being here for me whenever I felt sad or discouraged. I admire your ability to listen to me and all your advices, you showed me true compassion and empathy. I admire your discipline in work and your motivation. To my BESTIE whom was chosen as my office colleague but became my biggest cheerleader and supporter, Alejandra (as we call each other Habibtiiii). I cannot put words on how much I appreciate you as a human being and as a friend, you always put me before yourself, you always carried me with open arms. Thank you for all the laughs, cries (a lot of them) and brunches we shared (more to come!). Thierry, thank you for your warmth and mature advices and for always making fun of each other. Anna, you are like a little sister to me, although I bullied a lot (in a good way) you have a special place in my life, I'm sorry but this friendship is not over I will always annoy you and support you no matter what. Claire, you ray of sunshine, thank you for always being positive and being so sweet to the people around you. To Michael, thank you for all the good conversations that we shared and for trusting me and uplifting me. To Maryam, the sweetest and kindest person I have met here, thank you for always listening to me, you were as a big sister to me, I admire your resilience,

wisdom and authenticity. Especially in last few months, I learned a lot about you, we share this entire path together. To Doina, you were here for me since day 1, thank you for all the technical and experimental help, thank you for your open heart and for showing me love, as I used to call it mom's love. Samuel, thank you for helping me in my files and computer problems but most importantly, for your care and genuine love for others and to me, you deserve all the best in this world. I hope I did not forget any names, but thank you to Solene (my fellow swiftie), Saylor, Sadhan, Allan, Salma and Ana-Carolina for your friendships and the time we have spent. Thank you to Luc GUILLARD, Isabelle LE-ROUX, Nasser, and all others if I forgot a name for your support.

Finally, a special thanks for Cecile RANNOU, a research engineer with the Flavour team at Oniris. She conducted most of the analyses of the sensory analysis and assisting me in conducting the sensory trials. For your kind words that touched me and motivated me so much.

To my second family here in Nantes, my Lebanese friends that made this transition period and life easier and it gave me a better sense of home. Tania, Sarah, Samad, Issa, Hariri, Rachelle, Elie, Georges and you know yourselves thank you sincerely.

Last but not least, I want to thank me for believing in me. I want to thank me for doing all this hard work. I want to thank me for having no days off. I want to thank me for never quitting; I want to thank me for always being a giver. I want to thank me for just being me at all times (mic drop).

ABSTRACT

This PhD project, funded by GEPEA-ONIRIS (CNRS 6144) and the INRAE-BIA research unit, in partnership with TU Hohenheim, aimed to study bread dough kneading under pressure with various pure gases or gas mixtures, with the goal of modulating dough development and aeration. The main objective was to control and optimize the structure of the dough and the final bread by adjusting kneading parameters. Different gases (air, O_2, CO_2, N_2) and their mixtures, pressure levels, and mixing speeds were considered. Ascorbic acid (AH_2) was also used to study its behaviour under these modified kneading conditions. AH_2 acts as an oxidizing agent by promoting the oxidation of free thiol groups (-SH), leading to the formation of disulfide bridges (-S-S-) that strengthen the gluten network. Finally, the use of carbonated water saturated with CO_2 was also considered as an alternative to supplying CO_2 in gaseous form.

A calculation-based approach was first used to quantify the potential for gas solubilisation or consumption by the dough during kneading, across two kneading strategies—with or without gas purging. After optimizing the experimental parameters, particularly controlling fermentation expansion based on the dough's initial gas fraction, the main results showed that kneading under CO_2 did not have a positive effect on bread quality, whether introduced in gaseous or liquid form. However, modulating the amount of yeast helped mitigate the observed defects. The use of AH_2 had no significant effect on the kneading process or on bread quality, whether in the presence or absence of oxygen.

A study was also conducted to evaluate the effect of gases on bread staling, with interesting results. Finally, sensory analysis revealed good acceptance of the breads, with comments on crumb homogeneity, color, aroma, and an overall positive texture. This project contributed to a better understanding of the operation of non-conventional mixers and opened up many perspectives, particularly in terms of equipment design and implementation.

RÉSUMÉ

Ce projet de thèse, financé par GEPEA-ONIRIS (CNRS 6144) et l'unité de recherche INRAE-BIA en partenariat avec la TU Hohenheim visait à étudier le pétrissage de pâte à pain sous pression de divers gaz purs ou de mélanges en vue de moduler le développement de la pâte et son aération. L'objectif principal était de contrôler et d'optimiser la structure de la pâte et du pain en ajustant les paramètres de pétrissage. Divers gaz (air, O_2, CO_2, N_2) et leurs mélanges, les niveaux de pression et les vitesses de mélange ont été considérés. L'acide ascorbique (AH_2) a également été utilisé pour étudier son comportement dans ces conditions de pétrissage modifiées. L'AH_2 fonctionne comme un agent oxydant en favorisant l'oxydation des thiols libres (-SH), ce qui conduit à la formation de ponts disulfures (-S-S-) qui renforcent le réseau de gluten. Enfin, l'utilisation d'eau gazeuse saturée en gaz carbonique a également été considérée comme une alternative à l'apport de CO_2 sous forme de gaz.

Une approche calculatoire a tout d'abord permis de quantifier le potentiel de solubilisation ou de consommation des gaz par la pâte en cours de pétrissage autours de deux stratégies de pétrissage, avec ou sans balayage gazeux. Après avoir optimisé les paramètres expérimentaux, en particulier la maîtrise du taux d'expansion en fermentation en fonction de la fraction de gazeuse initiale de la pâte, les principaux résultats obtenus ont montré que le pétrissage sous CO_2 n'avait pas d'effet positif sur la qualité des pains, qu'il soit apporté par voie gazeuse ou liquide ; la modulation de la quantité de levure a permis de pallier aux défauts observés. L'utilisation d'AH_2 n'a pas eu d'effet significatif sur les étapes du procédé de pétrissage ni sur la qualité des pains, que ce soit en présence ou en absence d'oxygène. Une étude a été menée afin d'évaluer l'effet des gaz sur le rassissement des pains avec des résultats intéressants. Enfin, l'analyse sensorielle a révélé une bonne acceptation des pains, avec des remarques sur l'homogénéité de la mie, la couleur et l'odeur, et une texture généralement positive. Ce projet a permis de mieux comprendre le fonctionnement de pétrins non conventionnels et a ouvert de nombreuses perspectives en particulier sur le plan de la conception des équipements et sur leur mise en œuvre.

NOMENCLATURE

ADA	Azodicarbonamide
AH_2	Ascorbic Acid (ppm or % of flour dry weight)
AOX	Ascorbic acid oxidase
AX	Arabinoxylans
a*	The spectrum from green to red
BU	Brabender Unit
b*	The spectrum from blue to yellow
C	CO_2 solubility according to Henry's law ($mol \cdot L^{-1}$)
C_2H_5OH	Ethanol
$C_6H_{12}O_6$	Glucose
C_∞	Saturation concentration of gas in the liquid phase ($mol \cdot L^{-1}$ or $g \cdot L^{-1}$)
CarbD	Carbonated dough
CBP	Chorleywood Bread Process
$CO_2(aq)$	Dissolved molecular CO_2 in aqueous phase ($mol \cdot L^{-1}$)
CO_2*	Total dissolved CO_2 ($mol \cdot L^{-1}$)
CO_2	Carbon dioxide
CO_3^{2-}	Carbonate ion
Cys	Cysteine
D50	Median pore size or area at which 50% of total pore number falls under
D90	Median pore size or area at which 90% of total pore number falls under
DDT	Dough Development Time
DF	Dry Flour
DHA	Dehydroascorbic acid
dpi	Dots per inch (unitless)
DSC	Differential Scanning Calorimetry
f	Frequency (Hz)
FW	Free Water
G	Swelling
G''	Loss or viscous modulus (Pa)
G'	Storage or elastic modulus (Pa)
GH	Gas hydrates
GSH	Glutathione (reduced form)
GSSG	Glutathione (oxidized form)
H or KH	Henry's Law Constant ($MPa \cdot mol^{-1}$ or $Pa \cdot m^3 \cdot mol^{-1}$)
H+	Proton (Hydrogen ion) ($mol \cdot L^{-1}$)
H_0	Initial experimental height of the dough (cm)
H_2CO_3	Carbonic acid

HCO_3^-	Bicarbonate Ion
H_F	Final dough height after fermentation (cm)
H_I	Initial dough height before fermentation (cm)
H_{final}^{theo}	Theoretical final height of the dough in the flask at the end of fermentation (cm)
H_0^{theo}	Theoretical initial height of the dough in the flask (cm)
HMW	High Molecular Weight
HPF	High Protein Flour
HS	Headspace
Ie	Elasticity index
IPM	Ideal Profile Method
JAR	Just-About-Right
K	Time constant (unit in time, days in general)
K_0	Henry's constant ()
K_1	Equilibrium constant for CO_2/HCO_3^- ($mol \cdot L^{-1}$)
K_2	Equilibrium constant for HCO_3^-/CO_3^{2-} ($mol \cdot L^{-1}$)
K_C	CO_2 solubility Coefficient ($g_{CO2} \cdot g_{LPD}^{-1}$)
K_H	Henry's constant ($Pa \cdot m^3$ of LPD$\cdot mol^{-1}$)
KH_0	Reference Henry's constant at temperature T0 ($Pa \cdot m^3$ of LPD$\cdot mol^{-1}$)
L*	The spectrum of lightness to darkness
Latent heat (Lf)	Latent heat of fusion water ($333\ J \cdot g^{-1}$)
LMW	Low Molecular Weight
LOX	Lipoxygenase
LPD	Liquid Phase Dough
LPF	Low Protein Flour
LSF	Lubricated Squeezing Flow
L	Extensibility (mm)
m	Consistency coefficient ($Pa.s_n$)
m'_c	Mass of CO_2 in gaseous phase (g)
m''_c	Mass of dissolved CO_2 in aqueous phase (g)
m_1	Initial dough mass in ambient air (g)
m_2	Final dough mass in oil (g)
MC	Moisture content (%)
Mc	Molecular mass of CO_2 ($g \cdot mol^{-1}$)
m_c	Total mass of CO_2 (g)
m_D	Mass of dough in the flask (g)
MDD	Mechanical Dough Development
n	Cross exponent or flow index ($n \leq 1$)
n	Avrami exponent
n	Number of moles of gas (mol)

N	Expansion ratio of the dough during fermentation = X_f/X_i (dimensionless)
N_2	Nitrogen
NaCl	Sodium Chloride
nO_2	Moles of Oxygen (mol)
O_2	Oxygen
OM	Overpressure Mixing
P(t)	Instantaneous mechanical power (W)
P/L	Ratio between tenacity and extensibility
p	Partial pressure (Pa)
P	Tenacity
P	Pressure (Pa)
Pc	Partial pressure of CO_2 (Pa)
P_{dough}	Power associated specifically to the dough (tool power – satellite power) ($W \cdot kg^{-1}$)
P_{O2}	Partial Pressure of Oxygen (Pa)
$P_{satellite}$	Power of orbiting arm (W)
PSH	Protein-bound thiols
PSSG	Protein–glutathione mixed disulfides
P_{Tool}	Power of mixing tool (W)
QDA	Quantitative Descriptive Analysis
R	Perfect gas constant (8.314 $J \cdot mol^{-1} \cdot K^{-1}$)
RefD	Reference dough
RH	Relative humidity (%)
RPM	Revolution per Minute (tool rotational speed)
SDS-PAGE	Sodium Dodecyl Sulfate–Polyacrylamide Gel Electrophoresis
SEM	Scanning Electron Microscopy
SH	Sulfhydryl/thiol group
SME	Specific Mechanicl Energy ($kJ \cdot kg^{-1}$)
SME_0	Initial SME (intercept at start of kneading) ($kJ \cdot kg^{-1}$)
SME_{RATE}	Slope of SME over time ($kJ \cdot kg^{-1} \cdot min^{-1}$)
$SMEt_{PEAK}$	SME value at t_{PEAK} ($kJ \cdot kg^{-1}$)
SS	Disulfide bonds
SV	Specific volume of the bread ($cm^3 \cdot g^{-1}$)
T	Temperature (K)
T	Torque
t	time (days or s)
T0	Reference temperature (Kelvin, K)
TCD	Total Color Difference
t_{PEAK}	Optimal Mixing Time (min)
$t_{PEAK-DE}$	t_{PEAK} determined from double exponential fitting (min)
$t_{PEAK-EXP}$	Experimentally observed peak time (maximum point in raw power data) (min)

t_{PEAK-X}^2	t_{PEAK} determined from quadric polynomial fitting (min)
UY	Unyeasted dough
v/v%	Volume/volume Percentage (%)
V	Volume (m^3)
V_d	Volume of continuous dough (m^3)
Vc	Equivalent volume of dissolved CO_2 in unit mass of dough ($m^3 \cdot kg^{-1}$ or $L \cdot kg^{-1}$)
V_D	Volume of gassed dough (real dough containing gas cells) (cm^3)
V_{DD}	Volume of degassed dough or gas-free dough (cm^3)
V_{DF}	Final apparent volume of dough (cm^3)
V_{DI}	Initial apparent volume of dough (cm^3)
V_{dough}	Dough Volume
V_{gas}	gas volume entrapped in the dough to determine its void fraction (cm^3)
V_{GF}	Final gas volume inside the dough (cm^3)
V_{GI}	Initial gas volume in dough (cm^3)
V_{HS}	Volume of Headspace (L)
V_{HS-NET}	Net volume of Headspace (L)
V_iO_2	Instantaneous Oxygen Consumption rate ($\mu mol \cdot g_{DF}^{-1} \cdot s^{-1}$)
VOC	Volatile Organic Compounds
w.b	Wet Basis (%)
w/w%	Weight/Weight Percentage (%)
W	Baking strength ($x10^{-4}$ J)
WE-AX	Water-extractable arabinoxylans
w_f	Final weight after drying (g)
w_i	Initial weight before drying (g)
WU-AX	Water-unextractable arabinoxylans
X_c	Concentration of CO_2 in aqueous dough ($mol \cdot L^{-1}$)
XCO_2	Molar Ratio of CO_2 to H_2O ($mol_{CO2} \cdot mol_{H2O}^{-1}$)
X_{DF}	Total Water per gram of Dry Flour ($g_{water} \cdot g_{flour}^{-1}$)
X_{FW}	Free Water Content ($g_{water} \cdot g_{dry\ flour}^{-1}$)
X_i^V	Volumic fraction of the ingredient I in the dough (dimensionless)
XRD	X-ray Diffraction
Y	Yeasted dough

Greek Letters

ΔE	Energy (kcal)
ΔE	Total Colour Difference
ΔH	Enthalpy of retrogradation ($J \cdot g^{-1}$ dry matter or flour)
ΔH_0	Initial enthalpy ($J \cdot g^{-1}$ of dry flour)
Δ	Loss angle (rad)

ε	dough void fraction = ratio of entrapped gas divided by the dough volume (dimensionless)
ε'_I	Dough's void fraction at the end of mixing (dimensionless)
ε_C	Final crumb porosity at the end of baking (dimensionless)
ε_F	Final void fraction in the dough at the end of fermentation (dimensionless)
ε_I	Initial dough's void fraction at start of fermentation (dimensionless)
γ	Deformation rate
$\dot{\gamma}_0$	Critical shear rate
μ_0	Initial viscosity of the Newtonian plate
ρ_{app}	Apparent density ($g \cdot cm^{-3}$)
ρ_d	Density of aerated dough ($g \cdot cm^{-3}$)
ρ_{DD}	Density of degassed dough ($g \cdot cm^{-3}$)
ρ_{oil}	Density of sunflower oil ($g \cdot cm^{-3}$)
ρ_T	True density ($g \cdot cm^{-3}$)
τ	Stress applied
τ_0	is the yield stress (Pa)
τ'	Time constant characterising retrogradation kinetics rate (unit in time, days in general)
ω	Angular frequency ($rad \cdot s^{-1}$ or Hz)

TABLE OF CONTENTS

ACKNOWLEDGEMENT II
ABSTRACT IV
RÉSUMÉ V
NOMENCLATURE VII
TABLE OF CONTENTS XIII
LIST OF FIGURES XXI
LIST OF TABLES XXXI
GENERAL INTRODUCTION 1
CHAPTER 1 : STATE OF ART 5
1.1. Introduction 6
1.2. Bread & components 7
1.2.1. Wheat Flour 8
1.2.1.1. Gluten 9
1.2.1.2. Starch 10
1.2.1.2.1. Morphology, structure & ultrastructure 10
1.2.1.2.2. Crystallinity 13
1.2.1.2.3. Other flour components 13
1.2.2. Water 14
1.2.3. Yeast 15
1.2.4. Salt 15
1.2.5. Additives in bread 16
1.3. Interactions between dough ingredients during bread making 16
1.3.1. During kneading 17
1.3.1.1. Mixing speed & time 19
1.3.2. During shaping 19
1.3.3. During fermentation 20
1.3.4. During baking 21
1.3.4.1. Distribution of Water in Bread 23
1.3.5. During cooling 24
1.3.6. During storage 24
1.3.6.1. Basic Mechanisms of Starch Gelatinization 25
1.3.6.2. Retrogradation 25
1.3.6.3. Water Redistribution Within Bread 26
1.3.6.4. Influence of Water Partitioning and Salt on Starch Retrogradation in Bread 27

1.4. Dough aeration methods 27
1.4.1. Influence of conventional mixer parameters on dough aeration**Error! Bookmark not defined.**
1.4.1.1. Mixing speed & time 30
1.4.1.2. Dough temperature 32
1.5. Specific process 33
1.5.1. Partial vacuum aeration method 33
1.5.2. Vacuum combined with overpressure method 33
1.5.3. Injected gas 36
1.5.3.1. Carbon dioxide: CO_2 36
1.5.3.1.1. CO_2 solubility in water 40
1.5.3.1.2. Effect of solutes on CO_2 solubility in water 42
1.5.3.1.3. CO_2 solubility in bread dough 43
1.5.3.2. Oxygen: O_2 46
1.5.3.3. Nitrogen: N_2 49
1.5.4. Incorporation of Ascorbic acid: AH_2 or E300 as an additive 50
1.5.4.1. Ascorbic acid (AH_2) chemical properties 50
1.5.4.2. AH_2 mode of action 51
1.6. Rheological properties of dough 54
1.6.1. The Farinograph (Brabender) 56
1.6.2. The Chopin alveograph 56
1.6.3. Rheological Measurements 56
1.6.4. Viscoelastic properties (low deformations in dynamic regime) 58
1.6.5. Flow properties (large deformations) 59
1.7. The sensory aspect 61
1.7.1. Appearance 62
1.7.2. Texture 62
1.7.3. Odour/aroma 63
1.7.4. Taste 64
1.7.5. Evaluation of the sensory properties – Sensorial analysis 64
1.7.5.1. Discriminative tests 64
1.7.5.2. Descriptive tests 65
1.7.5.3. Hedonic Tests 65
SCIENTIFIC APPROACH 66
CHAPTER 2 : MATERIALS & METHODS 71
2.1. Part I 72
2.1.1. Ingredients 72
2.1.2. Breadmaking process summary 72
2.1.2.1. Dough mixing protocol 73

2.1.2.2. Determination of dough development time (t_{PEAK}) and the mechanical energy (SME) consumed by the dough 75
2.1.2.2.1. t_{PEAK} data treatment and processing 75
2.1.2.2.2. SME data treatment and processing 80
2.1.2.3. Shaping and resting 82
2.1.2.4. Sheeting and moulding 82
2.1.3. Determination of dough properties 82
2.1.3.1. Dough void fraction after mixing, sheeting and fermentation 82
2.1.3.2. Dough fermentation and determination of dough expansion ratio N 84
2.1.3.3. Quantifying Fermentation Kinetics through CO_2 Emission Measurements with Risograph 85
2.1.3.4. Measurement of dough pH before and after fermentation 86
2.1.3.5. Analysis of bubbles in dough under Photonic Optical Microscopy 86
2.1.3.6. Dough/bread colour 87
2.1.3.7. Dough Rheology 87
2.1.3.8. Determination of freezable water in Dough 89
2.1.4. Determination of bread properties 90
2.1.4.1. Breads Specific Volume (SV) 90
2.1.4.2. Determination of breadcrumb structure 90
2.1.4.3. Determination of bread porosity 92
2.1.4.4. Bread Staling 92
2.1.4.4.1. Determination of bread texture during storage 92
2.1.4.4.2. Determination of bread moisture content during storage 93
2.1.4.4.3. Microcalorimeter multicells µ-DSC 94
2.1.5. Sensorial analysis of breads 95
2.1.5.1. Objectives 95
2.1.5.2. Sensory analysis laboratory 95
2.1.5.3. Panellists 95
2.1.5.4. Product preparation 95
2.1.5.5. Triangular test 95
2.1.5.6. Flash Profile 96
2.1.5.7. Statistical analysis of the sensory analysis 97
2.2. Part II – Mobility Project by TU HOHENHEIM 97
2.2.1. Ingredients 97
2.2.2. Breadmaking process 98
2.2.3. Dough mixing 98
2.2.3.1. Determination of t_{PEAK} 98
2.2.3.2. Determination of dough void fractions 98
2.2.3.3. Determination of dough expansion ratio N at end of fermentation 99
2.2.3.4. Shaping of dough and fermentation 99
2.2.4. Baking 100

2.2.5. Determination of dough and bread properties 101
2.2.5.1. Measurement of dough pH before and after fermentation 101
2.2.5.2. Determination of doughs texture before and after fermentation 101
2.2.5.3. Dough colour measurement before and after fermentation 101
2.2.5.4. Texture profile analysis of bread 101
2.2.5.5. Determination of breads texture after baking 101
2.2.6. Statistical analysis 102
CHAPTER 3 : RESULTS & DISCUSSION 103
3.1. Part I – Article 1 104
3.1.1. Introduction 105
3.1.2. Materials & Methods 108
3.1.2.1. Ingredients 108
3.1.2.2. Mixing 109
3.1.3. Determination of the dough properties 111
3.1.3.1. Determination of dough void fractions 111
3.1.3.2. Determination of dough expansion ratio N in function of the initial and final dough void fractions after fermentation ε_I & ε_F 112
3.1.3.3. Bread baking and determination of bread properties 114
3.1.3.4. Determination of breads specific volumes (SV) 114
3.1.3.5. Determination of the breadcrumb aeration 114
3.1.4. Statistical analysis 114
3.1.5. Results & discussion 114
3.1.5.1. Determination of the dough optimum mixing time (t_{PEAK}) 114
3.1.5.2. Determination of the dough void fraction ε after mixing, sheeting & fermentation 116
3.1.5.3. Determination of the dough expansion ratio N in real conditions 117
3.1.5.4. Determination of bread specific volume SV 118
3.1.5.5. Determination of the breadcrumb structure 119
3.1.6. Conclusion 121
3.1.7. References 122
3.2. Part II – Dough results for all gas mixtures with the addition of ascorbic acid AH_2 123
3.2.1. Part A: O_2 consumption and CO_2 solubility in dough 125
3.2.1.1. Determination of the partial pressures of the different gases in function of the protocols 125
3.2.1.2. Determination of O_2 consumption by the dough during the kneading phase: A vs. Protocol B 125
3.2.1.3. Solubility in water and in bread dough 128
3.2.1.4. Experimental validation: CO_2 solubility using SodaStream at various salt (NaCl) concentrations 128
3.2.2. Part B: Main mixing tests and dough results 131

3.2.2.1. Effect of pressurized gas-composition and addition of AH_2 on t_{PEAK} and SME after kneading: A vs. B protocol 131
3.2.2.2. Effect of pressurized gas-composition and addition of AH_2 on dough void fraction ε after kneading, sheeting and fermentation 136
3.2.2.3. In absence of AH_2 137
3.2.2.4. In presence of AH_2 139
3.2.2.5. Effect of pressurized gas-composition and addition of AH_2 on dough expansion ratio N and effectively fermentation time 141
3.2.2.6. Measurement of CO_2 emission during fermentation by the Risograph equipment 143
3.2.3. Part C: effect of sheeting and additional analysis 146
3.2.3.1. Effect of the sheeting process on dough void fractions under air and CO_2-mixed doughs vs. without sheeting 146
3.2.3.2. Analysis of bubbles in dough observed under Photonic Optical Microscopy 148
3.2.3.3. Effect of pressurized gas-composition and addition of AH_2 on dough pH after fermentation 153
3.2.3.4. Effect of pressurized gas-composition and addition of AH_2 on dough storage modulus (G') after kneading 154
3.2.3.5. Effect of pressurized gas-composition and addition of AH_2 on dough color after kneading 156
3.3. Conclusion for Chapter 3 159
CHAPTER 4 : BREAD RESULTS 161
4.1. Part A – Bread results for all gas mixtures (air, 100%CO_2, 30%O_2 70%N_2) 162
4.1.1. Effect of pressurized gas conditions and the addition of AH_2 on bread specific volumes SV and porosity 162
4.1.2. Determination of Breadcrumb structure and pore distribution 163
4.1.3. Determination of breadcrumb porosity 166
4.1.4. Determination of bread colour 168
4.1.5. Bread Staling 170
4.1.5.1. Starch retrogradation 170
4.1.5.2. Determination of bread texture changes during storage 174
4.1.5.2.1. Firmness 174
4.1.5.2.2. Cohesiveness 177
4.1.5.3. Determination of moisture content during storage 178
4.2. Part B – Effect of reduction of yeast amount on bread SV and breadcrumb structure under CO_2-enriched environment 181
4.2.1.1. Determination of breads SV 182
4.2.1.2. Breadcrumb structure 184
4.3. Part C – Impact of mechanical dough sheeting 186
4.3.1. Determination of bread SV of sheeted vs. non-sheeted breads 186
4.3.2. Determination of breadcrumb structure of sheeted and non-sheeted doughs 187

4.4. Part D – Sensory analysis 190
4.4.1. The Triangular Test 190
4.4.2. Flash Profile 191
4.4.2.1. Results 191
4.4.2.2. Correlation with Instrumental Measurements 195
4.4.3. Conclusion 196
CONCLUSION OF CHAPTER 4 197
CHAPTER 5 : ARTICLE 2 199
5.1. Experimental strategy 200
5.2. Introduction 201
5.3. Materials & Methods 202
5.3.1. Experimental strategy 202
5.3.2. Ingredients 203
5.3.2.1. Experimental preparation protocol of carbonated water and the influence of salt concentrations on CO_2 solubility 203
5.3.2.2. Breadmaking process 204
5.3.2.2.1. Dough mixing 204
5.3.2.2.2. Determination of t_{PEAK} 204
5.3.2.2.3. Determination of dough void fractions 205
5.3.2.2.4. Determination of dough expansion ratio N at end of fermentation 205
5.3.2.2.5. Shaping of dough and fermentation 206
5.3.2.3. Baking 207
5.3.3. Determination of dough and bread properties 207
5.3.3.1. Measurement of dough pH before and after fermentation 207
5.3.3.2. Determination of doughs texture before and after fermentation 207
5.3.3.3. Dough colour measurement before and after fermentation 208
5.3.3.4. Texture profile analysis of bread 208
5.3.3.5. Determination of breads texture after baking 208
5.3.4. Statistical analysis 208
5.4. Results & Discussion 209
5.4.1. Dough properties 209
5.4.1.1. Assessment of CO_2 Solubility in Carbonated Water: Influence of Salt Concentration and Implications for Dough Formulation 209
5.4.1.2. Determination of t_{PEAK} 212
5.4.1.3. Measurement of dough void fractions after mixing, sheeting & fermentation 212
5.4.1.4. Measurement of dough expansion ratio (N) after sheeting 213
5.4.1.5. CO_2 measurement in the fermentation cabinet during fermentation 214
5.4.1.6. Measurement of dough texture before & after fermentation 216
5.4.1.7. Measurement of dough colour before and after fermentation 217

5.4.2. Bread properties 218
5.4.2.1. Breads specific volume SV 218
5.4.2.2. Breads texture 219
5.4.2.3. Breads upper crust and crumb colour 219
5.5. Conclusion 220
GENERAL DISCUSSION 222
CONCLUSION AND PERSPECTIVES 232
REFERENCES 236

LIST OF FIGURES

Figure 1.1 A bread advertisement for Sunbeam bread dates back to 1947 showing the appeal of aerated bread and the expectation of consumers for uniform and fine gas cells in crumb 7

Figure 1.2 Schematic Representation of Wheat Flour Components and Their Substructures (ref. A. Le-Bail- ONIRIS) 9

Figure 1.3 Schematic illustration of glutenin and gliadin when bonded together forming the gluten . 10

Figure 1.4 SEM native wheat starch granules images (Sujka and Jamroz 2013) 11

Figure 1.5 Primary structure of the two polymers amylose and amylopectin constituting the carbohydrate fraction of starch (Kim, Kim and Baik 2012) 12

Figure 1.6 Schematic representation of a starch granule (Jenkins and Donald 1995; Oostergetel and van Bruggen 1993) 12

Figure 1.7 Constituents of arabinoxylans (AX) in wheat flour (Courtin and Delcour 2002) 14

Figure 1.8 Flow diagram of the main operation units in breadmaking processing from wheat flour to the final product (Venturi et al. 2021) 16

Figure 1.9 Temperature profile during baking showing crust and crumb formation stages: the crust undergoes Maillard reactions, drying and caramelisation. While the crumb experiences starch gelatinisation, yeast inactivation, gluten changes and α-amylase inactivation. Key temperature points for biochemical transitions are also indicated along the crumb temperature curve (Source: A. Le-Bail, personal communication) 23

Figure 1.10 Mechanism of starch gelatinisation (Lai and Kokini 2008) 25

Figure 1.11 Amylose and amylopectin rearrangement during retrogradation 26

Figure 1.12 A diagram illustrating how the application of either overpressure or vacuum during mixing can influence dough aeration (Sadot, Cheio and Le-Bail 2017) 34

Figure 1.13 Fraction of solubilized carbon dioxide (CO_2), carbonic acid (H_2CO_3) and carbonate (CO_3^{2-}) in water as a function of pH (adapted from Daniels et al, 1985) 37

Figure 1.14 Effect of dough density on external pressure evolution at 20 °C for 30 g samples (Ben Aissa et al. 2010) for different volumes Vi of the dough 39

Figure 1.15. Solubility of CO_2 and O_2 in water as a function of temperature. The left y-axis indicates the concentration of CO_2 in $mg \cdot L^{-1}$, while the right y-axis corresponds to O_2 concentration in $mg \cdot L^{-1}$. The solubility of both gases decreases with increasing temperature. Red lines highlight the CO_2 solubility ($\approx 1450\ mg \cdot L^{-1}$) at approximately 25°C, demonstrating the inverse relationship between gas solubility and temperature (Gevantman 2011) 41

Figure 1.16. Henry's constant for CO_2 in water as a function of temperature. A fitted correlation curve is shown through the selected data points. The plot highlights the general trend of increasing Henry's constant with temperature, indicating decreasing gas solubility Gevantman (2011) 41

Figure 1.17. Effect of alcohol and sugar on CO_2 partial pressure in water. The bar graph shows the CO_2 partial pressure (in atm) for pure water and water containing either alcohol (11° or 40°) or sugar at concentrations of 10 $g \cdot L^{-1}$ and 40 $g \cdot L^{-1}$ Descoins et al. (2006) 43

Figure 1.18. schematic representation of the water distribution in the typical bread dough system. The "LPD" or Liquid Phase Dough concerns a priori the water added to the recipe (here 58 g water on 100 g flour wb). The "free water" represents the "freezable water", which is a priori mainly concerned by the solubilisation of CO_2 as well as other solute (salt in particular) during mixing... 43

Figure 1.19. Effect of temperature on the dissolved CO_2 Chiotellis & Campbell (2003) 45

Figure 1.20 O_2 consumption during kneading of yeasted vs. unyeasted dough (Buche 2011) 47

Figure 1.21 Oxygen consumption and total carbon dioxide production (sum of released and retained CO_2) during the mixing, fermentation, and second mixing of yeasted dough containing 1% dry yeast (Buche 2011) 49

Figure 1.22 Effect of different concentrations of AH_2 (0, 10, and 15 ppm) on dough rheological properties measured by Chopin's alveograph. Curves A, B, and C represent dough without ascorbic acid, with 10 ppm, and with 15 ppm AH_2, respectively. The addition of AH_2 increased dough strength (G) and baking strength (W), indicating improved gluten network formation and gas retention capacity. Extensibility (P) and elasticity ratio (P/L) also changed, reflecting enhanced dough elasticity (Calvel 2001)..... 50

Figure 1.23 Ascorbic acid (AH_2) isomers and their molecular structures (Raghavendra Rao et al. 2016) 51

Figure 1.24 Ascorbic acid (AH_2) molecular structure (Devaki and Raveendran 2017) 51

Figure 1.25 Reactions catalysed by ascorbic acid oxidase (Chen and Schofield 1996; Faccio et al. 2012; Guo et al. 2020)..... 53

Figure 1.26 The characteristic curve of dough measures tenacity (P), extensibility (L), and baking strength (W). Tenacity reflects resistance to deformation and depends on protein quality, starch damage, and fiber content. Extensibility indicates the dough's ability to stretch and retain gas, mainly influenced by protein. Elasticity, measured by the elasticity index (Ie = P200/P), shows how well the dough recovers after stretching. Baking strength (W), the area under the curve, represents the dough's total energy and overall performance in baking (KPM 2025) 54

Figure 1.27 Representative farinogram showing some commonly measured indices. (reproduced from Pomeranz, Y., ed. 1971. Wheat; Chemistry and Technology, 2nd ed. Am. Assoc. Cereal Chem., St. Paul, MN)..... 55

Figure 1.28 a) Rheogram for an ideal shear-thinning fluid (pseudo-plastic behaviour), b) Linear viscoelasticity domain. Adapted from (Steffe 1996) 57

Figure 1.29 Rheogram for a thixotropic shear-thinning fluid. Adapted from (Steffe 1996) 58

Figure 1.30 Flow curve (viscosity versus shear rate) of wheat flour dough (Lefebvre 2006)..... 60

Figure 1.31 Evolution of the apparent viscosity of the dough as a function of temperature (Bloksma 1990) 61

Figure 1.32. Schematic representation of CO_2 injection and pressure conditions during dough kneading under vacuum and gas composition. The chronological order of dough mixing starts by phase 1 and ends with phase 3: a) Effect of partially opening the mixer valve at atmospheric pressure throughout the entire mixing stages, where vacuum pressure at -500 mbar followed by atmospheric pressure (all air molecules evacuated) b) Effect of vacuum treatment at – 500 mbar by partially opening the mixer valve then closing it during the kneading phase where pressure reached a total of 1.5 bar within the chamber. This resulted in partial evacuation of air..... 66

Figure 1.33. Effect of exhaust valve closing of the mixer during vacuum and then slightly opening it when the mixing pressure was above atmospheric on the gas composition inside the kneader headspace. Phase (a) to evacuate ambient air, followed by CO_2 injection during pre-mixing (c) and kneading (d)..... 67

Figure 2.1 Breads making steps from mixing to baking..... 73

Figure 2.2 VMI prototype dough mixer used for the tests. The lid covering the mixing bowl (open position on picture) was equipped with a spiral tool. The mixer allowed control of the pressure in the headspace as well as a control of the gas composition. The mixer has a valve that opens and closes on its right side to control air and gas circulation, and the mixer is connected to gas bottles through a gas pump that controls the injected gas pressure..... 73

Figure 2.3 Example of a treatment applied to 3 replicated to determine the t_{PEAK}. The three tests underwent a sliding average to smooth the noise. Then the three measurements were averaged 76

Figure 2.4 Determination of $t_{PEAK-EXP}$ based on the maximum power level observed during dough mixing (kneading phase)..... 76

Figure 2.5 Schematic representation of the power function during mixing (kneading phase) in the case of data fitting with a quadratic polynomial function. The excess in time coverage during the mixing yielded in a shift of the t_{PEAK} to non-realistic values (doted red line ➔ $t_{PEAK\text{-}X^2}$ 100% considering all the data points) compared to the observed "Experimental maximum time" ($t_{PEAK-EXP}$ on the figure). Consequently, it was decided to use a shorter time coverage corresponding to two times the $t_{PEAK-EXP}$; this is $t_{PEAK\text{-}X^2\ 50/50}$. Still, the obtained values were around 1 minute longer than the $t_{PEAK-EXP}$ 77

Figure 2.6 Schematic representation of triplicate of t_{PEAK} of an air-mixed dough showing the difference between $t_{PEAK-EXP}$ and $t_{PEAK\text{-}X}^2$. As well as the average of the triplicate, and the polynomial regression R2..... 78

Figure 2.7 Schematic representation of a double exponential function..... 78

Figure 2.8 Schematic presentation of the type of fitting obtained with a double exponential model using a 50/50 approach = the number of points used for the fitting cover the double of the $t_{PEAK-EXP}$ observed (example here with $t_{PEAK-EXP}$ = 3 min and values up to 6 min used for the fitting of the double exp. model)..... 79

Figure 2.9 Example of a Cumulative linear exponential curve of SME in function of kneading time ... 81

Figure 2.10 Principle of the test used to determine the void fraction in a dough sample. The measurement is based on Archimedes principle with (a) mass m_1 of the sample and (b) mass perceived when the dough sample was immersed in the oil. For after kneading, a 30 g of dough was

measured, whereas after sheeting an entire piece of rolled/sheeted dough (150 g) was similarly measured 83

Figure 2.11 Apparatus used for measuring the dough void fraction after fermentation 84

Figure 2.12 Risograph apparatus showing the jars placed in the water bath connected with detection tubes 86

Figure 2.13 Thermo Scientific™ HAAKE™ RheoWin™ MARS 40 rheometer 88

Figure 2.14 Standard rheological measuring geometries, including cone-and-plate, parallel plates, and coaxial cylinders, each suited for different sample types and measurement conditions 88

Figure 2.15 Graphical illustration of the area under each endothermic peak for the reference dough. The two runs showing repeatability 90

Figure 2.16 Sliced bread showing the thickness of each slice prior to analysis 91

Figure 2.17 The process of image analysis using ImageJ software. (a) is the blue hue image, (b) is the inverted version and (c) is the outlined image 91

Figure 2.18 Compressive force as function of time 93

Figure 2.19 Sampling illustration from the sliced bread load: 3 slices taken from 3 distinct positions with the sampling illustration of 3 subsamples from each slice 93

Figure 2.20, Example of the evaluation sheet used in the first session of Profile Flash test 97

Figure 2.21 Picture of the inside of the fermentation cabinet; CO_2 sensors in yellow and Relative humidity sensors in blue 100

Figure 3.1 Evolution of the dough void fractions during the bread making process; this figure proposes a schematic evolution during mixing, sheeting - moulding, dough resting and fermentation (personal communication) 107

Figure 3.2. Fermentation flask used to monitor the expansion ratio of the dough during fermentation (internal ref.). Example of an expansion ratio N of 3 with $N = H_F / H_I$ 108

Figure 3.3. VMI prototype dough mixer used for the tests. The lid covering the mixing bowl (open position on picture) was equipped with a spiral tool. The mixer allowed control of the pressure in the headspace as well as a control of the gas composition 109

Figure 3.4. Principle of the test used to determine the void fraction in a dough sample. The measurement is based on Archimedes principle with (a) mass m_1 of the sample and (b) mass perceived when the dough sample was immersed in the colza oil. For after kneading, a dough piece of 30 g was considered, whereas after sheeting an entire piece of rolled/sheeted dough (150 g) was similarly considered 112

Figure 3.5. Illustrations of the evolution of the dough's void fractions during fermentation in a flask. The expansion ration N depends on the initial dough void fraction; it should be around 3.6 to reach 0.75 in the case of an initial void fraction of 0.1 113

Figure 3.6. This curve shows an exact representation of the evolution of the power of the mixer and the specific mechanical energy consumed by the dough during the mixing, kneading and over-mixing and the t_{PEAK} attained during the kneading phase 115

Figure 3.7. Theoretical vs. real dough profiles in the cylindrical flask 117

Figure 3.8. Bread loaves specific volumes under the different mixing parameters 119

Figure 3.9. Cumulative pore size distribution for breads mixed under different mixing parameters . 120

Figure 3.10. Scanned images of bread slices mixed under Air and CO_2 at atmospheric pressure and 0.5 bar gauge pressure with a scale of 10 mm for each treated image 121

Figure 3.11 O_2 consumption and instantaneous O_2 consumption rate (ViO_2) by the dough during kneading (1% dry yeast) (Buche 2011) 126

Figure 3.12 Schematic illustration of the VMI headspace volume showing the net volume occupied by the gas inside the headspace 127

Figure 3.13. Impact of the NaCl titrant of a water solution (tap water) on the CO_2 solubility at around 5 bar. Tests done with a sodastream equipment. The x-axis shows the titrant, essentially the mass fraction or titrant solution of NaCl in the solution 129

Figure 3.14. Evolution of average power (W) as a function of time (min) during dough kneading under air at 150 RPM. The solid line represents the measured values with standard deviation (shaded area), while the dotted line shows the quadratic regression fit 131

Figure 3.15. Evolution of Cumulative SME ($kJ \cdot kg^{-1}$) for all conditions without and with AH_2 with the A protocol 134

Figure 3.16. Cumulative SME ($kJ \cdot kg^{-1}$) for all conditions without and with AH2 with the B protocol.. 135

Figure 3.17. Evolution of gas bubbles in size, number and shape during the different breadmaking stages 137

Figure 3.18. Comparison of dough void fractions after kneading, sheeting and fermentation for air-mixed dough 0.5 bar gauge pressure between the A and B protocols without AH_2. Error bars represent standard deviation. Bars labelled with the same letter (a) are not significantly different ($p > 0.05$), indicating no statistical difference between the two protocols at each processing stage 137

Figure 3.19. Comparison of dough void fractions after kneading, sheeting and fermentation for CO_2-mixed dough 0.5 bar gauge pressure between the A and B protocols without AH_2. Error bars represent standard deviation. Bars labelled with the same letter (a) are not significantly different ($p > 0.05$), indicating no statistical difference between the two protocols at each processing stage 138

Figure 3.20. Comparison of dough void fractions after kneading, sheeting and fermentation for O_2-mixed dough 0.5 bar gauge pressure between the A and B protocols without AH_2. Error bars represent standard deviation. Bars labelled with the same letter (a) are not significantly different ($p > 0.05$), indicating no statistical difference between the two protocols at each processing stage 138

Figure 3.21. Comparison of dough void fractions after kneading, sheeting and fermentation for Air-mixed dough between the A and B protocols with AH_2. Error bars represent standard deviation. Bars labelled with the same letter (a) are not significantly different ($p > 0.05$), indicating no statistical difference between the two protocols at each processing stage 139

Figure 3.22. Comparison of dough void fractions after kneading, sheeting and fermentation for CO_2-mixed dough between the A and B protocols with AH_2. Error bars represent standard deviation. Bars labelled with the same letter (a) are not significantly different ($p > 0.05$), indicating no statistical difference between the two protocols at each processing stage..... 140

Figure 3.23. Comparison of dough void fractions after kneading, sheeting and fermentation for O_2-mixed dough between the A and B protocols without AH_2. Error bars represent standard deviation. Bars labelled with the same letter (a) are not significantly different ($p > 0.05$), indicating no statistical difference between the two protocols at each processing stage..... 140

Figure 3.24, Cumulative CO_2 production during fermentation under A (solid lines) and B (dashed lines) protocols for two gas conditions: air (orange) and 100% CO_2 (blue). Measurements were taken over 180 min using a Risograph 144

Figure 3.25 Production rate of CO_2 based on Hibberd & Parker equation of rate production and solubility of CO_2 (Hibberd and Parker 1976) in function of time 145

Figure 3.26. Comparison of dough void fractions after sheeting for sheeted doughs, after resting for doughs without sheeting and the final dough void fraction after fermentation under air and CO_2. Statistical comparisons were made separately within the “with sheeting” and “without sheeting” groups. Different lowercase letters above bars within each group indicate significant differences ($p < 0.05$), while bars sharing the same letter are not significantly different 146

Figure 3.27 Evolution of dough void fraction ε_i before sheeting for air and 100%CO_2 in function of time (atmospheric mixing pressure). The jump observed with the 100% CO_2 condition is maybe due to the re-expansion of the compressed gas nuclei entrapped in the dough; this could be explained maybe by a softer dough with a less cohesive gluten network (more a viscous dough with les elasticity). The air mixing condition resulted in a progressive rise at a higher rate than with CO_2 with no jump; it may be explained by a stronger gluten network with a more elastic dough 148

Figure 3.28 A schematic representation of a bubble containing CO_2 surrounded by the dough matrix (Shah et al. 1998) 149

Figure 3.29. Microscopic images of unyeasted doughs, air-mixed doughs (left in blue) and CO_2 (right in grey), with two observation times 0 min (post-mixing) and 5 min. The scale was set between 1 – 100 µm..... 150

Figure 3.30. Microscopic images of yeasted doughs, air-mixed doughs (left in blue) and CO_2 (right in grey), with two observation times 0 min (post-mixing) and 5 min. The scale was set between 1 – 100 µm..... 150

Figure 3.31. Microscopic images of unyeasted doughs, air-mixed doughs (left in blue) and CO_2 (right in grey), with two observation times 10 min and 15 min. The scale was set between 1 – 100 µm .. 151

Figure 3.32. Microscopic images of yeasted doughs, air-mixed doughs (left in blue) and CO_2 (right in grey), with two observation times 10 min and 15 min. The scale was set between 1 – 100 µm .. 151

Figure 3.33. Microscopic images of yeasted doughs, air-mixed doughs (left in blue) and CO_2 (right in grey), after 20 min of resting followed by sheeting. The scale was set between 1 – 100 µm 152

Figure 3.34. Dough pH after fermentation under different gas conditions comparing doughs without AH_2 (left group) and with AH_2 (right group). Error bars represent standard deviations. Bars within the same group with different letters (a, b, c) are significantly different ($p < 0.05$) 154

Figure 3.35. Effect of different pressurized gas compositions on the dough storage modulus G' after kneading, without the addition of AH_2 155

Figure 3.36. Effect of different pressurized gas compositions on the dough storage modulus G' after kneading, with the addition of AH_2 155

Figure 3.37. Effect of the different gas mixtures with & without the addition of AH_2 on dough lightness L* 157

Figure 3.38. Effect of the different gas mixtures with & without the addition of AH_2 on dough yellowness b* 157

Figure 4.1 Breads specific volumes (SV) in $cm^3 \cdot g^{-1}$ with and without AH_2 under the different gas mixtures. Letters indicate significant differences ($p < 0.05$) between gas conditions within each treatment (with or without AH_2) 162

Figure 4.2 Cumulative pore size distribution of all mixing conditions without and with AH_2 164

Figure 4.3 Median pore size D90 of all conditions. Values with different superscript lowercase letters in the same column for each condition are significantly different ($p < 0.05$). The values presented here are mean ± standard deviation 164

Figure 4.4 Scanned images of bread slices showing the breadcrumb structure of each condition without and with AH_2 166

Figure 4.5 Breadcrumb porosity for all conditions without & with AH_2. Values with different superscript lowercase letters in the same column for each condition are significantly different ($p < 0.05$). The values presented here are mean ± standard deviation 167

Figure 4.6 Breads upper crust lightness L* in function of injected gas mixtures and with the addition of AH_2. Values with different superscript lowercase letters in the same column for each condition are significantly different ($p < 0.05$). The values presented here are mean ± standard deviation 168

Figure 4.7 Breads crumb lightness L* in function of injected gas mixtures and with the addition of AH_2. Values with different superscript lowercase letters in the same column for each condition are significantly different ($p < 0.05$). The values presented here are mean ± standard deviation 169

Figure 4.8 Breads crumb yellowness b* in function of injected gas mixtures and with the addition of AH_2. Values with different superscript lowercase letters in the same column for each condition are significantly different ($p < 0.05$). The values presented here are mean ± standard deviation 169

Figure 4.9 Evolution of enthalpy of amylopectin retrogradation during storage under different gas composition without the addition of AH_2. Experimental enthalpy values (ΔH in $J \cdot g^{-1}$ per dry flour) are shown as data points, while corresponding model predictions are shown in the figure as fitted lines 171

Figure 4.10 Avrami model showing the time constant (τ in days) of all conditions stored at 10°C during 15 days 171

Figure 4.11 Evolution of enthalpy of amylopectin retrogradation during storage under different gas composition with the addition of AH_2. Experimental enthalpy values (ΔH in $J \cdot g^{-1}$ per dry flour) are shown as data points, while corresponding model predictions are shown in the figure as fitted lines 173

Figure 4.12 Avrami model showing the time constant (Ƭ in days) of all conditions with AH_2 stored at 10°C during 15 days..... 173

Figure 4.13 Comparison of starch enthalpies for all conditions with AH_2 (solid fitted lines) and without AH_2 (dashed fitted lines). In the colour legend, each gas mixture (air, 100%CO_2, 30%O_2 70%N_2) is represented by a specific colour, the breads without AH_2 are in a solid line with their corresponding calculated values from Avrami model: orange (air), blue (100%CO_2) and yellow (30%O_2 70%N_2), and the dashed lines with their corresponding calculated Avrami values are for the breads with $AH_2$174

Figure 4.14 Evolution of breadcrumb firmness for all conditions without the addition of AH_2 during storage days..... 175

Figure 4.15 Evolution of breadcrumb firmness for all conditions without the addition of AH_2 during storage days..... 176

Figure 4.16 Summary of breadcrumb firmness of all conditions under the different as conditions with and without the additions of AH_2..... 176

Figure 4.17 Breads cohesiveness for all conditions for all gas compositions without and with AH_2 .. 177

Figure 4.18 Evolution of moisture content MC (%) in bread slices for all gas conditions without the addition of AH_2 over 3 storage days (J0 (immediately after baking) , J1 (after 24 hours) & J7. MC is shown for two longitudinal positions (¼ and ½ slice) and 3 diagonal positions within the same slice (top, middle and bottom). Each point represents the mean moisture content at each time point with error bars indicating standard deviation 179

Figure 4.19 Evolution of moisture content MC (%) in bread slices for all gas conditions with the addition of AH_2 over 3 storage days (J0 (immediately after baking) , J1 (after 24 hours) & J7. MC is shown for two longitudinal positions (¼ and ½ slice) and 3 diagonal positions within the same slice (top, middle and bottom). Each point represents the mean moisture content at each time point with error bars indicating standard deviation 180

Figure 4.20 Difference in breads volume: Air (left) and collapsed CO_2 bread (right) 181

Figure 4.21 Summary of the experiment sets conducted with and without yeast, with and without fermentation 182

Figure 4.22 Breads SV ($cm^3 \cdot g^{-1}$) for the different conditions. Letters above the bars indicate statistical differences (a, b, c, d). Error bars represent standard deviation..... 183

Figure 4.23 Breads volumes after baking for the 4 tested conditions, starting from the left: air without yeast, 100%CO_2 without yeast, 100%CO_2 with east without fermentation and far right 100%CO_2 with ½-yeast amount with fermentation..... 183

Figure 4.24 Breads SV of CO_2-mixed dough with full yeast amount (blue bar) and ½-yeast amount (grey). Letters above the bars indicate statistical differences (a, b, c, d). Error bars represent standard deviation..... 184

Figure 4.25 Breadcrumb structure of scanned bread slices for all the experiments conducted with yeast. Starting from far left to right: (a) air without yeast, (b) 100%CO_2 without yeast, (c) 100%CO_2 with full yeast without fermentation, (d) 100%CO_2 with ½ yeast with fermentation and (e) 100%CO_2 full yeast with fermentation 185

Figure 4.26 Cumulative pore size distribution pattern of 100%CO_2 breads with the full yeast amount and ½ yeast amount 185

Figure 4.27 SV for breads mixed with air and 100%CO_2 with sheeting and without sheeting. Error bars represent standard deviation 186

Figure 4.28 Cumulative pore size distribution of sheeted and none-sheeted bread doughs mixed with air and 100%CO_2-mixed breads at 0.5 bar gauge pressure. The error bars confirm that these trends are reliable across measurements 187

Figure 4.29. Median pore size D50 of all conditions. Values with different superscript lowercase letters in the same column for each condition are significantly different ($p < 0.05$). The values presented here are mean ± standard deviation 188

Figure 4.30 Median pore size D90 of all conditions. Values with different superscript lowercase letters in the same column for each condition are significantly different ($p < 0.05$). The values presented here are mean ± standard deviation 188

Figure 4.31 Scanned breadcrumb images of bread slices mixed with air and CO_2 with sheeting and without sheeting 189

Figure 4.32 Generalized Procrustes Analysis (GPA) plot of bread samples based on sensory attributes obtained from the Flash Profile analysis 194

Figure 4.33 Biplot of the sensory attributes used to characterize bread samples. In order to simplify the interpretation, attributes are grouped using circles of different colours by characteristics such as softness, crumb colour, chew resistance, volume, gas cell size, acidity and firmness 194

Figure 5.1 Fermentation flask used to monitor the expansion ratio of the dough during fermentation (Raad, Alain Le-Bail and Le-Bail 2025) 206

Figure 5.2 Picture of the inside of the fermentation cabinet; (a) to the left, CO_2 sensors in yellow and Relative humidity sensors in blue and (b) to the right the moulded dough sticks at the end of fermentation with the expansion ratio monitoring flask 207

Figure 5.3 pH monitoring over 12 hours of carbonated water, where the bottles are stored at 4°C.. 209

Figure 5.4 Impact of the NaCl titant of a water solution (tap water) on the CO_2 solubility at around 5 Bar. Tests done with a sodastream equipment. The x-axis shows the titrant, essentially the mass fraction or titrant solution of NaCl in the solution 210

Figure 5.5 Dough pH of RefD and CarbD in absence and presence of CO_2 flow before and after fermentation 211

Figure 5.6 Average tool power during dough kneading in function of kneading time, representing the maximum point of the curve (t_{PEAK}) 212

Figure 5.7. Real-time CO_2 emission by RefD and CrabD during fermentation in absence of the CO_2 flow detected by the sensors at 30°C and RH of 90% 214

Figure 5.8. Real-time CO_2 emission by RefD and CarbD during fermentation in presence of the CO_2 flow at 30°C and RH of 90%..... 215

Figure 5.9. Colour parameter L* of dough CarbD and RefD before and after fermentation..... 218

Figure 5.10. Breads specific volume SV 218

Figure 5.11. L* values for Upper and crumb color of breads 219

Figure A Scheme presenting the prototype mixer showing the importance of the injected gases (CO_2, O_2 and N_2) during the kneading phase 223

Figure B Scanned images of bread slices mixed under Air and CO_2 at atmospheric pressure and 0.5 bar gauge pressure with a scale of 10 mm for each treated image 224

Figure C Difference in breads volume: Air (left) and collapsed CO_2 bread (right) 228

Figure D Breadcrumb structure of scanned bread slices for all the experiments conducted with yeast. Starting from far left to right: (a) air without yeast, (b) 100%CO_2 without yeast, (c) 100%CO_2 with full yeast without fermentation, (d) 100%CO_2 with ½ yeast with fermentation and (e) 100%CO_2 full yeast with fermentation 229

Figure E Scanned breadcrumb images of bread slices mixed with air and CO2 with sheeting and without sheeting..... 230

LIST OF TABLES

Table 1.1 Formulations (indicative values) of different types of bread (per 100 g of flour), excluding additives 7

Table 1.2. Summary of key dough mixing studies describing different mixing conditions applied with different dough recipes with observed impact of mixing parameters on the dough and bread properties 28

Table 1.3 The summarized results, showing the increasing solubility of CO_2 with pressure, consistent with Henry's Law (Carroll, Slupsky and Mather 1991) 42

Table 2.1 Dough recipe 72

Table 2.2. Table of the different mixing stages 75

Table 3.1. Dough recipe. The density of each ingredient are from a) for flour helium picnometry (ONIRIS-GEPEA), b) computed from eq. (1) assuming 70% water, 15% proteins, 13% sugars, 2% lipids, c) sodium chloride ref. Hazardous Substances Data Bank 109

Table 3.2. Different mixing stages 110

Table 3.3. Impact of gas-pressure mixing on the measured dough void fractions and the evolution of this parameter during the mixing stage, sheeting and fermentation. Values with different superscript lowercase letters in the same column for each condition are significantly different ($p < 0.05$) 116

Table 3.4. Effect of different pressure mixing on D50 and D90 values of crumb microstructure. Values with different superscript lowercase letters in the same column for each condition are significantly different ($p < 0.05$). The values presented here are mean ± standard deviation 120

Table 3.5. Comparison between Protocol A and B in terms of gases partial pressures (N_2, O_2 and CO_2)and the quantity in g of CO_2 needed for each protocol to be solubilized 130

Table 3.6. Values of t_{PEAK} and SME of the A protocol under different mixing parameters at a kneading speed 150 RPM and pressure of 0.5 bar gauge pressure with and without AH_2 for Air, 100%CO_2 and 30%O_2 70%N_2. Superscript letters (a–c) indicate significant differences ($p < 0.05$) among gas conditions, analysed separately for samples without AH_2 and with AH_2. For SME, comparisons were performed across all samples 131

Table 3.7. Values of t_{PEAK} and SME of the B protocol under different mixing parameters at a kneading speed 150 RPM and pressure of 0.5 bar gauge pressure with and without AH_2 for Air, 100%CO_2 and 30%O_2 70%N_2. Superscript letters (a–c) indicate significant differences ($p < 0.05$) among gas conditions, analysed separately for samples without AH_2 and with AH_2. For SME, comparisons were performed across all samples. The table summarizes mixing time for all conditions 133

Table 3.8. Dough expansion ratios N without AH_2. Superscript letters (a–c) indicate significant differences ($p < 0.05$) among gas conditions for each column 141

Table 3.9. Dough expansion ratios N with AH_2. Superscript letters (a–c) indicate significant differences ($p < 0.05$) among gas conditions for each column 142

Table 3.10. Rate of CO_2 emission of air and CO_2-mixed dough under the A vs. B protocols 144

Table 4.1 Summary of bread staling results 178

Table 4.2 Summary of median pore size D50 and D90 for the full yeast amount breads and ½ yeast amount breads. The table presents half the amount of pores size smaller than the median pore size D50 and the ones larger than D90 (representing 10% of pores population) 184

Table 4.3 Summary of Triangular test results for sensory discrimination, presenting the number of panellists, correct responses, statistical significance and the perceptible sensory differences 190

Table 4.4 Table summarising all sensory descriptors given by the panel for bread samples, categorized by aspect, odour, texture/mouthfeel, texture to touch and taste. The citation frequency is indicated for each attribute 192

Table 5.1 Doughs void fractions after mixing, sheeting and fermentation. This table also represents the dough expansion ratio N (computed with Eq. 5.6) during fermentation to reach a final void fraction of 0.75. Values with different superscript lowercase letters in the same column for each condition are significantly different ($p < 0.05$). The values presented here are mean ± standard deviation. 212

Table 5.2. Dough texture (Hardness, Springiness, Cohesiveness & Adhesiveness) before & after fermentation. Values with different superscript lowercase letters in the same column for each condition are significantly different ($p < 0.05$) before fermentation and after fermentation. The values presented here are mean ± standard deviation 216

Table 5.3. Breads texture analysis in terms of Hardness, springiness, cohesiveness & adhesiveness in absence and presence of CO_2 flow. 219

GENERAL INTRODUCTION

Bread has been a dietary cornerstone for millennia, integral not only as a source of nutrition but also culturally and economically worldwide. France is renowned for its rich bread heritage, with per capita bread consumption among the highest in Europe, adherence to traditional artisanal techniques with modern innovations to preserve quality and meet evolving consumer demands. Despite its long history, breadmaking remains a complex art and science wherein the interactions of ingredients and process variables. Among these, dough mixing is a pivotal stage where the fundamental structure, texture, flavour and shelf life of bread are established. Traditionally, these processes occur under ambient atmospheric conditions, but the baking industries emphasis on product consistency, sustainability and clean-label demands novel approaches that afford greater precision and control.

One of the most intriguing frontiers in cereal science and baking technology is the gas-pressure mixing under a controlled atmosphere during the mixing process. The injection of O_2, CO_2 and N_2 in the headspace of mixing vessels profoundly affects the biochemical and physical-chemical properties of the dough. O_2 for example is consumed by enzymatic oxidation reactions critical for gluten development and strengthening, while CO_2 modulated fermentation kinetics and dough aeration. The partial pressure of these latter gases influence their solubility and transfer rates into the dough liquid phase. Controlling O_2 levels may reduce the need for chemical oxidants; CO_2 can enhance dough gas retention and bread volume without the use of additives. Yet, practical application of these concepts is challenged by the complexity of gas-liquid phase interactions during mixing and fermentation requiring a detailed scientific investigation.

This thesis experimentally put into investigation to explore and valorise non-conventional bread dough mixing by focusing on gas-pressure injection during the mixing stage. Two distinct mixing protocols were developed, one allowing residual air to remain in the mixer headspace and another employing vacuum degassing with controlled vacuum or gas flushing to systematically investigate their effect on oxygen and CO_2 availability, solubility and consumption by the dough. Complementing these protocols, the study examined the role of ascorbic acid AH_2 under varying gas composition to evaluate if gas injection can mimic and replace traditional dough improvers.

This project was conducted through the complementarity of two research units (Oniris – GEPEA and INRAE), each contributing distinct and essential expertise in addressing scientific questions of this thesis. Oniris unit provided fundamental knowledge in cereal science, dough physico-chemistry and gluten development. Particularly, in mixing technology and gas-pressure control. The research unit of the co-supervisor, INRAE, contributed scientific expertise in cereal processing, dough aeration mechanisms and interpretation of gas-dough interactions, supporting the conceptual framework and analytical approach of the study.

In this context, this manuscript will be divided into:

- Studying the impact of two pressure levels with air and CO_2 injection on dough and bread properties & development of a calculation model based on dough void fraction after sheeting to estimate the actual fermentation time under given mixing parameters

- Studying the effect of different gases (air, 100%CO_2, 30%O_2 70%N_2 at 0.5 bar gauge pressure) with/without AH_2 addition on dough using the two mixing protocols
- Studying the effect of different gases (air, 100%CO_2, 30%O_2 70%N_2 at 0.5 bar gauge pressure) with/without AH_2 addition on bread using the two mixing protocols
- A sensory analysis
- Investigating the impact of carbonated water and CO_2-controlled fermentation chamber on dough and bread properties

The same bread dough recipe was used across all the axes mentioned above.

The first part focuses on determining the dough development time under the employed gases air and 100%CO_2 at two pressure level atmospheric and 0.5 bar gauge pressure and different tool mixing speeds 100, 150 and 200 RPM. The objective was to examine the influence of the headspace pressure and gas composition during dough mixing on dough and bread properties. A calculation model was employed based on dough void fraction after sheeting as a key parameter with a target final void fraction of 0.75 set for optimal bread volume and breadcrumb structure. This model allowed for more accurate estimation of the actual fermentation time under the specific mixing parameters, thereby linking process conditions with dough development and bread quality.

The second part focused on studying the impact of different gas mixtures at a fixed pressure level (0.5 bar gauge pressure) with two mixing protocols on dough properties specifically development time, specific mechanical energy (SME) and dough void fractions. Based on these results, additional tests were conducted by employing one protocol (protocol A).

The third part focused on studying the impact of these latter on bread properties and its shelf life. We also in this part conducted a sensory analysis to examine if consumers will be able to distinguish between the different bread samples mixed at different gas composition with/without AH_2.

The last part was investigating the combined effect of carbonated water with CO_2-controlled fermentation chamber on CO_2 solubilisation and its effect on dough properties mainly pH, dough colour, texture and void fractions as well as the final bread quality.

The first chapter provides a comprehensive state of art necessary for understanding and interpreting the results of this study. The general composition of bread, ingredients, interactions between ingredients during the key breadmaking stages. Special attention was given to dough aeration methods, including conventional mixing parameters and non-conventional ones. We also emphasized on the impact of each employed gas injected on dough aeration and structure.

The second chapter focuses on material and methods experimentally used during this project.

The third chapter presents the dough results which was divided into two parts. The first one the results of air and CO_2 mixing under two pressure levels with Protocols A, then the second part, focuses on the addition of a third gas mixture and AH_2 under two mixing protocols (Protocol A at 0.5 bar gauge pressure and Protocol B) on dough properties.

A fourth chapter focuses on the bread results of Part2 of Chapter 3 and its staling during storage, with a sensory analysis.

A fifth chapter about the effect of carbonated water which was conducted at Hohenheim University.

Finally, the manuscript was finalised by a general discussion of all of the results, with a conclusion and future perspectives.

CHAPTER 1 : **STATE OF ART**

1.1. Introduction

Bread is a staple food worldwide, consumed in different forms by different cultures with average annual consumption ranging from 59 to 70 kg per person (Mesta-Corral *et al.* 2024). This widespread consumption is largely due to its versatile preparation methods, affordable price, and high energy content (Mesta-Corral *et al.* 2024). A key reason for bread high consumption is that its primary ingredient is wheat, due to its mass production in Europe, thus making it an affordable cereal crop (Mesta-Corral *et al.* 2024; Sakandar *et al.* 2019).

For millennia, bread has been a cornerstone of human sustenance. Its origins date back to ancient civilizations, where it was not only a basic food source but also a symbol of culture, tradition, and social practices. Nutritionally, it is a source of carbohydrates, dietary fibres, vitamins (e.g., Vitamin B) and minerals (Belitz *et al.* 2004; Joye, Lagrain and Delcour 2009a; Zarzycki *et al.* 2024). The bread we eat today, is the result of a long agricultural, technological and gastronomic process; its preparation involves mechanical, fermentative and thermal actions carried out in a precise sequence (Moore 2016). Beyond nutrition, bread is deeply intertwined into religious rituals, social, and cultural identities across the globe. From sacred offerings in ancient temples to daily sustenance on the family table, bread has represented life, community, and prosperity. The countless forms of bread from the airy baguettes of France to dense rye breads in Eastern Europe, and flatbreads in the Middle East are a testament to the diverse cultural landscapes shaped by local ingredients, traditions, and culinary practices.

Although "bread" is a general term, it encompasses a wide range of varieties that reflect regional and cultural traditions. These breads are often distinguished by their unique aerated textures or by the characteristic shapes formed during the fermentation process (Cauvain 2020a). Historically, the process of leavening was viewed as mysterious, with fermentation perceived as both fascinating and unsettling (Campbell and Martin 2020). Over time, greater understanding of yeast fermentation and gluten network formation transformed this once-mystical process into a scientifically controlled technique.

Gas bubbles production and retention are essential to breadmaking, a thorough understanding of gas phase behaviour remains crucial for anyone aiming to truly master the breadmaking process (Cauvain 2020a). Dough aeration, therefore, is fundamental to bread quality. Historically, this was achieved through manual kneading a skilful method of mixing that incorporated air and helped develop the gluten network essential for trapping gas bubbles. Over time, innovations in mixing technology revolutionized this step. Mechanical mixers, by applying controlled shear and energy, improved the efficiency of gas incorporation and gluten development. This evolution transformed dough mixing from a traditional craft into a precisely controlled process, ensuring consistency and enhancing bread texture on an industrial scale.



Figure 1.1 A bread advertisement for Sunbeam bread dates back to 1947 showing the appeal of aerated bread and the expectation of consumers for uniform and fine gas cells in crumb

1.2. Bread & components

Feillet (2000) defines bread as "the result of highly complex physical transformations, chemical reactions and biological activity occurring within a mixture of flour, water, salt and yeast, and sometimes a few other ingredients (sugar, fat, milk powder, egg, antioxidants), under the action of a controlled supply of mechanical and thermal energy". Each ingredient plays a role in the properties of the dough and finished product developed during the various stages of the bread-making process. The formulation differs according to the type of bread (Table 1), with "traditional French bread" being free of sugar, milk and fat.

Table 1.1 Formulations (indicative values) of different types of bread (per 100 g of flour), excluding additives

Bread type	**"French", "pain de tradition française"**	**Viennese**	**Sandwich bread**	**Milk bread**	**Brioche**
Water (mL)	60	55-55	45-50	variable	35-45
Salt (g)	1,8-2,2	1,5-1,8	1,5-2	1,8-2	1,5-1,8
Yeast (g)	1-2	3-5	2-6	2-5	2-6
Sugar (g)	-	4-8	2-6	2-5	2-6
Fat (g)	-	5-15	0,5-10	5-10	10-20
Powdered milk (g)	-	3-5	variable	60-65	3-5
Eggs (g)	-	-	-	variable	10-20

The “pain de tradition française” (Traditional French bread) is an appellation defined by a regulation (Decree no. 93-1074 of September 13, 1993). This bread (in any form) must not have undergone any freezing treatment during production, and must be made exclusively from a mixture of bread-making wheat flours, drinking water, salt, and fermented with baker's yeast (Saccharomyces cerevisiae) and/or sourdough. This regulation also allows malted flours (0.3%), soya flours (0.5%) and fava bean flour (2%). Flours and Ingredients play an important role in the processing of the dough, in the workability of the dough to increase its volume and in the quality of the final product by extending its shelf life. Therefore, the role of each ingredient is explained in detail in the next chapter.

1.2.1. Wheat Flour

Wheat is the generic name for various wheat varieties (durum wheat / *Triticum turgidum* subsp. durum, soft wheat / *Triticum æstivum*, spelt / *Triticum spelta*). In France, the most commonly used flour is wheat flour from *Triticum æstivum*. Wheat flour is the basic ingredient in bread-making products (Gan, Ellis and Schofield 1995). Bread-making flour has the viscoelastic properties needed to hold ingredients together, enabling the formation of a dough capable of trapping air and thus making bread.

Flours are classified according to their ash content. Flours containing mineral matter from the bran (the grain husk) are reduced to mineral residues in the form of ash when incinerated at 900°C. The higher the ash content, the higher the flour number, and conversely, the whiter the flour. At the extremes, therefore, we have type 45 flour, the purest and whitest used for cake making mainly (even though type 35 exist too for ready to bake laminated dough), but which has lost many nutrients. Type 150 flour, known as wholemeal or integral, contains a larger portion of the wheat grain outer layer, and retains most of its minerals and vitamins (mainly vit B and E).

There are 6 main types of flour, starting with the "purest":

- Type 45: White pastry flour or "fleur de farine" for pastry making
- Type 55: Ordinary white flour for white breads, pastries and pizzas
- Type 65: White flour for special breads and pizzas
- Type 80: Beige or semi-complete flour for special breads
- Type 110: Wholemeal flour for brown and wholemeal breads
- Type 150: Wholemeal flour for bran breads

Wheat flour is made up mainly of carbohydrates (notably starch, 71-78%), water (13-14.5%), proteins (8-13%), lipids (1.0-1.5%) and fibre (around 0.2%), as well as various enzyme systems (amylases, proteases, lipases and lipoxygenases) (Cauvain and Young 2006). Each ingredient plays a direct or indirect role in structuring and aerating the dough, with starch and gluten remaining the main components of wheat flour.

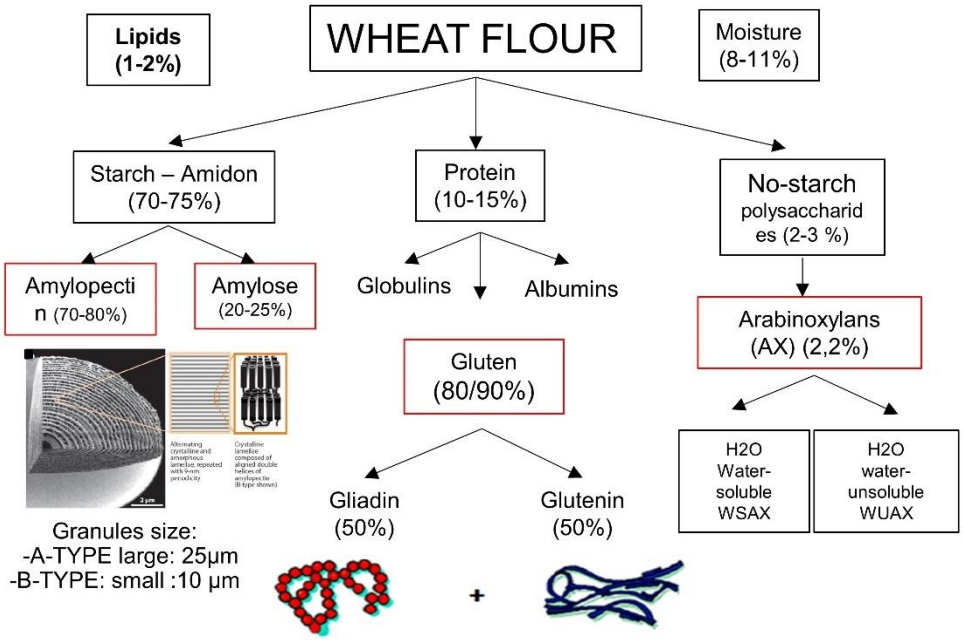


Figure 1.2 Schematic Representation of Wheat Flour Components and Their Substructures (ref. A. Le-Bail- ONIRIS)

Additionally, non-starch polysaccharides approximately 2-3%, mainly consisting of arabinoxylans (AX) and lipids 1-2%, are significant minor flour components important for the bread production and quality (Goesaert *et al.* 2005) (Figure 1.2).

1.2.1.1. Gluten

Apart from the significance of wheat as a source of energy for humans, it is also recognized for its distinctive functional characteristics, which are largely influenced by the proteins found in wheat gluten. These proteins are as crucial in the process of breadmaking (Johansson *et al.* 2013). In practice, the term 'gluten' denotes the proteins, as they significantly influence the distinct baking quality of wheat by providing water absorption capability, cohesiveness, viscosity, and elasticity to dough (Wieser 2007). Gluten can be described as the elastic substance in the dough (Wieser 2007). There are two functionally distinct groups of gluten proteins: gliadins (between 30 and 40% of total proteins) (Barak, Mudgil and Khatkar 2015) and glutenins (between 40 and 50% of total proteins) (Delcour *et al.* 2012; Johansson *et al.* 2013). Gliadins are monomeric proteins (single polypeptide chain) associated by hydrogen bonds and hydrophobic interactions; they contribute to dough viscosity. Glutenins are a heterogeneous family of polymers resulting from the polymerization of high- (HMW) and low-molecular-weight (LMW) glutenin subunits, and form highly complex aggregates; they contribute to the extensibility properties of doughs (Chen *et al.* 2019; Delcour *et al.* 2012; Wieser 2007). The glutenin fraction accounts for roughly half of the overall gluten proteins and is made up of polymers reinforced by inter-chain disulfide bonds (Shewry and Lafiandra 2022). High Molecular Weight Glutenin Subunits (HMW) in bread wheat are encoded by six genes with each locus typically expressing an x-type and a y-type subunit (Shewry and Lafiandra 2022; Shewry and Belton 2024; Wieser 2007). These two types differ in molecular mass x-types are about 80,000–100,000 Da, while y-types are around 60,000–80,000 Da and in cysteine content, which plays a key role in protein cross-linking (Shewry and Belton 2024). The number and type of HMW subunits significantly influence dough strength, both quantitatively

(based on how many subunits are expressed) and qualitatively (depending on which subunit alleles are present) (Shewry and Belton 2024). Gliadins can be categorized into different groups according to various studies: α-, β-, γ-, and ω-gliadins, depending on electrophoretic mobility (Johansson *et al.* 2013; Wieser 2007) and α/β-, γ-, ω1-, ω2-, and ω5-gliadins group, based on their sequences and amino acid makeup (Johansson *et al.* 2013). Thirdly, ω-gliadins group having low sulphur (S) content, while the other gliadins are comparatively rich in S (Johansson *et al.* 2013; Shewry and Belton 2024). The secondary structures of gliadin α/β-, γ-, contain α-helices and β-sheets, whereas ω-gliadins are governed by β-turns (Welc-Stanowska, Kłosok and Nawrocka 2023; Wieser 2007). The ability of free sulfhydryl (S-H) bonds in gluten proteins to form disulfide (S-S) bonds under oxidizing conditions during dough kneading is one of the factors contributing to the bread-making character of wheat (Cauvain and Young 2006). Hence, Gliadins and glutenins create a three-dimensional mesh-like gluten network stabilized by S-S bonds and non-covalent bonds (Figure 1.3) (i.e. hydrogen bonds, van der Waals forces, ionic bonds, and hydrophobic interactions) (Shewry *et al.* 2002; Welc-Stanowska, Kłosok and Nawrocka 2023).

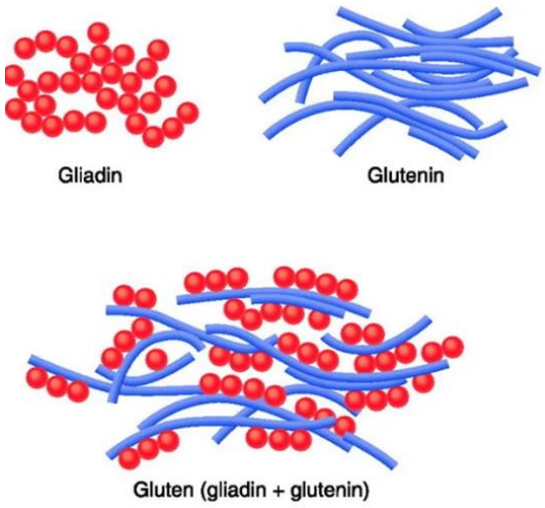


Figure 1.3 Schematic illustration of glutenin and gliadin when bonded together forming the gluten

1.2.1.2. Starch

Starch is a major source of energy for people all over the world and is produced by plants as a backup source of carbohydrates. Although starch is the most prevalent substance in wheat flour, it has not historically been believed to be the cause of variations in quality between wheat varieties (Eliasson 2012).

1.2.1.2.1. Morphology, structure & ultrastructure

Starch is organized into grains of varying sizes and shapes, depending on the starch botanical origins. Some cereals (barley, wheat, oats) exhibit two populations of granules size: A type granule (20 - 30 µm) and B type granule (≃ 4 µm). (Buléon *et al.* 1998; van de Velde, van Riel and Tromp 2002) have shown that potato starch grains are ellipsoidal, generally varying in size from 45 to 75 µm. Corn starch grains are polyhedral in shape with a size of around 15-20 µm.

Wheat starch consists of two types of relatively spherical granules: A-type granules, approximately 30 µm, and B-type granules, around 5 µm. The quaternary structure of starch is enormous and complex, ranging in size from 0 to more than 50 µm (Ball and Morell 2003), composed of two D-glucan polymers; amylose and amylopectin (Cornejo-Ramírez *et al.* 2018; Eliasson 2012; Liu *et al.* 2023; Sujka and Jamroz 2013).

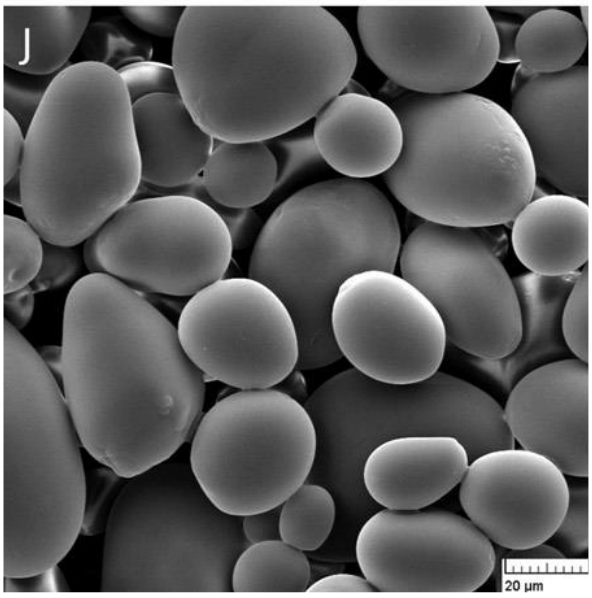


Figure 1.4 SEM native wheat starch granules images (Sujka and Jamroz 2013)

The two D-glucose homopolymers making up starch are amylose (1% to 40%) and amylopectin (99% to 60%) (Fredriksson *et al.* 1998). Amylopectin consists of a linear backbone of α-D-glucopyranosyl residues linked by α-D-(1→4) linkages, but 5-6% α-D-(1→6) linkages give amylopectin a branched structure (Figure 1.4) (Goesaert *et al.* 2009; Kim, Kim and Baik 2012). (Kainuma and French 1972) established a heterogeneous cluster model.

Amylose is a linear macromolecule made up of 500 to 6,000 α-D-glucopyranosyl units linked by α-D-(1→4) bonds (Figure 1.5). Randomly distributed α-D-(1→6)-type linkages in small quantities have also been described giving it a slight branched character (Putseys, Lamberts and Delcour 2010; Takeda, Maruta and Hizukuri 1992). Its predominantly linear conformation and the majority presence of α-D-(1→4) linkages enable amylose to complex with small hydrophobic molecules such as iodine or fatty acids. The presence of complexing agents leads to a change in the conformation of amylose (from a ball or double helix to a single-helix conformation) (Putseys, Lamberts and Delcour 2010). In this helical conformation of 6 glucose units/turn, the hydrophilic groups of the helix face outwards, while the hydrophobic groups face inwards (Buléon *et al.* 1998).

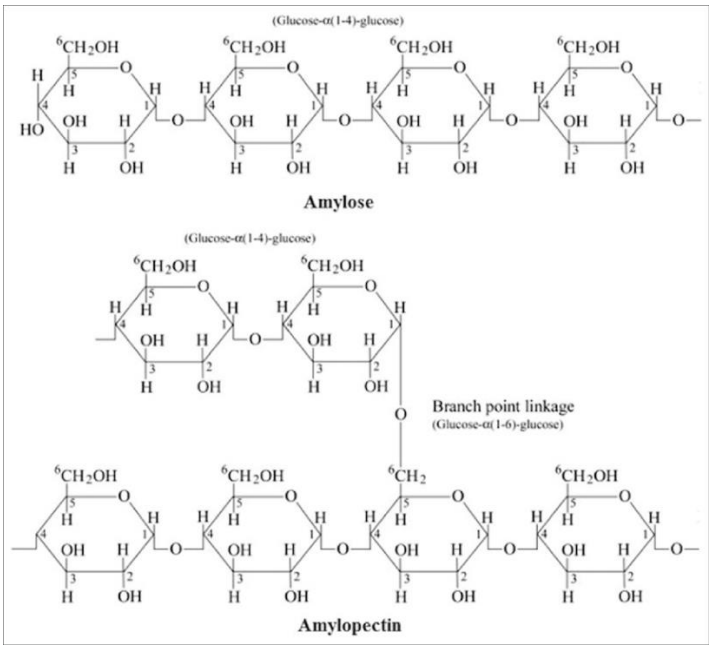


Figure 1.5 Primary structure of the two polymers amylose and amylopectin constituting the carbohydrate fraction of starch (Kim, Kim and Baik 2012)

By observing thin sections of partially hydrolyzed starch grains under transmission electron microscopy, an onion-like structure formed of amorphous and crystalline concentric layers is visible (Kainuma and French 1972) (Figure 1.6).

Several authors including Kim el al. (2012); Oostergetel and Van Bruggen (1993) showed by transmission electron microscopy that the crystalline rings were themselves semi-crystalline, consisting of a superposition of amorphous and crystalline lamellae (Figure 1.6).

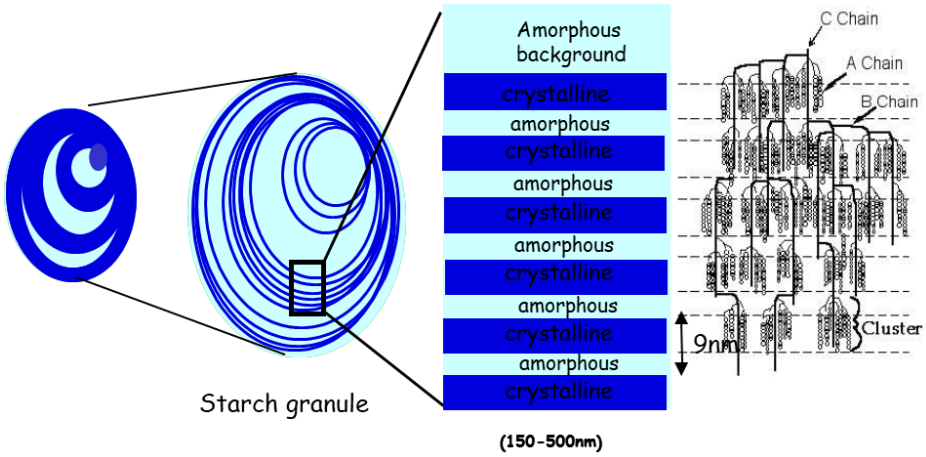


Figure 1.6 Schematic representation of a starch granule (Jenkins and Donald 1995; Oostergetel and van Bruggen 1993)

This repeat distance was detected by small-angle XRD and estimated at 9 nm (Jenkins and Donald 1995; Oostergetel and van Bruggen 1993). In the model proposed by Jenkins & Donald (1995), the structure of these semi-crystalline zones is coupled to the cluster structure of amylopectin (Figure 1.6).

Amylopectin makes up the majority of starch granules' weight, while amylose accounts for 15–30% of the total (Bertoft 2017). With the non-random distribution of linear chains and the clustering positioning of branch linkages, amylopectin exhibits a high degree of structural organization. High branching frequency regions alternate with regions devoid of branches, allowing intervening linear chains to align in parallel arrays of double helices (Belton 2007).

1.2.1.2.2. Crystallinity

Starch granules display an optical birefringence pattern called a "Maltese cross" when observed under polarized light, which suggests a high level of molecular order within the granule (Jane 2009; Pérez, Baldwin and Gallant 2009; Ratnayake and Jackson 2008; Wang *et al.* 2015; Zhong *et al.* 2020). In the starch granule, amylose and amylopectin polymers are arranged into a radially anisotropic, semi-crystalline unit. The recognizable maltese cross is a result of this radial anisotropy (Ratnayake and Jackson 2008).

The major differences between the two main allomorphic types A and B lie in the stacking of amylopectin double helices in the crystal lattice and the amount of water present between the double helices (Dome *et al.* 2020).

Cereal starches (such as wheat) typically have a crystalline structure of type A. Its X-ray diffraction pattern shows characteristic peaks at angles 2θ (λ = 0.15405 nm): 10.1; 11.3; 14.9; 17, 18.1; 23; 23.9 and 26°.

Type B essentially present in tubers and starches rich in amylose, gives characteristic diffraction peaks (λ = 0.15405 nm) at angles 2θ: 5.6; 10.1; 11.3 ;14; 14.9; 17 ;19.5; 22; 23.9 and 26°. Type C starch, generally found in legumes (smooth pea, bean), corresponds to a mixture of type A and type B within the same grain, as has been shown for smooth pea starch. Lipid-containing cereal starches (maize, wheat, barley...) may exhibit, in addition to type A, a different crystalline type (type V) characteristic of amylose-lipid complexes formed during heat treatment (Biliaderis, Page and Maurice 1986). These complexes do not generally exist in the crystalline state in native starches.

1.2.1.2.3. Other flour components

Flour contains between 1 and 1.5% lipids not included in the starch. These lipids are dispersed within the albumin and can react with other flour constituents. Another part of the lipids, very little reactive as it is, is located inside the starch granules in the form of inclusion complexes between amylose and monoacylated lipids, lisophosphatidylcholine in particular. Lastly, a third fraction is attached to the surface of starch granules, and is thought to be associated with proteins and may determine the brittleness or resistance of wheat varieties (Feillet 2000).

Amylolytic enzymes are of particular importance in bread-making, and include α- and β-amylase, which catalyze the hydrolysis of starch into oligosaccharides and, consequently, maltose (Cauvain and Young 2006). Proteases catalyze peptide hydrolysis within the gluten structure. The dough becomes flexible and is able to retain the gases produced by fermentation. Lipase activity determines flour stability during storage, while lipoxygenase contributes to the formation of unsaturated fatty acid hydroxydoxides and peroxides, which lighten flour color through β-carotene oxidation and stabilize dough structure. However, it is desirable that the activity of amylases, proteases, lipases and

lipoxygenase be average, as the application of flour with too high or too low enzyme activity generates a baked bread that does not meet specific quality requirements (Piechowiak, Józefczyk and Balawejder 2018).

Arabinoxylan (AX), a predominant hemicellulose in wheat bran, plays a key functional role in baked goods by influencing water retention, dough rheology, and starch retrogradation (Courtin and Delcour 2002; Izydorczyk and Biliaderis 1995; Pietiäinen *et al.* 2022). Consisting of D-xylopyranosyl units connected by β (1→4) glycosidic bonds, resulting in a linear chain structure (Courtin and Delcour 2002; Izydorczyk and Biliaderis 1995).

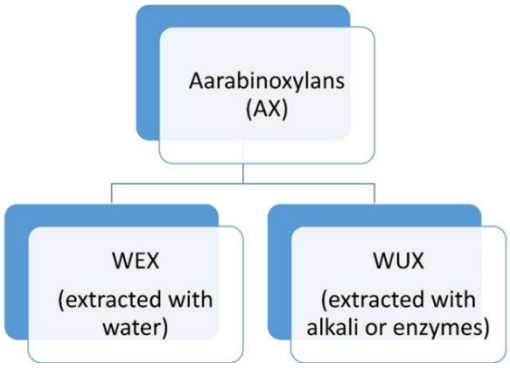


Figure 1.7 Constituents of arabinoxylans (AX) in wheat flour (Courtin and Delcour 2002)

AX exist in two main forms in cereal grains: water-extractable arabinoxylans (WE-AX) and water-unextractable arabinoxylans (WU-AX) (Figure 1.7). These forms differ in their solubility, molecular weight, and degree of cross-linking, which in turn influence their functional roles in dough and final baked products. WE-AX generally have lower molecular weights and higher solubility, contributing to increased water retention and viscosity in dough, which enhances dough extensibility and gas retention during fermentation (Courtin and Delcour 2002).

1.2.2. Water

Along with flour and air, water is one of the three essential elements in bread dough production. Dough temperature is controlled by water temperature (Feillet 2000; Moore 2016). In dough formation, water plays a major role as a plasticizer. It hydrates flour proteins and starch, and acts as a solvent for other ingredients (salt and sugar). As a reactive molecule, water also participates in the reactions that occur in the dough (Feillet 2000; Moore 2016). During baking, water also allows starch to gelatinize. Water plays a complex role in determining the conformational state of biopolymers, which affects the interaction between the various constituents and thus contributes to the structuring of the dough (Eliasson 1994). It is important that the ratio of water to flour and other ingredients is optimized so that the dough has the "correct" rheological characteristics after kneading. The optimal water level in a fermented dough depends on the properties of the flour used and certain other ingredients that may be present in the formulation (Cauvain and Young 2006). Within the dough, water is distributed into bound water and free water. Bound water contributes, along with other molecules, to the supramolecular organization of the dough; free water is responsible for its fluidity. For doughs intended for French breadmaking, the water content of a normally developed dough is between 40 and 46%. Below 35%, the dough does not form; around 50%, it becomes very difficult to handle; above this level, it is fluid (Feillet 2000).

1.2.3. Yeast

Commercial baker's yeasts are carefully selected strains of the *Saccharomyces cerevisiae* genus, which is used for bread fermentation all over the world and is essential to the bread's quality (Birch *et al.* 2013). Baker yeasts are found under 2 forms; compressed cakes or dry powder (Ali *et al.* 2012). The usual delivery method for the compressed form is in waxed paper-wrapped blocks. The recommended dry matter content for this product is between 28-30% (Cauvain 2015a). Yeast is thought to function as a catalyst in its natural, fresh form for the fermentation process that breaks down sugars (Ali *et al.* 2012). Yeast converts the fermentable glucose into carbon dioxide (CO_2) and ethanol, responsible for dough leavening during fermentation and oven rise during baking (Pfeiffer and Morley 2014; Struyf *et al.* 2017). By trapping carbon dioxide within the gluten network of the dough and increasing the volume of the dough, the carbon dioxide emissions act as a leavening agent. In presence of oxygen O_2, yeast initiates a cascade of enzymatic reactions, in which impart a major effect on dough aeration and gas bubbles formation (Birch *et al.* 2013; Boussard *et al.* 2012; Buche *et al.* 2011; Struyf *et al.* 2017). Yeast activity is not only limited in gas production, but also in production of a wide range of aromatic compounds as a result of the enzymatic reactions (Birch *et al.* 2013; Cauvain 2015a; Struyf *et al.* 2017). For example, alcohols, aldehydes, and ketones are important components of the breadcrumb aroma profile because they are by-products of the oxidation of flour lipids (Birch *et al.* 2013; Birch, Petersen and Hansen 2013). The temperature, duration, and yeast concentration of the fermentation process have a significant impact on the aroma compounds that are formed in the breadcrumb (Birch, Petersen and Hansen 2013; Maeda *et al.* 2009). However, yeast activity can be negatively influenced by such factors. In terms of gas production, a temperature of 40-45°C is ideal for yeast activity. Beyond 45°C, yeast activity starts to decline, and by the time the temperature reaches 55°C, the yeast is inactive (Cauvain 2015a). Sugar and salt have to some extent an effect on yeast' activity, thus adjusting the concentrations based on weight per flour is necessary in order to prevent changes in osmotic pressure due to high concentrations (Cauvain 2015a).

1.2.4. Salt

Salt main function is organoleptic; it usually enhances the flavour of bread. Following Baker's yeast and on the weight of the flour, 1.8 to 2 % of salt is used in bread dough recipe (Beck, Jekle and Becker 2012). Throughout the bread making process (mixing and dough formation, fermentation and proofing, baking, and storage), salt plays crucial technological roles in addition to its sensory contribution (Chen *et al.* 2019). Salt (NaCl) is required for the purpose of raising dough stability and fortifying the gluten network (Avramenko *et al.* 2018). Salt affects the charged amino acid of gluten proteins, thus changing the amount of salt in dough can affect the strength of the gluten network and the degree of protein-protein interactions by altering the hydration of the gluten (Avramenko *et al.* 2018). Salt ions exert their effect directly by interacting with the chemical groups of the protein, such as amino acids, peptide bonds, amino and carboxyl groups (Balla *et al.* 1998; Beck, Jekle and Becker 2012). By changing the level of gluten hydration, changing the salt content of dough can affect the degree of protein-protein interactions and the strength of the gluten network (Avramenko *et al.* 2018). Salt shields the charges of the gluten molecules when it is present in low concentrations. This lowers the electrostatic repulsion between proteins, allowing them to associate and form a stronger dough (Kinsella and Hale 1984). On the contrary, a high salt concentration slows the formation of the dough and significantly reduces the volume of the bread (Chen *et al.* 2018). Without enough salt, the gluten network (the dough structure)

will not form properly and the yeast will work harder, resulting in bread with poor texture, volume, flavour, and color (Farahnaky and Hill 2007).

1.2.5. Additives in bread

In addition to sugar and fat, a large number of minor ingredients are often used in bread making, such as ascorbic acid, enzymes, and emulsifiers. These ingredients are generally intended to improve the sensory properties, texture, color, shelf life, and volume of the bread (Cauvain and Young 2006). These include adjuvants (naturally occurring substances that correct, improve, or facilitate the production of a given product), additives (substances or mixtures of substances other than ingredients added to foods; additives are codified by references such as E---), and processing aids, which, like additives, are not usually food ingredients but are involved during production (e.g., enzymes). The concept of "improvers" is often used to define a mixture of these minority ingredients.

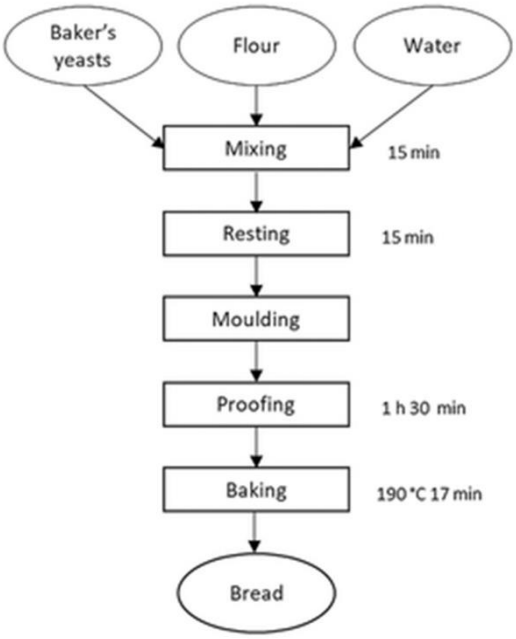


Figure 1.8 Flow diagram of the main operation units in breadmaking processing from wheat flour to the final product (Venturi et al. *2021)*

1.3. Interactions between dough ingredients during bread making

Bread making is a dynamic process characterized by continuous physicochemical, microbiological, and biochemical changes, caused by mechanical-thermal action and the activity of yeasts and lactic acid bacteria, as well as the activity of endogenous enzymes (Rosell 2011).

Most breadmaking processes generally consist of a central process, consisting of a number of common manufacturing steps, which allows for an understanding of the changes occurring during each step and their contribution to the quality of the finished product.

The stages of bread making include mixing ingredients in appropriate proportions and forming the dough during kneading, dividing and shaping the dough pieces during shaping, fermentation, and

baking (Cauvain 2015a; Rosell 2011). The differences between breadmaking processes are mainly related to the mixing of ingredients and kneading. The dividing and shaping processes contribute little to product quality, and the fermentation and baking processes are common to all breadmaking processes (Cauvain 2015a).

During the breadmaking process, several physical changes occur, with gluten proteins primarily responsible for forming the structure of the bread dough, while starch is primarily involved in the texture properties and final stability of the bread (Rosell 2011).

1.3.1. During kneading

The first step in bread making, kneading is one of the key steps that determine the mechanical properties of the dough and have a direct impact on the quality of the final product. It consists of two phases: the initial mixing of the ingredients, and the more intensive kneading. During kneading, the ingredients are hydrated and the liquid and solid phases (dry matter) are uniform. During the second phase, the dough gains strength and cohesion.

Flour owes its reactivity to the ability of its constituent molecules (primarily gluten proteins, but also pentosanes and lipids, and to a lesser extent starch) to form new bonds in the presence of water and to break old ones (Feillet 2000). These reactions are triggered during kneading (Gao *et al.* 2020; Wang, Zheng and Chao 2019; Wang and Copeland 2013) and continue during fermentation and baking of the dough (Jekle, Mühlberger and Becker 2016; Jekle and Becker 2012). In addition to mixing flour, water, and ingredients, kneading solubilizes and hydrates these ingredients, particularly gluten proteins and starch.

The movement of the mixer arms simultaneously homogenizes and incorporates air into the dough in the form of small spherical nuclei (10 to 100 µm) (Junge and Hoseney 1981). Kneading bread dough under vacuum (density = 1.25) or without vacuum (density = 1.15) shows that the introduced gas fraction occupies 8% of the total volume of a dough at the end of kneading at atmospheric pressure (Baker and Mize 1941). Relative volume, defined as the ratio of the total dough volume to the volume of dough without gas, is an indicator of the dough aeration rate. At the end of kneading, it is around 1.1 (Dobraszczyk and Morgenstern 2003; Vliet *et al.* 1992).

During kneading, more air is incorporated than during kneading, and therefore more oxygen. This introduction of oxygen will cause oxidation of the dough by attacking proteins, i.e., gluten and more specifically sulfur-containing amino acids, thus forming disulfide bonds, which are strong bonds. The formation of the protein film itself is due to the ability of glutenins and gliadins to associate with each other through these covalent bonds: disulfide bonds (-S-S-), within the same chain (intra-chain bonds) but especially between two neighboring chains (inter-chain bonds) to allow protein aggregation and contribute to the elongation and complexity of the protein network. At the end of kneading the gluten network will have all its strength (Feillet 2000).

The nuclei formed will be required for the carbon dioxide generated by yeast fermentation and for oxygen for oxidation and yeast activity.

Gliadins are primarily involved in the viscous component of gluten and are therefore largely responsible for the dough adhesive properties (Levavasseur 2007). Glutenins form intramolecular disulfide bonds, but they also form intermolecular disulfide bonds with other glutenins (Shewry and Tatham 1997).

They are rich in hydroxylated amino acids and glutamine, facilitating the formation of hydrogen bonds that provide gluten adhesive and cohesive properties. They are also rich in nonpolar amino acids, which enable protein aggregation and the binding of lipids and glycolipids through hydrophobic interactions. Glutenins provide elasticity and strength to dough, preventing it from expanding and collapsing during fermentation or baking (Khatkar 2002).

The interactions that develop between proteins, starch, and lipids during kneading also contribute to dough formation (Feillet 2000).

These three simultaneous actions (homogenization, dough aeration, and structuring of the protein network) result in a cohesive mixture with viscoelastic properties at the end of kneading, i.e., viscous at long times (flow) and elastic at short times (Dobraszczyk and Morgenstern 2003). This mixture, macroscopically homogeneous to the naked eye, appears at lower resolution as a dispersion of gas bubbles in a continuous matrix of swollen starch and proteins, where each of the constituents contributes to the dough's structuring (Della Valle *et al.* 2014). Each dough must be mixed for an optimal time to fully develop and provide maximum resistance to extension. Undermixing can result in small-unmixed portions. Conversely, if overmixing is performed, dough properties change from good (smooth and elastic) to poor (sluggish and sticky) (Sliwinski, Kolster and van Vliet 2004), and a decrease in consistency is observed, which is attributed to the weakening of the gluten network (Rosell 2011).

It is also important to maintain an optimal dough temperature during kneading and to achieve a suitable final dough temperature. Temperature has a direct impact on the production of chemical reactions, enzyme activity, yeast fermentation, dough consistency and rheology, and dough fermentation time (Cauvain and Young 2008). The final kneading temperature is generally between 20 and 30°C. The presence of water is essential since it is involved in all three levels of kneading action.

- Water ensures the dissolution of soluble compounds and is therefore essential for the homogeneity and cohesion of the dough. It is involved in most of the physicochemical reactions taking place in the dough (Eliasson 1994). Salt dissolved in water, for example, creates ionic bonds with flour proteins essential for dough development (Roussel and Chiron 2002).
- Water largely determines the rheological properties of the dough (cohesion, consistency, viscoelasticity, etc.): the energy required to deform the dough decreases exponentially with the increase in water added (WEBB *et al.* 2007). It acts as a plasticizer: its low molecular weight promotes the mobility of macromolecules (proteins, etc.) by increasing free volume and decreasing viscosity (Levine and Slade 1990).
- Finally, water indirectly influences gas retention: a dough with a total water content of 35% is no longer able to retain the gas bubbles introduced during kneading (MacRITCHIE 2007). This gas retention capacity then increases linearly with the dough water content up to 44%, the typical water content of bread dough (Gan, Ellis and Schofield 1995).

The traditional use of sodium chloride (NaCl) in bread dough produces various changes in its fundamental mechanical properties. The addition of NaCl results in increased osmotic pressure, which slows down the metabolism of bakery yeasts and thus the fermentation rate. It tends to improve the structure of the gluten network and contributes to a better technological suitability of bread doughs. Bread dough is generally considered a complex material consisting of a protein network, in which starch granules and insoluble flour particles are dispersed. Gluten proteins represent the determining fraction responsible for the viscoelastic properties of the dough. NaCl increases dough stability, extensibility

and strength, and increases kneading time due to a repulsion effect between gluten chains, which contributes to favoring S-H bonds over S-S bonds. Salt ultimately tends to decrease dough viscosity due to changes in the gluten network (Beck, Jekle and Becker 2012; McCann, Le Gall and Day 2016) and also has the effect of increasing dough cohesion and extensibility due to a better organized gluten network.

1.3.1.1. Mixing speed & time

Mixing speed, duration, and the energy applied significantly influence the rheological properties of dough, determining whether it develops optimally, remains underdeveloped, or becomes overmixed (Codina and Mironeasa 2013). Dough rheology and aeration are closely connected, as the rheological changes that occur during dough development influence both the incorporation of gas bubbles and their expansion into gas cells during baking (Chin and Campbell 2005a). As mixing progresses, the gluten network strengthens, increasing the dough resistance and the energy needed to maintain speed. Optimal dough development is reached at the peak mixing time (t_{PEAK}), where the dough achieves ideal consistency (Asaithambi *et al.* 2020; Decamps *et al.* 2016; Lancelot *et al.* 2021; Sadot, Cheio and Le-Bail 2017). Mixing beyond t_{PEAK} causes gluten breakdown (depolymerisation of the gluten network), resulting in sticky dough with reduced viscoelasticity. Conversely, insufficient mixing leaves unmixed areas, leading to poor gas holding capacity and fermentation performance (Parenti *et al.* 2021; Sun *et al.* 2022). Undermixed dough lacks a cohesive gluten network, reducing gas retention and yielding low-volume, dense bread. Overmixed dough releases excess free water and also produces poor-quality bread due to gluten degradation (Parenti *et al.* 2021; Sun *et al.* 2022). Codina et al. (2013) investigated the impact of mixing speed (80, 160, and 250 rpm) on dough microstructure and rheology using epifluorescence light microscopy and a Mixolab device. Results showed that higher mixing speeds, particularly at 250 rpm, produced a more compact and continuous protein network. Similarly, Chin and Campbell (2005a) investigated how mixing speed and work input affect the aeration and rheological properties of dough made from strong and weak flours. According to results, increased mixing speed had little impact on the density of gas-free dough but increased the amount of the gas void fraction inside the dough. Both aeration and dough rheology were influenced by the total energy input and mixing speed, with stronger flour showing higher strain hardening, failure strain, and stress that initially increased with work input before declining after reaching a peak. Another study conducted by Brabec et al. (2015), examined the effect of mixing time - undermining, optimal mixing (t_{PEAK}), and overmixing—on the bread properties. Varying the mixing time around the peak influenced experimental loaf volumes, with undermining or overmixing—especially beyond 40 seconds above t_{PEAK} causing the bread loaf volume decrease of 20–60 cm^3. High-protein flour was more sensitive to mixing variations, and while it produced larger crumb cell sizes overall, cell size distribution remained consistent across different mixing times and speeds. Sadot et al. (2017) an increase in rotation speed was found to accelerate gluten network formation, as higher speeds required fewer spiral agitator revolutions to reach maximum power during kneading.

1.3.2. During shaping

Once the dough is kneaded, it is cut into individual pieces. The main objective of the dividing process is to provide the products with the unit size for further processing without significantly altering the intrinsic properties of the matrix in question (Cauvain and Young 2006). Typically, the dough pieces

undergo two shaping processes separated by a short resting period. For many processes, the first shaping consists of a round or spherical shape. The resting period varies between approximately 15 and 20 minutes; longer periods encourage gas production by the yeast and the creation of more open cell structures in the final product. The second shaping stage establishes the final shape of the product, whether it is to be baked in a bread pan or on the oven floor. This process involves three main steps: the dough is first flattened by head rollers, then thinned into a sheet by sheeting rollers. Next, curling or threading rollers shape the dough into a cylinder, and a pressure plate completes the process by rolling and sealing it into a finished loaf (Campbell and Martin 2020; Cauvain 2020a).

1.3.3. During fermentation

Once the final shape is achieved, the dough pieces are transferred to the proofer for the final fermentation stage. Controlling the temperature within the dough allows the yeast to produce gas and controlling the humidity to prevent the surface of the dough from drying out.

This stage, specific to breadmaking, results in a total loss of material (approximately 2 to 3%) through the transformation of sugars into alcohol and carbonic acid (Chargelegue et al., 1994). The oxygen introduced during kneading allows baker's yeast to establish a respiratory metabolism:

Glucose (180 g) + oxygen → carbon dioxide + water + energy (688 kcal) (at 27°C)

$$C_6H_{12}O_6 + 6\,O_2 \rightarrow 6\,CO_2 + 6\,H_2O + \Delta E\ (27°C)$$

Shortly after kneading is complete, all the oxygen introduced is consumed by the yeast, whose metabolism then shifts toward alcoholic fermentation:

Glucose (180 g) → carbon dioxide + ethanol + energy (56 kcal) (at 27°C)

$$C_6H_{12}O_6 \rightarrow 2\,C_2H_5OH + 2\,CO_2 + \Delta E\ (27°C)$$

Carbon dioxide diffuses into air bubbles that are incorporated and dispersed throughout the dough during kneading. The elastic and extensible gluten network formed during kneading retains gas and allows the dough to rise (Poitrenaud 2004; Romano *et al.* 2007). The growth of gas bubbles during fermentation and baking determines the textural characteristics of the finished product (Birch *et al.* 2013; Rosell 2011). In general, an increase in protein content leads to an increase in the gas-retaining properties of the dough and therefore an increase in loaf volume. Volume is also influenced by the quality attributes of the proteins, namely their ability to form the gluten network (Cauvain and Young 2006). The concentration and type of yeast used, the salt content, and process variables (relative humidity, temperature, and fermentation time) will also influence dough expansion and the volume of the finished product (Birch *et al.* 2013).

In addition, a wide range of secondary products are produced during dough fermentation, particularly active compounds such as aldehydes, acids, esters, and ketones produced from yeast fermentative activity and flour lipid oxidation, which are very important for the overall aroma of bread (Birch *et al.* 2013). An increase in yeast concentration leads to an increased formation of most of the aroma compounds formed from yeast fermentation activity, while the concentration of lipid oxidation products increases with increasing fermentation temperature (Birch *et al.* 2013).

The expansion rate of the dough (ratio between final volume and initial volume) is generally 2 to 2.5 for a baguette-type product, 3 to 3.5 for sandwich bread-type products and 3.5 to 4 for hamburger bun-type products.

Salt also has an effect on the fermentation of the dough. Indeed, Lynch et al. (2009) observed a significant increase in maximum dough height when the salt content decreased and at the same time, an increase in the total volume of CO_2 released was observed. This can be explained by two opposing phenomena resulting from the effect of salt on yeast activity and the gluten network. At concentrations greater than 1 g per 100 g of flour (Jekle and Becker 2012), salt inhibits yeast activity. This is due to a decrease in water activity and an increase in osmotic pressure and the electrochemical potential of sodium and chloride ions on the yeast membrane (Matz, 1992). Dough expansion also depends on the strength of the gluten network, i.e., its ability to retain gas. Salt strengthens the gluten network, therefore improving CO_2 retention capacity.

1.3.4. During baking

Once fermentation is complete, a series of preliminary operations are required before baking the dough pieces: cutting the dough with a blade, bringing the oven to temperature, introducing steam into the oven (a steaming process), just before baking, then placing the dough pieces in the baking chamber (Therdthai and Zhou 2003).

Baking is the final step in manufacturing. It transforms a dough into an expanded, cellular solid. Baking is both a thermal and mass transfer process, in addition to chemical reactions. It acts simultaneously on the gas phase and the continuous phase. It determines the kinetics of a series of chemical and physical reactions (change in viscosity, expansion of the structure, browning, starch gelatinization and protein denaturation, etc.). Heat transfers occur from the oven walls to the surface of the product by radiation, from the mold to the product by conduction and within the product itself by thermal convection. Baking kinetics influence the physicochemical reactions and therefore the final properties of the baked product (Purlis 2010).

Structural expansion is an important phenomenon in baking. It depends on heat and mass transfers, but also on the rheological properties of the dough and its stability. Under the effect of temperature, the gases will expand, which increases the size of the bubbles, but it is the evaporation of water that contributes most to the expansion of the bubbles. Indeed, Dobraszczyk and Morgenstern (2003) modelled the expansion of bread during baking and showed that the vaporization of water contributed to more than half of the increase in volume, the rest being due to thermal expansion and the release of CO_2.

Just before baking, in the case of baguette-type products, the dough pieces are scored on the surface with a blade. Industrial bakeries also have scoring machines that automate this step. The scoring must be precise, clean, neither too deep nor too shallow, well-oriented, and regular. These scores will create the ridges on the crust of the baked bread, the so-called "grignes" (scratches), characteristic of French bread. The purpose of scoring is to artificially create areas of less resistance, which, by solidifying somewhat later than the rest of the walls, during baking allow the CO_2 to expand and thus contribute to the maximum development of the dough pieces. The dough pieces must be baked in a hot oven preheated to the chosen baking temperature: between 220 and 260°C (428 and 500°F) depending on their weight, shape, volume, and diameter.

It is not enough to preheat the oven before introducing the dough pieces; the baking chamber must also be saturated with water vapour. This is called steaming. Indeed, during baking, no additional water vapour is added. Steam plays an important role and influences the baking of bread. It softens the surface of the dough pieces, protects it from the intense heat of the oven, delays its solidification and thus promotes the rise of CO_2, thus better development of the dough pieces, and the development of the jets resulting from the blade strokes. It also promotes the caramelization of sugars, giving a more beautiful color to the breads, it allows obtaining after baking a thin crust with a slightly shiny and glazed appearance (Vanin, Lucas and Trystram 2009), it prevents the dough pieces from drying out during baking and that of the bread afterwards. Weight loss, due to water loss, is then limited and staling slows down. Baking is a complex step during which a series of physical, chemical, and biochemical transformations take place, such as product expansion, water loss through evaporation, the formation of a more or less developed honeycomb structure, protein denaturation, starch gelatinization, crust formation, and colouring reactions (Feillet 2000; Sablani *et al.* 1998).

The baking time-temperature relationship is not uniform throughout the dough. The surface of the dough undergoes a longer baking time at a higher temperature than the centre of the dough. The time-temperature relationship decreases toward the centre of the dough (Le-Bail *et al.* 2009). At the beginning of baking, the yeast continues to produce CO_2 until its deactivation temperature of around 50°C. The CO_2 and ethanol produced and dissolved in the dough evaporate and enrich the gas phase. The size, distribution and growth of the gas bubbles emitted during rising and baking will determine the texture and final volume of the bread (Cauvain 2020b).

In the crumb, enzymes are inactivated (α-amylase is destroyed at 70°C), starch gelatinized (between 65 and 80°C depending on local water availability), and proteins thermal rigidified (they coagulate between 70 and 90°C). When proteins are denatured, the gluten strands surrounding the individual gas cells are transformed into a semi-rigid structure that will give rise to the crumb (Rosell 2011). These modifications limit the extensibility of the dough. Any fats added to the formula melt (they lose their crystalline state) and temporarily contribute to the stability of the gas cells.

The initial structure, which was formed of closed pores separated by the dough, transforms into a porous structure with interconnected pores: this is the dough-crumb transition. Some of the alcohols and volatile acids are involved in esterification reactions and enhance the crumb aroma.

The water vaporizes on the surface and leads to the formation of a crust, which simultaneously undergoes coloring and aroma development, mainly due to Maillard reactions (Bolkvadze *et al.* 2024). The formation of a solid crust stops the dough from expanding and changes the pressure balance. An injection of water vapor into the oven, called a steam boost, produces a thin, shiny crust (Jefferson, Lacey and Sadd 2006). The temperature of the crumb gradually reaches 90°C at the center of the bread, while that of the crust rises to 250°C.

These different changes do not occur sequentially but overlap (Figure 1.9). Cooking temperature is the factor that dominates the quality of the finished product because it affects enzymatic reactions, volume expansion, starch gelatinization, protein denaturation, non-enzymatic browning reactions and water migration (Lucas, 2014).

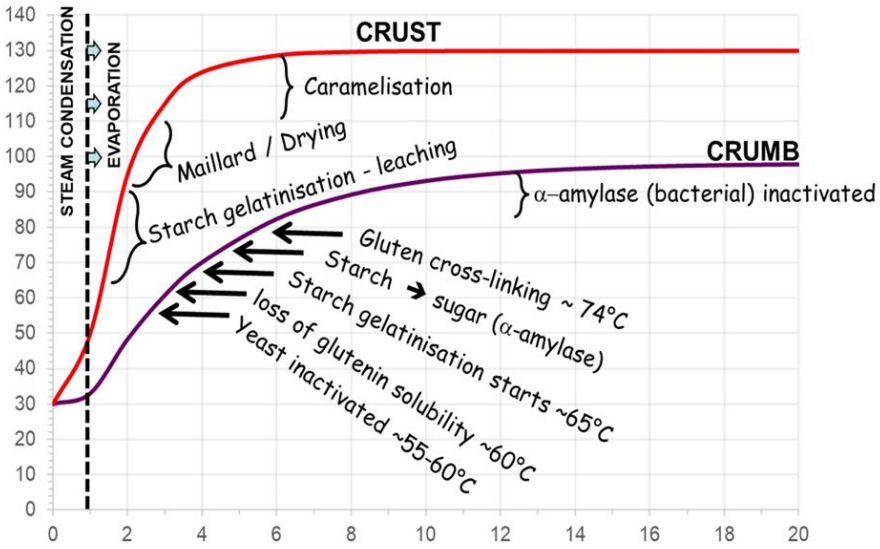


Figure 1.9 Temperature profile during baking showing crust and crumb formation stages: the crust undergoes Maillard reactions, drying and caramelisation. While the crumb experiences starch gelatinisation, yeast inactivation, gluten changes and α-amylase inactivation. Key temperature points for biochemical transitions are also indicated along the crumb temperature curve (Source: A. Le-Bail, personal communication)

1.3.4.1. Distribution of Water in Bread

During baking, the water in the dough evaporates (Dobraszczyk and Morgenstern 2003). Heat transfer occurs through heat conduction but also through evaporation-condensation due to temperature gradients between the outside of the dough and the center of the dough. Water evaporates first from the hottest walls of the gas cells. This water vapor migrates through the gas nuclei, driven by the vapor concentration gradient within the cell. The vapor then condenses on the coldest wall of the gas cells, releasing its latent heat. Finally, the condensed liquid water is transported by diffusion through the membrane to the hottest part of the neighboring gas cell, where the process restarts until the core temperature of the product reaches 98°C (Feillet 2000).

At the beginning of baking, the surface temperature of the bread hovers around the boiling point of water (in practice between 98 and 100°C) and then exceeds this temperature when there is no more free water in the skin (future crust) of the dough. At the beginning of baking, the skin of the dough is sufficiently impermeable to limit water loss from the dough (Cuq, Abecassis and Guilbert 2003).

Heat transport towards the center of the product during baking induces water transport and therefore a change in the water distribution in the bread. The initial water content generally varies between 38 and 48% for bread dough. After baking, the total water loss can be between 10 and 20% of the initial water content of the product on a wet basis (Besbes *et al.* 2013). This loss varies with the size, shape of the loaves and the baking temperature (Feillet 2000). The crust is the main part of the bread that loses water during baking, the water content of the crumb remaining slightly lower than that of the dough, or even higher, particularly at the geometric center of the products (Zhang *et al.* 2025).

1.3.5. During cooling

The cooling of bread after baking corresponds to the reduction in temperature of the loaves as soon as they are removed from the oven to room temperature. Upon removal from the oven, the amylose quickly structures, contributing to an initial stage of stiffening of the crumb over a time scale of around a few hours, visible on a macroscopic scale. The degree of firmness of the bread at this stage is therefore strongly associated with the amylose content released during baking. The longer the baking time, the higher the amylose content released, and the resulting loaf will be all the firmer.

Stear (1990) indicates that the spatial redistribution of water occurs significantly during the first two to four hours of cooling. During the first hour of cooling, water vapor is released from the bread; this is called sweating. According to Ruan et al. (1996), the rate of water migration towards the outside is a function of the storage temperature and the interactions between water and macromolecules. In parallel with sweating, a deformation of the sidewalls of the bread is sometimes observed; this is called corseting. This phenomenon causes a reduction in the volume of the bread and, above all, a deformation that we seek to avoid. The migration of water into the solid matrix, after baking, occurs by diffusion associated with a migration of water vapor into the empty spaces (Besbes *et al.* 2013). This temperature gradient between the crust and the crumb, as well as the difference in vapor pressure between these two parts of the bread, leads to a migration of free water from the center of the crumb towards the crust (Baik and Chinachoti 2000; Besbes *et al.* 2013). This mobility evolves gradually, until a thermodynamic equilibrium is reached in the bread during storage (Cuq, Abecassis and Guilbert 2003). Rapid during cooling, this mobility is reduced during storage.

Salt plays a very important role in the volume and texture of bread. Beck et al. (2012) showed that increasing the concentration of NaCl leads to a decrease in bread volume. This reduction in volume is accompanied by a reduction in the diameter of the crumb bubbles, and of course an increase in the crumb density, which results in an increase in the crumb's resistance to compression and its firmness.

1.3.6. During storage

Staling refers to the gradual decline in bread quality, particularly in flavor and texture, over time (Hug-Iten, Escher and Conde-Petit 2003). These textural changes occur in both the crust and crumb, the two main components of bread. Initially, the crust is dry, crisp, and brittle due to the glassy state of starch and protein. However, at room temperature, moisture moves from the crumb to the crust, triggering a transition from a glassy to a rubbery state in the macromolecules such as proteins and polysaccharides located in the amorphous regions (Primo-Martın *et al.* 2006). This transition leads to a loss of crispiness and results in a softer, more leathery crust texture. The softening is associated with a decline in the rigidity of gluten proteins, which exhibit rubber-like behaviour above their glass transition temperature (Hug-Iten, Escher and Conde-Petit 2003). Staling is largely driven by changes in the starch fraction, with key processes such as gelation and crystallization playing a major role, which were discussed about in previous sections above. These starch transformations; collectively known as retrogradation, contribute significantly to the aging of bread (Hug-Iten, Escher and Conde-Petit 2003).

1.3.6.1. Basic Mechanisms of Starch Gelatinization

At room temperature and in sufficient water, starch granules absorb up to 50% of their dry weight in water. When the starch suspension is heated, it undergoes a series of changes that lead to the irreversible disruption of the molecular order of the starch granule. This process is called gelatinization, and corresponds to a transition from an organized to a disorganized state of the starch grain (Renzetti, van den Hoek and van der Sman 2021).

Starch gelatinization involves three intertwined stages (Figure 1.10):

- Sorption, which consists of the absorption of water by the starch granules and their swelling;
- Stiffening, during which the water present in the amorphous lamellae creates a local disorganization of the amylose chains. The granules continue to swell, amylose begins to be released into the water, and the starch granules lose their crystalline structure and birefringence;
- Dispersion, during which amylose continues to be released into the water. The granules contain mainly amylopectin and collapse, held in a gel formed by the amylopectin. The gelatinization of the granules and the dissolution of the amylose contribute to the increase in dough viscosity during baking.

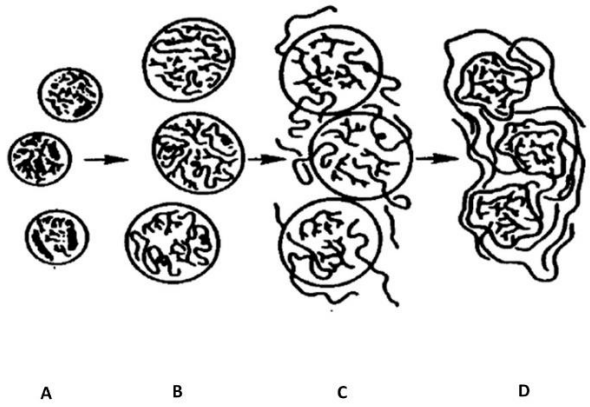


Figure 1.10 Mechanism of starch gelatinisation (Lai and Kokini 2008)

Based on the figure, A – raw starch granules made up of amylose (helix) and and amylopectin (branched), B - addition of water breaks up amylose crystallinity and disrupts helices. Granules swell. C - addition of heat and more water causes more swelling. Amylose begins to diffuse out of granule. D - granules, now containing mostly amylopectin, have collapsed and are held in a matrix of amylose forming a gel (Lai and Kokini 2008).

1.3.6.2. Retrogradation

During the cooling of bread, a starch gelation process occurs, in, which the amylose chains expelled outside the starch granules during heating tend to crystallize. The reassociation between starch molecules, particularly amylose, leads to the formation of a gel structure. This step is linked to the retrogradation and reordering of starch molecules (Rosell 2011).

Indeed, the linear amylose molecules, which diffuse with water towards the outside of the granules, associate randomly to form the rigid network of a gel while inside the granules, the branched amylopectin chains fold and associate, leading to a progressive rigidity of the whole Figure 1.11.

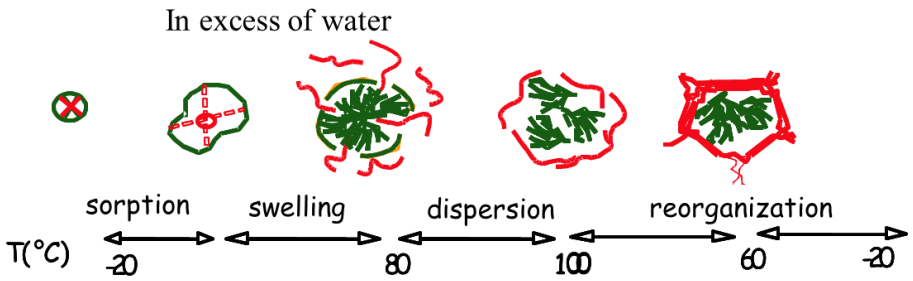


Figure 1.11 Amylose and amylopectin rearrangement during retrogradation

Retrogradation accelerates at temperatures between 0 and 5°C and when starch concentrations are high. It appears that the retrogradation of amylose, which occurs in the first hours after baking, is responsible for the structuring of the crumb and does not contribute to the staling of the bread. On the other hand, the recrystallization of the short side chains of amylopectin, being a much slower process (several days or weeks), would have a major role in the long-term staling of bread (Miles *et al.* 1985). Le Bail et al. (2009) showed that the firming of the crumb occurred after the retrogradation of amylopectin. This confirms that free water is trapped by the amylopectin crystals during storage leading to a stiffening of the structure.

1.3.6.3. Water Redistribution Within Bread

During cooling and storage, water is involved in the following changes in the bread matrix: drying, moisture balance between the crumb and crust, and moisture redistribution among bread components. Drying bread does not completely explain staling, but it can accelerate the reactions that lead to it (Gray and Bemiller 2003).

Besbes (2013) found that bread stored with its crust on became significantly firmer than bread stored without its crust and contained more recrystallized amylopectin, indicating that moisture redistribution from the crumb to the crust plays an important role in bread staling.

Another factor that can affect bread staling is the transfer of moisture from one crumb component to another. Water is a plasticizer, which makes bread components more flexible. Thus, as water is removed (from gluten or starch, or both), the firmness of the crumb increases (Gray and Bemiller 2003). Generally, the water that was bound to the gluten chains and provided an initial "soft" texture gradually becomes trapped in the recrystallized amylopectin during storage. This leads to dehydration of the matrix, particularly the gluten chains, and ultimately hardens the crumb (Baik and Chinachoti 2000).

In conclusion, the water that acts as a plasticizer will be trapped in the amylopectin crystals, in the crust, or will leave the product. This decrease in the amount of free water will lead to a hardening of the crumb.

1.3.6.4. Influence of Water Partitioning and Salt on Starch Retrogradation in Bread

The crystallization of starch that occurs during the staling phenomenon (overall retrogradation phenomenon) requires an addition of water which, by an increase in the strongly bound fraction, contributes to the crystalline structure. This water, which was bound to the gluten chains and which ensured an initial "soft" texture, will gradually become trapped in the recrystallized amylopectin during storage. This induces a migration of water from the gluten chains and the amylose gel present in the crumb towards these crystals. The water is still present in the crumb but being trapped in the amylopectin crystals, it no longer plays its plasticizing role, ultimately inducing a hardening of the crumb (Baik and Chinachoti 2000). Salt limits the phenomena of dehydration of bread thanks to its hygroscopic properties, it therefore delays the staling of the bread (Roussel & Chiron, 2002).

1.4. Dough aeration methods

As stated previously, kneading is the action that develops gluten in bread dough. Gluten acts like an elastic net that traps the gas bubbles created by fermentation. It is thanks to this elastic net that the bread rises and forms a honeycombed crumb rather than a compact block.

To provide an overview of the current understandings and key approaches used to improve dough aeration, Table 1.2 summarizes several studies conducted on the subject. These latter cover various mixer types, gas atmospheres, pressure levels and atmospheric conditions influencing gluten network development, gas bubble dynamics and product quality. It represents how different experimental approaches varying mixer type, mixing speed, gas composition, pressure levels, and dough formulations how they affect the gluten network development, gas bubble incorporation and the final product characteristics such as loaf volume and crumb structure.

Table 1.2. Summary of key dough mixing studies describing different mixing conditions applied with different dough recipes with observed impact of mixing parameters on the dough and bread properties

Study/ Authors	Product type	Mixer & mixing conditions	Gas atmosphere & pressure level	Dough recipe	Main finding & key observations
(Martin *et al.* 2008)	White wheat bread	Tweedy type 10 spiral mixer ; pressure varied from atmospheric to 2 bar; mixing with air and CO_2	Air and CO_2 at atmospheric pressure up to 2 bar	Strong wheat flour; standard white bread recipe with water, salt and yeast	CO_2-mixing reduced loaf specific volume by 17%, weakened gluten network. Air-mixing enhanced gas retention & bubble stability and breadcrumb structure was more homogeneous
(Varayil, Yadav and LeBail 2019)	Wheat bread	Spiral VMI mixer: Low mixing speed: 100 RPM (tool) and 10 RPM (bowl) High mixing speeds at 3 levels: 100, 150 & 200 RPM (tool) combines with 10, 15 & 20 RPM (bowl)	Air at 3 pressure levels: 50, 250 and 500 mbar	Standard wheat bread dough recipe with addition of oil and sugar	Higher pressure and mixing speed increased dough void fraction and loaf volume; pore size where larger with increased pressure
(Cappelli, Canessa and Cini 2020)	Wheat bread	Dry ice or CO_2 snow (solid CO_2)	Different % of CO_2 snow (0, 2, 4, 6, 8 & 10%)	Standard wheat bread dough with 2 types of flour: a moder wheat cultivar (bologna) and ancient wheat cultivar (verna)	Solid CO_2-mixing lowered dough temperature, increased load volume by 10-15%; and crumb density slightly decreased

Study/ Authors	Product type	Mixer & mixing conditions	Gas atmosphere & pressure level	Dough recipe	Main finding & key observations
(Sadot, Cheio and Le-Bail 2017)	White wheat bread	Spiral VMI mixer, cyclic vacuum and air pressure application (-960 to +500 mbar)	Mixing at 120 RPM (tool) and 10 RPM (bowl) 2 levels of overpressure and 3 levels of vacuum	Industrial bread recipe with some improvers such as ibis purple	Dough aeration was proportional to the number rotations of spiral tool The higher the spiral tool the higher the dough aeration
(Haridasan *et al.* 2025)	Pizza dough	Spiral VMI mixer, Vacuum applied during fermentation; batch and continuous mixing	-800 to + 500 mbar Stage 1: 4 min at 100 RPM at atmospheric pressure Stage 2: 4 min at 150 RPM	Typical pizza dough recipe	Higher salt and fat increased dough development time, fat lowered resistance to extension, lower gauge pressure reduced dough void fraction
(Palier *et al.* 2021)	Pound Cake compared to cakes without baking powder and industrial cakes with baking powder	VMI mixer	Air, CO_2 and N_2 with gauge pressures of 0.3 to 0.5 bar	Cake batter	Mixing with CO_2 at 0.3 and 0.5 bar yielded the best results in terms of highest specific volume and CO_2 was solubilised in the batter by evidence of decreased pH

In the breadmaking process, mixing and kneading are two distinct yet interconnected stages essential for developing dough with appropriate structural and rheological properties. Although the terms “kneading” and “mixing” are frequently used interchangeably in scientific literature, they in fact describe distinct, sequential physico-chemical stages within the dough development process (Parenti *et al.* 2021). The mixing stage is a fundamental operation in breadmaking, where flour, water, yeast, salt, and other ingredients are combined to form a homogeneous dough (Cauvain 2015a). During this stage, mechanical energy stimulates hydration**,** ingredient distribution, and initiation of gluten development, creating a viscoelastic network vital for gas retention and dough structure. Proper control of mixing time and intensity is essential to ensure optimal dough rheology: under-mixing may lead to weak, poorly aerated dough, while over-mixing can degrade gluten networks and reduce loaf volume (Sun *et al.* 2022). Also during this stage, dough aeration begins by the entrapment of air bubble that serve as nucleation sites for gas expansion during fermentation, contributing to the dough volume and the final bread structure (Martin *et al.* 2004). In contrast, kneading refers to the continued mechanical manipulation of the dough typically through stretching, folding, and compression to enhance the strength, elasticity, and extensibility of the gluten network (Cauvain 2015a). The two processes are also distinguished by their intensity and duration mixing is typically shorter and less vigorous, while kneading is usually done at end of mixing and is more vigorous. Despite these differences, both stages are essential and complementary to prepare dough that can trap gas during fermentation and expand properly during baking. Their combined effect determines dough machinability, fermentation behaviour, and ultimately, bread volume and texture (Belton 1999; Dobraszczyk and Morgenstern 2003). It is crucial to carefully monitor and adjust all controllable processing parameters to ensure a consistent and optimized bread production process. Among these, mixing variables such as mixing speed, dough temperature, and mixing duration play a critical role in determining both the technological performance and sensory quality of the final bread product. Sadot et al. (2017) found that by employing the VMI prototype spiral mixer, with air pressure cycling between -960 to + 500 mbar, that dough aeration was proportional to the spiral tool speed introducing higher dough void fraction.

1.4.1.1. Mixing speed & time

Mixing speed, duration, and the energy applied significantly influence the rheological properties of dough, determining whether it develops optimally, remains underdeveloped, or becomes overmixed (Codina and Mironeasa 2013). Dough rheology and aeration are closely connected, as the rheological changes that occur during dough development influence both the incorporation of gas bubbles and their expansion into gas cells during baking (Chin and Campbell 2005a). As mixing progresses, the gluten network strengthens, increasing the dough resistance and the energy needed to maintain speed. Optimal dough development is reached at the peak mixing time (t_{PEAK}), where the dough achieves ideal consistency (Asaithambi *et al.* 2020; Decamps *et al.* 2016; Lancelot *et al.* 2021; Sadot, Cheio and Le-Bail 2017). Mixing beyond t_{PEAK} causes gluten breakdown (depolymerisation of the gluten network), resulting in sticky dough with reduced viscoelasticity. Conversely, insufficient mixing leaves unmixed areas, leading to poor gas holding capacity and fermentation performance (Parenti *et al.* 2021; Sun *et al.* 2022). Undermixed dough lacks a cohesive gluten network, reducing gas retention and yielding low-volume, dense bread. Overmixed dough releases excess free water and also produces poor-quality bread due to gluten degradation (Parenti *et al.* 2021; Sun *et al.* 2022). Codina et al. (2013) investigated the impact of mixing speed (80, 160, and 250 rpm) on dough microstructure and rheology using

epifluorescence light microscopy and a Mixolab device. Results showed that higher mixing speeds, particularly at 250 rpm, produced a more compact and continuous protein network. Similarly, Chin and Campbell (2005a) investigated how mixing speed and work input affect the aeration and rheological properties of dough made from strong and weak flours. According to results, increased mixing speed had little impact on the density of gas-free dough but increased the amount of the gas void fraction inside the dough. Both aeration and dough rheology were influenced by the total energy input and mixing speed, with stronger flour showing higher strain hardening, failure strain, and stress that initially increased with work input before declining after reaching a peak. Another study conducted by Brabec et al. (2015), examined the effect of mixing time - undermining, optimal mixing (t_{PEAK}), and overmixing—on the bread properties. Varying the mixing time around the peak influenced experimental loaf volumes, with undermining or overmixing—especially beyond 40 seconds above t_{PEAK} causing the bread loaf volume decrease of 20–60 cm^3. High-protein flour was more sensitive to mixing variations, and while it produced larger crumb cell sizes overall, cell size distribution remained consistent across different mixing times and speeds. Sadot et al. (2017) an increase in rotation speed was found to accelerate gluten network formation, as higher speeds required fewer spiral agitator revolutions to reach maximum power during kneading.

Alongside flour hydration and formation of a viscoelastic dough matter, the primary function of kneaders during dough mixing is to deliver a specific amount of mechanical energy into the dough in order to modify its structure and achieve optimal consistency (Vidal *et al.* 2022). In all types of kneaders, the mechanical energy transferred to the developing dough involves a combination of tension, compression, and shear forces. Additionally, depending on the design of the kneader, the dough may undergo rigid body rotation during mixing (Buche 2011; Vidal *et al.* 2022). For example, the Chorleywood Bread Process (CBP), which relies on mechanical dough development, suggests that beyond a certain kneading speed threshold, dough can be fully developed using a constant amount of energy (Parenti *et al.* 2021). In contrast, the Mechanical Dough Development (MDD) approach emphasizes the need for preliminary assessment of a flour specific energy requirements, as the fixed energy input prescribed by the CBP may be inadequate for high-strength wheat flours (Wilson, Morgenstern and Kavale 2001).

SME is expressed in $kJ \cdot kg^{-1}$ following the equation (Buche 2011; Thompson and Williams 2021):

$$SME = \frac{P \cdot t}{m} \qquad \text{Eq. 1.1}$$

With P is the power of the kneader (kW); t is the kneading time and m is the dough mass (kg).

The power is usually considered as the electrical power consumed by the mixer. In principle, it should be the tool power that must be considered. In case the toll and bowl powers are known, a dough power is considered and is equal to the tool power minus the bowl power. In any case, the tool power represents the biggest part of the power consumed by the mixer and what is important is to observe the order of magnitude and to set up reference values to help supervising the mixing process along the production in a factory or at research level. The power can also be determined as follows in case the torque applied to the tool is known (Parenti *et al.* 2021)

$$P = T \cdot \omega \qquad \text{Eq. 1.2}$$

Where T represents the torque (Nm) and ω is the angular velocity in rad·s^{-1}, defined as below with rps being the number of rotation per second:

$$\omega = 2\pi \cdot rps \quad \text{Eq. 1.3}$$

The power is a function of time during the mixing process; therefore the specific energy is obtained by a progressive integration of the recorded or computed power in function of time. As the energy input per kilogram of dough increases during mixing, bread volume also rises, leading to smaller, more uniformly distributed gas cells in the crumb (Cauvain 2015a). Peighambardoust (2006) demonstrated that an energy input of around 30 kJ·kg^{-1} is typically sufficient to achieve optimal wheat dough development, this requirement can increase to as much as 100 kJ·kg^{-1} depending on the type of flour and the mixer employed. According to Shehzad et al. (2012), a general decrease in modulus ratio with increasing SME was observed, particularly for mixing times longer than 590 s. This decline suggests that higher SME values may inhibit dough stiffening during heating, likely due to limited cross-linking from an underdeveloped gluten network caused by excessive mixing. In contrast, lower SME values allowed for greater cross-linking and dough strength, as indicated by higher mixing scores and a well-developed gluten network.

1.4.1.2. Dough temperature

Controlling dough temperature is a critical factor in breadmaking, as it significantly influences dough rheology, fermentation kinetics, and final bread quality. During mixing, the temperature of the dough increases due to the energy transferred to the ingredients as they combine. It is essential for bakers to control the final dough temperature consistently to promote uniform processing and optimize the quality of the finished product (Cauvain 2015a). In high-speed mixers, this temperature increase is typically 5–7°C, while super-high-speed mixers can raise it by 10–20°C (Cappelli, Bettaccini and Cini 2020). Since protein swelling peaks between 20–30°C, temperatures above this range reduce gluten swelling due to protein denaturation. Lower dough temperatures have been shown to enhance gluten development (Cappelli, Bettaccini and Cini 2020; Quayson *et al.* 2015). Specifically, cooler conditions are thought to reinforce and increase the number of hydrogen bonds, which, despite being weaker than disulfide bonds, are more abundant and play a vital role in stabilizing and strengthening the gluten network (Cappelli, Bettaccini and Cini 2020; Quayson *et al.* 2015). Additionally, low temperatures encourage the formation of macromolecular aggregates, further supporting gluten development (Cappelli, Bettaccini and Cini 2020; Quayson *et al.* 2015). Basaran and Goçmen (2003) examined how different mixing temperatures (17°C, 23°C, and 30°C) affect dough rheology and bread quality. Dough mixed at 17°C produced the best results in terms of bread volume, weight, texture, elasticity, and crumb structure, while higher temperatures, particularly 30°C, led to a decline in overall bread quality. Therefore, the introduction of kneaders with temperature-controlled mixing bowls achieved through a circulating fluid system in a double-jacket design has enabled the quantification of heat loss to the surrounding environment, thereby allowing for accurate estimation of the energy absorbed by the dough (Buche 2011).

1.5. Specific process

1.5.1. Partial vacuum aeration method

Applying a partial vacuum to bread dough during kneading results in a reduction in the gas fraction in the dough and a reduction in bread volume, but results in a finer crumb structure (Shah *et al.* 1998). In addition to impacting the gas fraction, vacuum also modifies the rheological properties and color of the dough.

Liu et al. (2015), studied the impact of vacuum on Chinese noodles. They showed that vacuum mixing improved noodle quality. They noted three main effects. First, vacuum reduces protein oxidation by creating an anaerobic environment. This improves the colouring of the noodles: they are brighter and less yellow. Second, it improves cooking properties by reducing cooking loss and texture, and increasing firmness and extensibility. Cooking loss is defined as the amount of solid substance lost in the cooking water. Finally, vacuum improves water-solid interactions due to a decrease in water mobility and freezable water content. However, for noodles made with low protein flour (LPF), excessive vacuum causes cooking losses and a less firm texture.

To explain all these phenomena, this same group of researchers conducted a study on the structural changes in proteins induced by vacuum mixing (Liu *et al.* 2015). They showed that vacuum decreased the amount of free sulfhydryl (SH) groups for LPF noodles, but not significantly for HPF (high protein flour). However, there was an increase in disulfide bonds (SS) due to the likely proximity of cysteine residues and polymerization of large glutenin subunits, which resulted in large aggregates in SDS-PAGE. Finally, the microstructure of the vacuum-mixed dough (gluten network) was more continuous and compact, with higher tensile strength and extensibility.

In bread dough, Gao et al. (2017) also showed that the impact of vacuum mixing on dough properties, and therefore the finished product, depended on the flour type and mixing time. Indeed, oxygen availability, a critical point for gluten network development, depends on mixing time. The longer the mixing time, the more oxidation reactions occur, which can lead to over kneading. For LFPs, vacuum prevented over kneading, while for HPFs, vacuum reduced mixing time. As with Chinese noodles, vacuum increased extensibility and therefore decreased dough elasticity through greater development of the gluten network due to an increase in disulfide bonds and a higher ratio of β-sheets to β-bends. These results are consistent with those of Liu et al. (2015), who showed that the impact of vacuum and mixing time were dependent on flour protein content in Chinese noodles. High vacuum prevents overdevelopment of the gluten network (reduced disulfide bonds), particularly for weak flours, by reducing the amount of available oxygen, but this has a negative impact on dough elasticity, which can be offset by increasing kneading time.

In a second study, these same authors (Gao, Tay *et al.* 2017) also found that the effect of vacuum depended on mixing time and protein content. Increasing the mixing time increased dough development and air inclusion, resulting in a larger, less dense, and less hard loaf.

1.5.2. Vacuum combined with overpressure method

In baking, the Chorleywood bread process (CBP) is considered a benchmark for Anglo-Saxon bread making. The British invention led to a patent (GB 1044616 A – APV Corporation, 1992). This invention

involves applying a pressure/vacuum sequence to ensure adequate air intake from the atmosphere, followed by a rapid application of a partial vacuum to control bubble structure. However, this is a rapid process (mixing in 3 to 4 minutes).

The difference between CBP and conventionally fermented doughs lies in the rapid development of the dough in the mixer rather than during a prolonged resting time. Each kneading process is specific and allows in some way to modulate the degree of structuring of the gluten network. In the case of CBP, kneading is short and intensive, with a kneading time that does not exceed 5 minutes from the start of kneading (Martin *et al.* 2004; Cauvain 2015b; Trinh *et al.* 2015).

Several studies have shown that mixing under overpressure (OM) in the mixer headspace leads to an increase in the gas volume fraction and bubble size of the dough, as well as the final volume after baking (Brijwani, Campbell and Cicerelli 2008; Cappelli, Bettaccini and Cini 2020; Martin *et al.* 2008; Massey, Khare and Niranjan 2001; Sadot, Cheio and Le-Bail 2017). High pressure results in a larger dough volume. This is because, on the one hand, when gas at a higher pressure is mixed, it expands when the pressure is released to atmospheric pressure. On the other hand, if the gas used is soluble, an additional increase in volume is observed, due to the unsolubilization of the gas when the pressure is released. In the case of mixing with CO_2, a gas solubilization phenomenon was observed. Sadot, Cheio, and Le-Bail (2017) in bread, demonstrated that higher pressures increase the gas fraction by expanding the cells, while Martin et al. (2008) and Campbell et al. (1998) attributed this phenomenon to the increase in the number of bubbles, while an increase in mixing speed reduces the time required to reach the target gas volume fraction. Chin, Martin, and Campbell (2004) and Sadot, Cheio, and Le-Bail (2017) worked on kneading bread dough in OM followed by vacuum kneading compared to atmospheric pressure using air as the contact gas. They showed that overpressure increased the gas fraction of bread dough, following a model of entrainment and displacement of gases in a decreasing exponential order.

Sadot, Cheio, and Le-Bail (2017) showed that overpressure combined with vacuum had two effects on bread dough Figure 1.12. First, overpressure increases the volume of incorporated gas bubbles, which can then be subdivided by the spiral of the mixer during kneading. Second, the vacuum first increases the volume of the bubbles, which are divided by the rotation of the spiral. Then, the vacuum causes air to be released due to the pressure difference between the gas bubbles and the mixer head, but also due to the microporosity of the dough (Shah *et al.* 1998). The increased availability of oxygen allows for faster formation of the gluten network, which results from disulfide bond exchange reactions during mixing (Shewry and Tatham 1997).

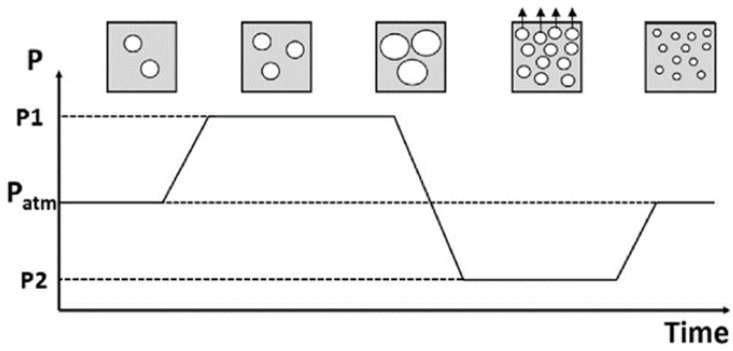


Figure 1.12 A diagram illustrating how the application of either overpressure or vacuum during mixing can influence dough aeration (Sadot, Cheio and Le-Bail 2017)

Baker Perkins Limited filed a patent in 1950 (GB677027 "Improvements in and relating to the manufacture of cake batter and apparatus therefore") that aimed to replace or reduce raising agents and emulsifiers in cake batters by a process of mixing under high pressure with compressed air or another gas such as CO_2 (0.2 to 1.3 bar above atmospheric pressure) and improve packaging. One of the advantages of this process is that the removal of baking powders improves the taste of cakes because the chemical yeast often leaves an aftertaste. Another advantage is that the cakes are moister and retain their soft texture for longer. In this invention, compressed air is preferred to CO_2, which acidifies the batter and would tend to whiten the cakes.

Massey et al. (2001) studied air inclusion in pressure-mixed sponge cake batter by measuring the gas volume fraction and studying the size distribution of gas bubbles. Following their experiments, like Sadot, Cheio, and Le-Bail (2017), they concluded that higher pressures increased the gas fraction through bubble expansion, while increasing the beating speed reduced the time required to reach a given gas volume fraction. The gas fraction was increased by bubble expansion rather than by an increase in the number of bubbles.

Allais and Dufour (2007) studied the impact of overpressure during mixing (air gas, pressure ranging from atmospheric pressure to + 0.4 bar) and the amount of water on various aspects of cake batter quality (porosity, color, spreading quality). The dough had a pound cake type formulation and included powdered eggs. The amount of water added allowed the dough viscosity and properties to be modulated. The aeration process was carried out after dough preparation, with a CDH brand mixer (France) thermostatically controlled at 2.5°C (20 minutes, 500 rpm). This article also included fluorescence spectrometry monitoring of various dough constituents. No interaction between the amount of water and kneading pressure was observed from the experimental design. By increasing the water content, the dough viscosity decreased while its porosity was not affected. On the other hand, a positive correlation (R^2 66%) was observed between the pressure level and the decrease in dough porosity. In return, the porosity of the dough had no effect on the spreading properties of the dough.

Brijwani, Campbell and Cicerelli (2008) studied the aeration of biscuit dough under different gases (CO_2, CO_2/N_2 (50/50) and N_2) and different pressures (0.5; 1; 1.5 and 2 bar). They found that mixing under gas pressure increased the volume of the biscuits. The higher the pressure, the thicker the biscuits. They also showed that the gas volume fraction is increased under a CO_2 atmosphere and a pressure higher than atmospheric pressure. At equilibrium, the amount of CO_2 solubilized in the dough increases as the pressure increases (Henry's Law, 1803). However, it appeared that the amount of gas solubilized in the dough mixed under partial vacuum and then under CO_2 overpressure was lower than that mixed under partial vacuum and N_2. They observed that the density of the dough decreased linearly with increasing mixing pressure with a poorly soluble gas such as nitrogen. Therefore, the gas volume fraction in the paste is proportional to the mixing pressure for insoluble gases (air and N_2) but not for CO_2.

Various models have been proposed to determine the aeration system of dough during pressure mixing:

- A bubble rupture model (Shah *et al.* 1998)
- A mass balance model (Shah *et al.* 1998)
- A bubble population equilibrium model (Martin *et al.* 2004)

In the bubble rupture model, the viscoelastic properties of the dough cause the bubbles to compress, causing them to rupture. The number of bubbles per volume of dough is almost proportional to the mixing pressure for the same volume fraction. Campbell et al. (1998) demonstrated the influence of mixing pressure on the bubble number distribution using optical microscopy. They formulated a theory explaining that the bubble size distribution does not vary with mixing pressure but rather with the number of bubbles. This means that bubbles have the same size distribution in doughs regardless of pressure. For the mass balance model proposed by Campbell and Shah (1998), dough aeration depends on a bubble entrainment and de-entrainment system. When two dough surfaces meet during mixing, a gas pocket is trapped between them. The gas de-entrainment mass flow rate is proportional to the gas mass in the dough. This is true when the probability of a bubble being "de-entrained" is equal for all bubbles.

Therefore, Chin et al. (2004) proposed a more appropriate model, the population equilibrium model, which included simultaneous bubble entrainment, de-entrainment, and breakage. X-ray computed tomography measurements of the number distribution of bubbles in the dough and their average volume during mixing are consistent with the simplified population equilibrium model: all entrained bubbles are of the same size, there is no breakage or coalescence, and the probability of de-entrainment is proportional to the bubble volume.

A more recent study by Palier et al. (2021) aimed to replace baking powders in pound cakes with a pressure-mixing process, while maintaining the best possible qualities. Three gases (air, CO_2, and N_2) and two pressure levels (300 and 500 mbar) were considered. The main results showed that cakes prepared without baking powders were denser than those with baking powders. The additional gas trapped in the dough during baking did not result in any gain in terms of baking expansion, except for cakes prepared using CO_2 baking.

1.5.3. Injected gas

As previously mentioned, during bread baking there are several gases that contribute to the leavening of bread dough. Carbon dioxide is the main gas associated with yeast leavened bread, however, other gases that play a crucial role such as O_2 and N_2. Controlling the gas composition during dough mixing through gas injection allows for precise manipulation of dough aeration and crumb structure. By replacing or supplementing atmospheric air with gases such as carbon dioxide or nitrogen or oxygen, it is possible to influence bubble size, distribution, and stability, which in turn affects fermentation dynamics, loaf volume, and texture.

1.5.3.1. Carbon dioxide: CO_2

CO_2 is a gas that is partially soluble in water at room temperature and atmospheric pressure (1.67 $g \cdot L^{-1}$). Its solubilization in water leads to a lowering of the pH (Figure 1.13).

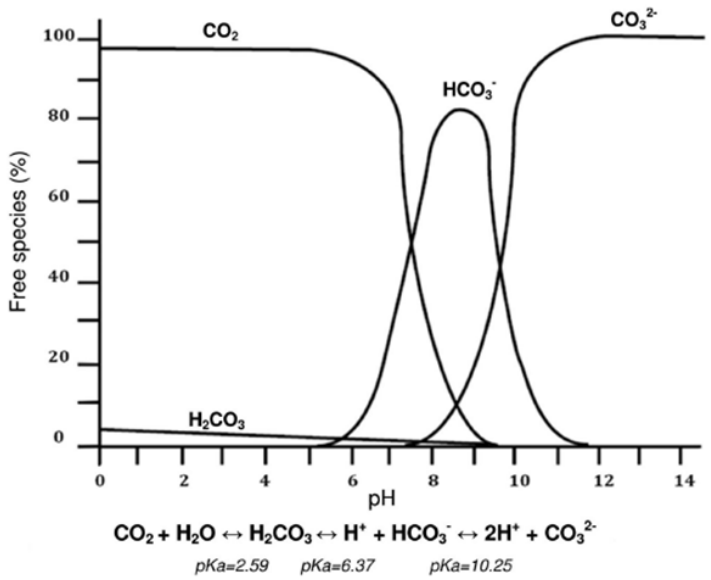


Figure 1.13 Fraction of solubilized carbon dioxide (CO_2), carbonic acid (H_2CO_3) and carbonate (CO_3^{2-}) in water as a function of pH (adapted from Daniels et al, 1985)

Solubility, or the amount of gas retained in the continuous phase, will also depend on many factors.

At low pressures, the relationship between the dissolved gas concentration, denoted C, and the partial pressure, denoted P, is expressed by Henry's law:

$$C = K_0 \cdot P \qquad \text{Eq. 1.4}$$

The K_0 constant, or Henry's constant, depends on the nature of the gas and its solvent, as well as the temperature. Numerous studies have therefore sought to define Henry's constants under different conditions, in order to list them in tables.

Once dissolved, a dissolved gas can then react with its solvent. This is the case for carbon dioxide in water, which dissociates into ions, releasing H+ ions. Several successive reactions then occur:

$$CO_2(g) + H_2O \Leftrightarrow CO_2(aq) + H_20$$
$$CO_2(aq) + H_2O \Leftrightarrow H_2CO_3$$

} Solubilization of gaseous CO_2 into H_2CO_3

$$H_2CO_3 \Leftrightarrow H^+ + HCO_3^-$$
$$HCO_3^- \Leftrightarrow H^+ + CO_3^{2-}$$

} Dissociation of H_2CO_3 to HCO_3^- and CO_3^{2-}

The idea of incorporating gas into a dough to increase the number of bubbles was first implemented in bread, following the work of Baker J.C. and Mize M., 1941, who discovered that the origin of the crumb cells are nucleation sites created during dough mixing. The Chorleywood Bread Process, a process consisting of mixing dough under pressure and then creating a partial vacuum to increase the

nucleation sites, has been the basis of numerous studies to improve the crumb texture of bakery products (Cauvain and Young 2006). It was later shown that the use of CO_2 at the end of mixing could replace the creation of a partial vacuum (Martin *et al.* 2008).

Through its solubilization and condensation properties, the type of gas influences the resulting foam or dough and its stability. For example, gas solubility can have a significant impact on dough characteristics. The more water-soluble a gas is, the faster the dough will drain, while adding a small proportion of insoluble gas prevents negative dough development (Weaire and Pageron 1990). However, it has also been shown that the lifespan of foam obtained by adding pressurized gas is limited by its condensation and evaporation. Adding a non-condensable gas such as nitrogen to a foam extends the lifespan of the bubbles (Chiotellis and G. M. Campbell 2003).

The pressure of the injected gas has a strong influence on the quantity of gas incorporated, but also on the incorporation rate and on the shape and number of gas bubbles created. Chiotellis and Campbell's study of bread dough kneading under CO_2 pressure demonstrated a positive correlation between headspace pressure and the amount of gas incorporated into the bread dough. They also showed that this pressure also influenced the rate of CO_2 incorporation (Chiotellis and G. M. Campbell 2003).

For Campbell and Mougeot (1999), mixing pressure influences the number of cells. For these authors, cell size does not vary with mixing pressure but rather with the number of cells, and therefore, cells have the same size distribution in prepared doughs regardless of the pressure applied. In their publication, Sadot et al. showed that kneading under pressure caused an increase in the volume of the incorporated gaseous alveoli and that it was the combination of vacuum and kneading at the end of the mixture which allowed a subdivision of the alveoli (Sadot, Cheio and Le-Bail 2017). These results had been shown by many authors such as Chiotellis and Campbell (2003), and Shah et al (1998).

Ben Aissa et al. (2010) measured the solubility of CO_2 in wheat flour bread dough mixed using a Diosna SP24 mixer using the theoretical model proposed by Hibberd and Parker. They considered a unit mass of dough with a total volume of V, with Vd representing the volume of continuous dough and the volume of gas given by V – Vd. CO_2 was assumed to be in equilibrium with the dissolved portion in the dough.

According to the ideal gas law, the mass of CO_2 in the gas phase, m'_c, was expressed in terms of partial pressure Pc, with R the gas constant (8.314 $J \cdot mol^{-1} \cdot K^{-1}$) and T the temperature (K):

$$m'_c = P_C \cdot (V - V_d) \cdot \frac{m_c}{R \cdot T} \qquad \text{Eq. 1.5}$$

Where M_c is the molecular weight of CO_2 in $g \cdot mol^{-1}$ and

$$P_c = K_H \cdot X_C \qquad \text{Eq. 1.6}$$

With K_H is Henry's constant and X_C is the concentration of CO_2 in aqueous dough, which varies depending on Arrhenius model:

$$K_H = K_{H0} \cdot e^{\frac{-\Delta Hc}{R \cdot T}\left(\frac{1}{T} - \frac{1}{T0}\right)} \qquad \text{Eq. 1.7}$$

Assuming that CO_2 solubility in the continuous dough phase followed Henry's law, the mass of dissolved CO_2, m''_c, was determined by:

$$m_c'' = K_c \cdot P_c \quad \text{Eq. 1.8}$$

With K_c is the solubility constant expressed as mass per unit of dough per unit pressure. Therefore, the total mass of CO_2 is:

$$m_c = P_c \cdot (V - V_d + V_c) \cdot \frac{M_c}{R \cdot T} \quad \text{Eq. 1.9}$$

Where

$$V_c = \frac{K_c \cdot R \cdot T}{M_c} \quad \text{Eq. 1.10}$$

Vc is the equivalent volume of dissolved CO_2 in a unit mass of dough.

The results reported that the pressure increased uniformly during the first 30 minutes. This rise in pressure for samples V1, V2, V3, and V4 was attributed to the diffusion of CO_2 from the dough's liquid phase into the gas bubbles Figure 1.14.

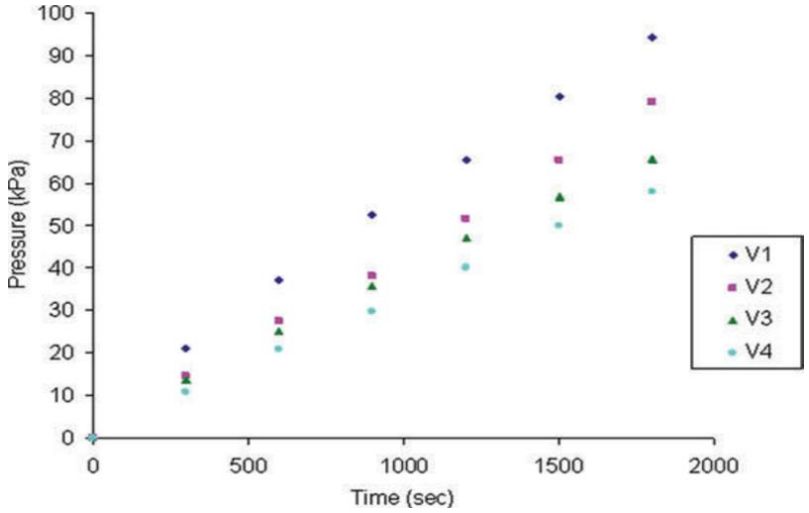


Figure 1.14 Effect of dough density on external pressure evolution at 20 °C for 30 g samples (Ben Aissa et al. *2010) for different volumes* Vi *of the dough*

Palier et al. (2021), used CO_2 as a substitution to baking powder in pound cake by mixing air, CO_2 and N_2 separately with a VMI spiral tool. Their results showed that CO_2-mixed cakes achieved the highest specific volume, which increased by 20% and gave finer breadcrumb structure than N_2-mixed cakes. Evidence of CO_2 solubilisation was marked by a decrease of dough batter pH, suggesting enhanced gas retention and batter expansion during baking. Contrarily, Martin et al. (2008) investigated the effect of CO_2 and air during mixing bread dough using a tweedy 10 type spiral mixer with controlled pressure varying between atmospheric up to 2 bar. Their results showed that CO_2-mixing decreased breads specific volume by about 17% than those mixed with air. In addition, based on C-Cell crumb observations, it showed coarser crumb structure and larger bubbles with CO_2 breads due to the weakened gluten network, whereas with air crumb was finer and more homogenous due to gas bubbles stability by the stable gluten network. They also concluded that depriving the dough from any source of O_2 would lead to detrimental results as observed.

1.5.3.1.1. CO_2 solubility in water

The solubility of CO_2 in water may play a significant role in gas retention and fermentation behaviour of the bread dough. The solubility is governed primarily by Henry's Law, which relates the concentration of dissolved gas in the liquid dough to its partial pressure in the surrounding gas phase. The CO_2 solubility is often reported in mole ratios ($mol_{CO2} \cdot mol_{H2O}^{-1}$), but this can be converted into mass-based unit using molar masses of CO_2 and water (H_2O), as follows:

$$\frac{g(CO_2)}{gH_2O} = mol\frac{CO_2}{H_2O} \cdot \frac{44}{18} \quad \text{Eq. 1.11}$$

Importantly, CO_2 solubility is not only a physical phenomenon but is also influenced by chemical reactions in the aqueous phase. The degree of CO_2 dissolution depends on multiple factors, including dough temperature, water content, and the presence of solutes such as proteins and salts (Poutanen, Flander and Katina 2009). Ben Aissa (2010), investigated the solubility of CO_2 in bread dough using a theoretical model based on Henry's law and ideal gas law. Considering both its physical dissolution and chemical dissociation in the aqueous phase. CO_2 exists as molecular CO_2 ($CO_{2(aq)}$) and carbonic acid (H_2CO_3), which further dissociates into bicarbonate (HCO_3^-) and carbonate (CO_3^{2-}) ions, releasing protons (H^+) and thus affecting pH (Ben Aissa *et al.* 2010).

$$[CO_2^*] = [CO_2]_{aq} + [H_2CO_3] \quad \text{Eq. 1.12}$$

$$[HCO_3^-] \leftrightarrow [CO_3^{2-}] + [H^+] \quad \text{Eq. 1.13}$$

The equilibrium of these reactions is governed by temperature, pressure, and ionic strength of the matrix.

The model proposed that in aqueous solution, the effective concentration of CO_2 is influenced by two sequential Eq. 1.14 & Eq. 1.15. The equilibrium constants of these are calculated by:

$$K_1^* = \frac{[H^+][HCO_3^-]}{[CO_2^*]} \quad \text{Eq. 1.14}$$

And

$$K_2^* = \frac{[H^+][CO_3^{2-}]}{[HCO_3^-]} \quad \text{Eq. 1.15}$$

This constant is dependent on temperature (T), pressure (P) and the ionic strength of the solution. Chiotellis et al. (2003; 2003) demonstrated that temperature significantly affects the concentration of dissolved CO_2 in the liquid phase of bread dough.

At standard conditions (25°C, 1 atm pressure), the solubility of CO_2 in pure water was reported to be approximately 1450 $mg \cdot L^{-1}$ or $1.45 \cdot 10^{-3}$ $g \cdot L^{-1}$ (Les eaux minérales et le gaz carbonique, MINEFI, 1997).

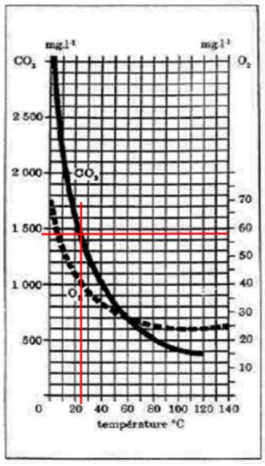


Figure 1.15. Solubility of CO_2 and O_2 in water as a function of temperature. The left y-axis indicates the concentration of CO_2 in mg·L^{-1}, while the right y-axis corresponds to O_2 concentration in mg·L^{-1}. The solubility of both gases decreases with increasing temperature. Red lines highlight the CO_2 solubility (≈ 1450 mg·L^{-1}) at approximately 25°C, demonstrating the inverse relationship between gas solubility and temperature (Gevantman 2011)

This value aligns with Gevantman (2011), who reported a solubility of 1.5 g·L^{-1} or 1500 mg·L^{-1}. Taking into consideration of temperature effect, Carrol et al. (1991) developed an empirical model that predicts the mole fraction of CO_2 dissolved in water as function of temperature and pressure up to 1 mPa. The relationship between the molar ratio of CO_2 to water (mol_{CO2}·mol_{H2O}^{-1}) as a function of temperature, providing values of the Henry coefficient in mole ratio per MPa. This formulation is valid for pressures up to 1 MPa (10 bar) and in the temperature range of 0°C to 160°C (i.e., 273–433 K) (Figure 1.16). The equation is as follows:

$$\ln\left(\frac{X_{CO_2}}{MPa}\right) = -6.8346 + 1.2817 \cdot \frac{10^{-4}}{T} - 3.7668 \cdot \frac{10^{6}}{T^{2}} + 2.997 \cdot \frac{10^{8}}{T^{3}} \qquad \text{Eq. 1.16}$$

Where XCO_2 is the molar ratio of CO_2 to water and T is the temperature in Kelvin. This value must be multiplied by the absolute pressure level to obtain the solubility.

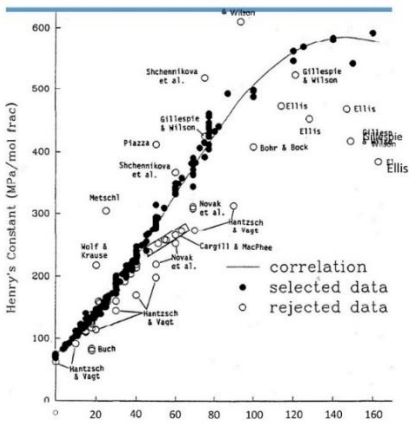


Figure 1.16. Henry's constant for CO_2 in water as a function of temperature. A fitted correlation curve is shown through the selected data points. The plot highlights the general trend of increasing Henry's constant with temperature, indicating decreasing gas solubility Gevantman (2011)

Using this model, the Henry's law constant at 25°C is calculated to be approximately 162 MPa·mol^{-1} fraction. Based on this value, the solubility of CO_2 in water was computed for different pressure conditions relevant to this study:

- **1 bar (atmospheric pressure)**
- **1.5 bar** (equivalent to + 0.5 bar gauge pressure used in carbonation tests)
- **6 bar** (approximate absolute pressure achieved using SodaStream equipment)

The results are summarized in Table 1.3 showing the increasing solubility of CO_2 with pressure, consistent with Henry's Law.

Table 1.3 The summarized results, showing the increasing solubility of CO_2 with pressure, consistent with Henry's Law (Carroll, Slupsky and Mather 1991)

Pressure condition (atm absolute pressure)	Solubility of CO_2 ($g_{CO2} \cdot g_{H2O}^{-1}$)
1	1.622
1.5	2.432
6	9.729

1.5.3.1.2. Effect of solutes on CO_2 solubility in water

Descoins et al. (2006) systematically investigated the impact of various solutes including proteins, alcohols and sucrose on CO_2 solubility in water. Their results have shown that increasing concentrations of these latter reduce the solubility by lowering partial pressure of CO_2 in solution. This phenomenon is attributed to the reduction in water activity and competition for hydration with dissolved species Figure 1.17.

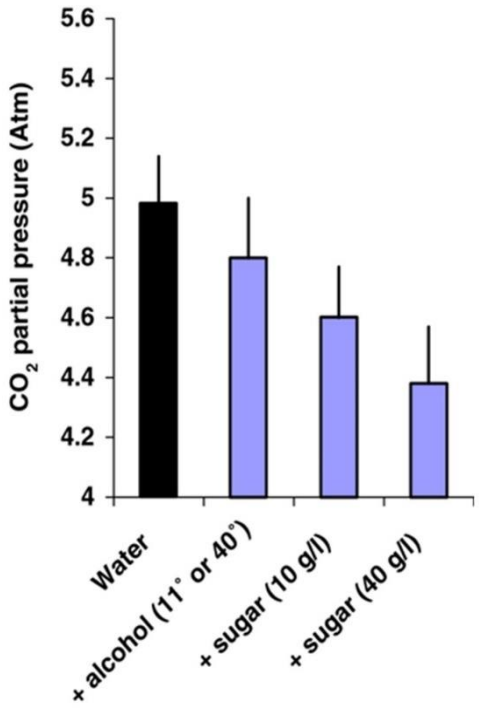


Figure 1.17. Effect of alcohol and sugar on CO_2 partial pressure in water. The bar graph shows the CO_2 partial pressure (in atm) for pure water and water containing either alcohol (11° or 40°) or sugar at concentrations of 10 $g \cdot L^{-1}$ and 40 $g \cdot L^{-1}$ Descoins et al. (2006)

The addition of alcohol or sugar reduces the CO_2 partial pressure, with higher sugar concentrations leading to a lower solubility.

1.5.3.1.3. CO_2 solubility in bread dough

Despite its critical role in bread and fermentation, CO_2 solubility has been only scarcely addressed in literature. A review of the most relevant and representative publication is presented below to benchmark existing data and highlight methodological and interpretative differences. The few available studies differ in terms of experimental setup, units of solubility and definition of the water phase used as a referenced medium.

Hibberd & Parker (1976) and Ben Aissa et al. (2010) both utilized the same methodology based on isochoric fermentation, which measures the pressure increase during fermentation at a constant volume. However, comparing these studies is complicated by differences in units, and by varying reference phases used to express solubility. Hibberd & Parker normalised CO_2 solubility to the dough mass, whereas Bloksma (1990) referred to the liquid phase of the dough (LPD) and Ben Aissa et al., used the total water content of the dough as a reference. The LPD lacks a precise definition in the literature but is generally assumed to correspond to the water added to the dough recipe. On the other hand, Chiotellis & Campbell (2003) reported values in mol/m^3 of the liquid phase without defining the liquid phase.

The water distribution within bread dough is a key factor in understanding CO_2 solubility. As illustrated in Figure 1.18, part of the water that was used to prepare the dough is considered free water, while the remainder is bound with the dough macromolecules. Free water is defined as water that can be frozen during food freezing processes and thus is accessible for CO_2 solubilisation. It is in this free water phase that CO_2, as well as solutes such as salt, dissolve during dough mixing. Moreover, the presence of salt introduces a competitive interaction that may reduce CO_2 solubility, suggesting that dough formulation, particularly salt content, can significantly influence CO_2 dissolution levels.

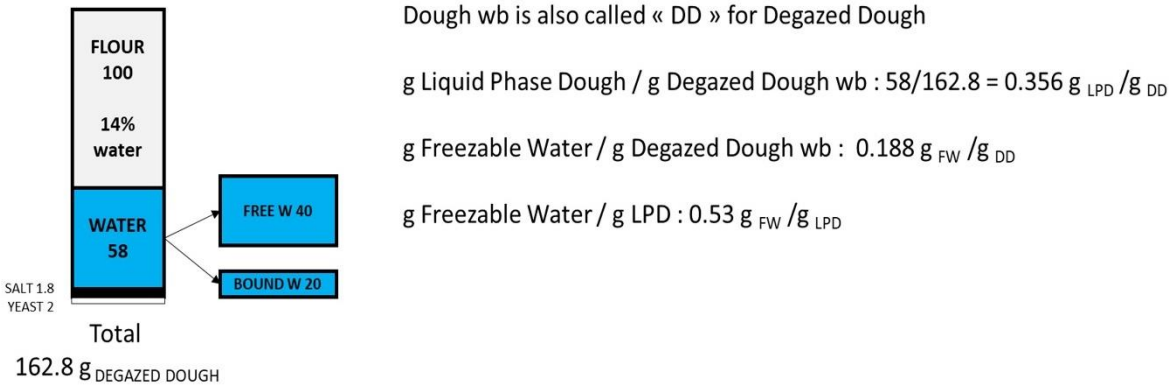


Figure 1.18. schematic representation of the water distribution in the typical bread dough system. The "LPD" or Liquid Phase Dough concerns a priori the water added to the recipe (here 58 g water on 100 g

flour wb). The "free water" represents the "freezable water", which is a priori mainly concerned by the solubilisation of CO_2 as well as other solute (salt in particular) during mixing

To better quantify free and bound water in dough systems, a study by Bushuk & Mehrotra (1977), provided foundational data. They measured the free water and bound water content of doughs made from various flours and investigated the effect of protein content, mixing time, salt concentrations and damaged starch. Notably, none of these factors significantly affected the amount of free water, their data showed a linear relationship between freezable and total water content. The following equation was used for the estimation of free water X_{FW} as function of total water per g of dry flour (X_{DF}):

$$X_{FW}\left(\frac{g_{FW}}{g_{DF}}\right) = 0.591 \cdot X_{DF}\left(\frac{g_{WATER}}{g_{DF}}\right) - 0.148 \qquad \text{Eq. 1.17}$$

Using this equation, and considering the reference dough recipe without AH2, it was found by using this equation that the free water accounted for 41.8% of the total water content and accounted for 53% of the LPD, with the LPD representing the added water in the recipe.

Hibberd & Parker (1976) developed their CO_2 solubility measurements by analysing pressure changes during fermentation at constant volume, assuming that the dough bubble structure and rheological properties did not change significantly during the experiments. Their dough recipe contained 58% water absorption (as LPD), 2% salt, 2%yeast, 2% fat and potassium bromate based on flour with 11.2% protein and 0.62% ash content. They reported a CO_2 solubility of 1.44 mg CO_2 per gram of dough at 27°C under atmospheric pressure. When normalized to the free water content derived from Bushuk & Mehrotra's model, this translated to an unexpectedly high solubility of 7.71 mg CO_2 per gram of free water. This value was approximately 4.76 times higher than the known CO_2 solubility in pure water under atmospheric pressure (1.62 $mg_{CO2} \cdot g_{water}^{-1}$), suggesting potential overestimation or methodological differences in their measurements.

Furthermore, Bloksma (1990) assumed that nearly all yeast-produced CO_2 dissolves in the liquid phase of the dough during fermentation. They estimated that saturation was achieved after about 50 min with a saturation concentration of $4.3 \cdot 10^{-5}$ $mol \cdot mL^{-1}$ LPD. Converting these units yields a value of approximately 1.89 g (1890 mg) CO_2 per g of water, slightly higher than CO_2 solubility in pure water but substantially lower than the values presented by Hibberd & Parker. The inconsistency between Bloksma's and Hibberd & Parker's numbers, despite referencing the same original data, underscores the ambiguity in defining the LPD and the difficulty in comparing these results directly.

Chiotellis & Campbell (2003) modelled the kinetics of fermentation and CO_2 accumulation by studying the effects of temperature, yeast concentration, bubble size, mixing speed, and pressure during mixing. Their simulations showed that at higher temperatures, yeast activity and CO_2 production accelerated, resulting in faster accumulation of CO_2 in LPD. However, the ultimate saturation concentration decreased with temperature, consistent with Henry's Law, which stated that that the gas solubility decreased as temperature increased. In the Figure 1.19 below, they show that at higher temperatures, the CO_2 concentration of the liquid phase accumulates faster at lower temperature. At 30°C (313 K), the saturation is reached at around 1500 s (25 min) and at 25°C (303 K) at 2500 s (42 min). This is due to the fact that at higher temperatures, yeast produces gas more rapidly. However, the higher is the temperature, the lower is the terminal value, which is determined by the Henry's law ($C\infty = P\infty / H$) with $C\infty$ the CO_2 concentration in the dough and $P\infty$ the CO_2 partial pressure in the gas cell embedded in the dough. Indeed, the Henry's law constant (H) increases with temperature. At 25 and 30°C, their

model predicted saturation of $3.2 \cdot 10^{-6}$ mol·mL^{-1} and $3 \cdot 10^{-6}$ mol·mL^{-1}, respectively; corresponding to 1.408 dough and 1.32 $mg_{CO2} \cdot g_{water}^{-1}$. These solubility values are roughly 5.5 times lower than those from Hibberd & Parker and closely align with the expected solubility in pure water under atmospheric pressure (1.62 $mg_{CO2} \cdot g_{water}^{-1}$).

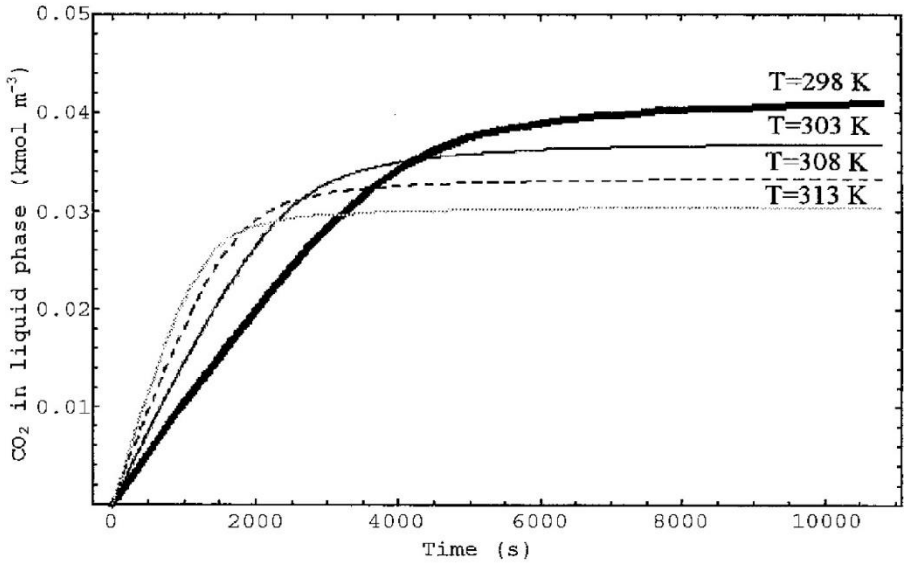


Figure 1.19. Effect of temperature on the dissolved CO_2 Chiotellis & Campbell (2003)

Ben Aissa et al. (2010) examined CO_2 solubility using a similar dough recipe as Hibberd & Parker; 100 g of flour, 58 g of water, 5 g of yeast, 2 g of salt and 1 g of improver. They proposed for the solubility factor K_C as a function of temperature in kelvin (K):

$$K_C = e^{\frac{2.0523 \cdot 10^{-3}}{\mathrm{T}} - 18.451} \qquad \text{Eq. 1.18}$$

The unit refers to the dough pressure in kPa, and also to the mass of LPD. At a temperature of 25°C and a pressure of $1.013 \cdot 10^5$ Pa or 101.3 kPa (atmospheric pressure), a value of solubility was found K_C at 25°C and atm. Pressure = $8.65 \cdot 10^{-6} \cdot 101.3$ kPa = $8.77 \cdot 10^{-4}$ $g_{CO2} \cdot g_{LPD}^{-1}$ = 0.877 $mg_{CO2} \cdot g_{LPD}^{-1}$.

In their conclusion, Ben Aissa proposed to convert the unit with respect to amount of free water present in the dough, which is (as mentioned earlier and *a priori)* the only water that can contribute to gas solubilisation, the remaining water being bounded to the dough constituents. Expressed per gram of dough, this corresponds to 0.306 $mg_{CO2} \cdot g_{dough}^{-1}$, considerably lower than the value reported by Hibberd & Parker but more consistent with CO_2 solubility in water. When adjusted for free water content (with free water being about 60.5% of LPD for Ben Aissa recipe), this corresponds to 1.45 $mg_{CO2} \cdot g_{free\ water}^{-1}$, closely matching pure water solubility (1.62 $mg_{CO2} \cdot g_{water}^{-1}$). The slightly lower solubility relative to pure water may be explained by the presence of salt: with 2 g of salt dissolved in approximately 35.09 g of free water, the salt concentration reaches a titrant of 0.0539 $g \cdot g^{-1}$, nearly double the salt concentration in seawater (0.0291 $g \cdot g^{-1}$). This elevated salt concentration could reduce CO_2 solubility.

In conclusion, the analysis of the aforementioned studies revealed significant discrepancies, many of which stem from differing definitions and measurements of the liquid phase or water reference. Hibberd & Parker reported that solubility is notably higher than theoretical and experimental values for water, due to overestimation or use of inappropriate reference phases. In contrast, Ben Aissa aligns

well with the solubility of CO_2 in pure water when normalized by free water content. The presence of salt and its interaction with dough components must also be considered, as it can reduce gas solubility. Overall, the free water fraction, rather than the total or added water (LPD), provides the most realistic basis for estimating CO_2 solubility in bread dough systems.

CO_2 is considered during dough mixing for its possible functional roles in:

1. Solubilisation into the dough matrix, resulting in the reduction of the dough pH which may interfere with the enzymatic activity. This pH reduction can have both positive and negative impacts on enzymatic activity in dough. On the positive side, due to the formation of carbonic acid, this acidification can enhance or create an environment suitable for the activity of proteases (pH range 4.0 – 5.0), which can modify the gluten proteins. This can improve dough extensibility and handling properties, making the dough easier to handle and thus, better gas retention during fermentation. Protease enzymes directly affect gluten proteins by hydrolysing peptide bonds (Rajendhran *et al.* 2024). According to Leitgeb et al. (2022), showed that CO_2 solubility alters the residual activity of proteases, leading to changes in ionization state of amino acid at the enzyme active sites, thus altering the enzymatic conformational and catalytic functions. These enzymatic changes could affect starch hydrolysis and gluten modifications by facilitating better gas retention during proofing. The measured pH in our dough was close enough to create an efficient environment for protease.
   On the negative side, the fungal α-amylase have optimal pH 5.5 – 6 and are mildly inhibited at our lower pH, thereby reducing starch hydrolysis and available sugars for fermentation, leading to slower fermentation and denser dough with less oven spring.
2. Stabilisation of gas nuclei, contributing to dough structure and gas retention.

The hypothesis of stabilisation is based on the fact that CO_2 will be present in the gaseous phase and also in the liquid phase of the dough. At start of fermentation, it takes some time for the CO_2 to be produced by yeast, diffuse in liquid state towards the gas cells and start to increase their initial pressure and then to increase their volume resulting in the dough expansion. During the onset period of CO_2 production, it is assumed that some gas cells may disappear because of the effect of the surface tension at the gas-dough interface because of a lack of internal pressure.

1.5.3.2. Oxygen: O_2

Oxygen O_2, a key constituent of atmospheric air, is indispensable in dough mixing due to its dual role in both aeration and gluten network development. As air is mechanically incorporated into the dough, O_2 facilitates the entrapment and stabilization of gas bubbles within the hydrated flour matrix (Joye, Lagrain and Delcour 2009a; Sun, Martin G Scanlon *et al.* 2023). These bubbles act as nucleation sites for carbon dioxide during fermentation and are essential for gas cell formation and bread volume (Cauvain 2015a; Chiotellis and G. M. Campbell 2003).

Oxygen availability during dough mixing plays a crucial role in determining the structural and functional quality of bread dough. During kneading, oxygen is not only incorporated into the dough matrix but also rapidly consumed by both yeast (through aerobic respiration) and oxidative enzymes such as lipoxygenase and glucose oxidase (Decamps *et al.* 2016). This creates a competition for oxygen between yeast and enzymes that are responsible for crucial biochemical modifications, particularly those involved in the formation of gluten and arabinoxylan networks (Buche 2011; Buche *et al.* 2011). O_2

consumption by dough proceeds via a two-step mechanism that ultimately limits the extent of dough oxidation. The initial step involves the physical incorporation of O_2 into the dough, which is predominantly influenced by the type of mixing apparatus employed and the rheological properties of the dough. The subsequent step entails the covalent binding of O_2 within the dough matrix, largely governed by the characteristics of the flour and the specific dough formulation (Buche *et al.* 2011).

In this context, a comprehensive study conducted by François Buche (2011), primarily focused on monitoring O_2 consumption using an airtight, instrumented kneader-fermenter called *sitoxygraph*. Similarly to any overhead pressure kneaders, this machine measured the time, temperature and pressure during the mixing phase, as well as the gas composition in the headspace. They aimed to examine the interactions with O_2 among dough components, the impact of O_2-enriched atmosphere or depleted on oxidation reactions and their subsequence effect on dough properties.

Kneading phase:

During kneading, the nitrogen content within the dough itself was regarded as negligible when compared to the nitrogen present in the surrounding gas phase. Consequently, the amount of nitrogen in the gas phase was assumed to stay constant. Therefore, at any time t, the amount of O_2 consumed was calculates per number of moles and the present amount of CO_2 in the headspace by the following:

$$O_{2\ consumed} = \frac{n_{O_2(initial)} - n_{O_2}(t)}{dry\ matter\ of\ flour} \qquad \text{Eq. 1.19}$$

Quantifying O_2 consumption, CO_2 production, and dough volume throughout mixing and fermentation was based on a six-step procedure incorporating gas composition (% O_2 and % CO_2), total chamber pressure (P), and gas phase temperature (T), as measured by gas analyzers and environmental sensors. Based on Figure 1.20, comparing yeasted and un-yeasted doughs, analysis of the average oxygen consumption at the end of kneading for doughs with and without yeast showed that adding yeast significantly increased the total O_2 consumed by 0.96 µmol O_2 per gram of dry flour after 15 minutes of kneading, representing a 24.5% increase.

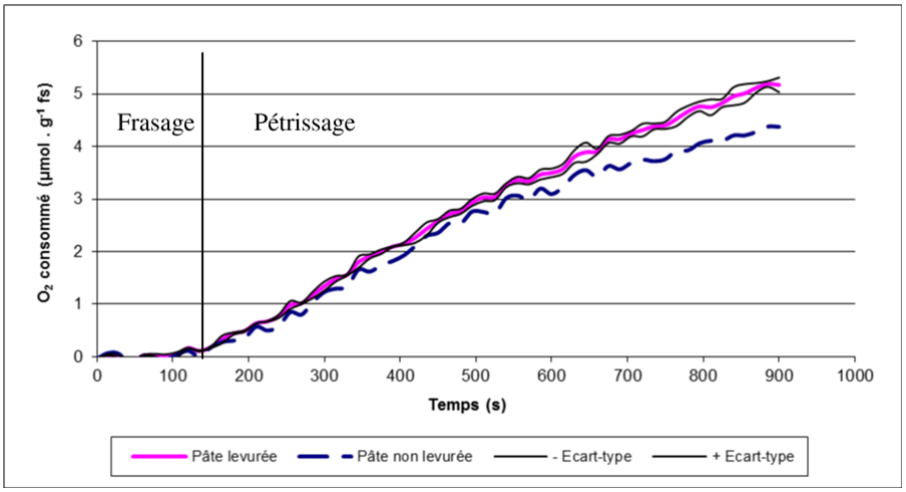


Figure 1.20 O_2 consumption during kneading of yeasted vs. unyeasted dough (Buche 2011)

In addition to the yeast consumption of O_2, LOX activity remained fully functional up to 400 seconds. This suggested that, unlike non-yeasted doughs, the presence of yeast introduced competition for O_2,

which delayed both the decline in substrate availability and LOX inactivation, thereby postponing the reduction in O_2 consumption rate.

Looking at Figure 1.20, after 15 min of kneading, CO_2 release was minimal in un-yeasted dough (0.12 µmol CO_2 per g of dry flour) but significantly higher in yeasted dough (4.30 µmol CO_2 per g of dry flour). In absence of yeast, the small amount of CO_2 detected was attributed to the metabolic activity of the endogenous microflora associated with the flour.

During kneading, the amount of CO_2 released over time was described by a second-degree polynomial equation of the form:

$$CO_{2\,released} = a \cdot t^2 + b \cdot t \qquad \text{Eq. 1.20}$$

Where t is time, and a and b are coefficients derived from experimental data.

At the end of dough kneading, the dough retained 0.09 µmol CO_2 per g of dry flour. This accumulation contributed to the increase in the breads specific volumes. However, this calculation likely underestimated the actual CO_2 retained without taking into account the dissolved HCO_3^-.

Fermentation phase:

During fermentation, the overall O_2 consumption remained unchanged, was attributed to the absence of air incorporation into the dough at the stop of mixing. Furthermore, increasing the O_2 concentration in the mixing atmosphere, either by adding more O_2 or increasing the mixing pressure through compressed air injection, enhanced the overall consumption for both yeasted and unyeasted doughs. These findings indicate that, under atmospheric pressure and with a mixing speed of 60 rpm in the *sitoxygraph*, oxygen transfer rate becomes a limiting factor during kneading (Buche 2011).However for CO_2, a small amount appeared in the gas phase (0.67 µmol CO_2 per g of dry flour), likely due to the partial retention in the gas cells inside the dough. After 30 min of fermentation, the amount retained increased significantly (+16.1 µmol), where the dough volume increased by 0.7L.

Buche adopted a 2 stages mixing in his experiments following a fermentation period; the rationale was to assess the impact of the re-introduction of oxygen in the dough. By referring to Figure 1.21, following the restart of kneading after fermentation, the O_2 consumption increased by 1.87 µmol CO_2 per g of dry flour within 5 min. This was attributed to the renewed yeast respiration due to air incorporation. Concurrently, the formed gas cells formed during fermentation were disrupted, releasing the CO_2 into the headspace resulting in a decrease of dough volume to 3.8 L (-12%). This CO_2 release was also marked by an increased production rate, surpassing levels observed at the end of the first kneading stage.

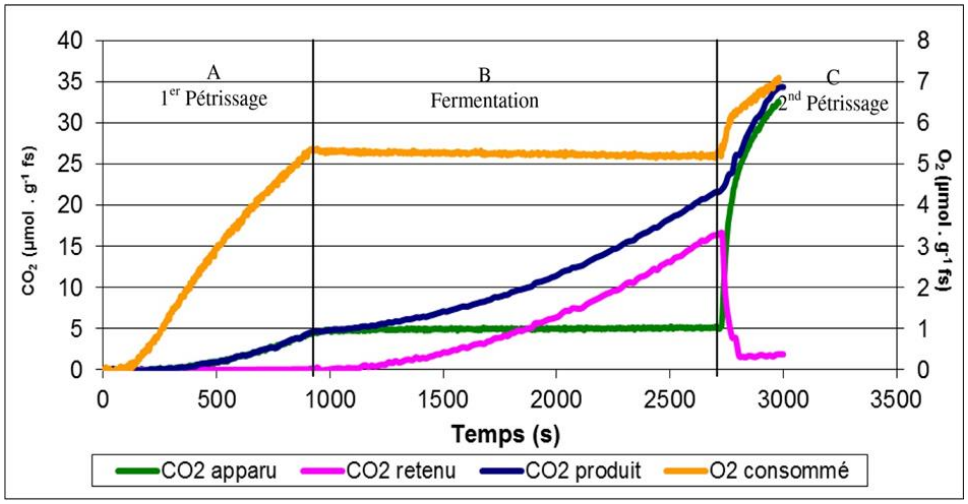


Figure 1.21 Oxygen consumption and total carbon dioxide production (sum of released and retained CO_2) during the mixing, fermentation, and second mixing of yeasted dough containing 1% dry yeast (Buche 2011)

1.5.3.3. Nitrogen: N_2

Air contains approximately 20%O_2 and 80%N_2. N_2, while relatively inert and poorly soluble in water compared to CO_2, can influence dough structure and gas retention during mixing and proofing (Chin, Martin and Campbell 2005; Chin and Campbell 2005b; Paulik *et al.* 2021). When dough is mixed in air, N_2 becomes trapped in gas cells because it does not participate in chemical reactions or dissolve significantly into the dough matrix (Beghin *et al.* 2022). Its low solubility and inertness make it stable within bubbles, providing a consistent gas phase that supports early-stage bubble formation and structure stabilization.

Unlike O_2, N_2 does not contribute to oxidative reactions important for gluten development. However, its presence in the gas phase (alongside CO_2 produced by yeast) helps maintain the mechanical integrity of gas cells, especially in the early stages before significant CO_2 accumulation (Beghin *et al.* 2022).

Chin et al. (2005; 2005b) in two-parts study, doughs were prepared with varying gas contents using a laboratory-scale Tweedy 1 mixer operated under different headspace pressures. Mixing conditions included air, pure nitrogen, and a controlled oxygen–nitrogen atmosphere with constant oxygen levels. Doughs void fraction exhibits a linear correlation with mixing pressure when mixed either in air or under a controlled O_2 environment. Results with N_2-mixing were not linear and lower than those with O_2-mixed. Also, doughs mixed in a pure N_2 atmosphere were soft, loose, and exhibited high viscosity and stickiness, with stickiness increasing at higher mixing pressures.

In summary, N_2 main roles in dough are:

- Acting as a filler gas in early-stage bubble formation
- Stabilizing gas cells due to its low solubility and inertness
- Having minimal impact on dough chemistry, unlike oxygen or CO_2

1.5.4. Incorporation of Ascorbic acid: AH_2 or E300 as an additive

Alongside hydrocolloids, oxidizing agents were the first dough conditioners used commercially. Initially, they were developed to serve as bleaching agents to eliminate the yellowish tint in flour, but it was later found that they also helped strengthen the gluten in dough (Bejosano and Alviola 2015; Liang *et al.* 2023; Wieser 2007). Oxidizing agents such as ascorbic acid, potassium bromate, and azodicarbonamide are commonly added to strengthen gluten networks by promoting disulfide bond formation, enhancing dough elasticity and gas retention (Every *et al.* 1999; Joye, Lagrain and Delcour 2009a; Decamps *et al.* 2012). For many years, potassium bromate and azodicarbonamide were the oxidants of choice, but their ban in most countries in the 1990s left bakers with only ascorbic acid (vitamin C) as the permitted oxidant during bread making (Joye, Lagrain and Delcour 2009a; Koehler 2003).

Ascorbic acid (AH_2) is very efficient in enhancing the performance of the flour as shown in the graph below obtained with Alveograph tests. The maximum amount allowed in Europe is 300 ppm based on the mass of flour. Usual dosages are below 100 ppm.

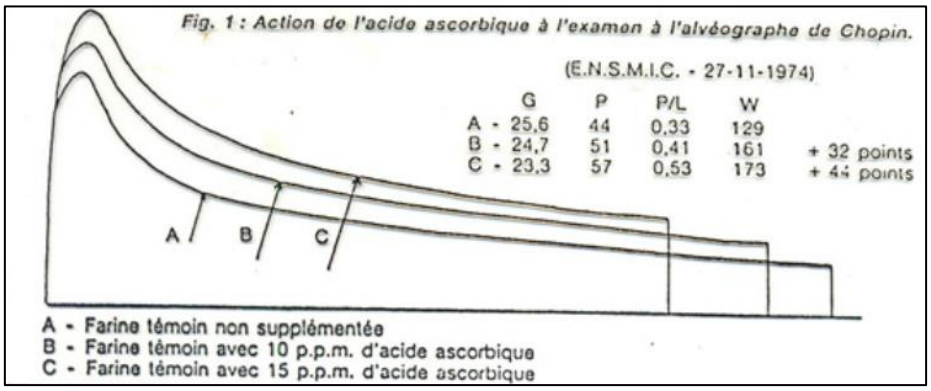


Figure 1.22 Effect of different concentrations of AH_2 (0, 10, and 15 ppm) on dough rheological properties measured by Chopin's alveograph. Curves A, B, and C represent dough without ascorbic acid, with 10 ppm, and with 15 ppm AH_2, respectively. The addition of AH_2 increased dough strength (G) and baking strength (W), indicating improved gluten network formation and gas retention capacity. Extensibility (P) and elasticity ratio (P/L) also changed, reflecting enhanced dough elasticity (Calvel 2001)

1.5.4.1. Ascorbic acid (AH_2) chemical properties

Ascorbic acid (AH_2) is a sugar acid monosaccharide (Raghavendra Rao *et al.* 2016). Pure ascorbic acid appears as a white crystalline powder and dissolves easily in water, forming a clear, colourless solution (Du, Cullen and Buettner 1826). AH_2, is a water-soluble antioxidant with strong reducing properties, primarily due to its enediol structure, which allows it to donate electrons and scavenge free radicals (Njus 2020; Smirnoff 2018). Chemically, ascorbic acid is a six-carbon compound with the molecular formula $C_6H_8O_6$ (Bradshaw *et al.* 2011). It exists in two forms: the reduced form (ascorbic acid) and the oxidized form (dehydroascorbic acid), and thus four stereoisomers exist as shown in the figure below (Figure 1.23) (Bradshaw *et al.* 2011; Du, Cullen and Buettner 1826; Raghavendra Rao *et al.* 2016). L-threo-AH_2 is the sole effective component of AH_2 that enhances the rheological properties of dough,

while D-erythro-AH_2 and D-threo-AH_2 are nearly powerless (Abedi and Pourmohammadi 2020; Dong and Hoseney 1995). This is also due to the high affinity of ascorbic acid oxidase (AO) to L-AH_2 than D-AH_2 (Every *et al.* 1999; Joye, Lagrain and Delcour 2009b).

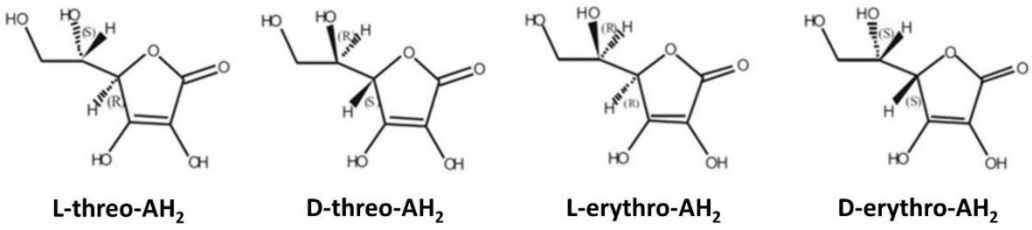


Figure 1.23 Ascorbic acid (AH_2) isomers and their molecular structures (Raghavendra Rao et al. *2016)*

AH_2 features an ethyldiol side chain, two hydroxyl groups, and a carbonyl group positioned around a γ-lactone ring Figure 1.24. The hydroxyl groups can function as both proton donors and acceptors in hydrogen bonding, while the carbonyl group serves as a proton acceptor. The flexibility of the ethyldiol side chain (a two-carbon chain (-CH_2OH) attached to the lactone ring) and hydroxyl groups allows for multiple intramolecular hydrogen bonding configurations, which influence the molecule's pKa values and electrochemical properties (Njus 2020; Tu, Njus and Schlegel 2017).

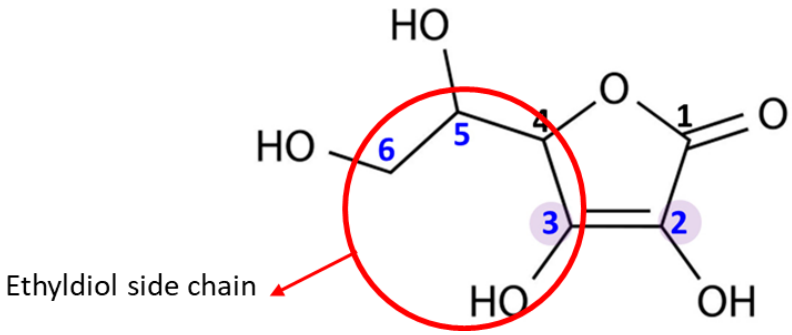


Figure 1.24 Ascorbic acid (AH_2) molecular structure (Devaki and Raveendran 2017)

1.5.4.2. AH_2 mode of action

Cysteine (Cys), an amino acid containing a sulfhydryl or thiol (SH) group, can function as both a reducing agent and a free radical scavenger during the extrusion processing of wheat flour (Angioloni and Dalla Rosa 2007; Sun *et al.* 2022). Three competitive thiol (–SH) mediated mechanisms significantly influence the structural integrity of the gluten matrix during dough development. These include (a) oxidation of free thiol groups, resulting in gluten polymerization; (b) interactions with non-functional “terminators” containing a single SH group that inhibit polymer formation; and (c) thiol–disulfide (SH/SS) exchange reactions involving low-molecular-weight thiols such as glutathione (GSH) and gliadins with an unpaired cysteine residue, leading to depolymerization (Joye, Lagrain and Delcour 2009a).

Glutathione (GSH), a tripeptide comprising glycine, cysteine, and glutamic acid, exists primarily in reduced (GSH) and oxidized (GSSG) forms (Mirończuk-Chodakowska, Witkowska and Zujko 2018). During dough mixing, the formation of disulfide (SS) bonds occurs both intra- and intermolecular within

glutenin subunits via oxidation of sulfhydryl groups and SH/SS interchange. The dough redox environment and the presence of redox-active agents influence these reactions (Joye, Lagrain and Delcour 2009b; Wieser 2007).

Although chemically a reducing agent, AH_2 exhibits an oxidative effect in bread dough through both enzymatic and non-enzymatic pathways, ultimately strengthening the gluten network (Beghin *et al.* 2022). AH_2 is quickly oxidized either by atmospheric oxygen or through enzymatic action to form dehydroascorbic acid, which enhances the formation of disulfide bonds SS between gluten proteins by reducing the thiol–disulfide (SH/SS) exchange involving endogenous glutathione (GSH) and the intermolecular disulfide bonds in gluten (Abedi and Pourmohammadi 2020). As a result, it contributes to the development of firmer and more robust dough (Grosch and Wieser 1999; Lucas, Becker and Jekle 2018; Wieser 2007).

Endogenous ascorbic acid oxidase (AOX) in wheat catalyzes the oxidation of L-threo-ascorbic acid to L-threo-dehydroascorbic acid (DHA) in the presence of molecular oxygen, a reaction that typically occurs during the latter stages of mixing (Beghin *et al.* 2022; Buche 2011; Joye, Lagrain and Delcour 2009b):

$$2L - threo - AH_2 + O_2 \rightarrow 2\ DHA + 2H_2O \qquad \text{Eq. 1.21}$$

AOX exhibits optimal activity between pH 5 and 6 and at approximately 40 °C (Decamps *et al.* 2016; Pfeilsticker and Roeung 1980). DHA subsequently functions as an electron acceptor in the oxidation of GSH, which is abundant in wheat flour, producing GSSG in a reaction catalyzed by glutathione dehydrogenase (Buche 2011; Every *et al.* 1999; Gao *et al.* 2020):

$$DHA + 2\ GSH \rightarrow AH_2 + GSSG \qquad \text{Eq. 1.22}$$

GSSG can further react with protein-bound thiols (PSH), yielding protein–glutathione mixed disulfides (PSSG) and regenerating GSH (Koehler 2003):

$$GSSG + PSH \rightarrow GSH + PSSG \qquad \text{Eq. 1.23}$$

The accumulation of PSSG has been shown to increase during mixing, particularly in dough systems treated with AH_2 (Abedi and Pourmohammadi 2020). GSH can disrupt glutenin polymer integrity by engaging in thiol–disulfide exchange reactions, forming protein–GS disulfides that result in depolymerization and a weakened gluten network (Guo *et al.* 2020). If not oxidized, GSH interferes with SS bond formation and inhibits gluten development (Decamps *et al.* 2016; Koehler 2003).

Reactions are summarized in the following scheme (Figure 1.25).

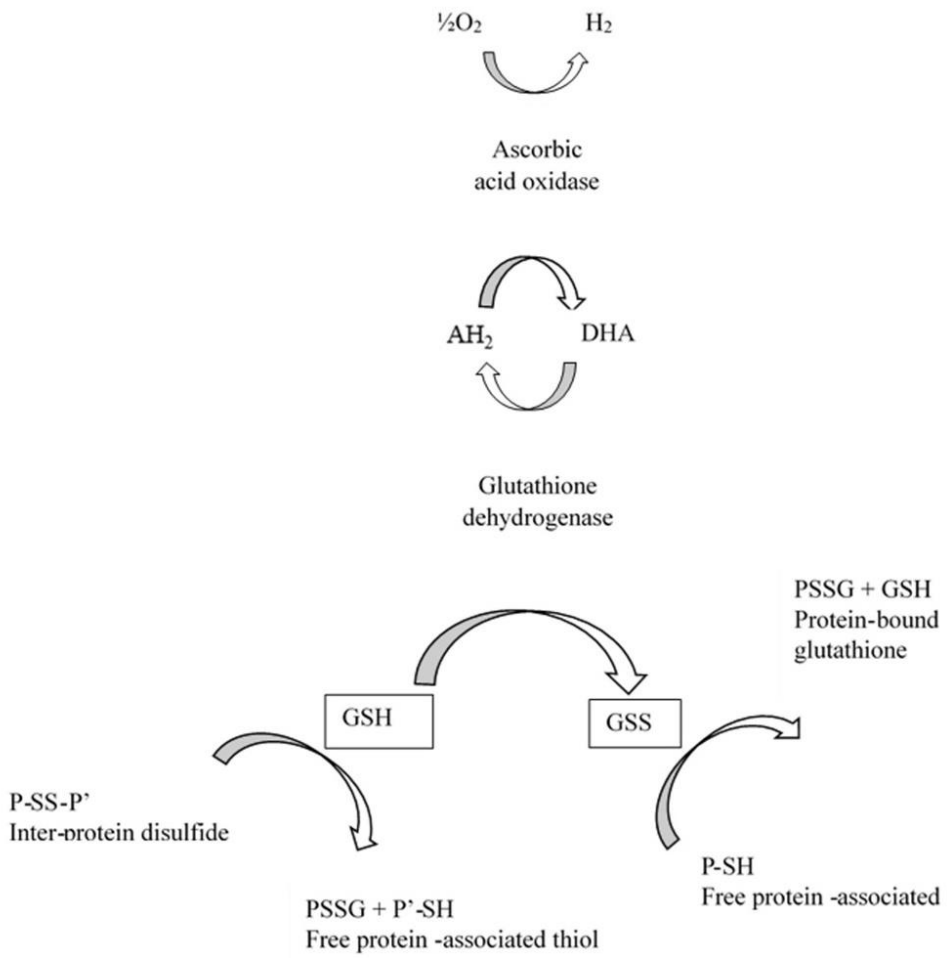


Figure 1.25 Reactions catalysed by ascorbic acid oxidase (Chen and Schofield 1996; Faccio et al. *2012; Guo* et al. *2020)*

The effect of AH_2 on dough strength relies on the quantity of oxygen introduced during mixing, identified as a limiting factor in AH_2 mechanism of action. Nonetheless, dough quickly turns anaerobic following mixing, since oxygen is mainly used by yeast and engaged in different enzyme-related reactions (Beghin *et al.* 2022; Decamps *et al.* 2016).

As previously mentioned, O_2 is indispensable in the activation/degradation of AH_2 into the active form DHA in order to exert its effect. During dough mixing, O_2 is supplied from both endogenous and exogenous sources. Endogenous oxygen may arise from biochemical reactions within the flour matrix, including those involving oxidases and other oxygen-releasing compounds naturally present in wheat flour. Exogenously, oxygen is incorporated from ambient air during mechanical mixing, which facilitates gas dispersion into the dough system (Joye, Lagrain and Delcour 2009a; Wieser 2007). Beghin et al., (2022), explored on how different levels of oxygen O_2 integration during mixing affect dough and bread characteristics, especially concerning the roles of azodicarbonamide (ADA) and AH_2. Results showed that greater incorporation of O_2 led to increased disulfide (SS) bond formation, which improved gas retention in the dough and resulted in higher bread specific volumes (BSVs).

1.6. Rheological properties of dough

Food products are extremely complex materials to study from a microstructural perspective. It is therefore difficult to establish exact cause-and-effect relationships between the initial structure and the texture of the finished product. Rheology is the science that studies the flow properties of bodies subjected to external forces or constraints, and deformations (Faridi and Faubion 1990). Three types of behaviour are distinguished: viscosity, elasticity, and viscoelasticity.

Analysis of flour properties is crucial for the breadmaking process, thus multiple rheological techniques could be implied. The “Chopin alveograph” (KPM 2025) can be used to determine the quality of a flour. The alveograph analyses the resistance to deformation of a strip of dough subjected to gaseous pressure. A typical plot is shown in Figure 1.26.

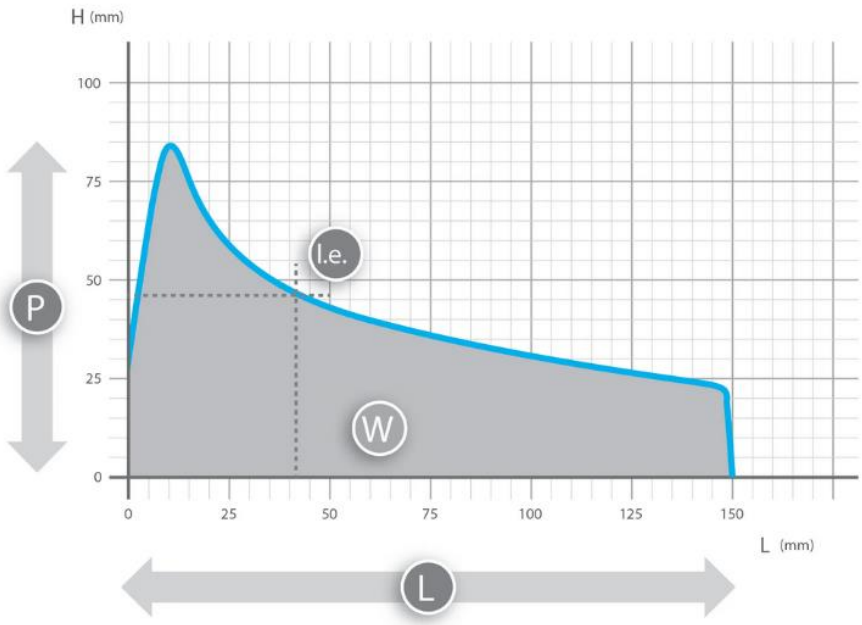


Figure 1.26 The characteristic curve of dough measures tenacity (P), extensibility (L), and baking strength (W). Tenacity reflects resistance to deformation and depends on protein quality, starch damage, and fiber content. Extensibility indicates the dough's ability to stretch and retain gas, mainly influenced by protein. Elasticity, measured by the elasticity index (Ie = P200/P), shows how well the dough recovers after stretching. Baking strength (W), the area under the curve, represents the dough’s total energy and overall performance in baking (KPM 2025)

The pressure applied to the dough strip (P) is measured as a function of time (parameter "L") under conditions specific to the equipment. In particular, this device can be used to determine flour strength (parameter "W" = area of the pressure – time record), the extensibility (parameter "P/L"). For bread-making applications, we look for a medium-to-high "W" parameter (160-250), reflecting a flour with a high gluten content (W can reach 400 for the strongest flours), and a medium P/L (P/L<1), reflecting good extensibility (ability to expand during fermentation and baking) (Roland Guinet & Bernard, 1994).

The Farinograph (BRABENDER-Germany), used routinely in many industries, is mainly designed to characterize the optimum level of hydration of a flour, as well as its rheological properties (Faridi and Faubion 1990). Two important pieces of information can be obtained from a farinograph curve (Koksel

and Scanlon 2012): The water absorption (the amount of water required for a dough to reach a specific consistency equal to 500 B.U or Brabender Unit) and the general mixing profile of the dough. It has been reported that water absorption affects dough consistency, dough development time (DDT) and dough density.

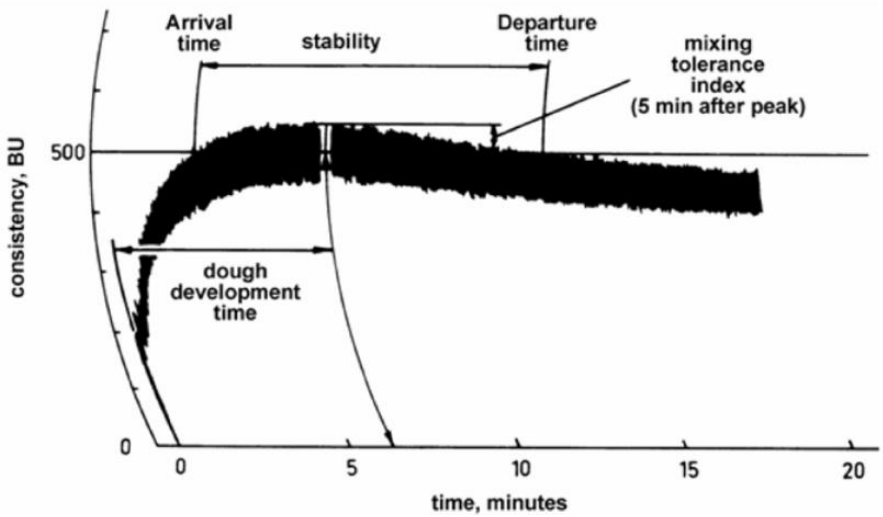


Figure 1.27 Representative farinogram showing some commonly measured indices. (reproduced from Pomeranz, Y., ed. 1971. Wheat; Chemistry and Technology, 2nd ed. Am. Assoc. Cereal Chem., St. Paul, MN)

Bread dough possesses the properties of both liquids (viscosity) and solids (elasticity): it is viscoelastic. The analysis of the rheological qualities of bread dough consists of measurements (or observations)

- Consistency, i.e., the firmness of the dough. Consistency is assessed during kneading (hydration readjustment) and at the end of kneading.
- Stickiness, or the adhesive strength of the dough. In general, stickiness is caused by: excess hydration, poor protein quality (insufficient strength of the dough), or excessive ambient relative humidity.
- Looseness, i.e., the flow of the dough under its own weight. It is assessed at the end of kneading, at the end of proofing, and at baking (after scoring the dough pieces).
- Extensibility, i.e., the dough's ability to elongate or deform. It can be assessed by stretching (uniaxial or biaxial), compression, or gas blowing.
- Elasticity, or the dough's ability to fully or partially regain its shape after a given deformation and the cessation of this deformation.
- Dough development or rise. This characteristic is assessed in the context of the breadmaking test using the AFNOR method. It involves measuring the rise volume (development) of the dough during fermentation (initial volume + volume gain after fermentation). This rise is related to the fermentative activity but also includes the dough's ability to deform and its gas retention.

1.6.1. The Farinograph (Brabender)

This test measures the variation in dough strength during kneading and provides information on the dough's behaviour during kneading. The maximum initial consistency of the dough is constant from one flour to another, but the hydration required to achieve this consistency varies. The strength measured by this test is a function of the closely intertwined viscosity (consistency) and elasticity characteristics of the dough.

1.6.2. The Chopin alveograph

This test aims to measure the baking quality of a flour, expressed by several parameters, including W:

- W corresponds to the work required to deform the dough bubble until it ruptures (related to the area of the curve obtained) and determines the baking strength.
- P, or Maximum Pressure, corresponds to resistance to deformation and measures tenacity. It depends on consistency (viscosity) and elastic resistance. It is correlated with the hydration potential of the dough in baking.
- Ie, or Elasticity Index, corresponds to the percentage of the pressure at 200 cm^3 of swelling over the maximum pressure. It highlights variations in the curve's drop (more or less hollow curve).
- G, or Swelling, corresponds to the amount of air injected into the bubble. It is correlated with the dough's extensibility and gas retention.
- P/L, or the ratio between tenacity and extensibility, is associated with a balance in the physical characteristics of the dough.

1.6.3. Rheological Measurements

As explained previously, rheology is defined as the science of the deformation and flow of solids and fluids under the influence of mechanical forces (Sumnu *et al.* 2007). Rheological properties are determined by measuring the applied stress and the resulting strain as a function of time. Rheological behaviours vary depending on the nature of the product studied. A solid is characterized by its modulus of elasticity (ratio of stress to strain), while a liquid is characterized by its viscosity (stress to strain rate). Most agri-food products, including bakery, biscuit or pastry dough, are complex rheological systems possessing both the properties of a solid (elastic component) and those of a shear-thinning liquid (viscous component): part of the energy is lost in viscous friction and part is conserved when a constraint is applied. The dough has a viscoelastic behaviour combining the properties of a Hooke solid and a non-Newtonian viscous fluid (Sumnu *et al.* 2007). During the flow of an ideal shear-thinning fluid, three distinct regions appear on the rheogram (Figure 1.28):

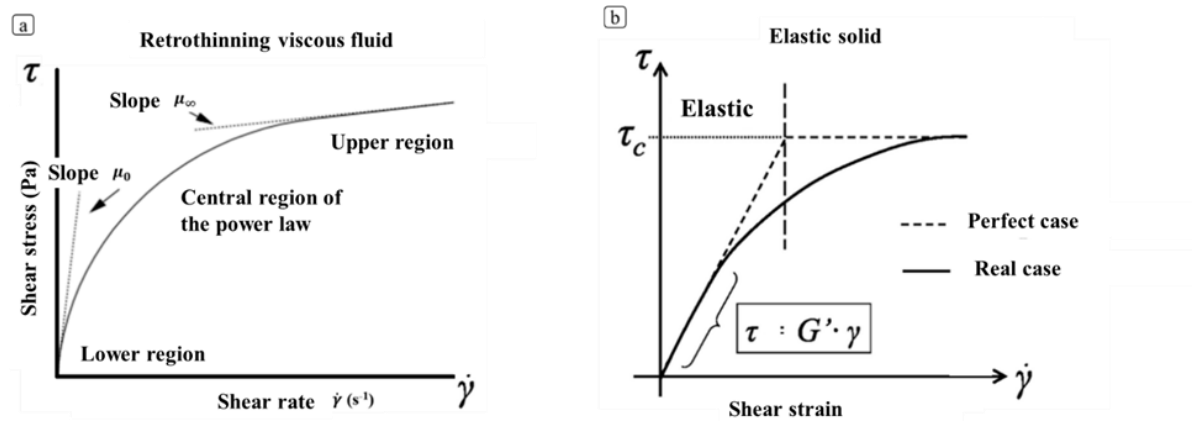


Figure 1.28 a) Rheogram for an ideal shear-thinning fluid (pseudo-plastic behaviour), b) Linear viscoelasticity domain. Adapted from (Steffe 1996)

- A lower Newtonian region where the apparent viscosity, called the zero shear rate limiting viscosity, is constant
- A middle (central) region where the apparent viscosity decreases with the shear rate
- An upper Newtonian region where the slope of the curve, called the infinite shear rate limiting viscosity, is constant as the shear rate changes

The central region is most often examined when studying the rheological behaviour of foods during processing (Steffe 1996). The viscoelastic behaviour of a material can be observed through its deformation response under a small stress amplitude; this small amplitude limit is that of linear viscoelasticity. For larger stress amplitudes, the material's deformation is no longer proportional to the excitation, and the material's behaviour is non-Newtonian; this is referred to as nonlinear viscoelasticity (Steffe 1996). Another phenomenon observed in viscoelastic materials is elastic recovery. Indeed, when the flow is stopped, the viscoelastic fluid recovers some of its deformation after the stresses are removed: the flow profile retracts; the tensile forces in the fluid cause the particles to recoil. However, viscous fluids remain where they are when their motion is stopped (Steffe 1996).

In the food industry, other types of behaviour can be encountered, notably thixotropic fluids, which are non-Newtonian fluids with time-dependent behaviour. These are fluids whose viscosity changes over time while the shear stress is constant: the structure of the fluid evolves under shear. Thixotropic behaviour is considered to occur when the stress under unloading (falling) is lower than that under loading (rising) for the same shear rate: the rheograms show hysteresis (Figure 1.29).

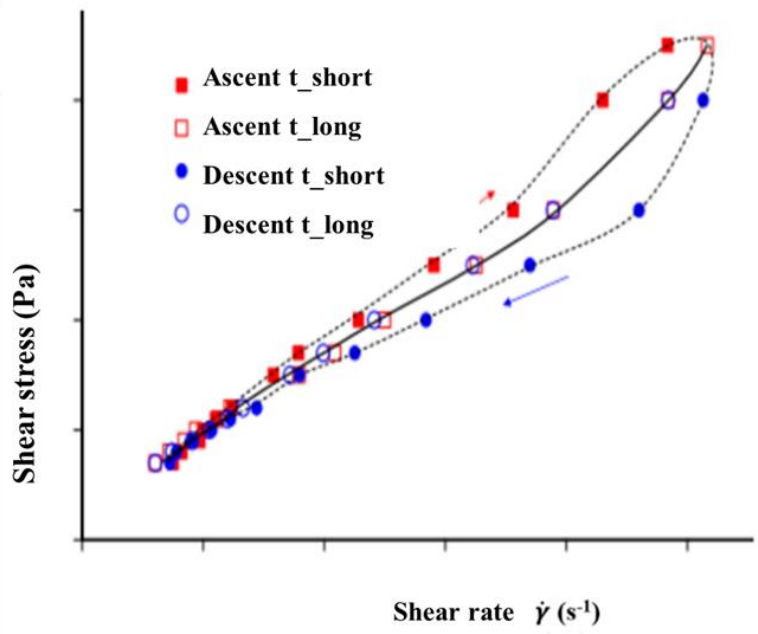


Figure 1.29 Rheogram for a thixotropic shear-thinning fluid. Adapted from (Steffe 1996)

Under certain temperature and shear conditions, starch pastes can exhibit a behaviour whose viscosity evolves over time: it is a thixotropic shear-thinning agent (Maache-Rezzoug *et al.* 2010; Nayouf, Loisel and Doublier 2003; Thebaudin, Lefebvre and Doublier 1998). Thixotropic phenomena depend on several factors: the volume fraction of swollen starch grains and their deformability (Doublier, Llamas and Meur 1987; Nayouf, Loisel and Doublier 2003). Maache-Rezzoug et al. (2010) demonstrated that their behaviour was thixotropic shear-thinning on starch suspensions from four different botanical sources. Two approaches then exist, depending on whether the focus is on the material structure or the definition of flow curves or behaviour laws:

- A low-strain rheology approach is required, meaning that the aim is to remain within the material's viscoelastic linearity (strains are less than 0.1%);
- Obtaining flow curves close to the usual process conditions, i.e., for significant strains, which in most cases result in the material destructuring (Shehzad *et al.* 2012).

Rheological measurements of pastes and gels after swelling can be carried out either in steady state to establish flow curves, or in harmonic state to allow non-destructive observation, due to the low deformation amplitudes used (Doublier, Llamas and Meur 1987). The objective of the next two paragraphs is to present the quantities and tools used for the rheological study of flour pastes.

1.6.4. Viscoelastic properties (low deformations in dynamic regime)

Large-strain measurements allow the determination of the apparent viscosity of the fluid but do not provide information on the viscoelastic behaviour of the bread dough. Viscoelastic property measurements are performed for very low-amplitude deformations, generally under shear, in harmonic regimes at very low deformations, and in the linear regime (Shehzad *et al.* 2012).

Tests use cone/plate or plate/plate rheometers, between which the dough sample is placed. These geometries allow precise control of the deformation γ (or the deformation rate $\dot{\gamma}$) or the stress τ

applied to the sample. Dynamic (or oscillating) rheometers allow a sample to be subjected to laminar shear movements whose amplitude varies sinusoidally with time. These sinusoids are characterized by the frequency f and the angular velocity ω = 2π·f.

In the domain of linear viscoelasticity, the resulting shear stress is also sinusoidal and of the same frequency f, but with a phase shift δ called the loss angle. The value of δ determines the behaviour of the material under study. If δ = 0, the system behaves like an ideal elastic solid (Hooke's law), if δ = π/2, the system behaves like a purely viscous (Newtonian) liquid, and if 0 < δ < π/2, the system exhibits viscoelastic behaviour.

The evolution of viscoelastic behaviour is expressed by the elastic modulus or storage modulus (G') and the viscous modulus or loss modulus (G''). The elastic modulus G' and the viscous modulus G" (or loss modulus) are calculated by:

$$(\mathrm{G})' = \frac{\tau_0}{\gamma_0} \cdot \cos\delta \qquad \text{Eq. 1.24}$$

$$(\mathrm{G})'' = \frac{\tau_0}{\gamma_0} \cdot \sin\delta \qquad \text{Eq. 1.25}$$

These modulus values reflect the fact that during harmonic stress, the material receives energy, part of which is stored G' and the other dissipated G" (essentially in the form of heat). These moduli make it possible to define the complex rigidity G*, the tangent of the phase shift angle tan δ (or loss angle) and the complex viscosity μ*.

$$\tan\delta = \frac{G''}{G'} \qquad \text{Eq. 1.26}$$

$$\mu^* = \frac{1}{\omega}\sqrt{\mathrm{G}' + \mathrm{G}''} \qquad \text{Eq. 1.27}$$

Where ω is the angular velocity in rad·s^{-1}. Typically, a frequency sweep is performed (10^{-1} to 100 rad·s^{-1}) to characterize the material in the linear domain.

Native or modified starch pastes often exhibit behaviour that can be described as weak gel with G' > G'' (Loisel *et al.* 2006; Tecante and Doublier 1999; Thebaudin, Lefebvre and Doublier 1998), and G' practically independent of frequency (Méndez-Montealvo *et al.* 2008; Nayouf, Loisel and Doublier 2003).

1.6.5. Flow properties (large deformations)

The actual deformations experienced by cereal pasta during the manufacturing process far exceed the order of magnitude of previous tests (≤ 0.2%), sometimes leading to material destructuring (including wall rupture) (Dobraszczyk and Morgenstern 2003).

To understand and predict the behaviour of the dough during the transformation process, the determination of the flow curve must cover the speed and deformation ranges applied during the process.

Experimental rheological measurement devices for large deformations seek to characterize the material under these conditions. Tests have been developed that take into account the nature of the stresses experienced by the dough, in shear or extension, during the process. Only two rheological

measurement tests at large deformations will be explained in this paragraph: the creep/recovery tests (creep test) in simple shear and the lubricated squeezing flow (LSF) tests for the bi-extensional mode. The creep-recovery tests, carried out at different stress values, make it possible to determine points ($\dot{\gamma}$, η) recorded once the steady state is reached. All of these points lead to a flow curve of a material, that is to say the expression of its viscosity as a function of its deformation rate. The Figure clearly shows that the paste has Newtonian behaviour at low deformation rates, less than 10^{-5} s^{-1} (its viscosity is independent of its deformation rate), we speak of a Newtonian plateau; then beyond, it has a fluid behaviour and the whole curve can be represented by a Cross model (Lefebvre 2006; Rouillé *et al.* 2005). For high values of the shear rate, the behaviour is comparable to that during kneading, while low values rather reflect the speeds of the upward movement of the alveoli during fermentation.

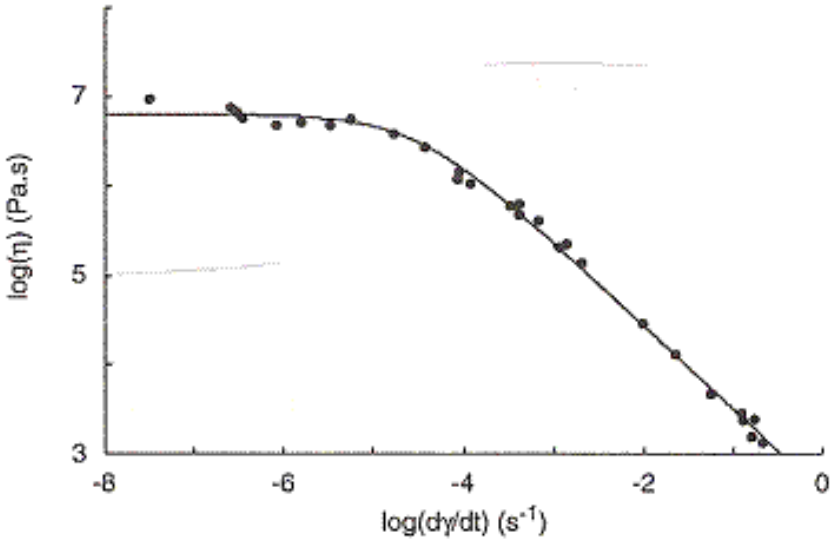


Figure 1.30 Flow curve (viscosity versus shear rate) of wheat flour dough (Lefebvre 2006)

The entire flow curve can be represented by a Cross model (Rouillé *et al.* 2005):

$$\mu = \frac{\mu_0}{1 + \left(\frac{\dot{\gamma}}{\dot{\gamma}_0}\right)^n} \qquad \text{Eq. 1.28}$$

Where μ_0 is the initial viscosity of the Newtonian plate; $\dot{\gamma}_0$ is the critical shear rate, and n is the Cross exponent or flow index ($n \leq 1$).

The shear-thinning behaviour is described in the case of starch pastes (EVANS and HAISMAN 2007; Giboreau, Cuvelier and Launay 1994; Maache-Rezzoug *et al.* 2010) and cake batters (Baixauli *et al.* 2008; Şakıyan *et al.* 2004; Turabi, Sumnu and Sahin 2008) by the power law model (Eq. 1.29):

$$\mu = m\,\dot{\gamma}^{(n-1)} \qquad \text{Eq. 1.29}$$

m is the consistency index and n is the flow index. When $n < 1$, the fluid exhibits shear-thinning behaviour and when $n > 1$, it exhibits shear-thickening behaviour.

The apparent viscosity of starch suspensions increases significantly when the shear rates applied to the flow tend to cancel out. The flow curves of shear-thinning liquids with a yield point can be described using the Herschel-Bulkley model (Doublier 1981):

$$\tau = \tau_0 + m\,\dot{\gamma}^n \qquad \text{Eq. 1.30}$$

Where τ_0 is the yield stress (Pa), m is the consistency coefficient (Pa.s_n), n; is the yield index.

Baik, Marcotte and Castaigne (2000) showed that pastes of different observed compositions have the behaviour at the yield stress limit and their stress-shear relationships are described with the Casson model:

$$\tau^{0.5} = \tau_0^{0.5} + m_c\,\dot{\gamma}^{0.5} \qquad \text{Eq. 1.31}$$

Where τ_0 is the yield stress of the Casson (Pa), m_c is the consistency coefficient (Pa·s).

In the case of cereal doughs, the rheological properties change during baking depending on the hydrothermal transformations undergone by starch and gluten. Their actions are located in the same temperature range, making it difficult to separate their effects. Dobraszczyk and Morgenstern (2003) showed that from the beginning of baking and up to a gelatinization temperature of approximately 60°C, the viscosity of bread dough decreases to a minimum of 5.104 N·s·m^{-2} (Figure 1.31). Thermal agitation is responsible for a major part of this. From 60°C, the progressive swelling of the starch grains and the beginning of coagulation of the three-dimensional gluten network are probably the cause of the rapid increase in the apparent viscosity value. The temperature at which viscosity increases varies with the heating rate.

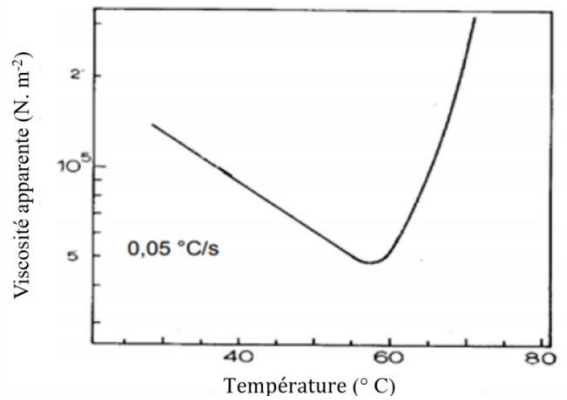


Figure 1.31 Evolution of the apparent viscosity of the dough as a function of temperature (Bloksma 1990)

1.7. The sensory aspect

Sensory perception is a complex process that extends beyond immediate sensory input, encompassing factors such as cultural background, emotional responses, and personal memories. Consumers evaluate product quality through a process that begins with identifying and perceiving both intrinsic and extrinsic attributes (Gellynck *et al.* 2009). The intrinsic attributes are a multifaceted process that involves the perception of appearance, smell, taste, colour, shape and texture (Heenan *et al.* 2008; Gellynck *et al.* 2009). Meanwhile the extrinsic attributes are external cues not related to the product but influential in perception, such as price, brand, production method and nutritional values (Gellynck *et al.* 2009). These sensory attributes are essential determinants of consumer preference and product acceptance and are shaped by a complex interplay of ingredients, processing techniques, fermentation,

and storage conditions. As bread loses its freshness, its sensory shelf life diminishes, which is closely linked to the changes in texture and aromatic parameters over time (García-Gómez *et al.* 2022; Lassoued *et al.* 2008). The different stages of the breadmaking process are designed to meet the consumer perception and preferences, which is marked by dynamic ongoing physicochemical, microbiological and biochemical transformations driven by mechanical actions such as kneading, fermentation, sheeting and baking (Mollakhalili-meybodi *et al.* 2023). This is essential to produce a high quality product. The effect of each stage will be discussed in correlation to the sensory attributes in the sections below.

1.7.1. Appearance

The appearance of bread is one of the first sensory cues that influence consumer perception and acceptance. A bread visual appeal can significantly influence a consumer decision to purchase or consume it. Key factors such as the color of the crust, the shape of the loaf, and the uniformity of the crumb contribute to the overall impression of freshness and quality. A golden-brown, well-baked crust, for example, is often associated with a freshly baked, high-quality product, while a dull or uneven appearance may suggest staleness or poor preparation (Callejo 2011). Most important perceived appearance attribute is the structure of the breadcrumb, which is linked to the mixing and fermentation stages (Mollakhalili-meybodi *et al.* 2023). The mixing stage is intended to deliver mechanical energy necessary for the development of the gluten network, which is crucial for gas retention during fermentation. To achieve optimal dough aeration and properties, mixing must be carried out at an appropriate duration, long enough to fully develop the gluten and to provide maximum extensibility and elasticity (Mollakhalili-meybodi *et al.* 2023). This well stable gluten will contribute to a final product with improved bread volume, structure and homogenised crumb with uniform gas bubbles in shape and size. In contrast, insufficient mixing time, will lead to underdeveloped gluten, in poorly incorporated flour patches that may disrupt the fermentation, whereas prolonged mixing can lead to weak unstable and sticky dough with reduced consistency. These will give a bread low in volume with heterogeneous breadcrumb structure. Surprisingly, a study conducted by García-Gómez et al. (2022) was to identify the key sensory attributes that influence consumer acceptance of various Galician bread and to find a correlation between these sensory characteristics and the specific ingredients and manufacturing processes. Based on the acceptability test with trained panels and hedonic tests, the acceptance rate was linked to the moisture content of the breadcrumb, a key indicator of freshness. In addition, breads with large and irregular gas cells gained higher acceptability.

1.7.2. Texture

Texture is one of the three key sensory qualities of food, alongside appearance and flavour. While appearance relates to what we see and flavour to what we taste and smell, texture is defined by how food feels when touched or chewed (Bourne 1993). It is fundamentally a sensory property that can only be perceived, described, and evaluated by humans (Stieger and van de Velde 2013; Szczesniak 2002).

In bread, the texture of breadcrumb is closely linked to perceived quality and is often a key factor to consumer perception (Lassoued *et al.* 2008; Callejo 2011). The crumb texture can be attributed to softness and hardness that are largely influenced by the size and structure of the breadcrumb cells.

These textural properties are strongly dependent on both the quantity and quality of gluten protein present in the dough (Callejo 2011).

One key element of the breadmaking process is fermentation, which enhances the texture, by slowing down firmness and staling during storage and increase bioavailability of nutrients (Mollakhalili-meybodi *et al.* 2023). The growth of gas bubbles during fermentation significantly influences the final volume and texture of wheat bread. Textural properties are strongly linked to the freshness and elasticity, although their deterioration over time decline the consumers' satisfaction (Angioloni and Collar 2009). Traditional bread tends to have short shelf-life due to physical and chemical changes most notable starch retrogradation which causes crumb firmness and dryness over time. These changes diminish the bread appeal and contribute to a perceived loss of freshness.

1.7.3. Odour/aroma

When we consumed food we engage multiple senses, we see, smell, taste and touch the food before deciding to swallow it. It is essential to distinguish between odour, aroma, taste and flavour. Odour refers to volatile compounds perceived by the olfactory receptors (Olfactory Epithelium) through the nose before ingestion (Delarue, Lawlor and Rogeaux 2015). Bread flavour is attributed to a complex mixture of volatile and non-volatile compounds mainly acids, alcohol, esters, ethers, etc. (Quilez, Ruiz and Romero 2006). Aroma compounds in bread are produced through various stages: enzymatic activity during kneading, fermentation by yeast and lactic acid bacteria, and chemical reactions such as lipid oxidation (Birch, Petersen and Hansen 2013). Organic volatiles (VOC) originate from metabolic yeast activity during fermentation, lipid oxidation of flour compounds during mixing, and during baking from Maillard reactions (Sanmartín *et al.* 2024). As the dough heats up, the Maillard reaction between reducing sugars and amino acids produce a variety of VOCs, including aldehydes, lactones, etc., which contribute to the nutty, roasted, caramel-like flavours (Bolkvadze *et al.* 2024) commonly associated with baked bread. Furthermore, thermal degradation of fats and carbohydrates generate compounds such as esters and alcohols that enhance the aroma profile of bread (Jiang *et al.* 2023).

For breadmaking, baker's yeast generate a diverse array of aroma compounds that contribute significantly to the overall flavour profile of bread (Birch *et al.* 2013). Birch et al. (2013) investigated the influence of baker's yeast on bread aroma by comparing it with seven different commercial compressed yeasts. Their results showed significantly differences between baker's yeast breads and the commercial ones, where higher concentration of fermentation aromas were detected with certain yeast strains. Therefore the bacteria strain is very important in respect for a specific bread aroma. Additionally, the ingredients and processing conditions used in the recipe significantly influence the final aroma (Belitz *et al.* 2004; Grosch and Schieberle 1997).

During baking, complex chemical reactions lead to the formation of both volatile and non-volatile compounds that significantly contribute to the overall flavour perception. Caramelization involves the thermal breakdown of sugars and the non-enzymatic Maillard reaction (Mollakhalili-meybodi *et al.* 2023). According to Birch et al. (2013), the most balanced aroma was with low lipid oxidation and the shortest fermentation time.

As previously mentioned, during storage, the aroma profile of wheat bread undergoes significant changes. Refrigeration allows a good preservation of volatile compounds (acids, esters, alcohols and ketones), especially in the first 3 weeks (Jensen, Oestdal and Thybo 2010). Whereas freeze storage

accelerated their loss due to starch retrogradation, which limits volatile retention and promotes oxidation (Jensen, Oestdal and Thybo 2010). As storage time increases, the pleasant, fresh bread aroma gradually fades and is replaced by less desirable notes often associated with staleness or rancidity (Jensen, Oestdal and Thybo 2010).

Due to the complex nature of flavour, its perception and control during fermentation process remains a significant challenge. However, the development of the flavour profile requires both mechanical and enzymatic breakdown of the raw bread ingredients (Mollakhalili-meybodi *et al.* 2023). This degradation is essential not only to generate the necessary precursors for flavour compound formation but also to eliminate the starchy aftertaste typically associated with untreated flour. Moreover, while acidity generated during fermetation plays a role in flavour enhancement, such as roasted noted in bread crust, its excess must be carefully monitored to avoid undesirable sour or pungent notes (Mollakhalili-meybodi *et al.* 2023; Callejo 2011). Therefore, optimzing the level of acidity is crucial to achieving a balanced and appealing flavour profile.

1.7.4. Taste

Taste is the fundamental sensory attribute that significantly influences consumer acceptance and preference for bread products. Taste is defined as our ability to detect five basic tastes, bitter, salty, sweet, sour and umami (Callejo 2011), which are detected by receptors on the tongues (Cauvain and Young 2006). These flavours arise from molecules which are released during the chewing process and dissolve in saliva (Hu *et al.* 2024). For example, sweetness in bread is often released from residual sugars and fermentation by-products (depending on the recipe) (Gray and Bemiller 2003). Sourness resulting from organic acids produced during yeast fermentation, which can be perceived negatively if it is in excess (Gänzle and Ripari 2016).

1.7.5. Evaluation of the sensory properties – Sensorial analysis

The purpose of sensory analysis is to obtain objective evaluations of food characteristics as experienced through the senses of sight, smell, taste, touch, and hearing. Sensory methods need to fulfil the criteria of measurement techniques by being accurate, consistent, and reliable (Piggott, Simpson and Williams 1998). They also need to meet the consumer perceptions and preferences to ensure real-world relevance.

Sensory analysis employs various standardized methods to assess food products, each designed to capture different aspects of human perception. According to the literature, these methods broadly fall into three categories: discriminative, descriptive and hedonic analysis. These tests are generally conducted in a sensory laboratory designed to maintain strict environmental control, including neutral surroundings with regulated lighting, temperature and humidity (Kemp, Hort and Hollowood 2017).

1.7.5.1. Discriminative tests

Discriminative tests are used to assess whether differences exist between product samples. The specific type of test depends on the complexity of the product such as ingredients substitutions, changes in production methods, or equipment (Marques *et al.* 2022). In addition, the test can be chosen based on other factors such as the number of samples to be tested, the availability of panellists and other

logistical considerations. One of the most popular test is the Triangular test, where 2 among 3 samples are identical. Assessors after being given samples in an equilibrated balance order (e.g. AAB, ABA, BAA) are asked to identify the odd sample by evaluating them from left to right (Marques *et al.* 2022).

1.7.5.2. Descriptive tests

Descriptive test is a sensory evaluation technique designed to objectively measure and characterize the specific attributes of a product, along with their intensities (Kemp, Hort and Hollowood 2017). This analysis firstly relies on trained human panelists as precise measuring instruments operating under controlled conditions to reduce bias and ensure data reliability (Kemp, Hort and Hollowood 2017). In approaches like Quantitative Descriptive Analysis (QDA) and profile-based methods, assessors can consistently and accurately evaluate the intensity and quality of sensory attributes, both within their own judgment and with others on the panel (Kemp, Hort and Hollowood 2017; Lawless and Heymann 2010). Other methods like Flash-Profile, use untrained or naïve participants instead trained panelists. These approaches rely on participants' intuitive perceptions to identify products based on overall similarities or differences (Varela and Ares 2012). These methods are quicker and more flexible than traditional descriptive analysis, making them valuable tools for exploratory product assessment.

1.7.5.3. Hedonic Tests

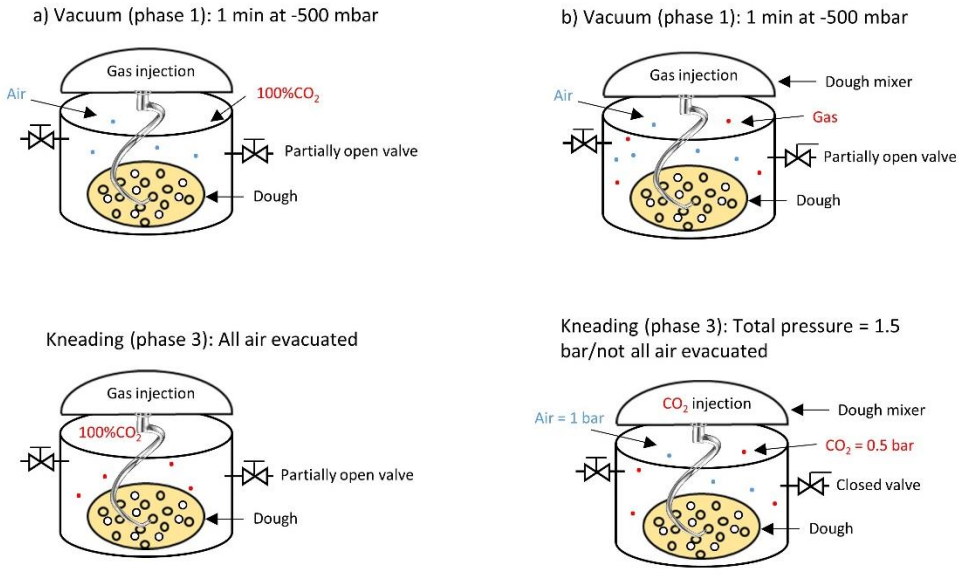
Hedonic tests are designed to capture the subjective response of consumers regarding their preference, acceptance, or liking of a product (Marques *et al.* 2022). Approaches like Just-About-Right (JAR) and the Ideal Profile Method (IPM) help to identify whether specific product attributes meet consumer expectations or require adjustment, providing valuable insights for product development and improvement (Marques *et al.* 2022). The JAR scale has a mid-point reflecting the just-right or ideal level, and two extreme points (Gere *et al.* 2017); for example, for the breadcrumb one extreme large gas cells and the other small gas cells. La croix et al. (2014) conducted an acceptability test for a total of 82 consumers in difference testing and 109 consumers in acceptability testing, for detecting differences in saltiness between control sandwich bread and bread with sodium reduction. Bread samples were evaluated by a nine-point hedonic scale, where participants ranked the key sensory attributes. Consumers did not perceive a 10% reduction in bread saltiness; however, a reduction up to 20 – 30% was detected without adverse effect on consumers acceptability.

SCIENTIFIC APPROACH

This thesis is part of a broader effort to explore and valorise non-conventional bread dough mixing processes, specifically those involving control over gas composition and pressure conditions during mixing. The scientific approach adopted throughout this work was exploratory, guided by a central objective: to evaluate how modulating the gas environment during mixing could affect dough development, fermentation dynamics, and final bread quality, while also contributing to cleaner label formulations. As part of the initial phase of this work, significant effort was dedicated to understanding and adapting the prototype mixer used for gas-pressure dough mixing. The mixer allowed for control over headspace gas composition and pressure, with adjustable parameters such as gas type (air, O_2, CO_2, N_2), pressure level (atmospheric and 0.5 bar gauge pressure), and mixing speed (typically 150 RPM). The approach is fundamentally exploratory, driven by one main question: *How does tailoring the gaseous environment inside the mixer affect dough development, fermentation and non-conventional breadmaking?*

In this context, the originality of this work lies in its systematic investigation of dough mixing under controlled gas composition and pressure as an approach that departs from conventional air-mixing into new perspectives on dough aeration, fermentation control and ingredients reduction.

1) Strategy 1: Protocol A – Exhaust valve partial opening during vacuum



Protocol A: atm pressure

Protocol A: 0.5 bar gauge pressure

Figure 1.32. Schematic representation of CO_2 injection and pressure conditions during dough kneading under vacuum and gas composition. The chronological order of dough mixing starts by phase 1 and ends with phase 3: a) Effect of partially opening the mixer valve at atmospheric pressure throughout the entire mixing stages, where vacuum pressure at -500 mbar followed by atmospheric pressure (all air molecules evacuated) b) Effect of vacuum treatment at – 500 mbar by partially opening the mixer

valve then closing it during the kneading phase where pressure reached a total of 1.5 bar within the chamber. This resulted in partial evacuation of air

Based on Protocol A, the mixer inner chamber was subjected to -500 mbar of vacuum to evacuate air molecules. Taking the example of CO_2 injection, at atmospheric pressure (a) the exhaust valve was kept partially open until the end of kneading with all air fully evacuated and only CO_2 present in the mixer headspace. In this scenario, the kneading was performed in an environment consisting purely of the injected gas (i.e. 100%CO_2) eliminating the influence of air. In the second scenario, at 0.5 bar gauge pressure (b), although vacuum was applied at – 500 mbar, when 100%CO_2 was introduced, the resulting pressure of 1.5 bar consisted of 1 bar from residual air and 0.5 bar only from the injected gas. This finding revealed that the gas atmosphere inside the kneader was not purely composed of the injected gas, despite pressure regulation. This technical limitation underscored the importance of optimizing both vacuum efficiency and valve operation. It also guided the refinement of subsequent experimental protocols, ensuring better control over gas composition during mixing and more reliable interpretation of results.

2) Strategy 2: Protocol B - Valve closing during vacuum

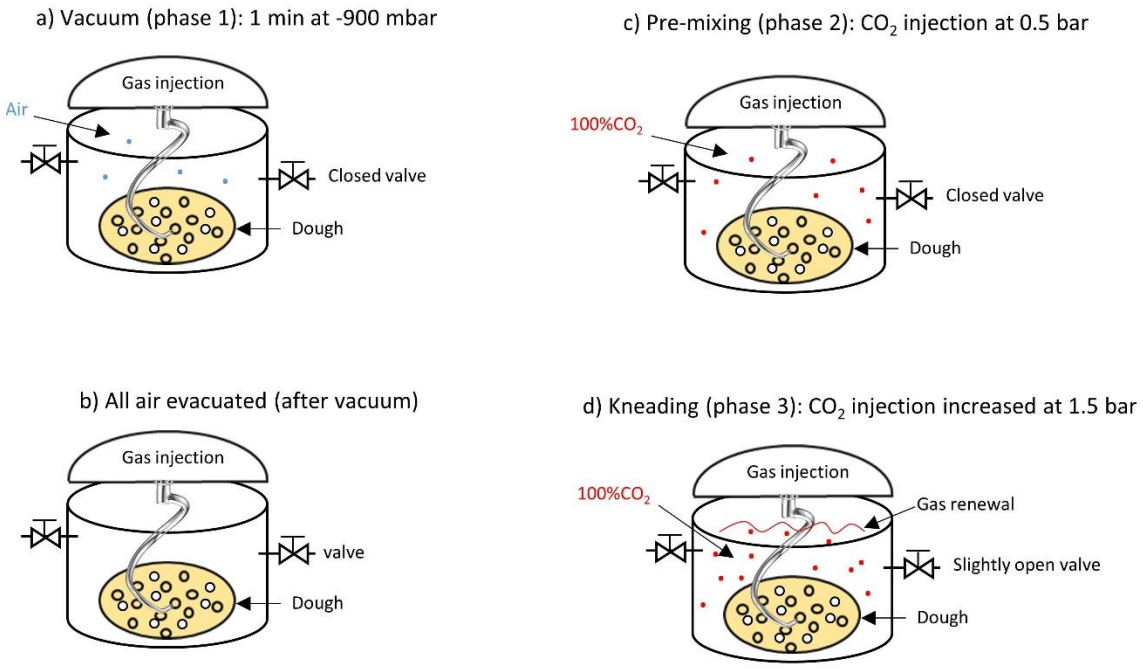


Figure 1.33. Effect of exhaust valve closing of the mixer during vacuum and then slightly opening it when the mixing pressure was above atmospheric on the gas composition inside the kneader headspace. Phase (a) to evacuate ambient air, followed by CO_2 injection during pre-mixing (c) and kneading (d).

The kneading sequence in both strategies begins with the application of vacuum at -500 mbar (Figure 1.32) and -900 mbar (Figure 1.33) to evacuate air from the mixer headspace.

In Protocol A, with the exhaust valve partially open, the injected CO_2 has 2 possible situations: at atmospheric pressure, continuous evacuation allows the headspace to be composed of 100% CO_2 during kneading (phase 3). However, at 0.5 bar gauge pressure, residual air is not completely removed.

When total pressure reaches 1.5 bar, the internal atmosphere consists of approximately 1 bar residual air and 0.5 of injected CO_2, resulting in incomplete gas removal during kneading.

In protocol B, the exhaust valve remains closed during vacuum, allowing a more effective air evacuation. After complete evacuation (phase 2), 100% CO_2 pressure is injected at 0.5 bar during pre-mixing while maintaining the valve closed. During kneading, CO_2 pressure increased to 1.5 bar and the valve was slightly opened to allow controlled gas renewal, ensuring a stable CO_2-enriched atmosphere throughout the entire kneading phase.

Maintaining a closed valve during key stages of the dough mixing process enables more effective control over the gaseous composition within the mixer headspace. This approach minimizes atmospheric interference and facilitates the creation of a modified atmosphere, particularly when introducing specific gases such as pure CO_2. In this approach, closing the mixer valve during vacuum prior to gas injection, evacuated all the ambient air particles from the mixer headspace, during the vacuum and pre-mixing phase (a) to (c). Thereby, preparing the environment for precise injection. Pure 100%CO_2 was introduced at 0.5 bar gauge pressure while maintaining the valves in a closed position to preserve gas purity within the bowl. In the final kneading phase (d), the CO_2 injection pressure was increased to 1.5 bar, and the outlet valve was slightly opened to allow controlled gas renewal. This setup was designed to ensure a stable CO_2-enriched environment throughout kneading by compensating for potential leaks and maintaining target gas composition during mechanical dough mixing.

Protocol A vs. Protocol B outcomes

In summary, Protocol A involves a partial vacuum with gas flushing at atmospheric pressure (with continuous gas flow and an open exhaust valve) and 0.5 bar gauge pressure (where the exhaust valve is closed during kneading). Protocol B employs a better vacuum control by closing the exhaust valve, evacuating residual air molecules before injecting the desired gas composition and maintains a continuous gas renewal through partially opening the exhaust valve.

The key difference lies in the degree of gas control: Protocol A mimics industrial variability with ample O_2, while Protocol B offers fine-tuned gas delivery, making it ideal for precise modulation of oxidation, fermentation, and the final properties of both dough and bread. The conducted measurements consisted of dough void fractions after mixing, sheeting and fermentation, CO_2 emission during fermentation by the Risograph, dough pH, dough rheology and colour, along with breads specific volumes, porosity, staling, texture and colour.

Effect of ascorbic acid AH_2 under variable gas composition and mixing protocols

To deepen the understanding of gas-additive interactions, both protocols A (0.5 bar gauge pressure) and B were further evaluated with the inclusion of ascorbic acid AH_2. We compared dough mixed under air, 100%CO_2 and the mixture 30%O_2 70%N_2 with and without the addition of AH_2 focusing on key parameters such as dough development time (t_{PEAK}), specific mechanical energy (SME), doughs void fractions after mixing, sheeting and fermentation as well as expansion ratios during fermentation. AH_2 is known as an oxidant that strengthens gluten network throughout oxidation reactions, thereby enhancing gas retention. The aim was to reveal if modifying the gas composition during mixing alone can replicate or compliment the biochemical effects traditionally achieved by AH_2. This could pave the way for more natural and label-friendly bread formulations, where controlled gas atmospheres reduce

or eliminate the need for chemical oxidants. The investigations offered valuable insights into the interaction between redox additives and atmospheric gases, highlighting opportunities for optimizing dough conditioning through process design.

In additions, supplementary experiments were conducted to address processing challenges observed under 100%CO_2 notable baking defects associated with excessive gas retention and fermentation imbalance. These trials focused on reducing yeast amount under CO_2-rich atmosphere for a better control of dough expansion and baking performance. Furthermore, the impact of mechanical processing was also investigated.

3) Strategy of carbonated water and modified fermentation atmosphere

This strategy or third part of this PhD project, was in collaboration with the University of Hohenheim to expand the research to include alternative gas-related techniques, like CO_2 injection during fermentation and the use of carbonated water, thereby broadening the scope and validating the applicability of the proposed mixing strategies across different processing contexts. The rationale for this investigation was based on environmental factors, including air renewal versus modified atmosphere in the fermentation chamber, due to their influence on dough color and gas exchange. Some studies revealed unexpected effects such as surface color darkening under air renewal conditions that were also observed in the crust and crumb of the final bread. These findings led to further experiments aimed at better controlling such external variables.

CHAPTER 2 : **MATERIALS & METHODS**

2.1. Part I

2.1.1. Ingredients

The flour used was Type 65 wheat flour supplied by Minoterie Giraudineau; The analytical characteristics of the flour carried out by Laboragro were as follows: the measured alveograph force W was 200.10^{-4} J and the water content 14.80 % w.b., Ash content 65 ppm, P/L: 1.68 and water absorption 57%. The flour was stocked at -20°C in order to prevent any quality changes, and then transferred at - 4°C for 24 hours before usage. The same analysis was carried out for flour with the addition of 80 ppm (0.08% of flour dry weight) of Ascorbic acid (AH_2) (Louis François – France), where W = 205, water content 14.28 % w.b., Ash content 65 ppm, P/L: 2.26 & water absorption 57%. The salt used was fine table salt (Sodium Chloride) (Cedot – France). The yeast is fresh pressed yeast (Hirondelle – France) and the water used was simply tap water.

Table.1 shows the list of ingredients used in the bread dough recipes. The degassed dough density was calculated using the following equation Eq. 2.1 (Sadot, Cheio and Le-Bail 2017) in which X_i^V is the volumic fraction of the ingredient i and ρ_i is the density of the ingredient i.

$$\rho_{DD} = \sum_i \rho_i . X_i^V \qquad \text{Eq. 2.1}$$

The density of the degazed dough was of ρ_{DD} = 1.250 ($g \cdot cm^{-3}$) was based on this computation.

Table 2.1 Dough recipe

Ingredients	per 100g flour	w/w%	Density $g \cdot cm^{-3}$	v/v%
Flour T65	100	61.51	1.45	53.53
Tap water	57	35.39	1	44.22
Compressed Yeast	2.1	2.00	0.95	1.62
Sodium chloride	1.8	1.10	2.17	0.63
Ascorbic acid (AH_2)	1.5	0.08	1.6	0.05
Total	162.48	100.08	/	100.02

2.1.2. Breadmaking process summary

The breadmaking process, involving mixing wet with the dry ingredients in one continuous step with the VMI prototype dough mixer, either with ambient air or gas injection. A resting period of 20 min was applied at the end of the mixing stage to allow dough relaxation, which is a usual practice in the baking industry.

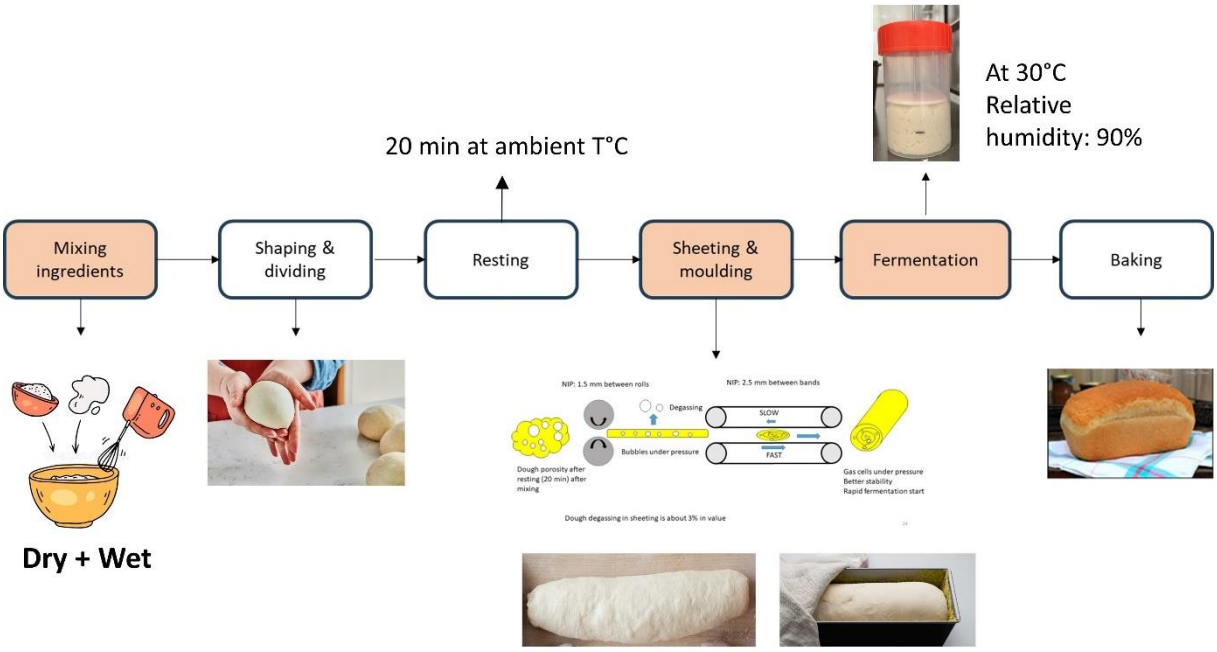


Figure 2.1 Breads making steps from mixing to baking

2.1.2.1. Dough mixing protocol

A VMI planetary prototype mixer (VMI, St Hilaire de Loulay-France), was used (Jha *et al.* 2022) (Figure 2.2).

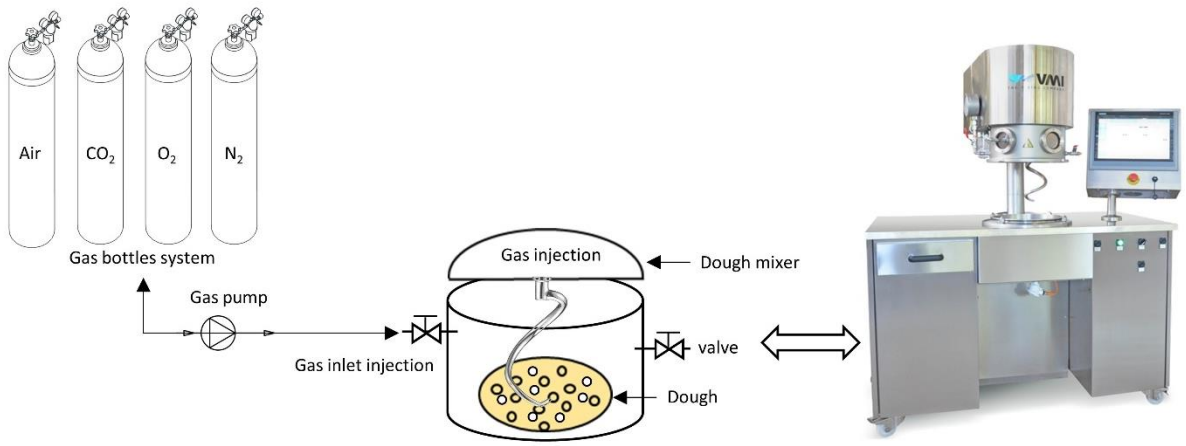


Figure 2.2 VMI prototype dough mixer used for the tests. The lid covering the mixing bowl (open position on picture) was equipped with a spiral tool. The mixer allowed control of the pressure in the headspace as well as a control of the gas composition. The mixer has a valve that opens and closes on its right side to control air and gas circulation, and the mixer is connected to gas bottles through a gas pump that controls the injected gas pressure

The mixer features separate controls for the bowl cycloidal movement and the spiral tool orbit, guaranteeing the tool sweeps the entire bowl. The mixing bowl was equipped with a double-jacket circulated by a fluid which temperature can be maintained constant during mixing. The fixed bowl has a capacity of 27 L and dough capacity of 5 kg. A lid attached to the mixing bowl allow control of the

headspace in contact with the dough during mixing. Both gas pressure (up to 0.5 bar gauge pressure) and gas composition were available. An infrared sensor, located at the top of the lid, measured the temperature inside the bowl. A supervision interface allowed the control of different parameters including the bowl temperature, operating pressure, mixing time, gyration speed, and tool rotational speed. The power consumed by the tool and by the gyration system were logged and the net tool power was computed from the difference between the tool power and the gyration power.

A set of experiments using an empty mixer was performed in order to obtain a matrix containing the offset values to apply depending on the tool, gyration speeds and headspace pressure (offset powers corresponded to the mechanical frictions caused by belts, gaskets friction on shaft and others). The temperature of the water used in the recipe was set in order to keep the sum of all ingredients and mixing temperature (25°C) to reach a dough temperature that was matching with temperature set point of the mixing bowl (which was 25°C for all tests). The mixer is connected to a WITT gas station consisting of gas bottles (CO_2, N_2 and O_2) where their different ratios can be controlled as desired from 0 to 100% of the gas to be injected.

Two distinct protocols were employed in this study (Table 2.2). The protocol A and B (with a variant of protocol A), to investigate the impact of injected gas composition on dough and bread properties. Both protocols followed a three-phases mixing structure: (1) pre-mixing at very low speed including a vacuum or partial vacuum, (2) mixing at moderate speed and (3) kneading at higher speed.

Protocol A atmospheric pressure: With partial vacuum and gas flushing

The protocol started with a pre-mixing stage (10 RPM tool, 3 RPM orbit speed); the headspace of the mixer was set under vacuum for 1 min (pressure level – 500 mbar) at slow speed with atmospheric air flowing through the head of the mixer (exhaust valve partly open at 1/4). Then mixing stage started at 100 RPM tool, 8 RPM orbit speed for 3 min; the pressure was set at atmospheric pressure with gas flow through the mixer head with exhaust valve partly open (at 1/4) to ensure renewal of the head space gas during mixing. Lastly, a kneading phase was used at higher speed (150 RPM tool, 16 RPM orbit speed with exhaust valve partly opened (at 1/4) for 10 min in order to be able to determine the optimal mixing time t_{PEAK}. and kneading. For further tests including baking tests, the t_{PEAK} was used for the kneading tests.

Protocol A 0.5 bar: With partial vacuum and gas flushing

The only difference with the previous protocol lies in the fact that the exhaust valve was closed for the last kneading phase.

Protocol B: With Vacuum and gas flushing

The protocol started with a pre-mixing stage (10 RPM tool, 3 RPM orbit speed); at first, the headspace was degassed or flushed by applying a 1 min vacuum stage (–900 mbar) in order to evacuate most of the headspace gas by making sure that the headspace exhaust valve was closed. Then a 3 min mixing stage at low-speed was applied during which the chosen gas was injected (100 RPM tool, 8 RPM orbit speed). During this stage, the exhaust valve was slightly open (1/4) once the pressure reached 0.5 bar gauge pressure and kept open until the end of kneading. Lastly, a kneading phase was used at higher speed (150 RPM tool, 16 RPM orbit speed with exhaust valve partly opened (1/4) for 10 min in order to be able to determine the optimal mixing time t_{PEAK}. and kneading. For further tests including baking tests, the t_{PEAK} was used for the kneading tests.

Two pressure levels (atmospheric and 0.5 bar) were tested. Three types of gas were considered in this study, air (atm and 0.5 bar gauge pressure), 100%CO_2 (atm and 0.5 bar gauge pressure), 30%O_2 70%N_2 (at 0.5 bar gauge pressure). The selected gas were introduced after the pre-mixing stage and maintained continuously until the end of the kneading phase. In each case, the kneading duration was adjusted to occur around the experimentally determined t_{PEAK} defined as the time point corresponding to the maximum gluten network development. The combination of protocols A and B with the different gases considered provided different mixes of gas in the mixer headspace with different gases partial pressures. It should be noted about this that the gas percentages mention the composition of the injected gas; the gas that was present in the mixer's headspace depends on the protocol used. More precision is provided about this point in the chapter 3.

The mixing was conducted for 10 min or 15 min for some trials and in triplicates for all the conditions in order to cross the time to peak. The plots of power in function of time were exploited to extract the maximum of each record. The corresponding average value was considered as the optimal mixing time. During mixing, the temperature-controlled water jacket was in charge of keeping the dough temperature constant at 25°C throughout the mixing. Under preliminary trials, at 150 RPM was the optimum speed for kneading.

Table 2.2. Table of the different mixing stages

Conditions	Phase 0 (Headspace vacuum or partial vacuum, pre-mixing)	Phase 2 (Mixing at low speed)	Phase 3 (kneading)
Mixing time (min) For the determination of the t_{PEAK}	1	3	10
Spiral agitator (RPM)	50	100	150
Satellite speed (RPM)	5	8	16
Mixing Pressure (bar)	-900 & - 500	0 or 0.5	0 or 0.5

2.1.2.2. Determination of dough development time (t_{PEAK}) and the mechanical energy (SME) consumed by the dough

2.1.2.2.1. t_{PEAK} data treatment and processing

Three different approaches have been considered; for each of them, 3 specific mixing tests were considered for each recipe or each mixing condition. A recording of the tool power and of the satellite power (cycloidal displacement of the tool in the bowl which was static) in function of time were available (1 Hz data acquisition rate). The dough power was computed based on the difference between the tool power and the satellite power and was used for the t_{PEAK}. The dough power was only considered during the last phase of mixing (kneading phase) and the time was accounted from the start of the kneading phase. The raw power data from the mixer tool was collected during the kneading phase, with the initial frasage in French or pre-mixing phase and slow mixing were excluded from analysis. To reduce noise and smooth the dataset, an average of 30 consecutive power readings was calculated. This moving average was applied repeatedly on the averaged data to further smooth the curve. The resulting smoothed power curve was then used to identify the dough development time,

t_{PEAK}, defined as the point of maximum power consumption during the kneading phase. This method improves the accuracy of t_{PEAK} determination by minimizing fluctuations and focusing solely on the kneading period. For each mixing condition, a triplicate measurements was conducted, below is an example of a triplicate of air-mixed dough at 150 RPM. An example of experimental data with the averaged function of power in function of time is plotted below Figure 2.3.

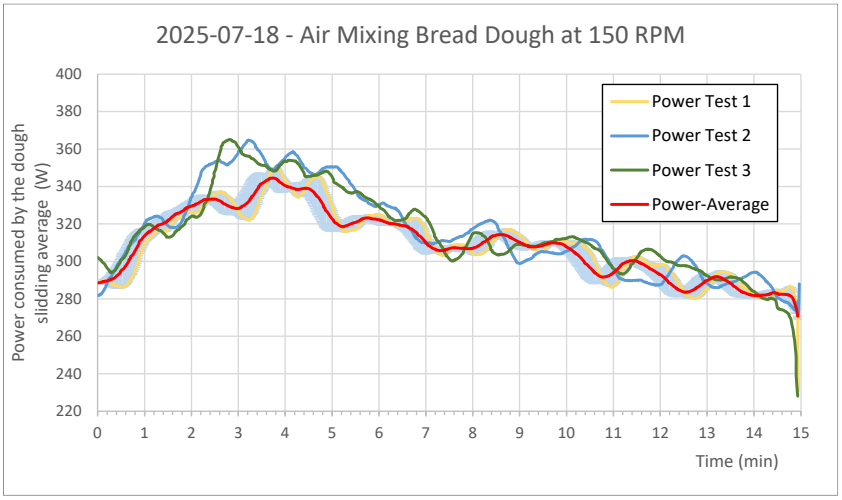


Figure 2.3 Example of a treatment applied to 3 replicated to determine the t_{PEAK}. The three tests underwent a sliding average to smooth the noise. Then the three measurements were averaged

Then three different approaches were applied:

- $t_{PEAK-EXP}$: Experimental t_{PEAK}
- t_{PEAK-X^2} from power function fitting using a quadratic polynomial equation
- $t_{PEAK-DE}$ from power function fitting using a double exponential equation

In the case of $t_{PEAK-EXP}$, the time corresponding to the maximum value of the power was simply attributed to the t_{PEAK} (Figure 2.4).

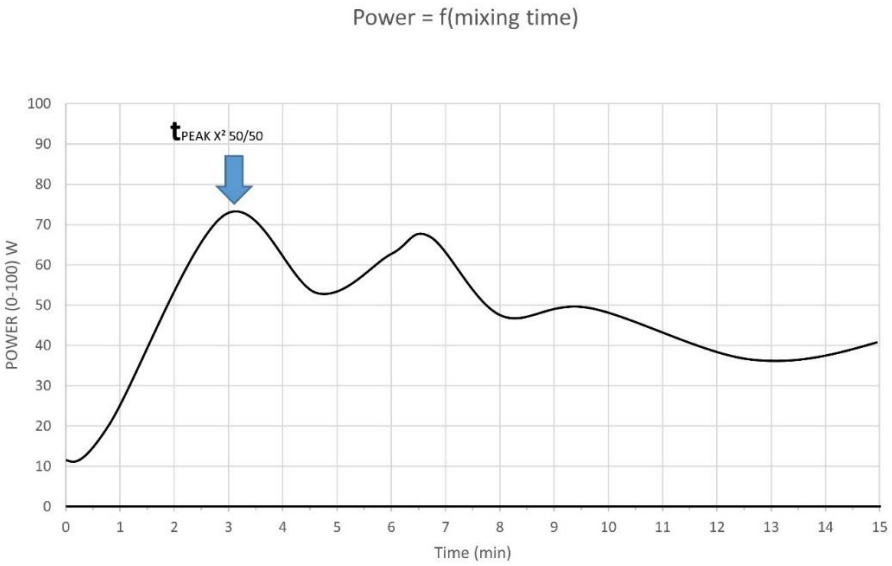


Figure 2.4 Determination of $t_{PEAK-EXP}$ based on the maximum power level observed during dough mixing (kneading phase)

Quadratic polynomial fitting of the power curve

To accommodate the oscillatory behaviour of the power function, a quadratic polynomial regression model (Power $P(t) = a \cdot t^2 + b \cdot t + c$) was fitted Figure 2.4. One of the challenges associated with fitting the power function using a quadric model lies in the selection of the time span used for regression. In several experimental runs, an extended kneading duration up to 10 min or even 15 min was used to ensure that the power peak t_{PEAK} was well covered, given that actual peak occurred between 3 and 5 min. It was initially assumed that a longer time span would improve the accuracy of t_{PEAK}.

However, as illustrated in the figure below Figure 2.5, this approach introduced distortions in the fitted curve, ultimately compromising the precision of t_{PEAK} estimation. This issue was only identified during the final stages of thesis preparation, requiring some experiments to be repeated. A corrective measure was applied by restricting the fitting interval to twice the experimental peak time ($2 \cdot t_{PEAK\text{-}EXP}$), which improved the accuracy of the regression. Nevertheless, even after correction, the t_{PEAK} values derived from the polynomial model remained approximately one minute longer than the experimentally observed t_{PEAK}.

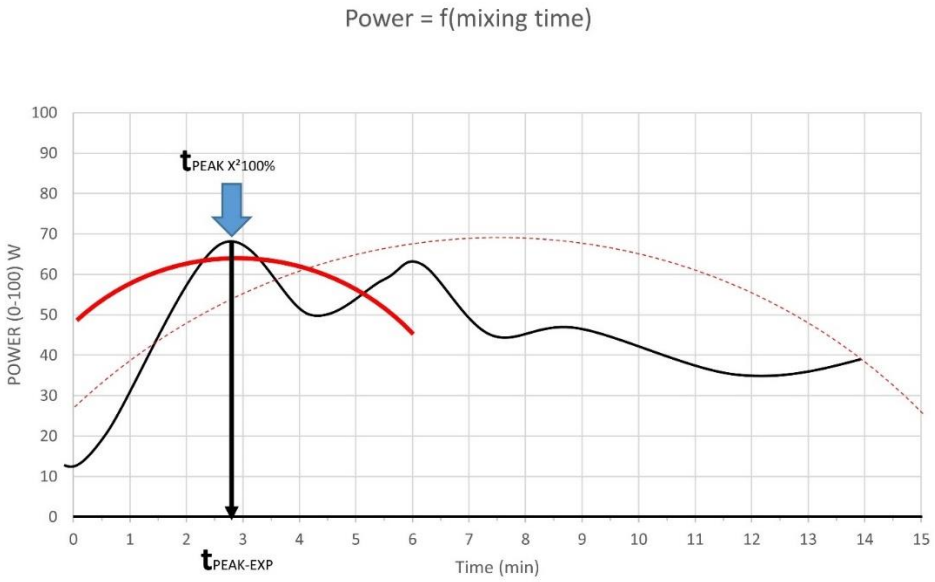


Figure 2.5 Schematic representation of the power function during mixing (kneading phase) in the case of data fitting with a quadratic polynomial function. The excess in time coverage during the mixing yielded in a shift of the t_{PEAK} to non-realistic values (doted red line ➔ $t_{PEAK\text{-}X^2}$ 100% considering all the data points) compared to the observed "Experimental maximum time" ($t_{PEAK\text{-}EXP}$ on the figure). Consequently, it was decided to use a shorter time coverage corresponding to two times the $t_{PEAK\text{-}EXP}$; this is $t_{PEAK\text{-}X^2\ 50/50}$. Still, the obtained values were around 1 minute longer than the $t_{PEAK\text{-}EXP}$

An example of the power curve during kneading under air mixing conditions over a 15-min duration is presented in Figure 2.6. The red curve corresponds to the average of three individual experimental plots shown in light blue, green, and orange. A quadratic polynomial regression was applied to the full dataset (up to 15 min), yielding a predicted peak time ($t_{PEAK\text{-}X^2\text{-}100\%}$) of 4.50 min. In comparison, the experimentally determined peak time ($t_{PEAK\text{-}EXP}$) was 3.73 min. To improve the accuracy of the fit, a second regression was performed using a restricted dataset limited to twice the experimental peak

time ($2 \cdot t_{PEAK\text{-}EXP}$ = 7.5 min). This approach resulted in a revised estimated peak time ($t_{PEAK\text{-}X^2\text{-}50/50}$) of 3.88 min, which more closely matched the experimental value.

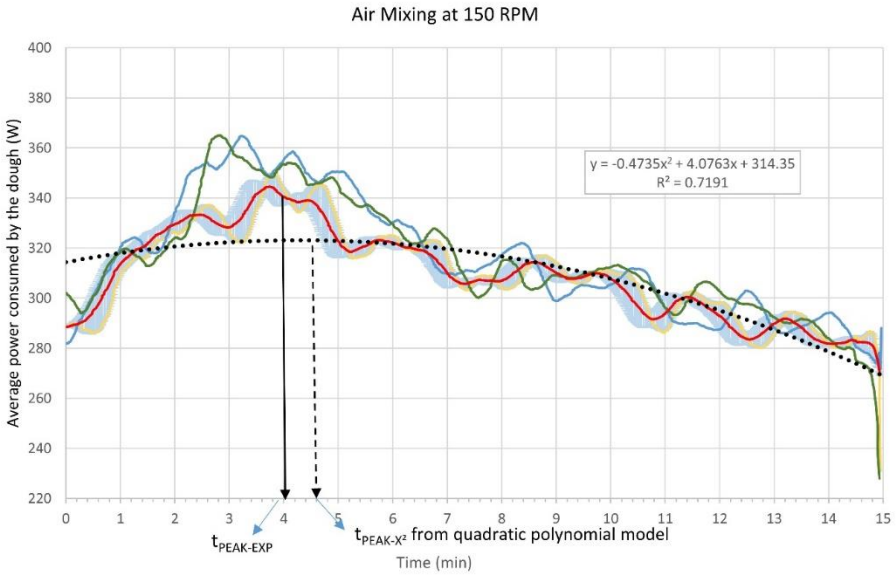


Figure 2.6 Schematic representation of triplicate of t_{PEAK} of an air-mixed dough showing the difference between $t_{PEAK\text{-}EXP}$ and $t_{PEAK\text{-}X^2}$. As well as the average of the triplicate, and the polynomial regression R2

Power fitting function using a double exponential function

To account for the oscillatory behaviour observed in the power function, a regression analysis was performed using Excel's Solver tool, applying a double exponential model. The general form of this function is illustrated in Figure 2.7.

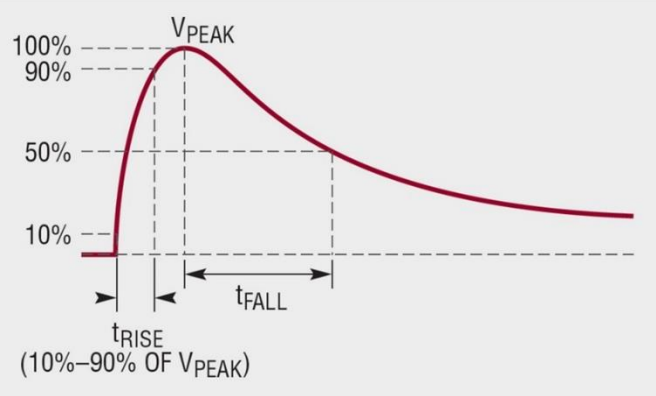


Figure 2.7 Schematic representation of a double exponential function

The rationale for using this function is that the power function usually raised quickly, went to a maximum value and tends to decrease slowly with a tailing effect. The objective was to improve the localisation of the t_{PEAK} compared to the simple quadratic model. The following equation was considered to fit the experimental date.

$$Power\ P(t) = A \cdot (e^{-a \cdot t} - e^{-b \cdot t}) \qquad \text{Eq. 2.2}$$

A schematic representation of this function in Figure 2.8:

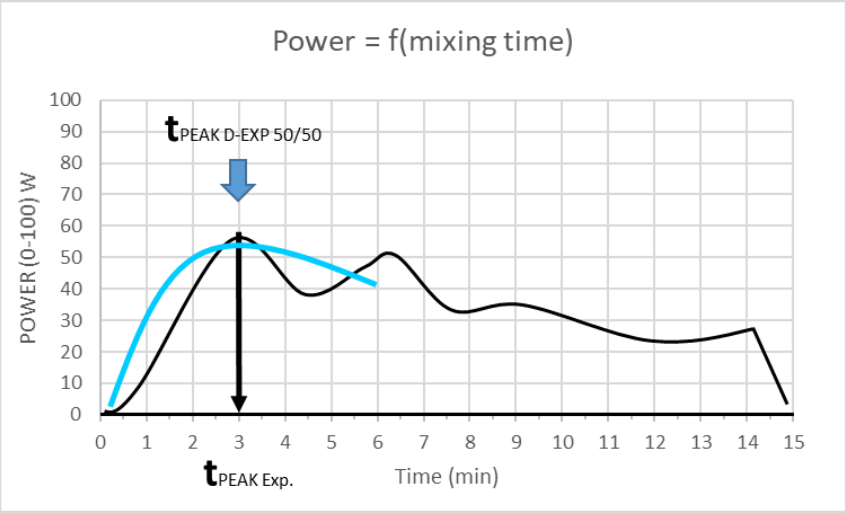


Figure 2.8 Schematic presentation of the type of fitting obtained with a double exponential model using a 50/50 approach = the number of points used for the fitting cover the double of the $t_{PEAK-EXP}$ observed (example here with $t_{PEAK-EXP}$ = 3 min and values up to 6 min used for the fitting of the double exp. model)

The maximum of this function is obtained when the derivative of the power function is equal to zero (Braide and Enoch 2018):

$$\frac{d}{dt}\mathrm{P(t)} = A \cdot \left(-a \cdot e^{-a \cdot t_{PEAK}} + b \cdot e^{-b \cdot t_{PEAK}}\right) = 0 \qquad \text{Eq. 2.3}$$

This yields in:

$$\left(-a \cdot e^{-a \cdot t_{PEAK}} + b \cdot e^{-b \cdot t_{PEAK}}\right) = 0 \qquad \text{Eq. 2.4}$$

Or

$$b \cdot e^{-b \cdot t_{PEAK}} = a \cdot e^{-a \cdot t_{PEAK}} \qquad \text{Eq. 2.5}$$

Or

$$\frac{a}{b} = \frac{e^{-b \cdot t_{PEAK}}}{e^{-a \cdot t_{PEAK}}} \qquad \text{Eq. 2.6}$$

Or

$$Ln(a) - Ln(b) = -b \cdot t_{PEAK} + a \cdot t_{PEAK} \qquad \text{Eq. 2.7}$$

Or

$$t_{PEAK-EXP} = \frac{Ln(a) - Ln(b)}{a - b} \qquad \text{Eq. 2.8}$$

Three different approaches were explored for determining the mixing time, including the use of a quadratic polynomial model. In some cases such as the experimental work conducted in Germany this method resulted in slightly extended mixing durations compared to other trials. Extending the kneading time beyond the "expected" t_{PEAK} may lead to overmixing, potentially increasing the dough void fraction and negatively impacting dough structure. Specifically, such conditions can reduce gas retention capacity and promote gas cell disproportionation during baking. However, all data sets were

analysed using the same protocol for t_{PEAK} determination, ensuring that any potential artefacts introduced by overmixing were consistently applied across all conditions, thereby allowing valid comparisons.

2.1.2.2.2. SME data treatment and processing

Once t_{PEAK} was identified for each condition, it served as the temporal reference point for subsequent analysis of mechanical energy input, particularly for calculating the Standard Deviation (SD) of SME values. The SME is a key parameter in dough processing, reflecting the energy required to develop the dough structure. The mixing trials were conducted using a VMI planetary mixer equipped with a double-tool system and integrated sensors for real-time monitoring. The mixer provided raw data output during operation, including the rotational speed (RPM) and torque-derived power of both the central mixing tool and the satellite arm. These measurements were recorded throughout the mixing process and exported as time-series datasets.

To evaluate the mechanical energy input delivered to the dough, the raw speed and power data were processed to calculate the Specific Mechanical Energy (SME). To ensure accurate SME determination, the data were first treated by isolating the kneading phase from the total mixing time. Only the period corresponding to effective dough development (i.e., kneading) was considered for subsequent analysis. The kneading time was standardized to the t_{PEAK} determined of each condition.

SME, expressed in $kJ \cdot kg^{-1}$, quantifies the mechanical work applied to the dough per unit mass and was computed using the following equation (Shehzad *et al.* 2012):

$$SME = \frac{\int P(t)\, dt}{m} \qquad \text{Eq. 2.9}$$

Where P(t) is the instantaneous mechanical power (W) recorded over time t, and m is the mass of dough (kg). The integral represents the cumulative energy input throughout the mixing duration.

The instantaneous mechanical power of the dough P_{dough} in $(W \cdot kg^{-1})$ was calculated by the following:

$$P_{dough} = \frac{P_{\text{tool}} - P_{satellite}}{m} \qquad \text{Eq. 2.10}$$

Where P_{tool} is the power given by the mixing tool (W) and $P_{Satellite}$ is the power given by the mixer (W). After which, this value was converted from $W \cdot kg^{-1}$ into $kJ \cdot kg^{-1}$ by dividing it with $3.6 \cdot 10^6$. Each calculation step has been conducted in triplicates for each mixing condition and then averaged. The average cumulative SME was plotted in function of time following a linear fit model of first-degree equation. The data was then given in an example below.

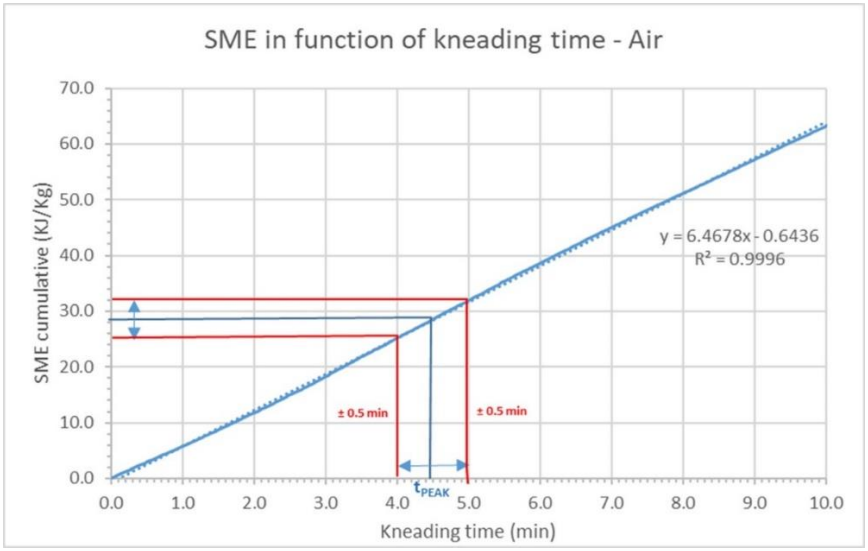


Figure 2.9 Example of a Cumulative linear exponential curve of SME in function of kneading time

By dissecting the linear-fit equation components, we obtain the value of each component:

y = the dependent variable which is the SME; a = the slope line which indicates the rate change which is dependent on the variable x and in our case, a represents or named SME_{rate} in kJ·kg^{-1}. It visualized how quickly the power increases over time during gluten development.

x = the SME at t_{PEAK}; b = y-intercept, is the initial condition at the start of mixing time SME_0.

Therefore, the equation will be as follows:

$$y = SME_{rate} \cdot SME_{t_{PEAK}} + SME_0 \qquad \text{Eq. 2.11}$$

To assess variability in mechanical energy input around dough development, the Standard Deviation (SD) of SME values was calculated in a defined time window centered around the t_{PEAK} of each condition. A time interval of ± 0.5 min around t_{PEAK} (i.e., a total window of 1 min) was then selected.

Within this 1 min interval, the SME values were modelled using the linear equation of the form SME (y = a / 2). The mean SME was calculated at the midpoint of the interval (0.5 min), and the SD was derived from the residuals of the data points relative to this linear fit. This approach allows a precise assessment of energy input variability during dough development, enabling comparison across different gas conditions.

By taking the example of Air in the figure above, t_{PEAK} was around 4.5 min, the selected analysis window ranges from 4.0 to 5.0 min. The fitted curve is then used to estimate the SME at t_{PEAK}. At t_{PEAK} = 4.5, this value was then used as the "a" input in the linear fit equation to calculate the corresponding SME at t_{PEAK}.

$$\mathrm{y} = 6.4678 \cdot 4.5 - 0.6436 = 28.6\ \mathrm{kJ} \cdot \mathrm{kg}^{-1} \qquad \text{Eq. 2.12}$$

Subsequently, the SD is calculated using the residuals—i.e., the differences between the actual SME values and the values predicted by the linear fit. Therefore, SME = 28 ± 3.2 kJ·kg^{-1} and SD = 6.4678 · 0.5 = 3.2.

The entire protocol was then applied for the different gas mixtures in triplicate.

2.1.2.3. Shaping and resting

After mixing, the dough was divided in pieces of 300 g, each dough piece was shaped into a ball-shape and covered with a piece of tissue to prevent dehydration and were let to rest for 20 min at ambient room temperature. Dough resting prior to sheeting promotes gluten formation by loosening the gluten structures formed during the mixing process and the handling of the dough (Fu and BeMiller 2017; Liu *et al.* 2021).

2.1.2.4. Sheeting and moulding

Principle of the method

The sheeting process has been reported to affect the behaviour of the dough in the subsequent stages especially proving and baking and the properties of the finished product (Engmann, Peck and Wilson 2005). In the breadmaking process, sheeting consists of shaping, rolling and stretching the dough before fermentation and baking. This affects both the cellular structure and rheological properties of the dough (Sandoval 2017). This step reinforces the gluten network around the formed gas bubbles from the mixing stage, and redistributed and reshaped the gas bubbles into smaller, spherical and more homogeneous bubbles

Protocol

After mixing, the doughs were shaped into balls and rested for 20 minutes at ambient temperature. Following this resting period, they were sheeted using a dough sheeter (MB 230, Bertrand Puma, France), by passing the doughs through counter rolling rollers with a space gap between the 2 rollers of 2.5 mm. The doughs was rolled into a dough stick with weight of 300 g each, which were installed in a pan (width w = 9.3 cm, height h = 10 cm and length L = 26.4 cm. Then the pans were installed in a fermentation cabinet (Hengel AR68, Paringy, France) at a temperature of 30°C and relative humidity of 90% for proofing. A piece of dough of 20 g was also installed in parallel in a fermentation flask to monitor the dough expansion. A thin film of sunflower oil lubricated the inner walls of the fermentation flask and a plastic disk was contacted on the top surface of the dough to monitor its expansion.

2.1.3. Determination of dough properties

2.1.3.1. Dough void fraction after mixing, sheeting and fermentation

The density of the dough was measured to estimate the amount of air incorporated into the dough (Campbell *et al.* 2001). First, based on Archimedes' principle (Figure 2.10) (Mohazzabi 2017), small dough samples (≈30 g) were weighed at ambient air using a precision balance (RADWAG, PS 6100.R2.M) this was the mass m_1. Then a beaker of 500 mL filled with colza oil with known density (916 g·cm^{-3}) was placed on the balance; a dough holder (steel wire) was introduced into the oil up to the level of the air-oil interface and the balance was then tared. Last, the piece of dough was fixed on the dough holder and was immersed in the oil. The resulting mass (m_2) corresponds to the buoyancy force caused by the volume of the tested dough sample (V_D), which is composed of the volume of the

degassed (gas free) dough (V_{DD}) previously calculated and of the volume of gas trapped in the dough (V_{gas}). The void fraction was then calculated using the difference in weight:

$$\varepsilon_{dough}(\emptyset) = 1 - \frac{\rho_D}{\rho_{DD}} \qquad \text{Eq. 2.13}$$

With the volume of gas-free dough

$$\mathrm{V_{DD}} = \frac{m_1}{\rho_{DD}} \qquad \text{Eq. 2.14}$$

In addition, the volume of gas trapped inside the dough can be calculated by the following

$$V_{gas} = \frac{m_2 - V_{DD} \cdot \rho_{oil}}{\rho_{oil}} \qquad \text{Eq. 2.15}$$

The void fraction of the dough (dimensionless) was finally determined as follows:

$$\varepsilon = \frac{\mathrm{V}_{gas}}{\mathrm{V_{gas}} + \mathrm{V_{DD}}} \qquad \text{Eq. 2.16}$$

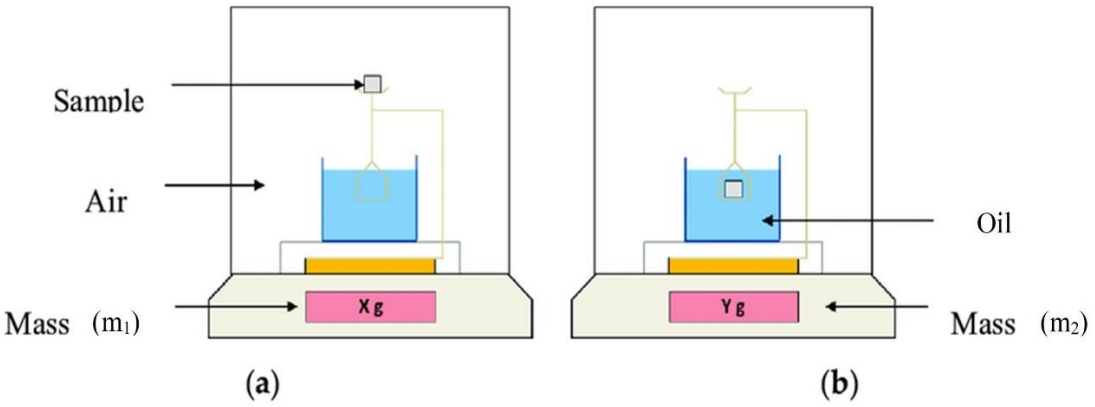


Figure 2.10 Principle of the test used to determine the void fraction in a dough sample. The measurement is based on Archimedes principle with (a) mass m_1 of the sample and (b) mass perceived when the dough sample was immersed in the oil. For after kneading, a 30 g of dough was measured, whereas after sheeting an entire piece of rolled/sheeted dough (150 g) was similarly measured

This measurement was carried out for all the tested recipes after mixing, sheeting and fermentation.

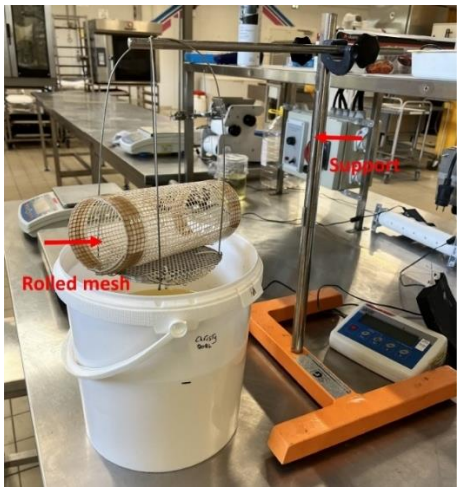


Figure 2.11 Apparatus used for measuring the dough void fraction after fermentation

The dough void fraction after fermentation was measured using this prototype apparatus, based also on Archimedes' principle. The rolled dough with weight of 150 g is weighed at ambient air as initial mass weight (m_1). The mesh network will always be immersed into the oil bucket until covered completely, will be tarred. After removal from the oil, it will be suspended on a support and left to dry completely. Any excess oil will be allowed to drip back into the bucket to prevent mass loss or measurement error. Then the mass is placed inside the mesh network and into the fermentation chamber. After fermentation, this network with the dough inside are immersed back into the oil bucket for measuring the mass (m_2). For each dough making, a triplicates were measured, for a total of 9 repetitions.

2.1.3.2. Dough fermentation and determination of dough expansion ratio N

During the fermentation phase, a piece of 20 g of dough was installed in a cylindrical flask (internal diameter of 5 cm). The dough in the flask started at an initial height of H_I (around 1 cm) until reaching an expansion of a final height of H_F cm. The expansion ratio N was defined as the ration of H_F to H_I and was tracked due to the vertical displacement of the disk contacting the upper dough surface in the flask. However, what is important is to reach the same void fraction in the dough before baking; this value was fixed at 0.75 and depends on the initial void fraction of the dough. The challenge that lies in determining in advance the N value based on the initial height of the dough in the flask, on the initial void fraction of the dough ε_i and on the targeted dough void fraction at the end of fermentation ε_F. The solution was obtained from the following calculation. The values of the effective dough density were ρ_D and ρ_{DD} respectively. The H_I was the initial dough height before starting the fermentation.

The initial apparent volume of the dough piece is (V_{DI}) with:

$$V_{DI} = V_{DD} + V_{GI} \qquad \text{Eq. 2.17}$$

For information, the volume V_{DD} of the degazed dough sample is detailed below (without the inserted void fraction):

$$V_D = \frac{m_D}{\rho_{DD}} \qquad \text{Eq. 2.18}$$

If we assume that the dough will expand by a ratio of N, the final dough volume will be:

$$V_{DF} = V_{DD} + V_{GI} + (N-1) \cdot (V_{DD} + V_{GI}) \quad \text{Eq. 2.19}$$

The initial void fraction of the dough is ε_I :

$$\varepsilon_I = \frac{V_{GI}}{V_{DI}} \quad \text{Eq. 2.20}$$

And the final void faction in the dough is ε_F :

$$\varepsilon_F = \frac{V_{GI} + (N-1) \cdot (V_{DD} + V_{GI})}{V_{DD} + V_{GI} + (N-1) \cdot (V_{DD} + V_{GI})} \quad \text{Eq. 2.21}$$

By combining the 2 previous equations, in particular in replacing V_{GI} by $\varepsilon_I . V_{DI}$ it comes:

$$N = \frac{(1-\varepsilon_I)}{(1-\varepsilon_F)} = \frac{H_F}{H_I} \quad \text{Eq. 2.22}$$

This calculation was applied for all the doughs mixed at 0.5 bar gauge pressure and 150 RPM for the following tested mixtures:

- Air
- 100%CO_2
- 30%O_2 70%N_2

Where the same recipes were repeated with addition of AH_2. Three dough batches were produced, where a triplicate for each measurement was conducted, therefore, a total of 9 repetitions was achieved.

2.1.3.3. Quantifying Fermentation Kinetics through CO_2 Emission Measurements with Risograph

Principle:

The Risograph is an electronic instrument designed to measure gas production from fermenting dough or chemical leavening agents. Initially developed by R-Design Co. (Pullman, WA, USA), it is now produced by the National Division of TMCO (Lincoln, NE, USA), with substantial upgrades to its software and hardware. The device allows for precise and rapid determination of carbon dioxide evolution, providing both the rate of gas release (in $mL \cdot min^{-1}$) and the cumulative volume over time.

The Risograph consists of several key components housed within a compact stainless steel casing. The dough samples are placed in sealed containers that are immersed in a water bath, which maintains a precise and stable temperature for optimal fermentation conditions. Thin tubes connect each container to the gas measurement system, allowing the carbon dioxide produced during fermentation to be transported and measured. As gas evolves from the fermenting dough, it generates back pressure in the sealed jars. This pressure is continuously measured by the Risograph and then converted into gas volume using the ideal gas law equation, PV = nRT (Hou and Hsu 2013; Rattin *et al.* 2009) following the general procedures of AACCI Approved Method 89-01.01.

The water bath ensures consistent temperature control, which is crucial for accurate and repeatable measurements of gas evolution. The tubes lead the released CO_2 to sensors that continuously record both the rate of gas production and the total volume evolved over time. The device top panel includes numbered ports corresponding to each sample container, enabling simultaneous monitoring of multiple dough samples. The entire system is linked to data acquisition software for real-time recording and analysis.



Figure 2.12 Risograph apparatus showing the jars placed in the water bath connected with detection tubes

Protocol:

Prior to the experiments, the Risograph was switched on to allow the water bath to reach a stable temperature of 30°C. Once the dough was sheeted and prepared according to the experimental protocol, 3 sheeted doughs of 50 g each were carefully weighed and placed into numbered jars. Each jar was then sealed tightly with a lid to prevent gas leakage. The sealed jars were subsequently immersed in the water bath, ensuring consistent temperature conditions during fermentation. The tubing connected to each jar allowed the CO_2 produced by the dough to be measured continuously by the Risograph. All measurements were conducted in triplicates and recorded over a period of 180 min to monitor the rate and total volume of gas evolved during fermentation.

2.1.3.4. Measurement of dough pH before and after fermentation

pH measurements were carried in triplicates for 3 dough pieces before and after fermentation for all the tested recipes, by using a penetration electrode (pHm 004 LMS). The instrument was calibrated before every measurement with distilled water and buffer solutions having a pH 4.0 and 7.0, respectively.

2.1.3.5. Analysis of bubbles in dough under Photonic Optical Microscopy

Microscopy analysis was carried out using a Linkam temperature-controlled stage set (Motic BA310E microscope, USA) at 27°C.

Protocol:

Microscopic observations were performed to evaluate the effect of gas mixing especially air and CO_2 on the behaviour of gas bubbles immediately after mixing under pressurized condition of 0.5 bar gauge pressure. The primary aim was to assess how the nature of the injected gas influences the characteristics of the gas cells in three distinct phases: (i) the size of gas bubbles initially entrapped within the dough matrix post-mixing, (ii) the persistence of these bubbles during the early stages of fermentation, and (iii) the evolution of bubble size following sheeting and throughout the final fermentation stage. Four conditions were tested using a standard reference dough (RD), with comparisons made between air and CO_2-mixed doughs and between yeasted and unyeasted doughs.

2.1.3.6. Dough/bread colour

The dough color measurements after mixing were performed using the KONICA MINOLTA colorimeter using illuminant D65 on the L*C*h color space in cylindrical coordinates. In this space, L* corresponds to lightness, C* to saturation (chroma), and h to chromatic hue. The difference between two colors (ΔE) is calculated from the L*C*h coordinates using an online calculator (ColorMine, n.d.) were it was used for the reference bread where ΔE values were calculated based relative to the reference air-mixed bread, according to the CIE76 formula proposed in Eq. 2.23, such that ΔL*, Δa*, and Δb* correspond to the differences of the L, a*, and b* coordinates in the color space, respectively. L for the Clarity level (which derives from luminance) from 0 to 100, a* for the color from red to green and b* for the color from blue to yellow (-128 to +127) in Cartesian coordinates. Measurements for each gas mixture were performed in triplicate.

A ΔE greater than “2” indicates a color difference perceptible to the human eye.

$$\Delta E = \sqrt{(\Delta L^*)^2 + (\Delta C^*)^2 + (\Delta h^*)^2} \qquad \text{Eq. 2.23}$$

2.1.3.7. Dough Rheology

Principle:

The Thermo Scientific™ HAAKE™ RheoWin™ MARS 40 rheometer measures the rheological properties of materials by applying controlled mechanical deformation between rotating and stationary geometries, such as cone-and-plate or parallel plates. It records the torque required to maintain this deformation, providing data on viscosity, viscoelasticity, and flow behaviour. The instrument features modular components with automatic recognition, precise temperature control from cryogenic to high temperatures, and supports various testing modes including oscillatory and rotational flow. This enables detailed analysis of a wide range of samples under realistic processing conditions.

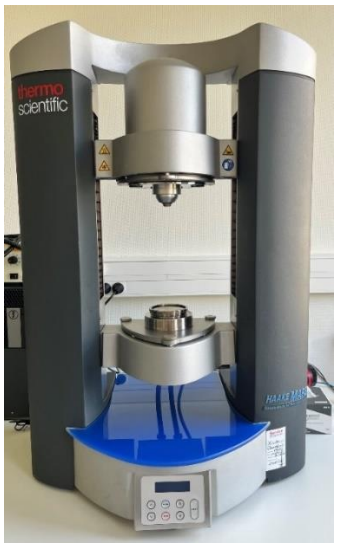


Figure 2.13 Thermo Scientific™ HAAKE™ RheoWin™ MARS 40 rheometer

Choosing the appropriate measuring geometry is crucial for accurate rheological measurements and depends on factors like the rheometer range, sample properties, and test parameters. Various standard geometries are available, each suited for different material types, as illustrated.



Figure 2.14 Standard rheological measuring geometries, including cone-and-plate, parallel plates, and coaxial cylinders, each suited for different sample types and measurement conditions

For more guidance, the application note "Well prepared – good results" offers further advice. Additionally, the Thermo Scientific™ HAAKE™ RheoWin™ software includes a range calculator that helps select the best geometry by estimating the optimal shear rate and stress based on the sample viscosity. If the chosen geometry range is insufficient, a different one should be used.

Protocol

The test was performed by a frequency sweep test. For dough analysis, a plate-to-plate application were used for the dough analysis, with P35/Ti/SE serrated and a 35 mm plate serrated. Roughly 2.5-5 g of dough was placed on the plate. The plate was then lowered at a constant speed 20 $mm \cdot min^{-1}$ to set the measurement at 1 mm gap, ensuring minimal compression to preserve the dough internal structure. Prior to the frequency sweep, an oscillation strain sweep was conducted at a fixed frequency of 1 Hz to determine the linear viscoelastic region (LVR), with strain amplitudes ranging from 0.01% to 50%. Measurements within the LVR were typically taken at a strain of around 0.01%. The frequency

sweep varied the angular frequency from 0.1 to 100 Hz, allowing determination of the storage modulus (G') and loss modulus (G").

During the test, excess dough was carefully trimmed from the edges to create a clean and uniform sample boundary as seen in **Error! Reference source not found.**. The test was performed at a constant t emperature 20°C and each measurement was conducted in triplicate to ensure repeatability.

2.1.3.8. Determination of freezable water in Dough

To determine freezable water in dough, a µDSC III (SETARAM, Caluire-et-Cuire, France) method is used. First, a sample of freshly mixed dough (160 mg) is carefully weighed and placed in a aluminium DSC pan, which is then sealed to prevent moisture loss. The reference cells were kept empty. The sample first calibrated at 20°C, then cooled at -40°C, held for 20 min, and then heated up to 20°C at a heating rate 1°C/min. During this process, the calorimeter records an endothermic peak corresponding to the fusion of the ice formed in the initial cooling phase. The area under this peak provides the fusion enthalpy, which, when divided by the latent heat of fusion of water (333 $J \cdot g^{-1}$), gives the freezable water content. During the heating run, the calorimeter recorded an endothermic peak corresponding to the melting of ice that was formed during the initial cooling phase Figure 2.15. The area under the peak was use for the calculation of enthalpy fusion which was then divided by the latent heat of fusion of pure water (333 $J \cdot g^{-1}$).

Once the analysis was complete, the freezable water was calculated as follow in triplicate:

$$\text{Freezable water (g freezable water/g dough)} = \frac{\text{area under peak}}{\text{Latent heat of fusion of water}} \qquad \text{Eq. 2.24}$$

Where,

$$\text{The area under endothermic peak} = \frac{\text{enthalpy of transition (J)}}{\text{mass of dough (g)}} \qquad \text{Eq. 2.25}$$

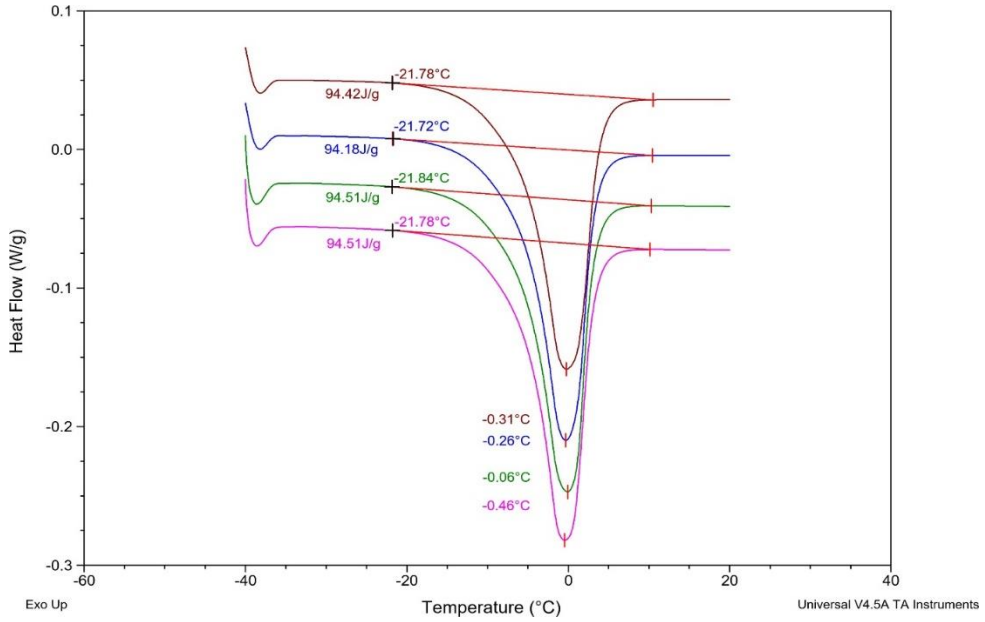


Figure 2.15 Graphical illustration of the area under each endothermic peak for the reference dough. The two runs showing repeatability

2.1.4. Determination of bread properties

Once fermentation was achieved, fermented doughs in the moulds were transferred into the baking over for a transition from dough into bread. Breads were baked in a MIWE deck oven (CO 1.1208 oven - Germany) at 230°C for 17 min according to the AACC method 10-10.03. Around 300 mL of water was injected in the steam box at start of baking to facilitate the oven rise. For each batch, 9 breads were baked. After baking, the bread was allowed to cool at ambient air temperature at 22°C for about 1 hour before measuring its properties. The cooled breads were then stored in sealed in zip-lock plastic bags for analysis.

2.1.4.1. Breads Specific Volume (SV)

The specific volume of a bread corresponds to the ratio of its volume to its mass, expressed in cm3/g.

The TexVol BVM-L370LC volumeter was used to determine the volume of the bread according to AACC Method 10-14.01. After baking, the bread sample was allowed to cool for approximately one hour, then placed onto the device's rotating platform. The volume was measured using an advanced laser sensor. The device was operated through Volcalc software, which automatically calculated the volume, weight, density, and the shape ratio (height-to-width). Additionally, the software generated a 3D image of the bread sample. For each batch, a triplicate of bread loaves were measured for a total of 9 repetitions.

2.1.4.2. Determination of breadcrumb structure

The bread crumb structure was determined after 24 hours of baking. The bread was cut to a thickness of 1.8 cm (Figure 2.16) by the help of a semiautomatic bread slicer PICO450 (JAC, France).



Figure 2.16 Sliced bread showing the thickness of each slice prior to analysis

The bread slices were then scanned using a flatbed scanner (EPSON Perfection V37), with images resolution 1200 pixel and 24-bits colour. Slices were collected from the middle (6th slice position counting from the left side of the loaf) to ensure representative sampling. The scanned images were subsequently analyzed using ImageJ software for further evaluation according to the AACC method 10-18.01.

ImageJ image treatment

In the first step of the analysis, images were calibrated by aligning a reference scale with the "Global" option enabled, then cropped to remove the scale bar. The pixel measurements were calibrated to millimetre units by including a ruler in the scan of the bread slice and digitizing the image accordingly. Color channels were split into black-and-white under the red, blue and green hues, where the images treatments were based on the blue hue. After this step, a threshold was fixed at a value of 140 using the Otsu method with manual adjustment. Median filtering (2 pixels radius) was applied, to eliminate any unnecessary noise below that value, images were inverted and analysed with showing the outlines of the bread slice and by excluding the edges to obtain the final measurements.

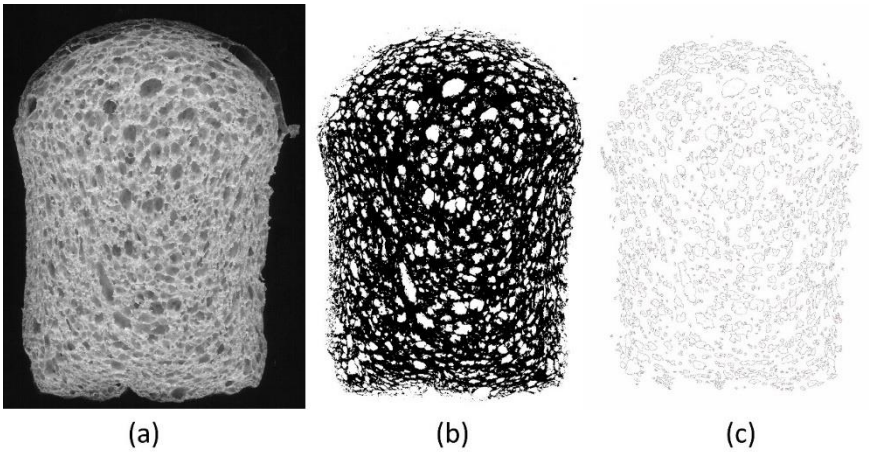


Figure 2.17 The process of image analysis using ImageJ software. (a) is the blue hue image, (b) is the inverted version and (c) is the outlined image

2.1.4.3. Determination of bread porosity

The true density of the bread sample was measured using the Helium Pycnometer (AccuPyc 1330), for gas displacement, that determines the actual density of solid materials. The bread sample was measured and placed on the sample holder, bread samples were prepared by cutting from the middle of the sliced bread a rectangle for a mass between 1 – 1.5 g. Next, the sample was placed in the Pycnometer and left to run for approximately 30 minutes, during which the instrument conducts 10 runs lasting 3 minutes each. The porosity of bread can be determined using the bread apparent and true density. The bread sample actual density is determined by the pycnometer. The measurement from the volumeter was used to calculate the apparent density. Measurements were conducted for 12 bread samples.

The porosity is:

$$\emptyset = 1 - \frac{\rho_{app}}{\rho_T} \qquad \text{Eq. 2.26}$$

Where:

ρ_{app} = Apparent density ($g \cdot cm^{-3}$) of bulk bread measured by $\rho_{app} = \frac{M}{V}$ with M is the bread total mass and V is volume including pore spaces obtained from the TexVol and ρ_T = True density ($g \cdot cm^{-3}$).

2.1.4.4. Bread Staling

Bread undergoes a natural aging process that affects its texture and quality over time. To monitor these changes, texture analysis, and moisture content and starch retrogradation measurements were conducted at specific time intervals following baking.

2.1.4.4.1. Determination of bread texture during storage

Principle

The texture of the bread was evaluated according to the AACC method 74-10.02 based on storage time (days 0, 1, 4, 7 & 15) and formulation using a Texture Profile Analysis (TPA) performed through a double compression test. This method allows the measurement of multiple textural parameters—such as hardness, springiness, cohesiveness, adhesiveness, and others—in a single analysis.

Protocol

Storage temperature plays a crucial role, as cold storage can accelerate texture changes and staling, primarily due to amylopectin retrogradation. Therefore, the bread was stored in plastic bags at 10°C to minimize these effects.

Bread slices were sliced on the day of analysis, keeping the crust intact, to obtain slices approximately 26 mm thick. From these slices, samples were taken from the crumb center using a 28 mm diameter cookie cutter and then placed at the center of a cylindrical probe for texture analysis.

The test was performed using a Texture analyser (AMETEK TA1 LLOYD) operated with Exponent software. A 50% deformation was applied to each slice at a speed of 1 $mm \cdot s^{-1}$ using a 25 mm cylindrical

probe equipped with a 5 kg force sensor. The double-compression was selected to simulated mastication and to allow calculation of hardness, springiness, and cohesiveness. Hardness corresponds to the maximum peak during the first compression. Springiness is expressed as the ratio of the distance travelled during the second compression to that of the first compression. Cohesiveness is defined as the ratio of the area under the curve of the second compression to that of the first compression (Figure 2.18). This measurement was repeated in triplicates.

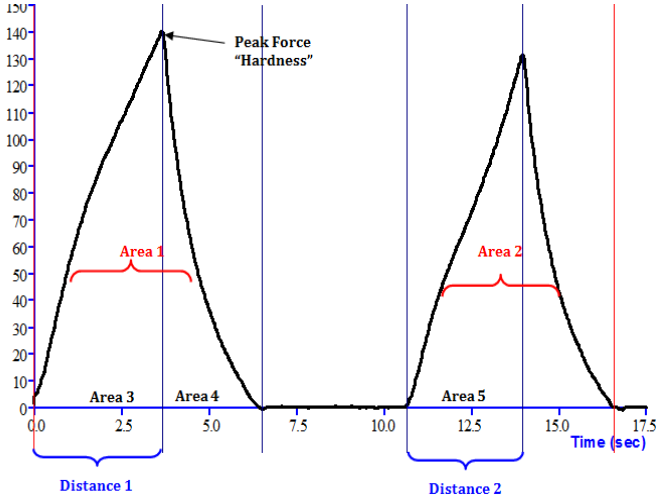


Figure 2.18 Compressive force as function of time

2.1.4.4.2. Determination of bread moisture content during storage

Moisture content measurements were conducted in parallel to bread staling according to the AACC method 44-15A drying method, measurements were carried out on specific days: day 0 (freshly baked out of the oven), 1, and 7. On each sampling day, bread slices were taken from three positions within the loaf**:** ¼ slice, ½ slice, and ¾ slice. From each of these slice positions, three subsamples (5 g each) were collected from distinct areas: the upper left**,** center**,** and lower right (Figure 2.19).

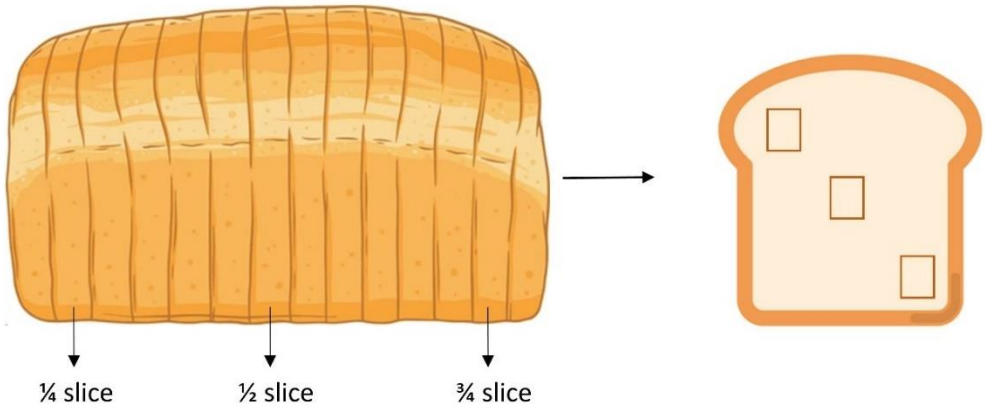


Figure 2.19 Sampling illustration from the sliced bread load: 3 slices taken from 3 distinct positions with the sampling illustration of 3 subsamples from each slice

The samples were dried in a hot air oven at 130°C for 2 hours. After drying, they were cooled in a desiccator to prevent moisture absorption from the air. Once cooled, the final weight of each sample

was recorded. The moisture content was then calculated using a standard formula, based on the difference between the initial and final weights of the samples.

$$\text{Moisture content (w. b \%)} = \frac{w_i - w_f}{w_i} \quad \text{Eq. 2.27}$$

Where w_i is the initial weight before drying and w_f the final weight after drying.

2.1.4.4.3. Microcalorimeter multicells µ-DSC

Principle

The µDSC III (SETARAM, Caluire-et-Cuire, France) calorimeter that simultaneously subjects a sample and an inert reference material to identical temperature variations over time. The instrument records differences in heat flow between the two, with deviations from the baseline indicating endothermic or exothermic transformations in the sample. The instrument consists of 4 capsules: 2 as reference and 2 for the samples.

Protocol – Starch retrogradation of the breadcrumb (Amylopectin)

For each condition, after 1 hour of cooling, one bread was sliced into five slices, each slice sealed in a plastic bag and stored at 10°C, where each slice represented a storage day: J0, J1, J4, J7 and J15.

For the analysis, at each assigned day, a piece of the middle breadcrumb around 170 – 175 mg was measured into the two sample capsules each and firmly closed. The other two reference samples were kept empty and sealed. After which, the capsules were placed in the calorimeter furnace.

The crumb was analysed at the various storage days, a heating rate of 1°C·min^{-1} was applied from 10°C to 120°C. Followed by cooling to 10°C at the same rate. The melting enthalpies of retrograded amylopectin were then determined using the CALISTO Processing thermal analysis software and expressed in J·g^{-1} of dry flour. The mass of each sample analysed was recorded to normalize the heat flow data per gram of dry flour.

The final enthalpy of retrogradation (ΔH) was thus calculated using the following equation:

$$\Delta H = \frac{Q\left(J/g_{dough}\right)}{\frac{g_{dry-flour}}{g_{dough}}} \quad \text{Eq. 2.28}$$

With Q is the heat value absorbed during melting of retrograded starch (J·g_{dough}^{-1}) from DSC .

The evolution curves of the fusion enthalpy of retrograded amylopectin as a function of storage time were modeled with the Avrami equation according to equation (4) (Le-Bail *et al.* 2009):

$$\Delta H(t) = \Delta H_\infty + (\Delta H_0 - \Delta H_\infty) \cdot e^{-\frac{t}{\tau}} \quad \text{Eq. 2.29}$$

With ΔH_0, ΔH_∞ the initial and final retrogradation enthalpy respectively, and τ the time constant.

2.1.5. Sensorial analysis of breads

2.1.5.1. Objectives

In this study, the sensory properties of bread samples with different production methods were evaluated to identify if differences were perceptible and to characterize the products. Specifically, we focused on assessing Ref bread (the reference bread) and gas-dough kneaded bread prepared with various gas mixtures ($O_2/CO_2/N_2$) and the addition of ascorbic acid (AH_2). The study employed two widely recognized sensory methods: the Triangular Test, to detect if differences are perceived between the samples, and the Flash Profile, to characterize the breads using sensory attributes.

2.1.5.2. Sensory analysis laboratory

All the tests were conducted in a sensory analysis laboratory complying with the requirements of the NF EN ISO 8589 (2010) standards. The lab is equipped with 30 booths. The light and temperature are controlled in order to ensure correct and reproducible evaluation conditions.

2.1.5.3. Panellists

The panellists were recruited through on-campus posters and via emails sent to staff and students at Oniris. Participation in the sensory analysis was open only to individuals who were legal in age, in good health, and have no food allergies or intolerances, not following any specific diet, with no oral conditions that could affect sensory perception. These inclusion and exclusion criteria clearly outlined in the information sheet provided to participants. Participants were informed about the purpose of the study through an information sheet. After reading the sheet, if they agreed to participate, the panellists signed a consent form, and if they had any concern or ambiguity in the consent. Personal data was stored and maintained following the guidelines outlined by the General Data Protection Regulation (GDPR).

2.1.5.4. Product preparation

The breads were produced the day before each analysis session, carefully sealed in plastic bag after cooling and refrigerated for the next day. They were prepared for tasting in the morning of the tests, in order to ensure freshness of the breads. The breads were sliced into 1.8 cm thickness using a slicing machine (PICO450, JAC, France). The slices taken from the extremes were not used. The remaining slices were cut vertically in half.

2.1.5.5. Triangular test

The objective was to determine if differences exist between a reference bread obtained with a classic kneading and breads mixed under gases, with and without AH_2.

The triangular test was conducted according to the NF EN ISO 4120 standard for sensory analysis methodology, with 30 panellists in one session. The panel was composed of 40% males and 60% females.

The samples were presented in a balanced random order, presented in identical cardboard boxes, each labelled with randomly assigned three-digit numbers. Each panellist evaluated half a slice of each sample. The following comparisons were tested:

- Ref vs O_2/N_2 with AH_2
- Ref vs O_2/N_2 without AH_2
- Ref vs CO_2 (Control)

2.1.5.6. Flash Profile

The objective was to characterize the sensory properties of breads with different kneading process using Profile Flash, which involves both descriptor generation and intensity ranking.

The method was divided into two sessions performed on two consecutive days: one for generating descriptors and the second for ranking the products according to the intensity of the identified attributes.

Session 1: Attributes generation

Although the recruited 17 panellists were untrained, they were familiar with sensory analysis tests from previous participations. This prior experience is important for ensuring the reliability of results in this type of evaluation. Participants were presented the sliced bread samples in the following:

1. REF bread
2. O_2/N_2 bread with AH_2
3. O_2/N_2 bread without AH_2
4. CO_2 bread

Each panellist individually generated a list of sensory descriptors they considered relevant for characterizing the perceived differences between bread samples. Following the individual generation, a group discussion was conducted to clarify the meaning of each terms and to ensure a shared understanding among panellists. During this discussion, participants were free to modify their descriptor lists by adding, removing or refining terms based on the collective response.

Afterwards, each panellist finalised their own descriptors list, which was then used during the evaluation phase. For each descriptor, panellists were asked to transfer the descriptors generated in the previous session onto a scale for each sensory attribute (e.g., color, texture, odour, and flavour). This approach ensured that each attribute was assessed with a specific scale tailored to the panellist own descriptor test, based on the Flash Profile methodology. Session 2: Samples ranking

The same 17 panellists returned for the second session, during which they ranked the samples according to the intensity of each of the attributes generated during Session 1. For each bread type, panellists used a 0-10 intensity scale to rank samples. Panellists were provided with one slice of each bread for ranking. The extremes of the scale were defined by the panellists to reflect their perception of the sensory characteristics.

Séance 2 – Evaluation des produits

Tout d'abord, veuillez reporter les descripteurs que vous avez notez dans votre liste définitive lors de la séance précédente, sur les pointillés en face de chaque échelle comme dans l'exemple ci-dessous. Vous pouvez encore modifier votre liste si vous le souhaitez.



Figure 2.20, Example of the evaluation sheet used in the first session of Profile Flash test

2.1.5.7. Statistical analysis of the sensory analysis

For the statistical analysis of the triangular test, the methodology was based on AFNOR standard NF ISO4120, which outlines the experimental procedure and statistical interpretation (binomial law) for determining whether the sensory difference exists between samples. For the Flash Profile analysis, a Generalized Procrustes Analysis (GPA) was performed using XLSTAT. In this study, GPA was used to obtain a consensus configuration from sensory profiles of the different samples evaluated by multiple panellists based on their descriptors.

2.2. Part II – Mobility Project by TU HOHENHEIM

2.2.1. Ingredients

The flour used was Fleur Tradition T65 (Moulins Soufflet – France), Universal fresh baker's yeast (Omas Ur-Hefe Universal, Lesaffre Deutchland GmbH, Kehl – Germany) was used as a leavening agent. Tap water was used. Fine table salt (Sodium Chloride) was used (Tafelsalz, Edeka – Germany).

Carbonated water

Carbonated water was prepared using a SODA-STREAM machine (SODA STREAM LtD-Israël). Tap water of temperature 22°C was used to fill up the bottles, which were then stored at 4°C overnight. The carbonated water preparation was done by applying four consecutive pumps per bottle (volume 0.84 L liquid content and 1 L total volume) to standardize gas pressure and CO_2 incorporation. Immediately after carbonation, the bottles were sealed and stored at 4°C. To monitor CO_2 dissolution over time, the pH of the carbonated water was measured at regular intervals (h0, h1, h2, h3, h24) to ensured reproducible carbonation conditions across all experimental batches.

2.2.2. Breadmaking process

2.2.3. Dough mixing

The dough was mixed using a DIOSNA SP 12 spiral mixer (Diosna, Germany). The mixer featured a rotating bowl made of stainless steel and a spiral-shaped mixing arm. A temperature sensor was installed flush within the arm, positioned approximately 2 mm above the bottom surface of the bowl. The mixer had a height of 21.2 cm and an internal bowl diameter of 37.4 cm, with a volume of 22 L. The supervision system enables real-time monitoring and documentation of key parameters such as mixing time, power consumption, dough temperature, and number of revolutions.

The dry and the wet ingredients are added together in one step and mixed. To ensure experimental consistency, mixing parameters (e.g., speed and duration) were carefully adjusted to reproduce the mixing conditions used in other tests.

A three-stage mixing protocol was applied:

- **Stage 1 – Start Phase**: 25 Hz (low speed = 75 RPM) for 1 min
- **Stage 2 – Pre-mixing phase**: 35 Hz (medium speed = 105 RPM) for 3 min
- **Stage 3 – Kneading phase**: 50 Hz (high speed = 150 RPM) for 10 min, during which the t_{PEAK} was determined based on the average power given by the mixer.

2.2.3.1. Determination of t_{PEAK}

The raw power data from the mixer tool was collected during the kneading phase. To reduce noise and smooth the dataset, an average of 30 consecutive power readings was calculated. This moving average was applied repeatedly on the averaged data to further smooth the curve. The resulting smoothed power curve was then used to identify the dough development time, t_{PEAK}, defined as the point of maximum power consumption during the kneading phase. A triplicate measurement was conducted to determine the t_{PEAK}, which corresponds to the time for which the power consumed by the mixer reaches a maximum value. This time was considered as an optimal mixing time based on (Lancelot *et al.* 2021). In order to accommodate the variability of the experimental records, the average of 3 power records was used. The highest power level during the kneading phase can be a first approach to determine the time at which the dough was supposed to be at its optimal texture (t_{PEAK}) (Lancelot *et al.* 2021; Sadot, Cheio and Le-Bail 2017). A second approach consisted in using the time of the maximum of a quadratic polynomial equation, which was used to fit the power data.

2.2.3.2. Determination of dough void fractions

The density of the dough was measured to estimate the amount of gas incorporated into the dough (Campbell *et al.* 2001), defined as the dough void fraction (ε_{dough}) with a procedure based on Archimedes' principle (Campbell *et al.* 2001; Chiotellis and G. M. Campbell 2003). First, after kneading, small dough samples (≈30 g) were weighed using a precision balance (RADWAG, PS 6100.R2.M) this was the mass m_1. Then a beaker of 500 mL filled with colza oil with known density (916 $g \cdot cm^{-3}$) was placed on the balance; a dough holder (steel wire) was immerged into the oil up to the level of the air-oil interface and the balance was then tared. Lastly, the piece of dough was fixed on the dough holder

and was immersed in the oil. The resulting mass (m_2) corresponds to the buoyancy force caused by the volume of the tested dough sample (V_D), which is composed of the volume of the degazed (gas free) dough (V_{DD}) previously calculated and of the volume of gas trapped in the dough (V_{gas}). The void fraction was then calculated using the difference in weight:

$$\varepsilon_{dough}(\emptyset) = 1 - \frac{\rho_D}{\rho_{DD}} \quad \text{Eq. 2.30}$$

With the volume of gas-free dough

$$\mathrm{V_{DD}} = \frac{m_1}{\rho_{DD}} \quad \text{Eq. 2.31}$$

Where ρ_{DD} = 1.250 g·cm^{-3} was based on the calculation:

$$\rho_{DD} = \sum_i \rho_i . X_i^V \quad \text{Eq. 2.32}$$

In addition, the volume of gas trapped inside the dough can be calculated by the following

$$V_{gas} = \frac{m_2 - V_{DD} \cdot \rho_{oil}}{\rho_{oil}} \quad \text{Eq. 2.33}$$

The void fraction of the dough (dimensionless) was finally determined as follows:

$$\varepsilon = \frac{\mathrm{V}_{gas}}{\mathrm{V_{gas}} + \mathrm{V_{DD}}} \quad \text{Eq. 2.34}$$

2.2.3.3. Determination of dough expansion ratio N at end of fermentation

The expansion ratio N corresponds to the ratio between the initial and final volume of the dough during fermentation. It was monitored in a fermentation flask (5 cm internal diameter) in which 20 g of dough was installed (dough considered after sheeting/shaping). The expansion ratio was calculated with the equation based on Raad et al. (2025), in which ε_I and ε_F are the initial and final void fractions of the dough respectively. The N value was computed to reach a final void fraction of 0.75 (Vliet *et al.* 1992).

$$N = \frac{(1 - \varepsilon_{\mathrm{I}})}{(1 - \varepsilon_{\mathrm{F}})} = \frac{\mathrm{H_F}}{\mathrm{H_I}} \quad \text{Eq. 2.35}$$

2.2.3.4. Shaping of dough and fermentation

After mixing, the dough was divided in pieces of 300 g, each dough piece was shaped into a ball-shape and covered with a piece of tissue to prevent dehydration and were let to rest for 20 min at ambient room temperature. After resting, the doughs were sheeted and moulded in a dough sheeter (Rondostar ECO SFE 6607H, GmbH, Burbach, Germany) by passing them through a pair of rollers maintained at a gap of 2.5 mm from each other. The dough was rolled to form a dough stick, which was installed in a pan (width w = 9.3 cm, height h = 10 cm and length L = 26.4 cm. Then the pans were installed in the fermentation cabinet at a temperature of 30°C and relative humidity of 90% for proofing at ambient air or with CO_2 flow. A piece of dough of 20 g was also installed in parallel in a fermentation flask to monitor

the dough expansion. A thin film of sunflower oil lubricated the inner walls of the fermentation flask and a plastic disk was contacted on the top surface of the dough to monitor its expansion.

CO_2 concentrations were measured using a digital non-dispersive infrared (NDIR) CO_2 sensor (model FYAD 00 CO_2) equipped with an integrated atmospheric pressure sensor for automatic compensation. The sensor features a 2-beam infrared measuring cell, measuring ranges up to 10,000 ppm (FYAD00CO2B10) or 5,000 ppm (FYAD00CO2B05), with typical accuracy of ± (100 ppm + 5%) or ± (50 ppm + 3%) of measured value, respectively. It operates in a temperature range from -40 to + 60°C and humidity up to 95% RH (non-condensing). A unique automatic calibration compensates for sensor ageing. Atmospheric pressure was measured and compensated automatically via a built-in digital pressure sensor (700 – 1100 mbar range, ± 2.5 mbar accuracy). Data logging was performed using an ALMEMO® data logger, recorded at 1-second interval, with each measurement based on a moving average reading window at 165 s (11 x 15 s reading). The sensor response time is less than 195 seconds, making it suitable for tracking dynamic changes in CO_2 concentration during fermentation or controlled atmospheric conditions. The sensors were installed into the fermentation cabinet as seen in the figure below; on the upper shelve one for CO_2 measurement and one for relative humidity measurement. The bottom shelve has the same two sensors mounted in parallel. A fan (visible at the back of the picture) ensured stirring of the gaseous ambiance contained in the cabinet.

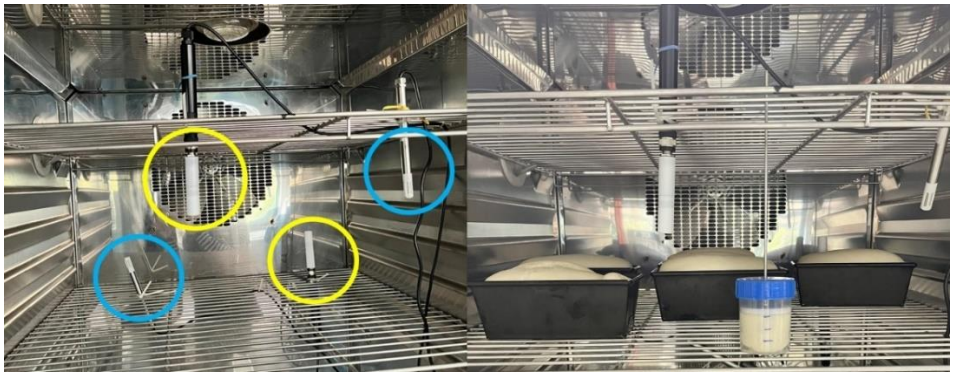


Figure 2.21 Picture of the inside of the fermentation cabinet; CO_2 sensors in yellow and Relative humidity sensors in blue

The fermentation cabinet was equipped with a CO_2 supply system, consisting of a pressurized CO_2 cylinder connected via a controlled tubing network, enabling the continuous introduction of CO_2 directly into the fermentation environment. Therefore, at the start of fermentation, the integrated sensors were activated to continuously monitor the CO_2 release in real time.

2.2.4. Baking

As previously described, baking was carried out for doughs after the fermentation stage. Baking was conducted in a deck oven (Piccolo I, Wachtel GmbH & Co.) for 17 min at 230°C with 300 mL of water vapour injected in the beginning. After baking, the bread was allowed to cool for about 1 hour before measuring its properties.

2.2.5. Determination of dough and bread properties

2.2.5.1. Measurement of dough pH before and after fermentation

pH measurements were carried in triplicates for 3 dough pieces before and after fermentation for all the tested recipes, by using a penetration electrode (Hanna Instrument HI98161 - France). The instrument was calibrated before every measurement with distilled water and buffer solutions having a pH 4.0 and 7.0, respectively.

2.2.5.2. Determination of doughs texture before and after fermentation

The texture profile analysis of doughs was determined by using texture analyser (TA-XT2, Stable Micro Systems, England) with a modified AACC method (74-09) for texture profile analysis (TPA). After kneading, 3 dough pieces around 50 g each were shaped and rounded for measurement. A 10 mm diameter probe and 5 kg load cell were used as measurement geometry. The three dough pieces were two times compressed up to 40% deformation with 15 s rest, the test speed was 1.7 $mm \cdot s^{-1}$. The same test was conducted for the dough pieces after fermentation to assess the impact of CO_2 flow on the dough textural profile. For each batch, a triplicate was conducted before and after fermentation.

2.2.5.3. Dough colour measurement before and after fermentation

Colour measurements were taken immediately after mixing the dough samples with a colorimeter Chroma Meter (CR-400, B 8212649; Konica Minolta, Tokyo, Japan) and after fermentation. The equipment was calibrated using a white reference plate. The color is quantified using the L*, a*, and b* values, where L* indicates lightness to darkness, a* represents the spectrum from green to red, and b* corresponds to the range from blue to yellow. The TCD (Total Color Difference) was calculated based on the equation below:

$$\Delta E = \sqrt{\Delta L^2 + \Delta a^2 + \Delta b^2} \qquad \text{Eq. 2.36}$$

Measurements for each recipe were performed in triplicate.

2.2.5.4. Texture profile analysis of bread

After 1 h of cooling, the breads were sliced (SOFRACA, France) to a thickness of 1.8 cm, and a 10 mm diameter cylindrical probe was employed along with a 5 kg load cell. Each of the three slices was compressed twice to 40% deformation with a 15-second rest between compressions. The test speed was set at 1.7 $mm \cdot s^{-1}$. The analysis was measured by using a texture analyser (TA-XT2, Stable Micro Systems, England) following a modified AACC method (74-09).

2.2.5.5. Determination of breads texture after baking

The texture profile analysis of breads was determined by using texture analyser (TA-XT2, Stable Micro Systems, England) with a modified AACC method (74-09) for texture profile analysis (TPA). After 1 hour of cooling, from each bread loaf 3 middle slices were taken for measurement. A 10 mm diameter probe

and 5 kg load cell were used as measurement geometry. The bread slices were two times compressed up to 40 % deformation with 15 s rest, the test speed was 1.7 $mm \cdot s^{-1}$.

2.2.6. Statistical analysis

Data were analysed using Statgraphics 19 – X64 software using one-way ANOVA and Tukey test. $P < 0.05$ was considered significant. 9 breads were baked for each condition and averaged.

CHAPTER 3 : **RESULTS & DISCUSSION**

Chapter 3 is divided into 2 main parts:

Part 1: Presents the dough and bread results of breads mixed under atmospheric and 0.5 bar gauge pressure with air and CO_2

« Impact of Dough Mixing Pressure with Air and CO_2 gases on Dough and Bread properties; A focus on Improved Control of Dough Aeration During the Baking Process »

Christy Raad, Patricia Le-Bail and Alain Le-Bail (Journal of Applied Food research)

Part 2: Focuses on the dough results from all gas mixtures at 0.5 bar gauge pressure

3.1. Part I – Article 1

This part of the chapter presents the results under the form of an article, it outlines the impact of gas atmosphere and pressure during dough mixing on dough aeration, gluten development and the final bread quality. The purpose of this present study is to fill this gap by systematically varying headspace composition and pressure during dough mixing.

In this study, air and CO_2 were investigated under two pressure levels: atmospheric and at 0.5 bar gauge pressure. A predictive model linking initial dough void fraction to final dough expansion is also proposed to optimise fermentation time and aeration under the tested parameters.

Protocol A atmospheric pressure: With partial vacuum and gas flushing

The protocol starts with a pre-mixing stage (10 RPM tool, 3 RPM orbit speed); the headspace of the mixer was set under vacuum for 1 min (pressure level – 500 mbar) at slow speed with atmospheric air flowing through the head of the mixer (exhaust valve partly open at 1/4). Then mixing stage started at 100 RPM tool, 8 RPM orbit speed for 3 min; the pressure was set at atmospheric pressure set point with gas flow through the mixer's head with exhaust valve partly open (1/4) to ensure renewal of the head space gas during mixing. Lastly, a kneading phase was used at higher speed (150 RPM tool, 16 RPM orbit speed with exhaust valve partly opened (1/4) for 10 min in order to be able to determine the optimal mixing time t_{PEAK} and kneading. For further tests including baking tests, the t_{PEAK} was used for the kneading tests.

Protocol A 0.5 bar: With partial vacuum and gas flushing

The only difference with the previous protocol lies in the fact that the exhaust valve was closed for the last kneading phase.

The tested hypotheses were the following:

- Controlling the headspace gas composition and pressure during dough mixing influences the initial dough void fraction
- The initial void fraction affects the final void fraction prior to baking
- Adjusting mixing times according to the optimal dough development time (t_{PEAK}) improves dough aeration and expansion
- Varying gases (air vs. CO_2) and pressure throughout mixing provides enhanced control over gas retention and dough structure, leading to optimized fermentation times and improved bread characteristics

We studied the impact of these mixing parameters on dough properties (t_{PEAK}, dough void fractions after mixing, sheeting and fermentation, and expansion ratio during fermentation) as well as bread properties such as breads specific volumes and crumb structure.

Title: Impact of Dough Mixing Pressure with Air and CO_2 gases on Dough and Bread properties; A focus on Improved Control of Dough Aeration During the Baking Process

Christy Raad[1], Patricia Le-Bail[2], Alain Le-Bail[1]

[1]Oniris - GEPEA UMR CNRS 6144, Nantes – France
[2]INRAE – ISD BIA, Nantes – France

Abstract

This study investigated the effect of controlling headspace pressure and gas atmosphere during dough mixing on dough aeration and bread quality. Using a specialized mixer, doughs were mixed with either air or CO_2 under atmospheric pressure and 0.5 bar gauge pressure. Dough aeration (void fraction) was monitored at key breadmaking stages; end of mixing, after sheeting and after fermentation with a target final void fraction of 0.75 for optimal bread volume. A predictive model estimated the expansion ratio needed to achieve this target void fraction. Although the target was not fully reached post-fermentation, doughs mixed with air at 0.5 bar gauge pressure demonstrated a higher $\varepsilon_F = 0.64 \pm 0.00$ and SV of 4.54 $cm^3 \cdot g^{-1}$ compared to those mixed with CO_2 at the same elevated pressure ($\varepsilon_F = 0.60 \pm 0.00$ & SV = 3.55 $cm^3 \cdot g^{-1}$). Lower SV and larger, irregular gas bubbles in CO_2 doughs were attributed to gas bubble disproportionation and loss during sheeting, as well as the weakening of the gluten network due to oxygen depletion. The calculated N required to reach the target void fraction was slightly lower for air (3.20 ± 0.06) than for CO_2 (3.36 ± 0.06), suggesting more efficient gas retention and dough expansion under air-enriched conditions. These finding suggest that while CO_2 may stabilize gas bubbles during mixing, oxygen from air is essential for a strong gluten network and uniform breadcrumb structure. Controlling the mixing atmosphere and pressure, offer a promising approach for optimizing dough aeration and bread quality.

keywords: Gas retention, fermentation dynamics, gas mixing, expansion ratio, CO_2-injection

Highlights:

- Bread dough mixing was carried in a pressure mixer with air and CO_2 as headspace gas
- The applied pressure was either atmospheric pressure or 0.5 bar gauge pressure
- A model was proposed to predict dough void fraction at end of fermentation
- CO_2 mixing yielded in less uniform crumb structure with disproportionation
- Air mixing yielded in bigger volume and a more uniform crumb structure

3.1.1. Introduction

Bread is a staple food whose final volume must be carefully controlled for several important reasons. Practically, the bread must fit its packaging. Additionally, crumb porosity is directly linked to texture, which influences the overall sensory experience. Recent research has also shown that bread density affects its glycaemic index (GI), with denser breads exhibiting a lower GI (Saulnier, Micard and Della Valle 2014). Therefore, controlling final bread volume is critical and is influenced by every stage of the production process.

The first major stage in bread making is dough preparation, particularly during mixing, which occurs in two phases. Initially, ingredients are mixed into a homogeneous dough mass in a slow-speed phase

called *mixing*. This is followed by a faster, more intensive phase called *kneading,* during which the final dough structure develops. For simplicity, the term *mixing* hereafter refers to the entire process comprising both premixing and kneading.

During mixing, the dough is aerated through continuous gas entrainment and distrainment. This dynamic circulation allows for the partial dissolution of soluble gases such as oxygen (in the case of air) or carbon dioxide (if used as an alternative headspace gas). Generally, a net positive gas incorporation is observed throughout most of the mixing phase, with a final dough void fraction in the range of 10% of the dough volume.

Incorporating air or other gases into the dough to create an aerated final structure will contribute to the final bread porosity and texture and therefore, to its sensory profile (Campbell and Martin 2012; Cauvain 2020b). Dough can be considered a dispersion of individual air cells in a viscoelastic gluten-starch matrix, hydrated with water and containing minor components such as lipids and hydrocolloids (Gan, Ellis and Schofield 1995; Grenier *et al.* 2021). During mixing, gluten proteins polymerize progressively until reaching a point known as the *time to peak* (t_{PEAK}), which represents the maximum dough consistency. This point can be identified by recording the power consumption of the mixer: t_{PEAK} corresponds to the maximum power input, indicating optimal gluten development.

Several studies have emphasized on the importance of t_{PEAK} in dough mixing, highlighting its crucial role in optimizing bread quality. For instance, (Lancelot *et al.* 2021) demonstrated that t_{PEAK} represents the optimal mixing time, during which the dough achieves its maximum viscoelastic properties. Exceeding this time results in a breakdown of the gluten network, leading to a weaker dough structure and suboptimal bread texture. Similarly, (Sadot, Cheio and Le-Bail 2017), confirmed that over-mixing beyond t_{PEAK} reduces dough strength and extensibility. Studies by (Asaithambi *et al.* 2020; Decamps *et al.* 2016) further emphasized that controlling t_{PEAK} through factors like mixing speed and pressure ensures proper gluten development and air incorporation, which are essential for achieving the desired crumb structure and rise. Overall, these studies highlight that accurately determining t_{PEAK} is essential for consistent dough quality, energy efficiency, and achieving the best possible bread texture.

Although void fraction typically continues to increase slightly beyond t_{PEAK}, this is accompanied by disproportionation—the growth of larger gas cells at the expense of smaller ones—due to gluten depolymerization. This leads to uneven gas distribution, which is undesirable in products like sandwich bread that require uniform crumb structure.

During fermentation, the baker's yeast (*saccharomyces cerevisiae*) uses the available sugars in the dough, primarily glucose and maltose released from the starch, and eventually by the added sugar (which may undergo hydrolysis into glucose and fructose) to produce carbon dioxide (CO_2)and ethanol under anaerobic conditions. The yeast activity is temperature-dependent and the baking industry often adopts high temperatures (≈35°C) to accelerate the fermentation process, while artisanal bakers often reduce the temperature to favour the organoleptic property of the bread. Ethanol, being highly volatile, mostly evaporates from the dough. In contrast, the CO_2 that is primarily solubilized in the liquid phase of the dough transitions to gaseous CO_2 at the interface with the gas nuclei embedded in the dough resulting in dough rise during fermentation.

An overview of the evolution of the dough aeration during the different stages of bread preparation is presented in Figure 3.1. The fermentation process is a crucial link between sheeting and the baking stages. Dough sheeting and shaping yields in a significant dough degassing. It also sets the gas nuclei

entrapped in the dough under pressure, which contributes to their stabilisation. Monitoring the extent of the dough expansion during fermentation is usually done as it indicates the right moment to transition to baking (Chevallier, Zuniga and Le-Bail 2009).

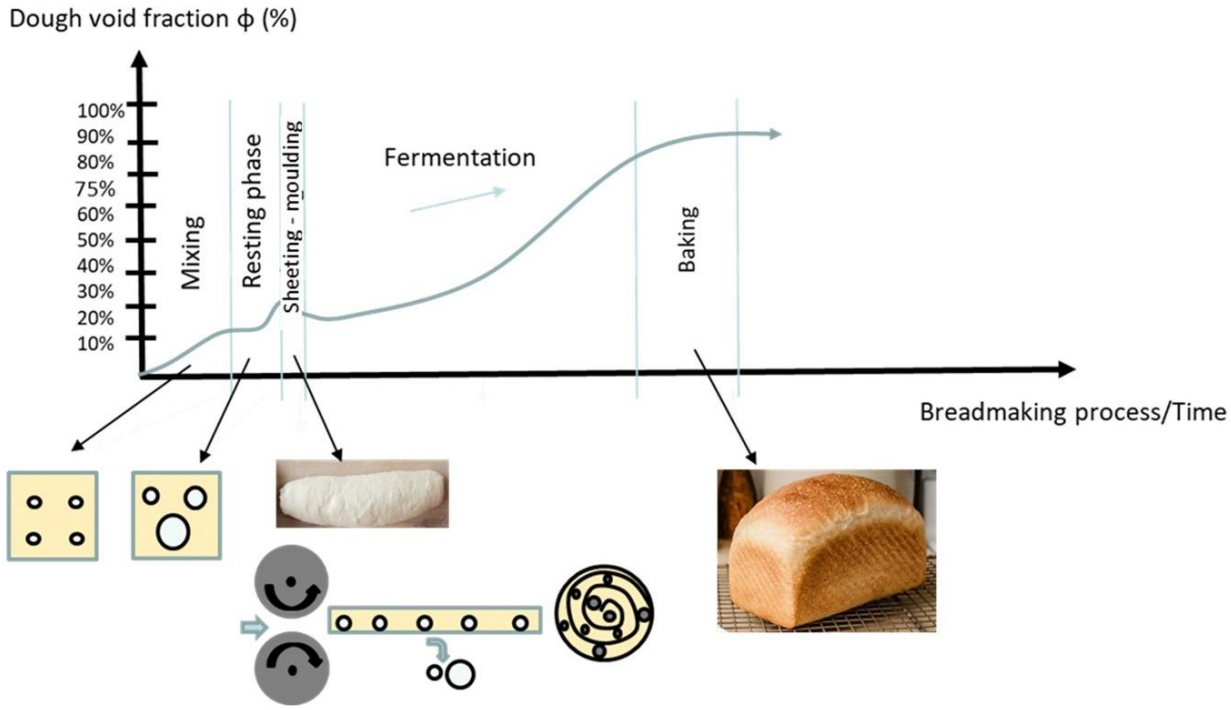


Figure 3.1 Evolution of the dough void fractions during the bread making process; this figure proposes a schematic evolution during mixing, sheeting - moulding, dough resting and fermentation (personal communication)

The dough volume expansion ratio (N) is most of the time monitored with a piece of dough installed in a cylindrical flask of constant section. Typical dimensions of a flask are 5 cm diameter and 10 cm height; a film of oil is installed inside to facilitate the dough installation and expansion. A disk is contacted onto the dough with a displacement guide (small metallic rod) travelling through a cap equipped with a hole at centre in order to visualize the vertical lift of the dough piece (typically around 20 g resulting in an initial height of ca. 1 cm). The dough undergoes volumetric expansion, which can be expressed as a vertical expansion ratio “N” in the case of a fermentation flask as detailed in Figure 3.2. This ratio, defined as the final dough height divided by the initial dough height, is a key parameter in assessing dough development (Kamel and Stauffer 1993; Pyler and Gorton 2008). By monitoring this ratio throughout the fermentation process, bakers can make adjustments to achieve the desired dough characteristics.

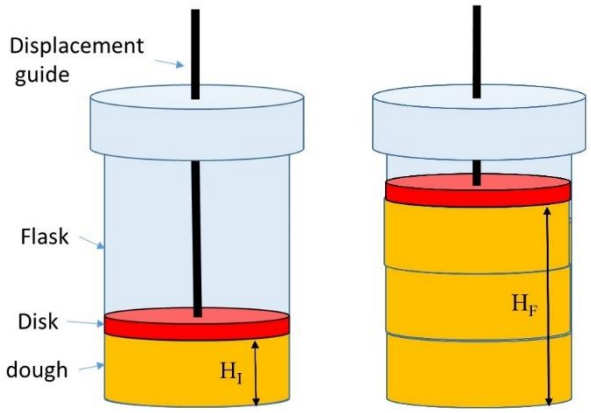


Figure 3.2. Fermentation flask used to monitor the expansion ratio of the dough during fermentation (internal ref.). Example of an expansion ratio N of 3 with $N = H_F / H_I$

The impact of gas-pressure mixing on dough aeration and its reflection on the final product has also been highlighted. Lu et al. (2013) used X-ray tomography to study how pressure step-changes during mixing influence dough density and bubble distribution, further emphasizing the importance of controlled pressure in achieving desirable bread characteristics (Lu *et al.* 2013). Sadot et al. demonstrated that pressure changes during mixing can significantly influence dough aeration, affecting the final baked volume and texture (Sadot, Cheio and Le-Bail 2017).

In light of the current state of the art, it appears that dough mixing under different gases has been investigated in few studies, and none have considered the impact of the initial void fraction of the dough on the final void fraction prior to baking. Moreover, these studies typically adopted a constant fermentation time. The present study aims to fill this gap with a strategy aiming to a better control of the void fraction of the dough during the entire mixing and fermentation process. This novel approach involves varying the headspace pressure and two different gases (air and CO_2) during dough mixing. A predictive model was introduced that links initial dough void fraction to the final void fraction through dough expansion. Furthermore, this study provides valuable insights into optimizing fermentation time based on the mixing parameters and their impact on the final bread quality. In addition, the impact of the different mixing conditions yielded in different mixing times, which were adjusted according to the time to peak corresponding to the optimal dough development in terms of dough rheology.

3.1.2. Materials & Methods

3.1.2.1. Ingredients

The ingredients used to make the bread dough were Type 65 wheat flour (Minoterie GIRARDEAU – France with a water content 14.80% w.b., Ash content 65 ppm, P/L: 1.68, W: 200.10^4 J & water absorption 57% obtained with a Farinograph test, fine table salt (Cedot – France), tap water and fresh compressed yeast (Hirondelle – France). The yeast content in this study (2%) was lower than 3 – 4% commonly used in commercial white pan bread; this dosage was preferred to have a better control of the fermentation stage, which was less reactive. Table 3.1 shows the list of ingredients used in the bread dough recipes. The degassed dough density was calculated using the following equation Eq. 3.1 (Sahin & al, 2006) in which X_i^V is the volumic fraction of the ingredient i and ρ_i is the density of the ingredient i.

$$\rho_{DD} = \sum_i \rho_i . X_i^V \qquad \text{Eq. 3.1}$$

The density of the degazed dough was of ρ_{DD} = 1.234 g·cm^{-3} was based on this computation.

Table 3.1. Dough recipe. The density of each ingredient are from a) for flour helium picnometry (ONIRIS-GEPEA), b) computed from eq. (1) assuming 70% water, 15% proteins, 13% sugars, 2% lipids, c) sodium chloride ref. Hazardous Substances Data Bank

Ingredients	per 100g flour	w/w%	Density g·cm^{-3}	v/v%
Flour T65	100	61.51	1.45	53.53
Tap water	57	35.39	1	44.22
Compressed Yeast	2.1	2.00	0.95	1.62
Sodium chloride	1.8	1.10	2.17	0.63
Total	160.98	100	/	100

3.1.2.2. Mixing

A VMI planetary prototype mixer (VMI, St Hilaire de Loulay-France), was used (Jha *et al.* 2017) (Figure 3.3).



Figure 3.3. VMI prototype dough mixer used for the tests. The lid covering the mixing bowl (open position on picture) was equipped with a spiral tool. The mixer allowed control of the pressure in the headspace as well as a control of the gas composition

The mixer features separate controls for the bowl cycloidal movement and the spiral tool's orbit, guaranteeing the tool sweeps the entire bowl. The mixing bowl was equipped with a double-jacket circulated by a fluid which temperature can be maintained constant during mixing. A lid attached to the mixing bowl allow control of the headspace in contact with the dough during mixing. Both gas pressure (up to 0.5 bar gauge pressure) and gas composition (using air or CO_2) were considered. An infrared sensor, located at the top of the lid, measured the temperature inside the bowl. A supervision interface allowed the control of different parameters including the bowl temperature, operating pressure, mixing time, gyration speed, and tool rotational speed. The power consumed by the tool and by the gyration system were logged and the net tool power was computed from the difference between

the tool power and the gyration power. A set of experiments using an empty mixer was performed in order to obtain a matrix containing the offset values to apply depending on the tool, gyration speeds and headspace pressure (offset powers corresponded to the mechanical frictions caused by belts, gaskets friction on shaft and others). The temperature of the water used in the recipe was set in order to keep the sum of all ingredients and mixing temperature (25°C) equal to 50°C to reach a dough temperature that was matching with temperature set point of the mixing bowl (which was 25°C for all tests). A headspace manual valve was installed on the mixer's headspace in order to adjust the headspace pressure (ie open position of open the mixer's lid) or to allow the circulation of the injected gas through the headspace. The mixing procedure was divided into 3 phases (Table 3.2). At first, the headspace was partially degassed by applying a 1 min partial vacuum (-0.5 atm) with the valve slightly open (1/4) in order to evacuate most of the headspace gas. Then a 3 min low-speed mixing was applied during which the chosen gas was injected (100 RPM tool, 8 RPM orbit speed) which the headspace manual valve kept slightly open until the end of this stage was closed. Lastly, a kneading stage (typically 150 RPM tool, 16 RPM orbit speed) was conducted. Whereas at atmospheric pressure, the manual valve was kept partially opened during the entire mixing phases to refresh the headspace gas and to maintain its composition constant. It should be mentioned that for the 100% CO_2 condition, the 100% refers to the gas that injected in the mixer's headspace. Some traces of gas may remain in the mixer's headspace. A constant pressure was applied during the pre-mixing and the kneading stages either at atmospheric pressure or at 0.5 bar gauge pressure. The mixing was conducted for 10 min and in triplicates for all the conditions in order to cross the time to peak. The plots of power in function of time were exploited to extract the maximum of each record. The corresponding average value was considered as the optimal mixing time. During mixing, the temperature-controlled water jacket was in charge of keeping the dough temperature constant throughout the mixing.

Table 3.2. Different mixing stages

Conditions	Phase 0 (Headspace vacuum, pre-mixing)	Phase 2 (Mixing at low speed)	Phase 3 (kneading)
Mixing time (min) For the determination of the t_{PEAK}	1	3	10
Spiral agitator (RPM)	50	100	150
Satellite speed (PRM)	5	8	16
Mixing Pressure (bar gauge pressure)	0.5	0 or 0.5	0 or 0.5

After mixing, the dough was collected, was covered with a piece of tissue to prevent dehydration and was left for resting for 20 min. in a fermentation cabinet at a temperature of 30°C and relative humidity of 90%. After resting, the dough was divided in pieces of 300 g. Each dough piece was sheeted and moulded in specific machine (MB 230 Bertrand, Puma – France) by passing them through a pair of rollers maintained at a gap of 2.5 mm from each other and nip between the conveying belts of 5 mm which correspond to usual values for this equipment as well as values observed in industry. The dough was rolled into a dough stick, which was installed in a pan (width w = 9.3 cm, height h = 10 cm and length L = 26.4 cm. Then the pans were installed in a fermentation cabinet at a temperature of 30°C

and relative humidity of 90% for proofing. The duration of the entire fermentation process including the resting period, ranged between 95 and 140 min. While 30°C is the optimal for many commercial bread making scenarios, it is important to recognize that certain industrial processes at a higher scale may employ higher temperatures to accelerate fermentation time, whereas artisanal and home bakers may prefer lower temperatures. In this study, the choice of temperature gave longer fermentation times for a better gas retention while higher temperatures can results in diminished gas retention, more rapid expansion and potentially over-proofing (Rathnayake, Navaratne and Navaratne 2018). However, having a fermentation temperature (30°C) close to the dough temperature at end of mixing (28°C in average) allows to align the time-temperature history of the dough. A piece of dough of 20 g was also installed in parallel in a fermentation flask to monitor the dough expansion. A thin film of sunflower oil lubricated the inner walls of the fermentation flask and a plastic disk was contacted on the top surface of the dough to monitor its expansion (see Figure 3.2).

3.1.3. Determination of the dough properties

3.1.3.1. Determination of dough void fractions

The density of the dough was measured to estimate the amount of air incorporated into the dough (Campbell *et al.* 2001). First, based on Archimedes' principle (Figure 3.4) (Mohazzabi 2017), small dough samples (≈30 g) were weighed at ambient air using a precision balance (RADWAG, PS 6100.R2.M) this was the mass m_1. Then a beaker of 500 mL filled with colza oil with known density (916 g·cm^{-3}) was placed on the balance; a dough holder (steel wire) was introduced into the oil up to the level of the air-oil interface and the balance was then tared. Last, the piece of dough was fixed on the dough holder and was immersed in the oil. The resulting mass (m_2) corresponds to the buoyancy force caused by the volume of the tested dough sample (V_D), which is composed of the volume of the degazed (gas free) dough (V_{Dgf}) previously calculated and of the volume of gas trapped in the dough (V_{gas}). The void fraction was then calculated using the difference in weight:

$$\varepsilon_{dough}(\emptyset) = 1 - \frac{\rho_D}{\rho_{DD}} \qquad \text{Eq. 3.2}$$

With the volume of gas-free dough

$$\mathrm{V_{DD}} = \frac{m_1}{\rho_{DD}} \qquad \text{Eq. 3.3}$$

In addition, the volume of gas trapped inside the dough can be calculated by the following

$$V_{gas} = \frac{m_2 - V_{DD} \cdot \rho_{oil}}{\rho_{oil}} \qquad \text{Eq. 3.4}$$

The void fraction of the dough (dimensionless) was finally determined as follows:

$$\varepsilon = \frac{\mathrm{V}_{gas}}{\mathrm{V_{gas}} + \mathrm{V_{DD}}} \qquad \text{Eq. 3.5}$$

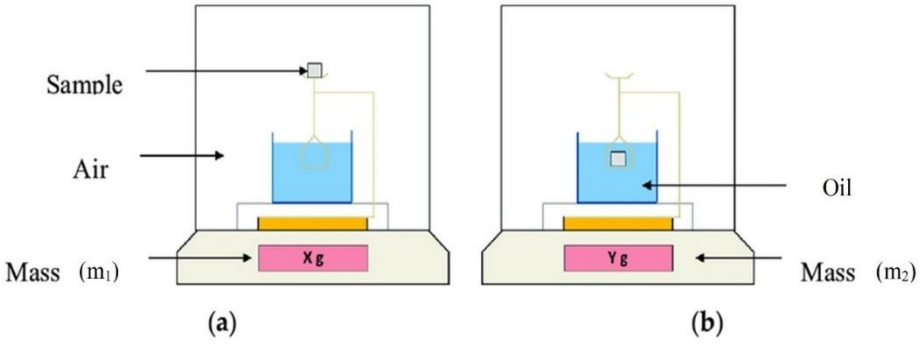


Figure 3.4. Principle of the test used to determine the void fraction in a dough sample. The measurement is based on Archimedes principle with (a) mass m_1 of the sample and (b) mass perceived when the dough sample was immersed in the colza oil. For after kneading, a dough piece of 30 g was considered, whereas after sheeting an entire piece of rolled/sheeted dough (150 g) was similarly considered

3.1.3.2. Determination of dough expansion ratio N in function of the initial and final dough void fractions after fermentation ε_I & ε_F

As mentioned previously, during the fermentation phase, a piece of 20 g of dough (done in duplicate) was installed in a cylindrical flask (internal diameter of 5 cm). The dough in the flask started at an initial height of H_I (around 1 cm) until reaching an expansion of a final height of H_F cm. The expansion ratio N was defined as the ratio of H_F to H_I and was tracked due to the vertical displacement of the disk contacting the upper dough surface in the flask. However, what is important is to reach the same void fraction in the dough before baking; this value was fixed at 0.75 based on the stated of the art. One point often omitted by bakers is that the expansion ratio needed to reach this value depends on the initial void fraction of the dough. The challenge lies in determining in advance the N value based on the initial height of the dough in the flask, on the initial void fraction of the dough ε_I and on the targeted dough void fraction at the end of fermentation ε_F. The solution was obtained from the following calculation. The values of the effective dough density were ρ_D and ρ_{DD} respectively. The H_I was the initial dough height before starting the fermentation. The initial apparent volume of the dough piece is (V_{DI}) with:

$$V_{DI} = V_{DD} + V_{GI} \qquad \text{Eq. 3.6}$$

For information, the volume V_{DD} of the degazed dough sample is detailed below (without the inserted void fraction):

$$V_D = \frac{m_D}{\rho_{DD}} \qquad \text{Eq. 3.7}$$

If we assume that the dough will expand by a ratio of N as shown in Figure 3.2, the final dough volume will be:

$$V_{DF} = V_{DD} + V_{GI} + (N-1) \cdot (V_{DD} + V_{GI}) \qquad \text{Eq. 3.8}$$

The initial void fraction of the dough is ε_I:

$$\varepsilon_I = \frac{V_{GI}}{V_{DI}} \qquad \text{Eq. 3.9}$$

And the final void faction in the dough is ε_F:

$$\varepsilon_F = \frac{V_{GI} + (N-1)\cdot(V_{DD} + V_{GI})}{V_{DD} + V_{GI} + (N-1)\cdot(V_{DD} + V_{GI})} \quad \text{Eq. 3.10}$$

By combining the 2 previous equations, in particular in replacing V_{GI} by $\varepsilon_I . V_{DI,}$ it comes:

$$N = \frac{(1-\varepsilon_I)}{(1-\varepsilon_F)} = \frac{H_F}{H_I} \quad \text{Eq. 3.11}$$

If one considers the height of the dough in the fermentation flask, with H_I and H_F being the initial and final height. As mentioned previously, it was hypothesised that ε_F was 0.75. Such value of void fraction is considered as a realistic value based on experience and was also mentioned by Vliet et al. (1992). By applying the previous equation with ε_I of 0.1 (a realistic value for a conventional dough mixer) and ε_F of 0.75, an N value of 3.6 is obtained, which is also a realistic value. These examples validate the applicability of the N equation. With a value of ε_I of 0.2, which can easily be obtained in the pressure mixer, the N value will turn to be 3.2 instead of 3.6. This example emphasized on the importance of adjusting the expansion ratio based on specific dough void fraction to ensure consistency in final product features, as shown in Figure 3.5.

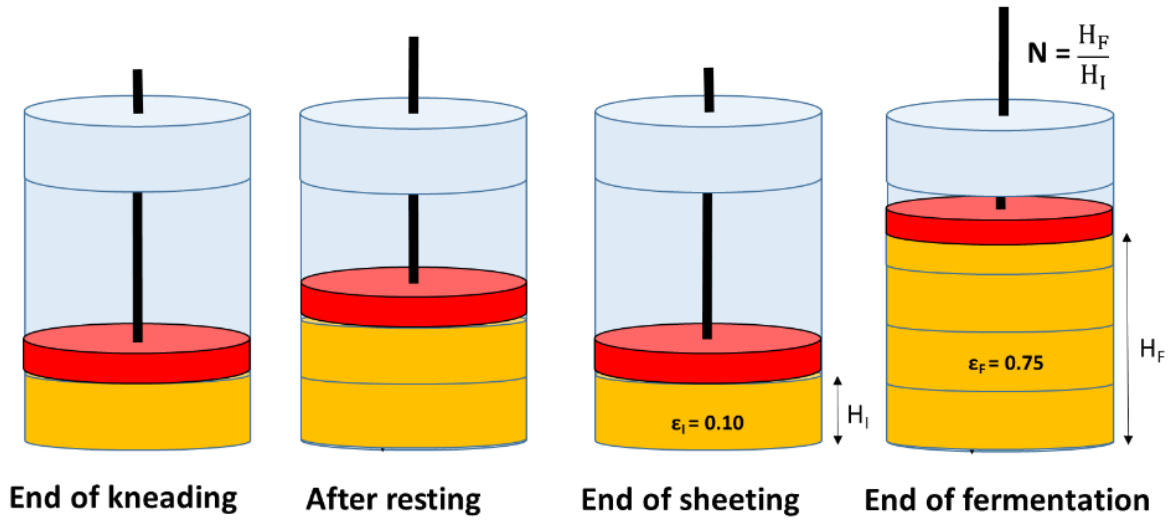


Figure 3.5. Illustrations of the evolution of the dough's void fractions during fermentation in a flask. The expansion ration N depends on the initial dough void fraction; it should be around 3.6 to reach 0.75 in the case of an initial void fraction of 0.1

As a consequence, the final fermentation time was not fixed as it appears in almost all papers on baking. The final fermentation time was function of the dough performance needed to reach the computed N value, which was supposed to yield in a final void fraction of 0.75.

The accuracy of fermentation modelling relies heavily on precise volume measurements, particularly when tracking dough expansion in the fermentation flask, in a precise determination of the initial height of the dough piece installed in the flask. In cylindrical fermentation flasks, theoretical models typically assume full adhesion of dough to the vessel walls. However, in practice, the expansion behaviour often reveals a discrepancy, leading to earlier termination of fermentation and possible misinterpretation of gas production. This aspect will be discussed in the results and discussion section.

3.1.3.3. Bread baking and determination of bread properties

Once the fermentation was achieved (reaching a predetermined N value), the fermented dough were baked in a MIWE deck oven (CO 1.1208 oven - Germany) at 230°C for 17 min. Around 300 mL of water was injected in the steam box at start of baking to facilitate the oven rise. After baking, the breads were allowed to cool for about 1 h before measuring its properties, packed in standard food grade plastic polyethylene bags (domestic freezer bags) with a double zip-lock providing an airtight sealing to maintain freshness.

3.1.3.4. Determination of breads specific volumes (SV)

After baking and cooling down for 1 h, a TexVol BVM-L370LC volumeter was used for measuring the breads specific volume. The Volcalc software was used to run the equipment, determining volume, weight, density, shape ratio (height / width), and displaying a three-dimensional image of the bread sample.

3.1.3.5. Determination of the breadcrumb aeration

Image analysis was used to evaluate the crumb microstructural characteristics of the final product crumb (Falcone *et al.* 2008; Rathnayake, Navaratne and Navaratne 2018). This technique highlighted on the bubbles characteristics and behaviour and the most common features to be analysed mainly cell size, cell size distribution, and number of cells per unit area, cell wall thickness, and finally void fraction ε_C of the crumb (Falcone *et al.* 2008; Rathnayake, Navaratne and Navaratne 2018). After cooling, breads are sealed and stored for 1 day at 4°C then cut into 1.8 cm thick slices and a slice from the middle of the bread loaf was scanned on a flatbed scanner (4800 x 9600 dpi hardware resolution HPScanjet G4010 – HP-USA). The scanned images were analysed using ImageJ software. Images were cropped to different field of view (FOV) as each bread mixed with different mixing parameters have different slice size and form. Image processing includes several actions including choosing a global scale for all the images based on pixels/mm-based unit and then a threshold was fixed for all the images giving a well observation of the gas bubbles and thus, eliminating unwanted ones. After the images were treated, data was collected about the number of cells and their respective mean area. Cells were divided into 2 populations, D50 (median) and D90 (90% of pores lie below this size).

3.1.4. Statistical analysis

Data were analysed using Statgraphics 19 – X64 software using one-way ANOVA and Tukey test. $P < 0.05$ was considered significant. Dough fermentation flasks were duplicated and 9 breads were baked for each condition and averaged.

3.1.5. Results & discussion

3.1.5.1. Determination of the dough optimum mixing time (t_{PEAK})

Doughs t_{PEAK} were therefore determined at different mixing speeds and pressures considering air and CO_2 as headspace gases. According to Figure 3.6, the mixing is carried out in the time interval (0 –

3 min) and corresponded to the homogenization of the dry and wet ingredients. The duration of this stage was not accounted in the t_{PEAK}. Following the mixing stage, the tool speed was increased and the mechanical energy consumed by the dough increased with the mixing time until reaching a maximum, where the dough had maximum viscoelastic properties – the kneading phase (Lancelot *et al.* 2021). After t_{PEAK}, a significant decrease in the power consumed was observed at over-mixing.

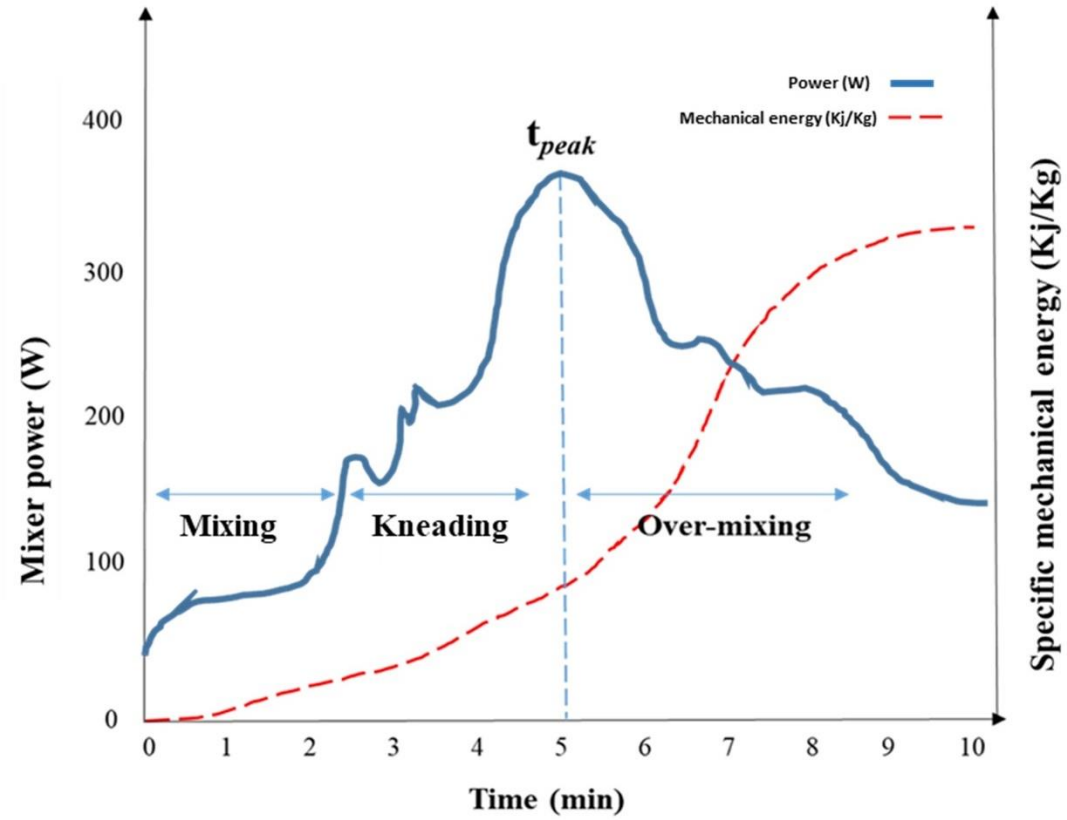


Figure 3.6. This curve shows an exact representation of the evolution of the power of the mixer and the specific mechanical energy consumed by the dough during the mixing, kneading and over-mixing and the t_{PEAK} attained during the kneading phase

The t_{PEAK} values corresponding to different kneading speeds were determined through preliminary trials conducted without gas injection during mixing. Based on the tests, 150 RPM offers a balance between mixing time and dough development, allowing the dough to reach its peak consistency quickly while minimizing the risks of over- or under-mixing. Therefore 150 RPM was considered at follow. The t_{PEAK} was determined using power data recorded by the VMI mixer during the kneading phase, excluding the initial pre-mixing steps. Tool power and satellite power were measured at 1 Hz, and dough power was calculated as their differences. To minimize noise, a moving average of 30 consecutive readings was repeatedly applied to smooth the power curve. The resulting smoothed power curve was then used to identify the dough development time, t_{PEAK}, defined as the point of maximum power consumption during the kneading phase. A quadratic polynomial regression Power $P(t) = a \cdot t^2 + b \cdot t + c$ was fitted to the smoothed data around this maximum. The vertex of the polynomial provided a more precise and robust estimation of t_{PEAK}. t_{PEAK} is important to determine since it accurately provides how much mixing time is needed and to avoid over or under-mixing.

3.1.5.2. Determination of the dough void fraction ε after mixing, sheeting & fermentation

The void fraction of the dough was tested according to different gas pressure levels during kneading (Air (0 bar) and CO_2 (0 bar): atmospheric pressure & Air (0.5 bar) and CO_2 (0.5 bar): 0.5 bar gauge pressure). Kneading was carried out at the previously determined t_{PEAK}. Table 3.3 lists the values of the void fraction of the dough after kneading, rolling and fermentation. Theoretical N values were calculated based on equation (11) based on the initial void fraction ε_I values after sheeting. The dough void fraction at the end of fermentation was measured with a full piece of dough (300 g dough stick) which was kept in a rolled piece of plastic net. The plastic net and the dough stick were then immerged in an oil bath as explained previously. The plastic net was previously tared (when immerged in the oil bath) and was needed to prevent dough floating in the oil bath. Its diameter was adjusted to the dough piece at the time of measurement.

Table 3.3. Impact of gas-pressure mixing on the measured dough void fractions and the evolution of this parameter during the mixing stage, sheeting and fermentation. Values with different superscript lowercase letters in the same column for each condition are significantly different ($p < 0.05$)

Conditions	ε'_I end mixing	ε_I after sheeting	ε_F end fermentation	N theoretical to reach $\varepsilon_F = 0.75$	Fermentation time
Air (0 bar)	0.13 ± 0.01^{a}	0.23 ± 0.02^{c}	0.57 ± 0.05^{a}	3.08 ± 0.07^{a}	1h15min
CO_2 (0 bar)	0.15 ± 0.07^{b}	0.19 ± 0.01^{ab}	0.58 ± 0.02^{a}	3.24 ± 0.03^{bc}	1h30min
Air (0.5 bar)	0.17 ± 0.01^{c}	0.20 ± 0.02^{bc}	0.64 ± 0.00^{a}	3.20 ± 0.06^{ab}	1h45min
CO_2 (0.5 bar)	0.23 ± 0.04^{d}	0.16 ± 0.02^{a}	0.60 ± 0.00^{a}	3.36 ± 0.06^{c}	2h

A first comment about this table is that the final dough void fraction of the dough did not reach the expected 0.75 value despite the computed N value was applied. Based on the values presented in the table above, the initial void fraction ε'_I at the end of mixing, at 0 bar mixing was higher with CO_2 injection than that without air-mixing (0.15 & 0.13 respectively). A similar trend was observed between mixing with CO_2 and air at higher pressure (0.5 bar gauge pressure). ε_I with CO_2 after mixing (0.23) was higher than the dough mixed with air (0.17). It was clear that mixing at a pressure above atmospheric pressure increased the dough aeration. (Chiotellis and G. M. Campbell 2003) reported that at low mixing pressures (low air content) the mass transfer rate within the relatively small number of bubbles is much slower. On the contrary, higher mixing pressure increased the number of bubbles, resulting in an initial increase in the CO_2 mass transfer rate within the bubbles, slowing down the accumulation of CO_2 into the liquid phase of the dough (Chiotellis and G. M. Campbell 2003). Martin et al, (2008), investigated the impact of controlled atmosphere on dough aeration under air & CO_2 (Martin *et al.* 2008).

Sheeting helps to divide large gas bubbles in the dough and ensures that the bubbles are evenly distributed throughout the entire piece of dough thus, a finer breadcrumb structure upon baking (Qi *et al.* 2008). After sheeting, a higher void fraction was observed under air at atm. pressure & 0.5 bar gauge pressure (0.23 & 0.20 respectively) than that with CO_2-mixing (0.19 & 0.16, respectively). These observations could be explained by the fact that sheeting removed a great amount of gas bubbles

formed during the mixing stage with CO_2 and the ones mixed with air are higher due to the presence of oxygen that helps to form and stabilize more disulfide (SS) bridges, which are the building units of a stable gluten network. According to literature, O_2 present in air and the O_2-enriched atmosphere helps in the oxidation of thiol (SH) groups and the more SH groups are oxidized the more SS bridges are formed and the more the gluten network is stable and thus more aeration or gas bubbles are retained (Chiotellis and G. M. Campbell 2003; Martin *et al.* 2008).

The fermentation process, as a link between kneading and baking, is a crucial step in the bread making process (Verheyen *et al.* 2015). During fermentation, the catalytic activity of yeast initiates a cascade of reactions that impart a great role in the dough aeration and expansion. This expansion is a result of the solubilisation of CO_2 by-product of yeast fermentation of glucose (Kulp and Lorenz 2003). Based on the values in Table 3, the final void fraction at the end of fermentation were higher at 0.5 bar gauge pressure than that at atm. pressure for air & CO_2 even though the observed differences were not significant. Comparing the values at 0.5 bar gauge pressure, it was lower with CO_2 maybe because of the loss of gas bubbles during sheeting. There is a link between the void fraction after sheeting and after fermentation, a high void fraction after sheeting leads to a higher void fraction at the end of fermentation, which was observed in the case of air. The CO_2-mixed dough at 0.5 bar gauge pressure resulted in the longest fermentation time (highest N value N = 3.36), but did not give the highest final void fraction ($\varepsilon_F = 0.60$) indicating that prolonged fermentation with CO_2 might hinder the yeast activity or compromise the gluten network integrity. Conversely, at the same pressure with air-mixed dough, the highest final void fraction ($\varepsilon_F = 0.64$) which was reached with faster fermentation time than that with CO_2. This suggests that although CO_2 slows down fermentation, it does not inherently improve the structural expansion of the dough, meaning that air with higher pressure is the optimal condition for achieving a balance between fermentation duration and dough aeration.

3.1.5.3. Determination of the dough expansion ratio N in real conditions

The important difference between the final dough void fraction and the expected one (0.75) required an explanation. An explanation lies in the fact that our computation of N is based on the assumption that the dough will fully occupy the flask interior during fermentation. In practice, a non-negligible gas pocket is present along the corners of the flaks and also along the disk contacting the upper surface of the dough piece as shown in the figure below.

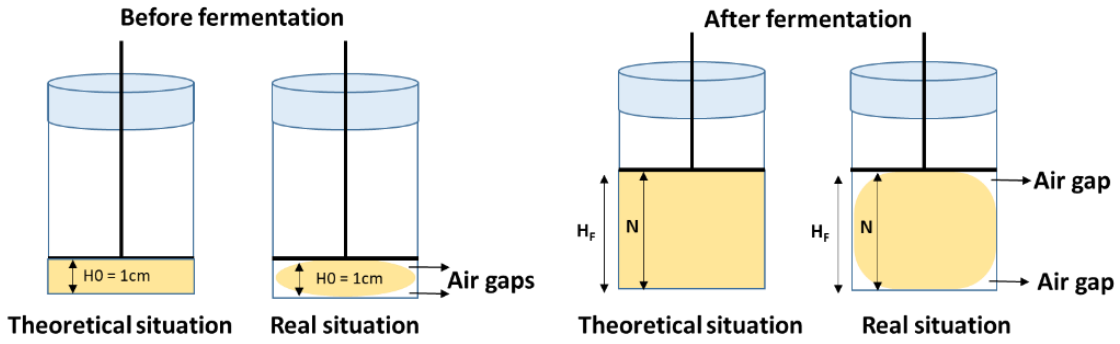


Figure 3.7. Theoretical vs. real dough profiles in the cylindrical flask

These air gaps or air pockets yields in a significant artefact on the accuracy of the N value determined by our model based on initial and final dough void fraction. As an illustration, let us consider a case

with a dough sample of 20 cm^3 with and initial void fraction of 0.1. Let us assume that 20% of the apparent dough volume (4 cm^3) corresponds to the air pockets located around the dough piece. Assuming a fermentation flask of 5 cm internal diameter, this will yield in an initial height of 1.22 cm (instead of 1.02 for perfect dough installation). The expansion ratio needed to reach a final void fraction of 0.75 is N = 3.6 for a perfect dough installation. Applying the same expansion ratio (N = 3.6) to the dough installed with air pockets will result in a final void fraction of 0.782 instead of 0.750 (+ 4.2%). Applying an N value of 3.18 instead of 3.6 for the imperfect dough installation will result in a final void fraction of 0.75. As a conclusion, the observed difference between the expected final void fraction of 0.75 and the effective void fraction shown in Table 3 (in the range of 0.6) cannot be explained by the imperfect installation of the dough in the fermentation flasks. Other source of explanation could be:

- The fact that gas nuclei are subjected to pressure during dough sheeting/rolling, results in an inaccurate determination of the initial dough void fraction at start of final fermentation. However, this would yield in a lower value of initial void fraction (compressed gas cells) and consequently, an overestimated N value. Therefore, it does not bring support to our observations.
- Hydrostatic effect of the immersion of the dough stick in oil, resulting in a compression of the dough stick and in a lower dough void fraction. In particular, the dough stick may have a lower density than the oil (the dough pieces were floating at around 0.3 void fraction) and was then compressed against the upper surface of the cylindrical plastic net used to maintain the dough stick. This brings to the same conclusion as previously.
- Temperature difference between the fermented dough (30°C) and the oil bath (20°C) resulting in a contraction of the gas cells at the surface of the dough stick. This brings to the same conclusion as previously.
- A final and most likely explanation could be that the time elapsed between the dough sheeting, sampling of the dough piece, and its installation in the fermentation flask resulted in a more aerated dough piece. These factors led to an inaccurate determination of the initial height of the dough piece installed in the fermentation flask, and in turn in caused an incorrect detection of the end of fermentation based on the computed N value.

To overcome this situation, alternative routes must be considered like:

- To compute the theoretical value of the dough height based on its initial void fraction and on the percentage of air pocket, which can be computed based on its mass.
- Image analysis using AI may also solve such issue and progressive training with artificial neurone network that will be trained by successive experiments.

3.1.5.4. Determination of bread specific volume SV

Based on our results in Figure 3.8, the highest values were observed with mixing under air at 0.5 bar gauge pressure (4.54). However, lower SV was observed with CO_2 at atm pressure & 0.5 bar gauge pressure (4.39 & 3.55, respectively) due to the sheeting process, which caused a large escape of the formed gas bubbles during mixing and resting. Breads mixed with CO_2 gave low SVs due to the collapsing of the upper crust of the loaves during baking. This phenomenon could be explained by the fragile gluten network or by an excess of injected CO_2, hence, depriving the gluten network of O_2, which is an essential contributor to the gluten network formation (Martin *et al.* 2008).

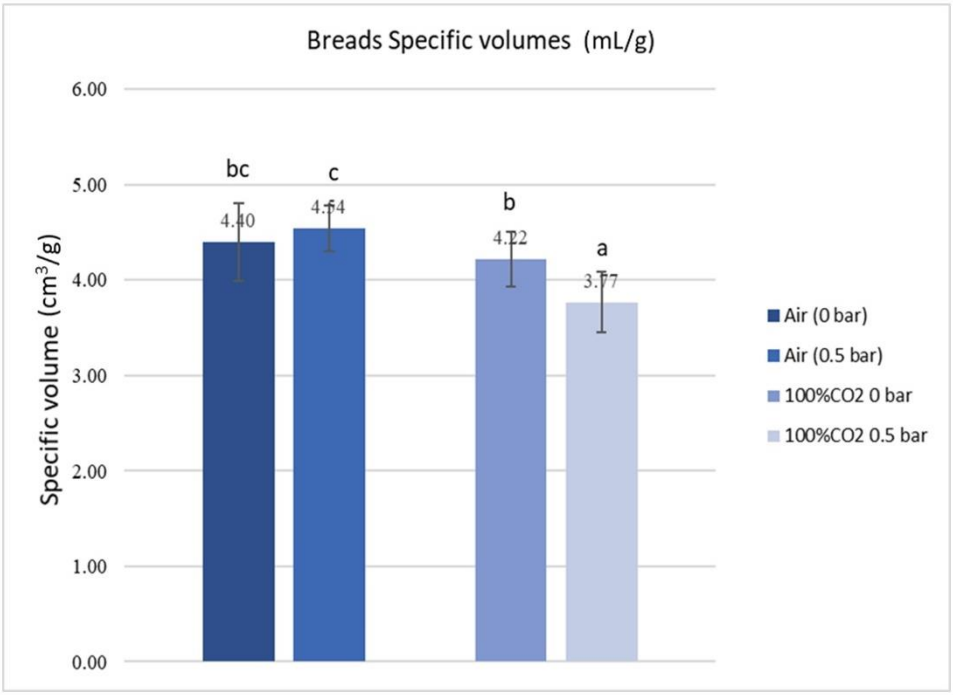


Figure 3.8. Bread loaves specific volumes under the different mixing parameters

A possible explanation could be due to over-expansion and bubble instability, could lead to weaker bubble walls, causing more collapse during baking, which reduces specific volume. This instability is related to the collapse of the gluten-starch matrix surrounding the individual gas bubbles due to the excess production of CO_2 toward the end of the fermentation phase and early baking (Mills *et al.* 2003; Sun, Martin Scanlon *et al.* 2023; Wilde 2012). The CO_2 generated by yeast fermentation and injected CO_2 dissolve into the aqueous phase of the dough surrounding the gas bubbles until saturation is reached, after which CO_2 diffuses into the nucleation cells by gradient concentration through Young-Laplace equation, raising the internal bubble pressure. According to Shah et al. (1998), gas stability depends on the strength and elasticity of the gluten network, which forms thin film layer around gas bubbles that assist in resisting this internal pressure. However, when this network is weakened and not well developed, the matrix loses its elasticity and strength, thus reducing its ability to resist internal pressure (Sroan, Bean and MacRitchie 2009). One logic explanation of this weakness besides deprivation from O_2, due to excess fermentation metabolites (succinic acid, ethanol, etc.). As a result, the gluten could not retain the excess internal pressure coming from both sources of CO_2, leading to overstretching and rupture of gas bubbles.

3.1.5.5. Determination of the breadcrumb structure

Based on Figure 3.9, among the mixing parameters presented above, breads mixed with CO_2 at atmospheric pressure gave the widest pore size distribution range in comparison to the rest conditions, thus reflecting larger pore size. There was no significant different between the cumulative pore size distribution range of the reference (air-mixed) breads, thus they showed the lowest distribution pore size range. From this point, pore size distribution was influenced by mixing conditions such as nature of mixing gas and pressure level.

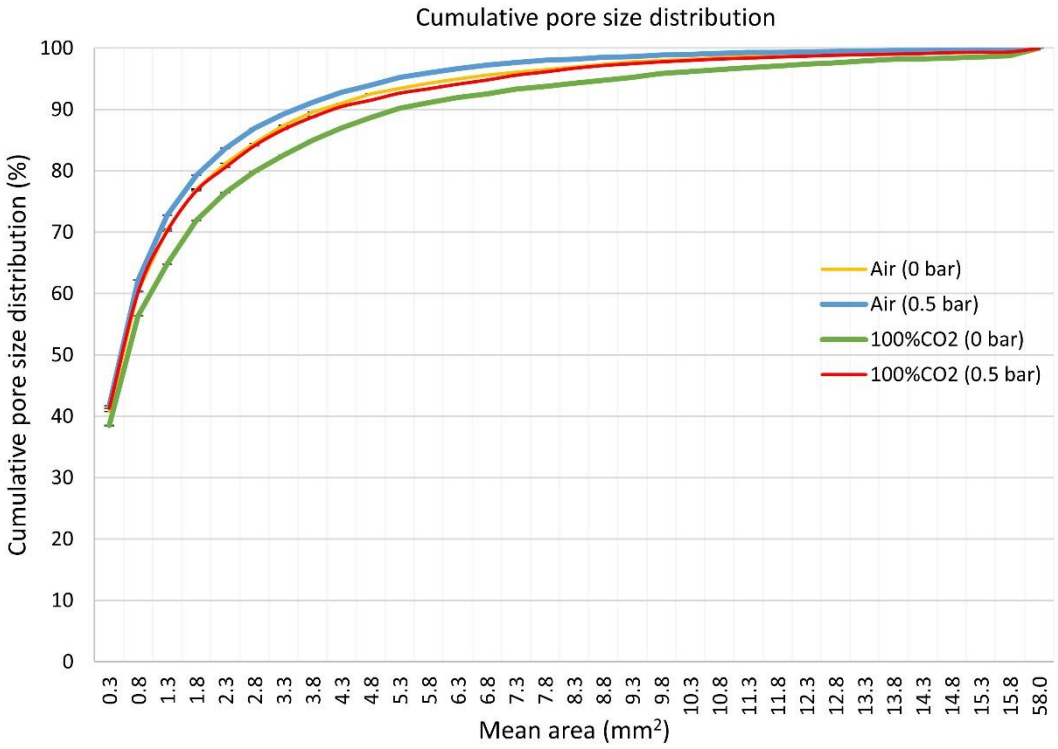


Figure 3.9. Cumulative pore size distribution for breads mixed under different mixing parameters

The Table 3.4 below presents the D50 (median) and D90 (90% of pore size lie below), which quantitatively supports the pore size for each condition. The median pore diameter (D50) was found to be close to the lower detection limit of the measurement method, suggesting that most pores fall within the smallest detectable size range of the imaging system. Breads mixed with CO_2 have a median pore size D50 for atmospheric pressure & 0.5 bar gauge pressure (0.57 & 0.59 respectively) higher than those mixed with air at both pressure levels (0.49 & 0.38 respectively). However, the lowest value was scored for air-mixed bread at 0.5 bar gauge pressure reflecting finer breadcrumb structure. Referring to the same table, there is statistical significance between all samples for D90 pores size ($p < 0.05$). For CO_2 at 0.5 bar gauge pressure, 90% of pores population had a pore size below 6.98 mm^2, which was the highest among all conditions, and for the air-mixed breads at 0.5 bar gauge pressure 90% of pore population had a pore size below 3.23 mm^2, which was the lowest value. In accordance to our results, a study conducted by Martin et al. (2008) , where this paper attempted to control crumb structure by mixing air and CO_2 in a variable modified atmosphere. In particular, this study examined whether the benefits of partial vacuum mixing can be replicated by mixing under a CO_2 atmosphere in the final stage. Based on the results of this study, mixed under air, the crumb cell structure becomes coarser as the pressure increases (0.3 to 2.0 bar). When mixed under CO_2, the crumb structure appears coarser over the entire range, but especially at lower pressure.

Table 3.4. Effect of different pressure mixing on D50 and D90 values of crumb microstructure. Values with different superscript lowercase letters in the same column for each condition are significantly different ($p < 0.05$). The values presented here are mean ± standard deviation

Samples Gauge pressures	Median pore size D50 (mm^2)	Pore size D90 (mm^2)
Air (0 bar)	0.49 ± 0.04^{b}	3.94 ± 0.23^{b}

Air (0.5 bar)	0.38±0.05[a]	3.23±0.23[a]
CO_2 (0 bar)	0.57±0.09[c]	5.20±0.62[c]
CO_2 (0.5 bar)	0.59±0.06[c]	6.98±1.10[d]

A foam goes through two basic stages: formation and stability (Wilde 2012). By definition, foam is a suspension of gas bubbles in an ongoing liquid phase, and in the case of bread can be a solidified foam due to baking (Wilde 2012). In the case of CO_2, the gluten network was deprived from an O_2 source, hence less stable gluten network leads to bubbles instability (Martin *et al.* 2008). As mentioned in previous parts, the catalytic activity of yeast initiate a cascade of reactions that impart a great role in the dough aeration and expansion during the fermentation period. This expansion is a result of the solubilisation of CO_2 by-product of yeast fermentation of glucose (Kulp and Lorenz 2003; Mills *et al.* 2003; Wilde 2012). Therefore, mixing under pure CO_2 in addition to the yeast fermentation, excess CO_2 will be produced and thus less gas bubbles will be available to act as nucleation sites. A study conducted by Martin *et al*. (2008), where this paper attempted to control crumb structure by mixing air and CO_2 in a variable modified atmosphere. In particular, this study examined whether the benefits of partial vacuum mixing can be replicated by mixing under a CO_2 atmosphere in the final stage (Martin *et al.* 2008). Based on the results of this study, mixed under air, the crumb cell structure becomes coarser as the pressure increases (0.3 to 2.0 bar). When mixed under CO_2, the crumb structure appears coarser over the entire range, but especially at lower pressure. The results showed that mixing solely under pure CO_2 is unlikely to produce an acceptable bread structure.

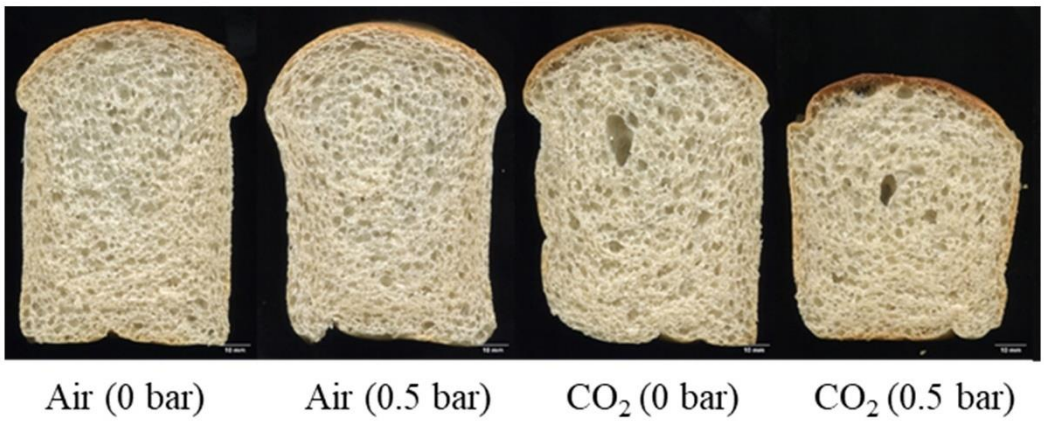


Figure 3.10. Scanned images of bread slices mixed under Air and CO_2 at atmospheric pressure and 0.5 bar gauge pressure with a scale of 10 mm for each treated image

Finally, Figure 3.10 represents the scanned images showing the ones mixed under CO_2, a smaller bread scan was observed at 0.5 bar gauge pressure reflecting the lower SV values due to the collapse of the dough during the baking stage, also, larger pores were observed on the scanned slices. Scanned slices for air breads showed a homogenous breadcrumb structure.

3.1.6. Conclusion

This study investigated the impact of pressure mixing and of two gases (air and CO_2) on dough and bread properties as well as fermentation duration. The results showed that mixing under higher mixing pressure (0.5 bar gauge pressure) significantly increased the initial void fraction of the dough after

mixing, particularly with CO_2. The optimum conditions for dough development depend on the used gas and pressure. For air, mixing at high pressure (0.5 bar gauge pressure) gave higher final void fraction $\varepsilon_F = 0.64$ with relatively shorter fermentation time than CO_2 at 0.5 bar gauge pressure. This condition is optimal for achieving bread with higher specific volume and finer breadcrumb structure.

In contrast, with CO_2 at 0.5 bar gauge pressure resulted in longer fermentation time (N = 3.36) with lower final void fraction $\varepsilon_F = 0.60$, likely due to gas bubbles loss during sheeting and possible yeast inhibition due to overwhelming CO_2 atmosphere in the dough. Thus, with CO_2 under high pressure dough expansion and fermentation were not very efficient.

Therefore, air mixing at higher pressure represents the condition for balancing fermentation duration and dough aeration to maximize the final bread. Future process optimization with CO_2 may require adjustment of fermentation parameters or dough formulation to overcome these challenges. Our additional findings suggest that while conventional fermentation relies on the yeast natural CO_2 production, direct CO_2 injection during mixing, offers an alternative means of improving dough aeration, especially if we consider of reducing the yeast concentration, which can further enhance gas retention and improve crumb structure. This alternative strategy may provide a better control over dough aeration and fermentation, and thus could be a potential for future process optimisation in baking industries.

Nevertheless, the stability of gas bubbles and strength of the gluten network were pivotal in determining the dough's development and its performance during the baking phase. A major novelty lies in a computation of the expansion ratio needed to reach a certain final void fraction before baking in function of the initial dough void fraction. In addition, the impact of imperfect dough installation in a fermentation flask has been investigated showing that a correction must be brought to the effective expansion ratio. Our results suggest that fermentation time and void fraction are interdependent, requiring adjustments based on aeration conditions; meaning mixing at atmospheric pressure resulted in shorter fermentation times but lower final void fractions. Meanwhile, mixing at 0.5 bar produced finer breadcrumb structures with smaller pore sizes, improving textural uniformity. These observations emphasize the importance of controlling pressure during mixing, in particular in the case of innovative mixer able to mix dough under pressure with non-conventional gases, to achieve a balance between aeration and final bread quality.

By systematically adjusting fermentation conditions, this study contributes to the optimization of bread making processes, improving both efficiency and product quality in the case of non-conventional mixing processes. Future research could explore the role of gas composition beyond air, including oxygen and carbon dioxide-enriched environments.

One major limitation encountered with the fermentation flask setup was the persistent presence of gas bubbles at the bottom of the flask that appear during the fermentation and other artefact as discussed, which introduced inaccuracies in assessing the true dough expansion value. To address this, future work will implement an alternative calculation model that compensates for or eliminates the effect of these gas bubbles. This improved model will then be integrated into the expansion ratio calculations to enhance the accuracy and reliability.

3.1.7. References

References are placed at the end in the References section p.236.

3.2. Part II – Dough results for all gas mixtures with the addition of ascorbic acid AH_2

This chapter presents the experimental findings designed to evaluate the influence of gas composition during kneading and oxidative supplementation on dough development and dough properties. Oxidative supplementation can be obtained by increasing the O_2 partial pressure in the mixer's headspace and/or by adding AH_2 in the dough formulation. The mixing protocols are reminded below:

As mentioned, the doughs were prepared considering the injection of three different gas and gas mixes with the following protocols as well:

- Air
- 100%CO_2
- 30%O_2 and 70%N_2 mixture

We applied two mixing protocols A at 0.5 bar gauge pressure with partial vacuum and Protocol B at 0.5 bar gauge pressure with full vacuum.

The level of oxygen in the 30%O_2 and 70%N_2 mix was set at 30% based on Buche work. Personal contacts with Air Liquide Company (taken after the tests) yielded in the fact that this percentage should be considered as a maximum due to explosion risk that could be initiated by static electricity accumulation in the flour particles or other external source resulting in explosion ignition. All these gaseous conditions were tested without and with the addition of AH_2 in the dough formulation, which is known to contribute to the dough development. A dosage of 70 ppm corresponding to the levels used in the baking industry was adopted. This dosage was not optimised.

Central to this investigation is the solubility of gases in bread dough primarily O_2 and CO_2 that are the most soluble gases in dough due to the aqueous environment. To quantify this, the amount of each gas (number of moles) present in the mixer headspace was first calculated based on partial pressures resulting from the way the mixer was operated. In addition, the evaluation of how much O_2 and CO_2 could be absorbed by the dough during mixing was quantified. During mixing, O_2 is solubilized in the liquid phase and trapped in gas bubbles of the dough; part of it is consumed by the chemical reactions in link with the dough development (gluten network polymerisation). CO_2 is also solubilized in the liquid phase and trapped in gas bubbles of the dough and may contribute to the onset of dough fermentation; indeed, during fermentation, the yeast works in anaerobic conditions and produces mainly CO_2 and ethanol which progressively reach a saturation level in the liquid phase resulting in the expansion of the gas bubbles entrapped in the dough. It can be assumed that having the dough already saturated at the end of mixing may have an impact on the kinetics of dough fermentation and on the cellular structure of crumb; this covers the concept of "dough stabilisation by CO_2 solubilisation".

An important point concerns the partial pressure of each soluble gas. We focused on the number of moles available in the headspace, but the partial pressure of those gases also very important to consider; indeed, the concentration of a given gas species that can be solubilized in the dough, with water being mainly concerned, is proportional to the partial pressure of the gas in the headspace.

An important point concerns the partial pressure of each soluble gas. We focused on the number of moles available in the headspace, but the partial pressure of those gases also very important to consider. Indeed, the concentration of a given gas species that can be solubilized in the dough, with water being mainly concerned, is proportional to the partial pressure of the gas in the headspace as shown by the Henry's law, which is reminded below:

$$C_\infty = \frac{P_\infty}{H} \qquad \text{Eq. 3.12}$$

where C_∞ is the concentration of the solubilized gas in the liquid phase, P_∞ is the partial pressure in the gaseous phase (dough's head space or inside the gas nuclei embedded in the dough) and H is the Henry constant. Depending on the source, this constant is referred also to K_H or K_c based on Bein Aissa et al. (2010) for example. The unit of the Henry's coefficient is in Pressure / concentration. The concentration is provided as a mole ratio (most frequent) or as a mass ratio. Some functions are available to accommodate the impact of temperature on the Henry's coefficient.

A special attention should be drawn to the case of O_2; beyond the simple solubilisation in the liquid phase of the dough, this gas is consumed by a cascade of chemical reactions as presented in the state of the art. As a consequence, no saturation is reached *a priori* during mixing and we took care about determining if there was enough O_2 in the mix of gas present in the mixer's headspace.

The overall dough preparation process was inspired from industry conditions and encompassed a rest period, a sheeting-rolling step, which was adopted for most cases. Some tests were also done without this step. A final fermentation, also named proving in some technical documentation of the baking process, was applied to reach a certain void fraction before switching to the baking phase. The obtained bread will be presented in the following chapter.

This part of the chapter is divided into 3 main parts:

- Part A: O_2 consumption and CO_2 solubility in dough
- Part B: Main mixing tests and dough results
- Part C: Effect of sheeting and additional analysis

The core section (Part II) covers the impact of varying gas-injection composition with and without the addition of AH_2 under both protocols on the dough mixing parameters namely t_{PEAK}, SME, dough void fractions after kneading, sheeting and fermentation kinetics. The part III covers additional tests, which were conducted including impact of sheeting and no sheeting process on dough void fractions, pH measurement before and after fermentation and dough rheology after kneading.

3.2.1. Part A: O_2 consumption and CO_2 solubility in dough

3.2.1.1. Determination of the partial pressures of the different gases in function of the protocols

Two main factors influence the solubilisation of gases within the dough matrix, or, in the case of oxygen, its consumption: (i) the number of moles available in the headspace gas, and (ii) the partial pressure of gaseous component. The Table below summarizes the expected partial pressures under the different experimental conditions. For Protocols A and B, the actual gas composition within the mixer headspace was not directly monitored.

In the mixing stage, it was assumed that the entire headspace volume of the mixer was replaced by the injected gas. Consequently, the partial pressures at the end of pre-mixing were added to the pressure contributed by the injected gas to attain the targeted pressure conditions for the mixing and kneading phases.

For the kneading phase, two particular situations were considered:

- Under **Protocol A at atmospheric pressure**, the injected gas continuously flowed into the mixer headspace. It was therefore assumed that the injected gas represented the total headspace composition.
- Under **Protocol A at 0.5 bar gauge pressure**, the exhaust valve was closed during kneading, consequently, the gas composition established during this phase was assumed to persist throughout kneading.
- Under **Protocol B**, the injected gas continuously flowed into the mixer headspace, leading to the assumption that the injected gas alone determined the headspace composition.

By comparing Protocol A atmospheric pressure with air and Protocol A 0.5 bar with 30%O_2, the increasing oxygen concentration to 30% resulted in substantial increase in the oxygen partial pressure (+114%).

Comparing mixing with 100%CO_2 with Protocol A and B at 0.5 bar gauge pressure, oxygen partial pressure did not change between these two conditions.

Comparing Protocol A with air and Protocol B with 30%O_2 at 0.5 bar gauge pressure, revealed also no change in oxygen partial pressure.

3.2.1.2. Determination of O_2 consumption by the dough during the kneading phase: A vs. Protocol B

The partial pressure of gases in the mixing environment especially O_2 influence the extent of gas dissolution in the dough. We did not do any focus on the solubility of O_2 in water or in the liquid phase of the dough. In fact, during mixing, the di-oxygen will be consumed during dough development, thereby impacting oxidative reactions and dough structure formation. It is likely that no saturation is obtained and there is no real interest to focus on O_2 solubility as such.

To apply this framework to our work, we first considered typical O_2 consumption rates from prior studies considering (Buche 2011) as a reference since no other studies were found. Buche determined the consumption of yeasted dough. The graph below, already shown in Chap 1 was analysed. Between 130 and 600 s of kneading (an interval of 8.3 min), the dough consumed approximately 3.5 µmol of O_2 per g of dry flour (µmol·g_{DF}^{-1}). This rate was then applied to the conditions of the current project to estimate the consumption rate of O_2 by the dough. This assumption provides a reasonable basis for comparison, particularly given similarities in mixing duration and dough formulation between Buche's study and our study.

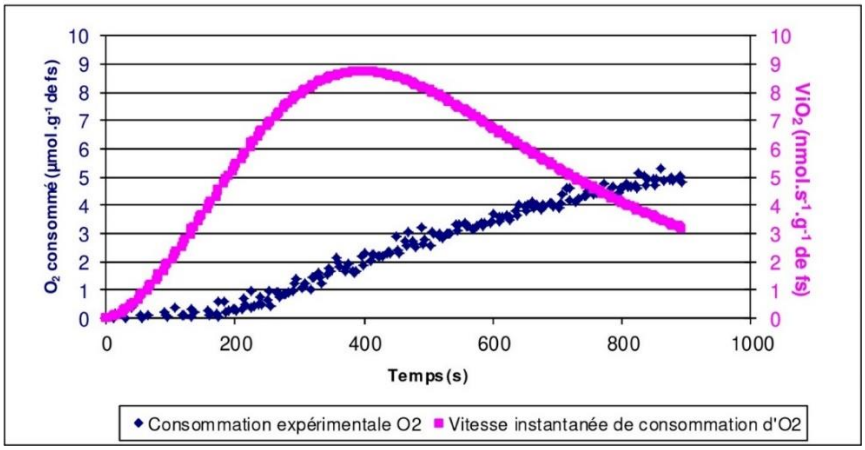


Figure 3.11 O_2 consumption and instantaneous O_2 consumption rate (ViO_2) by the dough during kneading (1% dry yeast) (Buche 2011)

Therefore, based on the calculations below, the rate of O_2 consumption rate would be:

$$O_2 \text{ consumption rate } = \frac{3.5\ \mu\text{mol} \cdot g_{DF}^{-1}}{(600-130)s} = 7.44 \cdot 10^{-3}\ \mu\text{mol} \cdot g_{DF}^{-1} \cdot s^{-1} \qquad \text{Eq. 3.13}$$

Taking into consideration that the VMI headspace mixer has internal volume of V_{HS} = 27 L, and the dough prepared of 3 kg of dough with gas-free dough density ρ_{DD} = 1250 kg·m^{-3}, the degassed dough volume represents:

$$V_{dough} = \frac{m_{dough}}{\rho_{DD}} = 2.4\ L \qquad \text{Eq. 3.14}$$

The remaining net headspace volume (V_{HS-NET}) Figure 3.12:

$$V_{HS-NET} = 27 - 2.4 = 24.6\ L \qquad \text{Eq. 3.15}$$

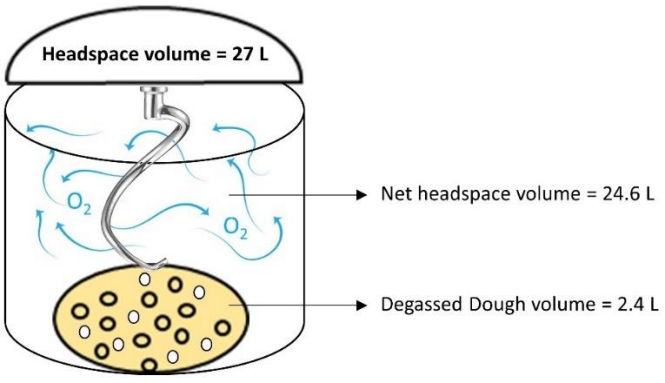


Figure 3.12 Schematic illustration of the VMI headspace volume showing the net volume occupied by the gas inside the headspace

By applying the ideal gas law, with atmospheric pressure (1 atm = 101325 Pa), with dough temperature in the mixer 25°C (298 K), where the O_2 has the partial pressure of P_{O2} = 0.21 atm = 21273 Pa, the number of moles of O_2 available in headspace would then be:

$$nO_2 = \frac{P \cdot V}{R \cdot T} = \frac{21273}{8.314 \cdot 298} = 0.211\ mol \qquad \text{Eq. 3.16}$$

With R is the ideal gas constant (8.314 $J \cdot mol^{-1} \cdot K^{-1}$), T is temperature in Kelvin (K), P is pressure of the gas (Pa) and V is the volume of the gas (m^3).

The dough contains 0.52 g of dry flour per gram of dough; this yield in an O_2 consumption rate per gram of dough of:

$$O_2\ consumption\ rate = 7.44\ \cdot 10^{-3}\ \cdot 0.52 = 3.874\ \cdot\ 10^{-3}\ \mu mol \cdot\ g_{DOUGH}^{-1} \cdot s^{-1} \qquad \text{Eq. 3.17}$$

However, for the 3 kg (3000 g) dough, the total O_2 consumption rate is:

$$O_2\ consumption\ rate\ (3\ kg\ dough) = 3.874\ \cdot\ 10^{-3}\ \cdot 3000 = 11.62\ \mu mol \cdot s^{-1} \qquad \text{Eq. 3.18}$$

For a total kneading time of 10 min, O_2 consumption by the dough is:

$$O_2\ consumption\ rate\ (3\ kg\ dough)\ for\ 10\ min = 11.62 \cdot 600\ s = 0.006272\ \text{moles of}\ O_2 \qquad \text{Eq. 3.19}$$

This amount represents only approximately 3.4% of the total O_2 (0.211 mol) available in the headspace. Therefore, during normal mixing under air, the oxygen present in the mixer headspace is more than sufficient to supply the dough O_2 consumption needs.

We then looked at the Protocol B, which provides a better control of the gaseous composition in the mixer's headspace. In protocol B, the headspace was vacuumed down to 0.1 atm (i.e., - 0.9 bar gauge pressure compared to - 0.5 bar for Protocol A) before injecting pure gas, representing the most critical situation regarding O_2 partial pressure.

In the case of CO_2 injection with protocol B, the residual air contains at start of the mixing stage only one tenth of the 0.211 mol obtained previously, or 0.0211 mol of O_2**.** Applying the same consumption rate, the dough would use about 34% of this O_2 over 10 min, adequate to fulfil the dough O_2 requirements during mixing. Therefore, the limiting parameter is mostly the dissolution of the O_2 contained in the gas cells entrapped in the dough and the consumption of the dissolved O_2 through the cascade of biochemical reactions.

According to the results reported by Buche (2011), he showed that increasing the O_2 concentration in the mixing atmosphere by increasing the partial O_2 pressure led to higher overall O_2 consumption by both yeasted and unyeasted doughs. These findings indicate that under atmospheric pressure and a mixing speed of 60 rpm (as used in the *sitoxygraph*), the rate of O_2 transfer becomes a limiting factor for dough oxidation. However, based on our calculations, in the Protocol A, the dough consumes only about 3.4% of the total O_2 available, and at most ≈34% of the O_2 in the vacuumed headspace (B protocol) over a 10-minutes kneading period. These results confirm that regardless of whether the headspace is vacuumed or not prior to gas injection, the amount of available O_2 in the mixer headspace remains sufficient to meet the O_2 consumption demands of the dough for its full development during

kneading. This indicates that O_2 availability should not be a limiting factor in dough oxidation or development under the tested gas mixing protocols; however, the partial pressure of O_2 may be a driving lever. One can see in the table of the partial pressure of gas that in the process B, the partial O_2 pressure may drop to zero depending on the flushing effect of the injected gas

Regarding the partial pressure of O_2, that will control the transfer of gaseous O_2 to the liquid phase of the dough, the O_2 partial pressure at start of mixing and during mixing, will be different for each protocol. For example, the option taken in rising the O_2 content in the tests done under gas mix of 30% O_2 and 70%N_2 will yield in a higher partial pressure of O_2, which may contribute to a reinforced O_2 solubilisation in the dough. In comparison, the protocol A or B with CO_2 injection will yield in a much lower partial pressure of O_2 in the headspace in particular during the kneading phase, and as a consequence in a lower amount of solubilized O_2 in the dough. In turn, this may yield in different results in terms of gluten network performance and baking results.

3.2.1.3. Solubility in water and in bread dough

3.2.1.4. Experimental validation: CO_2 solubility using SodaStream at various salt (NaCl) concentrations

To experimentally validate these observations and quantify the impact of salt, a series of carbonation tests were conducted using SodaStream equipment. Solutions were prepared using either distilled water, tap water or NaCl solutions at different concentrations. All experiments were performed at approximately 20°C, and each test involved 3-4 carbonation presses. The carbonated water bottles (1 L total volume, 840 mL water nominal capacity) were weighed before and after gas injection using precision balance (±0.01 g). Tests were performed in duplicate.

Initial comparisons between distilled and tap water revealed a slight difference in CO_2 solubility, 6250 $mg{\cdot}L^{-1}$ & 6120 $mg{\cdot}L^{-1}$, respectively. This difference is likely due to presence of minerals in tap water, which reduced the amount of free water available for dissolution. To further investigate this phenomenon, NaCl was added to tap water in increasing concentrations.

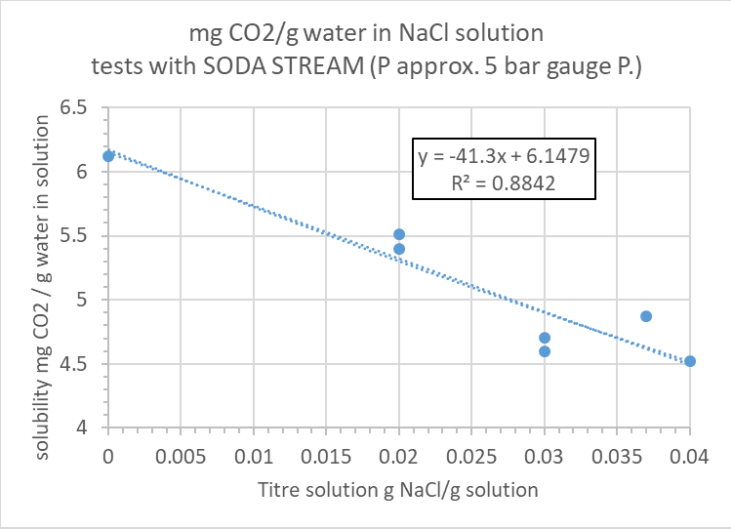


Figure 3.13. Impact of the NaCl titrant of a water solution (tap water) on the CO_2 solubility at around 5 bar. Tests done with a sodastream equipment. The x-axis shows the titrant, essentially the mass fraction or titrant solution of NaCl in the solution

Based on the results presented in Figure 3.13, a clear linear decrease in CO_2 solubility with increasing salt concentration. Specifically, a reduction of approximately of 25% was observed when comparing with pure water to a 40 g·L^{-1} NaCl solution (equivalent to 41.7 g per litre of water). The linear relationship observed under 5 bar gauge pressure is described by the following linear regression (Eq. 3.20):

$$\text{Solubility}\left(\frac{\text{mg}_{CO2}}{\text{g}_{\text{water-solution}}}\right) = -41.3 \cdot \frac{\text{g}_{\text{NaCl}}}{\text{g}_{\text{solution}}} + 6.148 \qquad \text{Eq. 3.20}$$

This finding is in agreement with literature that describes the salting-out effect, where dissolved salts reduce gas solubility in aqueous systems due to decreased water availability and modified ionic strength.

This section compares two CO_2 injection protocols (Protocol A and B), focusing on their effects on the gas composition inside the mixer headspace after reaching the target pressure of 0.5 bar gauge (i.e., 1.5 bar absolute).

Protocol recap:

- Protocol A: The mixer headspace is first partially vacuumed to -0.5 bar gauge pressure, leaving 0.5 bar of air partial pressure at the end of stage 1. CO_2 is then injected to reach atmospheric pressure (pressure of 1 bar absolute); therefore the partial CO_2 pressure is 0.5 bar.
- Protocol B: The mixer headspace is first vacuumed to -0.9 bar gauge pressure, leaving 0.1 bar of air partial pressure at the end of stage 1. CO_2 is then injected to reach the same final pressure of 1.5 bar absolute; therefore the partial CO_2 pressure is 1.4 bar.

In both configurations, the mixer headspace volume is fixed at 24.6 L, and the system is maintained at 25°C (298 K).

All values in the table below were calculated using the ideal gas law equation:

$$P \cdot V = n \cdot R \cdot T \qquad \text{Eq. 3.21}$$

And the total pressure by:

$$P_{TOT}.V = 1.5 \cdot 1.013 \cdot 10^5\, Pa = (P_{N2} + P_{O2} + P_{CO2}) \cdot V = (n_{N2} + n_{O2} + n_{CO2}) \cdot R \cdot T \qquad \text{Eq. 3.22}$$

Where:

P_{TOT}: final absolute pressure = $1.5 \cdot 1.013 \cdot 10^5\, Pa$

V: Volume of the mixer headspace ($24.6 \cdot 10^{-3}\, m^3$)

R: ideal gas constant (8.314 J·mol^{-1}·K^{-1})

T: absolute temperature (298 K)

Hence, these equations allow the determination of the amount of CO_2 injected and the corresponding partial pressures pO_2, PN_2 and pCO_2 in each protocol.

Table 3.5. Comparison between Protocol A and B in terms of gases partial pressures (N_2, O_2 and CO_2)and the quantity in g of CO_2 needed for each protocol to be solubilized

Parameter	Protocol A (at atm pressure) Stage 1 : vacuum at - 0.5 bar Stages 2 and 3 : atm pressure with gas flow stage 2 only	Protocol B (0.5 bar) Stage 1 : vacuum at - 0.9 bar Stages 2 and 3 : +0.5 bar with gas flow stages 2 and 3
CO_2 injected	0.503 mol (22.13 g)	1.408 mol (61.96 g)
CO_2 partial pressure (bar)	0.5	1.4 (tends to reach 1.5 = gas flow)
O_2 partial pressure (bar)	0.106	0.021 (tends to decline due to gas flow)
N_2 partial pressure (bar)	0.397	0.079 (tends to decline due to gas flow)
CO_2 needed for solubilisation (g)	1.37	1.37
Is CO_2 in excess?	yes	yes

In conclusion, for this section, both protocols supply more than enough CO_2 to satisfy the solubilisation within the dough (3 kg) which requires about 1.37 g of dissolved CO_2. However, the final gas compositions differ significantly:

- Protocol A at atmospheric pressure with a continuous flush of CO_2 tends to reach a point where the O_2 partial pressure may tend to zero, which does not support oxidative enzymes and yeast respiration.
- Protocol A at 0.5 bar with a continuous flush of CO_2 during stage 2 (3 min) and a stop of gas flush for stage 3 tends maintain a certain O_2 partial pressure during the mixing and kneading, which supports oxidative enzymes and yeast respiration.
- Protocol B, with a continuous flush of CO_2 tends to reach a point where the O_2 partial pressure may tend to zero, which does not support oxidative enzymes and yeast respiration. The partial pCO_2 pressure starts at 1.4 bar and tends to become 1.5 bar towards the end of the mixing resulting in zero the O_2 partial pressure.

Conclusion:

The comparison between protocols A & B reveals significant differences in terms of partial pressure of the different gases present in the mixer's headspace as shown in the related table at start of this section. Regarding the amount of gas available in the headspace, the computations done showed that there was enough dioxygen at least for the pre mixing and mixing stages and that this gas may reach critical values for protocols A and B in the case of CO_2 injection.

3.2.2. Part B: Main mixing tests and dough results

3.2.2.1. Effect of pressurized gas-composition and addition of AH_2 on t_{PEAK} and SME after kneading: A vs. B protocol

In the A protocol, t_{PEAK} was determined based on the power function fitting using a quadratic polynomial equation ($P(t) = a \cdot t^2 + b \cdot t + c$), using a 10 minutes mixing recording and using all the data points as shown in the figure below Figure 3.14.

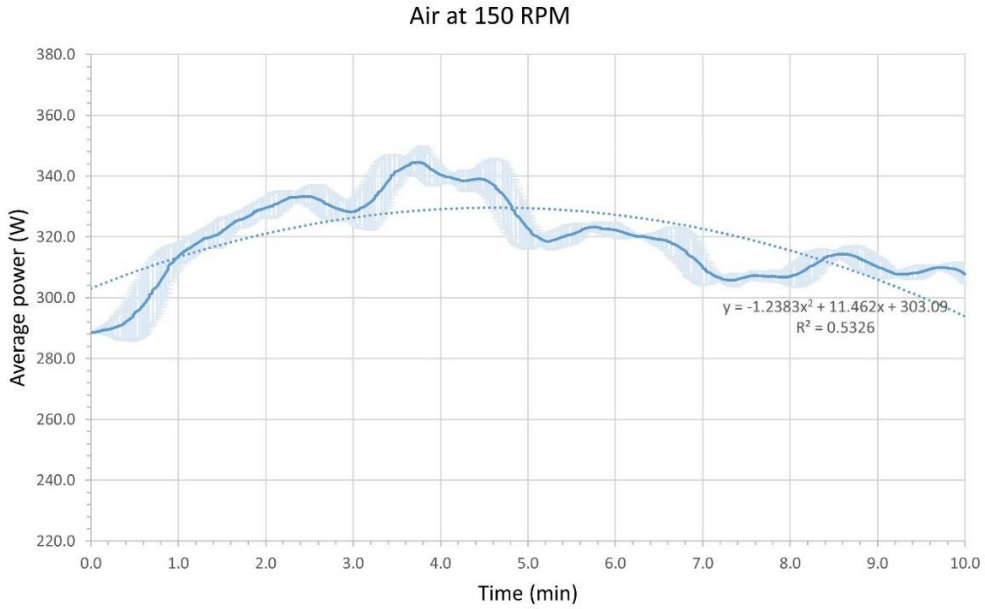


Figure 3.14. Evolution of average power (W) as a function of time (min) during dough kneading under air at 150 RPM. The solid line represents the measured values with standard deviation (shaded area), while the dotted line shows the quadratic regression fit

Table 3.6. Values of t_{PEAK} and SME of the A protocol under different mixing parameters at a kneading speed 150 RPM and pressure of 0.5 bar gauge pressure with and without AH_2 for Air, 100%CO_2 and 30%O_2 70%N_2. Superscript letters (a–c) indicate significant differences ($p < 0.05$) among gas conditions, analysed separately for samples without AH_2 and with AH_2. For SME*, comparisons were performed across all samples*

Protocol A	t_{PEAK} at 150 RPM (min ± SD)	t_{PEAK} at 150 RPM (min:s)	SME_{tPEAK} ± 0.5 min (KJ/Kg ± SD)
Air	4.63 ± 0.53^{a}	04:37	28.6 ± 3.2^{bc}
Air + AH_2	5.35 ± 0.21^{ab}	05:21	17.9 ± 1.6^{a}
100%CO_2	4.59 ± 0.51^{a}	04:35	25.4 ± 3.1^{b}
100%CO_2 + AH_2	5 ± 0.58^{ab}	05:00	17.9 ± 1.7^{a}
30%O_2 70%N_2	6.11 ± 0.64^{c}	06:07	32.5 ± 2.4^{c}
30%O_2 70%N_2 + AH_2	5.9 ± 0.25^{bc}	05:17	28.4 ± 2.3^{bc}

Without the addition of AH_2, t_{PEAK} value for dough mixed with 30%O_2 70%N_2 was the highest (6.11 ± 0.64 min) than the ones mixed with air and 100%CO_2 (4.63 ± 0.53 min and 4.59 ± 0.51 min, respectively). A possible explanation on the indifference of t_{PEAK} between air and CO_2, is the presence of residual air molecules in the mixer headspace with the CO_2 injected gas. The SME values at these t_{PEAK} were significantly influenced by the gas composition in the mixer headspace ($p < 0.05$), which was the highest with 30%O_2 70%N_2. Therefore, a longer dough development time (t_{PEAK}) will lead to higher SME.

In summary:

- 30%O_2 ➔ more oxidation ➔ stronger and polymerised gluten network ➔ higher SME
- Air (21%O_2) ➔ moderate oxidation ➔ moderate SME, not significantly different than 30%O_2
- CO_2 ➔ minimal oxidation could be due to residual air molecules ➔ lowest SME

In presence of AH_2, t_{PEAK} increased for all gas conditions except for 30%O_2 70%N_2 but not drastically, and SME values decreased for all gas conditions in comparison to the ones with AH_2, which was the highest with 30%O_2 70%N_2 (28.4 ± 2.3). Consequently, AH_2 exhorted its oxidative effect by oxidizing the thiol groups and therefore, lowering the mechanical energy needed at t_{PEAK}. The insignificant difference for the mixture 30%O_2 70%N_2 with and without AH_2 suggests that, its oxidative activity was hindered in the presence of an O_2-rich environment. The mechanical energy during mixing facilitates the formation of disulfide bonds, contributing to the progressive development of the gluten network. Differences in O_2 concentration within the dough could potentially affect the effectiveness of AH_2, given its role as an oxidizing agent. Beghin et al., (2022), explored on how different levels of oxygen O_2 integration during mixing affect dough and bread characteristics, especially concerning the roles of azodicarbonamide (ADA) and ascorbic acid (AH_2). Their study showed that greater incorporation of O_2 led to increased disulfide (SS) bond formation, which improved gas retention in the dough and resulted in higher bread specific volumes (BSVs). Although, under limited-O_2 atmosphere, AH_2 was still effective in enhancing BSVs, whereas no significant improvement was seen when AH_2 was added to dough with elevated oxygen levels (Beghin *et al.* 2022). In which this confirms our observations, were elevated O_2 levels was enough for the gluten network development and enough for the oxidation of available thiol groups.

Table 3.7. Values of t_{PEAK} and SME of the B protocol under different mixing parameters at a kneading speed 150 RPM and pressure of 0.5 bar gauge pressure with and without AH_2 for Air, 100%CO_2 and 30%O_2 70%N_2. Superscript letters (a–c) indicate significant differences ($p < 0.05$) among gas conditions, analysed separately for samples without AH_2 and with AH_2. For SME*, comparisons were performed across all samples. The table summarizes mixing time for all conditions*

Protocol B	t_{PEAK} at 150 RPM (min ± SD)	t_{PEAK} at 150 RPM (min:s)	SME_{tPEAK} ± 0.5 min (KJ/Kg ± SD)
Air	4.50 ± 0.22[a]	04:30	19.37 ± 2.15 [ab]
Air + AH_2	4.60 ± 0.32[a]	04:36	17.46 ± 2.52 [a]
100%CO_2	4.50 ± 0.11[a]	04:30	20.07 ± 2.23 [ab]
100%CO_2 + AH_2	5.30 ± 0.75[b]	05:18	24.14 ± 2.43 [c]
30%O_2 70%N_2	5.70 ± 0.24[c]	05:42	24.32 ± 2.21 [c]
30%O_2 70%N_2 + AH_2	4.80 ± 0.54[ab]	04:48	19.90 ± 2.12 [b]

On the other hand, t_{PEAK} in the protocol B was determined based on the power function fitting using a double exponential equation as shown in previous Chapter 2 with the option of 50/50 which means that the fitting was done considering 2 times the experimental value of the time to peak (simple reading of the maximal power level). Looking at the results of the B protocol, by referring to Table 3.7, in absence of AH_2, mixing with 30%O_2 70%N_2 resulted in higher t_{PEAK} (5.70 ± 0.24 min) than air and 100%CO_2-mixed doughs (4.50 ± 0.22 min & 4.50 ± 0.11 min, respectively). The same trend was observed where higher t_{PEAK} values requires higher SME value for the optimal dough development as we can observe with 30%O_2 70%N_2. This observation explains the strengthening effect of elevated oxygen in the headspace and the oxidation of SH groups essential for the gluten network polymerisation. There was no significant difference in t_{PEAK} values between Protocol A and B without and with AH_2. Although, as the protocol A, the mixture 30%O_2 70%N_2 significantly was higher than air and CO_2-mixed doughs.

Upon the addition of AH_2, t_{PEAK} values decreased consistently across all gas conditions, with the exception of 100%CO_2, where t_{PEAK} increased from 4.5 ± 0.11 min to 5.3 ± 0.75 min. In terms of SME at t_{PEAK} in presence of AH_2, all SME values decreased except for 100%CO_2. This suggests that based on literature, the activation of AH_2 in presence of O_2 is indispensable to exert its oxidative effect (Beghin *et al.* 2022; Grosch and Wieser 1999; Lucas, Becker and Jekle 2018; Wieser 2007). Therefore in the B protocol, the absence of O_2 with 100%CO_2 deprived the oxidation of thiol groups (SH), thus the dough needed more time to reach its optimum development (t_{PEAK}), which explains the pure CO_2 environment in the mixer headspace. This emphasises on the role of AH_2, where it accelerated in presence of O_2 the oxidation of disulfide bonds and thus, less SME was required for dough, thus, with 100%CO_2, AH_2 remained inactive (Beghin *et al.* 2022). According to Shehzad et al. (2012), longer mixing times combined with higher mechanical energy appear to limit gluten network development, likely due to protein aggregation caused by overmixing. Conversely, lower mechanical energy and adequate mixing time promotes better gluten formation. This aligns with our results, regardless of the protocol, mixing with 30%O_2 without the addition of AH_2, the observed longer t_{PEAK} values were due to limited gluten network development due to protein aggregation from overmixing.

Overall trends:

- Protocol B yielded lower SME across all conditions ➔ More efficient gluten network formation
- For both protocols, highest t_{PEAK} and SME observed with O_2-riched mixture ➔ increased disulfide bonds and more elastic gluten network
- AH_2 was hindered in elevated oxygen environment

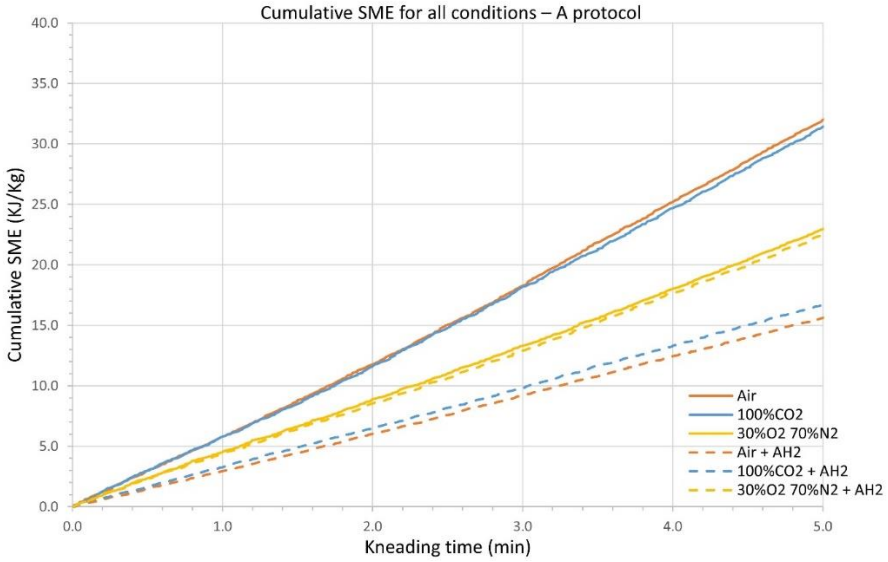


Figure 3.15. Evolution of Cumulative SME ($kJ \cdot kg^{-1}$) for all conditions without and with AH_2 with the A protocol

Graphical illustrations of the SME cumulative linear-exponential fits are shown for each condition with a corresponding SME value at t_{PEAK}. By looking at Figure 3.15, without AH_2, air and 100%CO_2 gave the highest exponential increase in comparison to the 30%O_2 70%N_2 mixture. Interestingly, in presence of AH_2, SME values were consistently lower across all gas conditions, creating a clear gap between the curves with and without AH_2. The presence of AH_2 resulted in a notable reduction in SME, creating a distinct gap between the curves with and without AH_2, except for the condition 30%O_2 70%N_2 where no significant difference was observed with and without AH_2. Suggesting a synergistic effect between O_2-rich environment and the oxidative action of AH_2. These findings align with oxygen partial pressures estimated for each experimental protocol and gas composition. For example, higher oxygen in 30%O_2 mixture resulted in 114% increase of pO_2 greatly enhancing oxidative reactions. Continuous gas renewal in Protocol B maintained a steady oxygen availability, enabling AH_2 to act efficiently and lower SME. In contrast, limited oxygen renewal with Protocol A, restricted oxidative reactions, resulting in higher SME values especially in absence of AH_2.

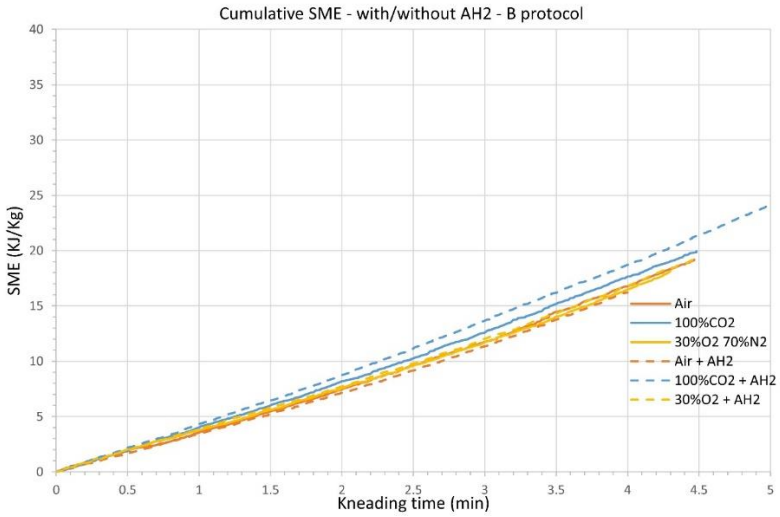


Figure 3.16. Cumulative SME (kJ·kg^{-1}) for all conditions without and with AH2 with the B protocol

By looking at Figure 3.16, showing the evolution of cumulative SME curves with the protocol B, unlike the Protocol A there is no significant gap between all conditions with and without AH_2. The SME values are very similar across all conditions. SME increases linearly with kneading time for all samples, with 100%CO_2 exhibiting the highest SME regardless of AH_2 presence. The air and 30%O_2 70%N_2 curves overlap closely, showing minimal influence from AH_2. This indicates that under the B protocol, AH_2 had little to no effect on mechanical energy input during mixing under the injected gases.

In the A protocol, the lack of gas renewal caused gradual decline in O_2 partial pressure within the mixer headspace, restricting oxidation reactions that are critical for gluten development. This resulted in tougher dough thus higher SME values especially with air and CO_2-mixed doughs. The addition of AH_2 compensated for the limited O_2 by promoting the oxidation of SH groups, which softened the dough and reduced SME. Under 30%O_2 the partial pressure pO_2 was sufficiently high to sustain the oxidation in absence of AH_2, diminishing the activity of this additive. The B protocol maintained gas renewal across all gas compositions and thus, eliminating SME differences. This reveals the crucial role of maintaining adequate oxygen partial pressure during mixing to optimize dough development.

It is widely recognized that thiol-disulfide exchange play a fundamental role in SME of the dough (Baudouin *et al.* 2020). Cauvain (2015a) stated that the substantial mechanical energy may contribute to the disruption of disulfide bonds stabilizing native protein conformations. This mechanical disruption can mimic the effects of natural or chemical reductants, thereby increasing the availability of thiol groups for subsequent oxidation. This hypothesis aligns well with our SME results, where higher SME potentially facilitates both the breaking and reformation of disulfide bridges during mixing. Such mechanochemical dynamics enhance dough development by allowing more SH groups to participate in oxidative cross-linking, particularly in presence of O_2 and AH_2. These molecular processes further explain the observed interactions between mixing protocol, gas atmosphere and AH_2.

Conclusion of this section:

- The comparative evaluation of dough mixing under varying gas compositions and mixing protocols demonstrated that both oxygen availability and AH_2 significantly influence gluten network dynamics. The results confirmed that an oxygen-enriched mixing atmosphere (30%O_2) enhanced thiol groups oxidation ad SS bridges formation, leading to stronger dough structure,

longer t_{PEAK} and higher SME. In contrast, with limited oxygen atmosphere (100%CO_2) oxidative reactions were inhibited, resulting in weaker dough and reduced energy consumption.

- The comparison between the A and the B mixing protocols revealed that the B protocol generally achieved a more efficient dough development as evidence by t_{PEAK} reduction, particularly under 30%O_2 and in presence of AH_2. This reduction in mixing time suggests improved dough development kinetics with the B protocol. Additionally, the B protocol consistently lowered the SME required to reach t_{PEAK} across most gas conditions, indicating enhanced energy efficiency and potentially less mechanical stress on the dough.
- Notably, the presence of AH_2 influenced both t_{PEAK} and SME by generally decreasing energy input and mixing times, with the Protocol B amplifying these effects except in the 100%CO_2 condition, where SME slightly increased. Moreover, without the addition of AH_2, in the A and B protocols, t_{PEAK} was influenced by the nature of the gas mixture injected during kneading ($p < 0.05$). Conversely, in the presence of AH_2, the influence of the gas mixture on t_{PEAK} was attenuated, indicating that AH_2 modulated or masked the gas-dependent variations in dough development. These findings demonstrate a synergic interplay between pO_2, AH_2 activity and the mixing protocol in shaping the mechanical dough development and energy requirements during dough mixing.

3.2.2.2. Effect of pressurized gas-composition and addition of AH_2 on dough void fraction ε after kneading, sheeting and fermentation

Following the characterization of the effects of gas composition and AH_2 on dough rheological properties, the impact of these modifications on gas retention was investigated through measurements of void fraction (ε) during kneading, sheeting, and fermentation. The figure below briefly shows at the end of dough kneading, the entrapped gas bubbles are small and unevenly distributed throughout the dough (Cauvain and Young 2006). Sheeting helps to alter the elongated and irregularly shaped bubbles due to resting phase into more regular, and spherical shaped bubbles. This deformation helps redistribute gas cells more uniformly, reducing large void fractions and improving dough structure before fermentation. During fermentation, bubbles continue to grow to become more uniform in size and distribution until reaching a maximum value of $\varepsilon_f = 0.75$, which was hypothesized as a fixed value.

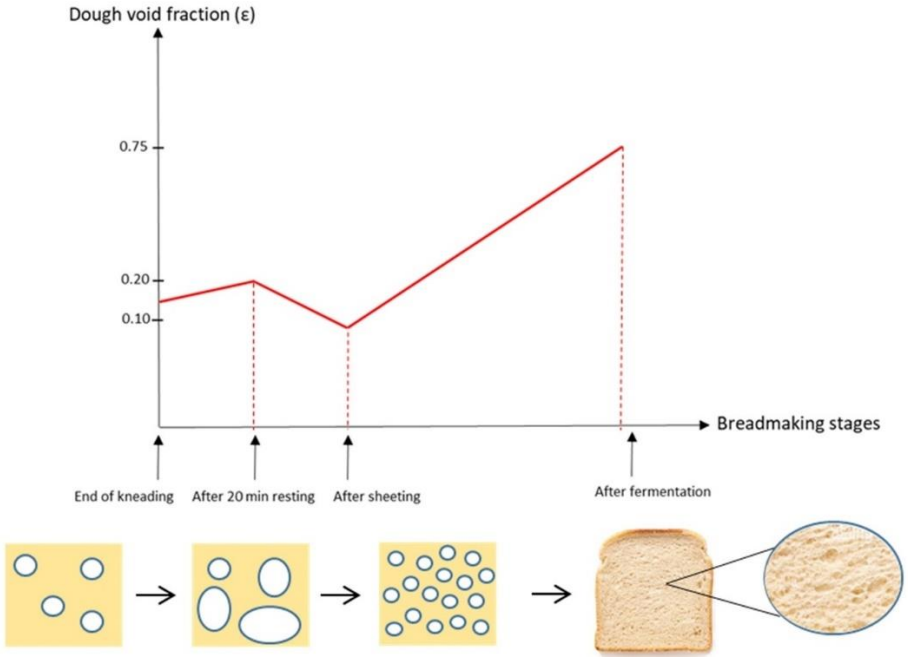


Figure 3.17. Evolution of gas bubbles in size, number and shape during the different breadmaking stages

To assess the influence of the two mixing protocols on dough aeration behaviour, a comparative analysis of dough void fraction was conducted under different gas atmospheres, both in the presence and absence of AH_2. Measurements were taken after kneading, sheeting, and fermentation to track structural changes throughout processing.

3.2.2.3. In absence of AH_2

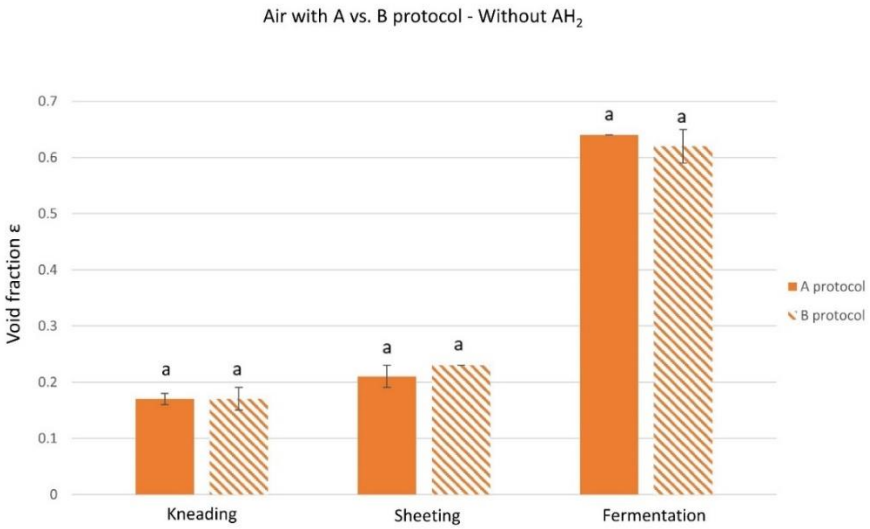


Figure 3.18. Comparison of dough void fractions after kneading, sheeting and fermentation for air-mixed dough 0.5 bar gauge pressure between the A and B protocols without AH_2. Error bars represent standard deviation. Bars labelled with the same letter (a) are not significantly different ($p > 0.05$), indicating no statistical difference between the two protocols at each processing stage

For both protocols, there was no statistical significance of void fractions at each processing stage ($p > 0.05$) Figure 3.18. In the A protocol, void fraction values rose from approximately 0.17 ± 0.01 after kneading ε_i to 0.22 ± 0.02 post-sheeting ε, and then markedly increased to around ε_f 0.64 ± 0.00 after fermentation. The B protocol followed a nearly identical trend, starting at ε 0.17 ± 0.02 post-kneading, increasing to 0.23 ± 0.00 after sheeting, and reaching ε_f 0.62 ± 0.03 at the end of fermentation.

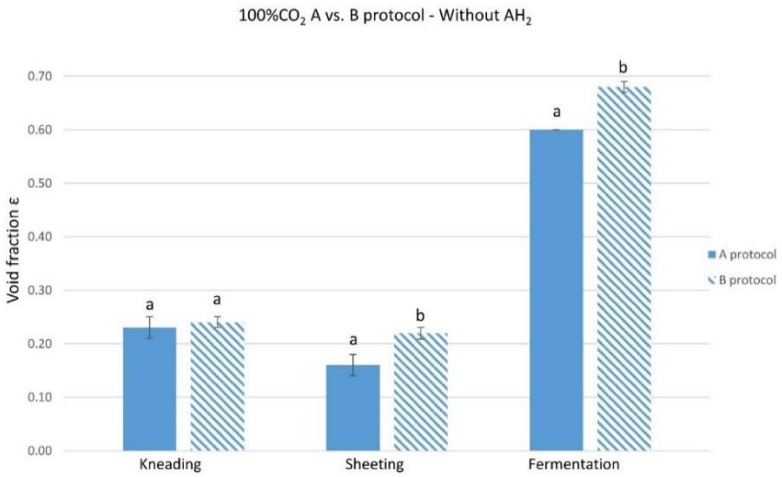


Figure 3.19. Comparison of dough void fractions after kneading, sheeting and fermentation for CO_2-mixed dough 0.5 bar gauge pressure between the A and B protocols without AH_2. Error bars represent standard deviation. Bars labelled with the same letter (a) are not significantly different ($p > 0.05$), indicating no statistical difference between the two protocols at each processing stage

By looking at Figure 3.19, no significant difference was observed between the two protocols for ε_i ($p > 0.05$). However, with the B protocol after sheeting, ε was higher than the one of A protocol (0.22 ± 0.02 and 0.16 ± 0.02, respectively). After fermentation, ε_f of the B protocol was higher than the A protocol (0.68 ± 0.01 and 0.60 ± 0.01, respectively) ($p < 0.05$).

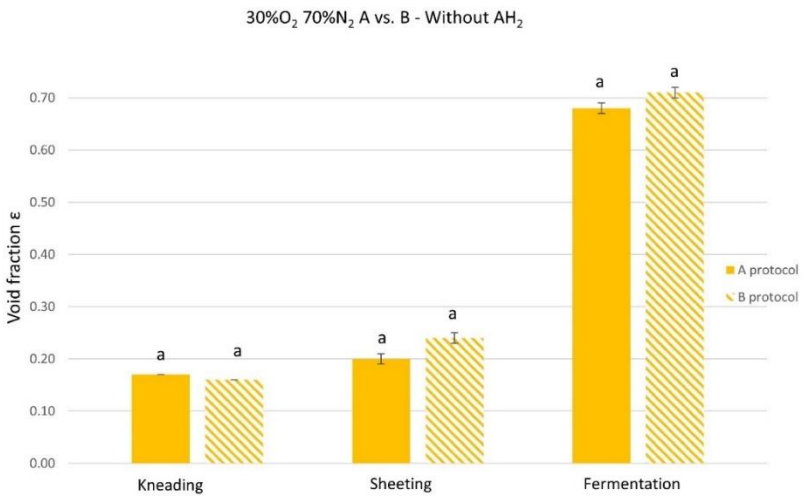


Figure 3.20. Comparison of dough void fractions after kneading, sheeting and fermentation for O_2-mixed dough 0.5 bar gauge pressure between the A and B protocols without AH_2. Error bars represent standard deviation. Bars labelled with the same letter (a) are not significantly different ($p > 0.05$), indicating no statistical difference between the two protocols at each processing stage

Based on Figure 3.20, in absence of AH_2, the evolution of void fractions followed a consistent upward trend from kneading through fermentation for both protocols, hence no significant difference ($p > 0.05$).

In the absence of AH_2, the comparison between *A* and *B protocols* showed no significant differences in void fractions for doughs mixed under air and 30%O_2 70%N_2 conditions at any stage of processing (kneading, sheeting, fermentation), indicating that the protocol change had no impact under these gas environments. However, under 100%CO_2 conditions, the B protocol resulted in significantly higher void fractions after both sheeting and fermentation compared to the *A protocol*, suggesting enhanced gas expansion and retention. Chin et al. (2005), showed how different ratios of N_2:CO_2 at pressure levels ranging from 0 – 2 atm pressure affect the dough void fractions. An increase in both the CO_2 concentration and applied pressure resulted in a higher dough void fraction. This phenomenon is attributed to the elevated solubility of CO_2 under high-pressure conditions, leading to greater amounts of dissolved gas within the dough matrix. This aligns with our results, the mixing at high pressure (0.5 bar gauge pressure) and pure CO_2 environment in the B protocol in the mixer headspace led to an increase of the final void fraction. In addition, during fermentation, the entrained gas bubbles during mixing act as nucleation sites for CO_2 produced by the yeast during fermentation (Shah *et al.* 1998). This confirms that the B protocol introduced a pure CO_2 atmosphere in the mixer headspace enabling a higher partial pressure of CO_2, which promoted greater dissolution of CO_2 into the dough liquid phase via Henry's law (Ben Aissa *et al.* 2010).

3.2.2.4. In presence of AH_2

Based on Figure 3.21, the dough void fractions with air-mixed doughs in presence of AH_2, show significant difference ($p < 0.05$) between both protocols after kneading were ε_i of the B protocol was lower (0.14 ± 0.01) than ε_i of the A protocol (0.17 ± 0.02). Whereas after sheeting and fermentation dough void fractions was not significantly different for both protocols. However, ε_f was slightly higher with the A protocol (0.71 ± 0.01).

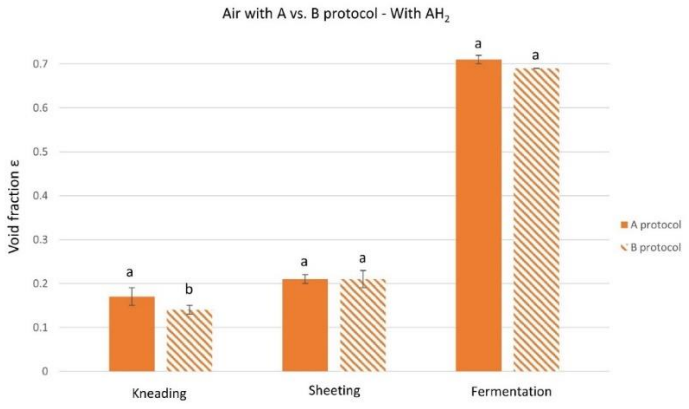


Figure 3.21. Comparison of dough void fractions after kneading, sheeting and fermentation for Air-mixed dough between the A and B protocols with AH_2. Error bars represent standard deviation. Bars labelled with the same letter (a) are not significantly different ($p > 0.05$), indicating no statistical difference between the two protocols at each processing stage

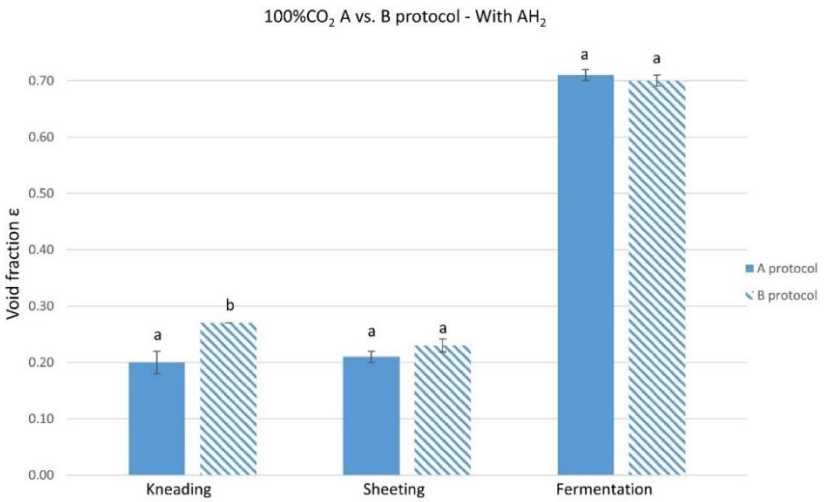


Figure 3.22. Comparison of dough void fractions after kneading, sheeting and fermentation for CO_2-mixed dough between the A and B protocols with AH_2. Error bars represent standard deviation. Bars labelled with the same letter (a) are not significantly different ($p > 0.05$), indicating no statistical difference between the two protocols at each processing stage

The *B protocol* of 100%CO_2 with AH_2 (Figure 3.22), gave a higher initial void fraction ε_i (0.27 ± 0.00) than the ε_i of the A protocol (0.20 ± 0.02). However, after sheeting and fermentation there was no significant difference ($p > 0.05$).

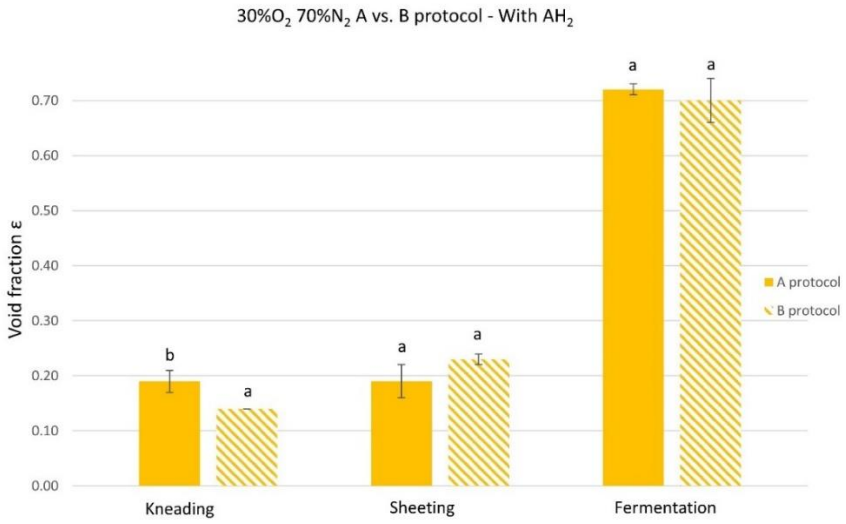


Figure 3.23. Comparison of dough void fractions after kneading, sheeting and fermentation for O_2-mixed dough between the A and B protocols without AH_2. Error bars represent standard deviation. Bars labelled with the same letter (a) are not significantly different ($p > 0.05$), indicating no statistical difference between the two protocols at each processing stage

Based on Figure 3.23, ε_i in the A protocol (0.19 ± 0.02) was higher than that of the B protocol (0.14 ± 0.00). However, after sheeting and fermentation there was no significant difference ($p > 0.05$).

In the presence of AH_2, the protocol influence was limited mainly to the kneading stage. Across all gas conditions and both protocols, AH_2 consistently led to higher ε_f compared to samples without AH_2. Therefore, with air and 30%O_2-mixed doughs, the formed gluten network was stable enough to retain the gas bubbles formed during the kneading phase and after sheeting. Sheeting contributes to partial degassing and helps redistribute the residual gas uniformly within the dough (Cauvain 2020a), while still maintaining the link between the aerated structure formed during mixing and the subsequent bubble expansion during proving (Campbell and Martin 2020). The addition of AH_2 enhanced dough stability and gas retention during fermentation. However, in the 30%O_2-mixed doughs, AH_2 role was less pronounced, likely because of the available O_2 was already sufficient to fully oxidize and stabilize the gluten network during kneading. In contrast, for CO_2-mixed doughs, the insignificant high ε_f could be due to the formation of large gas bubbles during the fermentation phase. Mixing under CO_2 limits O_2 availability, thus negatively impacting dough chemistry but facilitates CO_2 absorption and release depending on pressure changes, which can either shrink or expand gas bubbles and affect dough void fraction (Martin *et al.* 2008), which what we observed in according to our results. Nevertheless, none of the conditions regardless of the protocol or presence of AH_2, achieved a final void fraction of 0.75 as reported in literature as indicative optimal fermentation (Mills *et al.* 2003; Vliet *et al.* 1992).

3.2.2.5. Effect of pressurized gas-composition and addition of AH_2 on dough expansion ratio N and effectively fermentation time

After the determination of the dough void fractions ε, we examined its relationship with the dough expansion ratio during fermentation to elucidate how different gas conditions, combined with AH_2 addition, influence dough expansion ratio N and effectively fermentation time. The following results highlight how these variables affect N. We correlated the final expansion height with the fermentation time needed for each condition.

To illustrate the determination of N by the protocol calculation method, Air-mixed doughs without AH_2 from the *B protocol* was selected as a representative example. As described in the methodology chapter, N was determined based on the initial dough height (H_I = 1 cm) and dough void fraction ε ($\varepsilon_{I,air}$ = 0.23) after sheeting with the target of reaching ε_F = 0.75 at the end of the fermentation.

$$N = \frac{1-\varepsilon_I}{1-\varepsilon_F} = \frac{H_F}{H_I} = \frac{1-0.23}{1-0.75} = 3.08 \qquad \text{Eq. 3.23}$$

Table 3.8. Dough expansion ratios N without AH_2. Superscript letters (a–c) indicate significant differences ($p < 0.05$) among gas conditions for each column

Conditions without AH_2	ε_f (after fermentation)	Calculated expansion ratio N (Protocol A)	ε_f (after fermentation)	Calculated expansion ratio N (Protocol B)
Air	0.64 ± 0.00 ^{b}	3.18 ± 0.08 ^{abc}	0.62 ± 0.03 ^{a}	3.08 ± 0.00 ^{a}
100%CO_2	0.60 ± 0.00 ^{a}	3.36 ± 0.06 ^{c}	0.68 ± 0.01 ^{b}	3.16 ± 0.06 ^{ab}
30%O_2 70%N_2	0.72 ± 0.01 ^{d}	3.25 ± 0.12 ^{bc}	0.71 ± 0.01 ^{b}	3.06 ± 0.12 ^{a}

Effect of protocol and gas mixtures without AH_2

As shown in the table above (Table 3.8), the calculated expansion ratios N varied slightly between protocols and gas conditions. Under the A protocol, doughs mixed with 100%CO_2 exhibited the highest N (3.36 ± 0.06), suggesting a longer fermentation time than air and 30%O_2.

In contrast with the *B protocol*, N were slightly lower and showed reduced variability across gas conditions. Without AH_2, N values were generally higher, especially with 100%CO_2, and showed greater differences between both protocols, with the *A protocol* notably higher.

Table 3.9. Dough expansion ratios N with AH_2. Superscript letters (a–c) indicate significant differences ($p < 0.05$) among gas conditions for each column

Conditions with AH_2	ε_f (after fermentation)	Calculated expansion ratio N (Protocol A)	ε_f (after fermentation)	Calculated expansion ratio N (Protocol B)
Air	0.71 ± 0.01 [a]	3.18 ± 0.08 [a]	0.71 ± 0.01 [a]	3.16 ± 0.04 [a]
100%CO_2	0.71 ± 0.01 [a]	3.19 ± 0.06 [a]	0.71 ± 0.01 [a]	3.19 ± 0.06 [a]
30%O_2 70%N_2	0.70 ± 0.01 [a]	3.09 ± 0.05 [a]	0.70 ± 0.04 [a]	3.00 ± 0.00 [a]

Effect of addition of AH_2

The calculated expansion ratios N under different gas mixtures for both protocols showed no significant difference in presence of AH_2. This indicates that neither gas mixtures nor the change of protocol had an impact on N values. The expansion ratio N reflects the volume increase of dough during mixing and fermentation, primarily driven by gas bubble growth within the gluten network. Initially, CO_2 generated by yeast during its energy metabolism is first absorbed into the liquid phase of the dough. In this study, approximately 28% of the total 57% water content in the dough was identified as freezable water, representing the fraction of water more freely available for solubilisation. This free water provides the medium in which CO_2 can dissolve before diffusing into gas bubbles during fermentation. Therefore, the solubilisation capacity of the dough for CO_2 was partly limited by the amount of freezable water present. Moreover, Chin et al. (2005a, 2005b), reported that the aqueous phase of the dough does not need to be fully saturated with CO_2 for diffusion of the gas into existing air nuclei to occur during kneading. In fact, dough volume began to expand even before the liquid phase reached complete CO_2 saturation. Therefore, the increase in dough volume during fermentation is a result from the expansion of individual gas bubbles within the continuous gluten network.

The continuous CO_2 injection resulted in access or over-saturation of gas bubbles with CO_2. A possible explanation could be that regardless of the protocol, depriving the dough from O_2 during the early stages of dough processing, can switch the yeast into anaerobic mode, while continues to produce CO_2 leading to overwhelming the dough and weakening the gluten network (Cauvain 2017). Van Vliet et al. (2008; 1992) emphasized that the strain-hardening behaviour of the gluten matrix plays a crucial role in modulation bubbles expansion, although with CO_2-mixed doughs the weak gluten network may lead to less resistance against rupture of the liquid film between bubbles. Several studies reported that factors like water content, type of wheat or content of endogenous lipids affect the rate of bubbles growth during proving (Sahi 1994; Sroan, Bean and MacRitchie 2009). Our results suggest that the gas environment during kneading, especially under 100%CO_2, can slow bubble growth. Supporting

previous findings (Chiotellis and G. M. Campbell 2003; 2003), dough volume expansion starts prior to full CO_2 saturation of the liquid phase. Different gas mixtures can lead to variable N and fermentation times, as the gas composition influences bubble growth dynamics rather than overall CO_2 saturation.

Conclusion

The Protocol A, particularly under 100%CO_2, led to greater expansion and variability, suggesting longer fermentation due to weaker gluten network. In contrast, the Protocol B appeared to promote more uniform conditions, possibly due to vacuum and controlled gas injection, leading to reduced N and fermentation time. CO_2 solubility and bubble growth depend on the dough water structure and gluten strength, which were influenced by gas composition and oxidative treatment. Overall, gas environment and AH_2 together modulate dough structure and fermentation dynamics.

3.2.2.6. Measurement of CO_2 emission during fermentation by the Risograph equipment

The risograph equipment provides a global CO_2 production from a dough sample; it does not detect if the gas is inside the dough or outside the dough; however, we can assume that gas production occurs mainly inside the dough. The graph below illustrates the gaseous CO_2 production kinetics during fermentation under the two protocols, the gas detection was recorded every 1 min increment but the final cumulative data was presented every 15 min. Across all conditions, the highest production was observed with CO_2-mixed doughs in the B protocol. Where the opposite trend was observed in the A protocol, showing a higher kinetics release with air-mixed doughs.

Across both protocols, CO_2-mixed doughs showed the highest gas production although not significantly different between both protocols and with air-mixed doughs in the B protocol. Within the B protocol, CO_2-mixed doughs exhibited a markedly steeper incline starting from early stages of fermentation and continuing steadily towards the end (180 min). This suggests that the B protocol, when combined with CO_2 mixing, enhances the onset of dough expansion during fermentation thanks to the fact that the liquid phase of the dough was already saturated or close to saturation (assumption not verified). Also, the fact that the liquid phase of the dough was rich in CO_2 may have contributed to a direct release of CO_2 from the dough piece itself in the flask hosting the dough in the risograph. The B protocol yielded in the best results; this may be explained by the higher CO_2 partial pressure in the mixer's headspace. It shows that having enough moles of a given gas to be solubilised in the dough is one point; however, having a higher partial pressure of the given gas has obviously an impact on the solubilisation in the dough.

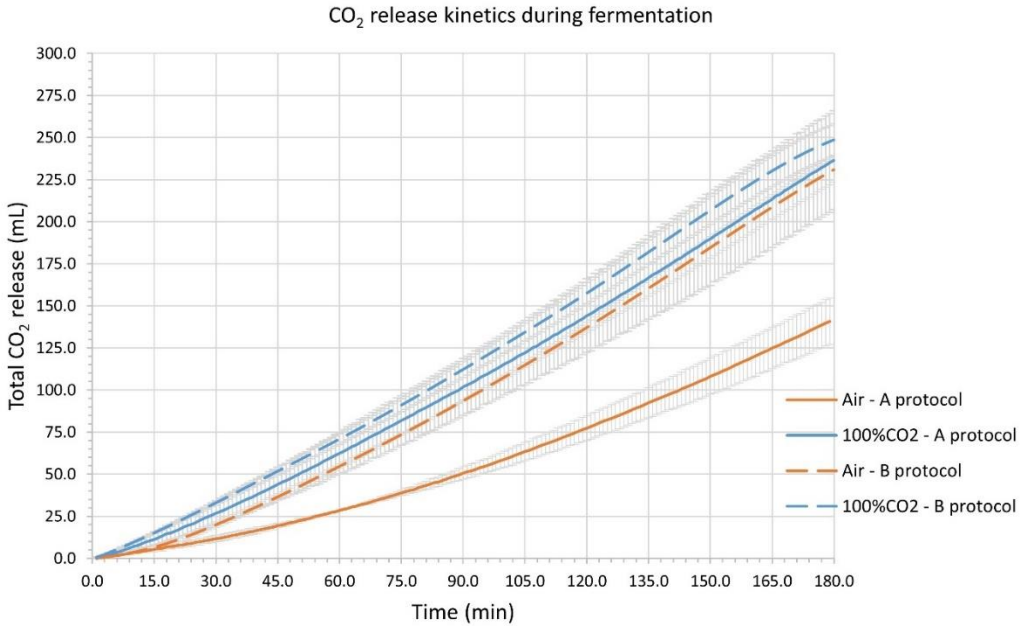


Figure 3.24, Cumulative CO_2 production during fermentation under A (solid lines) and B (dashed lines) protocols for two gas conditions: air (orange) and 100% CO_2 (blue). Measurements were taken over 180 min using a Risograph

Table 3.10. Rate of CO_2 emission of air and CO_2-mixed dough under the A vs. B protocols

Time (min)	Air (Protocol A) (mL)	100%CO_2 (Protocol A) (mL)	Air (Protocol B) (mL)	100%CO_2 (Protocol B) (mL)
0	0	0	0	0
15	5.00	11.25	6.65	12.77
30	11.17	26.83	20.01	28.27
45	18.67	44.00	36.60	45.01
60	27.67	62.42	54.73	62.60
75	38.17	81.92	73.62	81.32
90	49.67	101.83	93.63	101.03
105	62.50	122.08	114.89	121.68
120	76.50	144.08	137.16	143.73
135	91.33	166.67	160.49	166.85
150	106.83	189.75	184.65	190.31
165	123.67	213.33	208.71	213.07
180	140.83	236.42	230.98	233.13

The table above shows numerically the values of CO_2 production and release; there was no significant difference between CO_2-mixed doughs regardless of the protocol. At 15 min, the sudden incline was around 11.25 and 12.77 mL of released CO_2 for A and B protocols respectively. Whereas with air was significantly lower. These results confirm that regardless of the protocol, dough expansion together with CO_2 release in fermentation flask of CO_2-mixed doughs was enhanced. The contribution of the

release of solubilized CO_2 at the surface of the dough piece in the gaseous phase of the fermentation flask was impossible to quantify. According to Hibberd & Parker (1976), devices like Risograph measure only the undissolved CO_2, therefore, the observed pressure increase from the gradual release of dissolved CO_2 into the gas phase but also from the expansion of the dough piece itself; this process is a slow process when the dough liquid phase is not saturated in CO_2. These results support our observations, which under CO_2-rich environment the dough reached saturation more rapidly, leading to earlier dough expansion. In the A protocol with air-mixed doughs, the dough was under-saturated and the yeast probably was not fully active until 30 min into fermentation. A possible explanation could be the starting dough temperature was lower than the Risograph set temperature (Bloksma 1990).

Furthermore, Hibberd & Parker (1976), investigated CO_2 solubility in dough and estimated that saturated dough could dissolved up to 0.81 $mL \cdot g_{dough}^{-1}$. In our study, 50 g of dough samples based Hibberd & Parker equation based on Ideal Gas Law, we calculated the cumulative CO_2 gas release ($mL \cdot min^{-1}$) at each time interval (Figure 3.25), with the equation PV = nRT; at each time interval $V_t(CO_2)$ was measured and therefore $n(CO_2)$ was calculated.

Based on a constant CO_2 production rate of 0.78 – 1.30 $mL \cdot min^{-1}$ in a 50 g dough sample (Figure 3.25), it would theoretically take 17 min to reach saturation assuming no CO_2 was initially dissolved. However, gas release was detected by the Risograph within the first 5 min. This suggests that some CO_2 was already dissolved during mixing or that CO_2 started escaping before reaching full saturation.

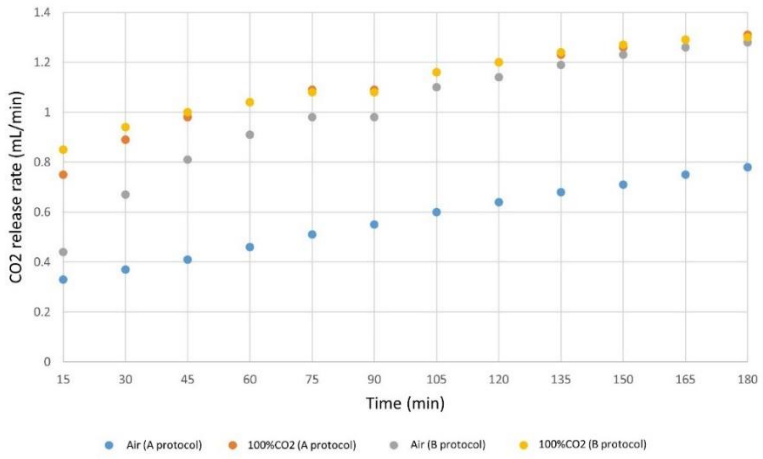


Figure 3.25 Production rate of CO_2 based on Hibberd & Parker equation of rate production and solubility of CO_2 (Hibberd and Parker 1976) in function of time

3.2.3. Part C: effect of sheeting and additional analysis

Therefore, based on the results above, the remainder of this study, the Protocol A was employed for all subsequent analyses to maintain methodological consistency. Although this method resulted in slightly higher SME values and longer t_{PEAK} times, it remains a validated and reliable approach for assessing the effects of gas composition and AH_2 supplementation on dough behaviour. Building on these results, the third and final section presents additional experiments aimed at investigating the effects of sheeting vs. no sheeting, pH changes during fermentation, and dough rheological properties under the selected protocol.

3.2.3.1. Effect of the sheeting process on dough void fractions under air and CO_2-mixed doughs vs. without sheeting

In this section, we examined the effect of the sheeting process on the dough void fractions under air and CO_2-mixed doughs. Both sheeted and non-sheeted doughs had a resting period of 20 min post-kneading; however, the sheeted doughs underwent a sheeting step prior to fermentation, while non-sheeted doughs straight to fermentation after resting. Void fractions were measured immediately after sheeting or resting, and again after fermentation, to evaluate how mechanical processing influences dough porosity throughout the fermentation process under different gas environments.

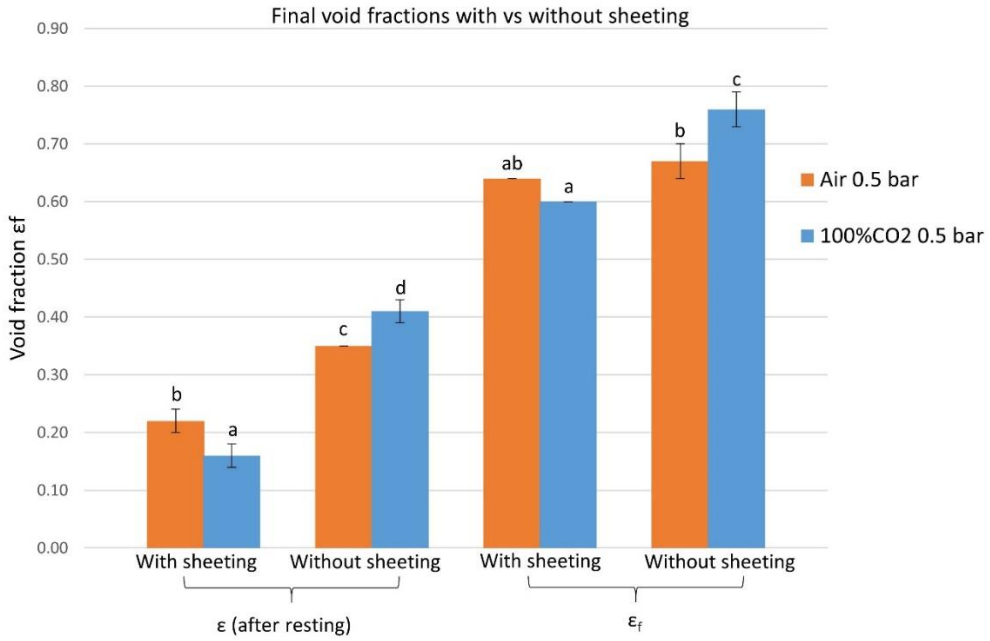


Figure 3.26. Comparison of dough void fractions after sheeting for sheeted doughs, after resting for doughs without sheeting and the final dough void fraction after fermentation under air and CO_2. Statistical comparisons were made separately within the "with sheeting" and "without sheeting" groups. Different lowercase letters above bars within each group indicate significant differences ($p < 0.05$), while bars sharing the same letter are not significantly different

By comparing ε after resting, non-sheeted doughs showed significantly higher ε than the sheeting doughs. With sheeting, CO_2-mixed dough had a lower ε (0.16 ± 0.02) than air-mixed doughs

(0.22 ± 0.02). The opposite trend was observed with non-sheeted doughs, where CO_2-mixed doughs scored a higher ε (0.41 ± 0.02) than air-mixed dough (0.35 ± 0.00).

After fermentation, ε_f increased under both atmospheres, although with sheeting, there was no significant difference ($p > 0.05$). Doughs without sheeting showed significantly higher ε_f for both atmospheres in comparison with sheeted doughs. CO_2-mixed doughs exhibited higher ε_f (0.76 ± 0.03) than air-mixed doughs (0.67 ± 0.03).

The comparison of void fractions (ε) between sheeted and non-sheeted doughs under different gas atmospheres revealed distinct structural differences influenced by both sheeting and gas composition. The results clearly showed that for both mixing conditions, without sheeting significantly resulted in higher void fractions, especially for CO_2-mixed doughs. This may be attributed to continued diffusion of CO_2 into nucleation sites and gas bubble growth during resting. However, the main role of sheeting is partial degassing and helping to redistribute the residual gas uniformly within the dough, dividing large gas bubbles into smaller and more uniformly ones (Cauvain 2020a), while still maintaining the link between the aerated structure formed during mixing and the subsequent bubble expansion during proving (Campbell and Martin 2020). Therefore, after sheeting, CO_2-mixed doughs exhibited lower void fractions, due to the loss of the large bubbles formed during resting and the dissolved CO_2 was more readily lost during mechanical sheeting than entrapped air. Leong and Campbell (2008), studied the effect of sheeting on internal density distribution of doughs made from weak and strong flours, with varying gas contents through the counter-rolling rolls set at different gaps (3.18, 3.96 and 4.76 mm). The results showed that gas content in dough generally decreased with smaller roll gaps during sheeting, due to increased pressure that compresses and expels gas from the dough. At higher pressure (2 bar headspace pressure during mixing) and across three different roll gap settings, doughs made from weak flour showed a more pronounced increase in density after sheeting, indicating they were degassed to a larger extent compared to those made from strong flour. This suggests that doughs with weaker gluten structures are more susceptible to gas loss under mechanical stress during sheeting. This aligns with our study, at a narrow gap of 2.5 mm and high mixing pressure at 0.5 bar, the weak doughs mixed under CO_2 exhibited larger degassing after sheeting, resulting to lower ε_f.

Overall, the results indicate that both the type of gas used during mixing and the application of sheeting significantly impact the dough ability to retain gas. Sheeting led to a reduction in void fraction due to partial degassing, particularly in CO_2-mixed doughs, which are more sensitive to mechanical stress. This suggests that doughs with weaker structures are more prone to gas loss during processing.

Building upon these finding, the calculation of N was based on void fraction after sheeting. However, it is notable that that the void fraction ε_f without sheeting reached up to 0.75, which appeared unexpectedly high. This discrepancy is likely due to compression of gas bubbles during the sheeting process, leading to underestimation of ε. Consequently, the void fraction measured after sheeting may not accurately reflect the true gas content within the dough structure. Tracking the void fraction in a dough slice before sheeting would provide further insight. Thus, it would be more accurate to calculate N from the measured ε before sheeting which aligns with the established role of sheeting in partially degassing the dough, redistributing gas bubbles and breaking large ones into more uniform and smaller ones (Campbell and Martin 2020; Cauvain 2020b).

To monitor the evolution of ε_i 30 g of dough was placed in the oil flask (based on Archimedes' principle). The weight of the dough was monitored for 10 min and recorded at each 1-min time interval. Changes

in the weight reflect variations in dough volume and gas retention over time. Therefore, based on the figure below, 100%CO_2 consistently exhibits higher ε and reached a higher ε_i (0.30 ± 0.04) than air-mixed dough (0.27 ± 0.01). At these ε_i values the expansion N of each would be 2.8 and 2.92 respectively.

The results can be explained that without sheeting, the void fraction ε_f reached a high value with 100%CO_2 to 0.75 due to the presence of intact large bubbles. With sheeting, mechanical compression reduced the gas bubbles in size and number, which resulted in a lowering of the final void fraction ε_f. This may mean that the void fraction measured after sheeting underestimated the true gas content of the dough, causing discrepancies in the calculations of N. Therefore, for accuracy, N should be calculated based on the void fraction of the dough before sheeting or applying a correction factor to account bubbles compression during sheeting. This highlights that sheeting not only redistributes gas bubbles but also compresses them, affecting how void fraction is interpreted in dough structure analysis.

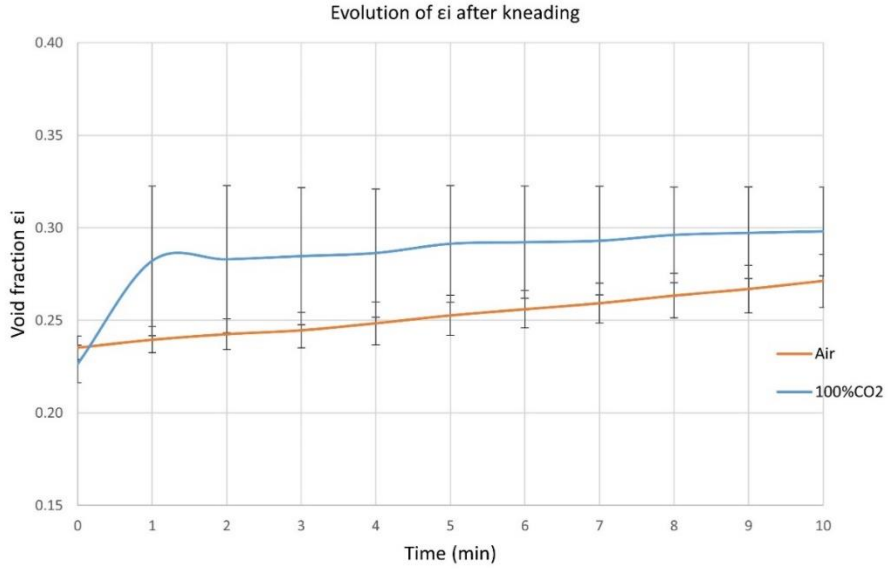


Figure 3.27 Evolution of dough void fraction ε_i before sheeting for air and 100%CO_2 in function of time (atmospheric mixing pressure). The jump observed with the 100% CO_2 condition is maybe due to the re-expansion of the compressed gas nuclei entrapped in the dough; this could be explained maybe by a softer dough with a less cohesive gluten network (more a viscous dough with les elasticity). The air mixing condition resulted in a progressive rise at a higher rate than with CO_2 with no jump; it may be explained by a stronger gluten network with a more elastic dough

3.2.3.2. Analysis of bubbles in dough observed under Photonic Optical Microscopy

Bubble growth during proving is influenced by several factors (1) the rate at which yeast produces CO_2 (2) the degree to which the dough retains the generated CO_2 (3) the rate at which CO_2 diffuses from saturated LDP to the formed gas nuclei and (4) bubble coalescence (Shah *et al.* 1998). The last two points are focused on the individual behaviour of gas bubbles.

Microscopic observations were conducted to test the hypothesis that CO_2 injection during mixing may enhance gas cell stability. According to this hypothesis, the stabilizing effect arises from both the physical injection of CO_2 into the gas phase of the dough and the simultaneous solubilisation of CO_2 into the liquid phase. The latter process could influence surface tension term of the Young Laplace equation which is reminded below. The size that separates growing bubbles from stable ones is called the critical bubble size and can be understood through the Young-Laplace equation:

$$P_b = P_\infty + \frac{4 \cdot \gamma}{D} \qquad \text{Eq. 3.24}$$

Where P_∞ is the surrounding dough pressure, γ is the surface tension and D is the bubble diameter. The foundational concept presenting the status of a gas nuclei in a bread dough is illustrated in the figure below (Figure 3.28), where Shah et al. (1998) described gas bubbles in the dough in equilibrium governed by Young-Laplace equation. The surface tension term of the Young-Laplace equation is reversely proportional to the bubble diameter; as a consequence, smaller bubbles require a higher internal pressure to stabilize in the dough in particular at the onset of fermentation (rest phase) and in particular after the sheeting step, during which the large bubbles are removed from the dough, whereas the smaller bubbles are set under pressure.

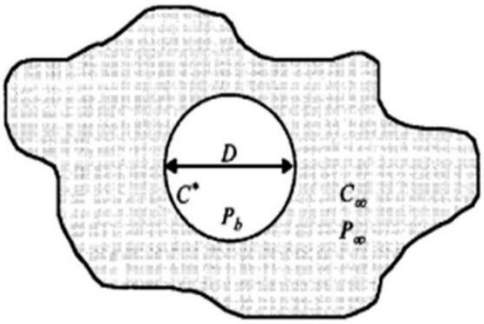


Figure 3.28 A schematic representation of a bubble containing CO_2 surrounded by the dough matrix (Shah et al. *1998)*

By comparing Figure 3.29 & Figure 3.30, with both mixing conditions Air and 100% CO_2, gas bubbles were higher in number with yeasted doughs than unyeasted doughs at both fermentation times, thus reflecting higher dough void fractions. This may be linked to the fact that yeast starts to produce CO_2 during mixing, and also to the time needed between the end of mixing and the start of image capturing with the microscope; the time interval is of around + 3-5 min., time needed to measure the initial void fraction and installation on glass plate + launching the image acquisition). After mixing (t = 0 min, which is in fact rather + 3/5 min), air-mixed doughs appeared to have higher number of small gas cells compared to the CO_2-mixed doughs which exhibited a lower number of gas cells with larger size. Also, the void fraction ε_i after mixing with CO_2 (0.23) was higher than that of air (0.17). The formed gas bubbles for yeasted and un-yeasted doughs, started to increase in size after 5 min of observation and smaller gas bubbles started to disappear. One can see with the 4 pictures below that a larger number of gas cells disappeared for the CO_2 dough compared to the air dough. Surprisingly, the gas cells were more stable in the air dough than in the CO_2 dough. It was also observed that the presence of yeast contributed to maintaining a larger amount of gas nuclei in both mixing conditions. This was clear in particular for the 100%CO_2 dough both at end of mixing (0 min) and after 5 min.

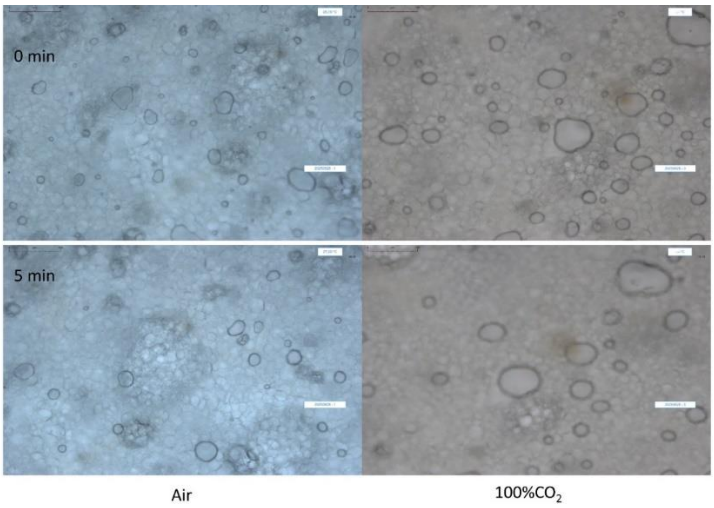


Figure 3.29. Microscopic images of unyeasted doughs, air-mixed doughs (left in blue) and CO_2 (right in grey), with two observation times 0 min (post-mixing) and 5 min. The scale was set between 1 – 100 µm

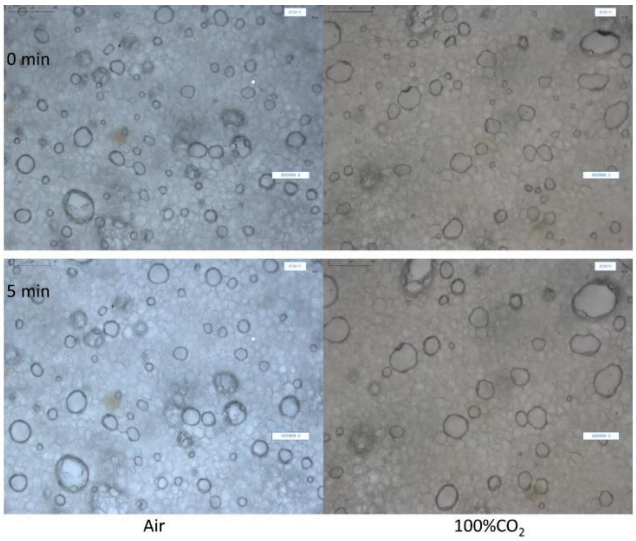


Figure 3.30. Microscopic images of yeasted doughs, air-mixed doughs (left in blue) and CO_2 (right in grey), with two observation times 0 min (post-mixing) and 5 min. The scale was set between 1 – 100 µm

The following images show the observation after 10 and 15 min. Compared to unyeasted doughs, yeasted doughs showed larger gas bubbles for air and CO_2-mixed doughs than unyeasted doughs. At the end of mixing, entrained gas bubbles become incorporated into the dough continuous network formed by the gluten-starch matrix and the dough liquid phase (Sun, Martin G Scanlon *et al.* 2023). Throughout fermentation, as observed below at 10 & 15 min, these gas bubbles start to grow in size due to the diffusion of formed CO_2 by the yeast activity into the formed nucleation sites. However, a significant portion of CO_2 generated at post-mixing dissolves into the dough liquid phase rather than immediately migrating into the entrained gas bubbles (Bloksma 1990; Chiotellis and G.M. Campbell 2003; Hibberd and Parker 1976). Unyeasted doughs showed slower bubbles growth due to the absence of yeast activity. These air mixing yielded in a more cohesive gluten network, which had a better capability to maintain small gas cells in place. On the opposite, at 15 min in yeasted doughs, larger bubbles and coalescence were observed with CO_2-mixed doughs.

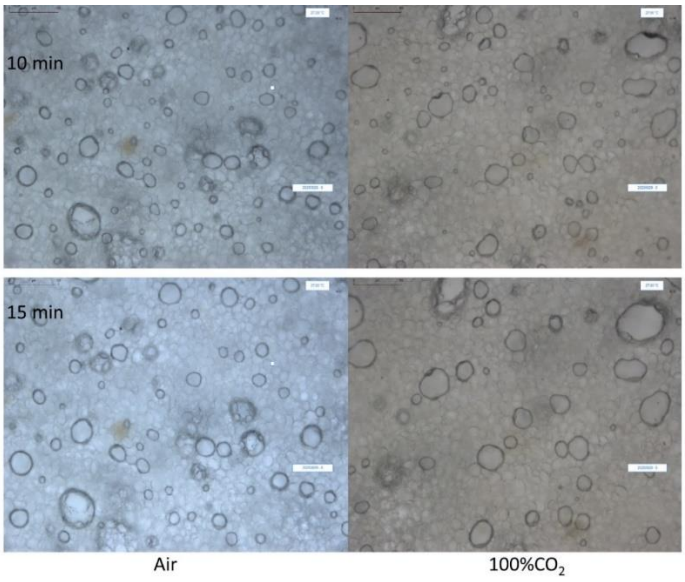


Figure 3.31. Microscopic images of unyeasted doughs, air-mixed doughs (left in blue) and CO_2 (right in grey), with two observation times 10 min and 15 min. The scale was set between 1 – 100 µm

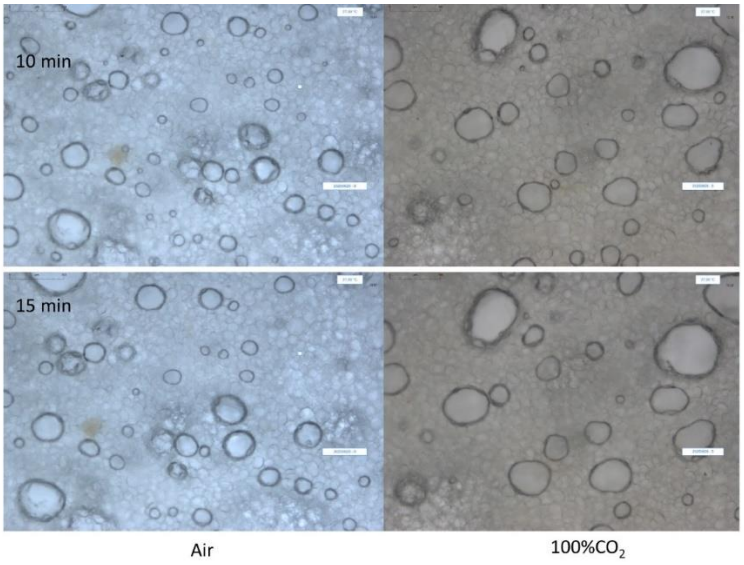


Figure 3.32. Microscopic images of yeasted doughs, air-mixed doughs (left in blue) and CO_2 (right in grey), with two observation times 10 min and 15 min. The scale was set between 1 – 100 µm

Microscopic observations were conducted for 20 min on yeasted CO_2 doughs to assess the impact of sheeting following a 20 min resting period. Based on Figure 3.33, further disproportionation was observed with both mixing conditions, thus with CO_2, bubbles were larger in size and irregular in shape, which was marked by high void fractions as discussed without sheeting results. After sheeting, large bubbles were broken down into smaller and uniform bubbles, which resulted in decreased void fractions after sheeting. This observation confirms the weak gluten network with CO_2-mixed doughs. The viscoelastic behaviour of gluten network plays a crucial role in enabling gas bubbles expansion and effectively trapping CO_2. The balance between dough elasticity and extensibility is important to avoid issues like coalescence and disproportionation (Verheyen *et al.* 2015). However, the gluten network with air was able to better maintain the initial small bubbles even after sheeting; this could be attributed to a higher partial pressure in dioxygen during mixing with air mixing conditions resulting in

more cohesive gluten network. Leong and Campbell (2008), examined how sheeting affects the density distribution and gas content in doughs made from weak and strong flour with and without yeast, mixed at various gas levels. Doughs prepared were made from wheat flour and mixed using Tweedy 1 mixer for 3 min under atmospheric pressure (1 bar) and high pressure (2 bar). Both unyeasted doughs (rested for 10 min) and yeasted doughs (sheeted immediately after mixing) were processed between counter-rotating rolls at different gaps. Results showed that doughs made from weak flour exhibited higher dough degassing, as indicated by a greater change in dough density following sheeting compared to those made with strong flour. The findings on how sheeting influences gas redistribution and degassing provide valuable insights into the behaviour of weak dough systems under mechanical processing.

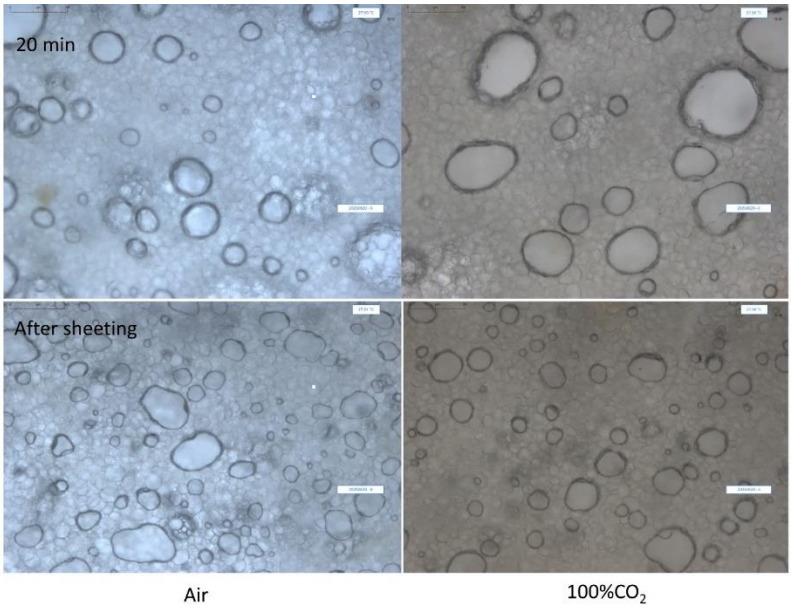


Figure 3.33. Microscopic images of yeasted doughs, air-mixed doughs (left in blue) and CO_2 (right in grey), after 20 min of resting followed by sheeting. The scale was set between 1 – 100 µm

Microscopy showed that CO_2 mixing yielded fewer, larger bubbles and air yielded more stable and smaller bubbles. Bubble disappearance during resting period with air-mixed doughs indicated better gas retention.

During mixing, the headspace gas entrapped in the dough bubbles partly dissolves (by Henry's law), where higher gas partial pressures increase solubilised CO_2 and O_2 in the LPD. Large bubbles in CO_2-mixed dough correspond to larger gas cells and lower specific volume compared to air dough. We propose two possible explanations:

- Mixing with air helps in the gluten network development, promoting gas retention and the stability of smaller stable gas bubbles. Initial solubilisation of CO_2 is low, throughout fermentation the yeast starts producing CO_2 where the LPD reaches saturation after 30 – 50 min.
- For dough mixed under CO_2, the solubilisation of CO_2 increases dough liquor viscosity, which in turn increases the viscosity of the liquid film surrounding the gas bubbles. This may yield in a higher value of the surface tension term of the Young Laplace equation; in turn, this phenomenon coupled with a weaker gluten network, resulted in the dissolution of the smaller gas bubbles and the

promotion and faster growth of large remaining bubbles. Indeed, the disappearance of small bubbles yielded in an increase of the concentration of CO_2 in the dough liquor.

The concept of "critical bubble size" was explained by Shah et al. (1998); it concerns the onset of fermentation (stability or disparition of the smaller bubbles according to the balance of the Young-Laplace equation). This concept also concerns the fact that bubbles stop growing until a certain point and until pCO_2 balances the concentration of CO_2 in the dough. Higher CO_2 concentration in the dough increased the critical bubble size, favouring the stability of the larger bubbles (and non-stability of the smaller ones). When CO_2 concentration is low, (like in air-mixed dough), the critical bubble size is smaller, hence the small bubbles tend to be more stable. Whereas large bubbles continue to grow when the internal pressure is low, thus allowing more CO_2 to enter the bubble. During growth, the CO_2 concentration at the bubble surface and inside the bubble changes in a complex way. When the CO_2 concentration at the bubble surface reaches the saturation point in the dough liquid, smaller bubbles stop growing. At this stage, CO_2 moves into the bigger bubbles or escapes the dough.

To sum up, the hypothesis that CO_2 solubilizes into the dough, stabilizing gas cells, was not supported by our results. Rather, it was found that dough mixed with air exhibited better gas stability. This stability was evident through reduced disproportionation, meaning that the air-mixed bubbles maintained their integrity over time, while CO_2 bubbles tended to be less stable and more prone to coalescing. Thus, contrary to expectations, air mixing was more effective in preserving gas cell structure during the mixing and early fermentation stages.

Another explanation for the reduced stability of gas cells could be initially attributed to a hypothesized decrease in the viscosity of the LPD due to CO_2 solubilisation. The assumption was that a lower viscosity could reduce surface tension forces at the gas-liquid interface (influenced by water, solutes, and interfacial components like proteins and lipids, which can act as surfactants) (Janssen, Wouters and Delcour 2021), compromising the structural integrity of gas bubbles and thus, leading to disproportionation. McBride-Wright et al. (2015) examined the viscosity and density of aqueous CO_2 solutions across a temperature range of 274 – 249 K and pressures up to 100 mPa. Their results showed that CO_2 solubilisation actually increased viscosity by approximately 6.25% for every 0.01 increment in mole fraction of CO_2. Thus, the idea that CO_2 reduces the viscosity of the LPD, thereby destabilizing gas cells, is not consistent with these findings.

3.2.3.3. Effect of pressurized gas-composition and addition of AH_2 on dough pH after fermentation

Following fermentation, dough pH was measured to evaluate how the different gas composition with the addition of AH_2 affect dough acidity.

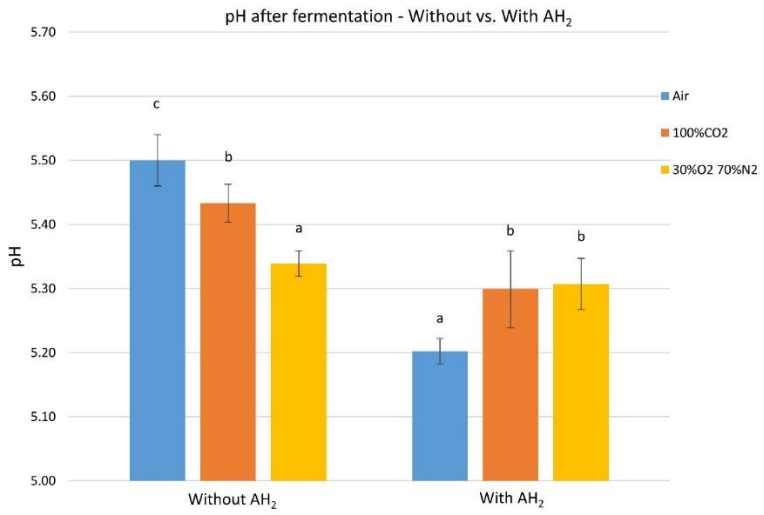


Figure 3.34. Dough pH after fermentation under different gas conditions comparing doughs without AH_2 (left group) and with AH_2 (right group). Error bars represent standard deviations. Bars within the same group with different letters (a, b, c) are significantly different ($p < 0.05$)

Under the conditions without AH_2, pH values are significantly different under the influence of gas mixtures ($p < 0.05$). The lowest pH values were achieved with gas mixtures $30\%O_2$ $70\%N_2$ (5.34 ± 0.02).

Under the conditions with AH_2, a further decrease was observed among all conditions ($p < 0.05$). The lowest pH was observed with air-mixed dough (5.20 ± 0.02).

Our results suggest that both gas composition and the presence of AH_2 significantly influence dough pH, with notable interactions between the two factors. With $30\%O_2$ $70\%N_2$ with and without AH_2 a minimal decrease of pH was observed, emphasizes on the hindering effect of AH_2 in presence of elevated O_2, may cause rapid AH_2 oxidation and depletion, reducing its efficacy. Therefore, ambient air with a pH decrease of 5.45% with and without AH_2 provides an optimal oxygen level that supports effective redox activity of AH_2.

These findings aligns with the solubility and chemical behaviour of the injected gases in the dough matrix; O_2 solubility increases with partial pressure and headspace gas composition, modulating the availability of dissolved O_2 necessary for oxidative reactions. High partial pressure pO_2 in the $30\%O_2$ $70\%N_2$ mixture accelerates AH_2 oxidation and depletion, thus, limiting further acidification and pH drop. Meanwhile, CO_2 solubility contributes directly to acidification through the formation of carbonic acid. The injected CO_2 with protocol B, had excess of CO_2 but differ in O_2 availability, thereby affecting the redox and acid-base equilibrium that governs pH.

3.2.3.4. Effect of pressurized gas-composition and addition of AH_2 on dough storage modulus (G') after kneading

Having established the impact of gas composition and AH_2 on dough t_{PEAK}, we next investigated how these factors affect the dough mechanical properties by analysing its rheological behaviour. Storage modulus (G'), representing the elastic response of the dough, was recorded across a logarithmic frequency sweep (approximately 0.1 to 100 Hz). Measurements were conducted both in the absence

and presence of AH_2 treatment. The following sections describe the observed rheological trends, including specific values at 10 Hz, as well as variability across conditions.

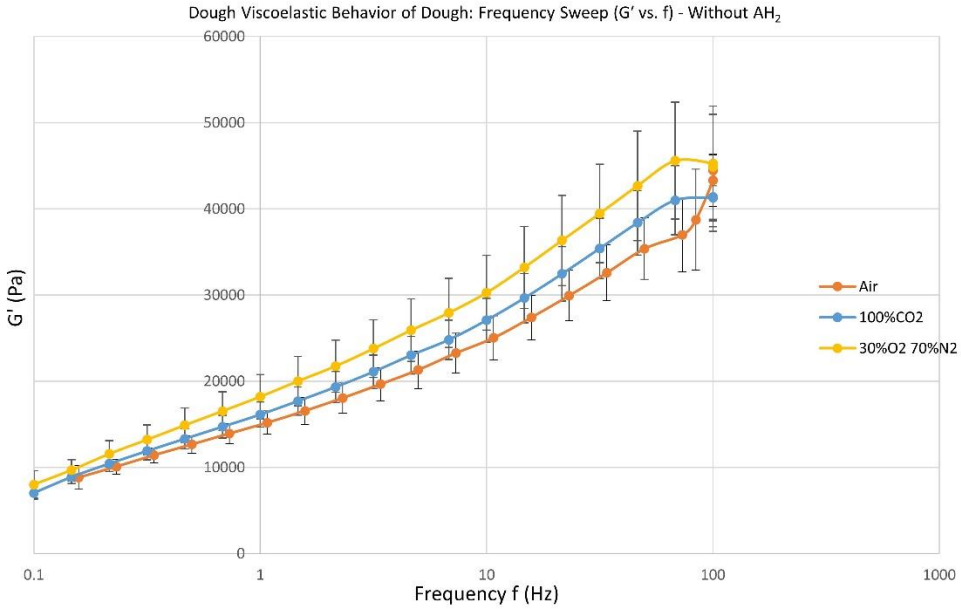


Figure 3.35. Effect of different pressurized gas compositions on the dough storage modulus G' after kneading, without the addition of AH_2

According to Figure 3.35, in absence of AH_2, the storage modulus G' exhibited a positive correlation with frequency across all gas conditions, reflecting a typical viscoelastic solid response. The extent of this increase varied depending on the gas atmosphere. Among all conditions, the doughs mixed with $30\%O_2$ $70\%N_2$ exhibited the highest G' values across the entire frequency spectrum in comparison to the reference (Air). At 10Hz, $30\%O_2$ $70\%N_2$ had G' values of 3000 Pa higher than that of air and CO_2 (2400 and 2700 Pa, respectively).

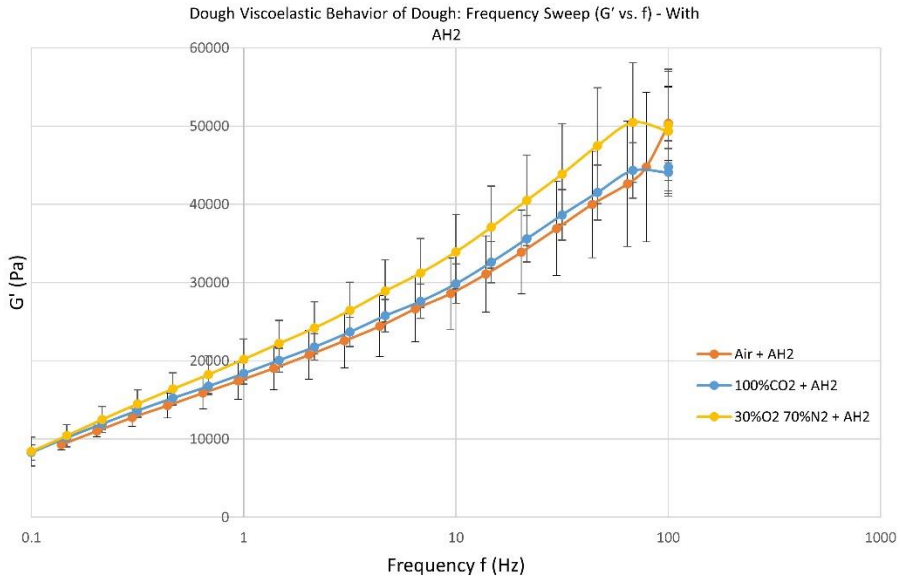


Figure 3.36. Effect of different pressurized gas compositions on the dough storage modulus G' after kneading, with the addition of AH_2

Based on the observations of Figure 3.36, across all gas conditions, G' increased with frequency, with curves rising smoothly and in parallel, exhibiting only minor offsets and indicating homogeneous viscoelastic responses. In other words, strain hardening was enhanced by the addition of AH_2. The G' values for air, 100% CO_2 was more closely aligned throughout the measured range. Doughs mixed with 30%O_2 70%N_2 gave the highest G' value at 10 Hz relative to the other conditions.

Dough mixed with O_2 becomes more elastic and exhibits greater resistance to extension compared to dough mixed without O_2 (Liang *et al.* 2023; Mirsaeedghazi, Emam-djomeh and Mousavi 2008). A similar pattern was observed by Chin et al. (2005), showed that when the dough was mixed under a steady partial O_2 pressure, the strain hardening index remained mostly unchanged despite higher gas levels. Within our linear strain range 0.01 s^{-1}, according to Meerts et al. (2017), at a small deformation range, dough extensional viscosity is primarily governed by short-range, non-covalent interactions such as van der Waals forces and hydrogen bonding. These interactions particularly between starch-starch, starch-gluten, and gluten – gluten components – play a key role in determining rheological behaviour. Therefore, the observed differences specifically with 30%O_2, likely reflect enhanced organization of the gluten-starch interactions due to mild oxidative effects.

Strain hardening is a key predictor of dough performance during breadmaking, as it reflects the dough ability to resist rupture during gas cell expansion (Meerts *et al.* 2017; van Vliet 2008; Vliet *et al.* 1992). This indicates that in accordance to our results, AH_2 enhanced the gluten network strength due to the SS bonds formation, which reinforced the dough matrix and improved gas retention capacity.

Based on Chin et al. (2005), doughs were prepared with different gas compositions using a laboratory-scale mixer, the Tweedy 1, operating at various headspace pressures. To evaluate the impact of oxidation, the doughs were mixed under different atmospheres: air, nitrogen, and a controlled O_2:N_2 environment with a constant O_2 partial pressure. Dough rheology was tested using constant airflow and constant strain rates of 0.1 and 0.05 s^{-1}. Under constant O_2 pressure, strain hardening stayed stable despite gas content, though failure strain and stress dropped. Gas flow affected aeration and work input, showing dough aeration affects rheology both during and after mixing. Another study conducted by Buche (2011), under 30% of O_2 at atmospheric pressure, doughs mixed in the presence of GOX exhibited high tenacity and poor extensibility, leading to tearing during handling. These results suggest that, under such enriched-oxygen conditions, the oxidative activity of GOX may be excessive, resulting in doughs with unsatisfactory rheological properties for breadmaking applications. Yeast and AH_2 both compete for the limited O_2 available in the dough. This competition reduces the amount of O_2 accessible for the full oxidation of AH_2. As a consequence, the intermediate by-product of AH_2 oxidation reduced glutathione (GSH) accumulates (Beghin *et al.* 2022). Since GSH is known to weaken the gluten network, its presence counteracts the strengthening role typically associated with AH_2.

3.2.3.5. Effect of pressurized gas-composition and addition of AH_2 on dough color after kneading

Building on the observed effects of gas composition and AH_2 on dough expansion and fermentation, the study also next examined dough color development, which provides insight in changes in dough color, which can ultimately affect the appearance of the final baked product. According to our knowledge, no previous studies have investigated the impact of modified atmosphere during dough kneading on dough colour.

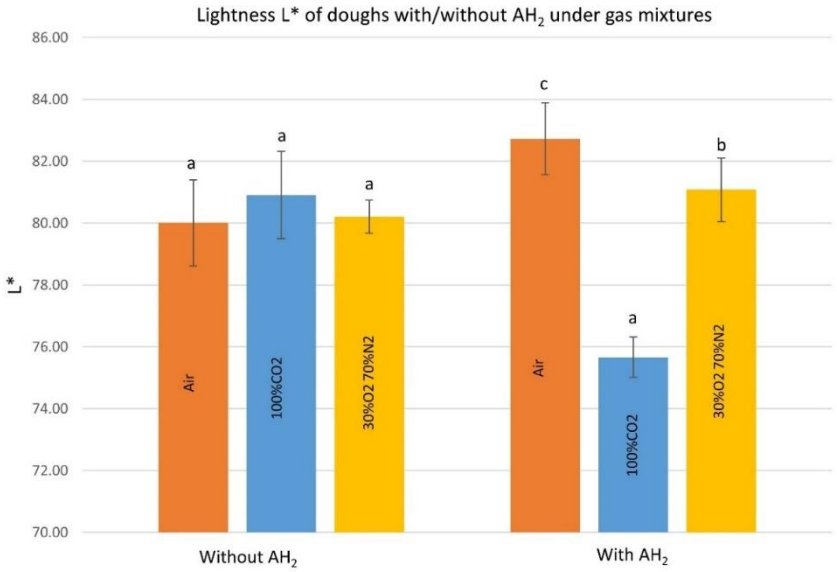


*Figure 3.37. Effect of the different gas mixtures with & without the addition of AH_2 on dough lightness L**

Dough lightness L* in absence of AH_2 was not statistically significant between all gas conditions ($p > 0.05$). The incorporation of AH_2 induced noticeable changes ($p < 0.05$). Dough with 100%CO_2, showed the darkest or lowest L* = 75 ± 0.65, whereas with air had the highest value of 82.72 ± 1.16.

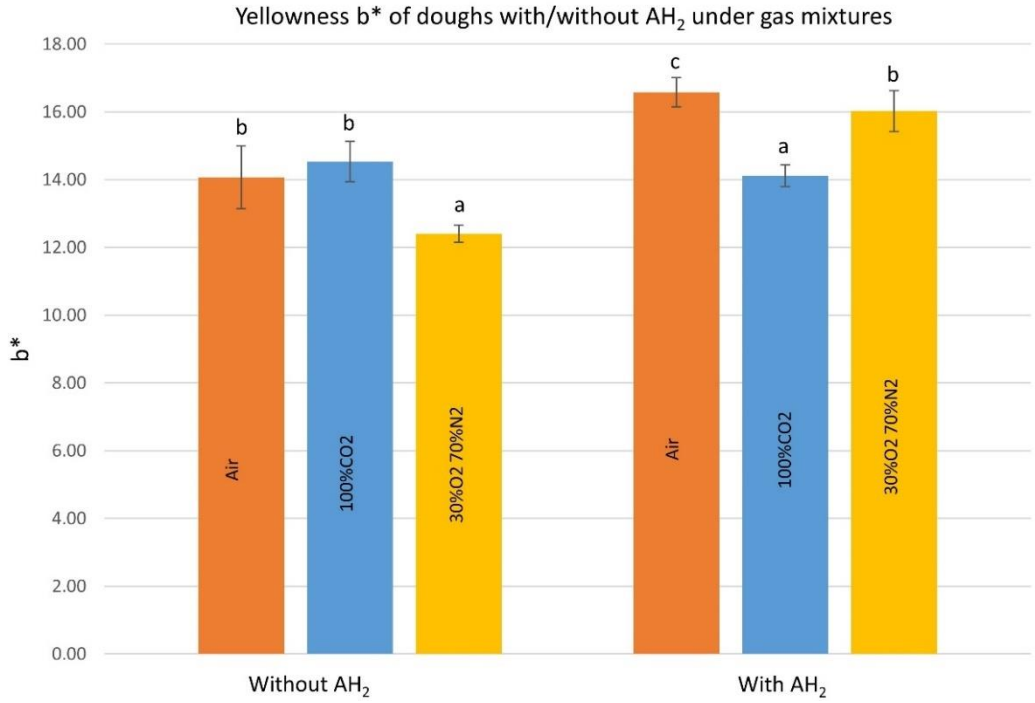


*Figure 3.38. Effect of the different gas mixtures with & without the addition of AH_2 on dough yellowness b**

In terms of yellow-blue axis b*, without AH_2 doughs mixed with 30%O_2 70%N_2 showed a lower yellow (12.40 ± 0.26) than air and 100%CO_2 with b* values (14.07 ± 0.92 and 14.52 ± 0.60, respectively).

The addition of AH_2 generally led to an increase in the b* value, this trend was observed across all gas conditions except under 100%CO_2, where b* remained nearly constant, having the lowest b* value 14.12 ± 0.32.

In absence of AH_2, dough yellowness was influenced by the gas composition, where elevated O_2 gas composition had bleaching effect. However, in presence of AH_2, the opposite trends could be explained by mixed under CO_2 will have less oxidation of pigments and phenolic compounds, resulting in a paler or less yellow color.

The darkening effect in presence of 100%CO_2 explains the inhibition activity of AH_2 in anaerobic conditions. In addition, the high O_2 levels in the O_2-enriched mixtures had no additional effect on the activity of AH_2 and coloration. Polyphenol oxidase (PPO) is a key enzyme responsible for browning in wheat products like pasta and bread (R. *et al.* 2023). Its activity depends on O_2 levels and can be inhibited by adjusting gas atmospheres, such as argon enrichment or higher O_2 (O'Beirne, Murphy and Ni Eidhin 2011). This aligns with our results, where lighter dough colours in presence of O_2 inhibited PPO, while darker dough with 100%CO_2. The similar pH and dough color between air and the 30%O_2 70%N_2 100%CO_2 mixture likely result from a balance between O_2-driven redox activity and CO_2-induced acidification, which together regulate AH_2 oxidation and enzymatic browning. Additionally, with air and O_2-mixed doughs, AH_2 act as bleaching agents which supports our results (Bejosano and Alviola 2015; Liang *et al.* 2023; Wieser 2007).

In summary, the results demonstrate that both gas composition and the presence of AH_2 significantly influence dough color, with the brightest doughs obtained under aerobic conditions with AH_2, and the darkest resulting from AH_2 addition in 100%CO_2-mixed doughs.

3.3. Conclusion for Chapter 3

The comprehensive findings of this two-part chapter provide an integrated understanding of the complex interplay between gas compositions, dough physical-chemical properties, and mechanical treatment and measurement limitations that govern dough aeration, gluten development and rheology.

The following points provide a summary of these findings:

Part I:

This part rigorously demonstrated how the combination of gas and pressure in the headspace of the mixer (air and CO_2) fundamentally alters dough development and fermentation performance.

- The main finding is that increasing mixing pressure to 0.5 bar gauge pressure led to a marked increase in dough initial void fraction with CO_2. However, the type of gas and pressure each dictated the optimal development time. With air, the dough achieved higher final void fraction ($\varepsilon_F = 0.64$) along with a comparatively shorter fermentation time, which favoured a higher SV with fine, uniform breadcrumb structure.
- By contrast, with CO_2 at elevated pressure, fermentation was longer and the final void fraction decreased, mainly due to gas loss during sheeting and yeast inhibition in the CO_2-rich environment.

The study also addressed why the actual measured void fractions did not reach the theoretical value of 0.75. Several hypothesis are proposed at follow and would require additional experimental investigations:

- First, the temperature of oil used to measure the final void fraction after fermentation was lower than the actual fermentation temperature, and eventually the dough temperature, which created a shock and thus shrinkage of many of the formed bubbles. This displayed an underestimated void fraction.
- Second, the presence of persistent gas bubbles at the bottom of the fermentation flask produced artefactual readings, inflating apparent dough expansion ratio but not presenting the real increase in gas volume within the dough matrix.
- Third, the mechanical sheeting applied prior to the measurement expelled some of the formed bubbles during mixing and pre-fermentation, resulting in a further reduction of observed void fraction.

Part II:

This part investigated the effects of gas environment (air, CO_2, O_2, N_2) at 0.5 bar gauge pressure (Protocol A and B) with the incorporation of ascorbic acid AH_2. Based on a summary of all the findings:

- The two mixing protocols A and B (0.5 bar gauge pressure) significantly influenced dough properties through the modulation of CO_2 and O_2 partial pressures.

- Both protocols supplied enough CO_2 for dough saturation, however Protocol A maintained a higher O_2 levels essential for enzymatic and oxidative reactions for the dough development, whereas Protocol B led to O_2 depletion, limiting these processes.
- Dough mechanical properties, SME and t_{PEAK}, varied with gas composition and the addition of AH_2, with AH_2 reducing SME especially in O_2-mixed doughs.
- CO_2 presence enhances bubble growth and dough expansion, though high CO_2 and low oxygen environments can impair gluten network development and fermentation kinetics, resulting in delayed dough expansion and development.
- Microscopic observations revealed that air-mixed doughs had smaller and more stable gas bubbles than CO_2-mixed doughs, where larger bubbles coalesce faster, and indicating instability.
- The decrease of pH with CO_2-mixed doughs was due to the formation of carbonic acid, which was intensified with the addition and conversion of AH_2 into DHA in presence of O_2.
- Dough colour is influenced by gas composition, with air and O_2 leading to lighter dough due to enzymatic bleaching, and CO_2 causing a darker dough due to pigments inhibition in absence of O_2.

Overall, these combined results illustrate the gas atmosphere during dough mixing can be strategically used to tailor dough microstructure, CO_2 solubilisations, mechanical properties, fermentation kinetics and colour. Air and O_2-riched environments favour balanced gluten development, stable aeration, and while with pure CO_2 through increasing gas solubility and initial expansion, compromise gas stability and uniformity.

We would like to shed the light on some experimental limitations, related to the final dough void fraction that did not reach the theoretical value of 0.75 under any condition or protocol. First, the oil temperature used to measure this value after fermentation was lower than the actual dough temperature, leading to contraction of formed gas bubbles as the dough was immerged into the oil. Second, slight mechanical degassing during sheeting especially with CO_2-mixed doughs, which may have resulted in partial gas loss. Finally, the appearance of gas bubbles at the bottom of the used fermentation flask likely introduced inaccuracies in the expansion ratio value. These combined limitations contributed to an underestimation of the true final void fraction.

CHAPTER 4 : BREAD RESULTS

This chapter presents the results obtained from baking tests done with some of the dough developed in the previous chapter 2 and 3. All breads examined here were produced by applying Protocol A at 0.5 bar gauge pressure with partial vacuum and gas flushing. This chapter consists of four parts:

- Part A: Bread results for all gas mixtures (air, 100%CO_2, 30%O_2 70%N_2) without and with AH_2 in terms of specific volume (SV), porosity, crust and crumb colour, breadcrumb structure as well as bread staling,
- Part B: Bread results of air and 100%CO_2 with variation of yeast concentration
- Part C: The impact of sheeting on breads mixed with air and 100%CO_2, focusing on how mechanical sheeting influences both SV and breadcrumb structure.
- Part D: Sensory analysis, integrating discriminative and descriptive assessments across all gas mixtures.

4.1. Part A – Bread results for all gas mixtures (air, 100%CO_2, 30%O_2 70%N_2)

4.1.1. Effect of pressurized gas conditions and the addition of AH_2 on bread specific volumes SV and porosity

All breads were evaluated after one hour of cooling after baking, to ensure comparable results of all conditions. After baking, breads showed significant difference in SV under the different gas compositions and with the addition of AH_2 (Figure 4.1) ($p < 0.05$).

The lowest significant value was scored with 100%CO_2 without and with AH_2 (3.24 ± 0.18 $cm^3 \cdot g^{-1}$ & 3.60 ± 0.45 $cm^3 \cdot g^{-1}$, respectively) than the rest of the conditions. Whereas the highest values were observed with air without AH_2 and 30%O_2 70%N_2-mixed breads with AH_2 (4.54 ± 0.24 $cm^3 \cdot g^{-1}$ & 4.53 ± 0.37 $cm^3 \cdot g^{-1}$, respectively). The addition of AH_2 had no significant differences with air and CO_2-mixed breads, except for 30%O_2 70%N_2 which was significantly different from 30%O_2 70%N_2 mixed breads without AH_2 (4.27 ± 0.29 $cm^3 \cdot g^{-1}$).

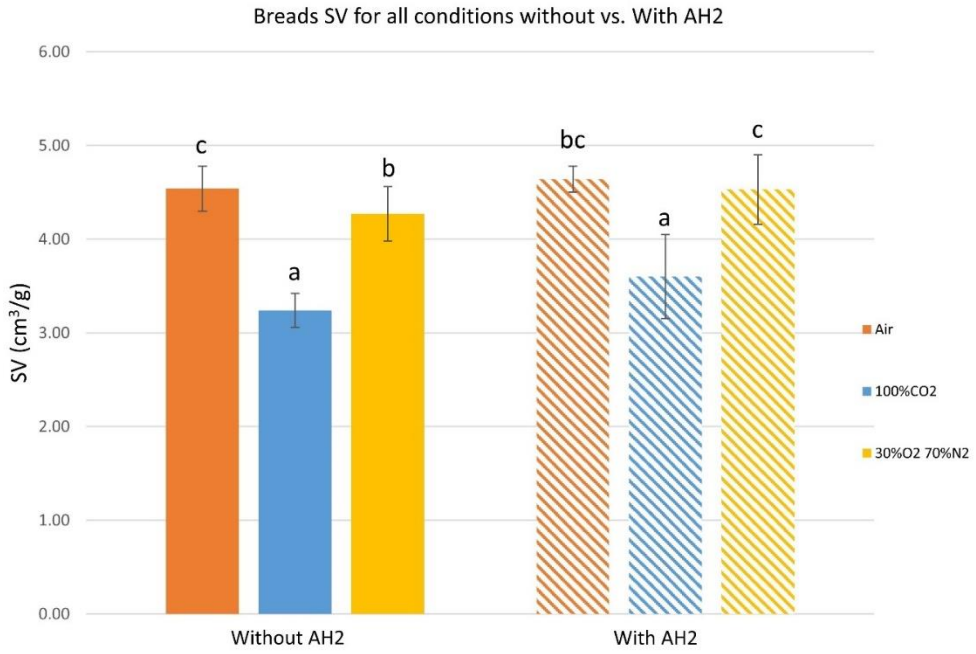


Figure 4.1 Breads specific volumes (SV) in $cm^3 \cdot g^{-1}$ with and without AH_2 under the different gas mixtures. Letters indicate significant differences ($p < 0.05$) between gas conditions within each treatment (with or without AH_2)

Based on these findings, bread loaves SV without AH_2 were primarily influenced by the gas composition injected during kneading. Martin et al. (2008) conducted a similar study by mixing bread dough with Tweedy type 10 mixer, under controlled air or CO_2 atmospheres with varying pressures. Experiments tested how changing the gas type and pressure during mixing affected dough structure and loaf volume. CO_2 was introduced at different times, and pressure was reduced mid-mixing to observe impacts on dough density and final loaf characteristics. Based on their results, high-pressure at 2 bar had more pronounced effect especially with CO_2-mixed doughs resulting in a decrease of 17% of bread

volume. In addition, loaves mixed with CO_2 were smaller than those with air, which was in accordance with our results with CO_2-mixed breads.

However, in the presence of AH_2, gas composition (the elevated O_2) hindered its effect, hence why no significance in SV between air and the gas mixture. Air (21% of O_2) was enough for the full development of the gluten network. Although it was anticipated that elevated O_2 incorporation during mixing would enhance the bread-improving effect of AH_2, its inclusion no longer influenced bread SV when the dough was mixed in an O_2-enriched environment. Based on Beghin et al. (2022), investigated the role of O_2 under different mixing times and AH_2 concentrations on breads SV. Results have shown that high levels of AH_2 resulted in increased breads SV up to a certain point. When doughs were mixed under low O_2 conditions, AH_2 continued to enhance SV until a certain extent. Additionally, this study also observed that variations in O_2 levels with extended mixing times (3, 4 & 6 min) led to higher breads SV. Their results align with our study that at a fixed mixing time and a fixed AH_2 concentration, the increased O_2 levels will hinder the effect of AH_2 and thus, O_2 alone is capable of the full oxidation of thiol SH groups. Cauvain and Young (2006) by using the CBP method, found that O_2-mixed doughs enhanced the effect of AH_2 which contradicted our results with the straight-dough recipe or rather, it showed no effect of AH_2 on breads SV especially with the 30%O_2.

To further elucidate these differences, it is important to consider how SV correlates to the injected gases partial pressures during mixing. The low SV in CO_2 aligns with very low partial pressure of O_2 (pO_2 = 0.14 bar), which may limit oxidative crosslinking, resulting in a weaker gluten network, less gas retention and thus reducing the breads SV. Higher SV with air and 30%O_2 corresponds with higher pO_2 (0.44 & 0.36, respectively) which was enough to promote the gluten network development and gas retention. High CO_2 levels additionally affect dough acidity and gluten functionality, contributing to lower SV independent of oxygen availability. Thus, bread SV reflects both the chemical strengthening via oxidation under different pO_2 and the physical stability of gas bubbles within the dough matrix.

4.1.2. Determination of Breadcrumb structure and pore distribution

The structure of bread is defined by size, distribution and shape of gas bubbles formed during mixing, fermentation and baking. A fine crumb structure features small, evenly distributed pores, while coarser crumb is characterised by larger and irregular pores. The porous structure of the bread is usually formed by the gluten network development and gas bubble nucleation during mixing; generation of CO_2 resulting from yeast fermentation; redistribution of gas bubbles during the shaping stage and internal water evaporation, expansion and combination of gas bubbles during baking (Aghajanzadeh *et al.* 2024; Gao, Wang *et al.* 2017). Quantitative analysis of breadcrumb structure was conducted by measuring pore surface area distribution. The results are illustrated by plotting the cumulative distribution of pores relative to their average pore area. As shown in Figure 4.2, different distribution patterns can be observed for the different mixing conditions.

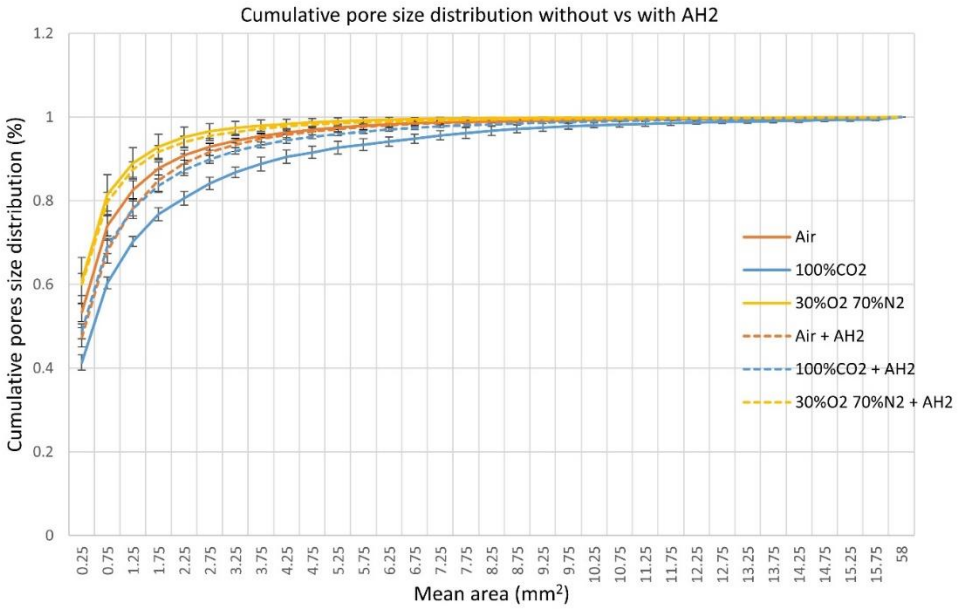


Figure 4.2 Cumulative pore size distribution of all mixing conditions without and with AH_2

Based on the observations, without AH_2, CO_2-mixed breads showed the widest pore size distribution pattern, thus reflecting largest pores size in comparison to all conditions and irregular distribution of gas bubbles. The narrowest pore size distribution was observed with 30%O_2 70%N_2. These observations reflect small and homogeneous breadcrumb structure. These results suggest that breadcrumb structure was influenced by the gas composition injected during mixing. The addition of AH_2 had no significant impact with 30%O_2 70%N_2 and with air. However, with air breadcrumb was less homogeneous than 30%O_2 70%N_2 and consistently, with CO_2 a wide distribution patter reflected large pores sizes. Based on these results, pore size distribution was then quantified into pores population groups according to their median sizes, allowing a clearer comparison of the structural differences between conditions. The population was based on D90 where 90% of pores fall, indicating the upper range of the pore size distribution.

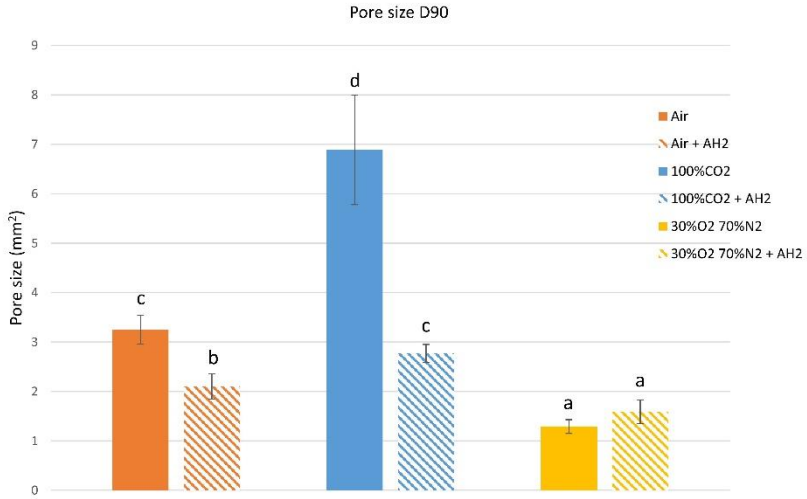


Figure 4.3 Median pore size D90 of all conditions. Values with different superscript lowercase letters in the same column for each condition are significantly different ($p < 0.05$). The values presented here are mean ± standard deviation

Based on results in Figure 4.3, without AH_2, for 100%CO_2, 90% of pores population were smaller than 6.89 ± 1.11 which was higher than air and 30%O_2 70%N_2 with 90% of pores population are smaller than 3.25 ± 0.29 & 1.29 ± 0.14, respectively. With the addition of AH_2, the same trend was observed where 100%CO_2 had 90% of pores population were smaller than 2.77 ± 0.18, which was a higher value than air and 30%O_2 70%N_2 with pores population was smaller than 2.10 ± 0.26 & 1.59 ± 0.24, respectively. Based on these results, AH_2 had no significant effect with 30%O_2 70%N_2, indicating that this gas composition alone was sufficient to produce a fine and homogeneous breadcrumb structure. Furthermore, with air and 100%CO_2 were significantly higher with and without AH_2, indicating larger pore sizes.

In the case of CO_2 mixing, the partial O_2 pressure is decreased, resulting in that the gluten network was deprived from an O_2 source. A weaker gluten network may explain bubbles instability (Martin *et al.* 2008). The catalytic activity of yeast initiates a cascade of reactions that impart a great role in the dough aeration and expansion during the fermentation period. This expansion is a result of the solubilisation of CO_2 by-product of yeast fermentation of glucose (Kulp and Lorenz 2003; Mills *et al.* 2003; Wilde 2012). Therefore, mixing under pure CO_2 in addition to the yeast fermentation, excess CO_2 will be produced and thus less gas bubbles will be available to act as nucleation sites. Gluten network acts as a physical barrier among other macromolecules between gas bubbles preventing coalescence. Coalescence was also defined by the rupture of the film between two gas cells thus they migrate together leading to irregular crumb structure (Dobraszczyk *et al.* 2003; Janssen, Wouters and Delcour 2021; Kokelaar, van Vliet and Prins 1996; van Vliet 2008; Vliet *et al.* 1992). Due to the weakened gluten network separating the gas bubbles, the stability of individual bubbles becomes compromised, facilitating disproportionation where smaller bubbles diminish and larger bubbles persist, resulting in less uniform and irregular breadcrumb structure (van Vliet 2008). In addition, based on the microscopic analysis of the doughs, CO_2 mixing showed a fewer number of gas bubbles with larger dimension, whereas air shower more and finer gas bubbles. These observations were translated into the breadcrumb structure as discussed above. The microscopic evidence of bubble disappearance and reduced coalescence in air-mixed dough aligns with higher gas retention capacity and smaller pore size distribution, reinforcing the connection between dough microstructure and breadcrumb.

In accordance to our results, a study conducted by Martin et al. (2008), aimed to explore the effects of controlled mixing atmosphere on bread dough, focusing on how mixing under air and CO_2 influences oxygen adsorption, bubble size distribution and finally their effect on the bread crumb structure. In particular, this study examined whether the benefits of partial vacuum mixing can be replicated by mixing under a CO_2 atmosphere in the final stage. Based on the results of this study, mixed under air, the crumb cell structure becomes coarser as the pressure increases (0.3 to 2.0 bar). When mixed under CO_2, the crumb structure appears coarser over the entire range, but especially at lower pressure. The results showed that mixing solely under pure CO_2 is unlikely to produce an acceptable bread structure. In the case of 30%O_2 70%N_2, O_2 helps in the oxidation of SH groups and the more SH groups are oxidized the more SS bridges are formed and the more the gluten network is polymerised and thus more aeration or gas bubbles are retained.

To better visualise these findings, scanned images of bread sliced were summarised in the Figure 4.4. These images are representative of all 9 samples for each gas condition. Visual examination confirmed that the samples within each group exhibited similar characteristics, indicating consistent breadcrumb structure across replicates. In addition, these scanned images give information concerning the crumb

colour and the height of the breads. As we observe, without AH_2, with the mixture 30%O_2 70%N_2 a finer and homogeneous breadcrumb was obtained, whereas more bubbles and a bit larger bubbles obtained with air and with 100%CO_2 we can observe coalescence. With AH_2, despite the disappearance of coalescence, the crumb was not homogeneous, although the coalescence phenomenon was observed on the crust. This could be due to the evaporation of excess CO_2 during baking, which likely accumulated and escaped through the crust. The release or evaporation of CO_2 disrupted its uniformity, contributing to low SV as observed. The extent of coalescence is influenced not only by bubbles size but also by the distribution of bubble sizes within the crumb (Sun, Martin Scanlon *et al.* 2023). When bubbles are consistent and similar in size, the mixture remains stable and uniform which was observed with 30%O_2 70%N_2, in contrast, when the bubbles distribution varies widely and large bubbles are present (in the case of 100%CO_2) the mixture is unstable and bubbles merge leading to uneven crumb structure. Interestingly, with the AH_2 breads, and particularly with 30%O_2, the crumb appeared slightly layered, as if the dough has been rolled prior to fermentation and baking. This visual feature suggests structural irregularities and possible heterogeneity in pores distribution.

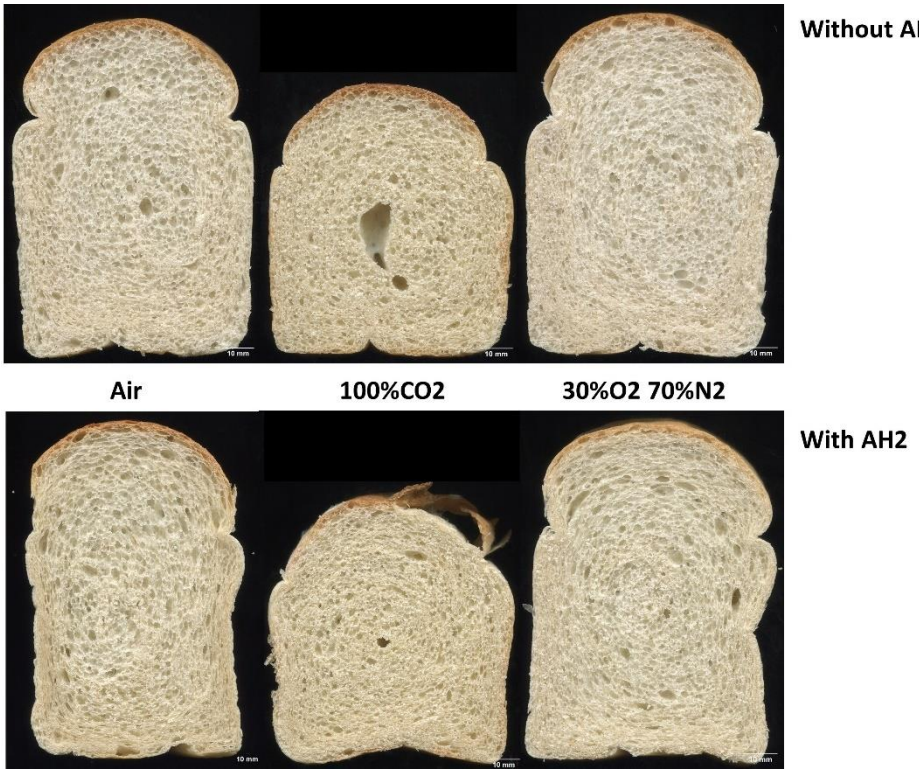


Figure 4.4 Scanned images of bread slices showing the breadcrumb structure of each condition without and with AH_2

4.1.3. Determination of breadcrumb porosity

There is a direct relationship between bubble size and overall porosity or density of the bread. As the average bubbles size increases and the distribution becomes broader, the crumb porosity rises leading to higher porosity and lower density. Conversely, a narrow distribution of small bubbles leads to a denser matrix with higher porosity. The figure below (Figure 4.5) presents the porosity values between all gas mixtures and with the addition of AH_2. The results of bread crumb porosity showed that both gas composition and the presence of AH_2 had a significant effect on bread porosity ($p < 0.05$). Evidently

without AH_2, the lowest crumb porosity was observed with 100%CO_2 (0.46 ± 0.04) reflecting larger chimney-like pores and irregular crumb distribution resulting in an overall denser crumb. In comparison to air and 30%O_2 70%N_2 (0.70 ± 0.02 & 0.70 ± 0.06, respectively), these latter reflected a less dense and finer breadcrumb distribution, as we observed in the breadcrumb structure in section 4.1.2. With AH_2, porosity values were higher under all gas compositions except for 30%O_2 70%N_2 which decreased with the addition of AH_2. There was no significant difference between air and 30%O_2 70%N_2 breads without AH_2 (0.70 ± 0.02 & 0.70 ± 0.06, respectively). However, with AH_2, air mixed breads achieved significantly higher porosity than 30%O_2 70%N_2, due to the higher SV than the rest of the conditions.

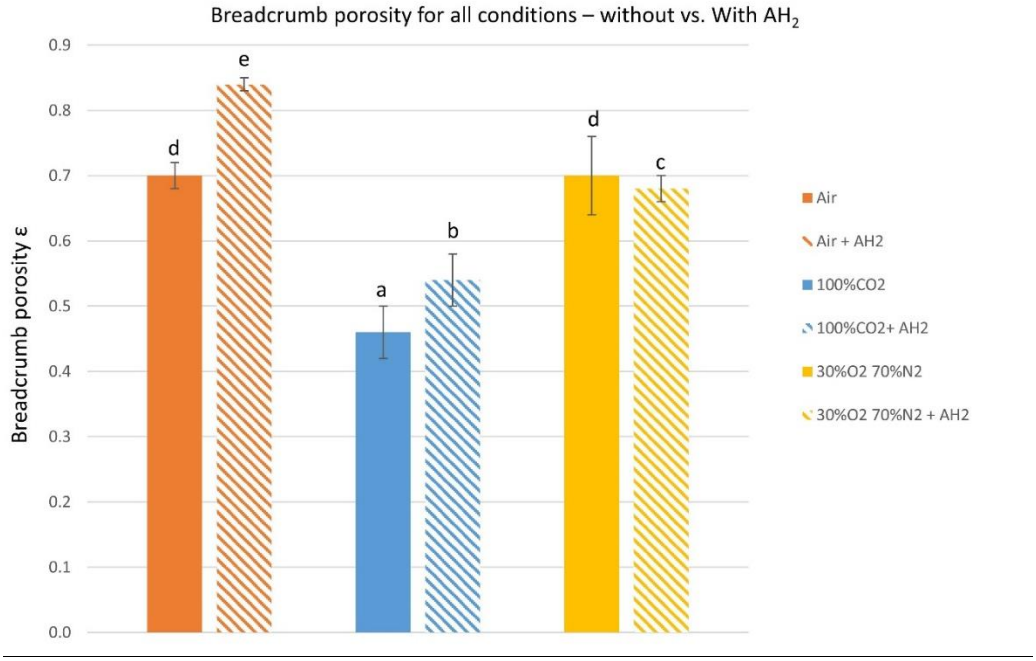


Figure 4.5 Breadcrumb porosity for all conditions without & with AH_2. Values with different superscript lowercase letters in the same column for each condition are significantly different ($p < 0.05$). The values presented here are mean ± standard deviation

Breadcrumb porosity is a reflection of bread dough aeration during mixing and fermentation (Shah *et al.* 1998; Martin *et al.* 2004). According to Wan et al. (2011) breadcrumb porosity represents 0.72 to 0.84 of the void fraction in crumb and is a single interconnected open pore network crucial for network strength and texture. Gao et al. (Gao, Tay *et al.* 2017) studied the effect of reduced headspace pressure during mixing and mixing duration on breads made from high protein flour (HPF) and low protein flour (LPF). Results have showed that HPF breads with longer mixing times (5 to 7 min) gave significantly higher porosity than LPF mixed at a shorter time (3 min). Our results align, where with air and 30%O_2 70%N_2 (with and without AH_2), had the longest mixing times, and thus higher SV and higher porosity. Palier et al. (2021) mixed cake batters with the same prototype where CO_2 and N_2 gases were the injected gases under different cake formulations under 0.3 and 0.5 bar gauge pressure. At 0.5 bar gauge pressure with CO_2-mixed cakes, showed a significant improvement in cakes SV and simultaneously crumb porosity. As seen in our study, there was a significant difference between air and CO_2 in terms of porosity with and without AH_2 suggesting that while CO_2 does not impact the overall porosity, it likely altered the gas cell distribution thus forming large gas bubbles, and due to a significantly lower SV after baking all the formed gas bubbles evaporated due to the depolemerized gluten network.

The reason why after the addition of AH_2 with air was the highest, could stem from its effectiveness depend on the gas atmosphere. With air, it provides sufficient amount of oxygen for AH_2 activation to exhert its strengthening effect, however it was observed lower with 30%O_2 70%N_2, likely due to the over-oxidation which led to less stabilisation of formed gas bubbles, explaining the significant decrease in porosity.

4.1.4. Determination of bread colour

Bread colour serves as an intermediate sensory attribute that reflects both the underlying chemical reactions during baking and the physical characteristics of the crumb and crust. In the following section, we will be presenting the impact of gas mixtures and with the addition of AH_2 on the upper crust and crumb lightness L* and yellowness b*.

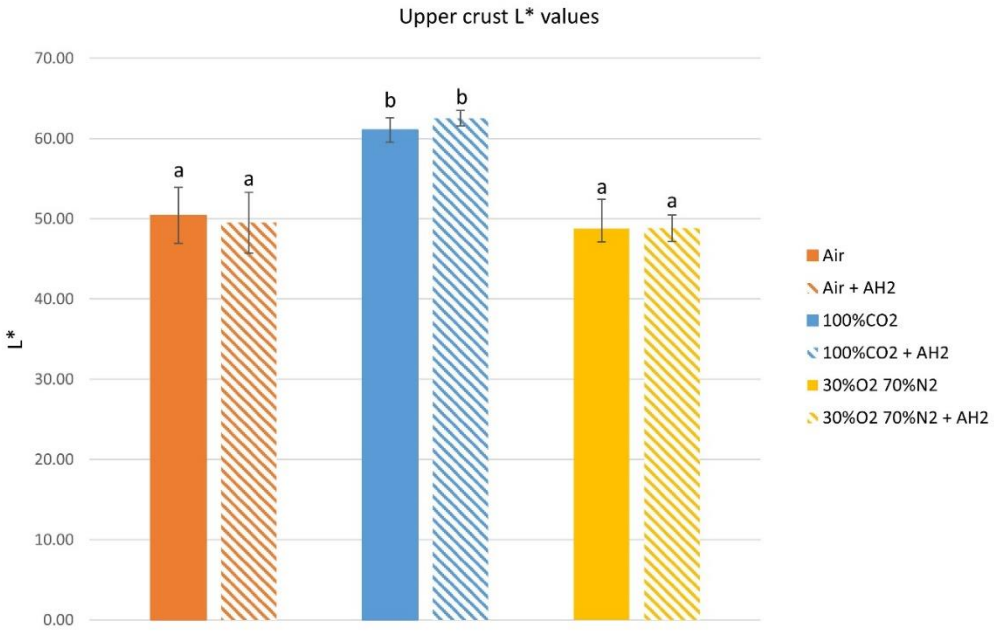


Figure 4.6 Breads upper crust lightness L in function of injected gas mixtures and with the addition of AH_2. Values with different superscript lowercase letters in the same column for each condition are significantly different ($p < 0.05$). The values presented here are mean ± standard deviation*

Figure 4.6 showed that gas mixtures alone have significantly influenced the lightness value L* of the upper crust after baking ($p < 0.05$). The highest L* value was observed with 100%CO_2 (61.08 ± 1.51) which was not significantly different after the addition of AH_2 (62.54 ± 0.95). There was no significant difference between air and 30%O_2 70%N_2 without and with AH_2, and thus demonstrating darker upper crust.

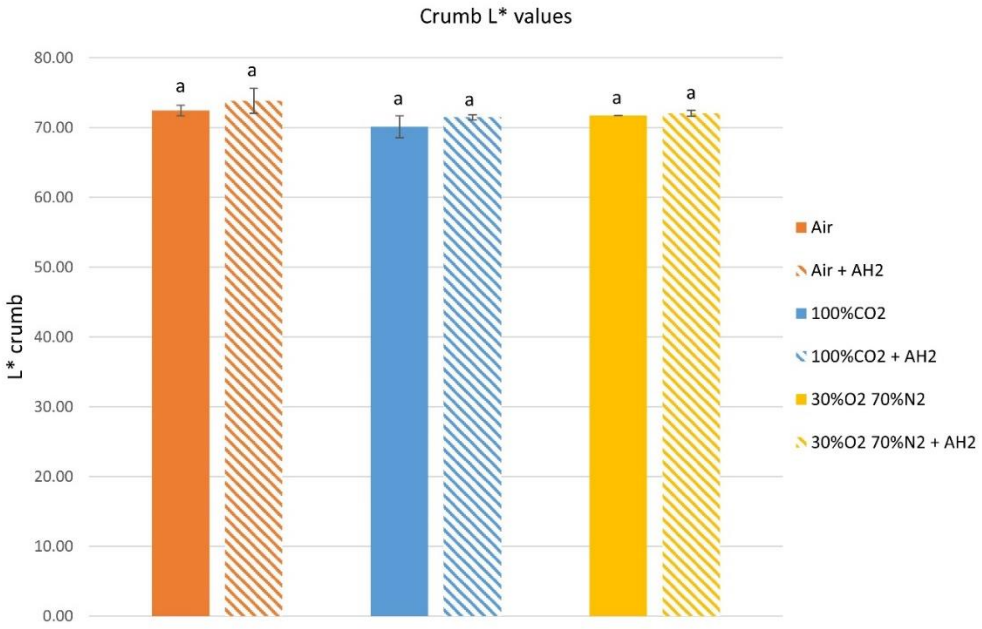


Figure 4.7 Breads crumb lightness L in function of injected gas mixtures and with the addition of AH_2. Values with different superscript lowercase letters in the same column for each condition are significantly different ($p < 0.05$). The values presented here are mean ± standard deviation*

There was no significant impact of gas mixtures and the additions of AH_2 on crumb L* ($p > 0.05$).

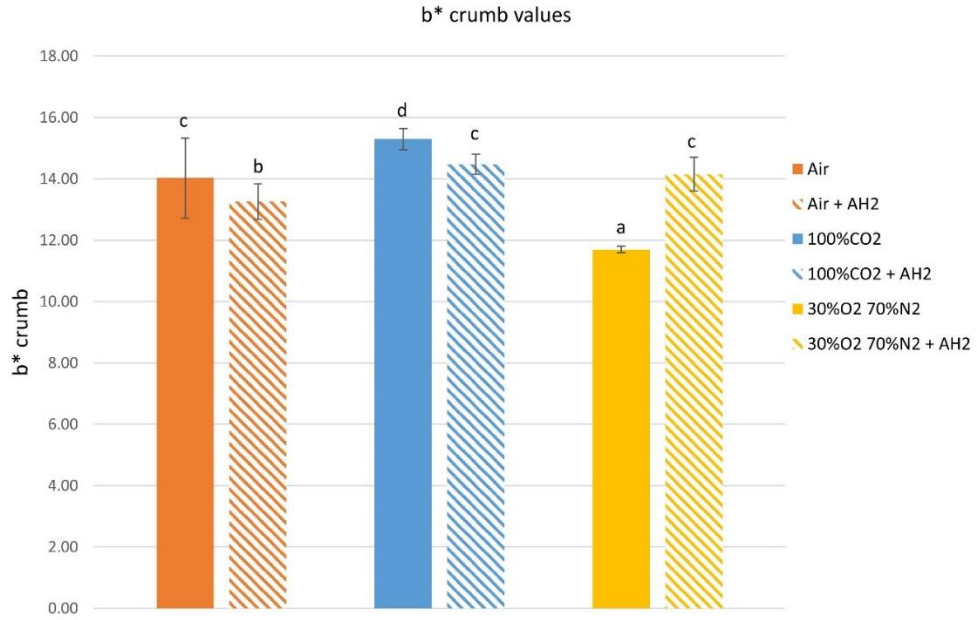


Figure 4.8 Breads crumb yellowness b in function of injected gas mixtures and with the addition of AH_2. Values with different superscript lowercase letters in the same column for each condition are significantly different ($p < 0.05$). The values presented here are mean ± standard deviation*

Based on Figure 4.8, breadcrumb yellowness b* was significantly influenced by the gas composition, with the highest value achieved with 100%CO_2 (15.30 ± 0.34) in comparison to air and 30%O_2 70%N_2 (14.03 ± 1.31 & 11.69 ± 0.11, respectively). The addition of AH_2 led to a higher b* value with 30%O_2 70%N_2 (14.15 ± 0.55) which was not significantly different from 100%CO_2 (14.48 ± 0.33).

Based on the results above, 100%CO_2 improved crust lightness L* and yellowness b* regardless to the addition of AH_2. CO_2 forms carbonic acid when dissociated in the dough (Chaix, Guillaume and Guillard 2014), and upon baking this acidity inhibits the Maillard browning reaction resulting in lighter crust. The presence of AH_2 did not significantly influence L* of crust, signifying the dominant influence of CO_2 and it confirms that this anti-oxidant is not active in absence of O_2.

4.1.5. Bread Staling

Right after baking, bread is at its peak with soft, air and flavourful. Nevertheless, within hours and days its texture and taste begin to decline, these undesirable changes are collectively called staling. This transformation is not just about bread drying out; it is mainly driven by starch retrogradation.

4.1.5.1. Starch retrogradation

Starch retrogradation was monitored over a 15-day storage period for all conditions on specific days J0, J1, J4, J7 and J15. The retrogradation kinetics were analysed using the Avrami model. The exponent of the time was fixed to n = 1. Some studies propose a determination of n; however, the interpretation of n is difficult and also it makes the comparison of the time constant more difficult. According to literature, an Avrami exponent n = 1 means that the formation of crystalline nuclei happens in one dimension, creating elongated, rod-shaped-like structures (Han *et al.* 2021; Li 2024). This kinetic model reflects the early rapid nucleation phase followed by linear elongation of amylopectin chains as they re-associate into double helices.

$$\Delta H(t) = \Delta H_\infty + (\Delta H_0 - \Delta H_\infty).e^{\left(-\frac{t^n}{\tau}\right)} \quad \text{Eq. 4.1}$$

Where ΔH_0 is the initial enthalpy and τ is the time constant characterising retrogradation kinetics rate. The higher the time constant, the slower will be the kinetics of staling. The higher the ΔH_∞, the higher will be the amount of retrogradated starch and the firmer should be the crumb, even though this correlation is not always observed. The ΔH_∞ and the τ values were obtained using the excel solver. This approach enabled precise quantification of starch retrogradation kinetics, elucidating how different processing conditions affect the rate and extent of bread staling.

Based on Figure 4.9, the evolution of enthalpy of 30%O_2 70%N_2 increased markedly after J1 until reaching a final enthalpy at J15 (4.64 ± 0.60 J·g^{-1} dry flour). In comparison, breads mixed with air and CO_2 exhibited a slower enthalpy increase, where it slowly started to increase until a sharp increase was observed between J5 and J7, reaching a higher final enthalpy of (5.03 ± 0.16 & 5.53 ± 0.39 J·g^{-1} dry flour, respectively). Despite the differences, all conditions exhibited continuous retrogradation from J7 to J15, without fully reaching a plateau by the end of storage, indicating ongoing amylopectin recrystallization during this later phase.

Based on Avrami model (Figure 4.10), it shows that 100%CO_2 gave the slowest kinetics rate and 30%O_2 70%N_2 the fastest with 9.44 and 4.67 days respectively. The retrogradation increased sharply during early storage, with the majority of amylopectin recrystallized after around 7 days of storage at 10°C. With air and 100%CO_2 the rate of retrogradation seemed slowed down until day 5; however, this was averaged in the Avrami model. Based on these finding, it can be concluded that gas composition had an effect on starch retrogradation rate and on the extent of starch recrystallization. The 100%CO_2 has staling effect with the highest level of retrogradated amylopectin; however, the staling rate was the

slowest and 100%CO_2 may contribute to a delayed staling. However, the lower development and the lower SV of 100%CO_2 is not in favour of this process.

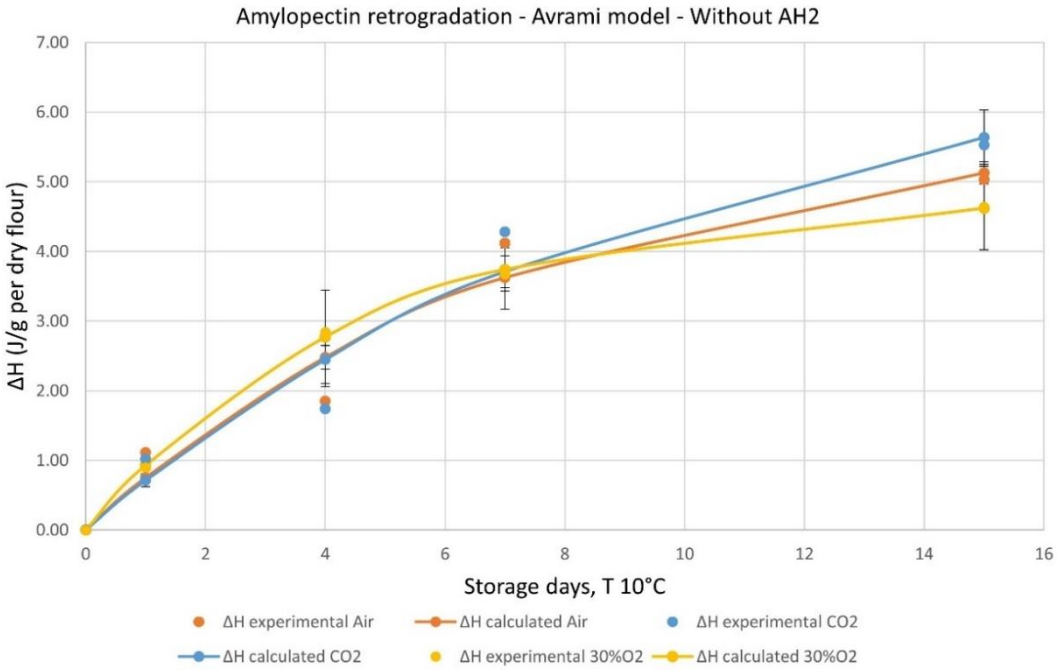


Figure 4.9 Evolution of enthalpy of amylopectin retrogradation during storage under different gas composition without the addition of AH_2. Experimental enthalpy values (ΔH in $J \cdot g^{-1}$ per dry flour) are shown as data points, while corresponding model predictions are shown in the figure as fitted lines

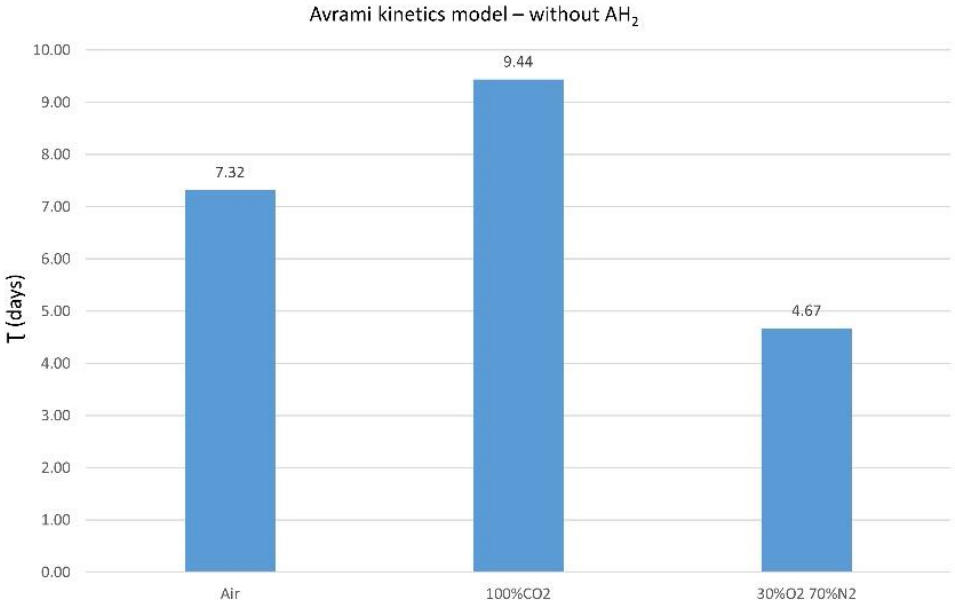


Figure 4.10 Avrami model showing the time constant (Ţ in days) of all conditions stored at 10°C during 15 days

One of the main factors of bread staling is the temperature storage (Le-Bail *et al.* 2009), affecting the retrogradation kinetics. Therefore, in our study, breads were stored at 10°C instead of 4°C in order to have a progressive staling which facilitated the monitoring the staling over a two weeks period of time

facilitating the implementation of the experimental work. One explanation could be that in the case of 100%CO_2, the injection of CO_2 was sufficient for its solubilisation in the dough (1.37 g) with moderate pCO_2, which led to acidification and altering plasticization of amylopectin chains. Acidification can weaken hydrogen bonds and the partially weakened gluten network may change starch-gluten interactions (Abedi and Pourmohammadi 2021). Several studies have highlighted the pivotal role of dough acidity in modulating starch retrogradation and thus bread staling. Li et al. (2024) showed that sourdough fermentation, by producing organic acids, lowers dough pH and delays amylopectin retrogradation, resulting in slower crumb firmness and extended freshness. Their work demonstrated that acidification modifies molecular mobility of starch chains and affects starch-protein interactions. Complementing this, Wang et al. (2024) found that dough acidity influences water distribution and amylopectin crystallinity during storage. In addition, Corsetti et al. (2000) investigated how sourdough fermentation and associated acidification influence starch retrogradation, bread firmness and staling. Their results showed that breads made with sourdough had a significant delay in retrogradation compared to chemically acidified or conventionally fermented breads. Furthermore, they demonstrated that the extent of retrogradation retardation depended on the level of acidification and the specific lactic acid bacteria strains involved. For example, sourdoughs containing *Lactobacillus sanfranciscensis* and *Lactobacillus plantarum* strains, especially when combined with fungal alpha-amylase or amylolytic bacteria such as *Lactobacillus amylovorus*, showed improved bread softness and delayed staling. The addition of pentosanes and endoxylanase enzymes to the sourdough gave a greater delay in starch retrogradation and firmness. Another explanation is that CO_2 does not interfere with amylopectin structure as other anti-staling gents (i.e. α-amylase), however due to its impact on dough liquor viscosity which physically limits amylopectin chain mobility and affecting their ability to re-associate into double helices. These structures are stabilised by hydrogen bonds and van der Waals interactions between hydroxyl groups of glucose, thus carbonic acid weaken or disrupt these bonds and reducing the stability and formation rate of amylopectin helices. According to Chen et al. (Chen *et al.* 2023), reported how high-pressure treatment disrupt the crystalline lamellae of amylopectin, altering the starch molecular mobility and retrogradation behaviour without breaking the double helix structure itself. Similarly, to our results, CO_2 delayed starch retrogradation physically by altering the surrounding environment. Gray and Bemiller (2003) also confirmed that during the first days of storage, bread staling is mainly due to structural changes in amylopectin molecules, whereas towards the last storage days is due to moisture loss from the gluten. Collectively, these studies provide a strong mechanistic support for the acidification effects observed in CO_2-mixed breads.

Based on the results with AH_2, the overall retrogradation enthalpy with 100%CO_2 and 30%O_2 70%N_2 was lower at early and mid-stages of storage between J0 and J5 (1.95 ± 0.48 & 1.78 ± 0.51 $J \cdot g^{-1}$ dry flour, respectively), whereas with air increased sharply by J5 (4.15 ± 0.25 J/g dry flour). By the end of the storage time, all conditions converged into a close value, suggesting that AH_2 is effective in slowing down retrogradation rate at early stages.

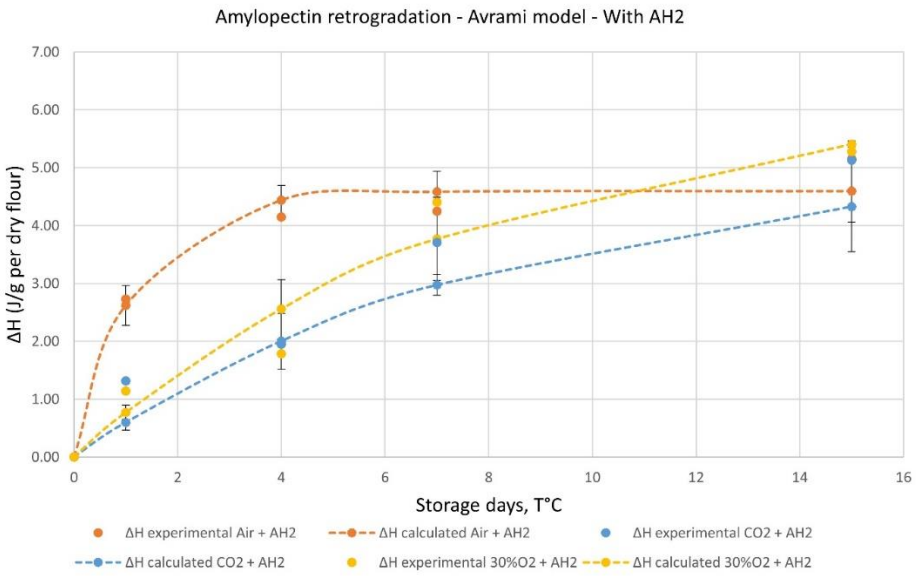


Figure 4.11 Evolution of enthalpy of amylopectin retrogradation during storage under different gas composition with the addition of AH_2. Experimental enthalpy values (ΔH in $J \cdot g^{-1}$ per dry flour) are shown as data points, while corresponding model predictions are shown in the figure as fitted lines

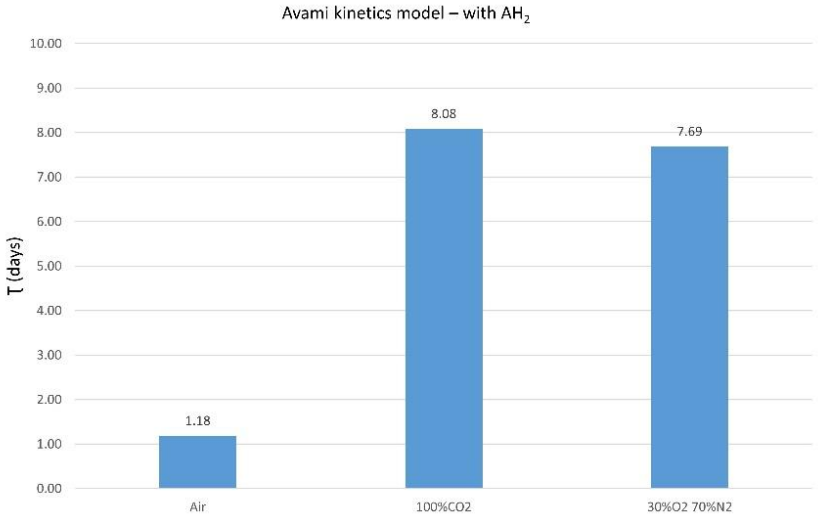


Figure 4.12 Avrami model showing the time constant (τ in days) of all conditions with AH_2 stored at 10°C during 15 days

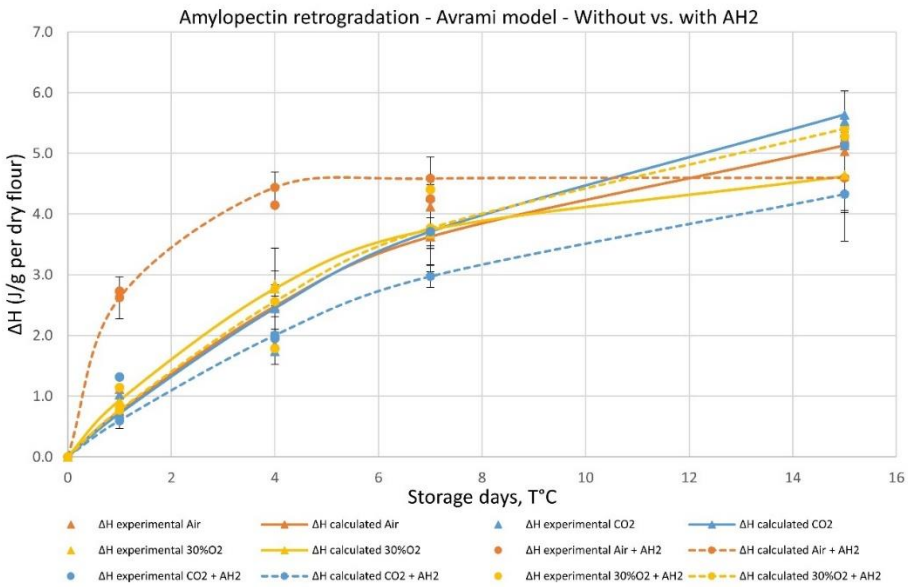


Figure 4.13 Comparison of starch enthalpies for all conditions with AH_2 (solid fitted lines) and without AH_2 (dashed fitted lines). In the colour legend, each gas mixture (air, 100%CO_2, 30%O_2 70%N_2) is represented by a specific colour, the breads without AH_2 are in a solid line with their corresponding calculated values from Avrami model: orange (air), blue (100%CO_2) and yellow (30%O_2 70%N_2), and the dashed lines with their corresponding calculated Avrami values are for the breads with AH_2

By comparing all conditions together, we can clearly observe an exponential increase of the retrogradation rate with air-mixed breads with AH_2. This explains a fast increase in retrogradation rate, whereas the opposite was observed with 100%CO_2 with AH_2, by a slower steady increase in the retrogradation rate. Studies conducted by Eliasson et al (1983a; 1983b), showed that gluten can interact with starch molecules via hydrogen bonds which partially delays retrogradation (J0 to J5 in our case with 100%CO_2 with AH_2). This interaction limits the ability of starch polymers (amylopectin) to re-associate into an ordered crystalline structure. Other studies elaborated that glutenin exhibits significant steric hindrance (physical obstruction) and forms continuous network that physically entangles or makes non-covalent bonds with starch molecules hindering their crystallisation (Jekle, Mühlberger and Becker 2016; Hu *et al.* 2025). This contributed into delaying starch retrogradation and firmness of the bread.

4.1.5.2. Determination of bread texture changes during storage

4.1.5.2.1. Firmness

Bread firmness during storage can be influenced by multiple factors beyond amylopectin retrogradation alone, including changes in moisture content over time (Gray and Bemiller 2003). Amylopectin recrystallization into double helices is a major factor in bread staling and crumb firming. However, variations in water redistribution and gluten network relaxation can also affect firmness, leading to differences solely explained by starch retrogradation rate. In the present section, we therefore examined the evolution of bread firmness during storage at 10°C for 15 days, in order to better understand the combined effects of gas composition and AH_2 addition on breadcrumb firmness. Based on Figure 4.14, bread firmness increased sharply with all conditions after J1. Although, breads

mixed with 100%CO_2 exhibited the highest firmness throughout the entire storage days reaching a final value of 9.8 ± 0.53 N, reflecting the firmest bread. Breads with 30%O_2 70%N_2 during the 7-days storage period gave the softest breadcrumb (5.57 ± 0.91 N), until it increased in firmness at J15 (7.84 ± 0.46 N).



Figure 4.14 Evolution of breadcrumb firmness for all conditions without the addition of AH_2 during storage days

Bread firmness also depends on crumb microstructure and changes in gluten network (Besbes *et al.* 2013; Chakrabarti-Bell, Wang and Siddique 2014). Gray and Bemiller (2003) described in their review that several studies concluded that gluten may serve as a moisture reservoir buffering changes in starch hydration capacity and it tends to reduce associations between swollen starch granules embedded within the network, thus retarding crumb firmness (Kulp, Ponte and D'Appolonia 1981).

Based on porosity results, it was significantly different between samples ($p < 0.05$) and that breadcrumb structure showed differences in pores distribution, thereafter, bread firmness is linked to porosity and structure. According to Jekle et al. (2018), the denser the breadcrumb, the more solid material is present under the cylindrical probe, resulting in greater force needed to compress the crumb. As previously concluded with 100%CO_2, the large gas cells led to lower crumb porosity coupled with a lower SV, resulting in a compact crumb structure. Together, these factors gave thicker and more rigid cell walls in the crumb that contributed to a faster increase in firmness during storage. The rate of firmness was slower in samples exhibiting a finer and homogeneous crumb structure and higher specific volume, as observed for breads mixed with 30%O_2 70%N_2. In such samples, this structure generally results in thinner and more elastic cell wall, which likely delayed the firming process by maintaining great moisture retention and flexibility within the matrix.

Srivastava et al. (2022) conducted a study similar to ours, but instead they used CO_2 gas hydrates (GH) as their leavening agent, which they compared to conventional breads made with baker's yeast. The breads hardness results showed that breads with different GH percentages scored significantly higher hardness values than the reference breads. They also concluded that under-developed or the absence of gluten network development was the main reason for the high hardness values.

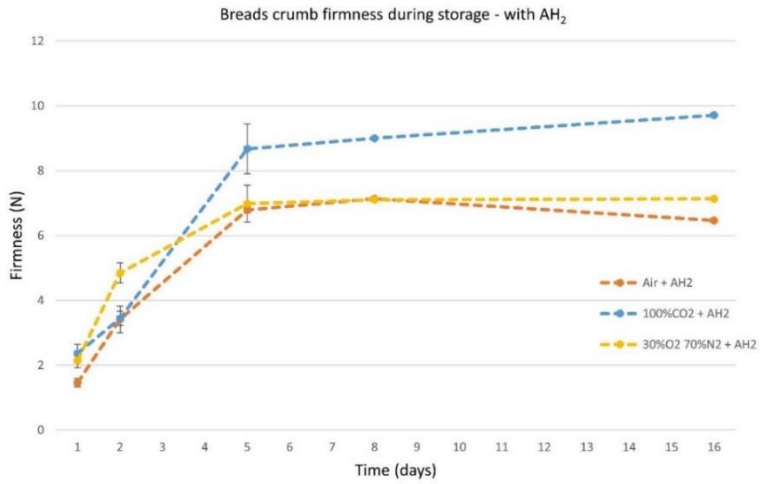


Figure 4.15 Evolution of breadcrumb firmness for all conditions without the addition of AH_2 during storage days

We can observe with the addition of AH_2, firmness with air and 30%O_2 70%N_2 mixed breads was lower than those without AH_2 while reaching plateau at J5 until the end of storage period. Breads mixed with CO_2 had the highest firmness which exponentially increased between J0 and J5 until reaching a plateau with final value at J15 of 9.71 ± 0.77 N, whereas air and 30%O_2 70%N_2 reached final values of 6.46 ± 0.10 N and 7.13 ± 0.57 N, respectively. There was no significant change for the 100%CO_2-mixed breads in comparison to the ones without AH_2. This confirms the effect of AH_2 on strengthening the gluten network in presence of O_2, leading to firmer breads. A study conducted by Sheikholeslami et al. (2020), investigated the effect of different concentrations of glycerol (0, 0.5 & 1%) and ascorbic acid (0, 75, 100 ppm) on the quality of Barbari bread. Results showed that control samples had the highest firmness, and as the amount of added ascorbic acid and glycerol increased as firmness decreased. Moreover, at 0 ppm of ascorbic acid, firmness decreased with solely increased glycerol concentration. They concluded that ascorbic acid could increase bread firmness if used alone, which was in accordance with our study. By comparing all gas composition with and without AH_2 in the figure below (Figure 4.16), we could significantly observe that the addition of AH_2 increased breads firmness for air and 30%O_2 70%N_2 and then decreased back to values closer to the ones without AH_2.

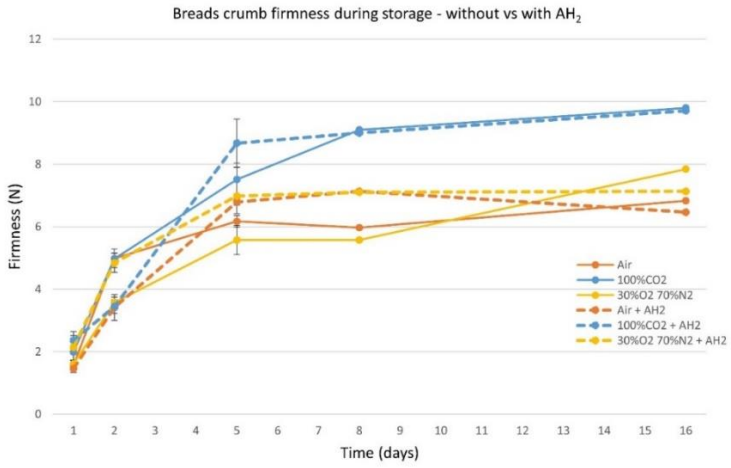


Figure 4.16 Summary of breadcrumb firmness of all conditions under the different as conditions with and without the additions of AH_2

4.1.5.2.2. Cohesiveness

Cohesiveness is another important texture parameter that reflects the internal strength within the breadcrumb structure, representing how well the sample withstands deformation and maintains integrity when compressed.

In the results below, all samples showed a significant initial drop during the first 4 days of storage. However, breads with air and 30%O_2 70%N_2 with AH_2, retained significantly the highest cohesiveness throughout the storage period in comparison to those without. The lowest cohesiveness was observed with 100%CO_2 breads with and without the addition of AH_2, which was not significantly different from those with air without AH_2.

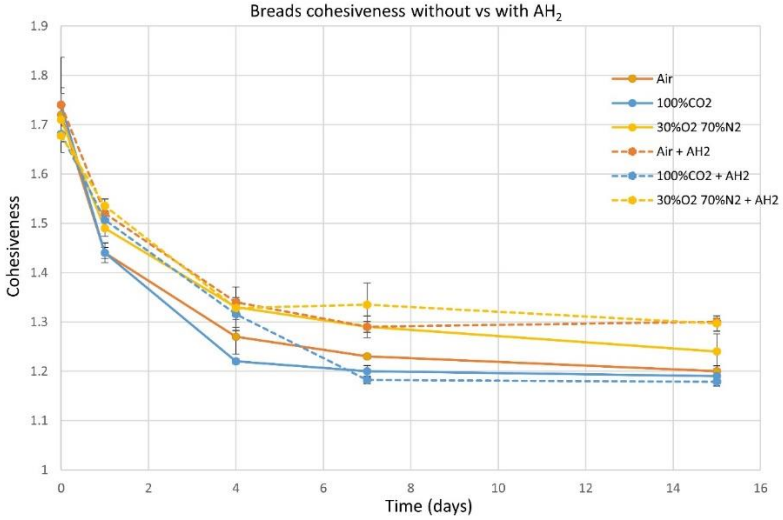


Figure 4.17 Breads cohesiveness for all conditions for all gas compositions without and with AH_2

Correlating these findings with firmness and retrogradation, it is evident that higher cohesiveness corresponds to slower increases in firmness and retrogradation, due to the reinforcement of gluten network constraining starch mobility and molecular re-association of amylopectin (Eliasson 1983a; 1983b).

<u>Conclusion for retrogradation and bread texture</u>

In conclusion, this study demonstrated that gas composition significantly influenced starch retrogradation kinetics and bread firmness during storage at 10°C. The 100%CO_2 exhibited anti-staling effect by delaying amylopectin recrystallization, thereby preserving bread longer than air and 30%O_2 mixture. The application of Avrami model allowed precise quantification of retrogradation rates, showing that 30%O_2 accelerated early retrogradation, while 100%CO_2 slowed the process. Texture analysis showed that despite slower retrogradation, 100%CO_2 maintained higher crumb firmness likely due to differences in SV and gas cells distribution. The application of AH_2 further supported gluten network strength, reducing early retrogradation. These results are summarized in the Table below.

Table 4.1 Summary of bread staling results

Parameter	Observations	Conclusion
Starch retrogradation	Retrogradation kinetics varied with gas composition: 30%O_2 70%N_2 showed fastest retrogradation rate, 100%CO_2 slowest	100% CO_2 atmosphere delays amylopectin recrystallization, exerting anti-staling effects
Enthalpy changes	Enthalpy increased over storage, with 100%CO_2 condition showing lowest retrogradation enthalpy early on	CO_2 solubilization acidifies dough, altering amylopectin plasticization and delaying staling
Firmness	Highest firmness observed with 100%CO_2	Crumb structure and porosity played a direct role in firmness
Effect of AH_2	AH_2 delayed early retrogradation, by strengthening gluten network, cohesiveness and firmness were delayed	Gluten network helped in restricting in starch mobility, reducing retrogradation rate and crumb firming
Breadcrumb structure	Higher porosity and larger gas cells in 100% CO_2 breads led to more compact crumb and rapid firmness increase	Crumb microstructure plays a major role in textural changes during storage

4.1.5.3. Determination of moisture content during storage

In this section, we studied the evolution of moisture content during storage at 10°C over a period of 15 days for all bread samples. This analysis was conducted, as reported by previous studies, that water plays a crucial role in the bread staling process by influencing starch retrogradation and the redistribution of water between the crumb and crust. Thus, monitoring moisture content (MC) provides essential insight into the mechanisms governing crumb firming and overall texture changes during storage.

Based on Figure 4.18, the moisture content MC% revealed distinct patterns influenced by both the diagonal position (top, middle and bottom) within the slice and longitudinal position (¼, ½ and ¾) of the slice within the bread loaf, showing that the rate of moisture loss is dependent on gas composition. Moisture distribution was evaluated at different positions within each loaf to understand how water migrated between the crumb and crust over time. Specifically, the analysis focused on slices taken from ¼ and halfway along the loaf length, and for each slice, 3 diagonal sampling points were analysed. All samples at J0 regardless of the slice position or gas conditions, showed similar initial MC %, around 46 – 48%, indicating uniform moisture distribution immediately after baking. By J1, differences among gas conditions were observed especially with 30%O_2 70%N_2 exhibited a significantly lower MC%, particularly at the top and bottom (near the crusts) of the bread loaf for both slices ¼ and ½. Whereas air and CO_2-mixed breads showed a steady decrease, maintaining a relatively higher MC%. By J7, 30%O_2 70%N_2 resulted in the lowest MC values across all slices positions and more specifically the middle and bottom positions of ¼ and ½ slices. In contrast, air and CO_2-mixed breads showed a better preservation of moisture content, especially in the middle position. This correlated with slower retrogradation rate observed. In addition, the ¼ and ½ slices for both conditions maintained a higher moisture content. The middle positions (crumb) tend to retain more moisture throughout storage, while the parts closer to the upper and lower crust are more prone for moisture loss due to proximity to the crust and environmental exposure (Piazza 1995).

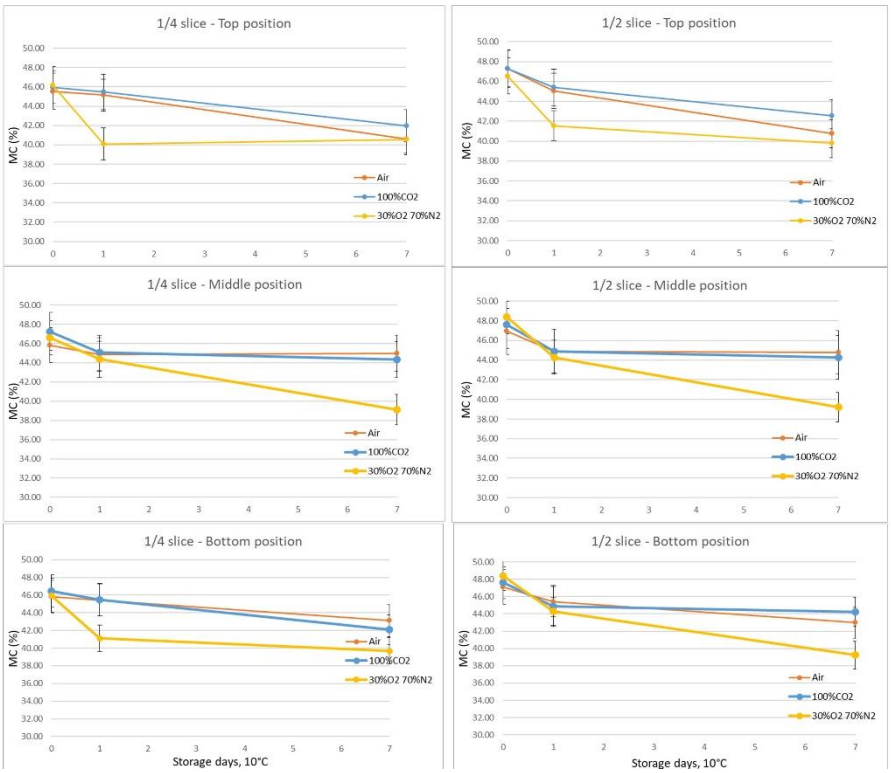


Figure 4.18 Evolution of moisture content MC (%) in bread slices for all gas conditions without the addition of AH_2 over 3 storage days (J0 (immediately after baking) , J1 (after 24 hours) & J7. MC is shown for two longitudinal positions (¼ and ½ slice) and 3 diagonal positions within the same slice (top, middle and bottom). Each point represents the mean moisture content at each time point with error bars indicating standard deviation

Effect of AH_2 on moisture retention

The MC% with the addition of AH_2 show distinct differences compared to those without AH_2, illustrating its biochemical impact on moisture retention (Figure 4.19). Across both slice positions ¼ and ½, there is less moisture migration and across the different positions within the slice, with 100%CO_2 increasing after 24 hours (J0 to J1) and then reaching a plateau at J7 for the top position (¼ slice) and bottom position (½ slice). An artefact due to moisture migration could explain this increase between J0 and J1 with 100% CO_2, from the bread to the packaging environment where breads needed more time to cool down. At J0, the higher MC% with 30%O_2 70%N_2 and air can be explained by the greater moisture retention due to the strong gluten network. In contrast with CO_2, the weak gluten can increase gas pressure inside the bubble and promote rapid moisture loss during baking, leading to lower MC at J0.

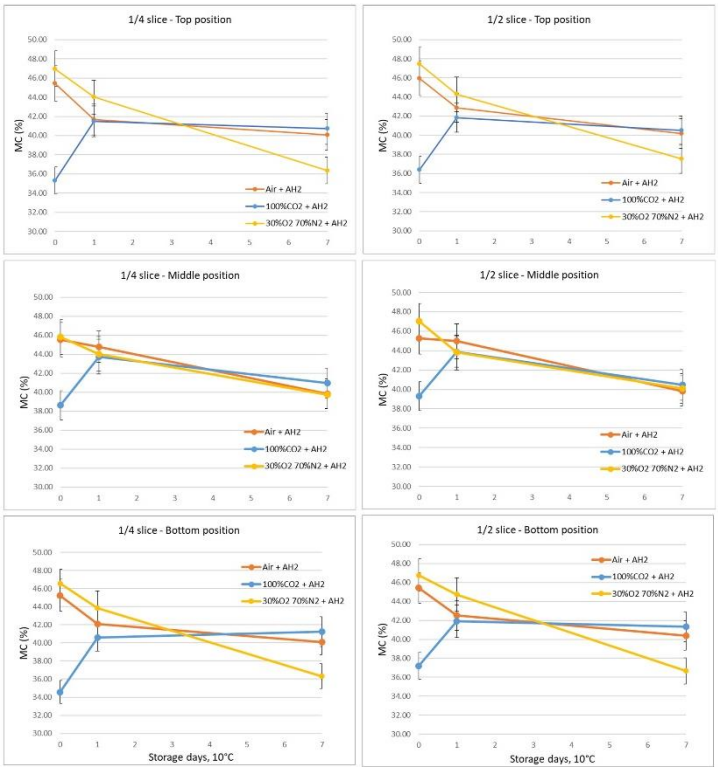


Figure 4.19 Evolution of moisture content MC (%) in bread slices for all gas conditions with the addition of AH_2 over 3 storage days (J0 (immediately after baking) , J1 (after 24 hours) & J7. MC is shown for two longitudinal positions (¼ and ½ slice) and 3 diagonal positions within the same slice (top, middle and bottom). Each point represents the mean moisture content at each time point with error bars indicating standard deviation

The distribution and moisture retention in bread during storage was significantly influenced by the gas composition and emphasized by the addition of AH_2. Breads mixed with 100%CO_2 consistently exhibited the least moisture loss across all slices positions and within the crumb which correlates with the slow starch retrogradation, when combined with AH_2, which further enhanced moisture retention. In contrast with 30%O_2 70%N_2, these breads showed a greater moisture loss, particularly at the top (closest to the upper crust) and bottom (closest to lower crust). In general, this gas mixture with or without AH_2 was the least effective in moisture retention, contributing to a fast retrogradation.

Studies have shown that moisture loss during storage is not uniform within the bread loaf, especially the crumb that tends to retain more moisture than regions closer to the crust. Srivastava at el. (2022) used CO_2 gas hydrates (GH) as a leavening agent instead of yeast. The results showed that breads prepare with 10 – 60% of GH had higher MC (38 – 44%) than traditional bread made with yeast (38%). This was in accordance with our study, at J7 MC with CO_2-mixed breads with AH_2 were higher than those with 30%O_2 70%N_2.

4.2. Part B – Effect of reduction of yeast amount on bread SV and breadcrumb structure under CO_2-enriched environment

In this section, we investigated the effect of reducing yeast amount on bread specific volume and crumb structure, with particular focus on the 100%CO_2 breads. This analysis aimed to determine whether lowering yeast activity could minimize excessive CO_2 accumulation during proofing and prevent structural collapse during baking. Comparing the appearance and volume of breads made under various gas conditions allowed us to assess how the balance between internal gas generation and dough gas-holding capacity affected the final loaf structure.

Based on our findings, with 100%CO_2 was due to a collapse of the top of the bread doughs during baking, which explains the low SV in absence and presence of AH_2. Notably, the pronounced negative impact of 100%CO_2 on SV and crumb structure suggests that the dough may be overwhelmed by the combined effect of exogenous CO_2 from the injected gas and endogenous CO_2 generated by yeast fermentation. The collapse indicated a potential imbalance between the CO_2 production and the dough ability to retain gas Figure 4.10.



Figure 4.20 Difference in breads volume: Air (left) and collapsed CO_2 bread (right)

The CO_2 generated by yeast fermentation and injected CO_2 dissolve into the aqueous phase of the dough surrounding the gas bubbles until saturation is reached, after which CO_2 diffuses into the nucleation cells by gradient concentration through Young-Laplace equation, raising the internal bubble pressure. According to Shah et al. (1998), gas stability depends on the strength and elasticity of the gluten network, which forms thin film layer around gas bubbles that assist in resisting this internal pressure. However, when this network is weakened and not well developed, the matrix loses its elasticity and strength, thus reducing its ability to resist internal pressure (Sroan, Bean and MacRitchie 2009). One logic explanation of this weakening of the gluten network besides deprivation from O_2, is the accumulation of fermentation metabolites (succinic acid, ethanol, etc.). As a result, the gluten network could not retain the excess internal pressure coming from both sources of CO_2 (injected during kneading and the yeast by-product of fermentation), leading to overstretching and rupture of gas bubbles. Oxygen is known to contribute to gluten network strengthening through oxidative cross-linking reactions involving thiol groups, which enhance dough elasticity and gas retention capacity. Therefore, under 100%CO_2, the absence of oxygen limited these oxidative reactions, while the accumulation of acidic metabolites further disrupted protein interactions. Consequently, the gluten

matrix could not withstand the internal pressure resulting from both exogenous CO_2 (introduced during mixing) and endogenous CO_2 (produced by yeast fermentation), leading to overstretching and eventual rupture of gas cells.

In the following set of trials, we investigated the effects of varying yeast content and fermentation on dough properties. We compared four different conditions:

- (1) No yeast, to assess the behaviour of dough without fermentation,
- (2) No yeast with fermentation, to evaluate how external fermentation affects the dough in the absence of yeast,
- (3) Yeast without fermentation, to isolate the impact of yeast without allowing fermentation to occur, and
- (4**)** Half the yeast amount (from 2% to 1%) with fermentation**,** to explore the effects of reduced yeast content while still allowing fermentation. Additionally, we compared the performance of half yeast content doughs to those made with full yeast in CO_2-mixed doughs. These experimental trials are summarised in the Figure 4.21.

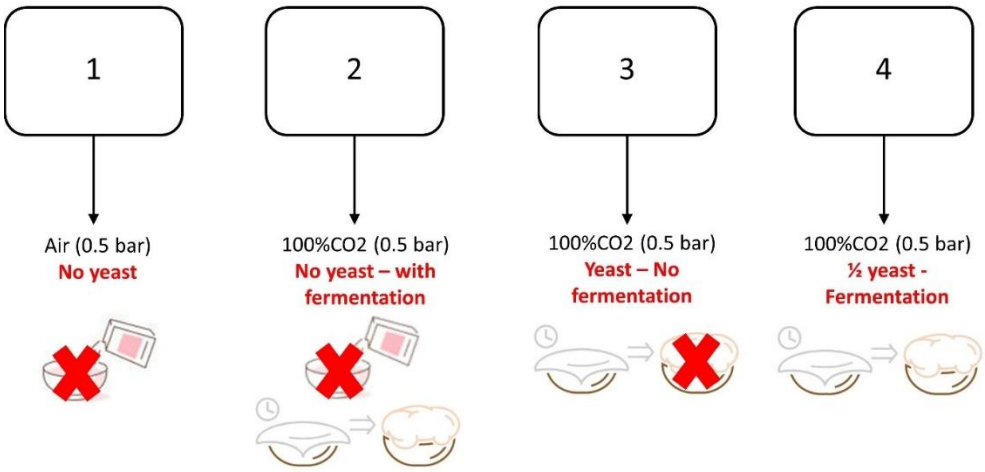


Figure 4.21 Summary of the experiment sets conducted with and without yeast, with and without fermentation

4.2.1.1. Determination of breads SV

Based on our observations (Figure 4.22 & Figure 4.23), breads SV were higher with 100%CO_2 (no fermentation than air-mixed doughs (1.56 ± 0.13 & 1.18 ± 0.03, respectively). By comparing CO_2- mixed doughs, with and without yeast, CO_2 with yeast gave higher SV. The highest value was achieved with ½-yeast amount and with fermentation.

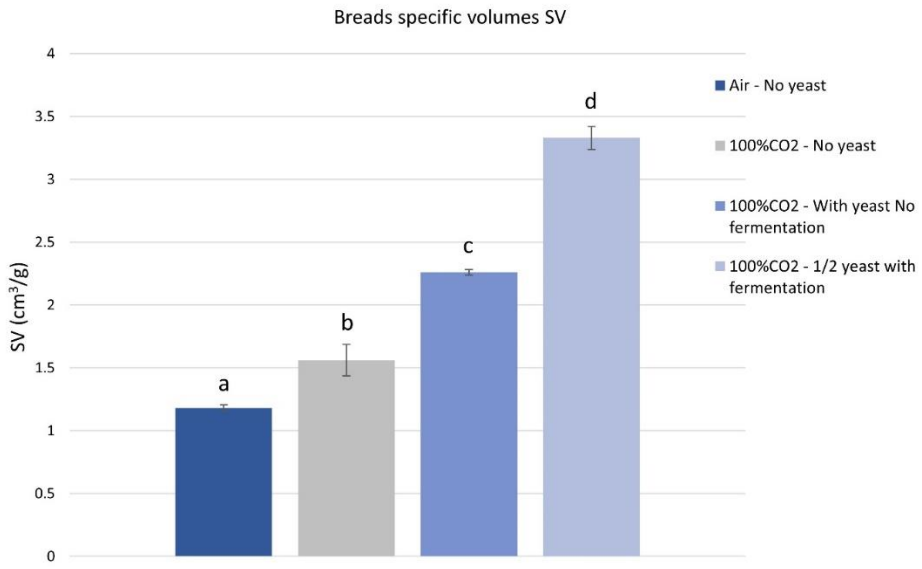


Figure 4.22 Breads SV ($cm^3 \cdot g^{-1}$) for the different conditions. Letters above the bars indicate statistical differences (a, b, c, d). Error bars represent standard deviation

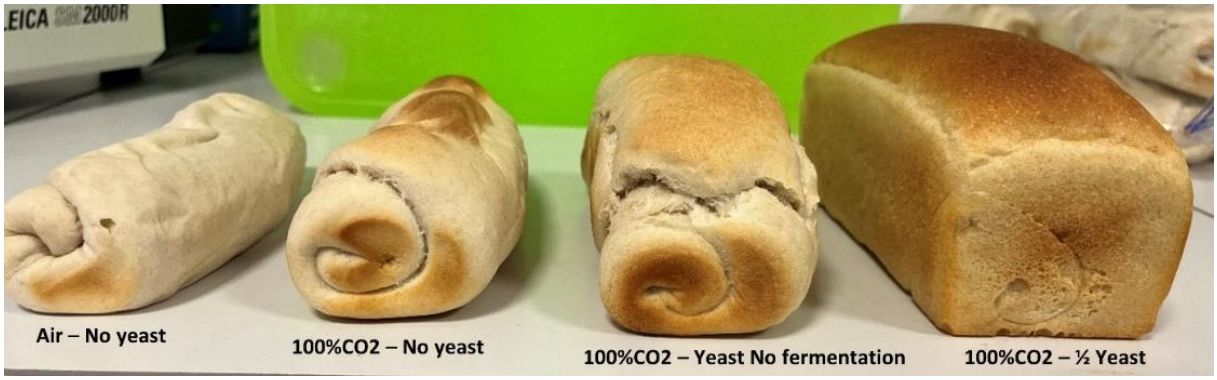


Figure 4.23 Breads volumes after baking for the 4 tested conditions, starting from the left: air without yeast, 100%CO_2 without yeast, 100%CO_2 with east without fermentation and far right 100%CO_2 with ½-yeast amount with fermentation

Therefore, the results showed that yeast addition and fermentation is inevitable for a high SV of breads. The SV increased significantly in the presence of 100% CO_2 without yeast, compared to air with no yeast. However, the highest SV value was achieved by reducing the yeast content and allowing fermentation. Reducing the yeast amount created more space for CO_2 bubbles to solubilize, preventing the dough from being overwhelmed by the high CO_2 levels. This balance allowed for better gas retention and improved bread volume, highlighting the benefit of modifying yeast levels in CO_2-mixed doughs. To further validate our hypothesis, we compared CO_2-mixed dough with the full yeast amount and ½-yeast amount.

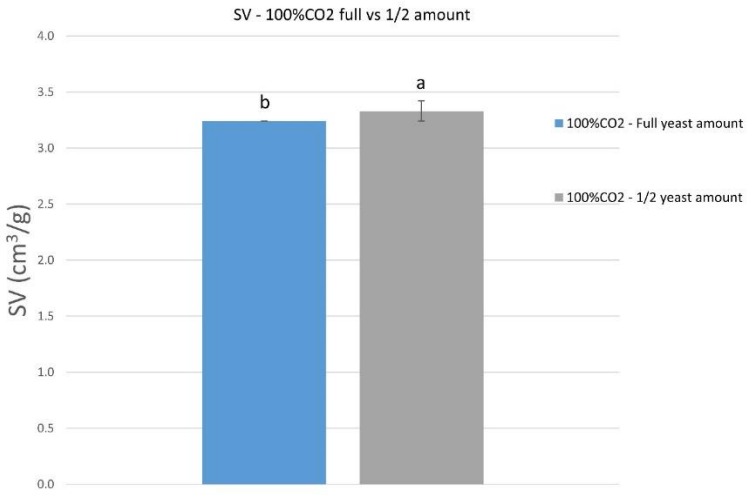


Figure 4.24 Breads SV of CO_2-mixed dough with full yeast amount (blue bar) and ½-yeast amount (grey). Letters above the bars indicate statistical differences (a, b, c, d). Error bars represent standard deviation

4.2.1.2. Breadcrumb structure

Based on the figure below, the pore size distribution of 100%CO_2 with the full yeast amount exhibited a wider pore size distribution range, indicating large pores size compared to breads mixed with the ½ yeast amount.

Table 4.2 Summary of median pore size D50 and D90 for the full yeast amount breads and ½ yeast amount breads. The table presents half the amount of pores size smaller than the median pore size D50 and the ones larger than D90 (representing 10% of pores population)

Conditions	Median pore size D50 mm^2	Pore size D90 mm^2
½ yeast amount	0.41 ± 0.09^b	2.52 ± 0.54^b
Full yeast amount	0.58 ± 0.06^a	6.86 ± 1.10^a

Based on Table 4.2, for ½ yeast breads, 50% of pore population had pores size below 0.41 mm^2 which was significantly smaller than the full yeast amount where 50% of pore population had pores size below 0.58 mm^2 demonstrating larger pores. Additionally, 90% of pore population in the ½ yeast breads had a median pore size smaller than 2.52 mm^2 significantly lower than the one with the full amount having median pores size smaller than 6.86 mm^2. These findings confirm our hypothesis that reducing yeast amount leads to a finer breadcrumb structure and a more homogenous crumb by limiting the formation of large pores during fermentation and baking.

Based on Figure 4.25, we can clearly visualize that gas bubbles are more prevalent in presence of CO_2 when comparing (a) and (b). In addition, breadcrumb structure was more developed in presence of yeast, furthermore, more homogenous with ½ yeast amount. The addition of yeast is inevitable for the breadcrumb structure formation and aeration; however, under 100%CO_2, a moderate reduction in yeast concentration produced finer and more stable crumb structure, likely due to its minimized excessive gas production and prevented structural collapse.

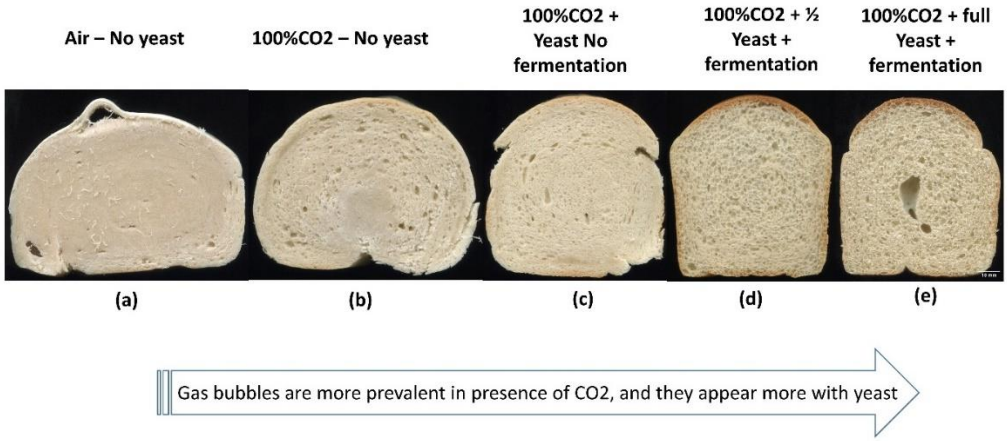


Figure 4.25 Breadcrumb structure of scanned bread slices for all the experiments conducted with yeast. Starting from far left to right: (a) air without yeast, (b) 100%CO_2 without yeast, (c) 100%CO_2 with full yeast without fermentation, (d) 100%CO_2 with ½ yeast with fermentation and (e) 100%CO_2 full yeast with fermentation

Fermentation is vital in bread making, but improper control of fermentation time or yeast concentration can lead to undesirable effects as observed in our Part 1 results. Wang et al. (2024) investigated the role of different yeast % (1.5%, 2%, 2.5% and 3%) under different fermentation times (60, 75, 90, 105, 120, 13 and 150 min) on the quality of the white bread properties. Results showed that obtaining optimal bread properties in terms of specific volume, texture and colour were achieved at a yeast concentration of 2-3% for a fermentation time of 90 – 105 min. Which was in accordance with our results for doughs mixed under air, were the optimal yeast concentration was 2%. However, with the additional source of CO_2 and based on the results of reducing yeast concentration to 1%, it gave the optimal conditions for breadcrumb structure. This balance of gas injection and yeast concentration enhanced gas retention and pore stability, emphasizing on the importance of tailoring yeast levels and fermentation conditions based on the leavening environment for the optimum dough and bread properties.

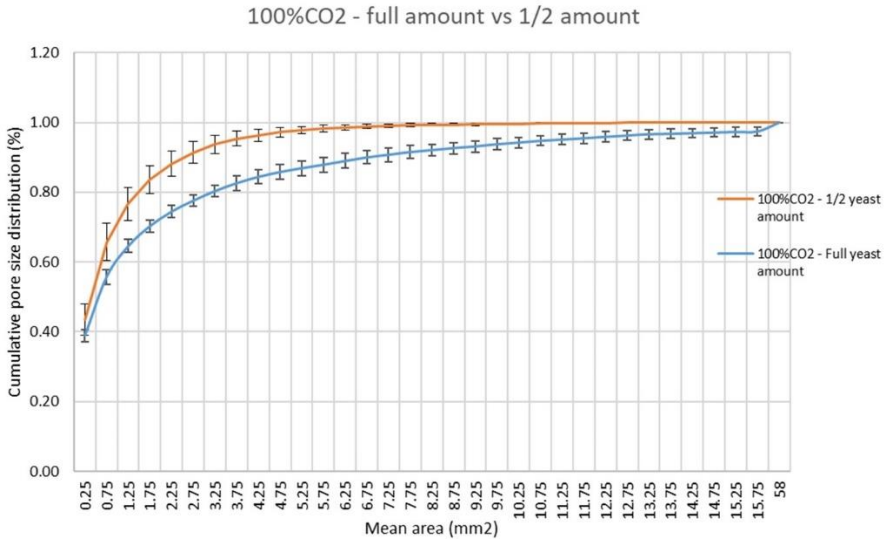


Figure 4.26 Cumulative pore size distribution pattern of 100%CO_2 breads with the full yeast amount and ½ yeast amount

Conclusion

Adjusting the yeast content proved to be a relevant means to adjust the specific volume of the bread. Reducing the yeast by 50% (from 2% to 1%) improved breadcrumb structure. A possible explanation would be that it would allow more gas to solubilise within the dough matrix. Another explanation is based on the critical radius theory developed by Shah. These findings underscore the critical balance required between gas composition and yeas concentration for optimal dough aeration and bread quality.

4.3. Part C – Impact of mechanical dough sheeting

Based on the findings above, we hypothesised that dough sheeting might play a significant role in modifying bubbles size distribution and aeration. Specifically, the mechanical stress and deformation induced by the sheeting process that could influence bubble coalescence, rupture and breadcrumb homogeneity. This hypothesis was built upon several literature studies, while this process offers clear benefits, it also carries the risk of damaging the quality of certain areas of the baked loaf (Cauvain 2015b). This negative effect stems from the intense deformation the dough goes through during the moulding process, along with the high efficiency of the sheeting process, which can both develop and damage the gluten network (Leong and Campbell 2008).

4.3.1. Determination of bread SV of sheeted vs. non-sheeted breads

Accordingly, doughs mixed with air and 100%CO_2 at 0.5 bar gauge pressure were processed both with and without sheeting. This approach provided information on how mechanical sheeting influence the quality of the final product in terms of SV and crumb structure.

Comparing breads without sheeting, there was no significant difference in SV ($p > 0.05$), whereas with sheeting, breads SV with 100%CO_2 was significantly lower than those mixed with air. The sheeting process degassed enormously the gas bubbles formed during the kneading and resting phase.

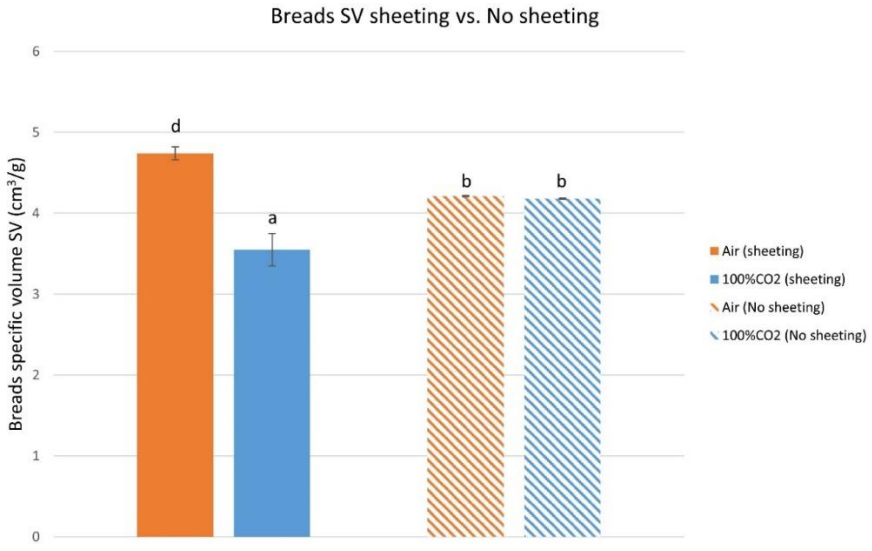


Figure 4.27 SV for breads mixed with air and 100%CO_2 with sheeting and without sheeting. Error bars represent standard deviation

Leong and Campbell (2008) studied the impact of sheeting on unyeasted doughs made from weak and strong flour and to investigate how the initial gas content affects the degree of degassing during the sheeting process. Results showed that at three different roll gap settings, doughs made from weak flour experienced greater degassing, indicating a larger density increase after sheeting to the ones made of strong flour at 2 bar. This trend was the opposite of observations made under atmospheric pressure. The same authors examined the extent of degassing in yeasted doughs mixed under atmospheric pressure. They observed that the continuous production of CO_2 from yeast fermentation during and after sheeting complicates the evaluation of gas loss as the bubble nuclei expand concurrently. However, according to our results, we observed a great difference of dough void fraction after sheeting and eventually SV. The authors suggested mimicking the yeast activity by mixing the dough under pure CO_2, which what was conducted, we observed that without yeast gluten network is not developed, and with full yeast amount, the gluten network was weakened. Therefore, weak doughs tend to have a reduced capacity to retain gas bubbles formed, as the gluten network is less elastic and less developed.

4.3.2. Determination of breadcrumb structure of sheeted and non-sheeted doughs

Based on Figure 4.28, the cumulative pore size distribution of air with and without sheeting was narrower than those with 100%CO_2 reflecting smaller pores size population. Additionally, 100%CO_2 without sheeting gave the widest pore size distribution, reflecting a greater proportion of large gas bubbles. This indicates that without sheeting, the high SV was due to large gas bubbles within the dough matrix.

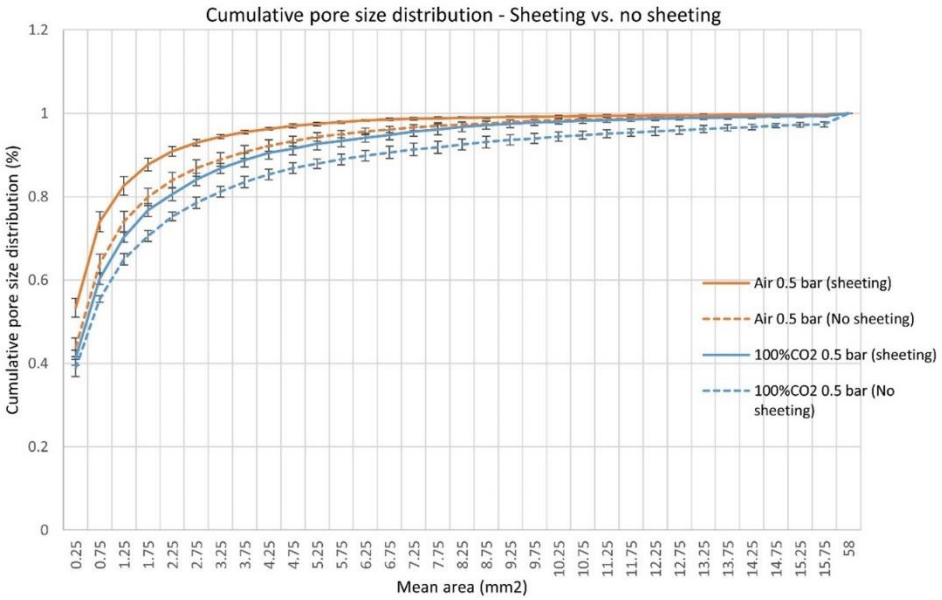


Figure 4.28 Cumulative pore size distribution of sheeted and none-sheeted bread doughs mixed with air and 100%CO_2-mixed breads at 0.5 bar gauge pressure. The error bars confirm that these trends are reliable across measurements

Based on median pore size (Figure 4.29), breads mixed with air regardless if sheeting was applied or not, had a lower median pore size were 50% of pore population had a median pore size of

0.37 ± 0.06 mm^2 (with sheeting) and 0.41 ± 0.04 mm^2 (without sheeting), than those mixed with CO_2 with and without sheeting (0.59 ± 0.06 mm^2 & 0.55 ± 0.10 mm^2, respectively).

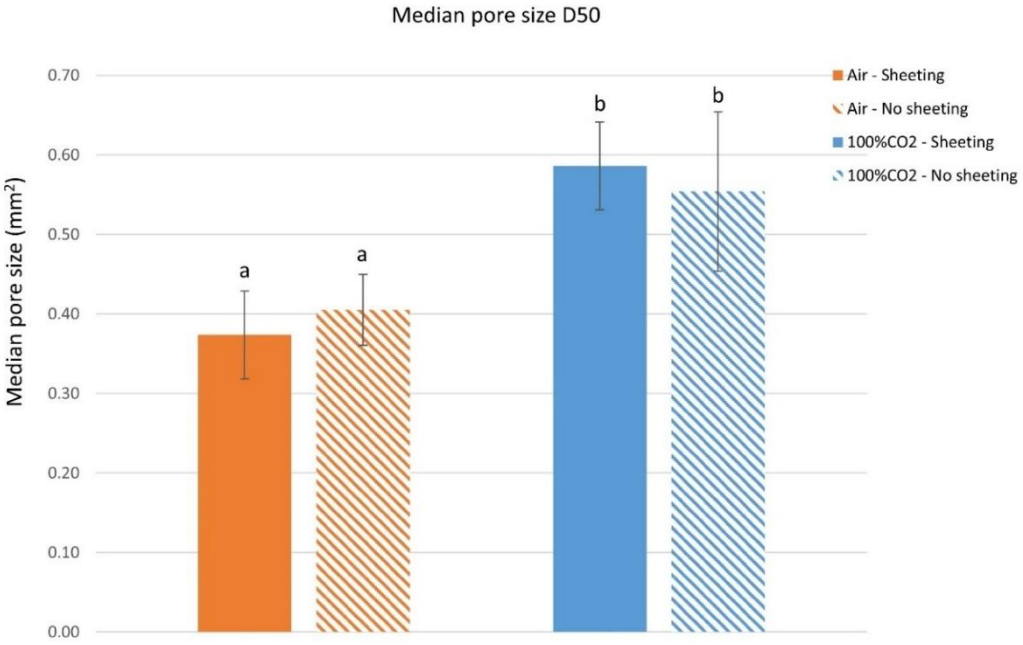


Figure 4.29. Median pore size D50 of all conditions. Values with different superscript lowercase letters in the same column for each condition are significantly different (p < 0.05). The values presented here are mean ± standard deviation

The same trend was observed where 90% of pore population of sheeted and none-sheeted air-mixed breads have median pore size smaller than 3.25 ± 0.29 mm^2 and 3.49 ± 0.23 mm^2 respectively, significantly lower than CO_2-mixed breads where 90% of pore population have median pore size smaller than 6.89 ± 1.11 mm^2 and 6.39 ± 0.82 mm^2 respectively Figure 4.30.

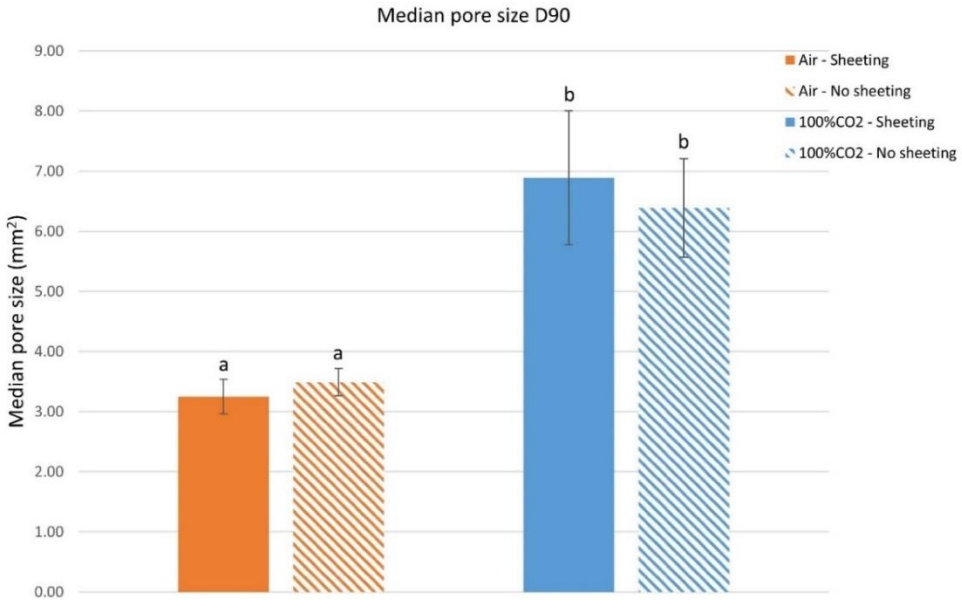


Figure 4.30 Median pore size D90 of all conditions. Values with different superscript lowercase letters in the same column for each condition are significantly different (p < 0.05). The values presented here are mean ± standard deviation

Based on Figure 4.31, we can clearly visualise that sheeting with air gave finer and more homogenous breadcrumb than without sheeting. Without sheeting with CO_2, we can clearly observe that the high SV was due to large gas bubbles and coalescence.

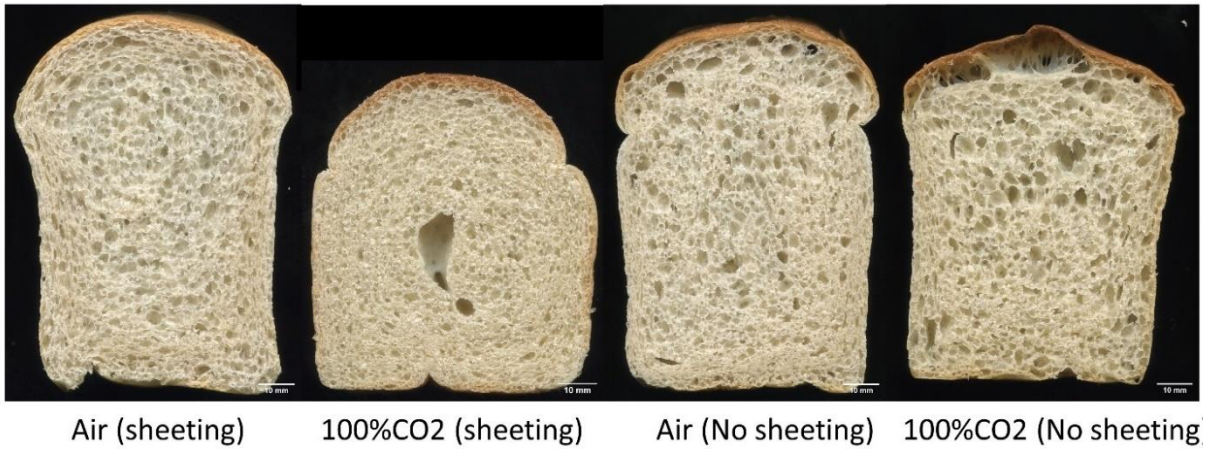


Figure 4.31 Scanned breadcrumb images of bread slices mixed with air and CO_2 with sheeting and without sheeting

The results demonstrated that sheeting, particularly under air, promoted a higher proportion of small pores and a uniform crumb structure. Conversely, with CO_2, sheeting led to pronounced degassing of the weak gluten network, as CO_2 solubility and diffusion into the dough promoted bubbles coalescence and rupture under the mechanical stress of sheeting. Verheyen et al. (2014), demonstrated a direct relationship between yeast metabolites-induced acidification and dough density, which indirectly reflected CO_2 content. They found that the rate of CO_2 production does not significantly affect gas retention; the total gas volume and the stability of the dough matrix limit it. They also found that the dough weakening was likely due to glutathione produced by yeast metabolism. This biochemical weakening renders the dough softer and pressure-sensitive to sheeting. In our study, with CO_2 this weakening effect was intensified, resulting in more pronounced degassing and large bubbles.

4.4. Part D – Sensory analysis

In this section of the chapter, we explored whether perceptible differences exist between bread samples with varying gas composition and formulation. To achieve this, a triangular test and Flash Profile methodology were implemented.

4.4.1. The Triangular Test

The triangular test was used as a rigorous sensory discrimination tool to determine if significant differences could be detected between:

- A reference bread (REF) and a bread containing ascorbic acid AH_2, kneaded under controlled gas composition (O_2/N_2 with AH_2);
- A reference bread (REF) and a bread not containing ascorbic acid AH_2, kneaded under controlled gas composition (O_2/N_2 without AH_2);
- A reference bread (REF) and a bread kneaded under CO_2 (CO_2)

This test was conducted with 30 panellists (12 male and 18 female) who were asked to identify the different sample among three coded samples (two identical and one different) for bread samples with varied gas composition and presence of AH_2. The table below summarises the results.

Table 4.3 Summary of Triangular test results for sensory discrimination, presenting the number of panellists, correct responses, statistical significance and the perceptible sensory differences

Comparison	Number of panellists	Number of correct responses	Significance level (α risk)	Conclusion
REF vs O_2/N_2 with AH_2	30	23	$\alpha < 0.001$ (very strong evidence)	Difference clearly perceived
REF vs O_2/N_2 without AH_2	30	14	$0.05 < \alpha < 0.10$ (weak evidence)	Poorly perceived
REF vs CO_2	30	13	$0.05 < \alpha < 0.10$ (weak evidence)	Poorly perceived

These results support that both gas composition and the addition of AH_2 during kneading significantly impact the sensory qualities of bread as detected by the panellists.

Complementing this, the Flash Profile method enabled a rapid and detailed characterization of the breads in order to determine *(i)* the impact of kneading under O_2/N_2 or CO_2 and *(ii)* the presence of AH_2 on their aspect, odour, flavour and texture. Four breads were characterized: REF, O_2/N_2 with AH_2, O_2/N_2 without AH_2 and CO_2. Panellists generated their own vocabulary and then ranked the products according to the descriptive sensory attributes relevant to each product.

4.4.2. Flash Profile

4.4.2.1. Results

For the Flash Profile, the panel consisted of 17 participants. Consequently, the data is robust for deriving meaningful insights into the impact of gas composition and antioxidant on bread sensory quality (Vilcanqui-Pérez *et al.* 2021). Based on the collected data, the panellists generated between 7 and 15 attributes each, with a mean value of approximately 11.8 attributes per assessor. This range suggested a good level of engagement across the panel (Lawless and Heymann 2010). In addition, data revealed that aspect-related attributes were the most frequently described, representing 35.6% of the total descriptors, followed by texture in mouth or mouthfeel by 31.68%. This indicates a strong emphasis on the visual and mouthfeel characteristics during the analysis. In contrast, odour was the least described modality with 12.38%.

Looking at the table below, the panel generated a total of 33 descriptors, by focusing on the visual aspect of bread samples, with 7 attributes representing 27.2% of the total 33 sensory attributes. Key aspect attributes included homogeneity of gas cells followed by bread volume and crumb colour. The texture/mouthfeel and texture to touch were the second most represented (21.2% & 18.2%, respectively), comprising respectively 7 and 6 attributes. Chewing resistance in the mouthfeel, crumb firmness and softness to touch were the most persistent . The remaining descriptors covered odour and taste attributes.

Table 4.4 Table summarising all sensory descriptors given by the panel for bread samples, categorized by aspect, odour, texture/mouthfeel, texture to touch and taste. The citation frequency is indicated for each attribute

Descriptors	Aspect	Odour	Texture / mouthfeel	Texture to touch	Taste
Aspect			-	-	-
Crumb colour	10	-	-	-	-
Crust colour	11	-	-	-	-
Crust thickness	4	-	-	-	-
Homogeneity of gas cells	16	-	-	-	-
Size of gas bubbles	9	-	-	-	-
Slice height/volume	10	-	-	-	-
Slice shape	3	-	-	-	-
Odour/aroma					-
Odour intensity	-	8	-	-	-
Yeast	-	3	-	-	-
Cereal	-	4	-	-	-
Freshness	-	3	-	-	-
Texture / mouthfeel					-
Soft	-	-	5	-	-
Dry	-	-	5	-	-
Sticky	-	-	4	-	-
Chew resistance	-	-	9	-	-
Elastic crumb	-	-	3	-	-
Elastic crust	-	-	2	-	-
Doughy	-	-	3	-	-
Texture to touch					
Firm crumb	-	-	-	9	-
Soft	-	-	-	8	-
Dry crust	-	-	-	3	-
Crumbly	-	-	-	5	-
Hard spots in crumb	-	-	-	3	-
Humidity	-	-	-	4	-
Taste					
Acidic	-	-	-	-	4
Salty	-	-	-	-	7
Yeast	-	-	-	-	1
Odour intensity	-	-	-	-	4
Total of attributes	9	4	7	6	4

The Flash Profile data were further analysed using Generalized Procrustes Analysis (GPA), with the first two components (F1 and F2) explaining a cumulative variance with 82.54% variance explained by the first two principal components F1 (61.36%) and F2 (21.17%) (Figure 4.32). The positioning of groups reveals key differences and similarities; the O_2/N_2 + AH_2 samples are clustered at the left quadrant, showing distinct characteristics along F1 with minimal variation with F_2, highlighting the significant influence of AH_2 with the gas mixture. Samples without AH_2 with O_2/N_2 mixture appear at the bottom left quadrant with a bit towards the centre separated from the samples with AH_2 by F2. The REF samples are located at the top right quadrant separated from both mixtures cited above, while CO_2-mixed samples are at the bottom right, emphasizing unique chemical or sensory effects related to high CO_2. Overall, F1 distinctly separates samples treated with AH_2 from REF and CO_2 samples, while F2 further differentiates between REF and CO_2 and between the presence and absence of AH_2. These results indicate that the antioxidant significantly influenced the bread features.

The biplot shows that F1 distinctly separates breads with high volume, slice height, crumb and crust colour (positive F1, right quadrant) from breads characterised by softness, homogeneity of gas cells and acidic/yeast/cereal notes (negative F2, left quadrant). F2 further differentiates based on chew resistance and crumb firmness, separating breads exhibiting firmer texture and chewiness (lower values) from those with more pronounced crumb colour and aroma intensity.

The reference bread (REF) is positioned in upper right quadrant, associated with attributes of crumb firmness, homogeneity of gas cells, crust and crumb colour (Figure 4.33). Panellists perceived REF bread as having a homogeneous breadcrumb structure with uniform gas cells size. These bread samples showed firmness in bread crumb with chewing and with touch indicating the bread had a firm, compact crumb; they noted pronounced crust and crumb colour, reflecting classical bread qualities.

The CO_2-mixed bread samples exhibited lighter crust colour with firmer and chewier crumb texture as perceived by the panellists. The sensory map also showed that these breads were perceived with the appearance of large gas cells reflecting heterogeneous crumb structure and acidic taste (Figure 4.33). In addition, panellists noted high intensity of crumb colour from the rest of the bread samples.

The O_2/N_2 bread samples without AH_2 form tight clusters in the lower left quadrant and is characterised by trends of increased chew resistance, firmer texture, higher acidity and yeast flavour. It was also perceived with less homogeneous crumb by the presence of larger gas cells. The negative position on both F1 and F2 for this group underscore their divergence from the soft and high intensity colour of REF breads. They also noted a higher bread volume and slice height than those with CO_2 and REF breads. The acidity was more pronounced than CO_2 mixed bread samples.

The O_2/N_2 bread samples with AH_2 showed markedly different sensory traits than the rest by clustering on the upper left quadrant, emphasizing on crumb softness, homogeneity of gas cells and an intent yeast and cereal aroma notes. Panellists noted that these breads have finer bread crumb structure with softer and lighter mouthfeel with less chewiness. Some panellists perceived a higher crust colour intensity than those without AH_2 but less intense than CO_2-mixed samples.

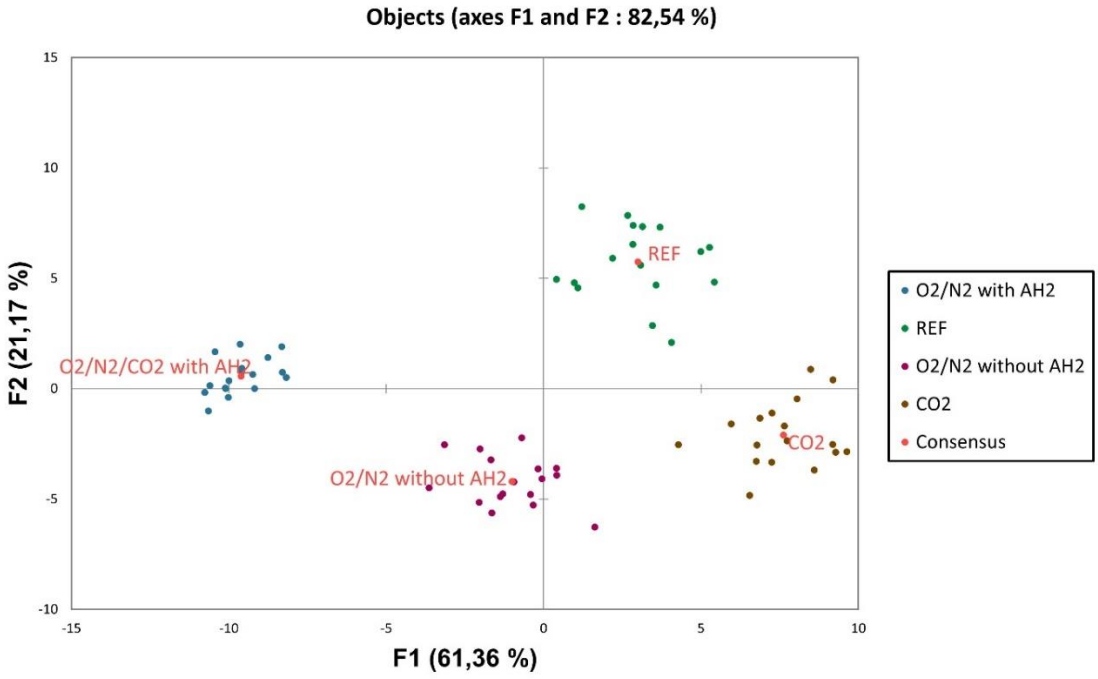


Figure 4.32 Generalized Procrustes Analysis (GPA) plot of bread samples based on sensory attributes obtained from the Flash Profile analysis

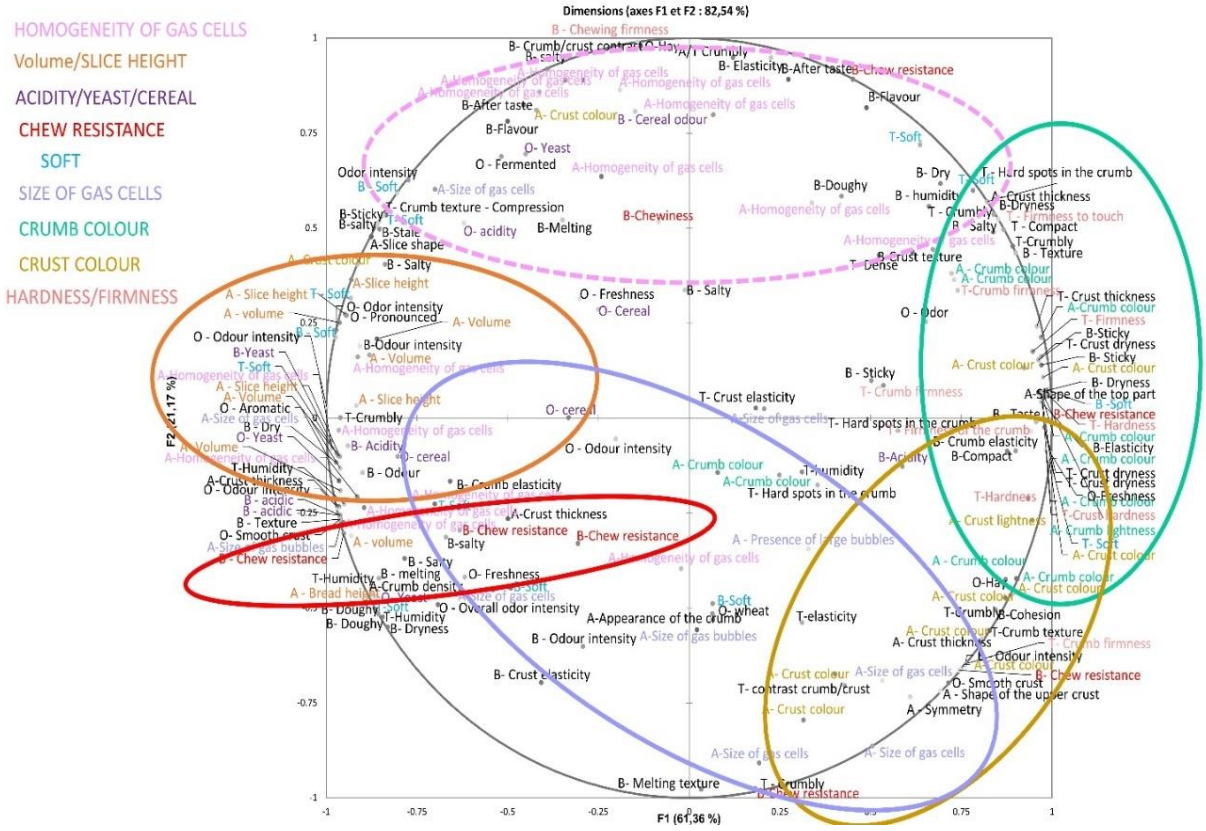


Figure 4.33 Biplot of the sensory attributes used to characterize bread samples. In order to simplify the interpretation, attributes are grouped using circles of different colours by characteristics such as softness, crumb colour, chew resistance, volume, gas cell size, acidity and firmness

4.4.2.2. Correlation with Instrumental Measurements

The observations of REF breads made by the panellists reflect the optimal gluten network formation under the classic kneading conditions, which effectively retained the gas bubbles formed during mixing and thus enabling the formation of a uniform breadcrumb structure. The Maillard reaction during baking gave the intense crust colour and crumb, contributing by the attractive visual and flavour qualities perceived by the panellists.

According to our knowledge, studies conducted on gas mixing atmosphere during bread kneading did not conduct a sensory analysis on the effect of gas-pressure mixing on sandwich bread qualities, which makes this study a first, and we will be correlating our results based on the observed results of previous studies conducted experimentally. The authors Sadot et al. (2017) and Martin et al. (2008) mixed pan bread dough under pressurised air which was similar to the conditions of REF breads. Their results showed that mixing with air supports the development of gluten network and at 0.3 bar breadcrumb appeared to be uniform and homogenous. The well-developed gluten supported uniform bubbles, leading to softness and desirable chewiness as observed by our panellists.

On the contrary with CO_2-mixed breads coarser breadcrumb with large gas bubbles was observed by the panellists. This was in accordance with Martin et al. (2008) where breads mixed with CO_2 appeared coarser at all pressure levels (0.3 and 2 bar). The lighter crust colour as explained by literature, is due to the dissolution of CO_2 into carbonic acid, which lowers pH and ultimately weakens the gluten network. This pH decrease reduces the Maillard reaction, a key browning reaction responsible for crust colour development, which is less favourable under acidic conditions (Martins, Jongen and Boekel 2000). The lower pH reduces the efficiency of reactions between reducing sugars and amino acids, leading to decreased formation of melanoidins (browning pigments) (Martins, Jongen and Boekel 2000). This weakening phenomenon negatively affects the crumb structure by reducing gas retention and producing a denser, less aerated crumb with coalescence (Chaix, Guillaume and Guillard 2014; Chiotellis and G. M. Campbell 2003). Based on texture analysis at J0, CO_2 mixed breads had a higher firmness than REF and O_2/N_2 although not significantly different, but it could explain the perception of sensory attributes made by the panellists is a comprehensive process influenced by cognitive interactions, which can account for some variability in the ratings.

Breads mixed with 30%O_2 70%N_2 with AH_2 were described as softer with a finer breadcrumb structure, due to the anti-oxidant activity of AH_2 that its strengthening role enhanced the mouthfeel texture and consistent pore size distribution (homogeneity of gas cells) (Beghin *et al.* 2022). Without AH_2 breads were perceived with presence of larger gas bubbles in comparison to the ones with AH_2, although they remained within the acceptable range of homogeneity of gas cells. Based on our breadcrumb results analysis, breads mixed with 30%O_2 70%N_2 with and without AH_2 showed a finer pore size distribution and more homogenous crumb structure, which were in correlation with the perceived sensory results. Both bread samples were described with higher bread volume and higher slice height in comparison to REF and CO_2 bread samples. According to Heuven et al. (2024), the visual appearance of bread affects the consumption behaviour, where they showed that bread volume and height are key physical parameters influencing bread consumption behaviour and sensory texture perception. Based on our results, we can hypothesize that breads mixed with 30%O_2 70%N_2 with and without AH_2, may be more appreciated by their height and volume. Experimental results further revealed that breads mixed with 30%O_2 70%N_2 and REF gave the highest loaf specific volume SV based on instrumental analysis, in

comparison to those mixed with CO_2. Instrumental texture analysis indicated that breads with AH_2 has reduced chewiness and higher softness than those without.

A differentiation of bread firmness was detected experimentally during storage, therefore, since in the sensory sessions breads were presented as fresh as possible, the panel did not detect this difference. This distinction between instrumental and sensory results highlights that firmness changes during storage may not be immediately detected in freshly baked breads. The structure of breadcrumb is determined by the number of gas cells, along with its uniformity of distribution, and it was found that the acceptance in terms of appearance and overall quality decreased when the cells were small and evenly distributed (García-Gómez *et al.* 2022). The crumb porous structure is also critical for moisture retention and staling properties, both of which influence texture during storage. However, in our study, the opposite perception was described, which a uniform breadcrumb was described by the panels.

The colorimetric analysis results showed that the highest L* value was observed with 100%CO_2 (61.08 ± 1.51) indicating a lighter crust and more yellow crumb, attributed to the induced acidification of CO_2 inhibiting Maillard reaction during baking, in which highest b* value achieved with 100%CO_2 (15.30 ± 0.34).

4.4.3. Conclusion

In conclusion, the bread with the mixture of 30%O_2 70%N_2 and AH_2 was the most positively evaluated by the sensory panel in terms of the descriptive attributes such as softness, volume crumb homogeneity and aroma. Panellists highlighted these breads for their softness in texture, uniform and homogenous breadcrumb, and mild and pleasant yeast and cereal aroma with higher volume. In contrast, bread with CO_2 were perceived as firmer, denser, chewier with lighter crust colour and more pronounced acidic aroma, which resulted in less favourable sensory perception. Similarly, breads mixed with 30%O_2 70%N_2 without AH_2, were firmer and exhibited strong acidic and yeast aromas, indicating the importance of presence of antioxidant for optimal sensory quality. For future perspectives, a hedonic test would allow direct consumer preference assessment, complementing panellists' descriptive data and would provide feedback for optimisation tailored to consumers liking and acceptance. We could also conduct a sensory analysis with the optimised formulation and process especially with the 100%CO_2 with ½ yeast amount, as well as adopting different gas composition and ratios.

CONCLUSION OF CHAPTER 4

The type of gas injected during kneading had a significant impact on bread specific volume SV, crumb porosity and crumb structure and aeration. Breads mixed with pure CO_2 consistently exhibited lower SV, coarser crumb, and larger, irregular pores due to the weakened gluten network and bubbles instability. In contrast, 30%O_2 70%N_2 gas mixture produced the densest and most homogeneous crumb structure, as indicated by low crumb porosity, regardless of whether ascorbic acid AH_2 was added or not. Under elevated O_2 (30%O_2 70%N_2), AH_2 efficacy was diminished due to the sufficiency of fully oxidizing thiol groups within the gluten.

Findings revealed that different gas composition significantly influenced the rate of starch retrogradation. The CO_2-mixed breads exhibited the slowest starch retrogradation, highest moisture retention but also developed the highest crumb firmness at the end of storage due to the heterogeneous crumb structure and the less elastic gluten network. The delayed retrogradation is related to the acidification and physical alteration of the dough liquor by the dissolved CO_2 into carbonic acid, which altered the mobility of amylopectin chains and disrupted the hydrogen bonds essential for starch crystallisation. The inclusion of AH_2 in oxygen-rich environment predominantly had no significant effect on starch retrogradation. These findings underscore the complex interplay between processing atmosphere, molecular interactions and starch-gluten interactions that govern bread staling.

Furthermore, yeast concentration within CO_2-mixed doughs was identified as critical parameter. Excessive yeast concentration led to destabilisation of gas cells and crumb collapse, owing to the combined effect of yeast-induced fermentation and exogenous CO_2. A reduction in yeast dosage corresponded to improved crumb structure, higher bread volume and gas retention, underscoring the necessity of optimizing fermentation with CO_2 enriched atmosphere to attain desirable bread quality.

Mechanical sheeting was observed to refine crumb structure in air-mixed breads, however, with CO_2 it induced pronounced degassing and bubbles coalescence, affecting the crumb uniformity due to the weak gluten network. This finding emphasize on the importance of tailoring mechanical processing parameters to the specific gas environment.

Based on the sensory analysis results, breads made with 30%O_2 70%N_2 with AH_2, was described as soft, with uniform crumb structure, greater loaf volume and pleasant yeast-cereal aroma. The ones without AH_2 with the same gas composition, were firmer, less homogenous and exhibited stronger acidic and yeast aromas. Finally, breads mixed with CO_2 were firmer, denser, chewy and more acidic with a lighter crust colour.

Building upon these findings, future research should explore a broader spectrum of gas ratios, particularly the integration of O_2 with CO_2 to optimize the dough aeration and rheology. Investigating intermediate pressure levels between atmospheric and 0.5 bar gauge pressure, combined with a final vacuum stage, which may significantly enhance the uniformity of gas bubbles. We also suggest studying the molecular interaction between carbonic acid and the gluten-starch matrix components, and how the gas composition induces conformational changes by using Confocal Laser Scanning Microscopy or Raman Spectroscopy. A further investigation on how CO_2 delayed starch retrogradation.

CHAPTER 5 : **ARTICLE 2**

This chapter presents part of the PhD project which took place in the University of Hohenheim (3 months stay / September – December 2024) under the supervision of Prof Mario JEKLE and Dr. Viktoria ZETTEL in partnership with my PhD supervisors, Dr Patricia LE-BAIL and Prof Alain LE-BAIL. The experimental work was carried out at the University of Hohenheim (Stuttgart, Germany) as a part of the MIGAP project, which explores innovative processing techniques for industrial bread production. This academic exchange took place within my AGRENIUM mobility program and was co funded by ONIRIS, University HOHENHEIM and AGRENIUM. The objective of this part of my PhD were as follows:

- To study the impact of carbonated water during dough preparation on dough and bread properties.
- To study the CO_2 exchange between dough and the ambiance of a fermentation cabinet
- To investigate the impact of gas composition in the fermentation cabinet on dough and bread properties.

In this section, the rationale consisted in using carbonated water as a source of CO_2 solubilisation in dough using conventional mixing, in replacement of gaseous CO_2 provided in the headspace of the mixer. The rationale was to assess the possible interest of CO_2 solubilisation on dough aeration and on the fermentation kinetics as well as bread properties.

5.1. Experimental strategy

Two main experimental strategies were considered:

- First, carbonated water was used during the mixing stage as a substitute to the effect of CO_2 injection under pressure; it was produced using a "SODA-STREAM" machine (SodaStream International Ltd). This method allowed for the incorporation of dissolved CO_2 directly into the dough before fermentation. A comparison was done using conventional dough mixer in comparison to a reference condition providing insights into their respective roles in dough development and gas retention.
- Second, different conditions of gaseous atmosphere were considered in the fermentation cabinet with a) regular condition in a closed fermentation cabinet and b) by introducing a continuous CO_2 flow into the cabinet, simulating an environment enriched in CO_2. This setup aimed to assess whether fermentation in the presence of CO_2 could enhance the solubilisation and stabilization of gas bubbles within the dough matrix.

These approaches were designed as alternative to experimental strategies based on CO_2 gas solubilisation during mixing. Quality assessments were done for dough and bread. A specific point for this study stemmed from the observation of possible colour change of dough pieces and of the bread crumb and crust. It is hypothesised that these colour change may be linked to either oxygen exposure and surface oxidation or to the impact of CO_2 gas on the dough pH.

The results are presented under the form of a manuscript that could be submitted to a scientific journal. This manuscript is organised as an independent section of the PhD and may contain some duplications in particular in the material and methods section.

Title: Impact of Carbonated Water and Gas Composition During Bread Dough Fermentation On Dough and Bread Properties: A Comprehensive Study

Christy Raad[1], Patricia Le-Bail[2], Alain Le-Bail[1]

[1]Oniris - GEPEA UMR CNRS 6144, Nantes – France
[2]INRAE – ISD BIA, Nantes – France

Abstract

This study explored the role of exogenous CO_2 in bread dough formulation and fermentation, with a focus on two novel interventions: the incorporation of carbonated water during dough preparation as a substitute to plain water and the application of a CO_2-enriched atmosphere during fermentation. Carbon dioxide (CO_2) produced endogenously during yeast fermentation, plays a critical role in dough expansion, gas cell formation and final bread structure. In addition to fermentation, exogenous sources such as carbonated water that could be used in replacement of plain water and CO_2-modified atmospheres may influence CO_2 solubilisation and retention in the dough matrix.

Doughs were mixed with plain water or with carbonated water and then fermented under with or without CO_2-flow in the fermentation cabinet. The incorporation of carbonated water resulted in lowered dough pH and increased initial CO_2 solubility. However, neither carbonated water nor the CO_2-flow consistently improved gas retention or the final loaf volume.

Overall, while exogenous CO_2 altered fermentation dynamics, it did not translate into better bread quality. Moreover, while the continuous CO_2 flow did not impact the bread SV, it improved crust appearance by increasing both brightness (L*) and yellowness (b*).

Keywords: Bread, Dough, CO_2, Carbonated water, Modified atmosphere

5.2. Introduction

Carbon dioxide (CO_2) and ethanol are produced by baker's yeast during bread dough fermentation. These chemical species exist in a gas/liquid equilibrium in the dough and play a pivotal role in the breadmaking process, from dough aeration, volume expansion during fermentation, to oven rise during baking. Ultimately, they significantly influence the final bread and crumb structure. (Campbell and Martin 2012; Chin and Campbell 2005b; Verheyen *et al.* 2015). This dissolved CO_2 diffuses into existing air nuclei created during mixing, even before the liquid phase reaches full saturation, as demonstrated by Chiotellis & Campbell (2003). This diffusion is governed by mass transfer principle, driven by partial pressure gradient, which yields in gas solubilisation and contributes to early-stage bubble nucleation (Chiotellis and G. M. Campbell 2003). The degree of CO_2 dissolution depends on multiple factors, including dough temperature, water content, and the presence of solutes such as proteins and salts (Poutanen, Flander and Katina 2009).

The solubility of CO_2 in water is governed by Henry's Law, which states that the amount of gas dissolved in a liquid is proportional to its partial pressure in the gas phase (Ben Aissa *et al.* 2010). In aqueous solutions, CO_2 exists not only in physical solution ($CO_{2(aq)}$) but also undergoes chemical transformation into carbonic acid (H_2CO_3), which dissociates into bicarbonate (HCO_3^-) and carbonate (CO_3^{2-}) ions depending on pH, temperature and ionic strength (Chiotellis and G. M. Campbell 2003; Chiotellis and G.M. Campbell 2003; Chaix, Guillaume and Guillard 2014). Under standard conditions (25°C, 1 atm),

the solubility of CO_2 in pure water was reported to be approximately 1.45 to 1.5 $g \cdot L^{-1}$ (Gevantman 2011). Descoins et al. (2006) showed that solutes such as NaCl, ethanol and sucrose significantly reduced CO_2 solubility by decreasing water activity and competing for hydration.

In bread dough systems, CO_2 solubility has been inconsistently reported due to differences in experimental methods and how the water phase was defined. Some studies referenced dough mass (Hibberd and Parker 1976), others used total water content (Ben Aissa *et al.* 2010) or an undefined Liquid Phase Dough (LPD) (Bloksma 1990; Chiotellis and G. M. Campbell 2003). The concept of free-water, which is the unbound portion to the dough constituents, was proposed as the most relevant reference.

Analysis of Henry coefficients reported by Hibberd & Parker and Ben Aissa et al., revealed the significance of units and reference phases in interpreting CO_2 solubility in dough. Expressing solubility per gram of dough as proposed by Hibberd & Parker offered practical metric for breadmaking applications, while expressing it per gram of free water allowed for more accurate scientific comparisons with pure water systems. According to Hibberd & Parker (1976), saturation occurred at approximately 1.44 $mg_{CO2} \cdot g_{dough}^{-1}$, which corresponded to about 7.71 $mg_{CO2} \cdot g_{free\ water}^{-1}$ based on free water content (computed from their recipe). In contrast, Ben Aissa et al. (2010), reported saturation at roughly 0.306 $mg_{CO2} \cdot g_{dough}^{-1}$ or 1.45 $mg_{CO2} \cdot g_{free\ water}^{-1}$ at 25°C, which is a value close to the solubility of CO_2 in water at atm. Pressure and 25°C. These differences reflect variations in experimental protocols and phase definitions but provide valuable boundaries for expected CO_2 solubility in dough. The value of Ben Aissa et al. appears as the closest one to water and was considered at follow.

CO_2 can be solubilized in a bread dough by applying a gas containing a partial pressure of CO_2 in the mixer headspace during mixing; eventually, this can be combined with a pressure above atmospheric pressure (Campbell and Martin 2012; Martin *et al.* 2008). Another mean consists in using carbonated water, which was considered in this project. While several studies have examined gas retention, bubble dynamics, and the effects of CO_2 during dough fermentation (Chiotellis and G. M. Campbell 2003; Koksel and Scanlon 2016), the use of carbonated water as an ingredient in bread dough has not been studied to our knowledge. No previous work has evaluated the effect of carbonated water on dough pH, CO_2 release kinetics, or void fraction in yeasted doughs. In addition, the study of the impact of CO_2 in the gaseous ambience surrounding the dough pieces in the fermentation cabinet has not been considered by previous researchers to our knowledge. CO_2 concentration can be considered an additional proving parameter, suitable for monitoring dough fermentation in relation to dough dimensions like height, volume and length. In this context, this study aims to:

- Investigate the impact of carbonated water in dough on dough and bread properties
- Quantify the CO_2 exchange between dough and the ambiance of a fermentation cabinet
- Assess the impact of gas composition in the fermentation cabinet on dough and bread properties

5.3. Materials & Methods

5.3.1. Experimental strategy

Two types of doughs were prepared:

- Reference dough (RefD): using regular tap water.

- Carbonated dough (CarbD): using carbonated water.

During fermentation, dough samples were placed in a fermentation cabinet under two different conditions:

1. Reference Fermentation in a closed cabinet, which gaseous ambiance was air at start of fermentation
2. Fermentation with a forced CO_2 flow in the cabinet (0.5 $l \cdot min^{-1}$) within a cabinet of 0.8 x 0.8 x 0.6 m corresponding to the injection of 0.13% of the cabinet volume per minute. This percentage is low but yielded in an atmosphere richer in CO_2. The CO_2 atmospheric partial pressure is 10^{-4} atm or 40.52 Pa. This corresponds to $6.17 \cdot 10^{-3}$ mol in the volume of the cabinet (0.384 m^3); applying the perfect's gas law, the number of moles in the fermentation cabinet at atm. pressure and 30°C is of 15.4 mol. The volume flow rate of 0.5 $l \cdot min^{-1}$ of pure CO_2 at atm pressure and at 30°C corresponds to flow rate of $1.98.10^{-2}$ $mol \cdot min^{-1}$. Over 1 min of CO_2 injection, the number of CO_2 moles is increased by 3.2 fold. The flow rate of $1.98 \cdot 10^{-2}$ $mol \cdot min^{-1}$ corresponds to the 0.13% mentioned earlier. In other words the CO2 partial pressure will rise by 0.13% per minute.

This resulted in **four experimental groups**:

- RefD + No CO_2
- RefD + CO_2 Flow
- CarbD + No CO_2
- CarbD + CO_2 Flow

In this study, the fermentation cabinet was equipped with CO_2 and air humidity sensors; this allowed the measurement of the CO_2 emitted by the dough during fermentation.

Additional post fermentation tests were done after the dough fermentation; these post-fermentation tests aimed at assessing the impact of the dough type and fermentation condition on the level of CO_2 saturation in the dough through a new experimental approach.

5.3.2. Ingredients

The flour used was Fleur Tradition T65 (Moulins Soufflet – France), Universal fresh baker's yeast (Omas Ur-Hefe Universal, Lesaffre Deutchland GmbH, Kehl – Germany) was used as a leavening agent. Tap water was used. Fine table salt (Sodium Chloride) was used (Tafelsalz, Edeka – Germany).

5.3.2.1. Experimental preparation protocol of carbonated water and the influence of salt concentrations on CO_2 solubility

Carbonated water was prepared using a SODASTREAM machine (SODASTREAM LtD-Israël). Tap water of temperature 22°C was used to fill up the bottles, which were then stored at 4°C overnight. The carbonated water preparation was done by applying 4 consecutive pumps per bottle (volume 0.84 L liquid content and 1 L total volume) to standardize gas pressure and CO_2 incorporation. Immediately after carbonation, the bottles were sealed and stored at 4°C. To monitor CO_2 dissolution over time, the

pH of the carbonated water was measured at regular intervals (h0, h1, h2, h3, h24) to ensured reproducible carbonation conditions across all experimental batches.

The focus of this work was on the use of carbonated water in dough formulation without salt as a strategy to enhance CO_2 solubility without altering dough composition. However, to validate the theoretical effect of salt (NaCl) on gas solubility, complementary carbonation tests were performed using distilled, tap and NaCl-containing solutions with varying concentrations. The CO_2 content was determined by measuring the mass difference of the bottles before and after carbonation. The experimental carbonation was with 4 consecutive pumps with SODASTREAM. All tests were conducted at ambient temperature 20°C and performed in duplicate for reliability. By comparing the mass difference corresponding to dissolved CO_2 between salt-free and salted carbonated water solutions, the impact of NaCl concentrations on CO_2 solubility was quantified.

5.3.2.2. Breadmaking process

5.3.2.2.1. Dough mixing

The dough was mixed using a DIOSNA SP 12 spiral mixer (Diosna, Germany). The mixer featured a rotating bowl made of stainless steel and a spiral-shaped mixing arm. A temperature sensor was installed flush within the arm, positioned approximately 2 mm above the bottom surface of the bowl. The mixer had a height of 21.2 cm and an internal bowl diameter of 37.4 cm, with a volume of 22 L. The supervision system enables real-time monitoring and documentation of key parameters such as mixing time, power consumption, dough temperature, and number of revolutions.

The dry and the wet ingredients are added together in one step and mixed. To ensure experimental consistency, mixing parameters (e.g., speed and duration) were carefully adjusted to reproduce the mixing conditions used in other tests.

A three-stage mixing protocol was applied:

- **Stage 1 – Start Phase**: 25 Hz (low speed = 75 RPM) for 1 min
- **Stage 2 – Pre-mixing phase**: 35 Hz (medium speed = 105 RPM) for 3 min
- **Stage 3 – Kneading phase**: 50 Hz (high speed = 150 RPM) for 10 min, during which the t_{PEAK} was determined based on the average power given by the mixer.

5.3.2.2.2. Determination of t_{PEAK}

The power consumed by the mixer was collected during the kneading phase. To reduce noise and smooth the dataset, an average of 30 consecutive power readings was calculated. This moving average was applied repeatedly on the averaged data to further smooth the curve. The resulting smoothed power curve was then used to identify the dough development time, t_{PEAK}, defined as the point of maximum power consumption during the kneading phase. A triplicate measurement was conducted to determine the t_{PEAK}, which corresponds to the time for which the power consumed by the mixer reaches a maximum value. This time was considered as an optimal mixing time based on (Lancelot *et al.* 2021). In order to accommodate the variability of the experimental records, the average of 3 power records was used. The highest power level during the kneading phase can be a first approach to determine the

time at which the dough was supposed to be at its optimal texture (t_{PEAK}) (Lancelot *et al.* 2021; Sadot, Cheio and Le-Bail 2017). A second approach consisted in using the time of the maximum of a quadratic polynomial equation, which was used to fit the power data. The maximum of this function was used to determine the t_{peak}.

5.3.2.2.3. Determination of dough void fractions

The density of the dough was measured to estimate the amount of gas incorporated into the dough (Campbell *et al.* 2001), defined as the dough void fraction (ε_{dough}) with a procedure based on Archimedes' principle (Campbell *et al.* 2001; Chiotellis and G. M. Campbell 2003). First, after kneading, small dough samples (≈30 g) were weighed using a precision balance (RADWAG, PS 6100.R2.M) this was the mass m_1. Then a beaker of 500 mL filled with colza oil with known density (916 g·cm^{-3}) was placed on the balance; a dough holder (steel wire) was immerged into the oil up to the level of the air-oil interface and the balance was then tared. Lastly, the piece of dough was fixed on the dough holder and was immersed in the oil. The resulting mass (m_2) corresponds to the buoyancy force caused by the volume of the tested dough sample (V_D), which is composed of the volume of the degazed (gas free) dough (V_{DD}) previously calculated and of the volume of gas trapped in the dough (V_{gas}). The void fraction was then calculated using the difference in weight:

$$\varepsilon_{dough}(\emptyset) = 1 - \frac{\rho_D}{\rho_{DD}} \quad \text{Eq. 5.1}$$

With the volume of gas-free dough

$$V_{DD} = \frac{m_1}{\rho_{DD}} \quad \text{Eq. 5.2}$$

Where ρ_{DD} = 1.250 g·cm^{-3} was based on the calculation:

$$\rho_{DD} = \sum_i \rho_i . X_i^V \quad \text{Eq. 5.3}$$

In addition, the volume of gas trapped inside the dough can be calculated by the following

$$V_{gas} = \frac{m_2 - V_{DD} \cdot \rho_{oil}}{\rho_{oil}} \quad \text{Eq. 5.4}$$

The void fraction of the dough (dimensionless) was finally determined as follows:

$$\varepsilon = \frac{V_{GAS}}{V_{GAS} + V_{DD}} \quad \text{Eq. 5.5}$$

5.3.2.2.4. Determination of dough expansion ratio N at end of fermentation

The expansion ratio N corresponds to the ratio between the initial and final volume of the dough during fermentation. It was monitored in a fermentation flask (5 cm internal diameter) in which 20 g of dough was installed (dough considered after sheeting/shaping). The expansion ratio was calculated with Eq. 5.6) below based on Raad et al. (2025), in which ε_I and ε_F are the initial and final void fractions of the dough respectively. The N value was computed to reach a final void fraction of 0.75 (Vliet *et al.* 1992).

$$N = \frac{(1-\varepsilon_I)}{(1-\varepsilon_F)} = \frac{H_F}{H_I} \qquad \text{Eq. 5.6}$$

5.3.2.2.5. Shaping of dough and fermentation

After mixing, the dough was divided in pieces of 300 g, each dough piece was shaped into a ball-shape and covered with a piece of tissue to prevent dehydration and were let to rest for 20 min at ambient room temperature. After resting, the doughs were sheeted and moulded in a dough sheeter (Rondostar ECO SFE 6607H, GmbH, Burbach, Germany) by passing them through a pair of rollers maintained at a gap of 2.5 mm from each other. The dough was rolled to form a dough stick, which was installed in a pan (width w = 9.3 cm, height h = 10 cm and length L = 26.4 cm. Then the pans were installed in the fermentation cabinet at a temperature of 30°C and relative humidity of 90% for proofing at ambient air or with CO_2 flow. A piece of dough of 20 g was also installed in parallel in a fermentation flask to monitor the dough expansion. A thin film of sunflower oil lubricated the inner walls of the fermentation flask and a plastic disk was contacted on the top surface of the dough to monitor its expansion.

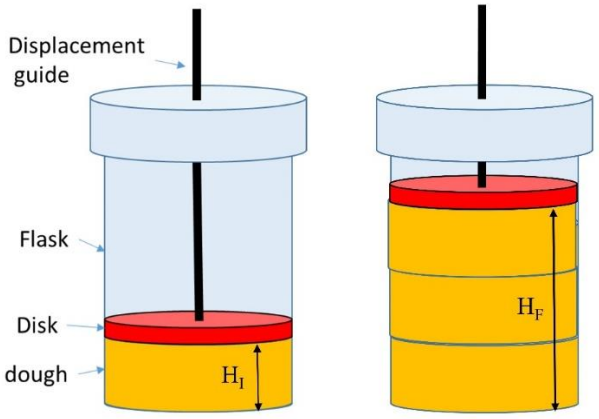


Figure 5.1 Fermentation flask used to monitor the expansion ratio of the dough during fermentation (Raad, Le-Bail and Le-Bail 2025)

CO_2 concentrations were measured using a digital non-dispersive infrared (NDIR) CO_2 sensor (model FYAD 00 CO_2) equipped with an integrated atmospheric pressure sensor for automatic compensation. The sensor features a 2-beams infrared measuring cell, measuring ranges up to 10,000 ppm (FYAD00CO2B10) or 5,000 ppm (FYAD00CO2B05), with typical accuracy of ± (100 ppm + 5%) or ± (50 ppm + 3%) of measured value, respectively. It operates in a temperature range from - 40 to + 60°C and humidity up to 95% RH (non-condensing).

A unique automatic calibration compensates for sensor ageing. Atmospheric pressure was measured and compensated automatically via a built-in digital pressure sensor (700 – 1100 mbar range, ± 2.5 mbar accuracy). Data logging was performed using an ALMEMO® data logger, recorded at 1 s interval, with each measurement based on a moving average reading window of 15 s. The sensors were installed into the fermentation cabinet as seen in the figure below; on the upper shelve one for CO_2 measurement and one for relative humidity measurement. The bottom shelve has the same two sensors mounted in parallel. A fan (visible at the back of the picture) ensured stirring of the gaseous ambiance contained in the cabinet.

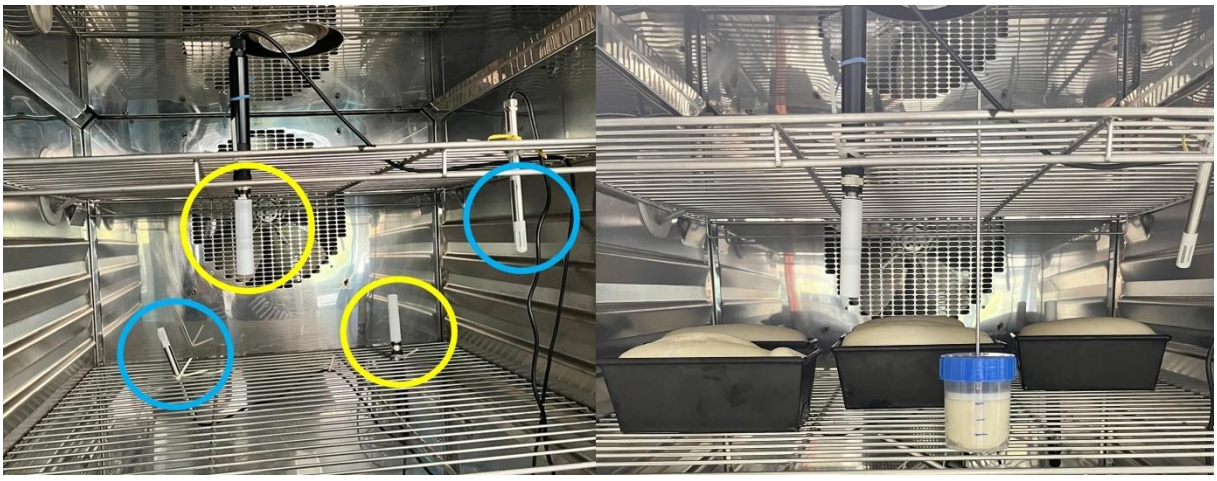


Figure 5.2 Picture of the inside of the fermentation cabinet; (a) to the left, CO_2 sensors in yellow and Relative humidity sensors in blue and (b) to the right the moulded dough sticks at the end of fermentation with the expansion ratio monitoring flask

The fermentation cabinet was equipped with a CO_2 supply system, consisting of a pressurized CO_2 cylinder connected via a controlled tubing network, enabling the continuous introduction of CO_2 directly into the fermentation environment at a low rate of 0.5 $L \cdot min^{-1}$. At the start of fermentation, the integrated sensors were activated to continuously monitor the CO_2 release in real time.

5.3.2.3. Baking

Baking was carried out for doughs after the fermentation stage. Baking was conducted in a deck oven (Piccolo I, Wachtel GmbH & Co.) for 17 min at 230°C with 300 mL of water vapour injected in the beginning. After baking, the bread was allowed to cool for about 1 hour before measuring its properties.

5.3.3. Determination of dough and bread properties

5.3.3.1. Measurement of dough pH before and after fermentation

pH measurements were carried in triplicates for 3 dough pieces before and after fermentation for all the tested recipes, by using a penetration electrode (Hanna Instrument HI98161 - France). The instrument was calibrated before every measurement with distilled water and buffer solutions having a pH 4.0 and 7.0, respectively.

5.3.3.2. Determination of doughs texture before and after fermentation

The texture profile analysis of doughs was determined by using texture analyser (TA-XT2, Stable Micro Systems, England) with a modified AACC method (74-09) for texture profile analysis (TPA). After kneading, 3 dough pieces around 50 g each were shaped and rounded for measurement. A 10 mm diameter probe and 5 kg load cell were used as measurement geometry. The three dough pieces were two times compressed up to 40% deformation with 15 s rest, the test speed was 1.7 $mm \cdot s^{-1}$. The same

test was conducted for the dough pieces after fermentation to assess the impact of CO_2 flow on the dough textural profile. For each batch, a triplicate was conducted before and after fermentation.

5.3.3.3. Dough colour measurement before and after fermentation

Colour measurements were taken immediately after mixing the dough samples with a colorimeter Chroma Meter (CR-400, B 8212649; Konica Minolta, Tokyo, Japan) and after fermentation. The equipment was calibrated using a white reference plate. The color is quantified using the L*, a*, and b* values, where L* indicates lightness to darkness, a* represents the spectrum from green to red, and b* corresponds to the range from blue to yellow. The TCD (Total Color Difference) was calculated based on the equation below:

$$\Delta E = \sqrt{\Delta L^2 + \Delta \mathrm{a}^2 + \Delta \mathrm{b}^2}$$

Measurements for each recipe were performed in triplicate.

5.3.3.4. Texture profile analysis of bread

After 1 h of cooling, the breads were sliced (SOFRACA, France) to a thickness of 18 mm, and a 10 mm diameter cylindrical probe was employed along with a 5 kg load cell. Each of the three slices was compressed twice to 40% deformation with a 15 s rest between compressions. The test speed was set at 1.7 mm·s^{-1}. The analysis was measured by using a texture analyser (TA-XT2, Stable Micro Systems, England) following a modified AACC method (74-09).

5.3.3.5. Determination of breads texture after baking

The texture profile analysis of breads was determined by using texture analyser (TA-XT2, Stable Micro Systems, England) with a modified AACC method (74-09) for texture profile analysis (TPA). After 1 hour of cooling, from each bread loaf 3 middle slices were taken for measurement. A 10 mm diameter probe and 5 kg load cell were used as measurement geometry. The bread slices were two times compressed up to 40% deformation with 15 s rest, the test speed was 1.7 mm·s^{-1}.

5.3.4. Statistical analysis

Data were analysed using Statgraphics 19 – X64 software using one-way ANOVA and Tukey test. $p < 0.05$ was considered significant. 9 breads were baked for each condition and averaged.

5.4. Results & Discussion

5.4.1. Dough properties

5.4.1.1. Assessment of CO_2 Solubility in Carbonated Water: Influence of Salt Concentration and Implications for Dough Formulation

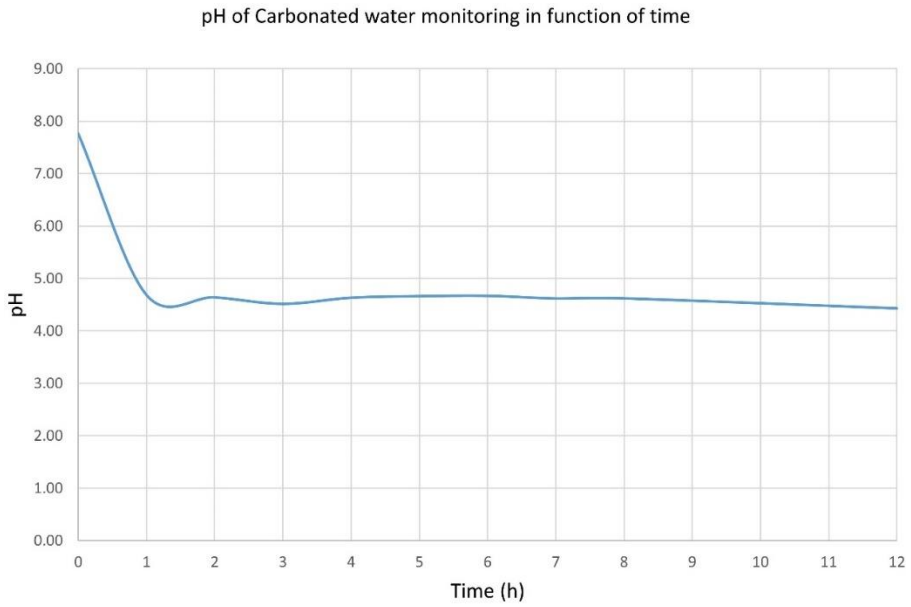


Figure 5.3 pH monitoring over 12 hours of carbonated water, where the bottles are stored at 4°C

After 2 hours, the pH stabilized at a value around pH = 4.6, before each dough production, carbonated water was prepared 2 hours before in order to have consistent pH and enough time for CO_2 solubilisation. Descoins et al. (2006), investigated the carbonation of several beverages among them tap water at different pH values, were the gas flow was set at 15 $g \cdot L^{-1}$ and CO_2 pressure at 6 bar. However, in our study, the pressure of CO_2 injection was not directly measured but according to the brand specification SODASTREAM the pressure is approximately 4-5 bars. The accuracy of these measurements was influenced by the amount of free gaseous CO_2 in the liquid, which depended on the solution pH. Results that are more accurate were obtained in acidic conditions, where CO_2 remained mostly in its dissolved form. When the pH exceeded 7, the formation of carbonates reduced measurement reliability (Descoins, Mathlouthi, Moual *et al.* 2006). Therefore, this highlighted the importance of pH control as a key factor in ensuring precise and reliable CO_2 detection in liquid samples, more specifically tap water (Descoins, Mathlouthi, Moual *et al.* 2006).

Building on this controlled acidic environment, the results of salting-out experiments showed a linear decrease in CO_2 solubility in sodastream processed NaCl solutions (around 5 bar) with increasing salt concentrations, with a decrease of 25% at 40 $g \cdot L^{-1}$ salt compared to pure water. Initial measurements showed CO_2 solubility of 6250 $mg \cdot L^{-1}$ in distilled water and slightly less with tap water (6120 $mg \cdot L^{-1}$) due to mineral content differences reducing available free water. Looking at Figure 5.4, the linear relationship confirms the salting-out effect, where dissolved salts reduced CO_2 solubility by limiting free water and altering its ionic strength. Despite its critical role in bread and fermentation, CO_2 solubility in bread dough has been only scarcely addressed in literature. A review of the most relevant and

representative publication is presented below to benchmark existing data and highlight methodological and interpretative differences. The few available studies differ in terms of experimental setup, units of solubility and definition of the water phase used as a referenced medium.

Hibberd & Parker (1976) and Ben Aissa et al. (2010) both utilized the same methodology based on isochoric fermentation, which measure the pressure increase during fermentation at a constant volume. However, comparing these studies is complicated by differences in units, and by varying reference phases used to express solubility. Hibberd & Parker normalised CO_2 solubility to the dough mass, whereas Bloksma (1990) referred to the liquid phase of the dough (LPD) and Ben Aissa et al., used the total water content of the dough as a reference. The LPD lacks a precise definition in the literature but is generally assumed to correspond to the water added to the dough recipe. On the other hand, Chiotellis & Campbell (2003) reported values in mol/m^3 of the liquid phase without defining the liquid phase.

To better quantify free and bound water in dough systems, a study by Bushuk & Mehrotra (1977), provided foundational data. They measured the free water and bound water content of doughs made from various flours and investigated the effect of protein content, mixing time, salt concentrations and damaged starch. Notably, none of these factors significantly affected the amount of free water, their data showed a linear relationship between freezable and total water content. The following equation was used for the estimation of free water X_{FW} as function of total water per g of dry flour (X_{DF}):

$$X_{FW}\left(\frac{g_{FW}}{g_{DF}}\right) = 0.591\,.X_{DF}\left(\frac{g_{WATER}}{g_{DF}}\right) - 0.148 \qquad \text{Eq. 5.7}$$

Using this equation, and considering the reference dough recipe, it was found by using this equation that the free water accounted for 41.8% of the total water content and accounted for 53% of the LPD, with the LPD representing the added water in the recipe. Overall, this experimental validation underscores the critical influence of salt on CO_2 dissolution, a factor important in both beverage carbonation and food fermentation contexts.

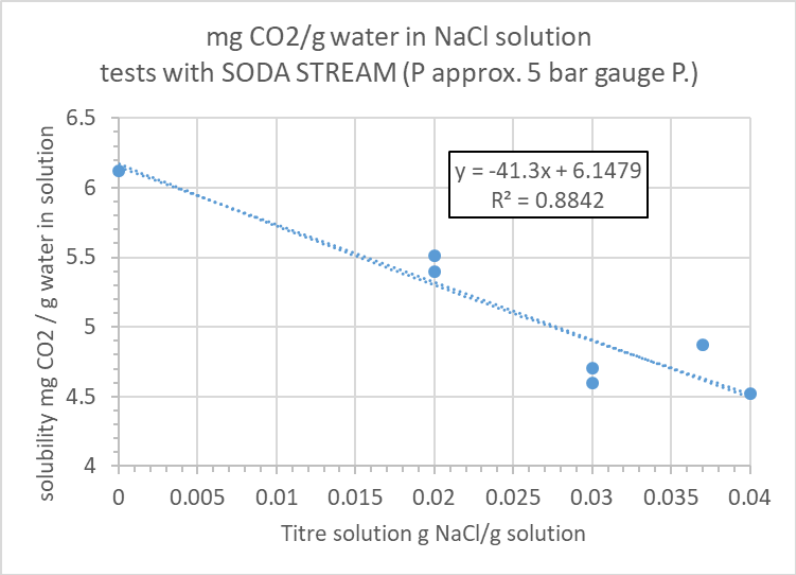


Figure 5.4 Impact of the NaCl titant of a water solution (tap water) on the CO_2 solubility at around 5 Bar. Tests done with a sodastream equipment. The x-axis shows the titrant, essentially the mass fraction or titrant solution of NaCl in the solution

Both graphs (Figure 5.3 & Figure 5.4), highlight how the environment affects dissolved CO_2, the physical-chemical state of water whether its ionic strength in case of NaCl or time-dependent CO_2 equilibrium, affects the state and retention of dissolved CO_2 either measured as pH change or reduction in solubility. Having established how CO_2 solubility and pH stabilize in carbonated water under different conditions, the subsequent section focuses on the effect of the carbonated water and CO_2 flow during fermentation on dough pH.

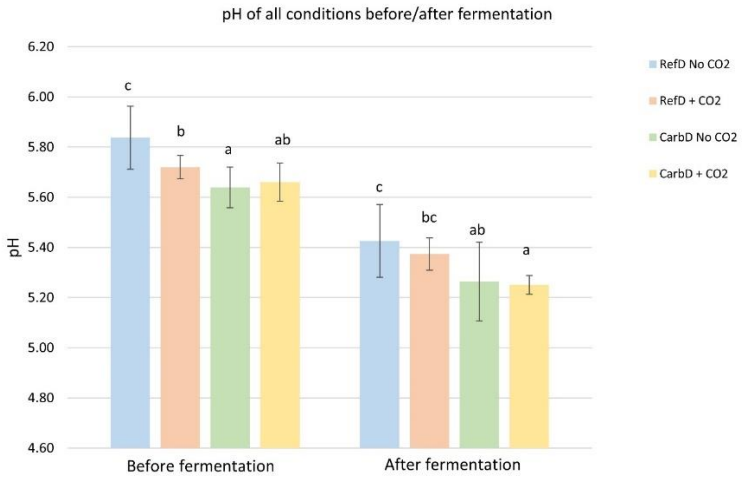


Figure 5.5 Dough pH of RefD and CarbD in absence and presence of CO_2 flow before and after fermentation

Before fermentation, without any CO_2 flow, we observed the impact of carbonated water on the RefD and CarbD doughs. Based on the figure above, before fermentation, the lowest pH values were achieved with CarbD recipes (5.64 ± 0.08 and 5.66 ± 0.08, respectively). The pH before fermentation was statistically significant between all the recipes ($p < 0.05$). The initial decrease in pH could be due to dissolution of CO_2 into H_2CO_3 (Ben Aissa *et al.* 2010).

The pH after fermentation was statistically significant between all the recipes ($p < 0.05$). However, the highest decrease in pH was for CarbD dough with and without CO_2 flow than the RefD doughs. In which, the lowest pH was achieved with CarbD + CO_2 flow (5.25 ± 0.04) which was not statistically significant with CarbD in absence of CO_2 flow (5.26 ± 0.16). The addition of continuous CO_2 flow during fermentation slightly intensified the pH reduction in CarbD dough, likely due to enhanced CO_2 dissolution. However, the dough intrinsic buffering capacity mainly provided by the dough constituents, tend to moderate such changes, which may explain why the final pH difference between CarbD with and without CO_2 flow was not statistically significant (Poutanen, Flander and Katina 2009). Exogenous CO_2 first dissolves into the liquid dough and then breaks into its different components as described, however, this breakdown is influenced by the pH level of the liquid, meaning that the pH of the food matrix significantly influence the amount of CO_2 that can be dissolved (Chaix, Guillaume and Guillard 2014). According to Chaix et al. (2014), decreasing the pH value leads to a reduction in CO_2 solubility, while increasing the pH value results in higher CO_2 solubility. These results confirm that pH is a key factor influencing CO_2 solubility and retention in dough, with acidic conditions favouring stable CO_2 dissolution, while the buffering constituents of the dough matrix prevent large pH fluctuations despite ongoing CO_2 exposure. This dynamic highlights the complex interplay between dough chemistry and gas solubility, which directly affects fermentation behaviour and dough characteristics.

5.4.1.2. Determination of t_{PEAK}

A record of the mixer power in function of time is shown in the figure below (Figure 5.6). This graph is the average of 3 records. The power is fluctuating depending on dough circulation in the mixer, which makes the determination of a precise value of the t_{PEAK} difficult. The determination of this parameter was crucial to have a fixed mixing time for all the dough conditions. To determine the optimal kneading time, average power was plotted over time and fitted with a second-degree polynomial regression (R^2 = 0.87). The t_{PEAK} representing the optimal mixing point, was identified at the vertex of the curve using the formula x = - b / 2a, yielding a t_{PEAK} value of 6 min.

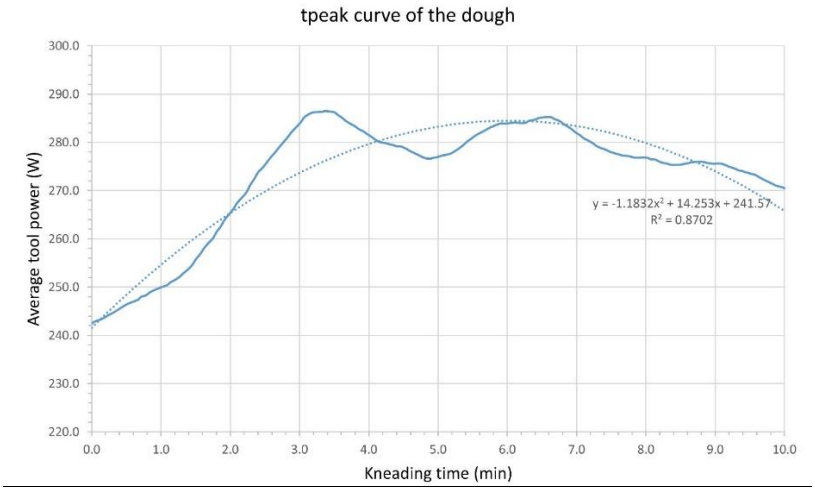


Figure 5.6 Average tool power during dough kneading in function of kneading time, representing the maximum point of the curve (t_{PEAK})

5.4.1.3. Measurement of dough void fractions after mixing, sheeting & fermentation

Table 5.1 Doughs void fractions after mixing, sheeting and fermentation. This table also represents the dough expansion ratio N (computed with Eq. 5.6) during fermentation to reach a final void fraction of 0.75. Values with different superscript lowercase letters in the same column for each condition are significantly different (p < 0.05). The values presented here are mean ± standard deviation

Conditions	Initial void fraction ε_i after mixing	ε after sheeting	Final ε_f after fermentation	Expansion ratio N
RefD No CO_2 flow	0.14 ± 0.53 ^{b}	0.23 ± 0.01 ^{a}	0.56 ± 0.05 ^{a}	3.07 ± 0.07 ^{b}
RefD+ CO_2 flow	0.12 ± 0.98 ^{a}	0.25 ± 0.01 ^{ab}	0.62 ± 0.03 ^{ab}	3.00 ± 0.02 ^{b}
CarbD No CO_2 flow	0.11 ± 0.22 ^{a}	0.26 ± 0.01 ^{b}	0.64 ± 0.04 ^{bc}	2.95 ± 0.07 ^{a}
CarbD + CO_2 flow	0.11 ± 0.06 ^{a}	0.26 ± 0.01 ^{b}	0.69 ± 0.01 ^{c}	2.96 ± 0.06 ^{a}

After mixing, ε_i (RefD) without CO_2 flow was significantly different from the rest of the conditions ($p < 0.05$).

After sheeting, ε was not statistically significant between all conditions ($p > 0.05$).

After fermentation, ε_f of RefD without CO_2 flow was the lowest in comparison to the rest. However, the highest value was observed with CarbD with CO_2 flow (0.69 ± 0.01), although not significantly different from CarbD without CO_2 flow (0.64 ± 0.04). By comparing doughs in presence of CO_2 flow, we observe that with CarbD, a higher ε_f was observed ($p < 0.05$). This aligns with Chiotellis & Campbell (2003), that stated increased CO_2 solubility and over-saturation within the dough matrix promote early-stage gas bubble nucleation and stability, particularly in viscoelastic systems like bread dough. Moreover, the presence of pre-dissolved CO_2 increased the probability of earlier gas nuclei formation during fermentation, which promoted a greater number of initial bubbles and contributed to a higher ε_f. This mechanism was particularly effective when paired with continuous CO_2 flow, which maintained a concentration gradient that derived further gas solubility.

These findings can be directly linked to the fundamental solubility behaviour of CO_2 in water and carbonated water. According to Henry's law, the concentration of dissolved CO_2 in the dough aqueous phase is proportional to the partial pressure of CO_2 in the surrounding gas. Carbonated water provides a pre-saturated dough with CO_2 compared to non-carbonated doughs. Comparisons across the literature, Hibberd & Parker (1976) reported high solubility when expressed relative to free water in the dough, whereas Chiotellis & Campbell (2003), provided values (1.32 – 1.40 $mg_{CO2} \cdot g_{water}^{-1}$) in closer agreement to Henry's law, where pressure during mixing varied between 0.133 – 2 bar and the final dough temperature was around 30 ± 1°C. In this context, carbonated water maximized CO_2 solubility and the availability of early gas bubbles. Despite the observed increase in ε_f with CO_2-enriched fermentation, the maximum ε_f did not reach the theoretical value of 0.75. This was consistent with Bellido et al. (2009) investigated the gas production and dough aeration properties of chemically leavened dough using a digital image analysis coupled with X-ray tomography. Their results showed that dough void fractions typically ranged between 5 and 67%. The limitation of not achieving a final ε_f of 0.75 arises from intrinsic factors related to dough rheology and gas cell stability. Specifically, a higher ε_f does not always mean a better bread aeration; it can result from fewer large gas bubbles, a consequence of a reduced gluten network extensibility that limited dough expansion during fermentation. When the gluten matrix becomes less extensible, gas cells tend to coalescence or grow disproportionally, which might lead to lower loaves volumes and irregular crumb structure (Verheyen *et al.* 2015).

5.4.1.4. Measurement of dough expansion ratio (N) after sheeting

Bubble growth during proving is influenced by several factors (1) the rate at which yeast produces CO_2 (2) the degree to which the dough retains the generated CO_2 (3) the rate at which CO_2 diffuses from saturated LDP to the formed gas nuclei and (4) bubble coalescence (Shah *et al.* 1998). By referring to Table 5.1, CarbD doughs with and without CO_2 flow reflected a higher ε after sheeting and thus, a higher ε_f after fermentation. This resulted to a lower calculated dough expansion ration (2.95 ± 0.07 and 2.96 ± 0.06, respectively) than RefD (3.07 ± 0.07 and 3.00 ± 0.02, respectively). These results are consistent with the findings of Chiotellis & Campbell (2003), who demonstrated that doughs with higher initial gas content, such as those mixed at elevated pressures, promote more uniform and continuous CO_2 transfer during proving. Similarly, the use of carbonated water and CO_2 flow in our study created a system rich in early bubble nuclei and elevated CO_2 saturation, accelerating void fraction formation after fermentation. This allowed the dough to reach its target expansion N in a

shorter time, reducing the necessary fermentation duration. The continuous CO_2 injection resulted in excess or over-saturation of gas bubbles with CO_2. Van Vliet et al. (2008; 1992) emphasized that the strain-hardening behaviour of the gluten matrix plays a crucial role in modulation bubbles expansion, although with CO_2-mixed doughs the weak gluten network may lead to less resistance against rupture of the liquid film between bubbles. Several studies reported that factors like water content, type of wheat or content of endogenous lipids affect the rate of bubbles growth during proving (Sahi 1994; Sroan, Bean and MacRitchie 2009).

5.4.1.5. CO_2 measurement in the fermentation cabinet during fermentation

CO_2 sensor readings were plotted as a function of fermentation time to monitor the dynamics of gas release for RefD and CarbD in the case of no CO_2 flow, as shown in Figure 5.7. The curves reflect the accumulation of CO_2 within the fermentation cabinet.

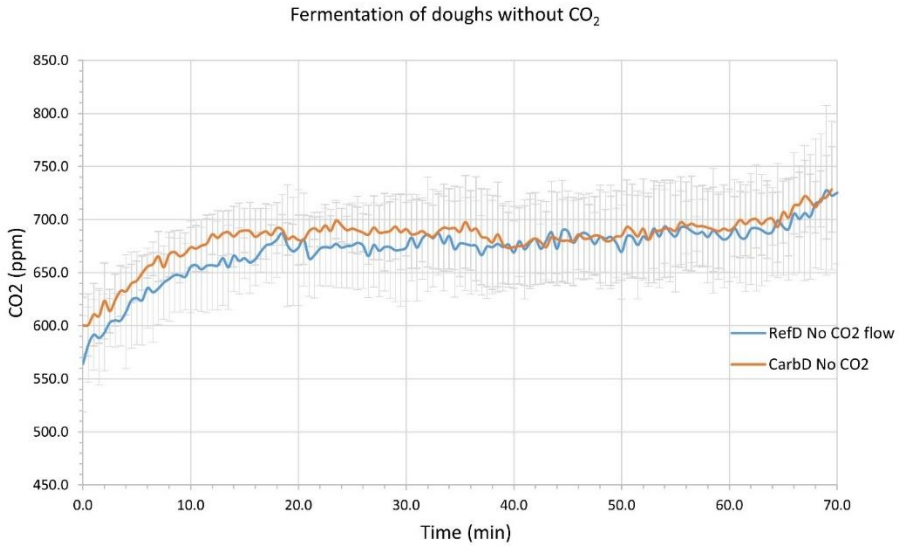


Figure 5.7. Real-time CO_2 emission by RefD and CrabD during fermentation in absence of the CO_2 flow detected by the sensors at 30°C and RH of 90%

The atmospheric CO_2 is $0.4.10^{-4}$ atm or 40 ppm; this does not match with the point at time zero and was attributed to the time needed to install the sample and start the experiment. Our results showed that the concentration of CO_2 in the fermentation cabinet did not exceed around 725 ppm. The maximum value detected was within the maximum range of the sensor (800 ppm) with a plateau observed at 700 ppm. This represents a partial CO_2 pressure of 7.10^{-4} atm compared to $0.4\ 10^{-4}$ atm for partial CO_2 pressure of atmospheric air on earth. This evidenced that the dough released some CO_2 in the ambiance of the fermentation cabinet. The cabinet was closed but was not sealed so that it is likely that some CO_2 escaped toward the external ambiance during fermentation, and that the value obtained at the plateau resulted from a balance between CO_2 released by the dough and CO_2 leaving the cabinet.

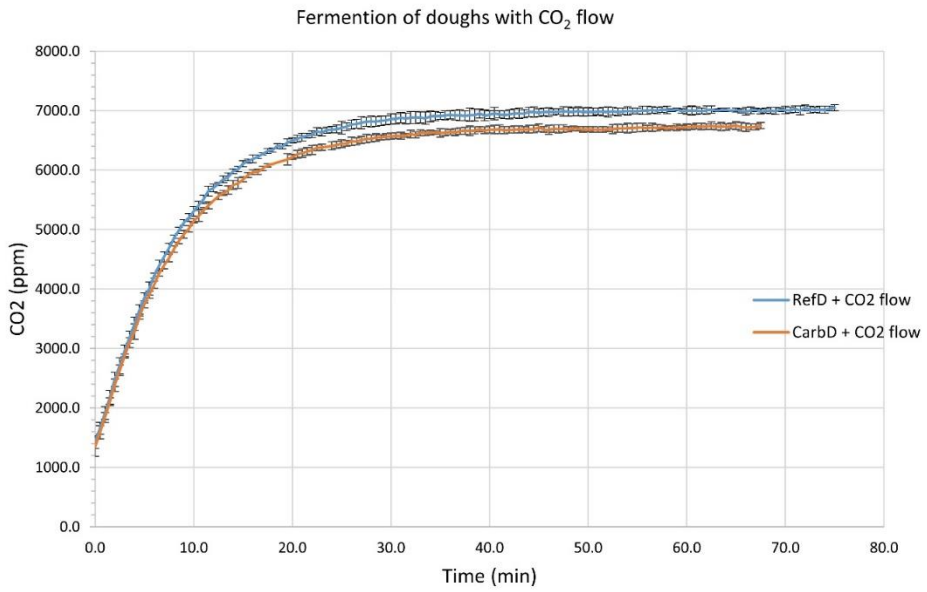


Figure 5.8. Real-time CO_2 emission by RefD and CarbD during fermentation in presence of the CO_2 flow at 30°C and RH of 90%

The results obtained with CO_2 flow are shown in Figure 5.8. The flow was adjusted to 0.5 L·min^{-1} in order to expose the dough to an ambiance enriched in CO_2, while keeping the concentration in the range of the CO_2 measuring equipment (8000 ppm). One can see that with the impose flow rate of CO_2, the ambiant partial pressure was magnified by a 10 factor, shwitching from 700 ppm to 7000 ppm after around 25 min in both cases. There was no significant difference between the two doughs (with tap water vs carbonated water), which both showed a similar trend over time. A small exponential increase in the beginning of fermentation (500 s) and then a plateau was reached after 1500 s (25 min of fermentation) at around 7000 ppm in volume. The plateau phase was slightly increasing over time. The plateau value was $7{\cdot}10^{-3}$ m^3·m^{-3} representing a partial CO_2 pressure of 7.10^{-3} atm compared to $0.4{\cdot}10^{-4}$ atm for atmospheric air on earth. Our computations showed an increase in partial pressure of CO2 of 0.13% per minute, or 3.25% after 25 min. 5 L·min^{-1} of CO_2 corresponds to $1.92.10^{-2}$ mol·min^{-1}; if we multiply this value by 25 min, we obtain the number of CO_2 moles released in the cabinet, which is proportional to the rise in CO_2 partial pressure. A value of 0.48 is obtained, resulting in an additional partial pressure of $32.1{\cdot}10^{-3}$ atm. considering the volume of the cabinet. What we observed is a irse by the difference between with and without flow (7000 - 700 = 6300 ppm = $6.3{\cdot}10^{-3}$ atm). The flow rate was thus influent on the CO_2 partial pressure in the fermentation cabinet. However, there is a discrepancy between the expected rise in CO_2 partial pressure (based on the flow rate) and the observed value. Further checking is needed with the flow rate and taking into consideration the fact that the cabinet was not sealed.

According to (Akdoğan and Ozilgen 1992), CO_2 production during fermentation is initially rapid, and then stabilizes. There was no significant different between the RefD and CarbD. However, the CO_2 concentration (around 6500 – 7000 ppm) was higher than the ones in absence of CO_2. This plateau as explained by Chiotellis & Campbell (2003), typically corresponds to the point which the dough becomes saturated with CO_2. The saturation and plateau occurred at 50 min. from the start of fermentation time. In contrast to our results, RefD and CarbD, reached saturation in RefD and CarbD earlier, around 25 min, likely due to the continuous CO_2 flow in the fermentation cabinet, which accelerated the saturation

process, although fermentation times based on the calculated N continued until 68 min for CarbD + CO_2 and 75 min for RefD + CO_2.

5.4.1.6. Measurement of dough texture before & after fermentation

Table 5.2. Dough texture (Hardness, Springiness, Cohesiveness & Adhesiveness) before & after fermentation. Values with different superscript lowercase letters in the same column for each condition are significantly different ($p < 0.05$) before fermentation and after fermentation. The values presented here are mean ± standard deviation

Before fermentation	**Hardness**	**Springiness**	**Cohesiveness**	**Adhesiveness**
RefD No CO_2 flow	2.33 ± 0.23^{b}	0.60 ± 0.10^{a}	0.53 ± 0.08^{b}	-0.10 ± 0.17^{ab}
RefD + CO_2 flow	2.14 ± 0.20^{a}	0.55 ± 0.06^{a}	0.46 ± 0.03^{a}	-0.26 ± 0.33^{ab}
CarbD No CO_2 flow	2.06 ± 0.22^{a}	0.98 ± 0.80^{b}	0.47 ± 0.03^{a}	-0.08 ± 0.06^{b}
CarbD + CO_2 flow	2.20 ± 0.20^{ab}	0.61 ± 0.11^{a}	0.49 ± 0.07^{ab}	-0.50 ± 0.96^{a}
After fermentation	**Hardness**	**Springiness**	**Cohesiveness**	**Adhesiveness**
RefD No CO_2 flow	1.28 ± 0.32^{a}	0.34 ± 0.11^{a}	0.29 ± 0.05^{a}	-0.05 ± 0.09^{a}
RefD + CO_2 flow	1.14 ± 0.24^{b}	0.42 ± 0.08^{b}	0.38 ± 0.08^{b}	-0.01 ± 0.01^{a}
CarbD No CO_2 flow	1.33 ± 0.26^{a}	0.36 ± 0.06^{ab}	0.33 ± 0.09^{ab}	-0.02 ± 0.05^{a}
CarbD + CO_2 flow	1.35 ± 0.22^{a}	0.38 ± 0.05^{ab}	0.34 ± 0.05^{ab}	-0.02 ± 0.01^{a}

Before fermentation, the texture profile of the doughs were compared based on the presence or absence of carbonated water. By comparing the results before and after fermentation, dough texture profile decreased for all conditions RefD and CarbD with and without CO_2 flow ($p < 0.05$) except for adhesiveness. Before fermentation, by comparing RefD and CarbD in absence of CO_2 flow, hardness was lower with CarbD (2.06 ± 0.22) than RefD (2.33 ± 0.23). In addition, with CarbD scored the highest springiness in comparison with RefD.

However, after fermentation, RefD with CO_2 flow showed the lowest hardness value (1.14 ± 0.24). For springiness, cohesiveness and adhesiveness there was significant difference after fermentation for all conditions ($p > 0.05$). Based on these observations, carbonated water softened the dough and gave the dough higher elasticity before fermentation, as seen by lower hardness and higher springiness compared CarbD with RefD without CO_2 flow. Fermentation reduced hardness across all samples

especially with RefD with CO_2 flow. This indicates carbonation and fermentation primarily affect dough softness without comprising its elastic recovery or adhesiveness.

Campbell & Mougeot (1999) demonstrated that the rheological properties of dough are influenced by its gas content, partly due to the physical presence of entrained bubbles. In addition, Rezaei et al. (2016) studied the changes of yeasted doughs after fermentation and its impact on the dough matrix. According to their findings, fermented dough resulted in a dough less fluid and more prone to deformation in comparison to unyeasted doughs. While fermentation generally leads to a weakening of the gluten network making dough less extensible and more prone to deformation, our results highlight that the presence of CO_2, especially from carbonated water and continuous CO_2 flow, can modify dough texture by introducing gas bubbles. These bubbles physically disrupt the dough matrix, leading to softer and more elastic dough characteristics. Therefore, the texture changes observed in our study are likely a combined effect of both fermentation-related gluten network alterations and gas bubble formation within the dough from the carbonated water and CO_2 flow. Another explanation could be that changes in dough pH over the course of fermentation time may play a crucial role in altering its rheological behaviour. Typically, dough pH declines to around 4 – 5.0, which is largely attributed to the formation of carbonic acid from CO_2 dissolution (Jayaram *et al.* 2013).

5.4.1.7. Measurement of dough colour before and after fermentation

Doughs lightness L* decreased after fermentation, however, CarbD with CO_2 flow had the smallest decrease. All the doughs had a shift to more yellow hue b* after fermentation, with the presence of CO_2 flow and more prominently with CarbD. The observed decrease in dough lightness L* indicated a darkening of the dough surface associated with fermentation. While these trends did not reach significance, they may point to a subtle effect of CO_2 flow in modulating dough surface colour, possibly through reduced oxidative browning or pigment degradation. Polyphenol oxidase (PPO) is a key enzyme responsible for browning in wheat products like pasta and bread (R. *et al.* 2023). Its activity depends on O_2 levels and can be inhibited by adjusting gas atmospheres, such as argon enrichment or higher O_2 (O'Beirne, Murphy and Ni Eidhin 2011). This aligns with our results, where darker dough with CO_2 rich environments. Another possible explanation is that the use of CarbD during mixing may have interrupted or reduced the availability of O_2 for the dough, thereby limiting oxidative reactions. As a result, less oxidation of the gluten network occurred, leading to a more compact structure consistent with the increased hardness observed in CarbD with CO_2 flow. Furthermore, the reduced O_2 levels likely created anaerobic conditions that inhibited the oxidation of carotenoids, preventing their typical degradation or bleaching. This lack of pigment oxidation could explain the darker dough color observed in these samples.

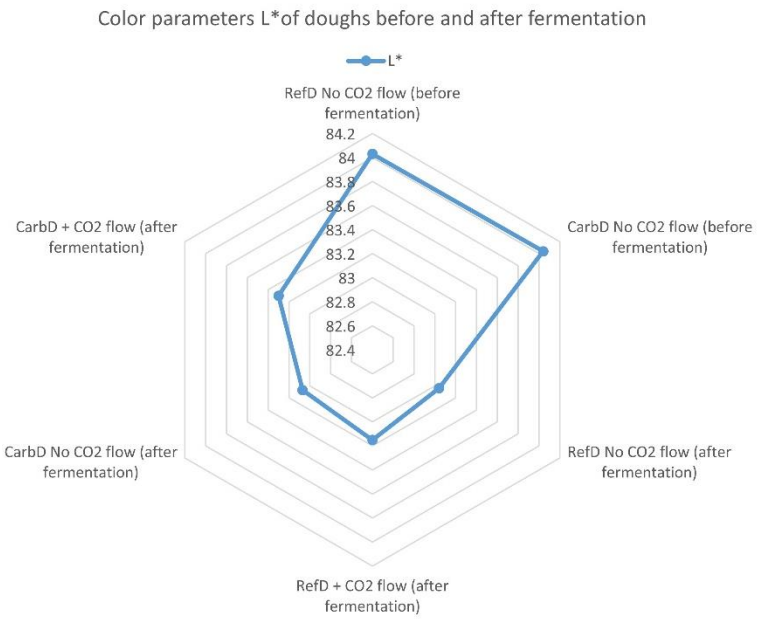


Figure 5.9. Colour parameter L of dough CarbD and RefD before and after fermentation*

5.4.2. Bread properties

5.4.2.1. Breads specific volume SV

The highest SV were scored with RefD with and without CO_2 low (3.15 ± 0.03 & 3.20 ± 0.04, respectively) in comparison with CarbD with and without CO_2 flow (2.97 ± 0.15 & 3.03 ± 0.04, respectively) Figure 5.10.

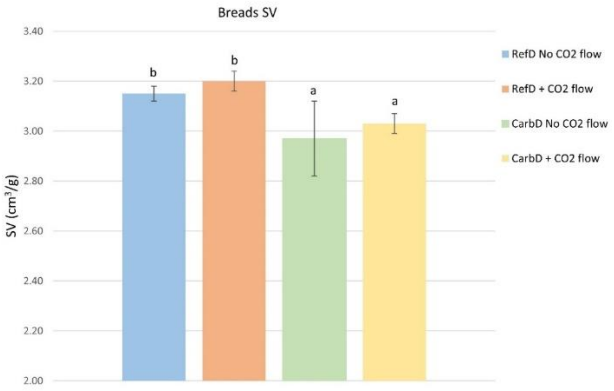


Figure 5.10. Breads specific volume SV

Adriana et al. (2020) observed changes in CO_2 release and bread volume with varying fermentation temperatures, our results showed no significant difference in CO_2 emission between samples. Notably, their findings indicated that bread volume increased alongside CO_2 concentration, with increments of 7.5% and 17.3% in volume corresponding to similar rises in CO_2 release at 33°C and 36°C, respectively. The presence of continuous CO_2 flow during fermentation did not significantly affect specific volume, indicating that the externally introduced CO_2 either escaped or had minimal structural influence. These results suggest that while CO_2 influences dough pH, its contribution to loaf volume is dependent on the

dough ability to retain gas, which may be compromised under acidic conditions. The observed differences in SV between RefD and CarbD can be explained by the influence of partial pressure of CO_2 on gas solubility and retention. Without CO_2 flow, the partial pressure of CO_2 remains relatively low, limiting CO_2 dissolution and gas retention. This allowed RefD with presumably stronger gluten network to maintain higher gas retention during baking. In contrast, with CarbD, the dough ability to retain the formed gas bubbles during baking was a limiting factor, as a result of the weakened gluten network. Therefore, even though CarbD was exposed to higher partial pressure due to carbonated water and the continuous CO_2 flow, the loaf volume does not only depend on the higher solubility but also on the integrity and rheological behaviour of the gluten network which governs the expansion during baking.

5.4.2.2. Breads texture

Table 5.3. Breads texture analysis in terms of Hardness, springiness, cohesiveness & adhesiveness in absence and presence of CO_2 flow.

Breads condition	Hardness	Springiness	Cohesiveness	Adhesiveness
Reference without CO_2 flow	2.18 ± 0.15[a]	7.13 ± 1.39[a]	0.93 ± 0.02[a]	0.01 ± 0.03[a]
Reference with CO_2 flow	2.57 ± 0.73[a]	6.75 ± 1.61[a]	0.92 ± 0.03[a]	0.01 ± 0.01[a]

Based on the Table 5.3, there was no statistical significance between all the tested parameters ($p > 0.05$); the presence of CO_2 has no impact on the bread texture. CO_2 plays a fundamental role in dough aeration and breadcrumb porosity, however, its direct effect on bread texture was pronounced. Our experimental work was conducted after cooling the breads, which could explain the reason why we could not detect significant differences. This could also explain the evaporation of CO_2 during baking and the amount of the solubilized CO_2 was not enough to induced changes at an early stage.

5.4.2.3. Breads upper crust and crumb colour

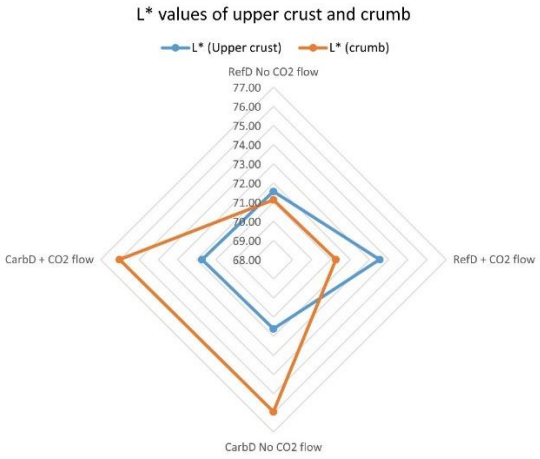


Figure 5.11. L values for Upper and crumb color of breads*

The results of the bread *L* (lightness)* after baking clearly demonstrate the significant impact of CO_2 flow and the use of carbonated water (CarbD) on the final crust color. Based on L* values of the upper

crust, RefD bread with CO_2 flow scored the highest L* values (73.53 ± 0.61) in comparison to the rest. In addition, L* values of CarbD breadcrumbs with and without CO_2 flow were significantly higher (75.94 ± 0.51 & 76.02 ± 0.08, respectively) than RefD breadcrumbs (71.12 ± 0.68 & 71.25 ± 0.25, respectively). The observed differences in L* values between breads could be attributed to the exogenous CO_2 in the dissolved carbonated water during mixing and the CO_2 flow during fermentation. The solubilized CO_2 is expected to result in a lower pH which is known to inhibit Maillard reaction, resulting in a lighter crust. In addition, the denser crumb observed for breads obtained with CO_2 resulted in a more heat conductive bread, which in turn made that the temperature rise of the bread surface (crust) was lower with CO_2 enriched process compared to control. Based on b* values of the upper crust, RefD breads with and without CO_2 flow scored the highest b* values (32.77 ± 0.21 & 32.81 ± 1.60, respectively) in comparison to CarbD breads. The opposite trend was observed in terms of breadcrumb b* values of CarbD with and without CO_2 flow (18.02 ± 0.95 & 18.31 ± 0.69, respectively) from the RefD breadcrumbs.

5.5. Conclusion

The combined use of carbonated water and continuous CO_2 flow resulted in over-saturation in the dough matrix, ultimately leading to structural collapse during baking and a significantly lower specific volume (SV) in CarbD breads prepared with carbonated water. This collapse was likely due to accumulation of CO_2 gas from three different sources: yeast fermentation, pre-dissolved CO_2 in carbonated water and the exogenous CO_2 flow. The excessive gas concentration appears to have exceeded the gluten network ability to stabilize and retain the formed gas bubbles, specifically if the dough lacked sufficient elasticity or strength. To further examine this, breadcrumb structure could be used for better identifying the pore cell distribution and size of gas bubbles within the crumb.

Despite this, carbonated water alone effectively reduced dough pH and enhanced crumb softness and porosity, suggesting improved microstructural development. When CO_2 flow was incorporated in the fermentation cabinet, an even great reduction in pH was observed, indicating increased CO_2 solubility in the dough matrix. However, this was not enough to improve dough properties and gas retention during baking, Real-time CO_2 sensor data further supported this, showing similar gas release profiles between RefD and CarbD across all conditions, with early increases attributed to system equilibration rather than active fermentation. Additionally, post-fermentation trials revealed comparable CO_2 release post-fermentation, reinforcing the conclusion that carbonation did not enhance long-term gas retention.

Interestingly, the increase in void fraction observed after fermentation in carbonated doughs regardless of CO_2 flow, did not lead to an increase in bread volume, likely because of gas bubble instability and coalescence during oven spring.

Moreover, while the continuous CO_2 flow did not affect the bread SV, it resulted in a lighter crust by increasing both brightness (L*) and yellowness (b*).

While this study highlights the potential and limitations of carbonation strategies in breadmaking, several avenues remain for future exploration, such as temperature and yeast concentration, to control gas production and prevent over-saturation. Future research could explore how precise control of CO_2 injection influences yeast metabolism and fermentation efficiency, potentially optimizing dough development and bread quality.

CO_2 solubility in water decreased significantly with increased salt concentration due to the salting-out effect, which was largely determined by the free water fraction approximately 42% of the total water content. When normalized to free water, CO_2 solubility values closely align with those of pure water but are further reduced by the dough elevated salt content. The sodastream results confirmed that increasing salt concentration linearly reduces CO_2 solubility due to the salting-out effect, decreasing free water available for gas dissolution by about 25% at 40 $g \cdot L^{-1}$ NaCl. Applying this to bread dough, where free water is the key medium for CO_2 solubilisation, highlighted that salt content significantly limited CO_2 uptake. Our result aligned with previous studies and emphasize on the importance of considering salt and free water when estimating and controlling CO_2 levels during dough fermentation and gas injection. Finally, it would be valuable to measure freezable water in carbonated dough to assess how much CO_2 could be solubilised within the dough matrix. This could help explain why the increase in CO_2 solubility from carbonated water did not translate into better gas retention or dough stability during baking. By measuring and controlling the freezable water content, it may be possible to prevent over-saturation of CO_2 in the dough, which can compromise gas retention and dough structure. Accurate measurement of freezable water in carbonated doughs would provide a more precise estimation of CO_2 solubility within the matrix. Excess dissolved CO_2 could cause over-saturation, thus compromising the stability of gas cells and weaken the gluten network.

GENERAL DISCUSSION

Bread dough mixing represents an initial and most critical stage in bread processing, that greatly influence the final bread attributes. Traditionally, mixing is done with the dough being exposed to the ambient air atmosphere. Bread dough mixing involves a combination of physical and biochemical phenomena interacting each other. The dough undergoes aeration with the introduction of gas cells, the development of a gluten network, together with the initiation of biochemical reactions. However, the pursuit of a consistent product with sustainability and clean-label formulations is urging the industry toward more controlled and precise methods.

Dough mixing represents an initial and most critical stage in bread processing, that greatly influence the final bread attributes. Traditionally, mixing with ambient air atmosphere, this process involves the formation of gas cells, development of gluten network, and initiation of biochemical reactions essential for the foundation of fermentation and baking. However, the pursuit of a consistent product with sustainability and clean-label formulations is urging the industry toward more controlled and precise methods.

Literature has shown growing interest in gas-pressure mixing under controlled atmosphere to enhance the physicochemical and structural properties of dough and bread of multiple matrices such as bread, cake, biscuits. Studies have shown that manipulating the headspace atmosphere of mixers with gases such as oxygen, carbon dioxide and nitrogen, can influence gas bubbles size and distribution and gluten network, thereby affecting the final crumb and bread volume. Other work has focused on solely the benefits of high-pressure mixing in improving loaf quality. Yet, a comprehensive understanding of the mechanisms governing gas solubility, oxidative effects, and process optimization remain incomplete.

This PhD project aims to advance this frontier by systematically investigating the interplay of gas composition, mixing pressure, oxidative supplementation (addition of ascorbic acid), and mechanical processing on dough aeration, how these mixing parameters affect fermentation kinetics and bread quality. Through rigorous experimental and analytical approaches, the research provides mechanistic insights and practical guidelines for optimizing breadmaking processes under novel gas-pressure conditions, meeting industrial and artisanal needs for enhanced quality, consistency, and sustainability. An illustration of the mixer headspace used throughout the entire study, highlighting the significant

importance of each injected gas during kneading as previously elaborated in the State of art chapter (Figure A).

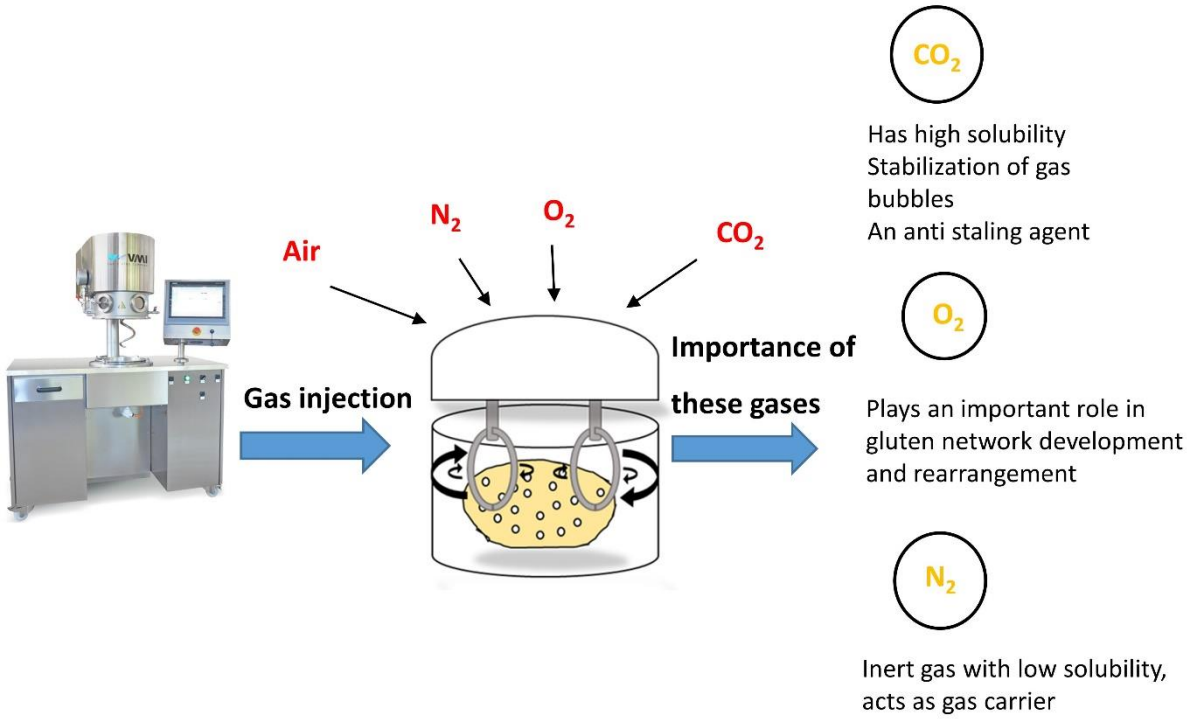


Figure A Scheme presenting the prototype mixer showing the importance of the injected gases (CO_2, O_2 and N_2) during the kneading phase

This PhD project consists of 5 main chapters. The state of art chapter integrates and discusses all experimental results presented throughout the thesis to provide a unified interpretation of how controlled mixing atmospheres influence dough development, fermentation behaviour, and the final bread quality. The experiments assessed how controlling headspace gas and pressure, as well as adjusting mixing to the optimal dough development time (t_{PEAK}), influenced dough properties such as void fractions and expansion, and how fermentation time varied as well as their impact on the final bread product. Determining t_{PEAK} is important, as it accurately indicates the appropriate mixing time to avoid over or under-mixing.

In the first part of our study, air and CO_2 were investigated under two pressure levels: atmospheric and at 0.5 bar gauge pressure. Two protocols were tested: both began with partial vacuum at – 500 mbar, followed by mixing and kneading stages, with only difference being that under 0.5 bar gauge pressure the exhaust valve remained closed during kneading. A predictive calculation model linking initial dough void fraction to final dough expansion is also proposed to optimise fermentation time and aeration under the tested parameters. The model was built to identify a correlation between early gas incorporation (during kneading) and later expansion (after fermentation), giving practical guidance for fermentation control.

Dough aeration, expressed as dough void fraction (ε), was measured throughout mixing, sheeting and fermentation to evaluate the effect of gas composition and pressure under the two protocols. Doughs mixed with air at an elevated pressure at 0.5 bar gauge pressure had a higher ε_F = 0.64 compared to CO_2-mixed doughs at the same pressure ε_F = 0.60. Results also showed that increasing pressure led to

higher initial gas incorporation, especially with CO_2-mixing, ε_I = 0.23 with CO_2 and ε_I = 0.17 with air. Sheeting effectively redistributed gas bubbles but resulted in a larger reduction in gas retention with CO_2-mixed doughs than with air, attributable to the oxygen role in promoting the polymerisation of gluten network.

Fermentation times also depended on gas composition, extending to 2 hours for CO_2-mixed doughs, versus 1 h 45 min for air. These findings suggest that fermentation time and void fraction are interdependent, requiring adjustments based on aeration conditions; meaning mixing at atmospheric pressure resulted in shorter fermentation times but lower final void fractions. Meanwhile, mixing at 0.5 bar produced finer breadcrumb structures with smaller pore sizes, improving textural uniformity. These observations emphasize the importance of controlling pressure during mixing, in particular in the case of innovative mixer able to mix dough under pressure with non-conventional gases, to achieve a balance between aeration and final bread quality.

Building on dough results, the resulting bread specific volumes SV and crumb structure were influenced by the gas composition and pressure during mixing. At 0.5 bar gauge pressure, breads mixed with air demonstrated the highest SV (4.54 $cm^3 \cdot g^{-1}$) in comparison to CO_2 breads (3.55 $cm^3 \cdot g^{-1}$). This was linked to larger, irregular bubbles and weakened depolymerized gluten network due to depletion from oxygen during mixing. This fragile network led to bubble instability and crust collapse during baking. These findings align with previous studies of Martin et al. (2008), where they observed that CO_2-mixed breads yielded 17% lower loaf volumes compared to air-mixed breads. Similarly, Varayil et al. (2019) reported that higher pressure and mixing speed enhanced aeration, although produced larger, less stable pores, suggesting that increased gas solubility should be balanced against mechanical stability.

Image analysis confirmed that air-mixed breads exhibited finer crumb, characterised by smaller median pore size (D50 = 0.38 mm^2) and narrower pore distribution. In contrast, broader pore size range with CO_2-mixed breads (D50 = 0.59 mm^2) (Figure B).

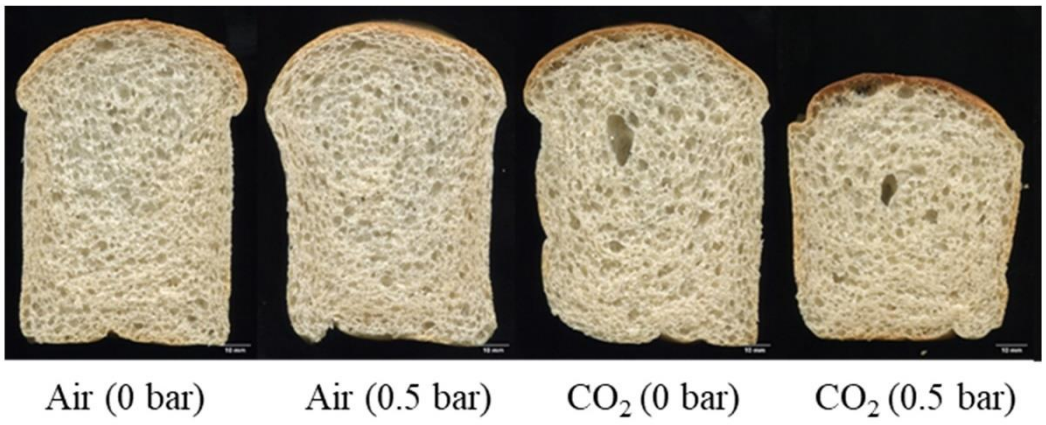


Figure B Scanned images of bread slices mixed under Air and CO_2 at atmospheric pressure and 0.5 bar gauge pressure with a scale of 10 mm for each treated image

Pressure itself has a positive effect on aeration, mixing at 0.5 bar produced finer breadcrumb structures with smaller pore sizes, improving textural uniformity. These findings highlight the critical importance of oxygen availability for dough and bread quality. Therefore, air mixing at higher pressure represents the condition for balancing fermentation duration and dough aeration to maximize the final bread.

Future process optimization with CO_2 may require adjustment of fermentation parameters or dough formulation to overcome these challenges.

The second part of our study represents a comprehensive investigation of gas composition during mixing and oxidative supplementation by either elevated O_2 in the injected gas composition or by adding AH_2 directly to the dough recipe, a commonly used oxidant in commercial baking.

Dough samples were prepared under three distinct gaseous conditions: air, 100%CO_2 and 30%O_2 70%N_2 with two mixing protocols at a controlled pressure of 0.5 bar gauge pressure: Protocol A, featuring partial vacuum and Protocol B a full vacuum. The oxygen level was carefully selected based on safety measures as advised by industry experts. AH_2 was introduced at an industry standard dosage of 80 ppm, aiming to quantify its synergic effect with various gas environments on gluten network formation and dough aeration. Central to the investigation, is the solubility behaviour of O_2 and CO_2 in the dough aqueous matrix. While O_2 is physically dissolved, it is concurrently consumed by enzymatic oxidation reactions critical for gluten development and is consumed by AH_2 for its activation in a cascade of reactions. Similarly, CO_2 dissolves and is solubilised into the nucleation sites formed during mixing and thus saturates the dough during mixing and fermentation, influencing yeast activity during fermentation and the physical expansion of gas bubbles.

The theoretical calculations showed that headspace gas composition and pressure significantly affected oxygen availability with overall O_2 consumption was limited to 3.4% for Protocol A and 34% for Protocol B, therefore, the partial pressure of O_2 proved to be critical for dough oxidation. This finding implies that O_2 availability in the headspace is generally sufficient to sustain oxidative reactions and gluten network development, in agreement with Buche (2011), who highlighted that O_2 transfer rates rather than total oxygen levels often limit dough oxidation. However, pO_2 differs markedly between protocols; for example, the 30%O_2 mixture yielded a higher pO_2 by +114%, likely promoting O_2 solubilisation and enhancing oxidative cross-linking. In contrast, CO_2 injection under both protocols resulted significantly lower pO_2 during kneading, reducing solubilized oxygen and potentially weakening the gluten network.

Comparisons of Protocols A and B showed that both protocols supplied enough CO_2 in the dough (1.37 g of dissolved CO_2 for 3 kg of dough). However, this differed with the different gas compositions at 0.5 bar gauge pressure: Protocol A (partial vacuum – 500 mbar) maintained a near zero pO_2, supporting yeast respiration and oxidative reactions, whereas with Protocol B with full vacuum (-900 mbar) gave a high pCO_2 (1.4 bar) with near zero pO_2 (0.021 bar) which eliminated the effect of O_2.

- ⇨ These differences highlight the importance of oxygen availability and CO_2 partial pressure in the mixer headspace that strongly depend on pressure and the mixing protocol.
- ⇨ Protocol A at 0.5 bar gauge pressure offers a good balance for industrial baking. It maintained sufficient oxygen partial pressure with adequate CO_2 for dough acidification and gas stabilisation. Protocol B despite supplying high CO_2, it reduced oxygen near to zero creating reductive conditions that may impair gluten strengthening.

The solubility in water and dough was found to be pivotal factor influencing dough gas retention and fermentation behaviour in this study, which was influenced by both pressure and formulation. We confirmed that CO_2 solubility was affected not only by its physical dissolution but also the chemical equilibria into carbonic acid, bicarbonate and carbonate ions, affected by the dough temperature, ionic strength and pH. Experimental validation with carbonation tests exhibited a linear decrease in CO_2 solubility with increased salt concentration, supporting a model where dough composition modulates

gas solubility though effects on water activity and ionic strength (Descoins, Mathlouthi, Moual *et al.* 2006). Furthermore, the analysis of free water content in the dough compared to the total water content was critical to correctly estimate CO_2 solubility. Free water, which accounted 41.8% of total water, provided the main solvent phase of gas dissolution.

Overall, Protocol B with a more pronounced vacuum application at the start of mixing (-0.9 mbar compared to -0.5 mbar in Protocol A), demonstrated a faster dough development shown by lower t_{PEAK} and and SME values, particularly under 30%O_2 70%N_2 and with the addition of AH_2, indicating improved mixing efficiency and potentially less mechanical stress on the dough. It also promoted greater gas retention and higher void fractions in CO_2-mixed doughs. On the other hand, Protocol A especially with air and 30%O_2 led to more polymerised gluten network, stable gas bubbles and a balanced oxidation and fermentation processes. Our results were consistent with literature, applying a partial vacuum to bread dough during kneading results in a reduction in the gas fraction in the dough as well as dough colour and rheological properties which was observed with Protocol A. Without AH_2, gas composition significantly affected t_{PEAK}, however, its presence masked these gas-dependent differences, illustrating synergic interaction between pO_2, AH_2 activity and the mixing protocol impacting dough mechanical development and energy.

Dough aeration further illustrated the role of gas composition and AH_2. Without AH_2, void fractions increased progressively from kneading to fermentation, with sheeting promoting bubbles redistribution and a more uniform gas cell size. The CO_2-mixed doughs under Protocol B, exhibited higher void fractions after fermentation compared to Protocol A, suggesting that continuous CO_2 gas renewal enhanced gas retention and dissolution, consistent with observations by Chin et al. (2005b) and Shah et al. (1998). Air and O_2-mixed doughs showed minimal differences, indicating that oxygen availability primarily influenced gluten network formation rather than initial gas entrapment. In the presence of AH_2, void fractions generally increased, reflecting improved network stability and gas retention during fermentation, and although its effect was less pronounced in O_2-rich doughs where oxidative reactions were already sufficient. These findings indicate that AH_2 acts synergistically with oxygen to stabilize entrapped gas and support dough expansion, whereas CO_2-enriched conditions limit oxidation but enhance gas solubilisation.

One of the main highlights of this project was the determination of dough expansion ratio (N) as a kay indicator of dough development during fermentation. Previous studies have hypothesized that N is a fixed value, where the end of fermentation time has a final fixed dough void fraction of 0.75. However, in our study, were we recently published a paper by Raad et al. (2025), we determined that N was calculated based on the relationship between the initial and final dough void fractions and that it varies according to the different mixing parameters such as pressure level and the used injected gas. This approach demonstrated that the expansion ratio required to reach a final target final void fraction of 0.75, depends strongly on the initial void fraction of the dough after mixing. For example, a conventional dough with $\varepsilon_I = 0.1$ has an expansion of N = 3.6, whereas in our case, under pressure, for $\varepsilon_I = 0.2$ has N = 3.2 to reach the same final void fraction.

Dough expansion (N) and fermentation kinetics were closely linked to void fraction and dough rheology. Without AH_2, CO_2-mixed doughs under Protocol A showed the highest N, reflecting longer fermentation time due to the weaker gluten and slower bubble growth. Protocol B reduced these differences, yielding more uniform expansion and shorter fermentation time across all gas compositions. With AH_2, N was similar for all conditions and protocols, indicating oxygen availability combined with oxidative

action of AH_2 governs the expansion of the dough. CO_2 solubilisation in the dough liquid phase, was assisted by the water content and bubbles nucleation, promoted early expansion in CO_2-mixed doughs.

The risograph analysis revealed distinct differences in CO_2 production kinetics between air and CO_2-mixed dough, where more CO_2 was released with CO_2-mixed doughs with Protocol B showing a steeper initial increase due to higher partial pressures, indicating a more rapid onset of expansion. While air-mixed doughs especially under Protocol A, release CO_2 more slowly due to a slower saturation. This behaviour suggests that the dough liquid phase was saturated with CO_2 before fermentation began, allowing rapid degassing at the start of fermentation. The difference between the two protocols highlights the importance of gas partial pressure in determining solubilisation during mixing. While the total moles of gas available for dissolution are important, the results demonstrate that the headspace partial pressure during mixing critically affects the amount of CO_2 actually absorbed by the dough matrix. Protocol B, with higher CO_2 pressure, therefore led to greater gas solubilisation and faster CO_2 evolution during fermentation. These findings reinforce the structural observations: CO_2-mixed doughs, already enriched in dissolved CO_2, exhibited faster initial expansion and release, but their weaker gluten matrix makes them prone to degassing under mechanical or thermal stress. Air-mixed doughs, in contrast, demonstrated slower gas evolution initially although more stable long-term gas retention due to stronger gluten reinforcement.

Microscopic analysis supported the macro-scale results of void fractions and risograph measurements. Air-mixed doughs contained smaller and more stable gas bubbles in the dough matrix, reflecting a strong gluten network. In contrast, with CO_2-mixed doughs, fewer larger bubbles were observed that were less stable and more prone to coalescence during resting. The assumption that CO_2 solubilisation would stabilize gas cells by modifying the surface tension at the bubbles interface (via the Young-Laplace law) was not supported, hence this behaviour likely arises from increased dough liquor viscosity and altered surface tension dynamics, promoting the merging of small bubbles into larger ones, as described by the critical bubble size concept. Therefore, rather than stabilizing gas cells, CO_2 mixing led to bubble disproportionation and coalescence, confirming that air mixing offers more favourable conditions for stable gas cell formation. The sheeting step partially degassed dough and redistributed gas bubbles. Doughs without sheeting had a higher dough void fraction, particularly with CO_2-mixed doughs, which showed more susceptibility for gas loss due to weakened gluten network.

In the last section of this subchapter, protocol A was used throughout additional analysis. The rheological findings showed that both gas composition and the addition of AH_2 by applying Protocol A (partial vacuum) that with elevated oxygen ($30\%O_2$ $70\%N_2$) increased the storage modulus (G') and enhanced elasticity compared to air and CO_2. AH_2 further reinforced G' across all conditions through promoting strain hardening and gluten network polymerisation. In accordance with literature, the microstructure of the vacuum-mixed dough (gluten network) was more continuous and compact, with higher tensile strength and extensibility.

The effect of gas composition and AH_2 on dough pH provided complementary biochemical evidence of gas-dough interactions. Under both conditions, gas composition significantly influenced pH, with the lowest values recorded under CO_2-rich and O_2-enriched environments. With AH_2 addition, air-mixed doughs reached the lowest pH (5.20 ± 0.02), suggesting enhanced acidification under balanced oxidative reductive conditions. The higher O_2 concentration (in $30\%O_2$ $70\%N_2$) accelerated AH_2 oxidation and depletion, limiting its reducing potential and thus moderating the pH decrease. In

contrast, ambient air provided an optimal O_2 level for continuous redox cycling of AH_2. CO_2 solubility further contributed to acidification by carbonic acid formation.

The third part of our study represents the bread results, where mixing was conducted at 0.5 bar gauge pressure by applying Protocol A (partial vacuum). For the first section of this chapter, the results showed that gas composition with the inclusion of AH_2 during dough mixing exerts a significant influence on bread properties, including specific volume, porosity, breadcrumb structure and crust/crumb colour. Breads mixed with 100%CO_2, gave the lowest SV and coarser crumb, attributed to deprivation of oxygen and excessive CO_2 accumulation within the dough matrix, which limited gluten polymerisation, and slowing down the yeast activity, thus a collapse was observed during baking (Figure C).

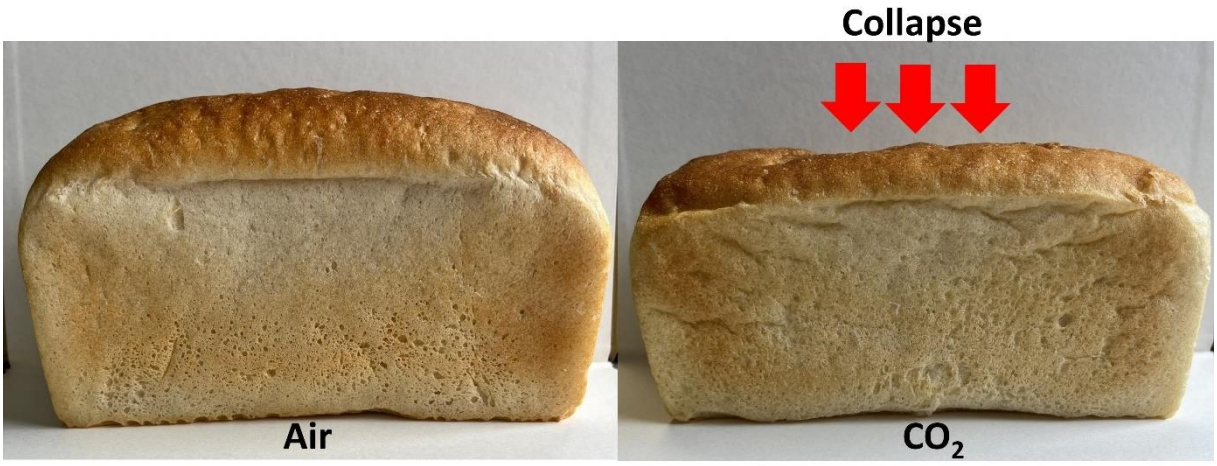


Figure C Difference in breads volume: Air (left) and collapsed CO_2 bread (right)

To mitigate these negative effects, reducing the yeast amount was investigated as a corrective approach to CO_2-mixed doughs. Conventional formulation using 2% yeast exhibited excessive CO_2 accumulation both from injected and endogenous yeast activity, leading to overexpansion and rupture of gas cells during baking. Reducing yeast to half (1%) proved efficient, providing a balanced endogenous and exogenous CO_2 production, improving SV and crumb structure. This allowed a better gas dissolution and bubble retention without structural collapse (Figure D).

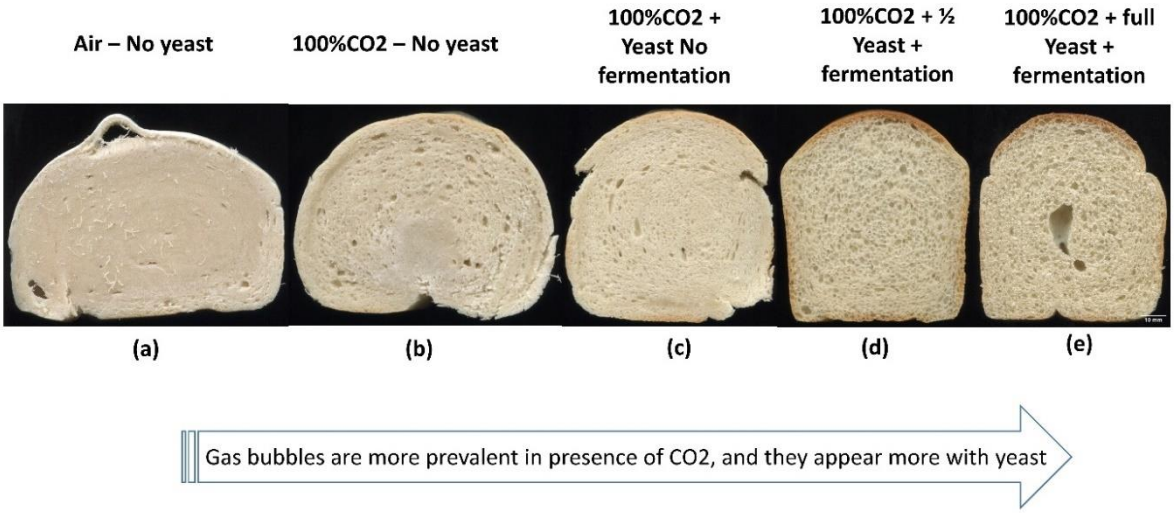


Figure D Breadcrumb structure of scanned bread slices for all the experiments conducted with yeast. Starting from far left to right: (a) air without yeast, (b) 100%CO_2 without yeast, (c) 100%CO_2 with full yeast without fermentation, (d) 100%CO_2 with ½ yeast with fermentation and (e) 100%CO_2 full yeast with fermentation

Breads with air and 30%O_2 70%N_2, gave optimal oxidation, resulting in polymerised and well-developed gluten network, higher loaf volume and fine, uniform crumb structure. The addition of AH_2 strengthened the gluten network only under air, while high O_2 reduced its effectiveness due to either to over-oxidation or inhibition of its activity.

Bread staling, characterized by changes in softness, structure and flavour, and remains a key challenge for maintaining bread quality during storage. In this study, staling predominantly driven by starch retrogradation monitored over a 15 days storage time, offering unique insights into how gas composition and the addition of AH_2 influence the rate of retrogradation and the extent of this process. The application of Avrami model gave a direct quantification of retrogradation kinetics, allowing direct comparison between gas compositions. Primarily, breads mixed with 100%CO_2 exhibited the slowest retrogradation rate, while the 30%O_2 70%N_2 was the fastest. Despite this, the 100%CO_2 breads showed the highest final retrogradation enthalpy (ΔH_{15} = 5.53 ± 0.39). The extension of staling with this condition is likely due to the CO_2 acidifying action, disrupting the hydrogen bonds and modifying the amylopectin-gluten interactions, which in turn slowed down the association of amylopectin chains.

Conversely, the use of AH_2 further delayed early retrogradation across all gas mixtures, with most pronounced effects during the beginning of storage. This supported the hypothesis that AH_2 strengthens the gluten network, confining the starch granules and retarding their structural reorganization. Towards the end of storage, retrogradation levels were converged.

Breads firmness increased across all gas conditions as staling progressed, although 100%CO_2 breads remained firmer overall, consistent with their lower porosity and denser crumb microstructure. In contrast, the 30%O_2 70%N_2 breads retained a softer and more elastic crumb, attributable to finer gas cell distribution and higher SV. AH_2 amplified firmness in oxygen mixtures (air and the 30%O_2 70%N_2), confirming its role in gluten strengthening and textural modifications. Bread cohesiveness was also higher with these latter with AH_2, emphasizing the role of reinforced gluten structure to bread elasticity.

Moisture dynamics during storage showed non-uniform migration, with the crumb retaining the most moisture and regions near the crust the greatest loss. Breads mixed with CO_2 preserved the most moisture, which coupled with the slower retrogradation. In contrast, the 30%O_2 70%N_2 prompted faster moisture loss, especially at the crust. The addition of AH_2 improved water retention for all gas compositions, and particularly in the crumb.

The hypothesis that dough sheeting significantly modifies bubble size distribution and bread aeration was supported by our findings. Mechanical stress and deformation induced by sheeting influenced bubble coalescence and rupture, impacting breadcrumb homogeneity and overall quality. This aligns with literature that while sheeting enhances dough processing efficiency, it has risks of damaging gluten structure and uneven quality development across the loaf due to intense deformation during moulding. The findings indicated that dough sheeting has a significant impact on bread structure. Breads mixed with air and CO_2, sheeting significantly reduced SV of CO_2-mixed breads, while no differences in SV was observed without sheeting. Analysis of pore size distribution showed that breads mixed with air showed fine and small gas bubbles regardless of sheeting, while CO_2-mixed breads had larger, more irregular pores. Median pore sizes were consistently smaller in air breads, indicating a more stable bubble population.

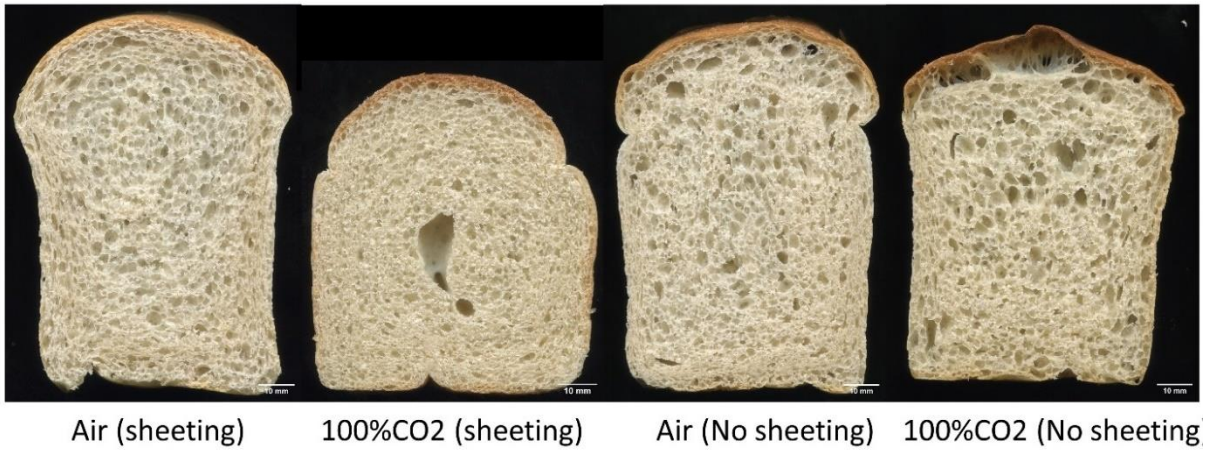


Figure E Scanned breadcrumb images of bread slices mixed with air and CO2 with sheeting and without sheeting

Interestingly, non-sheeted CO_2 doughs displayed high final void fraction ($\varepsilon_f \approx 0.75$), suggesting that sheeting under CO_2 led to pronounced gas degassing due to the weaker gluten network and increased susceptibility of bubble mechanical rupture. This resulted in underestimation of the true gas content and in lower SV and coarser crumb. The results emphasize the dough sheeting combined with gas composition critically determine the final loaf volume and crumb structure (Figure E).

Complementary to this section, **a sensory analysis** was conducted, to explore whether perceptible differences exist between bread samples with varying gas composition and formulation. To achieve this, a triangular test and Flash Profile methodology were implemented. The results revealed that bread mixed with 30%O_2 70%N_2 and AH_2 were the most positively perceived by the panel. These latter were characterised by a soft and elastic texture, uniform and homogenous crumb, pleasant cereal and yeast aroma, and higher loaf volume. Such sensory attributes align with the desirable qualities of sandwich bread.

In contrast, breads mixed with CO_2 were perceived as firmer and denser, with a chewier texture, lighter crust colour and more pronounced acidic aroma. These characteristics were consistent with the limited gas retention, reduced yeast activity and possible acidification effects associated with CO_2-enriched environments. Similarly, breads mixed with 30%O_2 70%N_2 without AH_2 were described as firm with strong acidic and yeast-like notes.

In the last part of our study, were we explored the role of exogenous CO_2 in bread dough formulation and fermentation, with a focus on two novel interventions: (1) the incorporation of carbonated water during dough preparation as a substitute to plain water and (2) the application of a CO_2-enriched atmosphere during fermentation. Carbon dioxide (CO_2) produced endogenously during yeast fermentation, plays a critical role in dough expansion, gas cell formation and final bread structure. In addition to fermentation, exogenous sources such as carbonated water that could be used in replacement of plain water and CO_2-modified atmospheres may influence CO_2 solubilisation and retention in the dough matrix.

The results showed that the combined use of carbonated water and continuous CO_2 flow markedly influenced dough and bread properties, revealing both advantages and limitations of carbonation strategies in breadmaking. Over-saturation from multiple CO_2 sources; exogenous CO_2, yeast CO_2 by-product and pre-dissolved CO_2 from carbonated water led to structural collapse during baking and reduced SV in CarbD breads. The excess gas likely exceeded the gluten network capacity to retain the gas bubbles due to the limited dough elastic capacity.

Carbonated water alone effectively decreased dough pH and enhanced crumb softness and porosity, reflecting improved microstructural development. However, the incorporation of continuous CO_2 led to further acidification of the dough without improving gas retention or bread expansion. Real-time CO_2 emission data indicated comparable gas release between the 2 recipes RefD and CrabD, suggesting that carbonation primarily affected dough chemistry rather than enhancing fermentation efficiency. Although high dough void fractions were recorded after fermentation with CrabD, these values did not correspond to higher loaf volumes, due to bubbles coalescence.

Complementary solubility measurements confirmed that CO_2 solubility decreased linearly with increasing NaCl concentration, showing a 25% reduction. Considering about 42% of the dough water is freezable, salt and water phase composition critically determine CO_2 solubilisation capacity.

Conversely, fermentation with CO_2 flow, improved breads crust colour characteristics, increasing both lightness L* and yellowness b*, due to reduced oxidative reactions and modified surface heat transfer. The lower pH inhibited Maillard reaction.

CONCLUSION AND PERSPECTIVES

Extensive research has previously examined how controlled gas-pressure mixing influences dough aeration, rheology, and bread quality. These studies have reported valuable insights into relationships between headspace gas, mixing pressures, and dough structure. However, most of these, focused on overpressure conditions or atmospheric and often neglected the combined effects of oxidative agents and different gas composition during mixing. In this project, we presented a simple bread recipe without any additive to the flour used, to solely investigate the effect of gas-pressure mixing on a clean additive-free recipe. Studies collectively demonstrated that gas-pressure mixing has been investigated across diverse bakery matrices, including white bread dough, pizza dough, and cake batters. For example, in pizza dough, gas-pressure mixing affected dough extensibility and resistance to deformation with higher salt and fat content extended dough development under pressure. Another study on cakes, demonstrated that mixing under pressurized CO_2 could partially replace baking powder by incorporating dissolved gas into the batter, enhancing loaf volume and microstructural homogeneity without the use of leavening agents.

Building on this foundation, the present thesis broadened the experimental scope by introducing controlled vacuum phases during mixing and systematically examining how both pressure and vacuum influence dough aeration, SME and t_{PEAK} were not previously evaluated in an integral framework. This thesis project has thoroughly explored the influence of gas composition, mixing protocols, mixing pressures, oxidative supplementation, and mechanical processing on dough aeration, fermentation kinetics and the final bread quality, significantly advancing the knowledge in controlled atmosphere breadmaking. By focusing on innovative gas-pressure mixing protocols combined with the addition of ascorbic acid, this work has elucidated how manipulating the mixer headspace gases and pressure affect the gluten network formation, gas bubbles stability, and fermentation behaviour, leading to impactful effects on bread volume, crumb structure and texture.

In the first part of this study, it was demonstrated that the combination of gas modified atmosphere and pressure in the mixer headspace significantly influenced dough development and fermentation behaviour. Increasing the mixing pressure led to a marked increase in initial void fraction with CO_2, whereas with air exhibited higher final void fractions and shorter fermentation times, which gave breads with finer, uniform crumb structures and higher specific volumes. At a higher pressure (0.5 bar gauge pressure), CO_2 mixed doughs had longer fermentation time and lower final void fraction, primarily due to the mechanical sheeting and yeast inhibition in the CO_2-rich environment.

The second part examined the effects of different gas compositions (air, CO_2, O_2, N_2) under elevated pressure of 0.5 bar gauge pressure, with the additional effect AH_2. Two mixing protocols, differing in vacuum application (partial and full vacuum), showed that while both supplied sufficient CO_2 for dough saturation, only the partial (Protocol A) maintained adequate oxygen levels essential for enzymatic and oxidative reactions for dough development. The dough mechanical properties, SME and t_{PEAK}, varied with gas composition and presence of AH_2. Microscopic analyses confirmed that air-mixed doughs contained smaller, more stable gas bubbles compared to the larger, irregular bubbles with CO_2-mixed doughs. The pH decrease in CO_2 doughs reflected its solubilisation and conversion into carbonic acid within the matrix.

For the bread results, the results showed the impact of the gas composition injected during kneading on bread characteristics such as specific volume, porosity, crumb structure and colour. Mixing with CO_2 consistently resulted in breads with lower SV, coarser crumb with larger and irregular pores. In contrast, the 30%O_2 70%N_2 mixture gave denser and uniform crumb, irrespective of AH_2 addition. Notably, under the elevated oxygen levels, the activity of AH_2 was reduced due to the fully oxidized thiol groups, diminishing its functional role. These findings suggest that while AH_2 remains an effective oxidative improver under controlled conditions, its functional role could potentially be replaced or complemented by alternative clean-label enzymatic oxidants capable of achieving a similar redox modulation. Such substitutions would align with clean-label and additive-free formulations in breadmaking.

Gas composition also played an essential role in starch retrogradation rates during bread storage. Breads mixed with CO_2 exhibited a delayed retrogradation and firmer crumb while maintaining higher moisture levels, reflecting heterogeneous crumb structure and less elastic texture. This delay was linked to the acidification from dissolved CO_2, which altered amylopectin mobility and disrupted hydrogen bonding essential for starch crystallisation. The addition of AH_2 with 30%O_2 70%N_2 mixture showed small effect on retrogradation, emphasizing the complex interplay between gas atmosphere and starch-gluten dynamics affecting staling.

Furthermore, the results showed that yeast concentration especially in CO_2-mixed doughs critically impacted gas cell stability and crumb structure. Excess yeast led to gas cell disproportionation and crumb collapse. Lower yeast concentration improved crumb uniformity, highlighting the importance of optimizing fermentation conditions in CO_2-rich environments. We also observed the necessity of tailoring the mechanical processing.

The sensory evaluation provided insights about consumers' perception, highlighting a clear difference between the different bread samples. Bread with the mixture of 30%O_2 70%N_2 and AH_2 was the most positively evaluated by the sensory panel in terms of the descriptive attributes such as softness, volume crumb homogeneity and aroma. Panellists highlighted these breads for their softness in texture, uniform and homogenous breadcrumb, and mild and pleasant yeast and cereal aroma with higher volume. In contrast, bread with CO_2 were perceived as firmer, denser, chewier with lighter crust colour and more pronounced acidic aroma, which resulted in less favourable sensory perception. Similarly, breads mixed with 30%O_2 70%N_2 without AH_2, were firmer and exhibited strong acidic and yeast aromas, indicating the importance of presence of antioxidant for optimal sensory quality.

In the final chapter, the results showed that the combined effect of carbonated water and continuous CO_2 flow can lead to over-saturation within the dough matrix, while carbonated water alone improved dough acidification, crumb softness and porosity, additional CO_2 further reduced pH without any impact on dough aeration or expansion. Salt content and free water availability significantly limited CO_2 solubility.

Despite the extensive experimental design and methodological rigor, certain limitations were encountered throughout this project. Ultimately, the study did not identify a completely novel pathway beyond general trends reported in literature. Most results confirmed established observations, and the additional experimental parameters such as broader variations in gas pressure, different partial pressure of gases and the incorporation of AH_2 did not give major modifications in dough and bread results. Nevertheless, several innovative findings emerged, notable combined effect of AH_2 and the

different gas compositions and the influence of CO_2 dissolved in water on dough behaviour and bread characteristics.

Some technical constraints of the equipment restricted the scope of the investigation. The mixing system did not allow rapid switching between different gases, limiting the ability to study transient gas effects within a single batch. Moreover, gas consumption could not be monitored, as no flow or mass sensors were available to quantify gas uptake or release.

Future work should aim to overcome these limitations by incorporating in situ gas composition monitoring within the mixer bowl and developing mixing systems capable of rapid gas switching or dynamic gas control. Quantifying gas flow, pressure variations, and solubilisation during mixing would provide valuable insights into gas dough interactions. Implementing a final vacuum phase at the end of mixing similar to that proposed by Sadot and already used in industrial systems could help mitigate disproportionation phenomena observed in CO_2-enriched doughs. Exploring the use of more oxidising gases, such as ozone, or introducing oxygen directly into process water could further enhance oxidative development, though such approaches must consider safety and regulatory constraints. Collectively, these methodological and process innovations would allow more precise control and a deeper mechanistic understanding of breadmaking under gas-modified atmospheres.

Beyond empirical optimization, future studies should also deepen the mechanistic understanding of gas-dough interactions. Investigating intermediate pressures between atmospheric and 0.5 bar gauge pressure, paired with a final vacuum stage, may enhance gas bubbles uniformity and dough structure. Using molecular techniques such as Confocal Laser Scanning Microscopy or Raman Spectroscopy could elucidate the interactions between carbonic acid, gluten and starch. Further work is also needed to investigate how dissolved CO_2 delays starch retrogradation, as this impacted bread staling on molecular level.

The precise measurement of dough void fraction remains challenging due to several factors. In order to minimize temperature shock, we propose installing an oil-bucket system inside the fermentation chamber; we also propose employing advanced imaging to monitor bubble dynamics such as acoustic and NIR technologies, which offer real-time monitoring of dough aeration. Installing gas sensors inside the mixer headspace in order to quantify the exact amount of injected gases.

For the sensory perspective, a hedonic test would allow direct consumer preference assessment, complementing panellists' descriptive data and would provide feedback for optimisation tailored to consumers liking and acceptance. We could also conduct a sensory analysis with the optimised formulation and process especially with the 100%CO_2 with ½ yeast amount, as well as adopting different gas composition and ratios.

Finally, it would be valuable to measure freezable water content in carbonated dough to more accurately assess the amount of CO_2 that could be solubilised into the dough matrix. This measurement would help clarify why the increased CO_2 solubility from using carbonated water did not translate into improved gas retention or dough stability during baking. By quantifying and controlling freezable water, it may be possible to prevent CO_2 over-saturation.

Future research should also extend investigations to industrial-scale dough mixing systems to validate these laboratory findings, and to investigate this novel gas-pressure mixing in gluten-free bread. Given the inherently weaker and less cohesive network structures in gluten-free doughs, manipulating the

gas environment and pressure could offer new ways to improve aeration and crumb structure without relying heavily on additives.

REFERENCES

[1] ABEDI, E. and POURMOHAMMADI, K., 2020. The effect of redox agents on conformation and structure characterization of gluten protein: An extensive review. *Food Science & Nutrition*. December 2020. Vol. 8, n° 12, pp. 6301–6319. [Accessed 2 June 2023]. DOI 10.1002/fsn3.1937. Available from : https://onlinelibrary.wiley.com/doi/10.1002/fsn3.1937

[2] ABEDI, E. and POURMOHAMMADI, K., 2021. Chemical modifications and their effects on gluten protein: An extensive review. *Food Chemistry*. May 2021. Vol. 343, pp. 128398. [Accessed 30 January 2023]. DOI 10.1016/j.foodchem.2020.128398. Available from : https://linkinghub.elsevier.com/retrieve/pii/S0308814620322603

[3] AGHAJANZADEH, S., SULTANA, A., ZIAIIFAR, A. and KHALLOUFI, S., 2024. Formation of pores and bubbles and their impacts on the quality attributes of processed foods: A review. *Food Research International*. 1 May 2024. Vol. 188, pp. 114494. DOI 10.1016/j.foodres.2024.114494.

[4] AKDOĞAN, H. and OZILGEN, M., 1992. Kinetics of microbial growth, gas production, and dough volume increase during leavening. *Enzyme and Microbial Technology*. February 1992. Vol. 14, pp. 141–143. DOI 10.1016/0141-0229(92)90172-K.

[5] ALI, A., SHEHZAD, A., KHAN, M.R., SHABBIR, M.A. and AMJID, M., 2012. Yeast, its types and role in fermentation during bread making process- A review. . 1 September 2012. Vol. 22, pp. 170–178.

[6] ALLAIS, I. and DUFOUR, E., 2007. Use of response surface methodology to study the influence of water content and air pressure on cake batter quality. *International Journal of Food Engineering*. 2007. Vol. 3, n° 6. [Accessed 7 September 2025]. DOI doi:10.2202/1556-3758.1195. Available from : https://doi.org/10.2202/1556-3758.1195

[7] ANGIOLONI, A. and COLLAR, C., 2009. Bread crumb quality assessment: A plural physical approach. *European Food Research and Technology*. 1 May 2009. Vol. 229, pp. 21–30. DOI 10.1007/s00217-009-1022-3.

[8] ANGIOLONI, A. and DALLA ROSA, M., 2007. Effects of cysteine and mixing conditions on white/whole dough rheological properties. *Journal of Food Engineering*. 1 May 2007. Vol. 80, n° 1, pp. 18–23. [Accessed 30 October 2025]. DOI 10.1016/j.jfoodeng.2006.04.050. Available from : https://www.sciencedirect.com/science/article/pii/S0260877406003852

[9] ASAITHAMBI, N., FONTAINE, J., LANCELOT, E., REBILLARD, A., VALLE, D.D., OGE, A., CHÉIO, J., VEERESH, C.D. and LE-BAIL, A., 2020. Evaluation of bread dough aeration during kneading by an air-jet impulse system. *Journal of Food Engineering*. August 2020. Vol. 278, pp. 109931. [Accessed 1 February 2023]. DOI 10.1016/j.jfoodeng.2020.109931. Available from : https://linkinghub.elsevier.com/retrieve/pii/S0260877420300303

[10] AVRAMENKO, N.A., TYLER, R.T., SCANLON, M.G., HUCL, P. and NICKERSON, M.T., 2018. The chemistry of bread making: The role of salt to ensure optimal functionality of its constituents. *Food Reviews International*. 3 April 2018. Vol. 34, n° 3, pp. 204–225. [Accessed 6 January 2023]. DOI 10.1080/87559129.2016.1261296. Available from : https://www.tandfonline.com/doi/full/10.1080/87559129.2016.1261296

[11] BAIK, M.-Y. and CHINACHOTI, P., 2000. Moisture redistribution and phase transitions during bread staling. *Cereal Chemistry Journal*. July 2000. Vol. 77, n° 4, pp. 484–488. [Accessed 13 January 2023]. DOI 10.1094/CCHEM.2000.77.4.484. Available from : http://doi.wiley.com/10.1094/CCHEM.2000.77.4.484

[12] BAIK, O.D., MARCOTTE, M. and CASTAIGNE, F., 2000. Cake baking in tunnel type multi-zone industrial ovens Part II. Evaluation of quality parameters. *Food Research International*. 1 August 2000. Vol. 33, n° 7, pp. 599–607. [Accessed 10 October 2025]. DOI 10.1016/S0963-9969(00)00096-X. Available from : https://www.sciencedirect.com/science/article/pii/S096399690000096X

[13] BAIXAULI, R., SALVADOR, A., MARTÍNEZ-CERVERA, S. and FISZMAN, S., 2008. Distinctive sensory features introduced by resistant starch in baked products. *LWT - Food Science and Technology*. December 2008. Vol. 41, pp. 1927–1933. DOI 10.1016/j.lwt.2008.01.012.

[14] BAKER, J.C. and MIZE, M.D., 1941. The origin of the gas cell in bread dough. *Cereal Chemistry*. 1941. Vol. 18, pp. 19–34. DOI https://www.researchgate.net/publication/284053347_The_origin_of_the_gas_cell_in_bread_dough.

[15] BALL, S.G. and MORELL, M.K., 2003. From Bacterial Glycogen to Starch: Understanding the Biogenesis of the Plant Starch Granule. *Annual Review of Plant Biology*. June 2003. Vol. 54, n° 1, pp. 207–233. [Accessed 15 February 2023]. DOI 10.1146/annurev.arplant.54.031902.134927. Available from : https://www.annualreviews.org/doi/10.1146/annurev.arplant.54.031902.134927

[16] BALLA, A., RAZAFINDRALAMBO, H., BLECKER, C. and PAQUOT, M., 1998. Interfacial properties of gluten monolayers spread on various chloride salt solutions. Effects of electrolytes, salt concentrations, and temperature. *Journal of Agricultural and Food Chemistry*. 1 September 1998. Vol. 46, n° 9, pp. 3535–3539. [Accessed 28 April 2023]. DOI 10.1021/jf971006j. Available from : https://pubs.acs.org/doi/10.1021/jf971006j

[17] BARAK, S., MUDGIL, D. and KHATKAR, B.S., 2015. Biochemical and functional properties of wheat gliadins: A review. *Critical Reviews in Food Science and Nutrition*. 23 February 2015. Vol. 55, n° 3, pp. 357–368. [Accessed 9 March 2023]. DOI 10.1080/10408398.2012.654863. Available from : http://www.tandfonline.com/doi/abs/10.1080/10408398.2012.654863

[18] BASARAN, A. and GOCMEN, D., 2003. The effects of low mixing temperature on dough rheology and bread properties. *European Food Research and Technology*. 1 August 2003. Vol. 217, pp. 138–142. DOI 10.1007/s00217-003-0717-0.

[19] BAUDOUIN, F., NOGUEIRA, T.L., VAN DER MIJNSBRUGGE, A., FREDERIX, S., REDL, A. and MOREL, M.-H., 2020. Mechanochemical activation of gluten network development during dough mixing. *Journal of Food Engineering*. 1 October 2020. Vol. 283, pp. 110035. [Accessed 13 October 2025]. DOI 10.1016/j.jfoodeng.2020.110035. Available from : https://www.sciencedirect.com/science/article/pii/S0260877420301333

[20] BECK, M., JEKLE, M. and BECKER, T., 2012. Impact of sodium chloride on wheat flour dough for yeast-leavened products. I. Rheological attributes. *Journal of the Science of Food and Agriculture*. February 2012. Vol. 92, n° 3, pp. 585–592. [Accessed 28 April 2023]. DOI 10.1002/jsfa.4612. Available from : https://onlinelibrary.wiley.com/doi/10.1002/jsfa.4612

[21] BEGHIN, A.S., OOMS, N., HOOYBERGHS, K., COPPENS, E., PAREYT, B., BRIJS, K. and DELCOUR, J.A., 2022. The influence of varying levels of molecular oxygen on the functionality of azodicarbonamide and ascorbic acid during wheat bread making. *Food Research International*. November 2022. Vol. 161, pp. 111878. [Accessed 9 December 2022]. DOI 10.1016/j.foodres.2022.111878. Available from : https://linkinghub.elsevier.com/retrieve/pii/S096399692200936X

[22] BEJOSANO, F. and ALVIOLA, J.N., 2015. Dough conditioners in flour tortilla processing. In : ROONEY, L. W. and SERNA-SALDIVAR, S. O. (eds.), *Tortillas*. AACC International Press. pp. 185–194. [Accessed 30 October 2025]. ISBN 978-1-891127-88-5. Available from : https://www.sciencedirect.com/science/article/pii/B9781891127885500086

[23] BELITZ, H.-D., GROSCH, W., SCHIEBERLE, P. and BELITZ, H.-D., 2004. *Food chemistry*. 3., rev. ed. New York Heidelberg : Springer. ISBN 978-3-540-40817-8.

[24] BELLIDO, G.G., SCANLON, M.G. and PAGE, J.H., 2009. Measurement of dough specific volume in chemically leavened dough systems. *Journal of Cereal Science*. 2009. Vol. 49, n° 2, pp. 212–218. DOI https://doi.org/10.1016/j.jcs.2008.10.002. Available from : https://www.sciencedirect.com/science/article/pii/S0733521008001665

[25] BELTON, Peter S. (ed.), 2007. *The chemical physics of food*. Oxford : Blackwell. ISBN 978-1-4051-2127-9.

[26] BELTON, P.S., 1999. Mini Review: On the elasticity of wheat gluten. *Journal of Cereal Science*. March 1999. Vol. 29, n° 2, pp. 103–107. [Accessed 9 March 2023]. DOI 10.1006/jcrs.1998.0227. Available from : https://linkinghub.elsevier.com/retrieve/pii/S0733521098902272

[27] BEN AISSA, M.F., BAHLOUL, S., MONTEAU, J.-Y. and LE-BAIL, A., 2010. Effect of Temperature on the Solubility of CO 2 in Bread Dough. *International Journal of Food Properties*. July 2010. Vol. 2010. DOI 10.1080/10942910903176360.

[28] BERTOFT, E., 2017. Understanding starch structure: Recent progress. *Agronomy*. 25 August 2017. Vol. 7, n° 3, pp. 56. [Accessed 15 February 2023]. DOI 10.3390/agronomy7030056. Available from : https://www.mdpi.com/2073-4395/7/3/56

[29] BESBES, E., JURY, V., MONTEAU, J.-Y. and BAIL, A.L., 2013. Water vapor transport properties during staling of bread crumb and crust as affected by heating rate. *Food Research International*. 2013. Vol. 50, n° 1, pp. 10–19. DOI https://doi.org/10.1016/j.foodres.2012.09.041. Available from : https://www.sciencedirect.com/science/article/pii/S0963996912004000

[30] BILIADERIS, C.G., PAGE, C.M. and MAURICE, T.J., 1986. On the multiple melting transitions of starch/monoglyceride systems. *Food Chemistry*. January 1986. Vol. 22, n° 4, pp. 279–295. [Accessed 30 March 2023]. DOI 10.1016/0308-8146(86)90086-5. Available from : https://linkinghub.elsevier.com/retrieve/pii/0308814686900865

[31] BIRCH, A.N., PETERSEN, M.A., ARNEBORG, N. and HANSEN, Å.S., 2013. Influence of commercial baker's yeasts on bread aroma profiles. *Food Research International*. June 2013. Vol. 52, n° 1, pp. 160–166. [Accessed 26 April 2023]. DOI 10.1016/j.foodres.2013.03.011. Available from : https://linkinghub.elsevier.com/retrieve/pii/S0963996913001749

[32] BIRCH, A.N., PETERSEN, M.A. and HANSEN, Å.S., 2013. The aroma profile of wheat bread crumb influenced by yeast concentration and fermentation temperature. *LWT - Food Science and Technology*. March 2013. Vol. 50, n° 2, pp. 480–488. [Accessed 27 April 2023]. DOI 10.1016/j.lwt.2012.08.019. Available from : https://linkinghub.elsevier.com/retrieve/pii/S0023643812003593

[33] BLOKSMA, A.H., 1990. Dough structure, dough rheology, and baking quality. *Cereal Foods World*. 1990. [Accessed 10 October 2025]. Available from : https://www.semanticscholar.org/paper/Dough-structure%2C-dough-rheology%2C-and-baking-quality-Bloksma/17b355e90dfbf3b76e56fd33d6dd438dd9822fb8

[34] BOLKVADZE, N., GVIDANI, S., URIDIA, R., TSERODZE, N., KAVTARADZE, N., TATIASHVILI, L. and KARKASHADZE, N., 2024. Formation of taste and aroma compounds by Maillard reaction during processing of food products. *GEORGIAN SCIENTISTS*. February 2024. Vol. 6. DOI 10.52340/gs.2024.06.01.14.

[35] BOURNE, M.C., 1993. Texture measurements on finished baked goods. In : KAMEL, Basil S. and STAUFFER, Clyde E. (eds.), *Advances in Baking Technology*. Boston, MA : Springer US. pp. 134–151. [Accessed 14 December 2022]. ISBN 978-0-7514-0055-7. Available from : http://link.springer.com/10.1007/978-1-4899-7256-9_6

[36] BOUSSARD, A., CORDELLA, C.B.Y., RAKOTOZAFY, L., MOULIN, G., BUCHE, F., POTUS, J. and NICOLAS, J., 2012. Use of chemometric tools to estimate the effects of the addition of yeast, glucose-oxidase, soybean or horse bean flours to wheat flour on biochemical bread dough characteristics. *Chemometrics and Intelligent Laboratory Systems*. April 2012. Vol. 113, pp. 68–77. [Accessed 9 December 2022].

DOI 10.1016/j.chemolab.2012.01.006. Available from : https://linkinghub.elsevier.com/retrieve/pii/S0169743912000172

[37] BRABEC, D.L., ROSENAU, S. and SHIPMAN, M., 2015. Effect of mixing time and speed on experimental baking and dough testing with a 200 g pin mixer. *Cereal Chemistry Journal*. 7 August 2015. Vol. 92, pp. CCHEM-02. DOI 10.1094/CCHEM-02-15-0021-R.

[38] BRADSHAW, M.P., BARRIL, C., CLARK, A.C., PRENZLER, P.D. and SCOLLARY, G.R., 2011. Ascorbic acid: a review of its chemistry and reactivity in relation to a wine environment. *Critical Reviews in Food Science and Nutrition*. July 2011. Vol. 51, n° 6, pp. 479–498. DOI 10.1080/10408391003690559.

[39] BRAIDE, S. and ENOCH, J., 2018. A mathematical modeling of double exponential voltage-waveshape (impulse generator) for power substations using laplace-transform. . 5 June 2018. Vol. 7.

[40] BRIJWANI, K., CAMPBELL, G. M. and CICERELLI, L., 2008. Aeration of biscuit doughs during mixing. In : CAMPBELL, Grant M., SCANLON, Martin G. and PYLE, D. Leo (eds.), *Bubbles in Food 2*. AACC International Press. pp. 389–402. American Associate of Cereal Chemists International. ISBN 978-1-891127-59-5. Available from : https://www.sciencedirect.com/science/article/pii/B9781891127595500419

[41] BUCHE, F., 2011. *Influence de la formulation de pâtes de farine de blé sur leur consommation d'oxygène et leur production de dioxyde de carbone au cours du pétrissage et de la fermentation : Conséquences biochimiques et rhéologiques*. These de doctorat. Paris, AgroParisTech. [Accessed 30 October 2025]. Available from : https://theses.fr/2011AGPT0033

[42] BUCHE, F., DAVIDOU, S., POMMET, M., POTUS, J., ROUILLÉ, J., VERTÉ, F. and NICOLAS, J., 2011. Competition for oxygen among oxidative systems during bread dough mixing: consequences of addition of glucose oxidase and lipoxygenase on yeasted dough rheology. *Cereal Chemistry Journal*. September 2011. Vol. 88, n° 5, pp. 518–524. [Accessed 9 December 2022]. DOI 10.1094/CCHEM-07-10-0106. Available from : http://doi.wiley.com/10.1094/CCHEM-07-10-0106

[43] BULÉON, A., COLONNA, P., PLANCHOT, V. and BALL, S., 1998. Starch granules: structure and biosynthesis. *International Journal of Biological Macromolecules*. August 1998. Vol. 23, n° 2, pp. 85–112. [Accessed 14 June 2023]. DOI 10.1016/S0141-8130(98)00040-3. Available from : https://linkinghub.elsevier.com/retrieve/pii/S0141813098000403

[44] CALLEJO, M.J., 2011. Present Situation on the descriptive sensory analysis of bread. *Journal of Sensory Studies*. 2011. Vol. 26, n° 4, pp. 255–268. DOI https://doi.org/10.1111/j.1745-459X.2011.00341.x. Available from : https://onlinelibrary.wiley.com/doi/abs/10.1111/j.1745-459X.2011.00341.x

[45] CALVEL, R., 2001. *The taste of bread: A translation of le goût du pain, comment le préserver, comment le retrouver*. ISBN 978-1-4757-6811-4. Available from : http://dx.doi.org/10.1007/978-1-4757-6809-1

[46] CAMPBELL, G.M., HERRERO-SANCHEZ, R., PAYO-RODRIGUEZ, R. and MERCHAN, M.L., 2001. Measurement of dynamic dough density and effect of surfactants and flour type on aeration during mixing and gas retention during proofing. *Cereal Chemistry*. May 2001. Vol. 78, n° 3, pp. 272–277. [Accessed 9 January 2023]. DOI 10.1094/CCHEM.2001.78.3.272. Available from : http://doi.wiley.com/10.1094/CCHEM.2001.78.3.272

[47] CAMPBELL, G.M. and MARTIN, P.J., 2012. Bread aeration and dough rheology: an introduction. In : CAUVAIN, Stanley P. (ed.), *Breadmaking*. Second edition. Woodhead Publishing. pp. 299–336. Woodhead Publishing Series in Food Science, Technology and Nutrition. ISBN 978-0-85709-060-7. Available from : https://www.sciencedirect.com/science/article/pii/B9780857090607500127

[48] CAMPBELL, G.M. and MARTIN, P.J., 2020. Bread aeration and dough rheology: an introduction. In : CAUVAIN, Stanley P. (ed.), *Breadmaking (Third Edition)*. Third Edition. Woodhead Publishing. pp. 325–371. Woodhead Publishing Series in Food Science, Technology and Nutrition. ISBN 978-0-08-102519-2. Available from : https://www.sciencedirect.com/science/article/pii/B9780081025192000116

[49] CAMPBELL, G.M. and MOUGEOT, E., 1999. Creation and characterisation of aerated food products. *Trends in Food Science & Technology*. 1999. Vol. 10, n° 9, pp. 283–296. DOI https://doi.org/10.1016/S0924-2244(00)00008-X. Available from : https://www.sciencedirect.com/science/article/pii/S092422440000008X

[50] CAPPELLI, A., BETTACCINI, L. and CINI, E., 2020. The kneading process: A systematic review of the effects on dough rheology and resulting bread characteristics, including improvement strategies. *Trends in Food Science & Technology*. 1 October 2020. Vol. 104, pp. 91–101. [Accessed 30 October 2025]. DOI 10.1016/j.tifs.2020.08.008. Available from : https://www.sciencedirect.com/science/article/pii/S0924224420305665

[51] CAPPELLI, A., CANESSA, J. and CINI, E., 2020. Effects of CO2 snow addition during kneading on thermoregulation, dough rheological properties, and bread characteristics: A focus on ancient and modern wheat cultivars. *International Journal of Refrigeration*. 1 September 2020. Vol. 117, pp. 52–60. DOI 10.1016/j.ijrefrig.2020.04.006.

[52] CARROLL, J.J., SLUPSKY, J.D. and MATHER, A.E., 1991. The solubility of carbon dioxide in water at low pressure. *Journal of physical and chemical reference data*. 1991. Vol. 20, n° 6, pp. 1201–1209.

[53] CAUVAIN, S., 2015a. *Technology of Breadmaking*. Cham : Springer International Publishing. [Accessed 22 December 2022]. ISBN 978-3-319-14686-7. Available from : http://link.springer.com/10.1007/978-3-319-14687-4

[54] CAUVAIN, S., 2015b. Mixing and Dough Processing. In : CAUVAIN, Stanley (ed.), *Technology of Breadmaking*. Cham : Springer International Publishing. pp. 101–146. [Accessed 6 February 2026]. ISBN 978-3-319-14687-4. Available from : https://doi.org/10.1007/978-3-319-14687-4_4

[55] CAUVAIN, S. and YOUNG, L., 2008. *Bakery Food Manufacture and Quality: Water Control and Effects: Second Edition*. ISBN 978-1-4051-7613-2.

[56] CAUVAIN, S.P., 2017. Bread and Other Fermented Products. In : *Baking Problems Solved*. Elsevier. pp. 153–234. [Accessed 14 December 2022]. ISBN 978-0-08-100765-5. Available from : https://linkinghub.elsevier.com/retrieve/pii/B9780081007655000047

[57] CAUVAIN, S.P. and YOUNG, L.S., 2006. *Baked products: science, technology and practice*. Oxford ; Ames, Iowa : Blackwell Pub. ISBN 978-1-4051-2702-8. TX552.15 .C375 2006

[58] CAUVAIN, Stanley P. (ed.), 2020a. *Breadmaking: improving quality*. Third edition. Kidlington, Oxford, United Kingdom : Woodhead Publishing an imprint of Elsevier. Woodhead Publishing Series in Food Science, Technology and Nutrition. ISBN 978-0-08-102519-2. TX769 .B77545 2020

[59] CAUVAIN, Stanley P. (ed.), 2020b. *Breadmaking: improving quality*. Third edition. Duxford Cambridge, MA Kidlington : Woodhead Publishing, an imprint of Elsevier. Woodhead Publishing series in food science, technology and nutrition. ISBN 978-0-08-102519-2. Available from : doi.org/10.1016/C2017-0-02039-6

[60] CHAIX, E., GUILLAUME, C. and GUILLARD, V., 2014. Oxygen and carbon dioxide solubility and diffusivity in solid food matrices: A review of past and current knowledge. *Comprehensive Reviews in Food Science and Food Safety*. May 2014. Vol. 13, n° 3, pp. 261–286. DOI 10.1111/1541-4337.12058.

[61] CHAKRABARTI-BELL, S., WANG, S. and SIDDIQUE, K.H.M., 2014. Flour quality and disproportionation of bubbles in bread doughs. *Food Research International*. October 2014. Vol. 64, pp. 587–597. [Accessed 26 January 2023]. DOI 10.1016/j.foodres.2014.07.025. Available from : https://linkinghub.elsevier.com/retrieve/pii/S096399691400502X

[62] CHEN, G., EHMKE, L., MILLER, R., FAA, P., SMITH, G. and LI, Y., 2018. Effect of sodium chloride and sodium bicarbonate on the physicochemical properties of soft wheat flour doughs and gluten polymerization. *Journal of Agricultural and Food Chemistry*. 5 July 2018. Vol. 66, n° 26, pp. 6840–6850. [Accessed 20 January 2023]. DOI 10.1021/acs.jafc.8b01197. Available from : https://pubs.acs.org/doi/10.1021/acs.jafc.8b01197

[63] CHEN, G., EHMKE, L., SHARMA, C., MILLER, R., FAA, P., SMITH, G. and LI, Y., 2019. Physicochemical properties and gluten structures of hard wheat flour doughs as affected by salt. *Food Chemistry*. March 2019. Vol. 275, pp. 569–576. [Accessed 20 January 2023]. DOI 10.1016/j.foodchem.2018.07.157. Available from : https://linkinghub.elsevier.com/retrieve/pii/S0308814618313128

[64] CHEN, X. and SCHOFIELD, J.D., 1996. Effects of dough mixing and oxidising improvers on free reduced and free oxidised glutathione and protein-glutathione mixed disulphides of wheat flour. *Zeitschrift für Lebensmittel-Untersuchung und Forschung*. 1 May 1996. Vol. 203, n° 3, pp. 255–261. [Accessed 30 October 2025]. DOI 10.1007/BF01192874. Available from : https://doi.org/10.1007/BF01192874

[65] CHEN, Z., YAO, Y., PU, H., HUANG, J. and ZHONG, H., 2023. The effects of high-pressure treatment on starch pasting, retrogradation, thermal, crystalline, rheological and digestive properties – A review. *International Journal of Food Science & Technology*. March 2023. Vol. 58. DOI 10.1111/ijfs.16342.

[66] CHEVALLIER, S., ZUNIGA, R. and LE-BAIL, A., 2009. Assessment of Bread Dough Expansion during Fermentation. *Food and Bioprocess Technology*. January 2009. Vol. 5, pp. 609–617. DOI 10.1007/s11947-009-0319-3.

[67] CHIN, N.L. and CAMPBELL, G.M., 2005a. Dough aeration and rheology: Part 2. Effects of flour type, mixing speed and total work input on aeration and rheology of bread dough. *Journal of the Science of Food and Agriculture*. October 2005. Vol. 85, n° 13, pp. 2194–2202. [Accessed 28 December 2022]. DOI 10.1002/jsfa.2237. Available from : https://onlinelibrary.wiley.com/doi/10.1002/jsfa.2237

[68] CHIN, N.L. and CAMPBELL, G.M., 2005b. Dough aeration and rheology: Part 1. Effects of mixing speed and headspace pressure on mechanical development of bread dough. *Journal of the Science of Food and Agriculture*. October 2005. Vol. 85, n° 13, pp. 2184–2193. [Accessed 28 December 2022]. DOI 10.1002/jsfa.2236. Available from : https://onlinelibrary.wiley.com/doi/10.1002/jsfa.2236

[69] CHIN, N.L., MARTIN, P.J. and CAMPBELL, G.M., 2005. Dough aeration and rheology: Part 3. Effect of the presence of gas bubbles in bread dough on measured bulk rheology and work input rate. *Journal of the Science of Food and Agriculture*. October 2005. Vol. 85, n° 13, pp. 2203–2212. [Accessed 28 December 2022]. DOI 10.1002/jsfa.2238. Available from : https://onlinelibrary.wiley.com/doi/10.1002/jsfa.2238

[70] CHIOTELLIS, E. and CAMPBELL, G. M., 2003. Proving of bread dough I: modelling the evolution of the bubble size distribution. *Food and Bioproducts Processing*. 1 September 2003. Vol. 81, n° 3, pp. 194–206. [Accessed 30 October 2025]. DOI 10.1205/096030803322437965. Available from : https://www.sciencedirect.com/science/article/pii/S0960308503703745

[71] CHIOTELLIS, E. and CAMPBELL, G.M., 2003. Proving of bread dough II. *Food and Bioproducts Processing*. September 2003. Vol. 81, n° 3, pp. 207–216. [Accessed 12 April 2023]. DOI 10.1205/096030803322437974. Available from : https://linkinghub.elsevier.com/retrieve/pii/S0960308503703757

[72] CODINA, G. and MIRONEASA, S., 2013. Influence of mixing speed on dough microstructure and rheology. *Food Technology and Biotechnology*. 1 October 2013. Vol. 51, pp. 509–519. Available from : https://www.researchgate.net/publication/293483413_Influence_of_Mixing_Speed_on_Dough_Microstructure_and_Rheology

[73] CORNEJO-RAMÍREZ, Y.I., MARTÍNEZ-CRUZ, O., DEL TORO-SÁNCHEZ, C.L., WONG-CORRAL, F.J., BORBOA-FLORES, J. and CINCO-MOROYOQUI, F.J., 2018. The structural characteristics of starches and their functional properties. *CyTA - Journal of Food*. January 2018. Vol. 16, n° 1, pp. 1003–1017. [Accessed 15 February 2023]. DOI 10.1080/19476337.2018.1518343. Available from : https://www.tandfonline.com/doi/full/10.1080/19476337.2018.1518343

[74] CORSETTI, A., GOBBETTI, M., DE MARCO, B., BALESTRIERI, F., PAOLETTI, F., RUSSI, L. and ROSSI, J., 2000. Combined effect of sourdough lactic acid bacteria and additives on bread firmness and staling. *Journal of Agricultural and Food Chemistry*. July 2000. Vol. 48, n° 7, pp. 3044–3051. DOI 10.1021/jf990853e.

[75] COURTIN, C.M. and DELCOUR, J.A., 2002. Arabinoxylans and endoxylanases in wheat flour bread-making. *Journal of Cereal Science*. March 2002. Vol. 35, n° 3, pp. 225–243. [Accessed 9 December 2022]. DOI 10.1006/jcrs.2001.0433. Available from : https://linkinghub.elsevier.com/retrieve/pii/S0733521001904333

[76] CUQ, B., ABECASSIS, J. and GUILBERT, S., 2003. State diagrams to help describe wheat bread processing. *International Journal of Food Science and Technology*. September 2003. Vol. 38, n° 7, pp. 759–766. DOI 10.1046/j.1365-2621.2003.00748.x. Available from : https://doi.org/10.1046/j.1365-2621.2003.00748.x

[77] DECAMPS, K., JOYE, I., NICOLAS, J., HALTRICH, D., COURTIN, C. and DELCOUR, J., 2012. Biochemical characteristics of Trametes multicolor pyranose oxidase and Aspergillus niger glucose oxidase and implications for their functionality in wheat flour dough. *Food Chemistry*. 1 April 2012. Vol. 131, pp. 1485–1492. DOI 10.1016/j.foodchem.2011.10.041.

[78] DECAMPS, K., JOYE, I.J., DE VOS, D.E., COURTIN, C.M. and DELCOUR, J.A., 2016. Molecular oxygen and reactive oxygen species in bread-making processes: scarce, but nevertheless important. *Critical Reviews in Food Science and Nutrition*. 3 April 2016. Vol. 56, n° 5, pp. 722–736. [Accessed 9 December 2022]. DOI 10.1080/10408398.2013.795929. Available from : http://www.tandfonline.com/doi/full/10.1080/10408398.2013.795929

[79] DELARUE, J., LAWLOR, J.B. and ROGEAUX, M., 2015. Rapid sensory profiling techniques and related methods: applications in new product development and consumer research. . January 2015. pp. 1–555.

[80] DELCOUR, J.A., JOYE, I.J., PAREYT, B., WILDERJANS, E., BRIJS, K. and LAGRAIN, B., 2012. Wheat Gluten Functionality as a Quality Determinant in Cereal-Based Food Products. *Annual Review of Food Science and Technology*. 10 April 2012. Vol. 3, n° 1, pp. 469–492. [Accessed 13 March 2023]. DOI 10.1146/annurev-food-022811-101303. Available from : https://www.annualreviews.org/doi/10.1146/annurev-food-022811-101303

[81] DELLA VALLE, G., CHIRON, H., CICERELLI, L., KANSOU, K., KATINA, K., NDIAYE, A., WHITWORTH, M. and POUTANEN, K., 2014. Basic knowledge models for the design of bread texture. *Trends in Food Science & Technology*. March 2014. Vol. 36. DOI 10.1016/j.tifs.2014.01.003.

[82] DESCOINS, C., MATHLOUTHI, M., LE MOUAL, M. and HENNEQUIN, J., 2006. Carbonation monitoring of beverage in a laboratory scale unit with on-line measurement of dissolved CO2. *Food Chemistry*. 1 April 2006. Vol. 95, n° 4, pp. 541–553. [Accessed 26 February 2026]. DOI 10.1016/j.foodchem.2004.11.031. Available from : https://www.sciencedirect.com/science/article/pii/S0308814604008805

[83] DESCOINS, C., MATHLOUTHI, M., MOUAL, M.L. and HENNEQUIN, J., 2006. Carbonation monitoring of beverage in a laboratory scale unit with on-line measurement of dissolved CO2. *Food Chemistry*. 2006.

[84] DEVAKI, S.J. and RAVEENDRAN, R.L., 2017. Vitamin C: Sources, functions, sensing and analysis. In : HAMZA, Amal H. (ed.). InTech. 2 August 2017. [Accessed 6 February 2026]. ISBN 978-953-51-3421-3. Available from : http://www.intechopen.com/books/vitamin-c/vitamin-c-sources-functions-sensing-and-analysis

[85] DOBRASZCZYK, B.J. and MORGENSTERN, M.P., 2003. Rheology and the breadmaking process. *Journal of Cereal Science*. 1 November 2003. Vol. 38, n° 3, pp. 229–245. [Accessed 30 October 2025]. DOI 10.1016/S0733-5210(03)00059-6. Available from : https://www.sciencedirect.com/science/article/pii/S0733521003000596

[86] DOBRASZCZYK, B.J., SMEWING, J., ALBERTINI, M., MAESMANS, G. and SCHOFIELD, J.D., 2003. Extensional rheology and stability of gas cell walls in bread doughs at elevated temperatures in relation to breadmaking performance. *Cereal Chemistry Journal*. March 2003. Vol. 80, n° 2, pp. 218–224. [Accessed 23 December 2022]. DOI 10.1094/CCHEM.2003.80.2.218. Available from : http://doi.wiley.com/10.1094/CCHEM.2003.80.2.218

[87] DOME, K., PODGORBUNSKIKH, E., BYCHKOV, A. and LOMOVSKY, O., 2020. Changes in the crystallinity degree of starch having different types of crystal structure after mechanical pretreatment. *Polymers*. 12 March 2020. Vol. 12, n° 3, pp. 641. [Accessed 15 February 2023]. DOI 10.3390/polym12030641. Available from : https://www.mdpi.com/2073-4360/12/3/641

[88] DONG, W. and HOSENEY, R., 1995. Effects of certain breadmaking oxidants and reducing agents on dough rheological properties. *Cereal Chemistry*. 1995. [Accessed 30 October 2025]. Available from : https://www.semanticscholar.org/paper/Effects-of-certain-breadmaking-oxidants-and-agents-Dong-Hoseney/9139ef50e21b7fa31b211465ac9fc8c9bd698d40

[89] DOUBLIER, J.-L., 1981. Rheological studies on starch — flow behaviour of wheat starch pastes. *Starch - Stärke*. 1981. Vol. 33, n° 12, pp. 415–420. [Accessed 10 October 2025]. DOI 10.1002/star.19810331205. Available from : https://onlinelibrary.wiley.com/doi/abs/10.1002/star.19810331205

[90] DOUBLIER, J.L., LLAMAS, G. and MEUR, M.L., 1987. A rheological investigation of cereal starch pastes and gels. Effect of pasting procedures. *Carbohydrate Polymers*. 1987. Vol. 7, n° 4, pp. 251–275. DOI https://doi.org/10.1016/0144-8617(87)90063-4. Available from : https://www.sciencedirect.com/science/article/pii/0144861787900634

[91] DU, J., CULLEN, J.J. and BUETTNER, G.R., 1826. Ascorbic acid: Chemistry, biology and the treatment of cancer. *Biochimica et Biophysica Acta*. 1826.

[92] ELIASSON, A.-C., 1983a. Differential scanning calorimetry studies on wheat starch—gluten mixtures: I. Effect of gluten on the gelatinization of wheat starch. *Journal of Cereal Science*. 1983. Vol. 1, n° 3, pp. 199–205. DOI https://doi.org/10.1016/S0733-5210(83)80021-6. Available from : https://www.sciencedirect.com/science/article/pii/S0733521083800216

[93] ELIASSON, A.-C., 1983b. Differential scanning calorimetry studies on wheat starch-gluten mixtures: II. Effect of gluten and sodium stearoyl lactylate on starch crystallization during ageing of wheat starch gels. *Journal of Cereal Science*. 1983. Vol. 1, n° 3, pp. 207–213. DOI https://doi.org/10.1016/S0733-5210(83)80022-8. Available from : https://www.sciencedirect.com/science/article/pii/S0733521083800228

[94] ELIASSON, A.-C., 1994. Interactions between starch and lipids studied by DSC. *Thermochimica Acta*. November 1994. Vol. 246, n° 2, pp. 343–356. [Accessed 30 March 2023]. DOI 10.1016/0040-6031(94)80101-0. Available from : https://linkinghub.elsevier.com/retrieve/pii/0040603194801010

[95] ELIASSON, A.-C., 2012. Wheat starch structure and bread quality. In : *Breadmaking*. Elsevier. pp. 123–148. [Accessed 15 February 2023]. ISBN 978-0-85709-060-7. Available from : https://linkinghub.elsevier.com/retrieve/pii/B9780857090607500061

[96] ENGMANN, J., PECK, M.C. and WILSON, D.I., 2005. An experimental and theoretical investigation of bread dough sheeting. *Food and Bioproducts Processing*. September 2005. Vol. 83, n° 3, pp. 175–184. [Accessed 25 January 2023]. DOI 10.1205/fbp.04184. Available from : https://linkinghub.elsevier.com/retrieve/pii/S0960308505704855

[97] EVANS, I. and HAISMAN, D., 2007. Rheology of gelatinized starch suspension. *Journal of Texture Studies*. January 2007. Vol. 10, pp. 347–370. DOI 10.1111/j.1745-4603.1980.tb00865.x.

[98] EVERY, D., SIMMONS, L., SUTTON, K.H. and ROSS, M., 1999. Studies on the mechanism of the ascorbic acid improver effect on bread using flour fractionation and reconstitution methods. *Journal of Cereal Science*. September 1999. Vol. 30, n° 2, pp. 147–158. [Accessed 15 February 2023]. DOI 10.1006/jcrs.1999.0248. Available from : https://linkinghub.elsevier.com/retrieve/pii/S0733521099902485

[99] FACCIO, G., FLANDER, L., BUCHERT, J., SALOHEIMO, M. and NORDLUND, E., 2012. Sulfhydryl oxidase enhances the effects of ascorbic acid in wheat dough. *Journal of Cereal Science*. January 2012. Vol. 55, n° 1, pp. 37–43. [Accessed 8 February 2023]. DOI 10.1016/j.jcs.2011.10.002. Available from : https://linkinghub.elsevier.com/retrieve/pii/S0733521011001676

[100] FALCONE, BAIANO, A., ZANINI, F., MANCINI, L., TROMBA, G., MONTANARI, F. and NOBILE, M.A., 2008. A Novel Approach to the Study of Bread Porous Structure: Phase-contrast X-Ray Microtomography. *Journal of Food Science*. June 2008. Vol. 69, pp. FEP38–FEP43. DOI 10.1111/j.1365-2621.2004.tb17865.x.

[101] FARAHNAKY, A. and HILL, S.E., 2007. The effect of salt, water and temperature on wheat dough rheology. *Journal of Texture Studies*. August 2007. Vol. 38, n° 4, pp. 499–510. [Accessed 2 May 2023]. DOI 10.1111/j.1745-4603.2007.00107.x. Available from : https://onlinelibrary.wiley.com/doi/10.1111/j.1745-4603.2007.00107.x

[102] FARIDI, Hamed and FAUBION, Jon M. (eds.), 1990. *Dough rheology and baked product texture*. Boston, MA : Springer US. [Accessed 26 December 2022]. ISBN 978-1-4612-8207-5. Available from : http://link.springer.com/10.1007/978-1-4613-0861-4

[103] FEILLET, P., 2000. *Le grain de blé: Composition et utilisation*. Quae. Mieux comprendre. ISBN 978-2-7380-0896-1. Available from : https://books.google.fr/books?id=b8eUc0Q_wP4C

[104] FREDRIKSSON, H., SILVERIO, J., ANDERSSON, R., ELIASSON, A.-C. and ÅMAN, P., 1998. The influence of amylose and amylopectin characteristics on gelatinization and retrogradation properties of different starches. *Carbohydrate Polymers*. March 1998. Vol. 35, n° 3–4, pp. 119–134. [Accessed 14 June 2023]. DOI 10.1016/S0144-8617(97)00247-6. Available from : https://linkinghub.elsevier.com/retrieve/pii/S0144861797002476

[105] FU, Z. and BEMILLER, J.N., 2017. Effect of hydrocolloids and salts on retrogradation of native and modified maize starch. *Food Hydrocolloids*. August 2017. Vol. 69, pp. 36–48. [Accessed 21 February 2023]. DOI 10.1016/j.foodhyd.2017.01.023. Available from : https://linkinghub.elsevier.com/retrieve/pii/S0268005X16306634

[106] GAN, Z., ELLIS, P.R. and SCHOFIELD, J.D., 1995. Gas cell stabilisation and gas retention in wheat bread dough. *Journal of Cereal Science*. May 1995. Vol. 21, n° 3, pp. 215–230. [Accessed 13 December 2022]. DOI 10.1006/jcrs.1995.0025. Available from : https://linkinghub.elsevier.com/retrieve/pii/S0733521085700252

[107] GÄNZLE, M. and RIPARI, V., 2016. Composition and function of sourdough microbiota: From ecological theory to bread quality. *International Journal of Food Microbiology*. 19 December 2016. Vol. 239, pp. 19–25. [Accessed 30 October 2025]. DOI 10.1016/j.ijfoodmicro.2016.05.004. Available from : https://www.sciencedirect.com/science/article/pii/S0168160516302148

[108] GAO, J., KOH, A., TAY, S. and ZHOU, W., 2017. Dough and bread made from high- and low- protein flours by vacuum mixing: Part 1: Gluten network formation. *Journal of Cereal Science*. 1 March 2017. Vol. 74. DOI 10.1016/j.jcs.2017.03.008.

[109] GAO, J., TAY, S.L., KOH, A.H.S. and ZHOU, W., 2017. Dough and bread made from high- and low-protein flours by vacuum mixing: Part 2. Yeast activity, dough proofing and bread quality. *Journal of Cereal Science*. September 2017. Vol. 77, pp. 275–283. [Accessed 26 December 2022]. DOI 10.1016/j.jcs.2017.08.015. Available from : https://linkinghub.elsevier.com/retrieve/pii/S0733521016304854

[110] GAO, J., WANG, Y., DONG, Z. and ZHOU, W., 2017. Structural and mechanical characteristics of bread and their impact on oral processing: a review. *International Journal of Food Science and Technology*. 2017.

[111] GAO, X., TONG, J., GUO, L., YU, L., LI, S., YANG, B., WANG, L., LIU, Y., LI, F., GUO, J., ZHAI, S., LIU, C., REHMAN, A., FARAHNAKY, A., WANG, P., WANG, Z. and CAO, X., 2020. Influence of gluten and starch granules interactions on dough mixing properties in wheat (Triticum aestivum L.). *Food Hydrocolloids*. September 2020. Vol. 106, pp. 105885. [Accessed 23 January 2023]. DOI 10.1016/j.foodhyd.2020.105885. Available from : https://linkinghub.elsevier.com/retrieve/pii/S0268005X19317473

[112] GARCÍA-GÓMEZ, B., FERNÁNDEZ-CANTO, N., VÁZQUEZ-ODÉRIZ, M.L., QUIROGA-GARCÍA, M., MUÑOZ-FERREIRO, N. and ROMERO-RODRÍGUEZ, M.Á., 2022. Sensory descriptive analysis and hedonic consumer test for Galician type breads. *Food Control*. 2022. Vol. 134, pp. 108765. DOI https://doi.org/10.1016/j.foodcont.2021.108765. Available from : https://www.sciencedirect.com/science/article/pii/S0956713521009038

[113] GELLYNCK, X., KÜHNE, B., BOCKSTAELE, F.V., WALLE, D.V. de and DEWETTINCK, K., 2009. Consumer perception of bread quality. *Appetite*. 2009. Vol. 53, n° 1, pp. 16–23.

DOI https://doi.org/10.1016/j.appet.2009.04.002. Available from : https://www.sciencedirect.com/science/article/pii/S0195666309000646

[114] GERE, A., SIPOS, L., KOVÁCS, S., KÓKAI, Z. and HÉBERGER, K., 2017. Which just-about-right feature should be changed if evaluations deviate? A case study using sum of ranking differences. *Chemometrics and Intelligent Laboratory Systems*. 2017. Vol. 161, pp. 130–135. DOI https://doi.org/10.1016/j.chemolab.2016.12.007. Available from : https://www.sciencedirect.com/science/article/pii/S016974391630538X

[115] GEVANTMAN, L.H., 2011. Solubility of selected gases in water. In : *CRC Handbook of Chemistry and Physics*. 92. CRC Press.

[116] GIBOREAU, A., CUVELIER, G. and LAUNAY, B., 1994. Rheological behaviour of three biopolymer/water systems, with emphasis on yield stress and viscoelastic properties. *Journal of Texture Studies*. 1994. Vol. 25, n° 2, pp. 119–138. [Accessed 30 October 2025]. DOI 10.1111/j.1745-4603.1994.tb01321.x. Available from : https://onlinelibrary.wiley.com/doi/abs/10.1111/j.1745-4603.1994.tb01321.x

[117] GOESAERT, H., BRIJS, K., VERAVERBEKE, W.S., COURTIN, C.M., GEBRUERS, K. and DELCOUR, J.A., 2005. Wheat flour constituents: how they impact bread quality, and how to impact their functionality. *Trends in Food Science & Technology*. January 2005. Vol. 16, n° 1–3, pp. 12–30. [Accessed 26 April 2023]. DOI 10.1016/j.tifs.2004.02.011. Available from : https://linkinghub.elsevier.com/retrieve/pii/S0924224404001906

[118] GOESAERT, H., SLADE, L., LEVINE, H. and DELCOUR, J.A., 2009. Amylases and bread firming – an integrated view. *Journal of Cereal Science*. November 2009. Vol. 50, n° 3, pp. 345–352. [Accessed 13 February 2023]. DOI 10.1016/j.jcs.2009.04.010. Available from : https://linkinghub.elsevier.com/retrieve/pii/S0733521009000757

[119] GRAY, J.A. and BEMILLER, J.N., 2003. Bread staling: Molecular basis and Control. *Comprehensive Reviews in Food Science and Food Safety*. January 2003. Vol. 2, n° 1, pp. 1–21. [Accessed 13 January 2023]. DOI 10.1111/j.1541-4337.2003.tb00011.x. Available from : https://onlinelibrary.wiley.com/doi/10.1111/j.1541-4337.2003.tb00011.x

[120] GRENIER, D., RONDEAU-MOURO, C., DEDEY, K.B., MOREL, M.-H. and LUCAS, T., 2021. Gas cell opening in bread dough during baking. *Trends in Food Science & Technology*. March 2021. Vol. 109, pp. 482–498. [Accessed 13 December 2022]. DOI 10.1016/j.tifs.2021.01.032. Available from : https://linkinghub.elsevier.com/retrieve/pii/S0924224421000327

[121] GROSCH, W. and SCHIEBERLE, P., 1997. Flavor of cereal products—A Review. *Cereal Chemistry*. 1997. Vol. 74, n° 2, pp. 91–97. [Accessed 30 October 2025]. DOI 10.1094/CCHEM.1997.74.2.91. Available from : https://onlinelibrary.wiley.com/doi/abs/10.1094/CCHEM.1997.74.2.91

[122] GROSCH, W. and WIESER, H., 1999. Redox reactions in wheat dough as affected by ascorbic acid. *Journal of Cereal Science*. January 1999. Vol. 29, n° 1, pp. 1–16. [Accessed 5 April 2023]. DOI 10.1006/jcrs.1998.0218. Available from : https://linkinghub.elsevier.com/retrieve/pii/S0733521098902181

[123] GUO, L., FANG, F., ZHANG, Y., XU, D., XU, X. and JIN, Z., 2020. Effect of glutathione on gelatinization and retrogradation of wheat flour and starch. *Journal of Cereal Science*. September 2020. Vol. 95, pp. 103061. [Accessed 9 December 2022]. DOI 10.1016/j.jcs.2020.103061. Available from : https://linkinghub.elsevier.com/retrieve/pii/S0733521020304240

[124] HAN, K.T., KIM, H.R., MOON, T.W. and CHOI, S.J., 2021. Isothermal and temperature-cycling retrogradation of high-amylose corn starch: Impact of sonication on its structural and retrogradation properties. *Ultrasonics Sonochemistry*. 2021. Vol. 76, pp. 105650. DOI https://doi.org/10.1016/j.ultsonch.2021.105650. Available from : https://www.sciencedirect.com/science/article/pii/S1350417721001929

[125] HARIDASAN, N., HAMDAMI, N., LÖSCHE, K. and LE-BAIL, A., 2025. Impact of salt and fat reduction under low pressure mixing on pizza dough properties. *LWT*. 1 February 2025. Vol. 217, pp. 117410. DOI 10.1016/j.lwt.2025.117410.

[126] HEENAN, S.P., DUFOUR, J.-P., HAMID, N., HARVEY, W. and DELAHUNTY, C.M., 2008. The sensory quality of fresh bread: Descriptive attributes and consumer perceptions. *Food Research International*. 2008. Vol. 41, n° 10, pp. 989–997. DOI https://doi.org/10.1016/j.foodres.2008.08.002. Available from : https://www.sciencedirect.com/science/article/pii/S0963996908001713

[127] HEUVEN, L.A.J., DEKKER, M., RENZETTI, S. and BOLHUIS, D.P., 2024. The eating rate of bread predicted from its sensory texture and physical properties. *Food & Function*. 9 December 2024. Vol. 15, n° 24, pp. 12244–12255. [Accessed 26 February 2026]. DOI 10.1039/D4FO04297B. Available from : https://pubs.rsc.org/en/content/articlelanding/2024/fo/d4fo04297b

[128] HIBBERD, G.E. and PARKER, N.S., 1976. Gas pressure-volume-time relationships in fermenting dough. Rate of production and solubility of carbon dioxide in dough. *Cereal Chemistry*. 1976.

[129] HOU, G.G. and HSU, Y.-H., 2013. Comparing fermentation gas production between wheat and apple sourdough starters using the Risograph. *Food Bioscience*. September 2013. Vol. 3, pp. 75–81. [Accessed 6 February 2026]. DOI 10.1016/j.fbio.2013.04.007. Available from : https://linkinghub.elsevier.com/retrieve/pii/S2212429213000333

[130] HU, N., QI, W., ZHU, J., ZHAO, F., XIU, L., ZHENG, M. and LIU, J., 2025. Mechanistic studies on the effect of endogenous proteins on the starch retrogradation characteristics of corn before and after postharvest ripening. *Food Chemistry: X*. 2025. Vol. 25, pp. 102088. DOI https://doi.org/10.1016/j.fochx.2024.102088. Available from : https://www.sciencedirect.com/science/article/pii/S2590157524009763

[131] HU, Y., BADAR, I., ZHANG, L., YANG, L. and XU, B., 2024. Odor and taste characteristics, transduction mechanism, and perceptual interaction in fermented foods: a review. *Critical reviews in food science and nutrition*. July 2024. Vol. 65, pp. 1–19. DOI 10.1080/10408398.2024.2377292.

[132] HUG-ITEN, S., ESCHER, F. and CONDE-PETIT, B., 2003. Staling of bread: Role of amylose and amylopectin and influence of starch-degrading enzymes. *Cereal Chemistry Journal*. November 2003. Vol. 80, n° 6, pp. 654–661. [Accessed 14 February 2023]. DOI 10.1094/CCHEM.2003.80.6.654. Available from : http://doi.wiley.com/10.1094/CCHEM.2003.80.6.654

[133] ISTUDOR, A., VOICU, G., MUSCALU, G. and TUDOR, P., 2020. Evaluation of carbon dioxide released by bread dough during proving stage. *E3S Web of Conferences*. 1 January 2020. Vol. 180, pp. 03012. DOI 10.1051/e3sconf/202018003012.

[134] IZYDORCZYK, M.S. and BILIADERIS, C.G., 1995. Cereal arabinoxylans: advances in structure and physicochemical properties. *Carbohydrate Polymers*. January 1995. Vol. 28, n° 1, pp. 33–48. [Accessed 9 February 2023]. DOI 10.1016/0144-8617(95)00077-1. Available from : https://linkinghub.elsevier.com/retrieve/pii/0144861795000771

[135] JANE, J., 2009. Structural features of starch granules II. In : *Starch*. Elsevier. pp. 193–236. [Accessed 16 February 2023]. ISBN 978-0-12-746275-2. Available from : https://linkinghub.elsevier.com/retrieve/pii/B9780127462752000069

[136] JANSSEN, F., WOUTERS, A.G.B. and DELCOUR, J.A., 2021. Gas cell stabilization by aqueous-phase constituents during bread production from wheat and rye dough and oat batter: Dough or batter liquor as model system. *Comprehensive Reviews in Food Science and Food Safety*. July 2021. Vol. 20, n° 4, pp. 3881–3917. [Accessed 3 January 2023]. DOI 10.1111/1541-4337.12761. Available from : https://onlinelibrary.wiley.com/doi/10.1111/1541-4337.12761

[137] JAYARAM, V.B., CUYVERS, S., LAGRAIN, B., VERSTREPEN, K.J., DELCOUR, J.A. and COURTIN, C.M., 2013. Mapping of Saccharomyces cerevisiae metabolites in fermenting wheat straight-dough reveals succinic acid as

pH-determining factor. *Food Chemistry*. 15 January 2013. Vol. 136, n° 2, pp. 301–308. [Accessed 26 February 2026]. DOI 10.1016/j.foodchem.2012.08.039. Available from : https://www.sciencedirect.com/science/article/pii/S0308814612013234

[138] JEFFERSON, D.R., LACEY, A.A. and SADD, P.A., 2006. Understanding crust formation during baking. *Journal of Food Engineering*. 2006.

[139] JEKLE, M. and BECKER, T., 2012. Effects of acidification, sodium chloride, and moisture levels on wheat dough: I. modeling of rheological and microstructural properties. *Food Biophysics*. September 2012. Vol. 7, n° 3, pp. 190–199. [Accessed 18 January 2023]. DOI 10.1007/s11483-012-9257-0. Available from : http://link.springer.com/10.1007/s11483-012-9257-0

[140] JEKLE, M., FUCHS, A. and BECKER, T., 2018. A normalized texture profile analysis approach to evaluate firming kinetics of bread crumbs independent from its initial texture. *Journal of Cereal Science*. 2018. Vol. 81, pp. 147–152. DOI https://doi.org/10.1016/j.jcs.2018.04.007. Available from : https://www.sciencedirect.com/science/article/pii/S0733521018300894

[141] JEKLE, M., MÜHLBERGER, K. and BECKER, T., 2016. Starch–gluten interactions during gelatinization and its functionality in dough like model systems. *Food Hydrocolloids*. March 2016. Vol. 54, pp. 196–201. [Accessed 23 January 2023]. DOI 10.1016/j.foodhyd.2015.10.005. Available from : https://linkinghub.elsevier.com/retrieve/pii/S0268005X15301119

[142] JENKINS, P.J. and DONALD, A.M., 1995. The influence of amylose on starch granule structure. *International Journal of Biological Macromolecules*. January 1995. Vol. 17, n° 6, pp. 315–321. [Accessed 14 June 2023]. DOI 10.1016/0141-8130(96)81838-1. Available from : https://linkinghub.elsevier.com/retrieve/pii/0141813096818381

[143] JENSEN, S., OESTDAL, H. and THYBO, A., 2010. Sensory profiling of changes in wheat and whole wheat bread during a prolonged period of storage. *Journal of Sensory Studies*. February 2010. Vol. 25, pp. 231–245. DOI 10.1111/j.1745-459X.2009.00254.x.

[144] JHA, P.K., CHEVALLIER, S., CHEIO, J., RAWSON, A. and LE-BAIL, A., 2017. Impact of resting time between mixing and shaping on the dough porosity and final cell distribution in sandwich bread. *Journal of Food Engineering*. February 2017. Vol. 194, pp. 15–23. [Accessed 24 January 2023]. DOI 10.1016/j.jfoodeng.2016.07.016. Available from : https://linkinghub.elsevier.com/retrieve/pii/S0260877416302667

[145] JHA, P.K., SADOT, M., CHEVALLIER, S., RAWSON, A. and LE-BAIL, A., 2022. Impact of Overhead Pressure During Mixing on the Quality of Sandwich Bread. *Food and Bioprocess Technology*. August 2022. Vol. 15, n° 8, pp. 1896–1906. [Accessed 26 February 2026]. DOI 10.1007/s11947-022-02846-9. Available from : https://link.springer.com/10.1007/s11947-022-02846-9

[146] JIANG, Z., HAN, Z., ZHU, M., WAN, X. and ZHANG, L., 2023. Effects of thermal processing on transformation of polyphenols and flavor quality. *Current Opinion in Food Science*. 1 June 2023. Vol. 51, pp. 101014. [Accessed 6 February 2026]. DOI 10.1016/j.cofs.2023.101014. Available from : https://www.sciencedirect.com/science/article/pii/S2214799323000280

[147] JOHANSSON, E., MALIK, A.H., HUSSAIN, A., RASHEED, F., NEWSON, W.R., PLIVELIC, T., HEDENQVIST, M.S., GÄLLSTEDT, M. and KUKTAITE, R., 2013. Wheat gluten polymer structures: The impact of genotype, environment, and processing on their functionality in various applications. *Cereal Chemistry Journal*. July 2013. Vol. 90, n° 4, pp. 367–376. [Accessed 13 March 2023]. DOI 10.1094/CCHEM-08-12-0105-FI. Available from : http://doi.wiley.com/10.1094/CCHEM-08-12-0105-FI

[148] JOYE, I.J., LAGRAIN, B. and DELCOUR, J.A., 2009a. Use of chemical redox agents and exogenous enzymes to modify the protein network during breadmaking – A review. *Journal of Cereal Science*. July 2009. Vol. 50, n° 1, pp. 11–21. [Accessed 7 February 2023]. DOI 10.1016/j.jcs.2009.04.001. Available from : https://linkinghub.elsevier.com/retrieve/pii/S0733521009000472

[149] JOYE, I.J., LAGRAIN, B. and DELCOUR, J.A., 2009b. Endogenous redox agents and enzymes that affect protein network formation during breadmaking – A review. *Journal of Cereal Science*. July 2009. Vol. 50, n° 1, pp. 1–10. [Accessed 8 February 2023]. DOI 10.1016/j.jcs.2009.04.002. Available from : https://linkinghub.elsevier.com/retrieve/pii/S0733521009000460

[150] JUNGE, R.C. and HOSENEY, R.C., 1981. A mechanism by which shortening and certain surfactants improve loaf volume in bread. *Cereal Chem 58:408 - 412*. 1981.

[151] KAINUMA, K. and FRENCH, D., 1972. Naegeli amylodextrin and its relationship to starch granule structure. II. Role of water in crystallization of B-starch. *Biopolymers*. November 1972. Vol. 11, n° 11, pp. 2241–2250. [Accessed 14 June 2023]. DOI 10.1002/bip.1972.360111105. Available from : https://onlinelibrary.wiley.com/doi/10.1002/bip.1972.360111105

[152] KAMEL, Basil S. and STAUFFER, Clyde E. (eds.), 1993. *Advances in Baking Technology*. Boston, MA : Springer US. [Accessed 14 December 2022]. ISBN 978-0-7514-0055-7. Available from : http://link.springer.com/10.1007/978-1-4899-7256-9

[153] KEMP, S., HORT, J. and HOLLOWOOD, T., 2017. *Descriptive analysis in sensory evaluation*. ISBN 978-0-470-67139-9.

[154] KHATKAR, B., 2002. Dynamic rheology of wheat flour dough. I. Non-linear viscoelastic behaviour. *Journal of The Science of Food and Agriculture*. 1 January 2002. [Accessed 6 February 2026]. DOI 10.1002/JSFA.1109. Available from : https://www.academia.edu/6637868/Dynamic_rheology_of_wheat_flour_dough_I_Non_linear_viscoelastic_behaviour

[155] KIM, H.-S., KIM, B.-Y. and BAIK, M.-Y., 2012. Application of Ultra High Pressure (UHP) in Starch Chemistry. *Critical Reviews in Food Science and Nutrition*. February 2012. Vol. 52, n° 2, pp. 123–141. [Accessed 16 February 2023]. DOI 10.1080/10408398.2010.498065. Available from : http://www.tandfonline.com/doi/abs/10.1080/10408398.2010.498065

[156] KINSELLA, J.E. and HALE, M.L., 1984. Hydrophobic associations and gluten consistency: effect of specific anions. *Journal of Agricultural and Food Chemistry*. September 1984. Vol. 32, n° 5, pp. 1054–1056. [Accessed 2 May 2023]. DOI 10.1021/jf00125a027. Available from : https://pubs.acs.org/doi/abs/10.1021/jf00125a027

[157] KOEHLER, P., 2003. Effect of ascorbic acid in dough: Reaction of oxidized glutathione with reactive thiol groups of wheat glutelin. *Journal of Agricultural and Food Chemistry*. 1 August 2003. Vol. 51, n° 17, pp. 4954–4959. [Accessed 8 February 2023]. DOI 10.1021/jf026061t. Available from : https://pubs.acs.org/doi/10.1021/jf026061t

[158] KOKELAAR, J.J., VAN VLIET, T. and PRINS, A., 1996. Strain hardening properties and extensibility of flour and gluten doughs in relation to breadmaking performance. *Journal of Cereal Science*. November 1996. Vol. 24, n° 3, pp. 199–214. [Accessed 23 December 2022]. DOI 10.1006/jcrs.1996.0053. Available from : https://linkinghub.elsevier.com/retrieve/pii/S0733521096900533

[159] KOKSEL, F. and SCANLON, M., 2016. Kinetics of bubble growth in bread dough and crust formation. In : *Food Engineering Series*. pp. 129–167. ISBN 978-3-319-24733-5.

[160] KOKSEL, F. and SCANLON, M.G., 2012. Effects of composition on dough development and air entrainment in doughs made from gluten-starch blends. *Journal of Cereal Science*. September 2012. Vol. 56, n° 2, pp. 445–450. [Accessed 11 January 2023]. DOI 10.1016/j.jcs.2012.05.013. Available from : https://linkinghub.elsevier.com/retrieve/pii/S0733521012001099

[161] KPM, 2025. Alveograph. *Alveograph*. 2025. [Accessed 1 July 2025]. Available from : https://www.kpmanalytics.com/products/functional-rheological/alveograph-test-series

[162] KULP, K., PONTE, J.G. and D'APPOLONIA, B.L., 1981. Staling of white pan bread: Fundamental causes∗. *C R C Critical Reviews in Food Science and Nutrition*. September 1981. Vol. 15, n° 1, pp. 1–48. [Accessed 22 February 2023]. DOI 10.1080/10408398109527311. Available from : http://www.tandfonline.com/doi/abs/10.1080/10408398109527311

[163] KULP, Karel and LORENZ, Klaus J. (eds.), 2003. *Handbook of dough fermentations*. New York : Marcel Dekker. Food science and technology, 127. ISBN 978-0-8247-4264-5. Available from : doi.org/10.1201/9780203911884TX770.S66 H36 2003

[164] LA CROIX, K., FIALA, S., COLONNA, A., DURHAM, C., MORRISSEY, M., DRUM, D. and KOHN, M., 2014. Consumer detection and acceptability of reduced-sodium bread. *Public health nutrition*. August 2014. Vol. 18, pp. 1–7. DOI 10.1017/S1368980014001748.

[165] LAI, L. and KOKINI, J., 2008. Physicochemical changes and rheological properties of starch during extrusion (A Review). *Biotechnology Progress*. September 2008. Vol. 7, pp. 251–266. DOI 10.1021/bp00009a009.

[166] LANCELOT, E., FONTAINE, J., GRUA-PRIOL, J., ASSAF, A., THOUAND, G. and LE-BAIL, A., 2021. Study of structural changes of gluten proteins during bread dough mixing by Raman spectroscopy. *Food Chemistry*. October 2021. Vol. 358, pp. 129916. [Accessed 22 December 2022]. DOI 10.1016/j.foodchem.2021.129916. Available from : https://linkinghub.elsevier.com/retrieve/pii/S0308814621009225

[167] LASSOUED, N., DELARUE, J., LAUNAY, B. and MICHON, C., 2008. Baked product texture: Correlations between instrumental and sensory characterization using Flash Profile. *Journal of Cereal Science*. 2008. Vol. 48, n° 1, pp. 133–143. DOI https://doi.org/10.1016/j.jcs.2007.08.014. Available from : https://www.sciencedirect.com/science/article/pii/S0733521007001646

[168] LAWLESS, H.T. and HEYMANN, H., 2010. Discrimination Testing. In : LAWLESS, Harry T. and HEYMANN, Hildegarde (eds.), *Sensory Evaluation of Food: Principles and Practices*. New York, NY : Springer. pp. 79–100. [Accessed 30 October 2025]. ISBN 978-1-4419-6488-5. Available from : https://doi.org/10.1007/978-1-4419-6488-5_4

[169] LE-BAIL, A., BOUMALI, K., JURY, V., BEN-AISSA, F. and ZUNIGA, R., 2009. Impact of the baking kinetics on staling rate and mechanical properties of bread crumb and degassed bread crumb. *Journal of Cereal Science*. 1 September 2009. Vol. 50, n° 2, pp. 235–240. [Accessed 26 February 2026]. DOI 10.1016/j.jcs.2009.05.008. Available from : https://www.sciencedirect.com/science/article/pii/S0733521009000861

[170] LEFEBVRE, J., 2006. An outline of the non-linear viscoelastic behaviour of wheat flour dough in shear. *Rheologica Acta*. 1 April 2006. Vol. 45, n° 4, pp. 525–538. [Accessed 10 October 2025]. DOI 10.1007/s00397-006-0093-3. Available from : https://doi.org/10.1007/s00397-006-0093-3

[171] LEITGEB, M., KNEZ, Ž. and GORDANA, H., 2022. Enzyme activity and physiochemical properties of flour after supercritical carbon dioxide processing. *Foods*. June 2022. Vol. 11, pp. 1826. DOI 10.3390/foods11131826.

[172] LEONG, S.S. and CAMPBELL, G.M., 2008. Degassing of dough pieces during sheeting. In : CAMPBELL, Grant M., SCANLON, Martin G. and PYLE, D. Leo (eds.), *Bubbles in Food 2*. AACC International Press. pp. 207–216. American Associate of Cereal Chemists International. ISBN 978-1-891127-59-5. Available from : https://www.sciencedirect.com/science/article/pii/B9781891127595500250

[173] LEVAVASSEUR, L., 2007. *Suivi simultané de la consommation d'oxygène et de la consistance des pâtes de farine de blé à l'aide d'un pétrin instrumenté (le sitoxygraphe) : tentative d'explication biochimique et rhéologique. Application à l'ajout de laccases*. phdthesis. AgroParisTech. [Accessed 10 October 2025]. Available from : https://pastel.hal.science/pastel-00004527

[174] LEVINE, H. and SLADE, L., 1990. Influences of the glassy and rubbery states on the thermal, mechanical, and structural properties of doughs and baked products. In : *Dough Rheology and Baked Product Texture*. pp. 157–330.

[175] LI, C., 2024. Unraveling the complexities of starch retrogradation: Insights from kinetics, molecular interactions, and influences of food ingredients. *Food Reviews International*. 2024. Vol. 40, n° 9, pp. 3159–3182. DOI 10.1080/87559129.2024.2347467. Available from : https://doi.org/10.1080/87559129.2024.2347467

[176] LI, M., ZHANG, H., LYU, L., DENG, Q., FAN, H., XU, X. and XU, D., 2024. Effects of sourdough on bread staling rate: From the perspective of starch retrogradation and gluten depolymerization. *Food Bioscience*. 1 June 2024. Vol. 59, pp. 103877. [Accessed 28 October 2025]. DOI 10.1016/j.fbio.2024.103877. Available from : https://www.sciencedirect.com/science/article/pii/S2212429224003079

[177] LIANG, Z., GAO, J., YU, P. and YANG, D., 2023. History, mechanism of action, and toxicity: a review of commonly used dough rheology improvers. *Critical Reviews in Food Science and Nutrition*. 2023. Vol. 63, n° 7, pp. 947–963. DOI 10.1080/10408398.2021.1956427.

[178] LIU, R., XING, Y., ZHANG, Y., ZHANG, B., JIANG, X. and WEI, Y., 2015. Effect of mixing time on the structural characteristics of noodle dough under vacuum. *Food Chemistry*. April 2015. Vol. 188. DOI 10.1016/j.foodchem.2015.04.045.

[179] LIU, S., LIU, Q., LI, X., OBADI, M., JIANG, S., LI, S. and XU, B., 2021. Effects of dough resting time on the development of gluten network in different sheeting directions and the textural properties of noodle dough. *LWT*. 1 April 2021. Vol. 141, pp. 110920. [Accessed 30 October 2025]. DOI 10.1016/j.lwt.2021.110920. Available from : https://www.sciencedirect.com/science/article/pii/S0023643821000736

[180] LIU, Y., ZHANG, Q., WANG, Y., XU, P., WANG, L., LIU, L. and RAO, Y., 2023. Enrichment of wheat bread with platycodon Grandiflorus Root (PGR) Flour: Rheological properties and microstructure of dough and physicochemical characterization of bread. *Foods*. 29 January 2023. Vol. 12, n° 3, pp. 580. [Accessed 6 February 2023]. DOI 10.3390/foods12030580. Available from : https://www.mdpi.com/2304-8158/12/3/580

[181] LOISEL, C., MAACHE-REZZOUG, Z., ESNEAULT, C. and DOUBLIER, J.L., 2006. Effect of hydrothermal treatment on the physical and rheological properties of maize starches. *Journal of Food Engineering*. 2006. Vol. 73, n° 1, pp. 45–54. DOI https://doi.org/10.1016/j.jfoodeng.2005.01.004. Available from : https://www.sciencedirect.com/science/article/pii/S0260877405000385

[182] LU, Huang, CHEN, J., LIU, G., LU, Huilin, LI, D. and ZHAO, F., 2013. Simulated second-order moments of clusters and dispersed particles in riser. *Chemical Engineering Science*. 2013. Vol. 101, pp. 800–812. DOI https://doi.org/10.1016/j.ces.2013.06.036. Available from : https://www.sciencedirect.com/science/article/pii/S0009250913004430

[183] LUCAS, I., BECKER, T. and JEKLE, M., 2018. Gluten polymer networks—A microstructural classification in complex systems. *Polymers*. June 2018. Vol. 10, n° 6, pp. 617. [Accessed 30 October 2025]. DOI 10.3390/polym10060617. Available from : https://www.mdpi.com/2073-4360/10/6/617

[184] LYNCH, E.J., DAL BELLO, F., SHEEHAN, E.M., CASHMAN, K.D. and ARENDT, E.K., 2009. Fundamental studies on the reduction of salt on dough and bread characteristics. *Food Research International*. 1 August 2009. Vol. 42, n° 7, pp. 885–891. [Accessed 10 October 2025]. DOI 10.1016/j.foodres.2009.03.014. Available from : https://www.sciencedirect.com/science/article/pii/S0963996909000866

[185] MAACHE-REZZOUG, Z., ZARGUILI, I., LOISEL, C. and DOUBLIER, J.-L., 2010. Study of DIC hydrothermal treatment effect on rheological properties of standard maize (SMS), waxy maize (WMS), wheat (WTS) and potato (PTS) starches. *Journal of Food Engineering*. August 2010. Vol. 99. DOI 10.1016/j.jfoodeng.2009.06.052.

[186] MACRITCHIE, F., 2007. Differences in baking quality between wheat flours. *International Journal of Food Science & Technology*. 28 June 2007. Vol. 13, pp. 187–194. DOI 10.1111/j.1365-2621.1978.tb00794.x.

[187] MAEDA, T., KIKUMA, S., ARAKI, T., IKEDA, G., TAKEYA, K. and SAGARA, Y., 2009. The effects of mixing stage and fermentation time on the quantity of flavor compounds and sensory intensity of flavor in white bread. *Food*

Science and Technology Research. 2009. Vol. 15, n° 2, pp. 117–126. [Accessed 27 April 2023]. DOI 10.3136/fstr.15.117. Available from : http://www.jstage.jst.go.jp/article/fstr/15/2/15_2_117/_article

[188] MARQUES, C., CORREIA, E., DINIS, L.-T. and VILELA, A., 2022. An overview of sensory characterization techniques: From classical descriptive analysis to the emergence of novel profiling methods. *Foods (Basel, Switzerland)*. 18 January 2022. Vol. 11, n° 3, pp. 255. DOI 10.3390/foods11030255.

[189] MARTIN, P.J., CHIN, N., CAMPBELL, G. and MORRANT, C.J., 2004. Aeration during bread dough mixing. *Food and Bioproducts Processing*. 1 December 2004. Vol. 82, pp. 282–290. DOI 10.1205/fbio.82.4.282.56408.

[190] MARTIN, P.J., TASSELL, A., WIKTOROWICZ, R., MORRANT, C.J. and CAMPBELL, G.M., 2008. Mixing bread doughs under highly soluble gas atmospheres and the effects on bread crumb texture: experimental results and theoretical interpretation. In : *Bubbles in Food 2*. Elsevier. pp. 197–206. [Accessed 22 December 2022]. ISBN 978-1-891127-59-5. Available from : https://linkinghub.elsevier.com/retrieve/pii/B9781891127595500249

[191] MARTINS, S.I.F.S., JONGEN, W.M.F. and BOEKEL, M.A.J.S. van, 2000. A review of Maillard reaction in food and implications to kinetic modelling. *Trends in Food Science & Technology*. 2000. Vol. 11, n° 9, pp. 364–373. DOI https://doi.org/10.1016/S0924-2244(01)00022-X. Available from : https://www.sciencedirect.com/science/article/pii/S092422440100022X

[192] MASSEY, A.H., KHARE, S. and NIRANJAN, K., 2001. Air inclusion into a model cake batter using a pressure whisk: Development of gas hold-up and bubble size distribution. *Journal of Food Science*. October 2001. Vol. 66, pp. 1152–1157. DOI 10.1111/j.1365-2621.2001.tb16097.x.

[193] MCBRIDE-WRIGHT, M., MAITLAND, G. and TRUSLER, M., 2015. Viscosity and density of aqueous solutions of carbon dioxide at temperatures from (274 to 449) K and at pressures up to 100 MPa. *Journal of Chemical & Engineering Data*. January 2015. Vol. 60, pp. 171–180. DOI 10.1021/je5009125.

[194] MCCANN, T.H., LE GALL, M. and DAY, L., 2016. Extensional dough rheology – Impact of flour composition and extension speed. *Journal of Cereal Science*. May 2016. Vol. 69, pp. 228–237. [Accessed 5 January 2023]. DOI 10.1016/j.jcs.2016.03.012. Available from : https://linkinghub.elsevier.com/retrieve/pii/S0733521016300443

[195] MEERTS, M., CARDINAELS, R., OOSTERLINCK, F., M. COURTIN, C. and MOLDENAERS, P., 2017. The interplay between the main flour constituents in the rheological behaviour of wheat flour dough. *Food and Bioprocess Technology*. February 2017. Vol. 10, n° 2, pp. 249–265. [Accessed 25 April 2023]. DOI 10.1007/s11947-016-1810-2. Available from : http://link.springer.com/10.1007/s11947-016-1810-2

[196] MÉNDEZ-MONTEALVO, G., GARCÍA-SUÁREZ, F.J., PAREDES-LÓPEZ, O. and BELLO-PÉREZ, L.A., 2008. Effect of nixtamalization on morphological and rheological characteristics of maize starch. *Journal of Cereal Science*. 2008. Vol. 48, n° 2, pp. 420–425. DOI https://doi.org/10.1016/j.jcs.2007.10.007. Available from : https://www.sciencedirect.com/science/article/pii/S0733521007002111

[197] MESTA-CORRAL, M., GÓMEZ-GARCÍA, R., BALAGURUSAMY, N., TORRES-LEÓN, C. and HERNÁNDEZ-ALMANZA, A.Y., 2024. Technological and nutritional aspects of bread production: An overview of current status and future challenges. *Foods (Basel, Switzerland)*. 28 June 2024. Vol. 13, n° 13, pp. 2062. DOI 10.3390/foods13132062.

[198] MILES, M.J., MORRIS, V.J., ORFORD, P.D. and RING, S.G., 1985. The roles of amylose and amylopectin in the gelation and retrogradation of starch. *Carbohydrate Research*. 1985. Vol. 135, n° 2, pp. 271–281. DOI https://doi.org/10.1016/S0008-6215(00)90778-X. Available from : https://www.sciencedirect.com/science/article/pii/S000862150090778X

[199] MILLS, E.N.C., WILDE, P.J., SALT, L.J. and SKEGGS, P., 2003. Bubble formation and stabilization in bread dough. *Food and Bioproducts Processing*. September 2003. Vol. 81, n° 3, pp. 189–193. [Accessed 20 December 2022]. DOI 10.1205/096030803322437956. Available from : https://linkinghub.elsevier.com/retrieve/pii/S0960308503703733

[200] MIROŃCZUK-CHODAKOWSKA, I., WITKOWSKA, A.M. and ZUJKO, M.E., 2018. Endogenous non-enzymatic antioxidants in the human body. *Advances in Medical Sciences*. March 2018. Vol. 63, n° 1, pp. 68–78. DOI 10.1016/j.advms.2017.05.005.

[201] MIRSAEEDGHAZI, H., EMAM-DJOMEH, Z. and MOUSAVI, S.M., 2008. Rheometric measurement of dough rheological characteristics and factors affecting it. *International Journal of Agriculture and Biology*. 2008. [Accessed 6 February 2026]. Available from : https://www.semanticscholar.org/paper/Rheometric-measurement-of-dough-rheological-and-it.-Mirsaeedghazi-Emam-djomeh/06a75d94b5c3fec41163ff6e8b36e3a9c0a1e6e1

[202] MOHAZZABI, P., 2017. Archimedes' principle revisited. *Journal of Applied Mathematics and Physics*. 27 April 2017. Vol. 5, pp. 836–843. DOI 10.4236/jamp.2017.54073.

[203] MOLLAKHALILI-MEYBODI, N., SHEIDAEI, Z., KHORSHIDIAN, N., NEMATOLLAHI, A. and KHANNIRI, E., 2023. Sensory attributes of wheat bread: a review of influential factors. *Journal of Food Measurement and Characterization*. 1 June 2023. Vol. 17, n° 3, pp. 2172–2181. DOI 10.1007/s11694-022-01765-9. Available from : https://doi.org/10.1007/s11694-022-01765-9

[204] MOORE, T.R., 2016. Breads. In : *Encyclopedia of Food Grains*. Elsevier. pp. 8–18. [Accessed 14 June 2023]. ISBN 978-0-12-394786-4. Available from : https://linkinghub.elsevier.com/retrieve/pii/B9780123944375001169

[205] NAYOUF, M., LOISEL, C. and DOUBLIER, J.L., 2003. Effect of thermomechanical treatment on the rheological properties of crosslinked waxy corn starch. *Journal of Food Engineering*. 2003. Vol. 59, n° 2, pp. 209–219. DOI https://doi.org/10.1016/S0260-8774(02)00460-0. Available from : https://www.sciencedirect.com/science/article/pii/S0260877402004600

[206] NJUS, D., 2020. Ascorbic acid_ The chemistry underlying its antioxidant properties. *Free Radical Biology and Medicine*. 2020.

[207] O'BEIRNE, D., MURPHY, E. and NI EIDHIN, D., 2011. Effects of argon enriched low-oxygen atmospheres and of high-oxygen atmospheres on the kinetics of polyphenoloxidase (PPO). *Journal of Food Science*. 2011. Vol. 76, n° 1, pp. E73-77. DOI 10.1111/j.1750-3841.2010.01964.x.

[208] OOSTERGETEL, G.T. and VAN BRUGGEN, E.F.J., 1993. The crystalline domains in potato starch granules are arranged in a helical fashion. *Carbohydrate Polymers*. January 1993. Vol. 21, n° 1, pp. 7–12. [Accessed 14 June 2023]. DOI 10.1016/0144-8617(93)90110-P. Available from : https://linkinghub.elsevier.com/retrieve/pii/014486179390110P

[209] PALIER, J., LE-BAIL, A., LOISEL, C. and LE-BAIL, P., 2021. Substitution of baking powders in a pound cake by an overpressure mixing process; impact on cake properties. *Journal of Food Engineering*. September 2021. Vol. 316, pp. 110824. DOI 10.1016/j.jfoodeng.2021.110824.

[210] PARENTI, O., GUERRINI, L., MOMPIN, S.B., TOLDRÀ, M. and ZANONI, B., 2021. The determination of bread dough readiness during kneading of wheat flour: A review of the available methods. *Journal of Food Engineering*. November 2021. Vol. 309, pp. 110692. [Accessed 6 January 2023]. DOI 10.1016/j.jfoodeng.2021.110692. Available from : https://linkinghub.elsevier.com/retrieve/pii/S026087742100217X

[211] PAULIK, S., PACZKOWSKI, C., LAUKEMPER, R., BECKER, T. and JEKLE, M., 2021. Texture design of gluten-free bread by mixing under controlled headspace atmosphere. *European Food Research and Technology*. 1 September 2021. Vol. 247. DOI 10.1007/s00217-021-03793-z.

[212] PEIGHAMBARDOUST, S.H., VAN DER GOOT, A.J., VAN VLIET, T., HAMER, R.J. and BOOM, R.M., 2006. Microstructure formation and rheological behaviour of dough under simple shear flow. *Journal of Cereal Science*. 1 March 2006. Vol. 43, n° 2, pp. 183–197. [Accessed 6 February 2026]. DOI 10.1016/j.jcs.2005.10.004. Available from : https://www.sciencedirect.com/science/article/pii/S0733521005001402

[213] PÉREZ, S., BALDWIN, P.M. and GALLANT, D.J., 2009. Structural features of starch granules I. In : *Starch*. Elsevier. pp. 149–192. [Accessed 15 February 2023]. ISBN 978-0-12-746275-2. Available from : https://linkinghub.elsevier.com/retrieve/pii/B9780127462752000057

[214] PFEIFFER, T. and MORLEY, A., 2014. An evolutionary perspective on the Crabtree effect. *Frontiers in Molecular Biosciences*. 21 October 2014. Vol. 1. [Accessed 5 June 2023]. DOI 10.3389/fmolb.2014.00017. Available from : http://journal.frontiersin.org/article/10.3389/fmolb.2014.00017/abstract

[215] PFEILSTICKER, K. and ROEUNG, S., 1980. Isolierung und Charakterisierung derl-Ascorbinsäureoxidase (EC 1.10.3.3) aus Weizenmehl. *Zeitschrift für Lebensmittel-Untersuchung und Forschung*. 1 December 1980. Vol. 171, n° 6, pp. 425–429. [Accessed 30 October 2025]. DOI 10.1007/BF01907233. Available from : https://doi.org/10.1007/BF01907233

[216] PIAZZA, L., 1995. Moisture redistribution throughout the bread loaf during staling and its effects on mechanical properties. *Cereal Chemistry*. 1 June 1995. [Accessed 30 October 2025]. Available from : https://www.academia.edu/127748863/Moisture_redistribution_throughout_the_bread_loaf_during_staling_and_its_effects_on_mechanical_properties

[217] PIECHOWIAK, T., JÓZEFCZYK, R. and BALAWEJDER, M., 2018. Impact of ozonation process of wheat flour on the activity of selected enzymes. *Journal of Cereal Science*. November 2018. Vol. 84, pp. 30–37. [Accessed 14 June 2023]. DOI 10.1016/j.jcs.2018.09.010. Available from : https://linkinghub.elsevier.com/retrieve/pii/S0733521018306167

[218] PIETIÄINEN, S., MOLDIN, A., STRÖM, A., MALMBERG, C. and LANGTON, M., 2022. Effect of physicochemical properties, pre-processing, and extraction on the functionality of wheat bran arabinoxylans in breadmaking – A review. *Food Chemistry*. July 2022. Vol. 383, pp. 132584. [Accessed 19 December 2022]. DOI 10.1016/j.foodchem.2022.132584. Available from : https://linkinghub.elsevier.com/retrieve/pii/S0308814622005465

[219] PIGGOTT, J.R., SIMPSON, S.J. and WILLIAMS, S.A.R., 1998. Sensory analysis. *International Journal of Food Science and Technology*. 1998. DOI https://doi.org/10.1046/j.1365-2621.1998.00154.x.

[220] POITRENAUD, B., 2004. Baker's Yeast. In : *Handbook of Food and Beverage Fermentation Technology*. CRC Press.

[221] POUTANEN, K., FLANDER, L. and KATINA, K., 2009. Sourdough and cereal fermentation in a nutritional perspective. *Food Microbiology*. October 2009. Vol. 26, n° 7, pp. 693–699. DOI 10.1016/j.fm.2009.07.011.

[222] PRIMO-MARTIN, C., VAN DE PIJPEKAMP, A., VAN VLIET, T., PLIJTER, J.J. and HAMER, R.J., 2006. The role of the gluten network in the crispness of bread crust. *Journal of Cereal Science*. 2006.

[223] PURLIS, E., 2010. Browning development in bakery products – A review. *Journal of Food Engineering*. 1 August 2010. Vol. 99, n° 3, pp. 239–249. [Accessed 6 February 2026]. DOI 10.1016/j.jfoodeng.2010.03.008. Available from : https://www.sciencedirect.com/science/article/pii/S0260877410001172

[224] PUTSEYS, J.A., LAMBERTS, L. and DELCOUR, J.A., 2010. Amylose-inclusion complexes: Formation, identity and physico-chemical properties. *Journal of Cereal Science*. May 2010. Vol. 51, n° 3, pp. 238–247. [Accessed 23 March 2023]. DOI 10.1016/j.jcs.2010.01.011. Available from : https://linkinghub.elsevier.com/retrieve/pii/S0733521010000354

[225] PYLER, E.J. and GORTON, L.A., 2008. *Baking Science & Technology: Formulation & production*. Sosland Pub. Baking Science & Technology. ISBN 978-0-9820239-1-4. Available from : https://books.google.fr/books?id=ts_rQwAACAAJ

[226] QI, F., DAI, S.-C., NEWBERRY, M.P., LOVE, R.J. and TANNER, R.I., 2008. A simple approach to predicting dough sheeting thickness. *Journal of Cereal Science*. May 2008. Vol. 47, n° 3, pp. 489–495.

[Accessed 25 January 2023]. DOI 10.1016/j.jcs.2007.05.015. Available from : https://linkinghub.elsevier.com/retrieve/pii/S0733521007001099

[227] QUAYSON, E., MARTI, A., BONOMI, F., ATWELL, W. and SEETHARAMAN, K., 2015. Structural modification of gluten proteins in strong and weak wheat dough as affected by mixing temperature. *Cereal Chemistry Journal*. 27 October 2015. Vol. 93. DOI 10.1094/CCHEM-06-15-0123-R.

[228] QUILEZ, J., RUIZ, J. and ROMERO, M.-P., 2006. Relationships between sensory flavor evaluation and volatile and nonvolatile compounds in commercial wheat bread type baguette. *Journal of Food Science*. July 2006. Vol. 71, pp. S423–S427. DOI 10.1111/j.1750-3841.2006.00053.x.

[229] R., H., SINGH, S., AHLAWAT, A., NARWAL, S., JAISWAL, J.P., SINGH, J., KUMAR, R., SINGHAL, S., P BALAKRISHNAN, A., SHUKLA, P., BHAVYA, B., AGRAWAL, A., SINGH, S.K. and SINGH, A., 2023. Elucidating the effects on polyphenol oxidase activity and allelic variation of polyphenol oxidase genes on dough and whole wheat-derived product color parameters. *International Journal of Food Properties*. 20 September 2023. Vol. 26, pp. 2716–2731. DOI 10.1080/10942912.2023.2252196.

[230] RAAD, C., LE-BAIL, P. and LE-BAIL, A., 2025. Impact of Dough Mixing Pressure with Air and CO2 gases on Dough and Bread properties; A focus on Improved Control of Dough Aeration During the Baking Process. *Applied Food Research*. 28 October 2025. pp. 101470. [Accessed 30 October 2025]. DOI 10.1016/j.afres.2025.101470. Available from : https://www.sciencedirect.com/science/article/pii/S2772502225007760

[231] RAGHAVENDRA RAO, K., SANATHKUMAR, R., BHAT, H.L. and ELIZABETH, S., 2016. The nonlinear optical properties of the monoclinic d-isoascorbic acid crystal. *Applied Physics B*. 14 October 2016. Vol. 122, n° 11, pp. 270. [Accessed 30 October 2025]. DOI 10.1007/s00340-016-6539-0. Available from : https://doi.org/10.1007/s00340-016-6539-0

[232] RAJENDHRAN, H.P., VAIDYANATHAN, V.K., VENKATRAMAN, S. and KARTHIK, P., 2024. Optimization of enzymatic hydrolysis by protease produced from Bacillus subtilis MTCC 2423 to improve the functional properties of wheat gluten hydrolysates. *International Journal of Food Science*. 30 June 2024. Vol. 2024, pp. 5053510. [Accessed 20 October 2025]. DOI 10.1155/2024/5053510. Available from : https://pmc.ncbi.nlm.nih.gov/articles/PMC11227950/

[233] RATHNAYAKE, H., NAVARATNE, S. and NAVARATNE, C., 2018. Porous crumb structure of leavened baked products. *International Journal of Food Science*. August 2018. Vol. 2018, pp. 1–15. DOI 10.1155/2018/8187318.

[234] RATNAYAKE, W.S. and JACKSON, D.S., 2008. Chapter 5 Starch Gelatinization. In : *Advances in Food and Nutrition Research*. Elsevier. pp. 221–268. [Accessed 16 February 2023]. ISBN 978-0-12-374120-2. Available from : https://linkinghub.elsevier.com/retrieve/pii/S1043452608004051

[235] RATTIN, G.E., FAUBION, J.M., WALKER, C.E. and MENSE, A., 2009. Measuring yeast CO2 production with the risograph. *Cereal Foods World*. November 2009. Vol. 54, pp. 261–265. DOI 10.1094/CFW-54-6-0261.

[236] RENZETTI, S., VAN DEN HOEK, I.A.F. and VAN DER SMAN, R.G.M., 2021. Mechanisms controlling wheat starch gelatinization and pasting behaviour in presence of sugars and sugar replacers: Role of hydrogen bonding and plasticizer molar volume. *Food Hydrocolloids*. October 2021. Vol. 119, pp. 106880. [Accessed 20 February 2023]. DOI 10.1016/j.foodhyd.2021.106880. Available from : https://linkinghub.elsevier.com/retrieve/pii/S0268005X21002964

[237] REZAEI, M.N., JAYARAM, V.B., VERSTREPEN, K.J. and COURTIN, C.M., 2016. The impact of yeast fermentation on dough matrix properties: Impact of yeast fermentation on dough properties. *Journal of the Science of Food and Agriculture*. August 2016. Vol. 96, n° 11, pp. 3741–3748. [Accessed 2 June 2023]. DOI 10.1002/jsfa.7562. Available from : https://onlinelibrary.wiley.com/doi/10.1002/jsfa.7562

[238] ROMANO, A., TORALDO, G., CAVELLA, S. and MASI, P., 2007. Description of leavening of bread dough with mathematical modelling. *Journal of Food Engineering*. 1 November 2007. Vol. 83, n° 2, pp. 142–148.

[Accessed 10 October 2025]. DOI 10.1016/j.jfoodeng.2007.02.014. Available from : https://www.sciencedirect.com/science/article/pii/S0260877407001008

[239] ROSELL, C.M., 2011. The science of doughs and bread quality. In : *Flour and Breads and their Fortification in Health and Disease Prevention*. Elsevier. pp. 3–14. [Accessed 17 April 2023]. ISBN 978-0-12-380886-8. Available from : https://linkinghub.elsevier.com/retrieve/pii/B9780123808868100017

[240] ROUILLÉ, J., VALLE, G.D., LEFEBVRE, J., SLIWINSKI, E. and VANVLIET, T., 2005. Shear and extensional properties of bread doughs affected by their minor components. *Journal of Cereal Science*. 2005. Vol. 42, n° 1, pp. 45–57. DOI https://doi.org/10.1016/j.jcs.2004.12.008. Available from : https://www.sciencedirect.com/science/article/pii/S0733521005000184

[241] ROUSSEL, P. and CHIRON, H., 2002. *Les pains français. Evolution, qualité, production*. Vesoul : Maé-Erti. ISBN 978-2-84601-693-3.

[242] RUAN, R., ALMAER, S., HUANG, V., PERKINS, P., CHEN, P. and FULCHER, R., 1996. Relationship between firming and water mobility in starch-based food systems during storage. *Cereal chemistry*. 1 January 1996. Vol. 73, pp. 328–332.

[243] SABLANI, S.S., MARCOTTE, M., BAIK, O.D. and CASTAIGNE, F., 1998. Modeling of simultaneous heat and water transport in the baking process. *LWT - Food Science and Technology*. 1 April 1998. Vol. 31, n° 3, pp. 201–209. [Accessed 10 October 2025]. DOI 10.1006/fstl.1997.0360. Available from : https://www.sciencedirect.com/science/article/pii/S0023643897903601

[244] SADOT, M., CHEIO, J. and LE-BAIL, A., 2017. Impact on dough aeration of pressure change during mixing. *Journal of Food Engineering*. February 2017. Vol. 195, pp. 150–157. [Accessed 19 December 2022]. DOI 10.1016/j.jfoodeng.2016.09.008. Available from : https://linkinghub.elsevier.com/retrieve/pii/S0260877416303132

[245] SAHI, S.S., 1994. Interfacial properties of the aqueous phases of wheat flour doughs. *Journal of Cereal Science*. 1 September 1994. Vol. 20, n° 2, pp. 119–127. [Accessed 30 October 2025]. DOI 10.1006/jcrs.1994.1052. Available from : https://www.sciencedirect.com/science/article/pii/S0733521084710526

[246] SAKANDAR, H., HUSSAIN, R., KUBOW, S., SADIQ, F., HUANG, W. and IMRAN, M., 2019. Sourdough bread: A contemporary cereal fermented product. *Journal of Food Processing and Preservation*. 1 March 2019. DOI 10.1111/jfpp.13883.

[247] ŞAKIYAN, Ö., SUMNU, G., SAHIN, S. and BAYRAM, G., 2004. Influence of fat content and emulsifier type on the rheological properties of cake batter. *European Food Research and Technology*. January 2004. Vol. 219, pp. 635–638. DOI 10.1007/s00217-004-1020-4.

[248] SANDOVAL, A.J., 2017. Cellular structure and rheological properties of shaped fermented wheat flour dough. *Journal of Cereal Science*. 2017.

[249] SANMARTÍN, G., SÁNCHEZ-ADRIÁ, I.E., SALVADOR, A., PRIETO, J.A., ESTRUCH, F. and RANDEZ-GIL, F., 2024. Quantitative Assessment of Volatile Profile and Sensory Perception of Artisan Bread Made in the City of Valencia. *Foods*. 29 November 2024. Vol. 13, n° 23, pp. 3872. DOI 10.3390/foods13233872.

[250] SAULNIER, L., MICARD, V. and DELLA VALLE, G., 2014. Structure du pain et index glycémique. *Cahiers de Nutrition et de Diététique*. 2014. Vol. 49, n° 2, pp. 61–66. [Accessed 6 February 2026]. DOI 10.1016/j.cnd.2014.01.004. Available from : https://hal.science/hal-01837408

[251] SHAH, P., CAMPBELL, G.M., MCKEE, S.L. and RIELLY, C.D., 1998. Proving of bread dough: Modelling the growth of individual bubbles. *Food and Bioproducts Processing*. 1998. Vol. 76, n° 2, pp. 73–79. DOI https://doi.org/10.1205/096030898531828. Available from : https://www.sciencedirect.com/science/article/pii/S0960308598700999

[252] SHEHZAD, A., CHIRON, H., DELLA VALLE, G., LAMRINI, B. and LOURDIN, D., 2012. Energetical and rheological approaches of wheat flour dough mixing with a spiral mixer. *Journal of Food Engineering*. 1 May 2012. Vol. 110, n° 1, pp. 60–70. [Accessed 30 October 2025]. DOI 10.1016/j.jfoodeng.2011.12.008. Available from : https://www.sciencedirect.com/science/article/pii/S0260877411006509

[253] SHEIKHOLESLAMI, Z., KARIMI, M. and HEJRANI, T., 2020. The effect of ascorbic acid and glycerol on quality of frozen barbari bread. . 1 May 2020. Vol. 7, pp. 1317–1321.

[254] SHEWRY, P.R. and BELTON, P.S., 2024. What do we really understand about wheat gluten structure and functionality? *Journal of Cereal Science*. 1 May 2024. Vol. 117, pp. 103895. [Accessed 30 October 2025]. DOI 10.1016/j.jcs.2024.103895. Available from : https://www.sciencedirect.com/science/article/pii/S0733521024000535

[255] SHEWRY, P.R., HALFORD, N.G., BELTON, P.S. and TATHAM, A.S., 2002. The structure and properties of gluten: an elastic protein from wheat grain. *Philosophical Transactions of the Royal Society B: Biological Sciences*. 28 February 2002. Vol. 357, n° 1418, pp. 133–142. [Accessed 30 October 2025]. DOI 10.1098/rstb.2001.1024. Available from : https://pmc.ncbi.nlm.nih.gov/articles/PMC1692935/

[256] SHEWRY, P.R. and LAFIANDRA, D., 2022. Wheat glutenin polymers 1. Structure, assembly and properties. *Journal of Cereal Science*. 1 July 2022. Vol. 106, pp. 103486. [Accessed 30 October 2025]. DOI 10.1016/j.jcs.2022.103486. Available from : https://www.sciencedirect.com/science/article/pii/S0733521022000753

[257] SHEWRY, P.R. and TATHAM, A.S., 1997. Disulphide bonds in wheat gluten proteins. *Journal of Cereal Science*. 1 May 1997. Vol. 25, n° 3, pp. 207–227. [Accessed 30 October 2025]. DOI 10.1006/jcrs.1996.0100. Available from : https://www.sciencedirect.com/science/article/pii/S0733521096901009

[258] SLIWINSKI, E.L., KOLSTER, P. and VAN VLIET, T., 2004. Large-deformation properties of wheat dough in uni- and biaxial extension. Part I. Flour dough. *Rheologica Acta*. August 2004. Vol. 43, n° 4, pp. 306–320. [Accessed 6 January 2023]. DOI 10.1007/s00397-003-0344-5. Available from : http://link.springer.com/10.1007/s00397-003-0344-5

[259] SMIRNOFF, N., 2018. Ascorbic acid metabolism and functions: A comparison of plants and mammals. *Free Radical Biology and Medicine*. 1 March 2018. Vol. 122. DOI 10.1016/j.freeradbiomed.2018.03.033.

[260] SRIVASTAVA, S., KOLLEMPAREMBIL, A.M., ZETTEL, V., CLASSEN, T., MOBARAK, M., GATTERNIG, B., DELGADO, A., JEKLE, M. and HITZMANN, B., 2022. An Innovative Approach in the Baking of Bread with CO2 Gas Hydrates as Leavening Agents. *Foods*. November 2022. Vol. 11, pp. 3570. DOI 10.3390/foods11223570.

[261] SROAN, B.S., BEAN, S.R. and MACRITCHIE, F., 2009. Mechanism of gas cell stabilization in bread making. I. The primary gluten–starch matrix. *Journal of Cereal Science*. January 2009. Vol. 49, n° 1, pp. 32–40. [Accessed 3 February 2023]. DOI 10.1016/j.jcs.2008.07.003. Available from : https://linkinghub.elsevier.com/retrieve/pii/S0733521008001136

[262] STEAR, C.A., 1990. Dough and bread preservation. In : STEAR, Charles A. (ed.), *Handbook of Breadmaking Technology*. Boston, MA : Springer US. pp. 679–714. [Accessed 10 October 2025]. ISBN 978-1-4615-2375-8. Available from : https://doi.org/10.1007/978-1-4615-2375-8_20

[263] STEFFE, J.F., 1996. *Rheological Methods in Food Process Engineering*. Freeman Press. ISBN 978-0-9632036-1-8.

[264] STIEGER, M. and VAN DE VELDE, F., 2013. Microstructure, texture and oral processing: New ways to reduce sugar and salt in foods. *Current Opinion in Colloid & Interface Science*. August 2013. Vol. 18, pp. 334–348. DOI 10.1016/j.cocis.2013.04.007.

[265] STRUYF, N., VAN DER MAELEN, E., HEMDANE, S., VERSPREET, J., VERSTREPEN, K.J. and COURTIN, C.M., 2017. Bread dough and baker's Yeast: An uplifting Synergy: Yeast and bread dough: The interaction.

Comprehensive Reviews in Food Science and Food Safety. September 2017. Vol. 16, n° 5, pp. 850–867. [Accessed 27 April 2023]. DOI 10.1111/1541-4337.12282. Available from : https://onlinelibrary.wiley.com/doi/10.1111/1541-4337.12282

[266] SUJKA, M. and JAMROZ, J., 2013. Ultrasound-treated starch: SEM and TEM imaging, and functional behaviour. *Food Hydrocolloids*. June 2013. Vol. 31, n° 2, pp. 413–419. [Accessed 12 June 2023]. DOI 10.1016/j.foodhyd.2012.11.027. Available from : https://linkinghub.elsevier.com/retrieve/pii/S0268005X12002925

[267] SUMNU, G., DATTA, A.K., SAHIN, S., KESKIN, S.O. and RAKESH, V., 2007. Transport and related properties of breads baked using various heating modes. *Journal of Food Engineering*. 2007. Vol. 78, n° 4, pp. 1382–1387. DOI https://doi.org/10.1016/j.jfoodeng.2006.01.010. Available from : https://www.sciencedirect.com/science/article/pii/S0260877406000550

[268] SUN, X., SCANLON, Martin, NICKERSON, M. and KOKSEL, F., 2023. The entrainment and evolution of gas bubbles in bread dough - A review. *Cereal Chemistry*. July 2023. Vol. 100. DOI 10.1002/cche.10699.

[269] SUN, X., SCANLON, Martin G, NICKERSON, M.T. and KOKSEL, F., 2023. The entrainment and evolution of gas bubbles in bread dough—A review. . 2023. Vol. 100, n° 5. DOI doi.org/10.1002/cche.10699.

[270] SUN, X., WU, S., KOKSEL, F., XIE, M. and FANG, Y., 2022. Effects of ingredient and processing conditions on the rheological properties of whole wheat flour dough during breadmaking - A review. *Food Hydrocolloids*. 1 September 2022. Vol. 135, pp. 108123. DOI 10.1016/j.foodhyd.2022.108123.

[271] SZCZESNIAK, A.S., 2002. Texture is a sensory property. *Food Quality and Preference*. 2002. Vol. 13, n° 4, pp. 215–225. DOI https://doi.org/10.1016/S0950-3293(01)00039-8. Available from : https://www.sciencedirect.com/science/article/pii/S0950329301000398

[272] TAKEDA, Y., MARUTA, N. and HIZUKURI, S., 1992. Structures of amylose subfractions with different molecular sizes. *Carbohydrate Research*. March 1992. Vol. 226, n° 2, pp. 279–285. [Accessed 14 June 2023]. DOI 10.1016/0008-6215(92)84076-5. Available from : https://linkinghub.elsevier.com/retrieve/pii/0008621592840765

[273] TECANTE, A. and DOUBLIER, J.L., 1999. Steady flow and viscoelastic behavior of crosslinked waxy corn starch-κ-carrageenan pastes and gels. *Carbohydrate Polymers*. 1999. Vol. 40, n° 3, pp. 221–231. DOI https://doi.org/10.1016/S0144-8617(99)00057-0. Available from : https://www.sciencedirect.com/science/article/pii/S0144861799000570

[274] THEBAUDIN, J.-Y., LEFEBVRE, A.-C. and DOUBLIER, J.-L., 1998. Rheology of starch pastes from starches of different origins: Applications to starch-based sauces. *LWT - Food Science and Technology*. 1998. Vol. 31, n° 4, pp. 354–360. DOI https://doi.org/10.1006/fstl.1998.0367. Available from : https://www.sciencedirect.com/science/article/pii/S002364389890367X

[275] THERDTHAI, N. and ZHOU, W., 2003. Recent advances in the studies of bread baking process and their impacts on the bread baking technology. *Food Science and Technology Research*. 2003. Vol. 9, n° 3, pp. 219–226. DOI 10.3136/fstr.9.219.

[276] THOMPSON, S.A. and WILLIAMS, R.O., 2021. Specific mechanical energy - An essential parameter in the processing of amorphous solid dispersions. *Advanced Drug Delivery Reviews*. June 2021. Vol. 173, pp. 374–393. DOI 10.1016/j.addr.2021.03.006.

[277] TRINH, L., LOWE, T., CAMPBELL, G.M., WITHERS, P.J. and MARTIN, P.J., 2015. Effect of sugar on bread dough aeration during mixing. *Journal of Food Engineering*. April 2015. Vol. 150, pp. 9–18. [Accessed 11 January 2023]. DOI 10.1016/j.jfoodeng.2014.10.020. Available from : https://linkinghub.elsevier.com/retrieve/pii/S0260877414004403

[278] TU, Y.-J., NJUS, D. and SCHLEGEL, H., 2017. A theoretical study of ascorbic acid oxidation and HOO / O 2 - Radical scavenging. *Org. Biomol. Chem.* 9 May 2017. Vol. 15. DOI 10.1039/C7OB00791D.

[279] TURABI, E., SUMNU, G. and SAHIN, S., 2008. Rheological properties and quality of rice cakes formulated with different gums and an emulsifier blend. *Food Hydrocolloids*. 2008. Vol. 22, n° 2, pp. 305–312. DOI https://doi.org/10.1016/j.foodhyd.2006.11.016. Available from : https://www.sciencedirect.com/science/article/pii/S0268005X06002864

[280] VAN DE VELDE, F., VAN RIEL, J. and TROMP, R.H., 2002. Visualisation of starch granule morphologies using confocal scanning laser microscopy (CSLM). *Journal of the Science of Food and Agriculture*. October 2002. Vol. 82, n° 13, pp. 1528–1536. [Accessed 14 June 2023]. DOI 10.1002/jsfa.1165. Available from : https://onlinelibrary.wiley.com/doi/10.1002/jsfa.1165

[281] VAN VLIET, T., 2008. Strain hardening as an indicator of bread-making performance: A review with discussion. *Journal of Cereal Science*. July 2008. Vol. 48, n° 1, pp. 1–9. [Accessed 23 December 2022]. DOI 10.1016/j.jcs.2007.08.010. Available from : https://linkinghub.elsevier.com/retrieve/pii/S0733521007001622

[282] VANIN, F.M., LUCAS, T. and TRYSTRAM, G., 2009. Crust formation and its role during bread baking. *Trends in Food Science & Technology*. 1 August 2009. Vol. 20, n° 8, pp. 333–343. [Accessed 30 October 2025]. DOI 10.1016/j.tifs.2009.04.001. Available from : https://www.sciencedirect.com/science/article/pii/S0924224409001307

[283] VARAYIL, H., YADAV, B. and LEBAIL, A., 2019. Impact of pressure change during dough mixing and characteristics of bread under high pressure. *International Journal of Pure & Applied Bioscience*. 30 June 2019.

[284] VARELA, P. and ARES, G., 2012. Sensory profiling, the blurred line between sensory and consumer science. A review of novel methods for product characterization. *Food Research International*. 1 October 2012. Vol. 48, n° 2, pp. 893–908. [Accessed 6 February 2026]. DOI 10.1016/j.foodres.2012.06.037. Available from : https://www.sciencedirect.com/science/article/pii/S0963996912002487

[285] VENTURI, M., GALLI, V., PINI, N., GUERRINI, S., SODI, C. and GRANCHI, L., 2021. Influence of different leavening agents on technological and nutritional characteristics of whole grain breads obtained from ancient and modern flour varieties. *European Food Research and Technology*. 1 July 2021. Vol. 247. DOI 10.1007/s00217-021-03740-y.

[286] VERHEYEN, C., ALBRECHT, A., ELGETI, D., JEKLE, M. and BECKER, T., 2015. Impact of gas formation kinetics on dough development and bread quality. *Food Research International*. October 2015. Vol. 76, pp. 860–866. [Accessed 27 December 2022]. DOI 10.1016/j.foodres.2015.08.013. Available from : https://linkinghub.elsevier.com/retrieve/pii/S0963996915301435

[287] VERHEYEN, C., JEKLE, M. and BECKER, T., 2014. Effects of Saccharomyces cerevisiae on the structural kinetics of wheat dough during fermentation. *LWT - Food Science and Technology*. 1 September 2014. Vol. 58, n° 1, pp. 194–202. [Accessed 30 October 2025]. DOI 10.1016/j.lwt.2014.02.050. Available from : https://www.sciencedirect.com/science/article/pii/S0023643814001261

[288] VIDAL, L.M., BRAUN, A., JEKLE, M. and BECKER, T., 2022. Micro-Scale shear kneading-gluten network development under multiple stress-relaxation steps and evaluation via multiwave rheology. *Polymers*. 21 February 2022. Vol. 14, n° 4, pp. 846. DOI 10.3390/polym14040846.

[289] VILCANQUI-PÉREZ, F., CHAQUILLA, L., SARMIENTO-CASAVILCA, V., CÉSPEDES-OROSCO, C. and VENTURA-SALDIVAR, Y., 2021. Nutritional, physical and sensory characteristics of bread with the inclusion of germinated basul (Erythrina edulis) flour. *Journal of Food Science and Technology*. August 2021. Vol. 59. DOI 10.1007/s13197-021-05246-7.

[290] VLIET, T., JANSSEN, A.M., BLOKSMA, A.H. and WALSTRA, P., 1992. Strain hardening of dough as a requirement for gas retention. *Journal of Texture Studies*. December 1992. Vol. 23, n° 4, pp. 439–460.

[Accessed 23 December 2022]. DOI 10.1111/j.1745-4603.1992.tb00033.x. Available from : https://onlinelibrary.wiley.com/doi/10.1111/j.1745-4603.1992.tb00033.x

[291] WANG, H., HAN, P., ZHANG, P. and LI, Y., 2024. Influence of yeast concentrations and fermentation durations on the physical properties of white bread. *LWT*. 2024. Vol. 198, pp. 116063. DOI https://doi.org/10.1016/j.lwt.2024.116063. Available from : https://www.sciencedirect.com/science/article/pii/S0023643824003426

[292] WANG, H., LIU, W., ZHANG, P. and LIAN, X., 2024. The mechanism underlying the increase in bread hardness in association with alterations in protein and starch characteristics during room-temperature storage. *Foods*. 4 December 2024. Vol. 13, n° 23, pp. 3921. [Accessed 28 October 2025]. DOI 10.3390/foods13233921. Available from : https://pmc.ncbi.nlm.nih.gov/articles/PMC11641183/

[293] WANG, S., AUSTIN, P. and BELL, S., 2011. It's a maze: The pore structure of bread crumbs. *Journal of Cereal Science*. 2011. Vol. 54, n° 2, pp. 203–210. DOI https://doi.org/10.1016/j.jcs.2011.05.004. Available from : https://www.sciencedirect.com/science/article/pii/S0733521011000956

[294] WANG, S. and COPELAND, L., 2013. Molecular disassembly of starch granules during gelatinization and its effect on starch digestibility: a review. *Food & Function*. 2013. Vol. 4, n° 11, pp. 1564. [Accessed 16 February 2023]. DOI 10.1039/c3fo60258c. Available from : http://xlink.rsc.org/?DOI=c3fo60258c

[295] WANG, S., ZHENG, M. and CHAO, C., 2019. Interactions between starch, proteins and lipids and the formation of ternary complexes with distinct properties. In : *Encyclopedia of Food Chemistry*. Elsevier. pp. 487–493. [Accessed 22 March 2023]. ISBN 978-0-12-814045-1. Available from : https://linkinghub.elsevier.com/retrieve/pii/B9780081005965214820

[296] WANG, Shujun, LI, C., COPELAND, L., NIU, Q. and WANG, Shuo, 2015. Starch retrogradation: A comprehensive review: Starch retrogradation. *Comprehensive Reviews in Food Science and Food Safety*. September 2015. Vol. 14, n° 5, pp. 568–585. [Accessed 16 February 2023]. DOI 10.1111/1541-4337.12143. Available from : https://onlinelibrary.wiley.com/doi/10.1111/1541-4337.12143

[297] WEAIRE, D. and PAGERON, V., 1990. Frustrated froth: Evolution of foam inhibited by an insoluble gaseous component. *Philosophical Magazine Letters*. 1 December 1990. Vol. 62, n° 6, pp. 417–421. [Accessed 10 October 2025]. DOI 10.1080/09500839008215544. Available from : https://doi.org/10.1080/09500839008215544

[298] WEBB, T., HEAPS, P., EGGITT, P. and COPPOCK, J., 2007. A rheological investigation of the role of water in wheat flour dough. *International Journal of Food Science & Technology*. 28 June 2007. Vol. 5, pp. 65–76. DOI 10.1111/j.1365-2621.1970.tb01543.x.

[299] WELC-STANOWSKA, R., KŁOSOK, K. and NAWROCKA, A., 2023. Insight into organization of gliadin and glutenin extracted from gluten modified by phenolic acids. *Molecules*. January 2023. Vol. 28, n° 23, pp. 7790. [Accessed 30 October 2025]. DOI 10.3390/molecules28237790. Available from : https://www.mdpi.com/1420-3049/28/23/7790

[300] WIESER, H., 2007. Chemistry of gluten proteins. *Food Microbiology*. April 2007. Vol. 24, n° 2, pp. 115–119. [Accessed 9 March 2023]. DOI 10.1016/j.fm.2006.07.004. Available from : https://linkinghub.elsevier.com/retrieve/pii/S0740002006001535

[301] WILDE, P., 2012. Foam formation in dough and bread quality. In : CAUVAIN, Stanley P. (ed.), *Breadmaking (Second Edition)*. Second Edition. Woodhead Publishing. pp. 370–399. Woodhead Publishing Series in Food Science, Technology and Nutrition. ISBN 978-0-85709-060-7. Available from : https://www.sciencedirect.com/science/article/pii/B9780857090607500152

[302] WILSON, A., MORGENSTERN, M. and KAVALE, D., 2001. Mixing response of a variable speed 125g laboratory scale mechanical dough development mixer. *Journal of Cereal Science - J CEREAL SCI*. 1 September 2001. Vol. 34, pp. 151–158. DOI 10.1006/jcrs.2001.0389.

[303] ZARZYCKI, P., WIRKIJOWSKA, A., TETERYCZ, D. and ŁYSAKOWSKA, P., 2024. Innovations in wheat bread: Using food industry by-products for better quality and nutrition. *Applied Sciences*. January 2024. Vol. 14, n° 10, pp. 3976. [Accessed 30 October 2025]. DOI 10.3390/app14103976. Available from : https://www.mdpi.com/2076-3417/14/10/3976

[304] ZHANG, L., YANG, W., XU, K., LONG, L. and YE, H., 2025. Study on moisture phase changes in bread baking using a coupling model. *Foods*. 2025. Vol. 14, n° 9. DOI 10.3390/foods14091649. Available from : https://www.mdpi.com/2304-8158/14/9/1649

[305] ZHONG, Y., BERTOFT, E., LI, Z., BLENNOW, A. and LIU, X., 2020. Amylopectin starch granule lamellar structure as deduced from unit chain length data. *Food Hydrocolloids*. November 2020. Vol. 108, pp. 106053. [Accessed 15 February 2023]. DOI 10.1016/j.foodhyd.2020.106053. Available from : https://linkinghub.elsevier.com/retrieve/pii/S0268005X20306640

Titre : Pétrissage de pâte à pain de mie sous gaz pressurisé

Mots clés : Pétrissage, Atmosphère gazeuse modifiée, Solubilisation des gaz, Gaz pressurisé, Pain de mie.

Résumé : Ce projet de thèse, financé par GEPEA-ONIRIS (CNRS 6144) et l'unité de recherche INRAE-BIA en partenariat avec la TU Hohenheim visait à étudier le pétrissage de pâte à pain sous pression de divers gaz purs ou de mélanges en vue de moduler le développement de la pâte et son aération. L'objectif principal était de contrôler et d'optimiser la structure de la pâte et du pain en ajustant les paramètres de pétrissage. Divers gaz (air, O_2, CO_2, N_2) et leurs mélanges, les niveaux de pression et les vitesses de mélange ont été considérés. L'acide ascorbique (AH_2) a également été utilisé pour étudier son comportement dans ces conditions de pétrissage modifiées. L'AH_2 fonctionne comme un agent oxydant en favorisant l'oxydation des thiols libres (-SH), ce qui conduit à la formation de ponts disulfures (-S-S-) qui renforcent le réseau de gluten. Enfin, l'utilisation d'eau gazeuse saturée en gaz carbonique a également été considérée comme une alternative à l'apport de CO_2 sous forme de gaz. Une approche calculatoire a tout d'abord permis de quantifier le potentiel de solubilisation ou de consommation des gaz par la pâte en cours de pétrissage autours de deux stratégies de pétrissage, avec ou sans balayage gazeux.

Après avoir optimisé les paramètres expérimentaux, en particulier la maîtrise du taux d'expansion en fermentation en fonction de la fraction de gazeuse initiale de la pâte, les principaux résultats obtenus ont montré que le pétrissage sous CO_2 n'avait pas d'effet positif sur la qualité des pains, qu'il soit apporté par voie gazeuse ou liquide ; la modulation de la quantité de levure a permis de pallier aux défauts observés. L'utilisation d'AH_2 n'a pas eu d'effet significatif sur les étapes du procédé de pétrissage ni sur la qualité des pains, que ce soit en présence ou en absence d'oxygène. Une étude a été menée afin d'évaluer l'effet des gaz sur le rassissement des pains avec des résultats intéressants. Enfin, l'analyse sensorielle a révélé une bonne acceptation des pains, avec des remarques sur l'homogénéité de la mie, la couleur et l'odeur, et une texture généralement positive. Ce projet a permis de mieux comprendre le fonctionnement de pétrins non conventionnels et a ouvert de nombreuses perspectives en particulier sur le plan de la conception des équipements et sur leur mise en œuvre.

Title : Mixing sandwich bread dough under pressurized gas

Keywords : Dough mixing, Modified gas atmosphere, Gas solubilisation, Pressurized gas, Sandwich bread.

Abstract : This PhD project, funded by GEPEA-ONIRIS (CNRS 6144) and the INRAE-BIA research unit, in partnership with TU Hohenheim, aimed to study bread dough kneading under pressure with various pure gases or gas mixtures, with the goal of modulating dough development and aeration. The main objective was to control and optimize the structure of the dough and the final bread by adjusting kneading parameters. Different gases (air, O_2, CO_2, N_2) and their mixtures, pressure levels, and mixing speeds were considered. Ascorbic acid (AH_2) was also used to study its behaviour under these modified kneading conditions. AH_2 acts as an oxidizing agent by promoting the oxidation of free thiol groups (-SH), leading to the formation of disulfide bridges (-S-S-) that strengthen the gluten network. Finally, the use of carbonated water saturated with CO_2 was also considered as an alternative to supplying CO_2 in gaseous form. A calculation-based approach was first used to quantify the potential for gas solubilisation or consumption by the dough during kneading, across two kneading strategies—with or without gas purging.

After optimizing the experimental parameters, particularly controlling fermentation expansion based on the dough's initial gas fraction, the main results showed that kneading under CO_2 did not have a positive effect on bread quality, whether introduced in gaseous or liquid form. However, modulating the amount of yeast helped mitigate the observed defects. The use of AH_2 had no significant effect on the kneading process or on bread quality, whether in the presence or absence of oxygen. A study was also conducted to evaluate the effect of gases on bread staling, with interesting results. Finally, sensory analysis revealed good acceptance of the breads, with comments on crumb homogeneity, color, aroma, and an overall positive texture. This project contributed to a better understanding of the operation of non-conventional mixers and opened up many perspectives, particularly in terms of equipment design and implementation.